

Chemistry Research and Applications

Polystyrene

Synthesis, Characteristics and Applications

Cole Lynwood
Editor

NOVA

CHEMISTRY RESEARCH AND APPLICATIONS

POLYSTYRENE
SYNTHESIS, CHARACTERISTICS
AND APPLICATIONS

No part of this digital document may be reproduced, stored in a retrieval system or transmitted in any form or by any means. The publisher has taken reasonable care in the preparation of this digital document, but makes no expressed or implied warranty of any kind and assumes no responsibility for any errors or omissions. No liability is assumed for incidental or consequential damages in connection with or arising out of information contained herein. This digital document is sold with the clear understanding that the publisher is not engaged in rendering legal, medical or any other professional services.

CHEMISTRY RESEARCH AND APPLICATIONS

Additional books in this series can be found on Nova's website under the Series tab.

Additional e-books in this series can be found on Nova's website under the e-book tab.

CHEMISTRY RESEARCH AND APPLICATIONS

POLYSTYRENE
SYNTHESIS, CHARACTERISTICS
AND APPLICATIONS

COLE LYNWOOD
EDITOR

The logo for Nova Publishers features the word "nova" in a bold, lowercase sans-serif font. The letter "o" is replaced by a stylized globe showing continents. To the left of the "nova" text is a decorative graphic consisting of a series of small dots arranged in a semi-circular pattern, resembling a sunburst or a molecular structure. Below "nova" is the word "publishers" in a smaller, lowercase sans-serif font.

nova
publishers

New York

Copyright © 2014 by Nova Science Publishers, Inc.

All rights reserved. No part of this book may be reproduced, stored in a retrieval system or transmitted in any form or by any means: electronic, electrostatic, magnetic, tape, mechanical photocopying, recording or otherwise without the written permission of the Publisher.

For permission to use material from this book please contact us:

Telephone 631-231-7269; Fax 631-231-8175

Web Site: <http://www.novapublishers.com>

NOTICE TO THE READER

The Publisher has taken reasonable care in the preparation of this book, but makes no expressed or implied warranty of any kind and assumes no responsibility for any errors or omissions. No liability is assumed for incidental or consequential damages in connection with or arising out of information contained in this book. The Publisher shall not be liable for any special, consequential, or exemplary damages resulting, in whole or in part, from the readers' use of, or reliance upon, this material. Any parts of this book based on government reports are so indicated and copyright is claimed for those parts to the extent applicable to compilations of such works.

Independent verification should be sought for any data, advice or recommendations contained in this book. In addition, no responsibility is assumed by the publisher for any injury and/or damage to persons or property arising from any methods, products, instructions, ideas or otherwise contained in this publication.

This publication is designed to provide accurate and authoritative information with regard to the subject matter covered herein. It is sold with the clear understanding that the Publisher is not engaged in rendering legal or any other professional services. If legal or any other expert assistance is required, the services of a competent person should be sought. FROM A DECLARATION OF PARTICIPANTS JOINTLY ADOPTED BY A COMMITTEE OF THE AMERICAN BAR ASSOCIATION AND A COMMITTEE OF PUBLISHERS.

Additional color graphics may be available in the e-book version of this book.

Library of Congress Cataloging-in-Publication Data

Polystyrene : synthesis, characteristics, and applications / editor, Cole Lynwood.

pages cm. -- (Chemistry research and applications)

Includes bibliographical references and index.

ISBN: ; 9: /3/85543/593/7 (eBook)

1. Polystyrene. 2. Polymers. 3. Chemistry, Inorganic. I. Lynwood, Cole, editor.

TP1180.S7P665 2014

668.4'233--dc23

2014022560

Published by Nova Science Publishers, Inc. † New York

CONTENTS

Preface		vii
Chapter 1	Waste/Contaminated Polystyrene Recycling through Reverse Polymerization <i>Piero Frediani, Andrea Undri, Luca Rosi and Marco Frediani</i>	1
Chapter 2	Polystyrene-Based Amphiphilic Block Copolymers: Synthesis, Properties and Applications <i>Patrizio Raffa</i>	31
Chapter 3	Expanded Polystyrene: Thermo-Mechanical Recycling, Characterization and Application <i>Matheus Poletto, Heitor L. Ornaghi Júnior and Ademir J. Zattera</i>	53
Chapter 4	Gigaporous Polystyrene Microspheres and Their Applications in High-Speed Protein Chromatography <i>Jian-Bo Qu, Fang Huang, Wei-Qing Zhou, Fei Gao and Guang-Hui Ma</i>	75
Chapter 5	Functional Structures Fabricated from Submicron-Scale Polystyrene Spherical Particles <i>Akira Emoto and Takashi Fukuda</i>	115
Chapter 6	Synthesis and Applications of Ionic Polystyrenes Derived from Imidazolium-Based Polymerizable Ionic Liquids <i>Jun-ichi Kadokawa</i>	129
Chapter 7	Hypercrosslinked Polystyrene: A New Life for the Old Polymer <i>M. P. Tsyurupa, A. V. Pastukhov, Z .K. Blinnikova, L. A. Pavlova, M. M. Il'in, Yu. A. Davidovich and V. A. Davankov</i>	143
Chapter 8	Synthesis and Characterization of Polystyrene Based Nanocomposites <i>Vesna V. Vodnik, Enis S. Džunuzović and Jasna V. Džunuzović</i>	201

Chapter 9	Polystyrene Spheres for Template in the Production of Nanostructured Materials <i>Asep Bayu Dani Nandiyanto, Takashi Ogi and Kikuo Okuyama</i>	241
Chapter 10	Applications of Polystyrene and Its Role as a Base in Industrial Chemistry <i>Tanvir Arfin, Faruq Mohammad and Nor Azah Yusof</i>	269
Chapter 11	A New Equation for Homogeneous Nucleation from Polystyrene Solutions <i>John H. Jennings</i>	281
Index		291

PREFACE

Polystyrene represents one of the oldest and the most widespread polymers in the world. Its starts as far back as 1839 when a German apothecary Edmon Simon distilled an oily liquid named styrol from the resin of Turkish sweet gum trees. In several days, the sterol converted into a jelly product that he thought resulted from the oxidation process. For that reason, the jelly product received the name styroloxide. This book discusses the synthesis of polystyrene, as well as the characteristics and applications of this polymer.

Chapter 1 - Polystyrene (PS) is the most employed aromatic thermoplastic polymer. PS finds a wide range of application from food contact packaging to thermal insulator in buildings. Its disposal is an environmental and social problem which is ceaselessly addressed from academic and industrial researchers.

Among several recycling processes exploited the most used is direct remanufacturing through milling, washing, drying, and moulding but this is possible only for un-contaminated waste.

Safeguarding of energy and material content of waste PS is a mandatory key to save oil stocks and contaminated PS may be disposed through conservation and valorisation of the phenyl moiety. Pyrolysis meets these requirements: it may convert waste PS into single ring aromatic compounds, together with low amount of char and gas, if appropriate pyrolysis conditions are employed.

Thermal pyrolysis is already active at 350 °C, where the main product is a dark viscous liquid rich in single ring aromatic compounds (benzene, toluene, ethylbenzene, and styrene). Char formation increases when pyrolysis temperature rises. Anyway different pyrolysis behaviour is observed for different classes of PS (virgin, expanded, and compacted from containers), especially for what concerning the composition and distribution of aromatics in the liquid fraction.

In the last few years microwave (MW) heating has encountered a sound and reliable application in polymeric waste treatment. Microwave assisted pyrolysis (MAP) encloses a number of advantages than classical methods. One of these is the direct and extremely fast heating in the presence of a MW absorber. MAP of PS has been investigated in the presence of a microwave absorber such as carbon, iron mesh, or aluminium, as coil or mesh.

Chapter 2 - Polystyrene is no longer only a commodity plastic. It has been long recognized that copolymerization of styrene with other monomers presenting different characteristics allows the production of new mate-rials, with improved or even completely new properties.

Of particular interest are block copolymers of styrene with hydro-philic monomers. The ability of these amphiphilic polymers to form stable self-assembled aggregates in water by association of the insoluble polystyrene blocks is the key feature of their interesting properties.

Especially in recent times, there has been a great interest in self-assembly, surface activity and rheology of polystyrene-based amphiphilic block copolymers in water. Because of their unique properties, polystyrene-based amphiphilic block copolymers can find applications as detergents, emulsifiers, stabilizers for emulsion polymerizations, nanoreactors, gelators, rheology modifiers and others.

The development of controlled radical polymerization methods (e.g., Atomic Transfer Radical Polymerization) in the last two decades provided powerful tools for the preparation of well-defined polymers and copolymers of styrene with tailored molecular weight, composition and architectures. Alongside the synthesis of an increasing number of polystyrene amphiphilic copolymers, an extensive knowledge of the self-assembly, surface and rheological properties of these materials has been gained, also in connection with the polymer composition and architecture.

Here, an overview of synthesis, properties and applications of amphiphilic copolymers containing at least one polystyrene block will be given, aimed at envisaging the impact of this kind of polymers in the future of science, industry and life.

Chapter 3 - Plastic materials are used in our daily lives in several applications. These include a substantial amount of polyolefins, which can potentially be recovered for recycling. Expanded polystyrene (EPS) is commonly used for insulation and packaging materials due some advantages as versatility, dimensional stability and low cost. However, in some countries, its inadequate disposal, mainly in landfills can cause serious environmental health concerns if modern regulations are not complied. Different characterization techniques, such as chemical and thermal ones, are available for recycling EPS waste. Nevertheless, chemical techniques usually involve the use of hazardous solvents meanwhile thermal recycling may cause gaseous pollution. So, in this work a methodology for thermo-mechanical recycling of EPS waste was presented in order to development composites based on recycled EPS and wood flour waste. The EPS wastes were processed by compression molding technique. So, they were grinded before processing with wood flour in a co-rotating twin-screw extruder. Consequently the composites were injection molding. The results showed that the process of compression molding led to a decreased in volume as well as a 25-fold increase in the density of the EPS waste when compared with the raw material. Thus, after compression molding and grinding, the EPS waste can be used directly in the extrusion process with the wood flour. This eliminates one process reducing the recycling costs. The composites showed increased in mechanical, thermo-mechanical and morphologic properties when coupling agent was used in the composite formulations. Based on the findings of this study, the methodology used for EPS recycling and for development of wood composites appears as an alternative for manufacture composites based on recycled materials with high properties without cause serious environmental problems.

Chapter 4 - Modern chromatography media have developed over the years, providing improved binding capacity, faster mass transfer, better chemical resistance, and greater selectivity. Compared with silica and conventional separation media (e.g. dextran and agarose), there is an increasing interest in the use of poly(styrene-divinylbenzene) (PS) microspheres as chromatographic packing materials for proteins and antibodies owing to their

excellent mechanical properties and good chemical stability over a wide pH range. However, for conventional porous microspheres with normal pore size of 10-100 nm, slow mass transfer rate is the factor that restricts their application in biomacromolecule separation. It is imperative to develop efficient separation media with high resolution, high speed and high capacity for a broad range of business areas including pharmaceuticals, nutrition and health products, bioenergy, environmental protection and so on.

Gigaporous PS microspheres with pore diameter around 300-500 nm are very promising in high-speed protein chromatography, which can effectively reduce the resistance from stagnant mobile phase mass transfer by inducing convective flow of mobile phase in the gigapores of medium. Unfortunately, the native PS beads are not suitable for protein chromatography medium due to their high hydrophobicity causing non-specific adsorption and denaturation of proteins. This chapter describes the current development of gigaporous PS microspheres and their application in high-speed protein chromatography, with emphasis on their recent contributions to this field.

Chapter 5 - Spherical polystyrene (PS) particles dispersed in colloidal suspensions have been used to fabricate photonic crystal structures, nano- and micro-scale templates, and functional surface structures. In this chapter, the authors describe methods for forming many of these functional structures from submicron PS spheres. They propose a thin sandwich-type cell to fabricate adjacent structures of different photonic crystals. In addition, the order of the crystals can be controlled by the evaporation rate of the colloidal suspension, creating unique, structure-dependent, optical characteristics. Monolayers of metal-coated PS spheres are also used for plasmonic sensor chips. A replication process using silicone rubber molds can form them repetitively and accurately. The resultant structures and optical characteristics can be modified *via* mold deformation during the replication process. In particular, significant anisotropic, dichroic reflections can be observed under certain elongation conditions. Finally, unique porous films can be formed with PS spheres. The authors discuss a simple method for the fabrication of pores having outer shells, and where submicron-scale pores are formed by spin-coating colloidal mixtures.

Chapter 6 - Polystyrene is one of the representative high-performance and commercially successful synthetic polymers. The main-chain structure of polystyrene has been employed in a variety of polymeric materials for carrying functional groups. For example, polymerization of styrene monomers, which have some substituted functional groups on the aromatic rings has led to polystyrene-based functional materials. On the other hand, ionic liquids, which are salts with a low melting point have been noted as new solvents and functional materials for the use as catalysts, environmentally benign solvents, photomaterials, and so on. One of the representative cationic structures in the ionic liquids is an imidazolium group. The polymer forms of ionic liquids, which are produced by polymerization of ionic liquids having polymerizable groups, are expected to lead to new functional polymeric materials.

On the basis of the above background, in this chapter, the author reviews the synthesis and applications of ionic polystyrenes derived from imidazolium-based polymerizable ionic liquids. For the study, vinylbenzylimidazolium ionic liquids have been prepared, which can be converted into a polystyrene main-chain by radical polymerization.

In the first topic in this chapter, the author describes the use of the vinylbenzylimidazolium ionic liquids for the production of composite materials with polysaccharides such as cellulose. The investigations have been based on the viewpoint that imidazolium ionic liquids have good affinity with polysaccharides and thus have been used as

good solvents for them. Consequently, the author found that polysaccharide-ionic polystyrene composite materials were facilely obtained by in-situ radical polymerization of the vinylbenzylimidazolium ionic liquids in the mixtures with polysaccharides. Clay-ionic polystyrene composite materials were also prepared by the similar in-situ polymerization approach. The second and third topics of this chapter deal with the applications of ionic polystyrenes derived from the vinylbenzylimidazolium ionic liquids as absorbents for CO₂ and sorbent coatings for microextraction, respectively.

Chapter 7 - Hypercrosslinked polystyrene (HP) has been obtained by an intensive crosslinking of strongly solvated pre-formed polystyrene chains with numerous rigid bridges. This approach results in obtaining uniformly crosslinked single-phase open-network polymers with developed intrinsic nanoporosity and a unique ability to swell in any liquid and gaseous media. Noteworthy, HP is characterized by a non-typical physical state, it belongs neither to glassy, nor rubber-like polymers. Owing to its special open network structure and high permeability, HP represents an excellent adsorbing material for large-scale water purification, separation of organic or inorganic compounds, solid-phase extraction of trace components in analytical chemistry, efficient detoxification of blood, etc. Polystyrene with ultimate crosslinking densities, up to a nominal 500%, displays a particularly high affinity even to small polar organic compounds and mineral electrolytes.

Chapter 8 - Polystyrene, one of the most important material in the modern plastic industry and one of the major synthetic polymer in use today, offers an extremely broad range of applications, due to its good physical properties and low-cost. Significant change of mechanical, rheological, thermal, optical, fire retardancy and barrier properties of polystyrene has been obtained by its combination with different nanoparticles. Due to the extremely high interface area between nanoparticles and polystyrene, some new properties could also be generated, which are often necessary to provide in order to meet current and future demands for various significant applications in different fields. In this review, recent advances on nanocomposites based on polystyrene and different kinds of nanoparticles will be presented through the results obtained by authors of this chapter and results given in other literature reports. This chapter reviews the current understanding of polystyrene based nanocomposites with three particular topics: (i) the preparation conditions of nanoparticles for their efficient, homogeneous incorporation in polystyrene matrix, (ii) different approaches for the synthesis of nanocomposites based on polystyrene and (iii) the influence of the type, size and shape of incorporated nanoparticles on the properties of the polystyrene based nanocomposites. The potential applications of these nanocomposites are also highlighted.

Chapter 9 - Research progress in developing synthesis of polystyrene spheres with controllable physicochemical properties (i.e. size and charge) and showing effectiveness of these properties as a template for assisting the creation of material with various morphologies and pore structures is the main topic in this chapter. The available process parameters (e.g. temperature, amount of styrene, and type and concentration of initiator) to achieve a smart strategy that is capable of regulating interaction, reaction, and growth of styrene are introduced. By controlling this smart strategy, control of the physicochemical properties is possible. Indeed, this control offers great advantages as the template for creating innovative materials that have advanced performances and are applicable for various practical applications, such as phosphors, photocatalysts, and adsorbents.

Chapter 10 - In recent years, the activities related to polystyrene (PS), both in the fields of academic research as well as industrial usage are impressive and are increasing by the number

of scientific papers and patent applications in general sense. The demanding interest of PS is due to its versatile applications and utility in various sectors is due to its hydrocarbon structure and ability to polymerize easily. PS is a thermoplastic polymer and is one of the most widely used plastic materials in the world, ranging from domestic, medical to automobiles. In addition, it is also an important ingredient in the manufacture of ionic membranes, disposable cutlery, plastic modelling, cases for compact disks, digital video disks, etc. The major application of PS is in packaging as an industrial base and specific additives are also included for achieving the product characteristics that are highly dependent on the usage at the end. It is transparent and can be fabricated easily to form products with enhanced mechanical and thermal properties. The chemical properties of PS are slightly brittle and soften at 100°C temperature and at higher temperatures, it gets degraded to a mixture of low molecular weight compound and styrene. The quality control and research protocols in the investigation of PS composition have resulted in different methodologies to be acting as a specific analyte. PS nanoparticles with some distinct particle morphology and surface composition can be achieved by using a simple and eco-friendly gentle free-radical micro-emulsion polymerization process. Based on these facts therefore, the current book chapter is aimed to demonstrate and discuss the applications and the role of PS in different aspect of analytical chemistry.

Chapter 11 - There have been various attempts since the two papers by (Han and Han) to predict the rise in superheat due to addition of polystyrene in solvents including toluene, benzene and cyclohexane. Calculation of the nucleation rate is a cumbersome way to attack the problem. The papers other than (Jennings) focus on getting a value for the nucleation rate J . In Jennings' formulation a simple vector calculus argument eliminates the need to calculate J . Each curve for (Jennings and Middleman) data is more or less a line and the object is to calculate the slope of the lines in the (w_2, T) plane where w_2 is the weight fraction polystyrene in cyclohexane and T is temperature Kelvin. All lines meet at the point $(0, T_1)$ where J is equal for all 4 molecular weights and T_1 is the limit of superheat of pure cyclohexane at 1 atm. This Short Communication shows how Jennings' approach is simple and gives a beautiful effective equation. In expanded form I am proposing a new equation for the limit of superheat T , by extending the limiting equation published by (Jennings) because the data are lines. Because they are lines the limiting slope would be the true slope. The additional temperature rise in the superheat limit is inversely proportional to MW polymer and directly proportional to weight fraction polymer in the solution. It is a semi-empirical argument. One would believe that experiments with polystyrene in cyclopentane, n-hexane and n-heptane would give the same lines in the data as cyclohexane in the experimental setup used by (Jennings and Middleman).

Chapter 1

WASTE/CONTAMINATED POLYSTYRENE RECYCLING THROUGH REVERSE POLYMERIZATION

Piero Frediani^{1,}, Andrea Undri¹, Luca Rosi¹ and Marco Frediani¹*

¹Department of Chemistry “Ugo Schiff”, University of Florence, Sesto Fiorentino, Firenze, Italy and Interuniversity Consortium on Chemical Reactivity and Catalysis – Florence section, Italy

ABSTRACT

Polystyrene (PS) is the most employed aromatic thermoplastic polymer. PS finds a wide range of application from food contact packaging to thermal insulator in buildings. Its disposal is an environmental and social problem which is ceaselessly addressed from academic and industrial researchers.

Among several recycling processes exploited the most used is direct remanufacturing through milling, washing, drying, and moulding but this is possible only for un-contaminated waste.

Safeguarding of energy and material content of waste PS is a mandatory key to save oil stocks and contaminated PS may be disposed through conservation and valorisation of the phenyl moiety. Pyrolysis meets these requirements: it may convert waste PS into single ring aromatic compounds, together with low amount of char and gas, if appropriate pyrolysis conditions are employed.

Thermal pyrolysis is already active at 350 °C, where the main product is a dark viscous liquid rich in single ring aromatic compounds (benzene, toluene, ethylbenzene, and styrene). Char formation increases when pyrolysis temperature rises. Anyway different pyrolysis behaviour is observed for different classes of PS (virgin, expanded, and compacted from containers), especially for what concerning the composition and distribution of aromatics in the liquid fraction.

In the last few years microwave (MW) heating has encountered a sound and reliable application in polymeric waste treatment. Microwave assisted pyrolysis (MAP) encloses a number of advantages than classical methods. One of these is the direct and extremely fast heating in the presence of a MW absorber. MAP of PS has been investigated in the

* E-mail: piero.frediani@unifi.it.

presence of a microwave absorber such as carbon, iron mesh, or aluminium, as coil or mesh.

1. INTRODUCTION

Nowadays polyolefins are the most produced and employed materials for application in everyday life for industrial, and technological applications [1]. They are thermoplastic polymers and are mainly used for packaging, disposed in short time after their production, and structural items (such as furniture, insulating materials, and so on), which may have a life cycle of decades before their disposal [1]. Therefore end life materials are largely produced on annual base and a large part must be disposed. Nevertheless their disposal must follow some principle which became mandatory in this period of financial, resources, and environmental crisis. Petrochemical feedstock ceaselessly increased their cost during last decades and consequently the price of monomers employed for polymer production, or to obtain finished product is rising as well. Moreover the environment is no longer able to receive the end life materials, without affecting our lifestyle, so must be avoided to send these end-life polymers as solid waste in landfills or burned and transformed in product of combustion (as CO₂, water and partially oxidated compounds). In fact landfill site are rapidly filled because most of the materials disposed in this way (such as polymers) are stable for a very long time in an anoxic, light free, and biotic environment such as a landfill. At the same time CO₂ is a greenhouse gas and its production must be reduced especially from fossil fuel (or material derived from fossil fuel such as polymers). So new worthwhile greener routes, which prevent dispose of waste polystyrene or their combustion must be found.

Anyway polymeric materials (Figure 1) can be, and are, recycled as reported in the following figures for production of renewed object so their life is prolonged and their landfilling or combustion is postponed [2] (Figure 2). Unfortunately only a minor fraction of waste polymers is eligible for a recycling process because only pure, not chemically and reologically degraded, nor contaminated polymers can be efficiently recycled to produce new objects with appealing performances [3].

Other friendly technologies have been proposed to deal with waste (Figure 3), often partially degraded and/or contaminated polymers. A pyrolysis process may be an appealing technology because it is realized through a high temperature cleavage of covalent bonds performed in an anoxic environment. In the course of a pyrolysis process bonds are broken without their oxidation so hydrocarbon moieties may be preserved in the form of a gas (C1 – C4 hydrocarbons and H₂), a liquid (hydrocarbons C4 - C20, liquid at room temperature), and a solid (high molecular weight hydrocarbons, products from aromatization/cooking of hydrocarbons, and inorganic fillers eventually present in the starting materials which are stable at pyrolysis conditions) [4]. These three classes of products may be useful as energy source (better than the initial solid waste polymer) but their use as source of chemicals is pretty more appealing.

Polystyrene (PS) within polyolefins is a very interesting material to be pyrolyzed due to the absence of a well-established protocol for disposal of waste and/or contaminated PS and the presence of an aromatic ring which is very attractive as feedstock for several industrial processes.



Figure 1. End-life polystyrene.

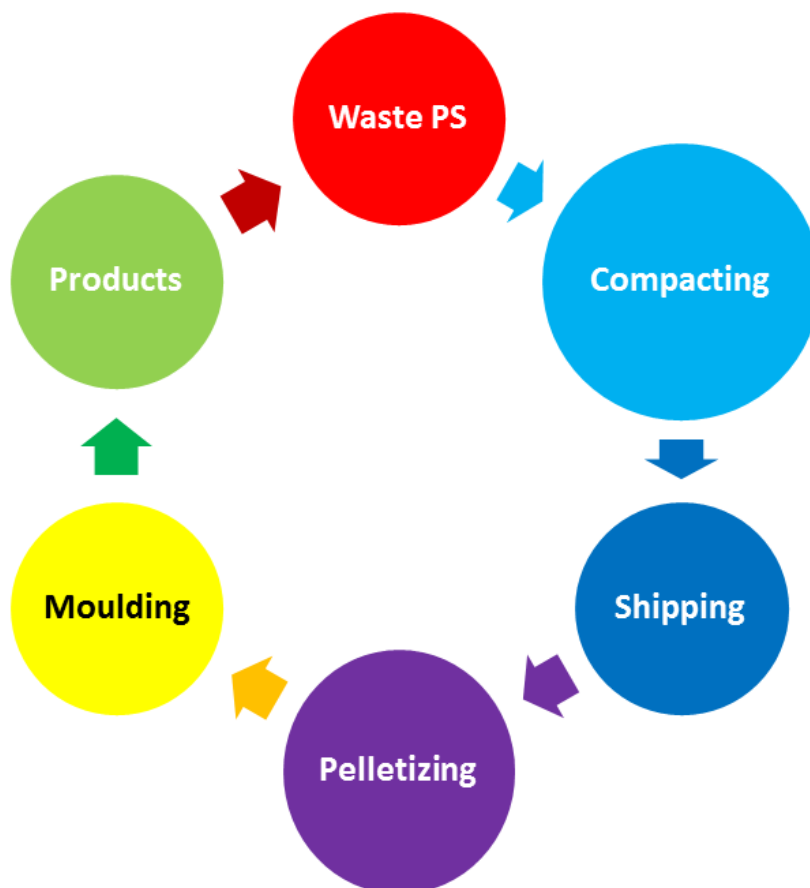


Figure 2. Recycle pathway of polystyrene.



Figure 3. Waste polystyrene.

Polystyrene is employed for outside housing of computers, other electronic devices and it also is used in the form of foam for packaging and insulation. Furthermore clear plastic drinking cups as well as a lot of the molded parts inside cars are made in PS, for instance radio knobs. Polystyrene is also used in toys, hairdryers, television, and kitchen appliances [1].

In this chapter several technologies for pyrolysis of PS are addressed with a specific attention to the heating technology (classical or microwave) and to the possibility to obtain a liquid with interesting application, among which the synthesis of new PS. Furthermore the pyrolysis of several form of PS such as crystalline or expandable PS (EPS), high-impact PS (HIPS), flame retarded PS (HIPS) are reviewed including the use of a catalytic systems to easier the process. Also pyrolysis of PS mixed with other polymers such as poly(ethylene) (PE), high density poly(ethylene) (HDPE), low density poly(ethylene) (LDPE), poly(propylene) (PP), poly(vinyl chloride) (PVC), poly(ethylene terephthalate) (PET), poly(acrylonitrile-butadiene-styrene) (ABS) or biomasses are reviewed. In this chapter pyrolysis of tires and other objects containing polystyrene copolymers are not reported. For a review of pyrolysis of these materials the reader may refer to the book edited by Scheirs and Kaminsky [4] or the chapter of Undri et al. [5].

2. PYROLYSIS OF POLYSTYRENE USING CLASSICAL HEATING

Pyrolysis was thoroughly investigated during the last 50 years and starting from the 1960s several patents were registered regarding different systems to carry out pyrolysis of coal and polymers among which PS [6- - 10]. These patents reported the design of various systems to recover products for energy and heat production and in some cases also as

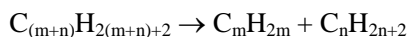
feedstock of chemicals especially for styrene production [11 - 13]. Most of the technological efforts were focused on overwhelming the poor heat conductivity of polymers, and more specifically of PS in this case [14-17].

Usually PS was mainly converted into a liquid rich in aromatic compounds (>80 wt % yield) and in minor extent to a solid (<10 wt % yield), non-volatile product, and a gas (<10 wt % yield).

Various mechanisms were proposed by several authors to explain PS degradation. In general a pyrolysis process involving any polymer is characterized by complex free-radical reactions. High molecular weight, polydispersity, and complexity of polymers might lead to a complex system of reactions giving up to thousands of species. The complexity of the reactions involved yielded a wide spectrum of products. Thus understanding the mechanism and reaction pathways via experimental studies was a challenging task.

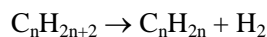
The first step of this process is a homolytic breaking of a C-C or a C-H bond as a function of the reaction conditions employed. C-C breaking is favored by a low temperature process while increasing the temperature the cleavage of the C-H bond becomes more important.

In fact the free energy of a general C-C breaking of a hydrocarbon, that is the reaction:



may be evaluated in a simplified approach by the following equation $\Delta G^\circ = 19100 - 36.7 T$ and consequently the equilibrium of the reaction ($\Delta G^\circ = 0$) is reached at 294 °C.

In the same way the free energy of a dehydrogenation of an alkane, that is the reaction:



may be represented by the equation $\Delta G^\circ = 31600 - 33.6 T$ and the equilibrium is reached at 669 °C.

Pyrolysis of PS yields few products, if compared to pyrolysis of other polymers such as polyethylene (PE) [18] and polypropylene (PP) [19] due to the relatively high stability of the radical intermediates formed. In fact due to the possible conjugation of radicals with the aromatic rings present in the molecule [20] these intermediates are relatively stable. The main products of PS pyrolysis are: styrene, toluene, α -methylstyrene, and diphenylpropane together with the dimer and trimer of PS. A representative gas chromatogram of a liquid obtained from microwave assisted pyrolysis of PS is shown in Figure 4 [20].

Styrene is primarily formed via chain unzipping (end-chain β -scission) (Figure 5).

Dimer and trimer were formed via backbiting reactions followed by β -scission of mid-chain head radicals in the third or fifth position, respectively (Figure 6) [21].

Furthermore any C-C bond along the polymer backbone could be broken by binary random scission. So far most of the reactions which might be involved in PS degradation are listed in the following schemes: chain random cleavage (Figure 7a), and the reverse radical recombination (Figure 7b), carbon-hydrogen bond cleavage with hydrogen abstraction (Figure 8), radical transfer (Figure 9), mid-chain β -scission (Figure 10a), and the reverse radical addition (Figure 10b), disproportionation (Figure 11), end-chain β -scission (Figure 12), and addition of mid-chain radical to chain-end double bonds (Figure 13) [22].

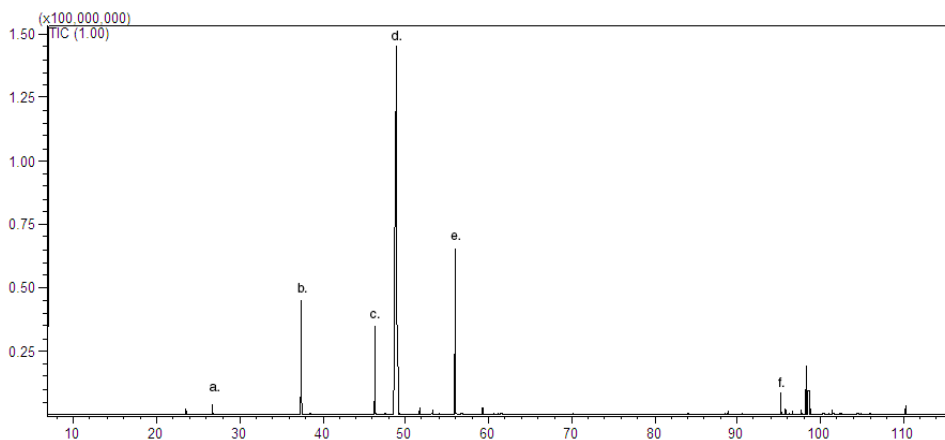


Figure 4. Total ion chromatogram of a liquid obtained from microwave assisted pyrolysis of PS. a) benzene; b) toluene; c) ethylbenzene; d) styrene; e) α -methylstyrene; f) styrene dimer [20].

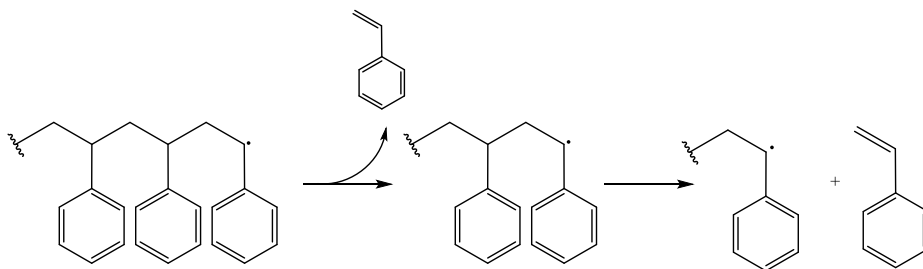


Figure 5. Back biting degradation of polystyrene to yield styrene.

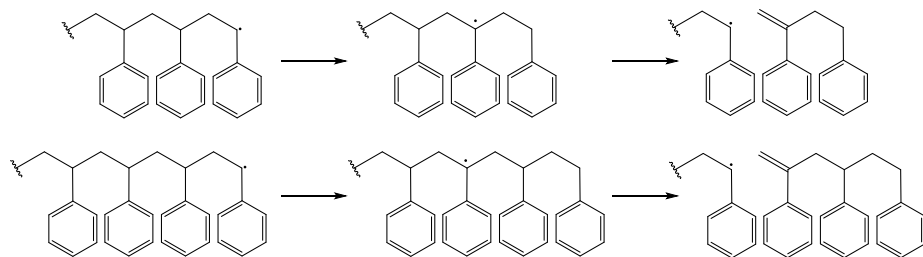


Figure 6. Dimer and trimer formation from backbiting degradation of polystyrene.

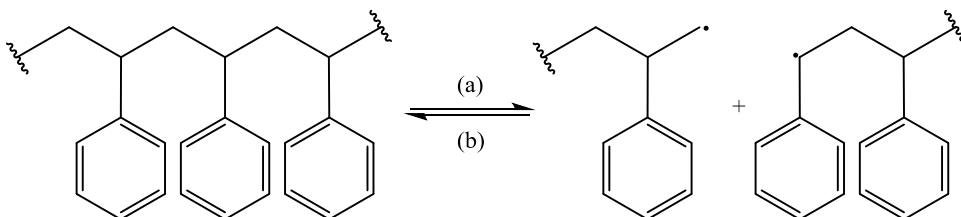


Figure 7. Polystyrene degradation through: a) chain random cleavage; b), radical recombination.

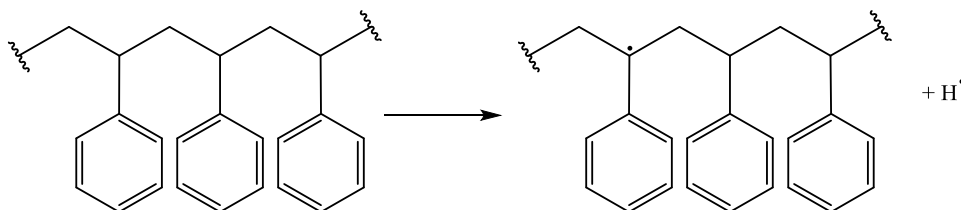


Figure 8. Polystyrene degradation through carbon-hydrogen bond cleavage with hydrogen abstraction.

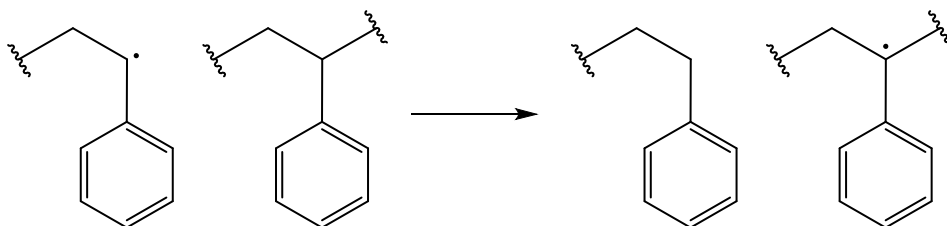


Figure 9. Radical transfer in polystyrene degradation.

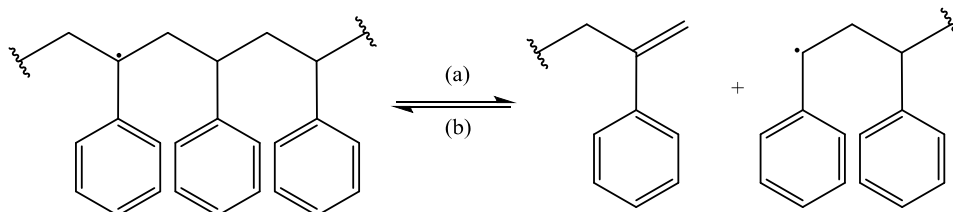


Figure 10. Polystyrene degradation through: a) mid-chain β -scission; b) radical addition.

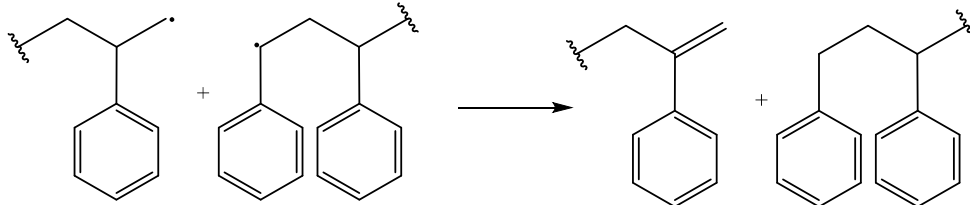


Figure 11. Polystyrene degradation through disproportionation among radicals.

Furthermore different kind of PS such as virgin PS, EPS, or waste PS from containers, showed different pyrolytic behaviors [23].

Starting from these proposed reactions several kinetic models were proposed and developed to improve the design of pyrolysis reactors and experiments [24-36], and they were reviewed by Kennan et al. [37] and Westerhout et al. [38].

In the following sections the behavior of PS pyrolysis using classical heating methods (external electrical resistances or burners) followed by unusual methods (microwave) are addressed with specific regards to formation of styrene and other interesting aromatic compounds which may find direct application in industrial processes.

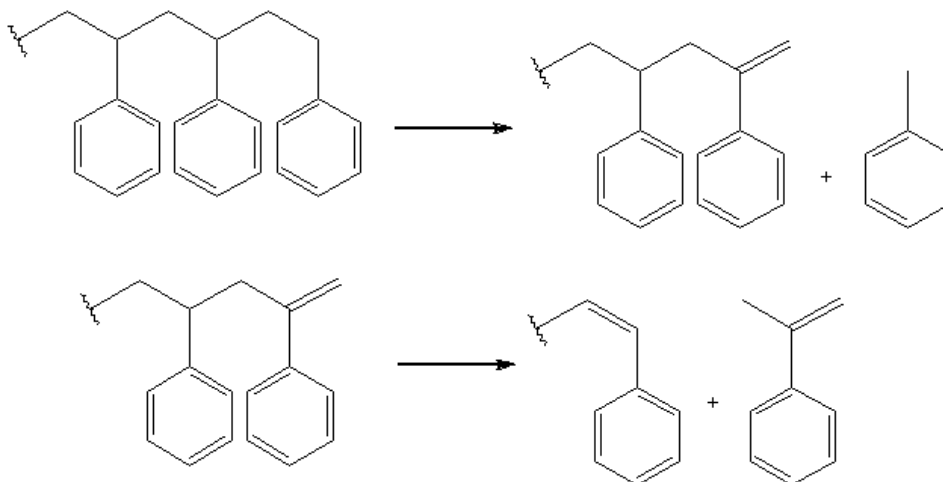
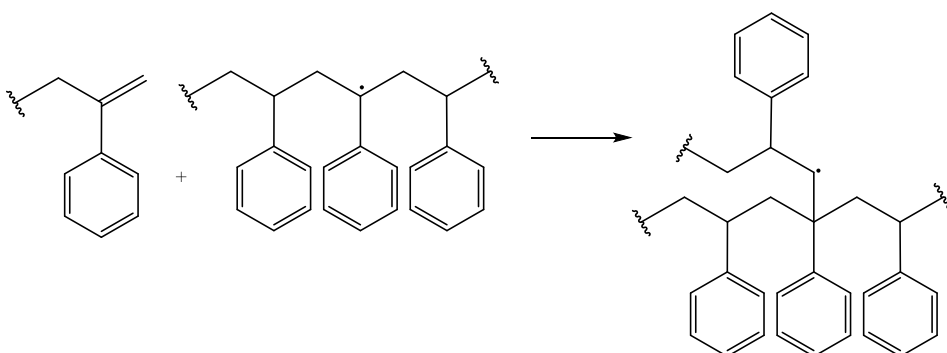
Figure 12. End-chain β -scission.

Figure 13. Addition of mid-chain radical to chain-end double bonds.

Pyrolysis of PS is first reported as single polymer, then mixed with other polymeric materials with various experimental set-ups, and finally pyrolysis in the presence of several catalytic systems. Pyrolysis using microwave assisted system was presented in the last part of this chapter.

2.1. Polystyrene Alone

Pyrolyses were carried out using batch, fluidized bed, and other kind of reactors. Processes summarized in the following paragraphs employed a nitrogen flow to assist the outlet of products from the oven. A detailed description of reaction parameters may be found in the original papers.

2.1.1. Autoclave Reactors

PS was pyrolyzed by Pinto et al. in an autoclave at 430 °C, thus vapors remained at pyrolysis temperature for all time of the whole reaction [39]. In this way styrene was detected

in minimum amount because it had enough time to react giving toluene, xylenes, and other aromatic compounds. In the same time gas was formed with a yield below 10 wt %.

In a closed pressurized batch reactor Onwudili et al. pyrolyzed PS in a temperature range of 300 – 500 °C [40]. At 300 °C no reaction was observed, while the maximum conversion of PS into a liquid product was obtained at 425 °C with a 97 wt % yield. As reported by Pinto et al. [39], in these conditions, the formation of styrene was low and it decreased if the temperature was improved. Secondary reactions involving styrene took place increasing the formation of toluene and ethylbenzene.

Also Williams and Slaney pyrolyzed PS in an autoclave at 500 °C for 1 h. Yields of liquid and solid were 71 and 27 wt %, respectively. PS pyrolyzed and the products initially formed reacted further increasing the yield of solid, however the liquid contained single (74.5 wt %), double (12.5 wt %), and triple (13.1 wt %) ring aromatic compounds [41].

2.1.2. Batch Reactors

Pyrolysis of PS was performed by Karaduman et al. in a free-fall reactor, where a feeder dropped particles of PS in the middle part of a vertical reactor kept under vacuum [42]. They investigated temperatures in the range 700 – 875 °C obtaining a 32 wt % yield of liquid at 750°C and a 18 % yield of styrene. Yield of styrene rose up to 32 % when the temperature of the pyrolysis was improved up to 825 °C.

A stirred batch reactor heated from room temperature to a range of temperatures among 370 – 400 °C was employed by Kim et al. [43]. They reported a first order kinetic law, an activation energy of 224 kJ/mol, and the yield of styrene was 70 wt %, independent from reaction temperature.

A liquid containing styrene as the main compound (composition was not reported) together with other single-ring and polycyclic aromatic hydrocarbons was obtained by Williams and Williams in a batch reactor at 700 °C. In these conditions a low yield of gas was formed while char was not present [44].

Kiran et al. obtained a low yield of styrene (37 %) in the pyrolysis of PS using a Gray–King apparatus, a tubular furnace without any carrier gas, heated at 600 °C [45].

Different kind of PS in a bench scale fixed bed reactor without or in the presence of a basic or a zeolitic catalysts were pyrolyzed by Achilias et al. obtaining a styrene rich liquid (up to 70 %). The liquid was employed as starting material, without any further purification, for styrene polymerization [46]. This polymer had similar characteristics with respect to the original PS. However the other aromatic compounds present, worked as chain transfer agents, lowering the average molecular weight of the PS. Therefore the synthesized PS had lower performances than a polymer prepared from virgin styrene.

Expanded PS was pyrolyzed by Chauhan et al. in a pebble bed reactor at 500 °C under vacuum reducing the working temperature and maximizing the yield of liquid and styrene [47]. The heat required for pyrolysis was partially supplied by combustion of the gas obtained and the highest yield of liquid was 91.7 % at 500 °C together with a yield of styrene of 85.5 %.

Expanded PS and a general purpose PS was also pyrolyzed by Park et al. in a semi-batch reactor with a continuous flux of nitrogen at a temperature between 350 and 480 °C. They achieved the best conversion of expanded PS at 450 °C (95.1 wt %) together with the highest yield of styrene, 76.3 wt %. At the same temperature general purpose PS gave lower yield of liquid (92.5 wt %) and styrene (65.5 wt %) while working at higher temperature the reaction

time decreased considerably but also the production of styrene and other single ring aromatics decreased while increased the yield of liquid [48].

A stainless steel tube heated in the range between 400 and 600 °C was used by Demirbas for the pyrolysis of PS obtaining a maximum yield of styrene of 64.6 % at 470 °C [49].

Lomakin et al. pyrolyzed PS in a tubular cell using an air flux in a broad range of temperatures (300 – 800 °C) [50] and the highest yield of styrene (75.6 wt %) was obtained at 400 °C. Raising the temperature styrene concentration decreased, meanwhile other single ring aromatic compounds were present in major amount.

2.1.3. Fluidized Bed Reactors

A sand fluidized bed reactor, that is a well-established technology, was used Sinn et al. [51] for the pyrolysis of PS obtaining a 76.2 wt % yield of styrene when working at 532 °C while no solid was collected. Fifteen years later Scott et al. obtained similar achievements, in terms of conversion and styrene yields, confirming the data of Sinn et al. [52]. Using a pilot plant with a fluidized bed reactor, Kamisky et al. confirmed the previous achievements obtaining a 76.8 wt % yield of styrene at 520 °C [53].

Also Liu et al. tested a fluidized bed reactor in a range of temperatures among 450 and 700 °C. Raising the reaction temperature the yield of liquid dropped from 98 to 90 wt % without an increase in solid formation. They reported a maximum yield of styrene of 78.7 wt % at 600 °C [54]. Over this temperature the yield of styrene decreased due to its involvement in secondary reactions, as proposed by Pinto et al. in an autoclave reactor [39], with an increasing formation of other single ring aromatics.

Fire retarded polystyrene (HIPS) (that is PS with bromo and antimony containing compounds) was pyrolyzed by Hall and Williams in a sand fluidized bed reactor between 450 – 550 °C [55]. PS was mainly converted to liquid (yield 89.9 wt % at least), but, surprisingly the highest yield of styrene does not exceed 19 % at 550 °C. Brominated compounds were present in liquid and gas, furthermore antimony bromide was identified in the liquid.

Pyrolysis of HIPS were also investigated by Jung et al. in a fluidized bed reactor obtaining the highest yield of liquid at 474 °C and in these conditions, a 50 % yield of styrene [56] was obtained.

2.1.4. Special Mediums

A special riser simulator (patented) which allowed a precise control of contact time between the feed and a fluidized bed as well as an optimal mixing between feed and fluidized bed was proposed by Arandes et al. They worked between 450 and 550 °C in the presence of a light cycle oil (a secondary product of a fluid catalytic cracking unit in the refinery) [57]. This riser simulator let to Arandes et al. to overwhelm some technical problems concerning the pyrolysis of solid plastics and lowering energy requirements. Furthermore PS was pyrolyzed giving products in comparable yields to those of other similar fluidized bed pyrolysis without the light cycle oil, but solid and undesired aromatic compounds were formed in lower yield. Anyway, in this case also, a very low yield of styrene was achieved and it never exceed 15 %.

Pyrolysis of PS was also carried out using supercritical fluids. Degradation of PS in supercritical methanol was carried out under reaction temperatures ranging from 340 to 420°C and pressures of 10–30 MPa by Shin and Bae [58]. The formation of styrene and other compounds from pyrolysis of PS occurred in the first steps of pyrolysis, and in the course of

the reaction their concentration declined. Intramolecular reactions among intermediates and reactions between aromatic compounds and methanol were suggested.

Pyrolysis of PS in supercritical hexane was also investigated by Hwang et al., in the range of temperatures among 330 and 390 °C and pressures of 10–30 MPa [59]. They reported a high (over 90 %) and rapid (below 30 min) conversion of PS, with small influence of pressure variations on conversion of PS, but the selective formation of styrene decreased with increasing temperature and reaction time. The highest yield of styrene (34.7 wt %) was reported at 350 °C after 30 min.

Reaction mechanisms of pyrolysis of waste PS using several supercritical solvents (benzene, toluene, ethylbenzene, and p-xylene) were studied by Ke et al. working at in the range of temperature among 310 - 370 °C and pressures among 4.0 - 6.0 MPa using a stainless steel reactor heated by molten salts. Toluene was proved to be the more efficient supercritical solvent and the yield of styrene was 77 wt % working at 360 °C for 20 min [60].

A medium of coal tar pitch or pitch prepared from tar coming from ethylene production, was used by Andreikov et al. to pyrolyze PS in the temperature range 360–420 °C in a Pyrex glass reactor [61]. Mixing PS with tar pitches shifted toward higher temperatures the maximum of weight loss rate and the main products were formed by hydrogen transfer from the solvents to radicals or unsaturated intermediates. These reactions affected also the characteristics of initial tar pitches. The selectivity towards styrene formation was very low when tar pitches were present: among 1.0 – 6.9 % with respect to 72.5 % without tar pitches [61].

2.1.5. Other Pyrolysis of PS

Production of hydrogen was investigated by Ahmed and Gupta in the pyrolysis or gasification (reaction with steam) of PS. Pyrolysis showed a mild linear dependency of temperature on syngas and energy yield. Meanwhile gasification was active only over 800 °C and hydrogen formation showed an exponential tendency with temperature. However the yield of syngas was higher in gasification than in pyrolysis reaction (61.1 versus 24.4 %) [62].

A facile method for synthesis of carbon nanosheets through pyrolysis of PS in the presence of iron particles and organophilic montmorillonite at 900 °C was proposed by Hong et al. Iron catalyzed the dehydrogenation of aromatic ring while organophilic montmorillonite contributed to keep pyrolysis products inside the reactor [63].

2.2. Pyrolysis of PS Mixed with Other Plastics

Mixed plastic were pyrolyzed as well as polystyrene alone, however some influences among intermediates formed in the course of the process were reported. Additive eventual presents in waste polymers may also affect the pyrolysis as reported in the following paragraphs.

2.2.1. Autoclave Reactors

In a pyrolysis carried out in an autoclave reactor PS was initially cleaved into styrene and α -methylstyrene, as main degradation products and these compounds further reacted because

they were still in the pyrolysis conditions. Infact Pinto et al. reported reactions between pyrolysis products of PS and PP or PE to form alkyl benzene derivatives [39]. On the contrary working in a closed reactor no interactions were observed by Onwudili et al. [40] who pyrolyzed PS together with PE in a range of temperature between 300 – 500 °C.

Also Siddiqui proposed a pyrolysis process in an agitated micro autoclave at a temperature of 420 °C but in the presence of 5 wt % of azobisisobutyronitrile as radical initiator of pyrolysis [64]. PS showed high conversions when it was used as the sole polymer. In the same apparatus and using similar operating conditions Siddiqui and Redhwi pyrolyzed PS mixed with PE, PP, and PET obtaining a liquid with feasible properties [65]. The use of hydrogen in the catalytic system seemed to improve the efficiency of the pyrolysis and it let to recover liquid useful as fuels or chemical feedstock (even if the nature of compounds formed and their distribution was not deeply investigated).

The major plastics present in municipal solid waste and three samples of mixed waste polymers (PE, PP, PS, PET, and PVC) were pyrolyzed in an autoclave at 500 °C for 1 h by Williams and Slaney [41]. The composition of the gas obtained from a simulated plastic mixture was close to that calculated from the gas compositions obtained from individual polymers, thus no interaction was highlighted. The liquids formed by pyrolysis of mixed waste plastics contained alkanes and single ring aromatic compounds. However cross reactions attributable to the presence of different plastics giving different composition of the liquid formed (for instance the amount of styrene) was not investigated [41].

2.2.2. Batch Reactors

In a batch reactor pyrolysis of mixed plastics such as HDPE, LDPE, PP, PVC, or PET in a 1:1 mixture with PS was studied by Williams and Williams. The yield of gas was higher than that one predicted from data of the single plastic pyrolysis suggesting a reciprocal influence among different plastics and different from results observed by Williams and Stanley [41] working in an autoclave. These data were confirmed by the increased concentration of alkenes in the gas of the pyrolysis due to the presence of PS and other polymers [44].

Several mixtures of PS and PE were also tested in a tubular furnace without a carrier gas by Kiran et al. [45]. The presence of degradation products of PS improved the cleavage of PE macromolecules.

Demirbas pyrolyzed a real waste samples of polymers containing a mixture of PS, PE and PP in a stainless steel tube, between 400 and 600 °C. A liquid was obtained but it showed limited applications due to the presence of additives initially present in the plastic stream. However information were not given on the composition of the liquid collected [49].

Also Angyal et al. investigated the pyrolysis of PS and PP in a horizontal tubular reactor working at a temperature of 510–520 °C and residence time of 15–30 min. The presence of PS affected the quantity and quality of products and the degradation rate of PP was enhanced [66].

Virgin and waste PP was pyrolyzed in the presence of waste PS by Kiran Ciliz et al. [67] in a modified Gray–King apparatus starting from room temperature up to 600 °C with a heating rate of 5 °C/min. The mixture of the polymers and the ratio between PP and PS influenced the yield and composition of the aliphatic, mono- and poly-cyclic aromatic compounds present in the liquid fraction collected together with the alkene/alkane ratio in the gas formed [67].

A mixed stream of plastics coming from a waste packaging separation and classification plant was pyrolyzed by de Marco et al. in an autoclave under a N_2 flux. A waxy liquid was obtained which solidified at room temperature, however it contained only 37.4 % of styrene (by chromatographic area) [68].

Also PS mixed with ABS containing polybrominated epoxy flame retardants was pyrolyzed in a batch reactor at 450 °C by Brebu et al. [69]. Styrene and other C9 aromatic hydrocarbons represented up to 70 wt % of the liquid, however they were partially formed by pyrolysis of the aromatic moieties of ABS. No specific information was supplied on the composition of the liquid collected.

Pyrolysis of a mixture of PS with HIPS containing brominated flame retardants and PP, PE, PVC, and PET was carried out in a batch reactor at 430 °C by Bhaskar et al. [70]. PET showed several influences on the pyrolysis results: it reduced the yield of liquid while increased the yield of gas, a waxy liquid was formed together the solid, $SbBr_3$ was not detected in the liquid collected and the yield of halogenated branched alkanes increased significantly. Styrene and other C9 aromatic hydrocarbons represented up to 40 wt % of the liquid, however no specific information on single aromatic compounds were given. The same authors reported another study on the pyrolysis of PS in the presence of HIPS containing decabromodiphenylethane as flame retardant, antimony trioxide, PE and PP using the same operating conditions [71]. Surprisingly styrene and α -methylstyrene were not observed in the liquid collected when antimony trioxide was present and the major amount of brominated hydrocarbons was observed in the liquid collected in the first phase of the pyrolysis as well as antimony containing compounds.

Pyrolysis of HIPS containing other two brominated flame retardants (decabromodiphenyl ether or decabromodiphenyl ethane) with or without antimony trioxide (5 wt %) was performed at 430 °C in the presence of 0.1 wt % of PET in a batch reactor by Bhaskar et al. Surprisingly in this case the presence of PET decreased the yield of gas and increased the yield of solid as well as the formation of brominated compounds. The presence of antimony trioxide decreased the decomposition temperature of 50 °C, and the yield of gas, while styrene was not present in the liquid collected. On the contrary styrene was present, even if in a relatively low amount (16 wt %) when antimony oxide was absent [72].

The pyrolysis of mixed plastic waste (PS with PE, PP, and PVC) using a long residence time (25 min) in a horizontal tube reactor at 530 °C has been investigated by Miskolczi et al. The liquid was separated into heavy oil, light oil, and gasoline. Styrene was found always in the gasoline fraction in a low amount between 5.8 and 7.0 %. This liquid was corrosive and its corrosiveness increased as well as its chlorine containing compounds when the initial amount PVC in the starting mixture was increased [73].

The pyrolysis of PS blended with an organosilicon polymeric additive, polydimethylsiloxane, was investigated by Lomakin et al. in a tubular cell using an air flow and working in a broad range of temperatures (300 – 800 °C) [50]. The organosilicon additive affected the heat resistance of PS which was stabilized (due to kinetic factors) and was pyrolyzed at higher temperatures than single PS while the temperature of pyrolysis of polydimethylsiloxanes was reduced. This behavior was explained by cross reactions between intermediates formed by pyrolysis of PS and polydimethylsiloxanes. These reactions reduced also the amount of styrene in the liquid [50].

A mixture of waste car lubricating oil and PS was pyrolyzed in a stirred batch reactor, at atmospheric pressure by Kim et al. They worked with an increased heating between 300 and

500 °C, using several heating rates. Hydrocarbons with a large distribution of carbon atoms were present in the liquid collected and the mean distribution of carbon atoms shifted slightly towards light hydrocarbons when the heating rates was decreased. The selectivity towards styrene formation was high even in the presence of the waste car lubricating oils [74].

2.2.3. Continuous Process Using a Fluidized Bed Reactors

The pyrolysis of waste PS blended with PE and PP has been carried out in an experimental continuous reactor at 550 °C by Miskolczi and Bartha. They collected three liquid fractions according to their petrochemical characteristics (naphtha, middle distillates, and heavy oil) with a total yield of 90.3 wt %. The products contained aromatic and aliphatic hydrocarbons, in the naphtha and heavy oil fractions. Information on the type and amounts of single compounds were not given [75].

A mixture of several polymers, including PS, were pyrolyzed in a fluidized bed reactor by Kaminsky and Kim in a range of temperature between 685 – 740 °C which proved to be a key parameter to control final products properties. They obtained a liquid rich in aromatics which might be used as feedstock for petrochemical process [76]. The same fluidized bed reactor was employed by Kim et al. to convert large amount of mixed polymers into an aromatic rich liquid and its aromatic content was increased when pyrolysis temperature was improved [77]. Using the same apparatus but in the presence of steam, Simon et al., were able to pyrolyze a mixture of waste polymers into low molecular weight olefins (C₂ – C₄ hydrocarbons) with minimal formation of styrene [78]. Using a very close fluidized bed pyrolysis unit, Predel and Kaminsky pyrolyzed a mixture of PE, PP and low amount of PS at 500 °C [79]. PS amount was set to 10 wt % of the feed and the yield of styrene was lower in the presence of PE than in the presence of PP. Unsaturated waxes were formed in high amount when PS was co-pyrolyzed in the presence of PP. A mixture of polymers containing a higher amount of PS (20 wt %) with PE, PP, and PET was pyrolyzed by Grause et al. in a fluidized bed reactor with a hard burnt lime in the presence of steam as well as nitrogen at 600 and 700 °C. Hard burnt lime together with steam as fluidizing gas reduced the yields of waxes by decarboxylation of the terephthalic moiety of PET (increasing the yields of gas) and improved the formation of styrene (up to 12 wt %). Furthermore hard burnt lime showed at 600 °C a behavior comparable to those at 700 °C when quartz sand was used as bed material [80].

A similar approach to a fluidized bed reactor was proposed by Bockhorn et al., using three well stirred reactors filled with glass spheres and heated at different rising temperatures [81]. Two mixtures of poly(vinyl chloride) (PVC), PS, poly(amide), and PE were melted and adhered to the glass spheres and the resulting composite was introduced into the system and in the same time it was stepwise pyrolyzed. A styrene yield of 58 vol. % was reported for pyrolysis products collected from the second reactor heated at 380 °C. The methodology adopted let to Bockhorn et al. to use a temperature considerably lower than those reported by the group of Kaminsky [79], however the system was very complicated for a practical application.

2.2.4. Pyrolysis of PS Mixed with Biomasses

A mixture of cellulose and PS was pyrolyzed in a vertical reactor by Rutkowski and Kubacki using an argon flux and a heating rate of 5 °C min⁻¹ up to 500 °C and keeping the mixture at the final temperature for 1 h. The addition of PS to cellulose had a beneficial effect

on the yield and physical properties of bio-oil (density, pour point, and total acid number were improved). The composition of liquids was close to that one obtained from pure PS, however information concerning the amount and composition of the liquid were not given [82].

Fast simultaneous pyrolysis of a mixture of pine wood/waste plastics (50:50, w/w, plastics: PS, PE, and PP) was realized by Bhattacharya et al. in an auger-fed reactor at 450 and 525 °C, with a short residence time of the vapors in the reactor. The liquid showed high performances (higher carbon and hydrogen content, lower oxygen content, higher heating value and heat of combustion and lower water content), than liquid from pyrolysis of pine wood alone. However the formation of cross-reaction products was negligible. Another benefit of the co-pyrolysis was the ability to avoid the agglomeration of molten plastic particles into larger mass that might be the cause of a variety of processing problems. Styrene was formed only in amount of 12.7 wt % at 450 °C [83].

A mixture of palm shell and PS was also pyrolyzed by Abnisa et al. in a tubular reactor to improve the characteristic of the liquid as a fuel. Three parameters were investigated: temperature, feed ratio, and reaction time. The maximum yield of the liquid fraction was 68.3 wt % in the following conditions: a temperature of 600 °C, a palm shell/PS ratio of 40:60, and a reaction time of 45 min. The liquid was mainly composed by aliphatic and aromatic hydrocarbons, with low water and oxygen content [84].

2.3. Catalytic Pyrolysis

A mixture of PE, PP, and PS was pyrolyzed in autoclave by Pinto et al. using a large plethora of catalysts such as zeolites and metals containing compounds (ZnCl_2 , iron and molybdenum-cobalt oxides) [85]. The use of catalysts did not improve the conversion nor affect the distribution of products. Styrene was presumably formed but it was not reported as pyrolysis product independently of the use, of a catalyst [39, 85]. Probably styrene was initially formed but it was transformed in other products in the reaction conditions tested.

A mixed stream of plastics coming from a waste packaging separation and classification plant was pyrolyzed by de Marco et al. in an autoclave with a N_2 flux in the presence of HZSM-5, red mud and AlCl_3 as catalysts. The use of each catalyst reduced the formation of styrene even if they improved the quality of the liquid obtained and HZSM-5 improved also the formation of single ring aromatic compounds [68].

A solution of PS in benzene was pyrolyzed by Puente and Sedran at 550 °C using several commercial acid catalyst [86] in a batch system working as a continuous unit. High amount of coke was always formed due to secondary oligomerization reactions followed by further cracking. Styrene was recovered in low yield if compared to results of other experiments without the presence of a catalyst.

PS was also pyrolyzed in a fixed bed reactor by Williams and Bagri using two zeolitic catalysts, ZSM-5 and Y-zeolite. The influence of temperature, type of catalyst, amount of catalyst, and use of a mixture of two catalysts were tested. These catalysts increased the gasification of the polymer, that is the yield of gas and consequently reduced the yield of liquid together with significant formation of carbonaceous coke on the catalysts. These zeolite catalysts did not improve the amount and quality of liquid nor the formation of styrene [87].

Expanded PS was pyrolyzed by Park et al. in a semi-batch reactor with a continuous flux of nitrogen at temperature between 350 and 480 °C in the presence of several catalyst: Al₂O₃, ZrO₂, Fe₂O₃, ZnO, BaO, Fe/Alumina or Fe/Alumina modified with a basic additive. Pyrolysis was already active at 350 °C in the presence of BaO giving a liquid (yield 73.2 wt %) containing an 84.3 % of styrene [48].

Pyrolysis of expanded PS was also investigated by Lee et al. in a swirling fluidized-bed reactor testing the influence of temperature and the presence of Fe₂O₃, BaO, or zeolite HZSM-5 as catalyst. The yields of liquid and styrene were increased while increasing the ratio of swirling gas in different experiments. Working with Fe₂O₃ at 450 °C the highest yield of liquid (96.7 %) with a styrene concentration of 73.7 % were obtained [88].

HIPS and crystal PS were pyrolyzed in the presence of zeolites and aluminosilicates by Marcilla et al. in a thermogravimetric balance increasing the temperature from 30 to 550 °C. They showed that the polymer-catalyst contact affected the decomposition of PS giving three steps of pyrolysis which might be used to characterize this material [89].

Pyrolysis of PS was carried out using a modified silicon mesoporous molecular sieve containing KNO₃ as catalyst by Xie et al. This new catalyst showed better catalytic activity and selectivity, if compared to other molecular sieves, giving a yield of liquid of 85.7 %, and a yield of styrene up to 69.0 % [90].

Also co-pyrolysis of PS with ABS containing a polybrominated epoxy flame retardant was carried out by Brebu et al. in a batch reactor in the presence of iron and calcium based catalysts with the aim to obtain a liquid without bromine containing compounds [69]. These authors showed that iron based catalysts, placed inside the reactor in the stream of vapors, reduced the amount of nitrogen and bromine containing compounds in the liquids without affecting the amount and distribution of aromatics.

In the same way Bhaskar et al. investigated the pyrolysis of PS and HIPS containing brominated flame retardants in a mixture with PP, PE, PVC, and PET. Pyrolysis were carried out in the presence of a composite of calcium carbonate and carbon using a batch reactor at 430 °C with the aim to obtain a liquid without halogenated (Cl, Br) compounds [70]. The presence of this catalytic system eliminated completely Br and Cl containing compounds in the liquid when PET was not present among the starting materials and reduced the content of these Cl and Br compounds when PET was present in the feeding materials. Furthermore the catalyst increased the yield of liquid products of 3 – 6 wt %, as well as enhanced the formation of gaseous product and decreased the amount of residue. In the same time the amount of C9 hydrocarbons was reduced [70].

A mixture of plastics (PS, 18 wt %, PE, PP, PVC, and PET) and real sample plastics from a sorting facility were pyrolyzed by Adrados et al. in a batch non stirred reactor at 500 °C (heating rate 20 °C/min) in the presence of red mud (a by-product of aluminum industry) as catalyst. Cracking and aromatization reactions were promoted increasing the yield of gas, light liquid, aromatics, furthermore liquid was more fluid (waxy products were not present). Indeed styrene was obtained up to 42.3 % (by chromatographic analysis) in the presence of red mud using the simulated plastic mixture [91].

A mixture of plastics (PS, 18 wt %, PE, PP, PVC, and PET) was also stepwise pyrolyzed by Lopez-Urionabarrenechea et al. in a semi-batch reactor at 440 °C for 30 min using a ZSM-5 zeolite catalyst [92]. The best results were obtained using a first step at 300 °C for PVC dechlorination without catalyst followed by the catalytic pyrolysis. The catalyst enhanced the production of liquid having a low density and containing an increased amount of aromatic

hydrocarbons together with a C3–C4 rich gas. Indeed styrene concentration in the liquid was 44.9 % (by chromatographic analysis) [92].

Pyrolysis of PS was carried out also in a fluidized-bed reactor using a catalyst obtained with the residue of a precedent pyrolysis process of PS by Lee et al. They reported an optimum temperature of 500 °C and using a gas velocity of 0.2 m/s the maximum yields of liquid (20 wt %) and styrene (11 wt %) was obtained working in the presence of two silica/alumina catalysts [93].

The catalytic decomposition of PS with special regards to the role of an acid or a basic catalyst was investigated by Marczewski et al. in a tubular reactor at 450 °C. They proposed two main reaction routes, one thermal and the other catalytic. The first one involves two main reaction pathways: gradual depolymerization to styrene and pyrolysis leading to low molecular weight compounds and only reactions of these compounds were affected by the presence of the catalyst. Consecutive reactions were claimed to form coke together with hydrogen (H^+ or H^-) which most probably promoted hydrogenation of styrene to ethylbenzene. In the presence of basic catalysts selective styrene formation took place and coke formation was low while formation of ethylbenzene was suppressed. Acid catalysts were less selective in styrene formation [94].

PS thoroughly mixed with manganese sulfate was pyrolyzed by Wei and Lee reducing the formation of soot and polycyclic aromatic hydrocarbons (PAHs). These results were attributed to a ring opening of the aromatic fraction or to a slow rate of ring formation [95], however information concerning other products present in the reaction mixture was not reported.

PS and flame-retarded PS composite containing magnesium hydroxide ($Mg(OH)_2$) were pyrolyzed in an off-line furnace-type reactor at 700 °C for 10 min by Hu and Li. $Mg(OH)_2$ did not contribute to the formation of new products, but increased the concentration of all compounds already present with the exception of styrene which markedly decreased. In PS/ $Mg(OH)_2$ composite, due to a cage and an endothermal effect, depolymerization reactions were restrained while intermolecular reactions took place and condensed aromatic compounds were formed [96].

Pyrolysis–gasification of PS, PP, PE, a real-world waste plastics and mixed plastics was investigated by Wu and Williams with or without a Ni–Mg–Al catalyst for hydrogen production in a two-stages reaction system (first pyrolysis at 500 °C then gasification at 800 or 850 °C in the presence of the catalyst). Low gas yield was obtained in the absence of steam and catalyst. At the gasification temperature of 850 °C, 50.2 wt % of liquid from PS was collected working in the absence of a catalyst. The presence of the catalyst improved the yield of gas and hydrogen production, however PS showed the lowest hydrogen production among tested polymers of 0.155 and 0.196 (g H_2 /g PS) at the gasification temperatures of 800 and 850 °C together with the lowest coke formation on the catalyst [97].

3. MICROWAVE ASSISTED PYROLYSIS

Microwave (MW) heating showed a sound and worthwhile application in several fields due to benefits enclosed with this heating technology among which a fast and localized heating. It has been developed and used in several applications such as food baking, vacuum

drying, tempering and thawing, pasteurization, and sterilization [98]. Furthermore it is used in polymer industries (for rubber vulcanization, polymerization or curing of resins and polymers by elimination of polar solvents), chemical reactions and so on [99].

In recent years there was a growing interest toward developing a microwave assisted pyrolysis (MAP) processes [5, 100, 101] for tire [102 - 104], PE and PP [105 - 107], and PS [20, 108 - 110]. With the exception of tire all these polymeric materials did not absorb MW thus they could not be directly heated. This limitation was overcome by adding a MW absorber in order to perform the pyrolysis process which focuses on the MW irradiation of the sample [5].

MW heating might overcome all problems concerning with heat transfer and diffusion related to pyrolysis of polymers by localizing the energy directly on MW absorbers that were thoroughly mixed with polymers. In addition MAP might allow a careful control of pyrolysis parameters to maximize one of the products. The reader must be take into account that operating parameters might induce and/or alter particular chemical reactions, resulting in different chemical paths and composition of the products [111]. Furthermore feedstock for MAP requires few pretreatment and conditioning steps (such as grinding or chopping) with respect to conventional pyrolysis. These benefits might reduce time and energy, and allowed a cleaner conversion to valuable products than conventional pyrolysis.

MW heating shows further differences and unique features with respect to conventional and other heating methods. MW heating is possible on materials which possess electrons able to move freely in its structure such as carbon or metals. These moving charges may cause the formation of arcing or microplasmas on the surface of the absorber [106, 112 - 116]. Also compounds having a dipole inside the material may adsorb microwave radiations. The dipole present inside the material tries to align in phase with the oscillating electromagnetic field of the MW. The friction due to the dipole movements cause a heating of the material and in this way energy is transferred from the microwave field to the material itself.

Anyway switching from a classical to a MW heated system may present some new problematic issues. Homogeneity of MW radiation and heating could be a problem on large sample and a mixing system might solve it. However the mixing system should be transparent to MW, otherwise it might interfere with the behavior of the pyrolysis itself. The formation of char might cover the quartz windows from which the MW was delivered into the oven. So the char might absorb the MW preventing their introduction inside the oven and this deposit might damage the windows themselves or the generator if the MW was reflected inside it. Two comprehensive reviews on MW interactions with several materials are already present in literature [117 - 119] and this aspect is not discussed in this chapter.

MAP of PS was reported by Hussain et al. in three different papers in the presence of different metals as MW absorbers [108 - 110]. A domestic oven was arranged to host a baked clay vessel (thus a batch reactor) which was filled with PS, together with a coal or a metal as MW absorber (Figure 14).

In a first set of experiments iron mesh were used as a MW absorber. In this way high temperature was achieved due to MW-metal interactions and they claimed that these interactions had a catalytic effect on the pyrolysis process and product distribution. Indeed when placing a copper wire in contact with the iron mesh it was melted so temperature about 1100 – 1200 °C were achieved [108]. A crucial role was attributed to the shape of the mesh and the best arrangement was a cylindrical form which showed best results. Furthermore the

mesh form was mandatory because a solid iron cylinder increased the reaction time. Probably the increased surface area of the powder improved the transfer of the heat to the plastic.

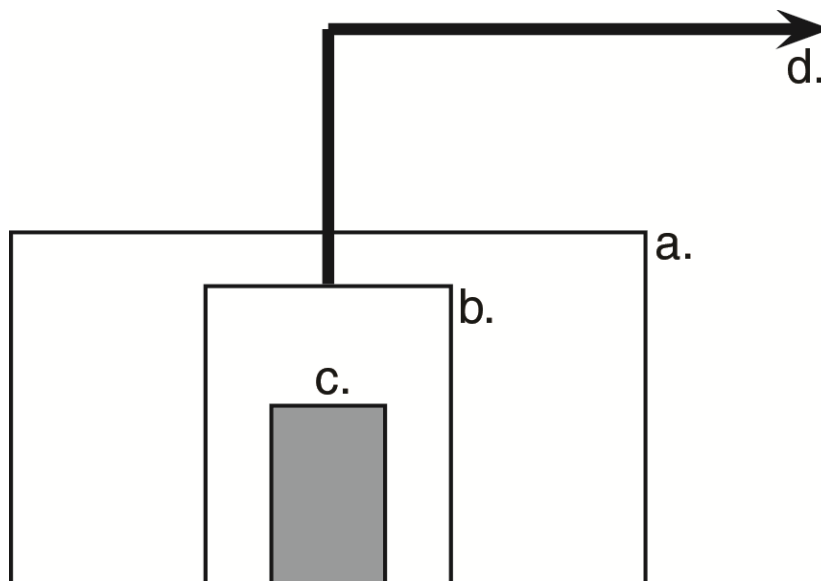


Figure 14. Scheme of the batch system employed by Hussain et al. [108]. a) MW oven; b) clay reactor; c) MW absorber; d) liquid to the condensing system.

In the best condition PS was pyrolyzed in 10 min to 80 wt % of liquid, 15 wt % of gas, and 5 wt % of solid.

The liquid obtained contained monocyclic (styrene and ethylbenzene), polycyclic and condensed rings aromatic compounds. However they did not report any information about composition of the liquid formed. Furthermore they observed the formation of oxygenated and chlorinated products due to reactions with atmospheric oxygen and chlorinated products present in plastic additives [108].

PS was also co-pyrolyzed with Makarwal coal in the presence of copper coil to yield 66 wt % of an oily liquid which was a mixture of tar and oil, 10 wt % of an aqueous liquid mainly composed of sulfides from Makarwal coal, 6 wt % of gas, and 18% of solid [109]. The temperature reached was close, but not above the melting point of the copper. The co-pyrolysis improves the yield of liquid due to probable interactions among radicals formed by the two materials in the course of the pyrolysis. The initially formed gaseous products reacted together via coupling reactions and improved the yield of liquid. The main compounds identified, but not quantified by any means, were aromatics. They were formed by cracking of PS in the presence of coal [93].

PS was also pyrolyzed at the temperature of the melting point of aluminum [110]. PS was mixed with aluminum in the form of tightly coiled wire, strips, and cylinder. The coil shaped aluminum showed the fastest pyrolysis rate while strips did not show any heating. Also the gauge of the aluminum wire used to prepare the coil played a role, indeed increasing the gauge, the rate of pyrolysis increased. Furthermore the formation of aluminum oxide, due to the presence of residual oxygen in the reactor, might facilitate the heat generation and also catalyze the cracking.

In the best conditions PS was pyrolyzed in 10 min to 88 wt % of liquid, 10 wt % of gas and solid residue. The liquid was a dark brownish liquid containing substituted aromatics (such as styrene) and polycyclic aromatics but no information was given about the composition of products [110].

Undri et al. reported a batch system for the MAP of PS in the presence of tire or carbon as MW absorber (Figure 15) [20]. They worked with a glass reactor placed in an oven able to deliver a MW power up to 6 kW and, in some experiment, a fractionating column was inserted between the oven and the coolers which increased the residence time of high boiling compounds inside the reactor [100, 101]. These pyrolysis were run without a gas flow and in an anoxic environment on the contrary of experimental conditions reported by Hussain et al. [108-110].

The pyrolysis took place in a very short time (22 min) using 100 g of PS and a MW power of 3 kW in the presence of carbon as MW absorber. The highest liquid yield was 96.1 wt % working with very low MW power (from 1.2 to 3.0 kW) for longer time (185 min). The liquids obtained in the presence of carbon were clear pale-yellow solutions in contrast with the results reported by Hussain et al.

Density of liquids was in a narrow range among 0.891–0.923 g/cm³ and viscosity was also in a very thin interval (0.79–0.91 cP). Furthermore they showed that pyrolysis may be run in the presence of tire as MW absorber.

Tire slightly affected the yield of MAP thus these authors conclude that PS might be pyrolyzed even when large amount of inorganic and/or organic compounds were present as contaminants. Using a MW power of 3 kW and a ratio of 2.0 between PS and carbon as MW absorber, the styrene in the liquid was 66.0 % as evidenced by the chromatographic analysis.

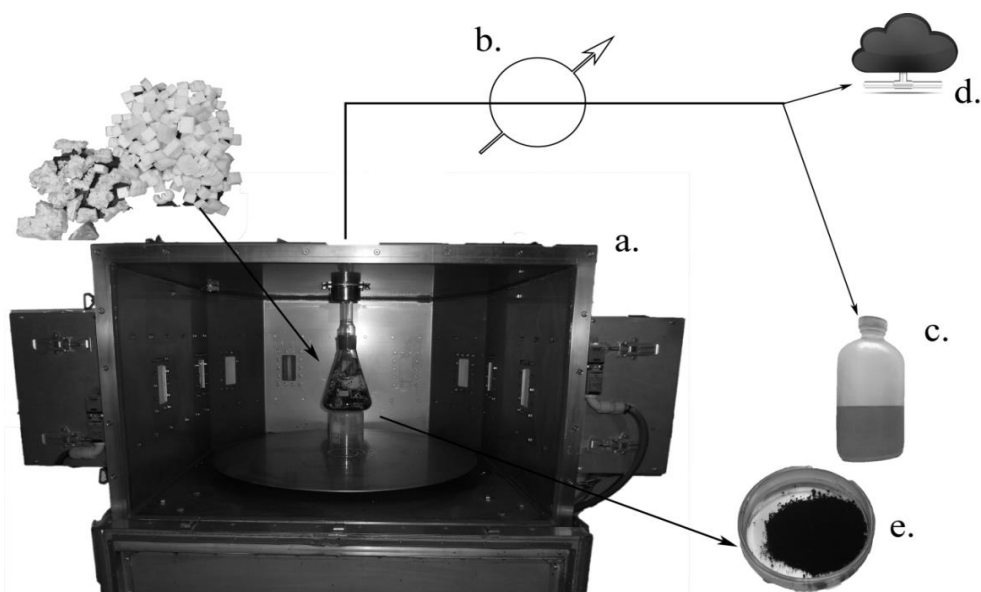


Figure 15. Scheme of the batch system employed by Undri et al. [20]. a) MW oven; b) heat exchanging systems; c) liquid collecting system; d) gas collecting system, e) char collecting system.

Table 1. Main compounds identified^a in liquid from MAP of PS in the presence of carbon as MW absorber and the conditions employed by Undri et al. [20]

Entry	1	2	3	4	5	6
Presence of a fractionating system	no	no	no	no	no	yes
MW power (kW)	3.0-6.0	1.2-3.0	3.0	3.0	3.0	3.0
Reaction time (min)	59	185	22	22	23	28
PS (g)	196.3	160.3	100.4	100.1	50.3	100.3
MW Absorber (g)	106.7	81.8	47.3	100.0	100.0	50.2
Liquid (wt %)	89.3	96.1	86.5	82.2	73.5	83.6
Solid (wt %)	6.8	0.9	9.8	11.1	16.7	10.0
Gas (wt %)	3.9	3.0	3.7	6.7	9.8	6.4
No.	Substance					
1	Benzene					
2	Toluene					
3	Ethylbenzene					
4	1,4-Dimethylbenzene					
5	Styrene					
6	1,2-Dimethylbenzene					
7	Cumene					
8	α -Methylstyrene					
9	1,3-Diphenylpropane					
10	3-Butenylbenzene					
11	Cyclopropane-1,1-diyldibenzene					
12	2-Phenylnaphtalene					
	Total identified aromatics					
	93.1	92.9	96.4	100.0	96.5	95.8

^a Compositions were reported by percent peak areas without any response factors correction; other peaks in concentration lower than 0.2 % were not reported.

The fractionating system reduced the density and viscosity of liquids as shown by the lower amount of high molecular weight compounds present in the liquid.

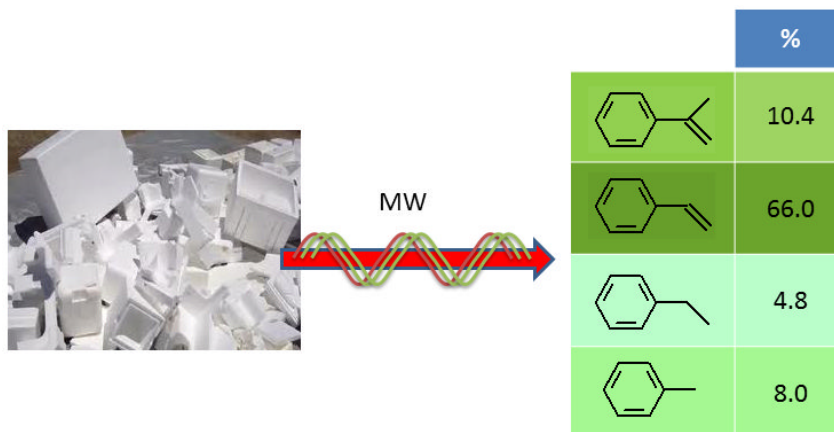


Figure 16. Results obtained by Undri et al. [20].

Indeed liquid obtained in the presence of the fractionating system contained up to 92.7% of single ring aromatic compounds among which styrene, toluene, ethylbenzene, and α -methylstyrene in high amount. (Figure 16). The composition of some liquids together with the pyrolysis condition and yields are reported in Table 1.

CONCLUSION

Polystyrene (PS) is a versatile polymer which is employed in several forms (general purpose PS, expandable PS, high impact PS) to realize objects for many applications such as packaging, electronic devices, insulators and its recycling pose a great challenge for the scientific world.

Pyrolysis showed promising and appealing feature among the possible technologies available or under development. Indeed it is a high temperature treatment which is able to cleave the C-C and C-H bonds of polymers thus to transform them into low molecular weight compounds with potential use as chemical feedstock or fuel.

Several reactors (such as autoclave, fixed bed, fluidized bed, and spouted bed reactors) and heating technologies (classical and microwave) were investigated. PS was usually converted in a liquid containing large amount of single ring aromatics and a special attention was devoted to the recovery of styrene. Indeed the degradation mechanism of PS led to the formation of large amount of styrene if appropriate condition were employed.

PS was mainly converted into a liquid (up to 92 wt %) using short residence time and MW heating. Using long reaction time (achieved in autoclave) a low amount of styrene was recovered because secondary reaction involving styrene took place.

When PS was pyrolyzed with other polymeric materials it improved the rate of pyrolysis due to interactions within radical intermediates formed in the course of the pyrolysis.

The pyrolysis was also investigated in the presence of several catalytic systems and only in some cases improved the quality of the final products, always with detriment to styrene recovery, suggesting a role of the catalyst in secondary reactions involving styrene.

The substitution of a classical heating method with a microwave assisted process showed a considerable reduction of pyrolysis reaction time and avoiding any pretreatment on the starting PS but requiring the addition of a MW absorber. The heat necessary to carry out the pyrolysis was obtained through a MW absorbing material mixed with the feed because PS was transparent to MW radiation. Indeed PS was just place in contact or mixed with the MW absorber and any problem due to poor thermal conductivity of PS, was overwhelmed.

The pyrolysis of waste PS obtaining large amount of styrene may be claimed as a reverse polymerization, so far pyrolysis may be a worthwhile technology to recover useful chemicals (styrene and aromatics) from a waste or a contaminated PS, even when it was mixed with other inorganic or organic materials.

ACKNOWLEDGMENT

The authors want to thanks Cooperativa Autotrasportatori Fiorentini – CAF Scral; Fondazione Ente Cassa di Risparmio di Pistoia e Pescia; and Fondazione Ente Cassa di

Risparmio di Firenze for financial support. A.U. thanks Interuniversity Consortium on Chemical Reactivity and Catalysis – Florence section for a three months grant.

REFERENCES

- [1] Maul, J., Frushour, B. G., Kontoff, J. R., Eichenauer, H., Ott, K.-H., and Schade, C. Polystyrene and Styrene Copolymers. In Ullmann's Encyclopedia of Industrial Chemistry. Wiley-VCH Verlag GmbH & Co. KGaA, 2000.
- [2] Fletcher, B. L. and Mackay, M. E. A model of plastics recycling: does recycling reduce the amount of waste? *Resour. Conserv. Recy.*, 17 (1996), 141-151.
- [3] Khait, K. Recycling, Plastics. In Encyclopedia of Polymer Science and Technology. John Wiley & Sons, Inc., 2002.
- [4] Scheirs, J. and Kaminsky, W. Feedstock Recycling and Pyrolysis of Waste Plastics: Converting Waste Plastics into Diesel and Other Fuels. John Wiley & Sons Ltd, The Atrium, Southern Gate, Chichester, West Sussex PO19 8SQ, UK, 2006.
- [5] Undri, A., Rosi, L., Frediani, M., and Frediani, P. Microwave Pyrolysis of Polymeric Materials. In Microwave Heating. InTech, Janeza Trdine 9, 51000 Rijeka, Croatia, 2012.
- [6] Ammann, P. R., Baddour, R. F., and Mix, T. W. Coal conversion to lower-molecular-weight hydrocarbons. US3384467A (1968).
- [7] Bergstrom, E. V. and Mitchell, J. G. Hydrocarbon pyrolysis reactor. US3283028 (1966).
- [8] Collins, R. N. and Zack, R. S. Increasing olefin yields in hydrocarbon pyrolysis. GB1051478 (1966).
- [9] Eddinger, R. T., Jones, J. F., and Seglin, L. Pyrolysis of coal to obtain liquid hydrocarbons. GB1090728 (1966).
- [10] Liu, G. Y. T. and Strange, C. P. Pyrolyzed blend of polyethylene and polypropylene for blow molding. US3420916A (1969).
- [11] Wingfield, R. C., Jr., Braslaw, J., and Gealer, R. L. Pyrolysis of plastic and rubber waste to hydrocarbons with basic salt catalysts. US4515659A (1985).
- [12] Lyakhevich, G. D., Khimanych, A. P., Suzanskii, V. G., and Kovalerchik, V. P. Apparatus for thermal decomposition of polymers. GB2144047A (1985).
- [13] Grispin, C. W., Jr. Pyrolytic process and apparatus. EP162802A2 (1985).
- [14] Ferrari, A., Lucchesi, A., Maschio, G., and Nardini, G. Apparatus and process for disposal of wastes of mixed polymeric materials. WO8808020A1 (1988).
- [15] Agarwal, K. B. Pyrolysis process and apparatus. CA2025705A1 (1991).
- [16] Chum, H. L. and Evans, R. J. Process for controlled catalytic and sequential pyrolysis and hydrolysis of mixed polymer wastes. WO9222528A2 (1992).
- [17] Kirkwood, K. C., Leng, S. A., and Sims, D. W. Thermal degradation of polymers in fluidized beds. EP502618A1 (1992).
- [18] Elordi, G., Olazar, M., Lopez, G., Artetxe, M., and Bilbao, J. Product Yields and Compositions in the Continuous Pyrolysis of High-Density Polyethylene in a Conical Spouted Bed Reactor. *Ind. Eng. Chem. Res.*, 50 (2011), 6650-6659.

-
- [19] Donaj, P. J., Kaminsky, W., Buzeto, F., and Yang, W. Pyrolysis of polyolefins for increasing the yield of monomers' recovery. *Waste Manage.*, 32 (2012), 840-846.
- [20] Undri, A., Rosi, L., Frediani, M., and Frediani, P. Reverse Polymerization of Waste Polystyrene through Microwave Assisted Pyrolysis. *J. Anal. Appl. Pyrol.*, 105 (2014), 35-42.
- [21] Levine, S. E. and Broadbelt, L. J. Reaction pathways to dimer in polystyrene pyrolysis: A mechanistic modeling study. *Polym. Degrad. Stabil.*, 93 (2008), 941-951.
- [22] M. Kruse, T., Sang Woo, O., and J. Broadbelt, L. Detailed mechanistic modeling of polymer degradation: application to polystyrene. *Chem. Eng. Sci.*, 56 (2001), 971-979.
- [23] Mo, Y., Zhao, L., Chen, C.-L., Tan, G. Y. A., and Wang, J.-Y. Comparative pyrolysis upcycling of polystyrene waste: thermodynamics, kinetics, and product evolution profile. *J. Therm. Anal. Calorim.*, 111 (2013), 781-788.
- [24] Song, H.-S. and Hyun, J. An optimization study on the pyrolysis of polystyrene in a batch reactor. *Korean J. Chem. Eng.*, 16 (1999), 316-324.
- [25] Sterling, W. J., Walline, K. S., and McCoy, B. J. Experimental study of polystyrene thermolysis to moderate conversion. *Polym. Degrad. Stabil.*, 73 (2001), 75-82.
- [26] Cha, W., Kim, S., and McCoy, B. Study of polystyrene degradation using continuous distribution kinetics in a bubbling reactor. *Korean J. Chem. Eng.*, 19 (2002), 239-245.
- [27] Song, H.-S., Lee, J., and Hyun, J. A kinetic model for polystyrene (PS) pyrolysis reaction. *Korean J. Chem. Eng.*, 19 (2002), 949-953.
- [28] Aguado, R., Olazar, M., Gaisán, B., Prieto, R., and Bilbao, J. Kinetics of polystyrene pyrolysis in a conical spouted bed reactor. *Chem. Eng. J.*, 92 (2003), 91-99.
- [29] Kim, S.-S. and Kim, S. Pyrolysis characteristics of polystyrene and polypropylene in a stirred batch reactor. *Chem. Eng. J.*, 98 (2004), 53-60.
- [30] Poutsma, M. L. Further considerations of the sources of the volatiles from pyrolysis of polystyrene. *Polym. Degrad. Stabil.*, 94 (2009), 2055-2064.
- [31] Kannan, P., Biernacki, J. J., and Visco, D. P. Fast pyrolysis kinetics of expanded polystyrene foam. *AIChE J.*, 56 (2010), 1569-1577.
- [32] Kruse, T. M., Levine, S. E., Wong, H.-W., Duoss, E., Lebovitz, A. H., Torkelson, J. M., and Broadbelt, L. J. Binary mixture pyrolysis of polypropylene and polystyrene: A modeling and experimental study. *J. Anal. Appl. Pyrol.*, 73 (2005), 342-354.
- [33] Costa, P., Pinto, F., Ramos, A. M., Gulyurtlu, I., Cabrita, I., and Bernardo, M. S. Study of the Pyrolysis Kinetics of a Mixture of Polyethylene, Polypropylene, and Polystyrene. *Energy Fuels*, 24 (2010), 6239-6247.
- [34] Siddiqui, M. N. and Redhwi, H. H. Catalytic coprocessing of waste plastics and petroleum residue into liquid fuel oils. *J. Anal. Appl. Pyrol.*, 86 (2009), 141-147.
- [35] Snegirev, A. Y., Talalov, V. A., Stepanov, V. V., and Harris, J. N. Formal kinetics of polystyrene pyrolysis in non-oxidizing atmosphere. *Thermochim. Acta*, 548 (2012), 17-26.
- [36] Miranda, M., Cabrita, I., Pinto, F., and Gulyurtlu, I. Mixtures of rubber tyre and plastic wastes pyrolysis: A kinetic study. *Energy*, 58 (2013), 270-282.
- [37] Kannan, P., Biernacki, J. J., and Visco Jr, D. P. A review of physical and kinetic models of thermal degradation of expanded polystyrene foam and their application to the lost foam casting process. *J. Anal. Appl. Pyrol.*, 78 (2007), 162-171.

- [38] Westerhout, R. W. J., Waanders, J., Kuipers, J. A. M., and van Swaaij, W. P. M. Kinetics of the Low-Temperature Pyrolysis of Polyethene, Polypropene, and Polystyrene Modeling, Experimental Determination, and Comparison with Literature Models and Data. *Ind. Eng. Chem. Res.*, 36 (1997), 1955-1964.
- [39] Pinto, F., Costa, P., Gulyurtlu, I., and Cabrita, I. Pyrolysis of plastic wastes. 1. Effect of plastic waste composition on product yield. *J. Anal. Appl. Pyrol.*, 51 (199), 39-55.
- [40] Onwudili, J. A., Insura, N., and Williams, P. T. Composition of products from the pyrolysis of polyethylene and polystyrene in a closed batch reactor: Effects of temperature and residence time. *J. Anal. Appl. Pyrol.*, 86 (2009), 293-303.
- [41] Williams, P. T. and Slaney, E. Analysis of products from the pyrolysis and liquefaction of single plastics and waste plastic mixtures. *Resour. Conserv. Recy.*, 51 (2007), 754-769.
- [42] Karaduman, A., Şimşek, E. H., Çiçek, B., and Bilgesü, A. Y. Flash pyrolysis of polystyrene wastes in a free-fall reactor under vacuum. *J. Anal. Appl. Pyrol.*, 60 (2001), 179-186.
- [43] Kim, Y., Hwang, G., Bae, S., Yi, S., Moon, S., and Kumazawa, H. Pyrolysis of polystyrene in a batch-type stirred vessel. *Korean J. Chem. Eng.*, 16 (1999), 161-165.
- [44] Williams, P. T. and Williams, E. A. Interaction of Plastics in Mixed-Plastics Pyrolysis. *Energy Fuels*, 13 (199), 188-196.
- [45] Kiran, N., Ekinçi, E., and Snape, C. E. Recycling of plastic wastes via pyrolysis. *Resour. Conserv. Recy.*, 29 (2000), 273-283.
- [46] Achilias, D. S., Kanellopoulou, I., Megalokononimos, P., Antonakou, E., and Lappas, A. A. Chemical Recycling of Polystyrene by Pyrolysis: Potential Use of the Liquid Product for the Reproduction of Polymer. *Macromol. Mater. Eng.*, 292 (2007), 923-934.
- [47] Chauhan, R. S., Gopinath, S., Razdan, P., Delattre, C., Nirmala, G. S., and Natarajan, R. Thermal decomposition of expanded polystyrene in a pebble bed reactor to get higher liquid fraction yield at low temperatures. *Waste Manage.*, 28 (2008), 2140-2145.
- [48] Park, J. J., Park, K., Kim, J.-S., Maken, S., Song, H., Shin, H., Park, J.-W., and Choi, M.-J. Characterization of Styrene Recovery from the Pyrolysis of Waste Expandable Polystyrene. *Energy Fuels*, 17 (2003), 1576-1582.
- [49] Demirbas, A. Pyrolysis of municipal plastic wastes for recovery of gasoline-range hydrocarbons. *J. Anal. Appl. Pyrol.*, 72 (2004), 97-102.
- [50] Lomakin, S. M., Koverzanova, E. V., Shilkina, N. G., Usachev, S. V., and Zaikov, G. E. Thermal Degradation of Polystyrene-Polydimethylsiloxane Blends. *Russ. J. Appl. Chem.*, 76 (2003), 472-482.
- [51] Sinn, H., Kaminsky, W., and Janning, J. Processing of Plastic Waste and Scrap Tires into Chemical Raw Materials, Especially by Pyrolysis. *Angew. Chem., Int. Ed.*, 15 (1976), 660-672.
- [52] Scott, D. S., Czernik, S. R., Piskorz, J., and Radlein, D. S. A. G. Fast Pyrolysis of Plastic Wastes. *Energy Fuels*, 4 (1990), 407-411.
- [53] Kaminsky, W., Predel, M., and Sadiki, A. Feedstock recycling of polymers by pyrolysis in a fluidised bed. *Polym. Degrad. Stabil.*, 85 (2004), 1045-1050.

-
- [54] Liu, Y., Qian, J., and Wang, J. Pyrolysis of polystyrene waste in a fluidized-bed reactor to obtain styrene monomer and gasoline fraction. *Fuel Process. Technol.*, 63 (2000), 45-55.
- [55] Hall, W. J. and Williams, P. T. Pyrolysis of brominated feedstock plastic in a fluidised bed reactor. *J. Anal. Appl. Pyrol.*, 77 (2006), 75-82.
- [56] Jung, S.-H., Kim, S.-J., and Kim, J.-S. The influence of reaction parameters on characteristics of pyrolysis oils from waste high impact polystyrene and acrylonitrile-butadiene-styrene using a fluidized bed reactor. *Fuel Process. Technol.*, 116 (2013), 123-129.
- [57] Arandes, J. M., Erena, J., Azkoiti, M. J., Olazar, M., and Bilbao, J. Thermal recycling of polystyrene and polystyrene-butadiene dissolved in a light cycle oil. *J. Anal. Appl. Pyrol.*, 70 (2003), 747-760.
- [58] Shin, H.-Y. and Bae, S.-Y. Thermal decomposition of polystyrene in supercritical methanol. *J. Appl. Polym. Sci.*, 108 (2008), 3467-3472.
- [59] Hwang, G.-C., Choi, J.-H., Bae, S.-Y., and Kumazawa, H. Degradation of polystyrene in supercritical n-Hexane. *Korean J. Chem. Eng.*, 18 (2001), 854-861.
- [60] Ke, H., Li-hua, T., Zi-bin, Z., and Cheng-fang, Z. Reaction mechanism of styrene monomer recovery from waste polystyrene by supercritical solvents. *Polym. Degrad. Stabil.*, 89 (2005), 312-316.
- [61] Andreikov, E. I., Amosova, I. S., Dikovinkina, Y. A., Krasnikova, O. V., and Pervova, M. G. Pyrolysis of polystyrene in coal tar and ethylene tar pitches. *Russ. J. Appl. Chem.*, 85 (2012), 89-97.
- [62] Ahmed, I. I. and Gupta, A. K. Hydrogen production from polystyrene pyrolysis and gasification: Characteristics and kinetics. *Int. J. Hydrogen Energy*, 34 (2009), 6253-6264.
- [63] Hong, N., Wang, B., Song, L., Hu, S., Tang, G., Wu, Y., and Hu, Y. Low-cost, facile synthesis of carbon nanosheets by thermal pyrolysis of polystyrene composite. *Mater. Lett.*, 66 (2012), 60-63.
- [64] Siddiqui, M. N. Conversion of hazardous plastic wastes into useful chemical products. *J. Hazard. Mater.*, 167 (2009), 728-735.
- [65] Siddiqui, M. N. and Redhwi, H. H. Pyrolysis of mixed plastics for the recovery of useful products. *Fuel Process. Technol.*, 90 (2009), 545-552.
- [66] Angyal, A., Miskolczi, N., and Bartha, L. Petrochemical feedstock by thermal cracking of plastic waste. *J. Anal. Appl. Pyrol.*, 79 (2007), 409-414.
- [67] Kiran Ciliz, N., Ekinçi, E., and Snape, C. E. Pyrolysis of virgin and waste polypropylene and its mixtures with waste polyethylene and polystyrene. *Waste Manage.*, 24 (2004), 173-181.
- [68] de Marco, I., Caballero, B. M., Lòpez, A., Laresgoiti, M. F., Torres, A., and Chomòn, M. J. Pyrolysis of the rejects of a waste packaging separation and classification plant. *J. Anal. Appl. Pyrol.*, 85 (2009), 384-391.
- [69] Brebu, M., Bhaskar, T., Murai, K., Muto, A., Sakata, Y., and Uddin, M. A. Thermal degradation of PE and PS mixed with ABS-Br and debromination of pyrolysis oil by Fe- and Ca-based catalysts. *Polym. Degrad. Stabil.*, 84 (2004), 459-467.

- [70] Bhaskar, T., Kaneko, J., Muto, A., Sakata, Y., Jakab, E., Matsui, T., and Uddin, M. A. Pyrolysis studies of PP/PE/PS/PVC/HIPS-Br plastics mixed with PET and dehalogenation (Br, Cl) of the liquid products. *J. Anal. Appl. Pyrol.*, 72 (2004), 27-33.
- [71] Bhaskar, T., Hall, W. J., Mitan, N. M. M., Muto, A., Williams, P. T., and Sakata, Y. Controlled pyrolysis of polyethylene/polypropylene/polystyrene mixed plastics with high impact polystyrene containing flame retardant: Effect of decabromo diphenylethane (DDE). *Polym. Degrad. Stabil.*, 92 (2007), 211-221.
- [72] Bhaskar, T., Mitan, N., Onwudili, J., Muto, A., Williams, P., and Sakata, Y. Effect of polyethylene terephthalate (PET) on the pyrolysis of brominated flame retardant-containing high-impact polystyrene (HIPS-Br). *J. Mater. Cycles Waste Manage.*, 12 (2010), 332-340.
- [73] Miskolczi, N., Bartha, L., and Angyal, A. Pyrolysis of Polyvinyl Chloride (PVC)-Containing Mixed Plastic Wastes for Recovery of Hydrocarbons. *Energy Fuels*, 23 (2009), 2743-2749.
- [74] Kim, S.-S., Kim, J., Jeon, J.-K., Park, Y.-K., and Park, C.-J. Non-isothermal pyrolysis of the mixtures of waste automobile lubricating oil and polystyrene in a stirred batch reactor. *Renew. Energ.*, 54 (2013), 241-247.
- [75] Miskolczi, N. and Bartha, L. Utilization of Hydrocarbons Obtained by Waste Plastic Pyrolysis: Energetic Utilization (Part I). *J. Power Energy*, 6 (2012), 1204-1210.
- [76] Kaminsky, W. and Kim, J.-S. Pyrolysis of mixed plastics into aromatics. *J. Anal. Appl. Pyrol.*, 51 (1999), 127-134.
- [77] Kim, J.-S., Kaminsky, W., and Schlesselmann, B. Pyrolysis of a fraction of mixed plastic wastes depleted in PVC. *J. Anal. Appl. Pyrol.*, 40-41 (1997), 365-372.
- [78] Simon, C. M., Kaminsky, W., and Schlesselmann, B. Pyrolysis of polyolefins with steam to yield olefins. *J. Anal. Appl. Pyrol.*, 38 (1996), 75-87.
- [79] Predel, M. and Kaminsky, W. Pyrolysis of mixed polyolefins in a fluidised-bed reactor and on a pyro-GC/MS to yield aliphatic waxes. *Polym. Degrad. Stabil.*, 70 (2000), 373-385.
- [80] Grause, G., Matsumoto, S., Kameda, T., and Yoshioka, T. Pyrolysis of Mixed Plastics in a Fluidized Bed of Hard Burnt Lime. *Ind. Eng. Chem. Res.*, 50 (2011), 5459-5466.
- [81] Bockhorn, H., Hornung, A., and Hornung, U. Stepwise pyrolysis for raw material recovery from plastic waste. *J. Anal. Appl. Pyrol.*, 46 (1998), 1-13.
- [82] Rutkowski, P. and Kubacki, A. Influence of polystyrene addition to cellulose on chemical structure and properties of bio-oil obtained during pyrolysis. *Energ. Convers. Manage.*, 47 (2006), 716-731.
- [83] Bhattacharya, P., Steele, P. H., Hassan, E. B. M., Mitchell, B., Ingram, L., and Pittman Jr, C. U. Wood/plastic copyrolysis in an auger reactor: Chemical and physical analysis of the products. *Fuel*, 88 (2009), 1251-1260.
- [84] Abnisa, F., Wan Daud, W. M. A., Ramalingam, S., Azemi, M. N. B. M., and Sahu, J. N. Co-pyrolysis of palm shell and polystyrene waste mixtures to synthesis liquid fuel. *Fuel*, 108 (2013), 311-318.
- [85] Pinto, F., Costa, P., Gulyurtlu, I., and Cabrita, I. Pyrolysis of plastic wastes 2. Effect of catalyst on product yield. *J. Anal. Appl. Pyrol.*, 51 (1999), 57-71.

- [86] Puente, G. d. I. and Sedran, U. Recycling polystyrene into fuels by means of FCC: performance of various acidic catalysts. *Appl. Catal., B*, 19 (1998), 305-311.
- [87] Williams, P. T. and Bagri, R. Hydrocarbon gases and oils from the recycling of polystyrene waste by catalytic pyrolysis. *Int. J. Energ. Res.*, 28 (2004), 31-44.
- [88] Lee, C.-G., Cho, Y.-J., Song, P.-S., Kang, Y., Kim, J.-S., and Choi, M.-J. Effects of temperature distribution on the catalytic pyrolysis of polystyrene waste in a swirling fluidized-bed reactor. *Catal. Today*, 79-80 (2003), 453-464.
- [89] Marcilla, A., Gómez-Siurana, A., Quesada, J. C. G., and Berenguer, D. Characterization of high-impact polystyrene by catalytic pyrolysis over Al-MCM-41: Study of the influence of the contact between polymer and catalyst. *Polym. Degrad. Stabil.*, 92 (2007), 1867-1872.
- [90] Xie, C., Liu, F., Yu, S., Xie, F., Li, L., Zhang, S., and Yang, J. Study on catalytic pyrolysis of polystyrene over base modified silicon mesoporous molecular sieve. *Catal. Commun.*, 9 (2008), 1132-1136.
- [91] Adrados, A., de Marco, I., Caballero, B. M., López, A., Laresgoiti, M. F., and Torres, A. Pyrolysis of plastic packaging waste: A comparison of plastic residuals from material recovery facilities with simulated plastic waste. *Waste Manage.*, 32 (2012), 826-832.
- [92] Lopez-Uriónabarrenechea, A., de Marco, I., Caballero, B. M., Laresgoiti, M. F., and Adrados, A. Catalytic stepwise pyrolysis of packaging plastic waste. *J. Anal. Appl. Pyrol.*, 96 (2012), 54-62.
- [93] Lee, C.-G., Kim, J.-S., Song, P.-S., Choi, G.-S., Kang, Y., and Choi, M.-J. Decomposition characteristics of residue from the pyrolysis of polystyrene waste in a fluidized-bed reactor. *Korean J. Chem. Eng.*, 20 (2003), 133-137.
- [94] Marczewski, M., Kaminska, E., Marczewska, H., Godek, M., Rokicki, G., and Sokolowski, J. Catalytic decomposition of polystyrene. The role of acid and basic active centers. *Appl. Catal., B*, 129 (2013), 236-246.
- [95] Wei, Y.-L. and Lee, J.-H. Manganese sulfate effect on PAH formation from polystyrene pyrolysis. *Sci. Total Environ.*, 228 (1999), 59-66.
- [96] Hu, Y. and Li, S. The effects of magnesium hydroxide on flash pyrolysis of polystyrene. *J. Anal. Appl. Pyrol.*, 78 (2007), 32-39.
- [97] Wu, C. and Williams, P. T. Pyrolysis-gasification of plastics, mixed plastics and real-world plastic waste with and without Ni-Mg-Al catalyst. *Fuel*, 89 (2010), 3022-3032.
- [98] Meredith, R.,. The Engineers' Handbook of Industrial Microwave Heating. The Institution of Electrical Engineers, London, United Kingdom, 1998.
- [99] Tierney, J. P. and Lidstrom, P. Microwave Assisted Organic Synthesis. Blackwell Publishing Ltd, Oxford, UK, 2005.
- [100] Frediani, P., Rosi, L., Frediani, M., Undri, A., Occhialini, S., and Meini, S. Production Of Hydrocarbons From Pyrolysis of Tyres. WO2012110991 (2012).
- [101] Frediani, P., Rosi, L., Frediani, M., Undri, A., and Occhialini, S. Production of Hydrocarbons from Copyrolysis of Plastic and Tyre Material with Microwave Heating. WO2012110990 (2012).

- [102] Undri, A., Meini, S., Rosi, L., Frediani, M., and Frediani, P. Microwave Pyrolysis of Polymeric Materials: Waste Tires Treatment and Characterization of the Value-Added Products. *J. Anal. Appl. Pyrol.*, 103 (2013), 149-158.
- [103] Undri, A., Rosi, L., Frediani, M., and Frediani, P. Upgraded Fuel from Microwave Assisted Pyrolysis of Waste Tire. *Feul*, 115 (2014), 600-608.
- [104] Undri, A., Sacchi, B., Cantisani, E., Toccafondi, N., Rosi, L., Frediani, M., and Frediani, P. Characterization of Carbon from Microwave Assisted Pyrolysis of Tires. *J. Anal. Appl. Pyrol.*, 104 (2013), 396-404.
- [105] Ludlow-Palafox, C. and Chase, H. A. Microwave-Induced Pyrolysis of Plastic Wastes. *Ind. Eng. Chem. Res.*, 40 (2001), 4749-4756.
- [106] Russell, A. D., Antreou, E. I., Lam, S. S., Ludlow-Palafox, C., and Chase, H. A. Microwave-assisted pyrolysis of HDPE using an activated carbon bed. *RSC Advances*, 2 (2012), 6756-6760.
- [107] Undri, A., Rosi, L., Frediani, M., and Frediani, P. Efficient Disposal of Waste Polyolefins through Microwave Assisted Pyrolysis. *Fuel*, 116 (2013), 662-671.
- [108] Hussain, Z., Khan, K. M., and Hussain, K. Microwave-metal interaction pyrolysis of polystyrene. *J. Anal. Appl. Pyrol.*, 89 (2010), 39-43.
- [109] Hussain, Z., Khan, K. M., Basheer, N., and Hussain, K. Co-liquefaction of Makarwal coal and waste polystyrene by microwave-metal interaction pyrolysis in copper coil reactor. *J. Anal. Appl. Pyrol.*, 90 (2011), 53-55.
- [110] Hussain, Z., Khan, K. M., Perveen, S., Hussain, K., and Voelter, W. The conversion of waste polystyrene into useful hydrocarbons by microwave-metal interaction pyrolysis. *Fuel Process. Technol.*, 94 (2012), 145-150.
- [111] Luque, R., Menendez, J. A., Arenillas, A., and Cot, J. Microwave-assisted pyrolysis of biomass feedstocks: the way forward? *Energ. Environ. Sci.*, 5 (2012), 5481-5488.
- [112] Menéndez, J. A., Arenillas, A., Fidalgo, B., Fernández, Y., Zubizarreta, L., Calvo, E. G., and Bermúdez, J. M. Microwave heating processes involving carbon materials. *Fuel Process. Technol.*, 91 (2010), 1-8.
- [113] Menéndez, J. A., Juárez-Pérez, E. J., Ruisánchez, E., Bermúdez, J. M., and Arenillas, A. Ball lightning plasma and plasma arc formation during the microwave heating of carbons. *Carbon*, 49 (2011), 339-342.
- [114] Horikoshi, S., Osawa, A., Abe, M., and Serpone, N. On the Generation of Hot-Spots by Microwave Electric and Magnetic Fields and Their Impact on a Microwave-Assisted Heterogeneous Reaction in the Presence of Metallic Pd Nanoparticles on an Activated Carbon Support. *J. Phys. Chem. C*, 115 (2011), 23030-23035.
- [115] Dawson, E. A., Parkes, G. M. B., Barnes, P. A., Bond, G., and Mao, R. The generation of microwave-induced plasma in granular active carbons under fluidised bed conditions. *Carbon*, 46 (2008), 220-228.
- [116] Tsukahara, Y., Higashi, A., Yamauchi, T., Nakamura, T., Yasuda, M., Baba, A., and Wada, Y. In Situ Observation of Nonequilibrium Local Heating as an Origin of Special Effect of Microwave on Chemistry. *J. Phys. Chem. C*, 114 (2010), 8965-8970.
- [117] Bykov, Y. V., Rybakov, K. I., and Semenov, V. E. High-temperature microwave processing of materials. *J Phys. D Appl. Phys.*, 34 (2001), R55.

- [118] Lam, S. S. and Chase, H. A. A Review on Waste to Energy Processes Using Microwave Pyrolysis. *Energies*, 5 (2012), 4209-4232.
- [119] Khaghanikavkani E., and Farid M. M. Mathematical modelling of microwave pyrolysis. *Int. J. Chem. React. Engin.*, 11 (2013), 543-569.
- [120] Yan, Y.-W., Huang, J.-Q., Guan, Y.-H., Shang, K., Jian, R.-K., and Wang, Y.-Z. Flame retardance and thermal degradation mechanism of polystyrene modified with aluminum hypophosphite. *Polym. Degrad. Stabil.*, 99 (2014), 35-42.

Chapter 2

POLYSTYRENE-BASED AMPHIPHILIC BLOCK COPOLYMERS: SYNTHESIS, PROPERTIES AND APPLICATIONS

*Patrizio Raffa**

Department of Chemical Engineering - Product Technology,
University of Groningen, Groningen, The Netherlands

ABSTRACT

Polystyrene is no longer only a commodity plastic. It has been long recognized that copolymerization of styrene with other monomers presenting different characteristics allows the production of new materials, with improved or even completely new properties.

Of particular interest are block copolymers of styrene with hydrophilic monomers. The ability of these amphiphilic polymers to form stable self-assembled aggregates in water by association of the insoluble polystyrene blocks is the key feature of their interesting properties.

Especially in recent times, there has been a great interest in self-assembly, surface activity and rheology of polystyrene-based amphiphilic block copolymers in water. Because of their unique properties, polystyrene-based amphiphilic block copolymers can find applications as detergents, emulsifiers, stabilizers for emulsion polymerizations, nanoreactors, gelators, rheology modifiers and others.

The development of controlled radical polymerization methods (e.g., Atomic Transfer Radical Polymerization) in the last two decades provided powerful tools for the preparation of well-defined polymers and copolymers of styrene with tailored molecular weight, composition and architectures. Alongside the synthesis of an increasing number of polystyrene amphiphilic copolymers, an extensive knowledge of the self-assembly, surface and rheological properties of these materials has been gained, also in connection with the polymer composition and architecture.

* Corresponding author: Patrizio Raffa. Department of Chemical Engineering - Product Technology, University of Groningen, Nijenborgh 4, 9747 AG Groningen, The Netherlands. E-mail: p.raffa@rug.nl, phone: +31 (0)50 363 4462, fax: +31 (0)50 363 4479.

Here, an overview of synthesis, properties and applications of amphi-philic copolymers containing at least one polystyrene block will be given, aimed at envisaging the impact of this kind of polymers in the future of science, industry and life.

1. INTRODUCTION

Polystyrene (PS) is a cheap and largely available commodity plastic, which has been used in countless applications for almost a century now.

Properties and applications of Polystyrene alone are outside the scope of this chapter. Physical blends of Polystyrene with other polymers will not be considered here as well. Here we will focus on amphiphilic block copolymers that contain at least one Polystyrene chain in their chemical structure. Unlike a blend, a block copolymer is constituted by different macromolecular chains connected by a chemical bond. The simplest case is a diblock, when only two blocks are connected, but also tri or more block can be connected, giving multiblock structures (triblock, tetrablock and so on). The blocks can also be connected in a non-linear way (graft or star copolymers). Schematic structures are given in Figure 1.

Since Polystyrene is highly hydrophobic, the copolymers described here will include an hydrophilic (water soluble) block as the other partner.

As we will see, these polymers possess unique properties that allow the use of Polystyrene in even more applications.

It has been long recognized that copolymerization of styrene with other monomers (such as butadiene, acrylonitrile or maleic anhydride) greatly expands the possibility for its applications. For instance, the very well-known high impact polystyrene (HIPS) is constituted by a polystyrene backbone with grafted polybutadiene (PBD) chains. The interesting properties of such material come from the immiscibility of PS and PBD, which causes the formation of two distinct phases.

A classic example of PS-containing block copolymer is given by SBS rubbers. These are triblock styrene-butadiene-styrene copolymers. The terminal PS blocks tend to aggregate into the BD rubbery matrix, making the rubber more resistant and durable.

Analogously, phase segregation is observed when polystyrene (hydro-phobic) is combined with an hydrophilic polymer (the most common being ethylene oxide, acrylic acid, methacrylic acid, 4-vinylpyridine and styrene sulfonate) in a block copolymer.

An important feature of these amphiphilic block copolymers is their ability to form micellar aggregates in water, similarly to what happens to low-molecular weight amphiphilic molecules (a.k.a. surfactants).

The self-assembly of amphiphilic block copolymers in water result in very interesting interfacial and rheological properties, which makes them interesting for applications in many diverse areas, such as emulsion stabilization, coatings, biotechnology, nanotechnology, medicine, pharmacology, cosmetics, agriculture, water purification, electronic, optoelectronic, and enhanced oil recovery.

In this chapter, synthesis, relevant properties and applications of this class of polymers based on polystyrene will be reviewed.

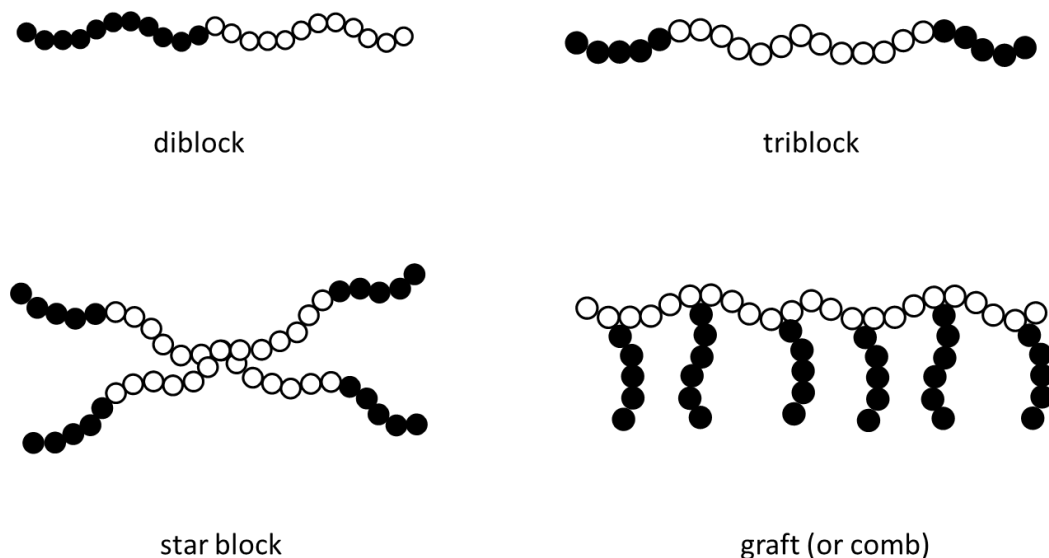


Figure 1. Schematic structures of a diblock, triblock, star block and graft copolymers. White and black circles represent chemically different monomers.

2. SYNTHESIS OF POLYSTYRENE-BASED AMPHIPHILIC BLOCK COPOLYMERS

It is not possible to achieve the synthesis of a perfect block copolymer with conventional radical polymerization methods. Block copolymers (amphi-philic or not) containing polystyrene as one of the blocks can conveniently be prepared by living polymerization methods. Historically, living anionic polymerization has been the most used, but with the advent of free-radical controlled method such as nitroxide-mediated polymerization (NMP), atomic transfer radical polymerization (ATRP) and reversible addition-fragmentation chain-transfer polymerization (RAFT), these last started to be the preferred ones, mainly because they are more tolerant of functional groups and impurities and usually require milder experimental conditions.

Moreover, controlled free-radical methods are more suitable to build well-defined complex architectures (star blocks, comb, miktoarm, etc.).

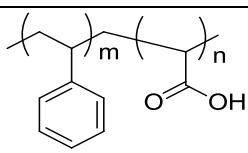
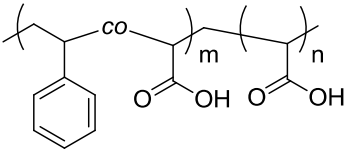
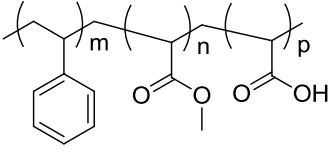
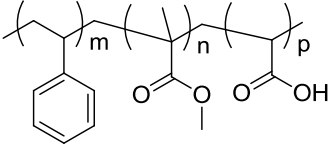
In fact, the discovery of controlled free-radical polymerizations gave a big boost in the study of properties of polymers and copolymers characterized by non-linear structures.

In Table 1, the most studied amphiphilic block copolymers containing at least a PS moiety are reported.

For the synthesis of copolymers containing MAA or AA as the hydro-philic partner, which are probably the most common block polyelectrolytes (block copolymers containing a polyelectrolyte block), a problem may be represented by the dramatically different polarity of the two blocks, which gives them a very different solubility in most solvents. This problem is usually solved by using a non-polar acrylic ester as source of the acidic monomer. Once polymerized, the polyester block can be hydrolyzed to the corresponding acid. A particularly

suitable monomer is the *tert*-butyl acrylate (or methacrylate), which is polymerizable with basically any known method and easily hydrolyzed in relatively mild conditions. Standard procedures involve the use of HCl in dioxane/water mixture or TFA in CH₂Cl₂.

Table 1. Most common amphiphilic copolymers based on PS

Polymer	References
 <p>PS-b-PAA</p>	[1-31]
 <p>P(S-co-AA)-b-PAA</p>	[28, 32-34]
PAA-PS-PAA	[3, 22]
PS-PAA-PS	[35-37]
PS-PAA-PBA	[38, 39]
Polymer	References
 <p>PS-b-PMA-b-PAA</p>	[40]
 <p>PS-b-PMMA-b-PAA</p>	[18]

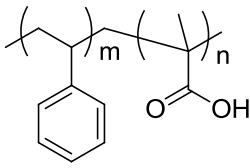
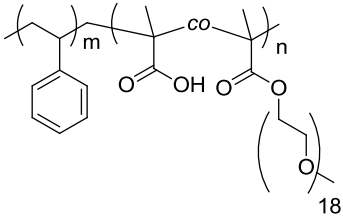
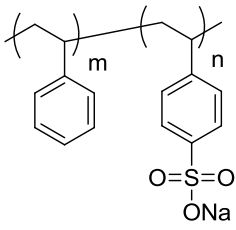
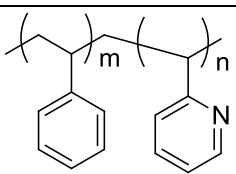
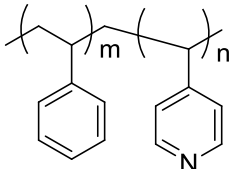
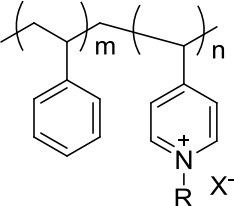
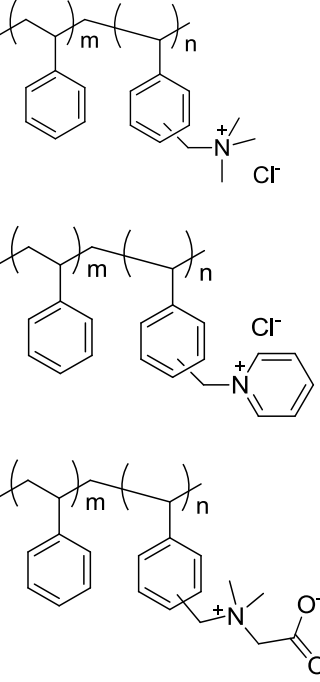
Polymer	References
 <p>PS-b-PMAA</p>	[8, 30, 41-46]
 <p>PS-b-P(PEO18MA-co-MAA)</p>	[30]
 <p>PS-b-PSS</p>	[47-49]
 <p>PS-b-P2VP</p>	[53]
 <p>PS-b-P4VP</p>	[54-56]

Table 1. (Continued)

Polymer	References
 <p> $RX = MeI$ $RX = C_4I$ $RX = C_6I$ $RX = C_{10}I$ $RX = C_{10}Br$ $RX = C_{18}I$ </p>	[11, 21, 57-62]
	[63]

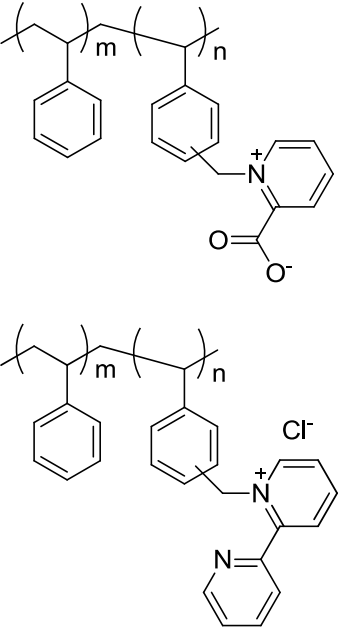
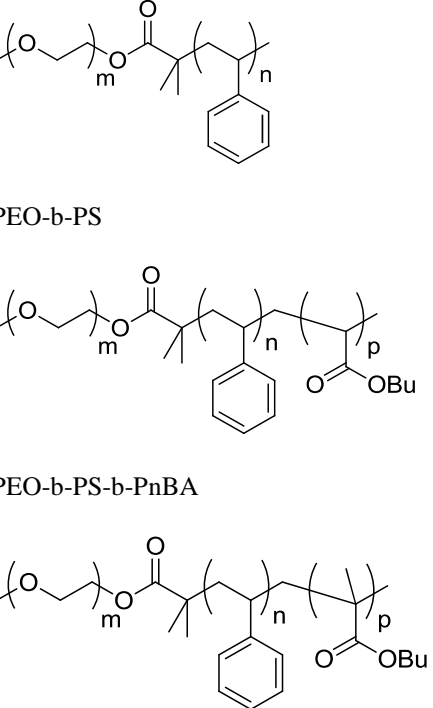
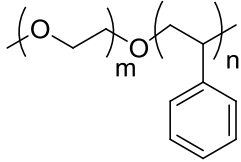
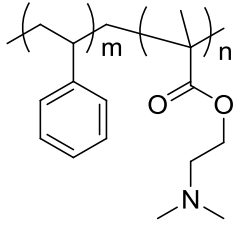
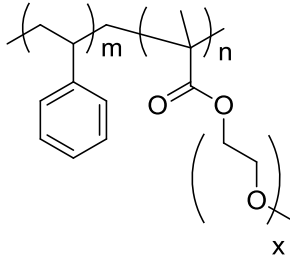
Polymer	References
	[63]
 <p>PEO-b-PS</p> <p>PEO-b-PS-b-PnBA</p> <p>PEO-b-PS-b-PnBMA</p>	[64]

Table 1. (Continued)

Polymer	References
 <p>PEO-b-PS</p>	[65, 66]
 <p>PDMAEMA-b-PS</p>	[67, 68]
 <p>PEGMA-b-PS</p> <p>$x = 4.5, 23$</p>	[69, 70]
PEGMA-PS-PEGMA	[71]
PEGMA-b-PS	[72]
$x = 23$	
PS(PEO) ₂	[73]
Gemini	
PS _n (PEO) _m	[74-77]
3 and 4 arm star block PS-PEO	[78]
PMMA-PEO-PS μ -star miktoarm	[79]

Polymer	References
PS(PAA) ₂ gemini	[80]
Star block PS-PAA	[3, 5, 22]
Dendrimeric (calix arene) PS-PAA	[81, 82]
Dendrimeric (PAMAM) PS-PAA	[83]

2.1. Anionic Polymerization

Anionic addition polymerization is a form of chain-growth polymerization or addition polymerization that involves the polymerization of vinyl mono-mers with strong electronegative groups. This polymerization is carried out through a carbanion active species. Living polymerizations, which lack a formal termination pathway, occur in many anionic addition polymerizations.

The advantage of living anionic addition polymerizations is that they allow for the control of structure and composition. A major drawback is the high reactivity of the anionic species, which requires protection from oxygen and moisture and very low process temperatures (several degrees below zero Celsius).

Eisenberg's group studied extensively PS-b-PAA copolymers of various compositions prepared by anionic living polymerization using sec-butyllithium as initiator. [6-21, 84] LiCl and α -methylstyrene were used to prevent side reactions during polymerization of tBA. [7, 84] The hydrolysis of the tBA block was performed with pTSA in refluxing toluene.

Block copolymers with a broad range of compositions and low dispersities have been successfully prepared, allowing a systematic and extensive study of their properties. Polymers with long PS chains and short PAA [9, 13, 20], as well as short PS and long PAA [10, 12] have been synthesized.

Ring-opening anionic polymerization is often used to prepare PEG-containing block copolymers, using ethylene oxide as the monomer. PEO-b-PS [65, 66] has been prepared this way.

Even if more complicated, also non-linear structures can be made by anionic polymerization.

A miktoarm PS(PEO)₂ copolymer was prepared via two rather complicated alternative procedures involving several protection-deprotection steps, anionic polymerization of styrene and ring-opening polymerization of ethylene oxide [73].

2.2. Nitroxide-Mediated Radical Polymerization (NMP)

Nitroxides are relatively stable radicals with the general formula R₂NO. They are generally derived from alkoxyamines by hemolytic scission of the C-O bond. Nitroxide-

mediated radical polymerization is a method of radical polymerization that makes use of such alkoxyamines to keep the concentration of free radicals low, reducing chain transfer and termination reactions, in order to generate polymers with low polydispersity index.

It is a type of controlled/ living radical polymerization, probably the first one of its kind to appear in literature.

Styrene is very efficiently polymerized by NMP. There are, thus, several examples of amphiphilic block copolymers of styrene prepared by NMP. PS-*b*-PAA was successfully synthesized via NMP of a PS macroinitiator, and direct polymerization of AA. [24] The same group reported NMP of latexes based on amphiphilic block copolymers with short AA block and long hydro-phobic block, by using a nitroxide-terminated PAA macroinitiator in a water emulsion and surfactant-free conditions at alkaline pH. [25, 26] Also diblock, triblock and star amphiphilic PS-*b*-PAA copolymers has been prepared by NMP of a PS macroinitiator and chain extension with PtBA, followed by hydrolysis. [22] In this case, a small amount of styrene is added in the second polymerization step, in order to decrease the propagation rate, which results in incorporation of some styrenic units in the PtBA block. Star block PS-*b*-PA can also be made by NMP. [22]

Sodium styrenesulfonate can be directly polymerized by NMP in a water/ ethylene glycol mixture. [47] Molecular weights up to 900 KDa and low dispersities can be obtained. The PSSNa prepared by this procedure can be used as macroinitiator for the growth of the hydrophobic block of PS in emulsion, [48] or other styrenic type block of various hydrophilicity. [49] It is also possible to add the PSSNa block in three steps, passing through the neo-pentyl and the trimethylsilyl derivatives of SS. [50, 51]

TEMPO mediated NMP of 4-vinylpyridine has been found to proceed in a controlled manner [56, 85] and the resulting polymer has been used success-fully as a macroinitiator for a polystyrene block. [56]

2.3. Atom Transfer Radical Polymerization (ATRP)

Atom Transfer Radical Polymerization (ATRP) is among the most effecti-ve and most widely used methods of controlled radical polymerization.

The key step in ATRP is the atom transfer, that is responsible for uniform polymer chain growth.

It proceeds through a redox equilibrium between Cu(I) and Cu(II) species (other transition metals also work, but Copper is by large the most used), that keeps under control the amount of available radicals, thus reducing drastically the possibility for chain transfer of chain termination reactions.

Matyjaszewski's group (one of the pioneers of ATRP) firstly reported the successful preparation of amphiphilic block copolymers (diblock, star, ABA and ABC triblock) by ATRP following this approach [1, 86, 41] The polymeri-zation of tBA present a good living character up to relatively high molecular weight and good blocking efficiency when the acrylate block is used as macro-initiator. Both addition of small amounts of Cu(II) and use of polar solvents (which enhance the solubility of the deactivator), decrease the reaction rate and afford polymers with narrower molecular weight distribution.

Diblock, triblock and three-arm star PS-*b*-PAA and PS-*b*-PMAA whitin a quite extended range of molecular weights and low polydispersities have been prepared *via* ATRP with a

standard CuBr/PMDETA catalytic system in bulk, either starting from the styrenic [3, 44] or the acrylic block. [2]

Several studies have been performed in order to find the optimal conditions for the polymerization to occur with reasonable rates, high molecular weight and low dispersities. The CuBr/PMDETA systems proved to work better for the synthesis of PtBA macroinitiator in a polar solvent (dibenzyl-ether) and in presence of small amounts of CuBr₂ as deactivator. [1] CuCl proved to be superior to CuBr in CuX/PMDETA catalyzed ATRP of tBMA on a PS-Br macroinitiator, again due to halogen exchange effects. [43]

Halogen terminated PEG has been used as ATRP macroinitiator for amphiphilic block PS-*b*-PEG copolymers. [64]

Nowadays, especially thanks to the availability of controlled radical polymerization methods and “click” chemistry, the preparation of complex copolymers can be achieved with relatively simple methodologies. [74, 75]

For example, various PS_n(PEO)_m heteroarm copolymers have been made by combinations of ring opening polymerization of EO and ATRP of styrene using opportune multifunctional cross-linkers. [76, 77]

Another strategy based on ATRP has been used to synthesize block tri- and four-arm star of PS-*b*-PEO.

The PEO blocks were made by anionic ring-opening polymerization after modification of the terminal bromides with ethanolamine. [78]

An interesting example of the synthesis of a PMMA-PEO-PS μ -star miktoarm polymer based exclusively on ATRP was recently reported. [79]

Due to the high deactivation constant and the low propagation rate of styrene with the CuBr/PMDETA catalyst at room temperature, the authors were able to incorporate only one styrene terminated PEO unit on the macroinitiator.

Star block copolymers constituted by vinylic monomers both as hydrophilic and hydrophobic partner are generally prepared by anionic polymerization or ATRP.

ATRP has been used to prepare Gemini [80] and star block PS-PAA. [5, 3]

The synthesis and study of a complex PS-PAA made by ATRP, which can be considered as a joining link between block star and dendrimeric polymer, has been recently reported. [81, 82]

The synthesis is based on the use of multihalogenated calixarenes for the preparation of the PS core with 2 to 8 arms followed by a two-step chemical modification of the terminal bromide into a difunctional ATRP initiator for the growth of tBMA chains.

A dendrimeric PS-PAA has been also synthesized again via ATRP, starting from a poly(propylene imine) dendrimer with 64 NH₂ functionalities. The polymerization involved, as usual ATRP of styrene followed by ATRP of tBMA and hydrolysis. [83] However, from their studies on the behavior of the prepared polymers the authors concluded that only a minor fraction of the 64 active sites was actually initiated, leading to polymers with a low (not specified) number of branches. On the other hand, an initiator with 8 sites provided an 8-arm star copolymer.

2.4. Reversible Addition-Fragmentation Chain Transfer (RAFT)

Reversible Addition-Fragmentation chain Transfer (RAFT) is also a commonly employed controlled radical polymerization method. It makes use of a chain transfer agent in the form of a thiocarbonylthio compound (or similar) to afford control over the generated molecular weight and polydispersity during a free-radical polymerization.

RAFT is also suitable for the synthesis of PS-based amphiphilic block copolymers, with the advantage over the others methods that acidic monomers such as AA and MA can be polymerized directly, since the polymerization conditions are not affected by the presence of their functional groups.

Preparation of polystyrene-containing amphiphilic block copolymers co-polymers by RAFT has been reported. [23, 28, 32-34] In this cases, precursors were firstly synthesized in aqueous emulsion and then hydrolyzed in basic conditions (NaOH at 90-95°C). Small amounts of AA were added for the synthesis of the second PEA block (for polymerization stability).

Nevertheless, the dispersity indices are always greater than 2. PS-*b*-PAA can be directly synthesized by RAFT in dioxane. The conversion reached 40% for AA and 10% for Styrene. [27-29] PS-*b*-PMAA and similar polymers can be synthesized either in water or dioxane. [30] This is the first report of direct RAFT synthesis of PMAA in water.

Recently, RAFT has been used to prepare PSS-TOA, which can be subsequently used as macro RAFT agent for a second block of PS of various lengths. The controlled nature of both polymerization steps has been emphasized. [52] This system can be easily converted to the corresponding Na salt by ion exchange. The use of the TOA salt of styrene sulfonate is required in order to solubilize the monomer and perform the polymerization in a non-polar organic solvent.

3. PROPERTIES OF POLYSTYRENE-BASED AMPHIPHILIC BLOCK COPOLYMERS

3.1. Interfacial Properties

As for many others amphiphilic block copolymers, also for the ones based on polystyrene the most interesting (or, at least, the most studied) properties comes from their ability to form self-assembled aggregates in water (Figure 2). In diluted solutions they tend to form spherical micelles with a “frozen” poly-styrene core (at temperatures below the glass transition) if the PS block is long enough. In some cases, especially if the hydrophilic block is relatively short, direct dissolution in water is kinetically hampered, but the copolymers can be dissolved in different solvent (e.g. dioxane), where also PS is soluble, and subsequently transferred into an aqueous phase by dialysis.

The critical micelle concentration (CMC) can be determined by measuring the concentration dependence of surface tension or by fluorescence measurements using an hydrophobic fluorescent probe.

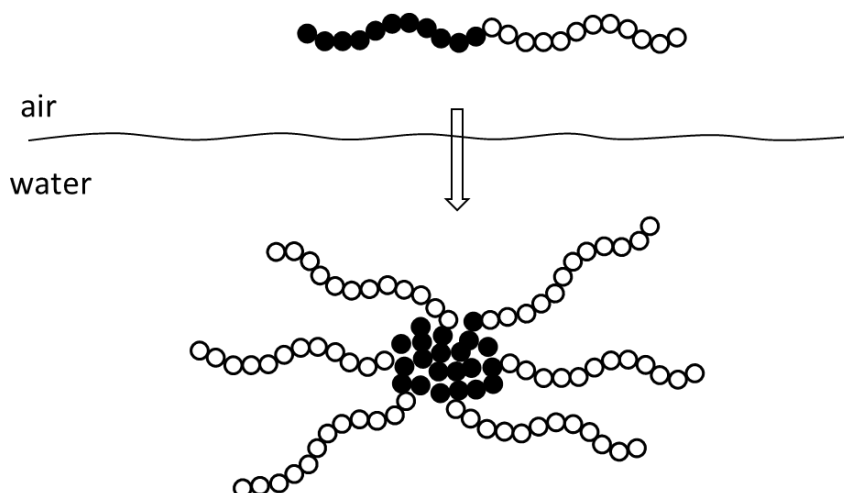


Figure 2. Self-assembly of amphiphilic block copolymers in water.

The latter is used for very low values of CMC and/or when the amphiphilic copolymers are surface inactive or have a very low surface activity.

Theoretical treatments of CMC for both small molecules and macrosurfactants predict that the CMC should decrease exponentially with the length of the hydrophobic group (or block), while the dependence from the hydrophilic block length is much less pronounced. [87] Experimentally, it has been shown that CMC is proportional to $\exp(-cN)$ - where c is a parameter dependent on the Flory-Huggins interaction parameter and N the length of hydrophobic group, but this is valid only for small N . For bigger N the dependence becomes weaker and CMC scales with $\exp(-cN^{1/3})$. This behaviour seems to be general, as shown by the data collected for many systems. [87]

A theoretical model has been proposed to explain this dependence, but it is based on an unusual aggregation mechanism. [88]

The relationship between surface properties and polymer structure is still far from being completely clarified. The picture becomes much more obscure when non linear structures are considered. For example, polymers having roughly the same monomer composition and molar mass, and thus the same HLB, but different architecture, can show different CMCs and surface tension values. S.Gibanel et al. [73] studied PS-*b*-PEO copolymers with different geometry, namely a linear diblock and a Gemini-like one. CMC and surface activity in water solution are completely different. In particular the non-linear polymer shows an higher value of CMC and low surface tension over the all range of concentrations.

The higher CMC for the gemini derivative is attributed to the higher steric hindrance preventing aggregation of the macromolecules.

It has been often observed that PS based block polyelectrolytes do not present a measurable surface activity, that is, their water solutions have the same surface tension of pure water.

An explanation has been proposed for PS-*b*-PSS block copolymers. [50] This model involves the use of an imaginary charge at the water/air interface (a typical concept in electromagnetism to solve the problem of an electrical charge at the interface).

The interface typically consists of two media (in this case water and air) with different relative dielectric constants. A relevant number of electrical charges (q) of the hydrophilic

block are present very close at the interface. In this situation the magnitude of the image charge (q') is given by:

$$q' = -\left(\frac{\varepsilon_a - \varepsilon_w}{\varepsilon_a + \varepsilon_w}\right)q$$

By inserting the known dielectric constant values for water ($\varepsilon_w = 78$) and air ($\varepsilon_a = 1$), one easily obtains that the image charge is of the same sign and almost the same magnitude of the real one ($q' = 0.97q$), thus generating an electrical repulsion at the interface.

The proposed explanation seems to be supported by some experimental observations. For example, for some charged polymeric surfactants the surface activity decreases upon addition of salts, contrarily to what happens for low-molecular weight surfactants. [89]

According to the authors, this can be explained by an electrostatic screening effect caused by salt ions on the electrostatic image charge repulsion. The decrease of surface activity in presence of salts seems to be a general rule for macrosurfactants. [89-92] To support their theory of image charges, the authors also mention a study performed on PhIP-PSS, [90] in which the hydrophobic block length has been systematically changed.

In this case, surface activity has been detected only when the hydrophobic block was at least three times longer than the hydrophilic one. The non-surface activity is believed to result from the balance between hydrophobic adsorption and image charge repulsion.

However, more recent experiments (by the same group) show that in most cases the surface activity of macrosurfactants arises when the hydrophobic block is sufficiently short (below 20 units in case of PBA-PSS).

3.2. Solution Rheology

Besides the interfacial properties, amphiphilic block copolymers containing polystyrene have raised a lot of interest for what concerns their rheological behaviour in water solution. The rheology of water solutions is very important for many applications such as paints and coatings or enhanced oil recovery. The most studied systems in this regards are block polyelectrolytes, where the hydrophilic block is constituted again by PAA or PMAA.

Rheology of block polyelectrolytes is particularly interesting because of the charged nature of the hydrophilic corona: the micelle arms are completely extended in water solution because of osmotic pressure, leading to jammed solutions, and thus gelation, at relatively low concentration.

Also, the conformation of the polyelectrolyte blocks is strongly dependent on salinity and pH of the solution. Consequently, the rheology can be tuned by acting on these parameters, providing the basis for responsive behaviour and “smart” materials.

Of particular interest are amphiphilic triblock copolymers (Figure 1) with a central hydrophilic block. In this case the two associative end blocks can assemble either into the same core, forming “flower-like” micelles or into different cores, forming bridges and thus a gel via formation of transient net-works, depending on the concentration and the compatibility of the hydrophobic blocks. [39] A PS-PAA-PnBA triblock copolymer show a similar viscosity profile of the analogous PS-PAA-PS system, but a lot higher absolute values of viscosity and yield stress at the same concentration. [39] According to the authors, the

incompatibility between the PS and the PnBA blocks would favour the intermolecular aggregation over the intramolecular one, explaining the observed behaviour.

When the hydrophilic block is constituted by a charged polyelectrolyte, it is expected to have an extended conformation in water due to repulsive electrostatic interactions. As a consequence, PS-*b*-PAA-*b*-PS exhibits a gel concentration about 1 order of magnitude lower than that of the latter PEO derivative in which the middle block has comparable length. [37]

Diblock copolymers aggregates in solution are normally constituted by a dense rigid core surrounded by a hydrophilic corona. The rheological properties of these polymers are determined by the interactions between the coronas, but little is known about the interaction mechanism. [93]

Anyway, at sufficiently high concentrations the micelles are jammed and the solution stop flowing, forming a viscoelastic gel. [94] A relatively short PS₂₀-PAA₈₅ polymer has been studied by Korobko et al. [93]

It exhibits Newtonian plateau at low shear in a large interval of concentrations and shear thinning at high concentrations. Also in this case, the zero shear viscosity increases dramatically with polymer concentration, from 1 to 4 orders of magnitude greater than water. Addition of salt (1 M KBr), yield solutions with a zero shear viscosity comparable to that of water. This behaviour is explained in terms of chain collapse due to shielding effects, with a consequent weaker interaction between the micelles. [93, 95]

If hydrophobic groups are present in the polyelectrolyte block they can act as “stickers”, favouring the gelation of the system. [95] PS-*b*-(AA-co-EA) copolymers show a decrease in the gelation concentration and an increase in viscosity and elastic moduli by increasing the amount of EA groups scattered along the AA block. [95]

Rheology of star PAA polymers capped with short PS ends has been also studied. [5, 96] Also these polymers form elastic gels in water at relatively low concentration (around 2.2 weight %). [5] As for other PAA based copolymers, a drop in viscosity is observed upon addition of salt (0.1 – 0.9 M NaCl), but the system still present the characteristic of a gel, showing that the polyelectrolyte screening upon salt addition shrunk the PAA chains but did not affect the hydrophobic association. [5]

The authors compared their findings with other results published by other groups for analogous linear systems. Elastic moduli of the studied star polymers are comparable with those of diblock PS-*b*-PAA and triblock PS-*b*-PAA-*b*-PS copolymers, but the gelation concentration is sensibly higher. This difference can be attributed to the different topology, as starlike polymer are likely to have a smaller hydrodynamic radius than a corresponding linear one, but the longer length of the hydrophobic blocks and the higher molecular weight of the linear polymer, make the two systems difficult to compare. [5]

When a linear PS-*b*-PAA-*b*-PS copolymer with comparable PS end blocks length and PS/PAA ratio is considered, the star polymer results in more effective network formation and more elastic gel. [96]

The solutions of polymer with longer PS ends form gels characterized by short linear viscoelastic region, more pronounced shear thinning and less marked gel softening with temperature.

This behaviour is rationalized by the authors considering that longer PS chains lead to stronger hydrophobic association. [96]

A systematic study of the rheology of block PS-*b*-PMAA copolymers characterized by different architecture (diblock, triblock and four arm star block) and block length (in case of the diblocks) has been performed in the research group of the author of this chapter. [44]

It has been shown that the viscosity versus concentration profile is dependent on both the block length of the hydrophilic block and the number of hydrophilic arms (1, 2 in the case of the triblock and 4 in the case of the four-arm star), while is less affected by the length of the polystyrene block.

Analogously to other amphiphilic block polyelectrolyte of different nature and structure, these polymers form strong viscoelastic gels at relatively low concentration, due to formation of micelles with highly stretched corona. The viscosity versus concentration profile shows at least three different regimes.

The transition from the diluted to the semi-diluted regime has been interpreted in terms of overlapping concentration, derived from scaling theory for polymers solutions, while the transition from semi-diluted to concentrated regime can be rationalized in terms of percolation theory for gelation of hard spheres. The rheological behavior for the triblock and the star copolymers is basically equivalent to that of a diblock copolymer with respectively half and one-fourth the concentration.

Preliminary investigations show that - as expected - pH and ionic strength have a great influence on the rheology of the prepared systems.

Despite the fact that the great importance of block polyelectrolytes for many applications is related to their rheology, the literature concerning this subject is still far from exhaustive. In particular, systematic studies about the dependence of rheology on the macromolecular structure are rare. Our focus is on providing more insight in the influence of the molecular architecture of amphiphilic block polyelectrolytes on their rheological behaviour.

In our work, [44] various amphiphilic diblock PS-*b*-PMAA copolymers characterized by different length of hydrophobic and hydrophilic blocks have been prepared by ATRP. The influence of the blocks length on the rheological properties of their water solutions was investigated. Previous work on the rheology of block polyelectrolytes based on PAA or PMAA were focused on the effect of the different polymer architecture.

The sol-gel transition and the gel characteristics have been found to be dependent on the polymer composition. In particular, polymers with longer PMAA blocks start to form gels at lower concentrations. This was already known for neutral amphiphilic block copolymers but never reported for block polyelectrolytes. On the other hand, in the concentrated region, the polymers with shortest PMAA blocks form stronger gels at the same weight concentration. The length of the hydrophobic block, although it seems to influence the micellar core size, does not show a relevant effect on the final rheological properties.

Remarkably, this is different to what reported for neutral block copolymers, where the hydrophobic block length (or, more precisely, the HLB ratio) plays a relevant role in the gelation properties. [44]

The behavior of the prepared polymer solutions can be interpreted in terms of a simple model which takes into account the different aggregation numbers, the corona shrinking at increasing concentration and the dependence of volume fraction from these two parameters. It is assumed that at high concentration the shrinking merely derives from the screening effect exerted by the interpenetrating charged coronas. Consequently, the micelles radius are leveled and the packing start to be more dependent on the micelles concentration and thus on the aggregation number. The aggregation numbers of the diblock copolymers seems to be

sensibly higher than those of corresponding triblock and four arm star previously reported as expected by geometric considerations. Further investigations are required in order to understand the effect of the different hydrophilicity of MAA with respect of AA on the micelles interactions and thus on the rheology of the systems.

Fine-tuning of the rheological properties is of great importance for many applications, such as coatings or enhanced oil recovery. [44]

Summarizing, the main rheological features seem to be dependent on several structural factors including: 1) the geometry of aggregation into micelles; 2) the aggregation number of the polymers; 3) the extension of the hydrophilic charged corona in solution; 4) the shrinking of the corona at increasing concentration, due to their interpenetration and shielding of the charges. As for many other block polyelectrolytes, the properties of these polymers are very dependent on salinity.

The viscosity drops down quite quickly if salt are added to the solution. Also, given the nature of weak acid of MAA, decreasing the pH has an analogous effect: protonation decreases the charge density and thus it favours corona shrinking and eventually precipitation.

4. APPLICATIONS

Amphiphilic block copolymers have a long history as industrial surfac-tants. [97, 98] The major types of block copolymers, such as those made from ethylene oxide (EO) and propylene oxide (PO) or EO and styrene, are cheap and easy to tailor-make for specific applications (see synthesis section).

Polymer containing PPO as the hydrophobic partner are by far the most studied and used, but the use of a more hydrophobic segment in the block copolymer becomes important for other applications, such as emulsion polymerization. Thus, PS-b-PEO copolymers are preferred for this purpose. EO-styrene block copolymers have also been used to formulate water-in-oil microemulsions. Such microemulsions have been used as minireactors for polymerization of acrylamide, for example. [97]

Amphiphilic polymers containing polystyrene blocks are also effective stabilizers for emulsion. [97, 99] This application is related to the previously mentioned emulsion polymerization, but in this case the emulsion is formed by intimate mixing of two immiscible liquid phases and not by polymerization of an hydrophobic monomer in aqueous phase in order to prepare latexes. It is important in this case that the hydrophobic (polystyrene) block is long enough to ensure steric stabilization of the non-aqueous phase but not too long, to avoid bridging flocculation. [97]

Due to the permanently hydrophobic nature of the polystyrene, its high glass transition temperature and its toxicity in living organisms, applications as drug carriers and drug delivery systems does not seem to be practicable for PS-based amphiphilic block copolymers.

Nevertheless, the ability of such polymer to solubilize hydrophobes in their PS core (e.g.: benzene, hexane) makes them suitable systems for applica-tion in separation systems, as alternative to liquid-liquid extractions.

Due to the affinity of the PS block for components of crude oil, and the rheological and interfacial properties of amphiphilic block copolymers, poten-tial application of PS-

containing amphiphilic block copolymers for enhanced oil recovery can also be envisaged. This potential, however, at the present day has not been fully disclosed yet.

REFERENCES

- [1] Davis, K. A.; Matyjaszewski, K. *Macromolecules*. 2000, 33, 4039.
- [2] Burguiere, C.; Pascual, S.; Coutin, B.; Polton, A.; Tardi, M.; Charleux, B.; Matyjaszewski, K.; Vairon, J. P. *Macromol. Symp.* 2000, 150, 39.
- [3] Davis, K. A.; Charleux, B.; Matyjaszewski, K. *J. Polym. Sci., Part A: Polym. Chem.* 2000, 38, 2274.
- [4] Burguiere, C.; Chassenieux, C.; Charleux, B. *Polymer*. 2003, 44, 509.
- [5] Hietala, S.; Mononen, P.; Strandman, S.; Jarvi, P.; Torkkeli, M.; Jankova, K.; Hvilsted, S.; Tenhu, H. *Polymer*. 2007, 48.
- [6] Terreau, O.; Bartels, C.; Eisenberg, A. *Langmuir*. 2004, 20, 637.
- [7] Terreau, O.; Luo, L. B.; Eisenberg, A. *Langmuir*. 2003, 19, 5601.
- [8] Desjardins, A.; Eisenberg, A. *Macromolecules*. 1991, 24, 5779.
- [9] Zhong, X. F.; Varshney, S. K.; Eisenberg, A. *Macromolecules*. 1992, 25, 7160.
- [10] Astafieva, I.; Zhong, X. F.; Eisenberg, A. *Macromolecules*. 1993, 26, 7339.
- [11] Gao, Z. S.; Varshney, S. K.; Wong, S.; Eisenberg, A. *Macromolecules*. 1994, 27, 7923.
- [12] Astafieva, I.; Khougaz, K.; Eisenberg, A. *Macromolecules*. 1995, 28, 7127.
- [13] Zhang, L. F.; Eisenberg, A. *J. Am. Chem. Soc.* 1996, 118, 3168.
- [14] Zhang, L. F.; Eisenberg, A. *Macromolecules*. 1996, 29, 8805.
- [15] Yu, Y. S.; Eisenberg, A. *J. Am. Chem. Soc.* 1997, 119, 8383.
- [16] Yu, Y. S.; Zhang, L. F.; Eisenberg, A. *Langmuir*. 1997, 13, 2578.
- [17] Zhang, L. F.; Shen, H. W.; Eisenberg, A. *Macromolecules*. 1997, 30, 1001.
- [18] Yu, G. E.; Eisenberg, A. *Macromolecules*. 1998, 31, 5546.
- [19] Yu, Y. S.; Zhang, L. F.; Eisenberg, A. *Macromolecules*. 1998, 31, 1144.
- [20] Zhang, L. F.; Eisenberg, A. *Polym. Adv. Technol.* 1998, 9, 677.
- [21] Lysenko, E. A.; Bronich, T. K.; Slonkina, E. V.; Eisenberg, A.; Kaba-nov, V. A.; Kabanov, A. V. *Macromolecules*. 2002, 35, 6351.
- [22] Burguiere, C.; Pascual, S.; Bui, C.; Vairon, J. P.; Charleux, B.; Davis, K. A.; Matyjaszewski, K.; Betremieux, I. *Macromolecules*. 2001, 34, 4439.
- [23] Bendejacq, D.; Ponsinet, V.; Joanicot, M.; Loo, Y. L.; Register, R. A. *Macromolecules*. 2002, 35, 6645.
- [24] Laruelle, G.; Francois, J.; Billon, L. *Macromol. Rapid Commun.* 2004, 25, 1839.
- [25] Delaittre, G.; Nicolas, J.; Lefay, C.; Save, M.; Charleux, B. *Chem. Comm.* 2005, 5, 614.
- [26] Delaittre, G.; Nicolas, J.; Lefay, C.; Save, M.; Charleux, B. *Soft Matter*. 2006, 2, 223.
- [27] Lu, F.; Luo, Y.; Li, B. *Macromol. Rapid Commun.* 2007, 28, 868.
- [28] Theodoly, O.; Jacquin, M.; Muller, P.; Chhun, S. *Langmuir*. 2009, 25, 781.
- [29] Ganeva, D. E.; Sprong, E.; de Bruyn, H.; Warr, G. G.; Such, C. H.; Hawkett, B. S. *Macromolecules*. 2007, 40.
- [30] Chaduc, I.; Zhang, W.; Rieger, J.; Lansalot, M.; D'Agosto, F.; Charleux, B. *Macromol. Rapid Commun.* 2011, 32, 1270.

- [31] He, W.; Sun, X.; Wan, W.; Pan, C. *Macromolecules*. 2011, 44, 3358.
- [32] Bendejacq, D.; Ponsinet, V.; Joanicot, M.; Vacher, A.; Airiau, M. *Macromolecules*. 2003, 36, 7289.
- [33] Bendejacq, D. D.; Ponsinet, V.; Joanicot, M. *Langmuir*. 2005, 21, 1712.
- [34] Bendejacq, D. D.; Ponsinet, V. *J. Phys. Chem. B*. 2008, 112, 7996.
- [35] Zaruslov, Y. D.; Fytas, G.; Pitsikalis, M.; Hadjichristidis, N.; Philippova, O. E.; Khokhlov, A. R. *Macromol. Chem. Phys.* 2005, 206, 173.
- [36] Tsitsilianis, C.; Iliopoulos, I. *Macromolecules*. 2002, 35.
- [37] Tsitsilianis, C.; Iliopoulos, I.; Ducouret, G. *Macromolecules*. 2000, 33.
- [38] Tsitsilianis, C.; Katsampas, I.; Sfika, V. *Macromolecules*. 2000, 33.
- [39] Katsampas, I.; Tsitsilianis, C. *Macromolecules*. 2005, 38.
- [40] Ma, Q. G.; Wooley, K. L. *J. Polym. Sci., Part A: Polym. Chem.* 2000, 38, 4805.
- [41] Zhang, X.; Xia, J. H.; Matyjaszewski, K. *Abs. Pap. Am. chem. Soc.* 1999, 218, U543.
- [42] Wang, G. J.; Yan, D. Y. *J. Appl. Polym. Sci.* 2001, 82, 2381.
- [43] Krishnan, R.; Srinivasan, K. S. V. *Eur. Polym. J.* 2004, 40, 2269.
- [44] Raffa, P.; Brandenburg, P.; Wever, D. A. Z.; Broekhuis, A. A.; Picchio-ni, F. *Macromolecules*. 2013, 46, 7106; Raffa, P.; Stuart, M. C. A.; Broekhuis, A. A.; Picchioni, F. *J. Coll. Interf. Sci.* 2014, in press.
- [45] Qin, A. W.; Tian, M. M.; Ramireddy, C.; Webber, S. E.; Munk, P.; Tuzar, Z. *Macromolecules*. 1994, 27, 120.
- [46] Van Stam, J.; Creutz, S.; De Schryver, F. C.; Jerome, R. *Macromolecules*. 2000, 33, 6388.
- [47] Keoshkerian, B.; Georges, M. K.; Boilsboissier, D. *Macromolecules*. 1995, 28, 6381.
- [48] Bouix, M.; Gouzi, J.; Charleux, B.; Vairon, J. P.; Guinot, P. *Macromol. Rapid Commun.* 1998, 19, 209.
- [49] Gabaston, L. I.; Furlong, S. A.; Jackson, R. A.; Armes, S. P. *Polymer*. 1999, 40, 4505.
- [50] Matsuoka, H.; Maeda, S.; Kaewsaiha, P.; Matsumoto, K. *Langmuir*. 2004, 20, 7412.
- [51] Okamura, H.; Takatori, Y.; Tsunooka, M.; Shirai, M. *Polymer*. 2002, 43, 3155.
- [52] Liu, Y.; Pollock, K. L.; Cavicchi, K. A. *Polymer*. 2009, 50, 6212.
- [53] Choi, M.; Chung, B.; Chun, B.; Chang, T. *Macromol. Res.* 2004, 12, 127.
- [54] Yang, R. M.; Wang, Y. M.; Wang, X. G.; He, W. D.; Pan, C. Y. *Eur. Polym. J.* 2003, 39, 2029.
- [55] Yuan, J. J.; Ma, R.; Gao, Q.; Wang, Y. F.; Cheng, S. Y.; Feng, L. X.; Fan, Z. Q.; Jiang, L. *J. Appl. Polym. Sci.* 2003, 89, 1017.
- [56] Bohrisch, J.; Wendler, U.; Jaeger, W. *Macromol. Rapid Commun.* 1997, 18, 975.
- [57] Shen, H. W.; Zhang, L. F.; Eisenberg, A. *J. Am. Chem. Soc.* 1999, 121, 2728.
- [58] Zhu, J. Y.; Eisenberg, A.; Lennox, R. B. *J. Am. Chem. Soc.* 1991, 113, 5583.
- [59] Zhu, J.; Lennox, R. B.; Eisenberg, A. *Langmuir*. 1991, 7, 1579.
- [60] Zhu, J.; Hanley, S.; Eisenberg, A.; Lennox, R. B. *Macromol. Symp.* 1992, 53, 211.
- [61] Zhu, J.; Eisenberg, A.; Lennox, R. B. *Macromolecules*. 1992, 25, 6547.
- [62] Zhu, J.; Eisenberg, A.; Lennox, R. B. *Macromolecules*. 1992, 25, 6556.
- [63] Wendler, U.; Bohrisch, J.; Jaeger, W.; Rother, G.; Dautzenberg, H. *Macromol. Rapid Commun.* 1998, 19, 185.
- [64] Li, W.; Min, K.; Matyjaszewski, K.; Stoffelbach, F.; Charleux, B. *Macromolecules*. 2008, 41, 6387.

- [65] Yu, K.; Eisenberg, A. *Macromolecules*. 1998, 31, 3509.
- [66] Xie, H. Q.; Xie, D. *Prog. Polym. Sci.* 1999, 24, 275.
- [67] Zhang, X.; Matyjaszewski, K. *Macromolecules*. 1999, 32, 1763.
- [68] Lokaj, J.; Vlcek, P.; Kriz, J. *Macromolecules*. 1997, 30, 7644.
- [69] Munoz-Bonilla, A.; Ali, S. I.; del Campo, A.; Fernandez-Garcia, M.; van Herk, A. M.; Heuts, J. P. A. *Macromolecules*. 2011, 44, 4282.
- [70] Munoz-Bonilla, A.; van Herk, A. M.; Heuts, J. P. A. *Macromolecules*. 2010, 43, 2721.
- [71] Holder, S. J.; Durand, G. G.; Yeoh, C.; Illi, E.; Hardy, N. J.; Richardson, T. H. *J. Polym. Sci., Part A: Polym. Chem.* 2008, 46, 7739.
- [72] Cheng, Z. P.; Zhu, X. L.; Kang, E. T.; Neoh, K. G. *Langmuir*. 2005, 21, 7180.
- [73] Gibanel, S.; Forcada, J.; Heroguez, V.; Schappacher, M.; Gnanou, Y. *Macromolecules*. 2001, 34, 4451.
- [74] Khanna, K.; Varshney, S.; Kakkar, A. *Polym. Chem.* 2010, 1, 1171.
- [75] Hadjichristidis, N.; Pitsikalis, M.; Iatrou, H. *Adv. Polym. Sci.* 2005, 189, 1.
- [76] Peleshanko, S.; Jeong, J.; Shevchenko, V. V.; Genson, K. L.; Pikus, Y.; Ornatska, M.; Petrash, S.; Tsukruk, V. V. *Macromolecules*. 2004, 37.
- [77] Peleshanko, S.; Jeong, J.; Gunawidjaja, R.; Tsukruk, V. *Macromolecules*. 2004, 37, 6511.
- [78] Francis, R.; Taton, D.; Logan, J.; Masse, P.; Gnanou, Y.; Duran, R. *Macromolecules*. 2003, 36, 8253.
- [79] Dong, Y.; Dong, B.; Du, F.; Meng, J.; Li, Z. *Polymer*. 2009, 50.
- [80] Francis, R.; Lepoittevin, B.; Taton, D.; Gnanou, Y. *Macromolecules*. 2002, 35.
- [81] Matmour, R.; Lepoittevin, B.; Joncheray, T. J.; El-Khoury, R. J.; Taton, D.; Duran, R. S.; Gnanou, Y. *Macromolecules*. 2005, 38.
- [82] Joncheray, T. J.; Bernard, S. A.; Matmour, R.; Lepoittevin, B.; El-Khoury, R. J.; Taton, D.; Gnanou, Y.; Duran, R. S. *Langmuir*. 2007, 23.
- [83] Kim, Y. H.; Ford, W. T.; Mourey, T. H. *J. Polym. Sci., Part A: Polym. Chem.* 2007, 45, 4623.
- [84] Zhang, L. F.; Eisenberg, A. *Macromolecules*. 1999, 32, 2239.
- [85] Fischer, A.; Brembilla, A.; Lochon, P. *Macromolecules*. 1999, 32, 6069.
- [86] Davis, K. A.; Matyjaszewski, K. *Macromolecules*. 2001, 34, 2101.
- [87] Mok, M. M.; Thiagarajan, R.; Flores, M.; Morse, D. C.; Lodge, T. P. *Macromolecules*. 2012, 45, 4818.
- [88] Gao, Z. S.; Eisenberg, A. *Macromolecules*. 1993, 26, 7353.
- [89] Matsuoka, H.; Chen, H.; Matsumoto, K. *Soft Matter*. 2012, 8, 9140.
- [90] Kaewsaiha, P.; Matsumoto, K.; Matsuoka, H. *Langmuir*. 2005, 21, 9938.
- [91] Matsumoto, K.; Ishizuka, T.; Harada, T.; Matsuoka, H. *Langmuir*. 2004, 20, 7270.
- [92] Su, T.; Styrkas, D.; Thomas, R.; Baines, F.; Billingham, N.; Armes, S. *Macromolecules*. 1996, 29, 6892.
- [93] Korobko, A. V.; Jesse, W.; Lapp, A.; Egelhaaf, S. U.; van der Maarel, J. R. C. *J. Chem. Phys.* 2005, 122, 024902.
- [94] Chassenieux, C.; Nicolai, T.; Benyahia, L. *Curr. Opin. Colloid Interface Sci.* 2011, 16.
- [95] Kimerling, A. S.; Rochefort, W. E.; Bhatia, S. R. *Ind. Eng. Chem. Res.* 2006, 45.
- [96] Hietala, S.; Strandman, S.; Jarvi, P.; Torkkeli, M.; Jankova, K.; Hvilsted, S.; Tenhu, H. *Macromolecules*. 2009, 42.

-
- [97] Alexandridis, P.; Lindman, B. In: *Amphiphilic Block Copolymers: Self-Assembly and Applications*; Elsevier: Amsterdam, 2000; p. 448.
- [98] Alexandridis, P. *Curr. Opin. Colloid Interface Sci.* 1996, 1, 490.
- [99] Hamley, I. W. In: *Block Copolymers in Solution: Fundamentals and Application*; Wiley: 2005; p. 300.

Chapter 3

EXPANDED POLYSTYRENE: THERMO-MECHANICAL RECYCLING, CHARACTERIZATION AND APPLICATION

Matheus Poletto*, Heitor L. Ornaghi Júnior and Ademir J. Zattera

Laboratory of Polymers (LPOL), University of Caxias do Sul (UCS)
Rua Francisco Getúlio Vargas, Caxias do Sul/RS, Brazil

ABSTRACT

Plastic materials are used in our daily lives in several applications. These include a substantial amount of polyolefins, which can potentially be recovered for recycling. Expanded polystyrene (EPS) is commonly used for insulation and packaging materials due some advantages as versatility, dimensional stability and low cost. However, in some countries, its inadequate disposal, mainly in landfills can cause serious environmental health concerns if modern regulations are not complied. Different characterization techniques, such as chemical and thermal ones, are available for recycling EPS waste. Nevertheless, chemical techniques usually involve the use of hazardous solvents meanwhile thermal recycling may cause gaseous pollution. So, in this work a methodology for thermo-mechanical recycling of EPS waste was presented in order to development composites based on recycled EPS and wood flour waste. The EPS wastes were processed by compression molding technique. So, they were grinded before processing with wood flour in a co-rotating twin-screw extruder. Consequently the composites were injection molding. The results showed that the process of compression molding led to a decreased in volume as well as a 25-fold increase in the density of the EPS waste when compared with the raw material. Thus, after compression molding and grinding, the EPS waste can be used directly in the extrusion process with the wood flour. This eliminates one process reducing the recycling costs. The composites showed increased in mechanical, thermo-mechanical and morphologic properties when coupling agent was used in the composite formulations. Based on the findings of this study, the methodology used for EPS recycling and for development of wood composites appears as an alternative for manufacture composites based on recycled materials with high properties without cause serious environmental problems.

* Corresponding author: M. Poletto Email: mpolett1@ucs.br.

EXPANDED POLYSTYRENE

History

Polystyrene (PS) was first commercially produced in the United States in 1938, about eight years after its introduction in Germany [1, 2]. Earlier British patents issued in 1911 describe polystyrene resin, and literature references go back to the mid-nineteenth century [1, 2]. In 1941, the research chemist Ray McIntyre invented a process for extruding polystyrene to achieve closed-cell foam that resists moisture [3]. The first application was as an "unsinkable" buoyancy billet by the U.S. Coast Guard in their six-man life rafts [3], in 1942. Impact grades (PS enhanced with rubber to improve impact strength) have been commercialized in the United States after World War II. Before 1949, the chemical engineer Fritz Stastny developed pre-expanded PS beads by incorporating aliphatic hydrocarbons, such as pentane. By the 1950s, expanded polystyrene products started making a significant impact in the U.S. construction market, replacing cork in varied low-temperature applications, and as a thermal barrier in the walls and roofs of institutional and commercial buildings [3].

EPS has captured a large market since their introduction at about 60 years ago. Polystyrene foam is mostly manufactured from atactic polystyrene prepared via free radical polymerization in a suspension process. The molar mass and the molar mass distribution of the polystyrene matrix play a vital role in the properties of the foam [1, 4]. Since polystyrene is an organic material, it burns and since it is thermoplastic, it melts. The excellent balance of cost and thermal insulation properties of polystyrene foams make it competitive with other commercial insulating materials, such as polyurethane foam. The apolar characteristics of polystyrene in combination with a closed-cell structure make it water resistant at ambient temperatures [4]. For this reason it can be used for e.g. food packaging and coating applications. Since polystyrene foam has excellent shock-absorbing properties with low costs and high insulation efficiency, it is ideal for low-temperature insulation [4].

Description

EPS is the international abbreviation used for expanded polystyrene according to ISO 1043-1:2011 standard. The final product consists of beads of up to 3 mm in diameter, which is intended for expansion. In the transformation process, these beads are undergoing expansion up to 50 times its original size. This occurs by heating a blowing agent (pentane) that boils and produces a steam, creating a closed cell honeycomb structure. It can be molded in different ways. After expanded, the beads comprise up to 98% air and only 2% polystyrene. For example, in 1m³ expanded EPS there are 3 to 6 billion cells closed and filled with air.

METHODS FOR MANUFACTURING EPS

Basic Materials

EPS foams are generally made of very small beads of polystyrene (94 % by weight) with a molecular weight of 160000-260000. They are blown with pentane up to 6 % by weight - which is partly released during or (shortly) after production. The most commonly used flame retardant is hexabromocyclododecane (HBCD), present at ca. 0.6 % by weight [5]. In addition to the basic materials, the manufactures can also used waste EPS from packaging.

Preparation of Expandable Polystyrene Beads

A batchwise radical polymerization in a suspension process is a standard route for producing spherical expandable polystyrene beads [4]. This route starts by using liquid styrene monomer dispersed in an aqueous medium containing a suitable suspension stabilizer, a hydrocarbon foaming agent and a radical initiator [4]. The mixture is heated to an appropriate polymerization temperature. During the polymerization process a controlled pressure is applied to incorporate approximately 6 wt% of the blowing agent in the beads [4]. A wide variety of hydrocarbons have been applied as the blowing agent, e.g. butane, propane, propylene or more exotic ones like alcohols, esters and ketones. The most frequently used are pentane isomers since they possess the best cost/performance ratio [4, 5].

Manufacturing Process

The EPS product manufacturing process is typically a three-step process, as can be seen in Figure 1.

- 1) Pre-expansion: the expansion process occurs due to the inclusion of a blowing agent (typically pentane) within the bead boiling-off in presence of steam at temperatures of between 80-100°C, and thus causing the expansion [6]. The pentane and steam are normally exhausted from the process. The pre-expansion of the compact beads in steam atmosphere is the most preferable way since a relatively large amount of energy is quickly transferred to the beads. It is important that the beads are quickly heated to make sure that no blowing agent is lost, in order to generate foam with as low density as possible [4]. Steam diffuses into the PS beads, ensuring a relatively uniform temperature profile in the beads. In addition, the steam diffused into the beads increases its expandability. Several stages of the pre-expansion process are presented in Figure 2. Polystyrene beads with the size of a grain of sand are expanded to around 50 times their original size on contact with steam, as shown in Figure 2(e). The density of the final foam is determined in this stage. The density of the material generally falls from some 630kg/m³ to values of between 10 and 35kg/m³ [6].

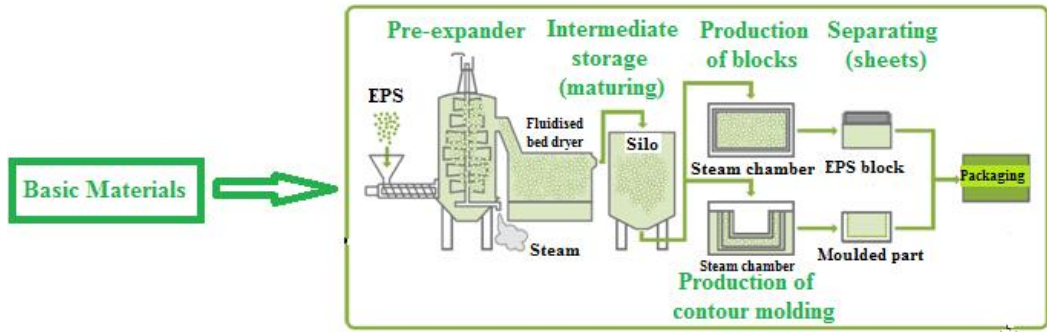


Figure 1. EPS product manufacturing process, adapted from [5].

- 2) Conditioning: the expanded beads are then stored in hoppers for a period to mature before the molding process [4]. Due to passive off-gassing, some pentane gas may be present in and around the storage hoppers. After the pre-expansion, the beads contain approximately 4 wt% of pentane and air at atmospheric pressure. On cooling, the recently expanded particles form a vacuum in their interior and this must be compensated by air diffusion [6]. This process is carried out during the material's intermediate maturing in aerated silos [6]. The beads are dried at the same time. This is how the beads achieve greater mechanical elasticity and improve expansion capacity, with is very important in the following transformation stage [6].

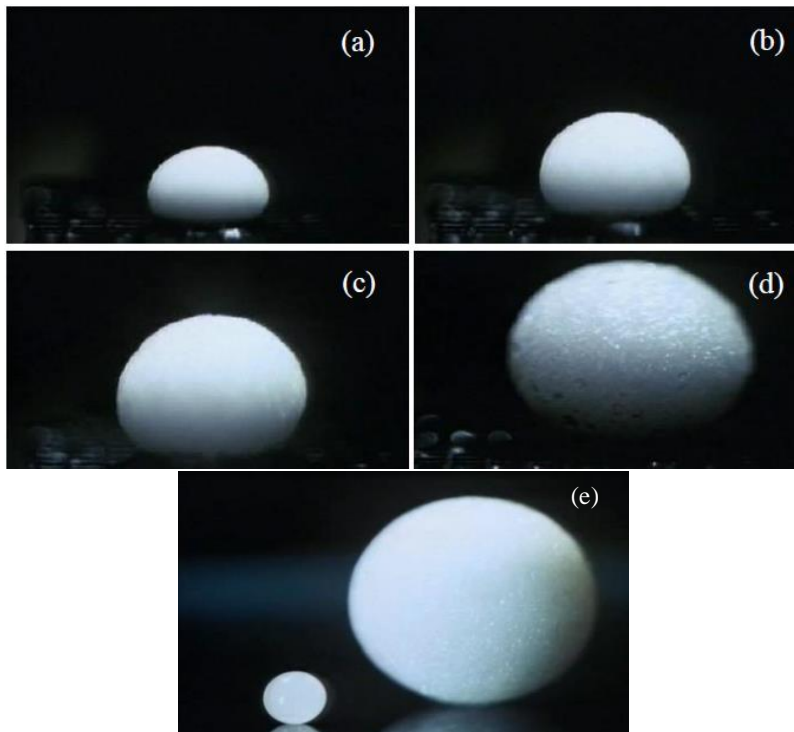


Figure 2. EPS pre expansion stage, from (a) to (d) and the final result (e) after expansion, adapted from [7].

- 3) **Molding:** subsequently, the beads are matured, after which the pre-expanded beads are entered into a mold [4]. Steam is injected into the mold, allowing the beads to expand further and melt together to fill the mold completely [4], as presented in Figure 3. The pressure of pentane and air are reduced while the steam pressure is maintained. After the foaming process has been completed, a controlled cooling of the system is of major importance since it determines the final performance of the foam and the production capacity [4]. The expanded beads are molded either into blocks or customized in shaped products such as food boxes, waffle pods, packaging materials, stubby holders etc [6].

APPLICATIONS AND PROPERTIES

There are a wide range of applications for expanded polystyrene. Many industries use EPS due some advantages as versatility, dimensional stability, cleanliness and low cost. However, three main applications can be highlighted: packaging, construction and other applications.

Packaging

Nowadays EPS is used in packaging for almost any high value industrial product. It provides protection and safety from risk during transport and handling. EPS ranges from fragile pharmaceutical products to electronic components, electrical consumer goods and toys since horticultural until gardening products [5, 6]. All of these items are able to arrive at their destination (either industry or consumer home) in perfect conditions when the product is packaging with EPS [6]. The material can be designed to fit perfectly into automated production lines, which include the packing of the product [6]. In addition, EPS packaging system is often an alternative in terms of cost, versatility and efficiency. It is easy for workers to handle with no sharp edges or staples and it can work equally well with sophisticated machinery [5, 6].

On the other hand, EPS packaging keep the foodstuff fresh. The material offers a protection against hazards, breakages and wastage in the different stages of production and transport [6]. Every day EPS packaging is ensuring that many different types of food reach the retailer or the final consumer in perfect conditions. Food safety is paramount; a badly protected or poorly insulated product could arrive in a substandard condition [6]. It could entail a serious health risk to consumers or a serious waste of food for supermarkets or food suppliers. EPS has the capacity to conserve food, reducing wastage of food and consequently saving money.

Due to some unique characteristics and the relationship between structure and properties EPS is an excellent choice for packaging material. So, several EPS properties are useful for food storage and others applications. The following properties can be emphasizing when EPS is used as a packaging material:

Shock absorption: the material has a high energy absorption index, due its cellular structure [6]. This makes it the ideal material for protecting sensitive products during transport and storage. This unique level of protection also makes EPS ideally suitable for safety and sports helmets and for children's car seats.

Thermal insulation: this is due to its closed cell structure which inhibits the passage of heat or cold. It protects products such as vaccines or other pharmaceutical items and conserves food such as fish and meat from sudden temperature changes [6].

Low weight: EPS is made of 98% air, making it extremely light and providing savings in weight and in fuel consumption [5, 6]. Consequently there is a reduction in the environmental impact of transporting products.

Resistance to humidity: the excellent mechanical and thermal properties are unaffected by humidity because EPS does not absorb water or water vapor [5, 6].

Compressive resistance: the ability of EPS to resist compression makes it ideal for packing large items such as cookers and washing machines [6]. It not only protects the products in transport, but they can be stacked in the warehouse, saving on space and without any damage to the items.

Chemical resistance: allows many products to be packed without the goods being affected [6]. In addition, EPS can easily be printed or coloured, it has a clean appealing appearance and can be used in many different ways to garnish products aiming to attract customers. Besides EPS is completely inert and innocuous, it meets all the food contact regulations and requirements and can be used to package food or pharmaceutical products [5].

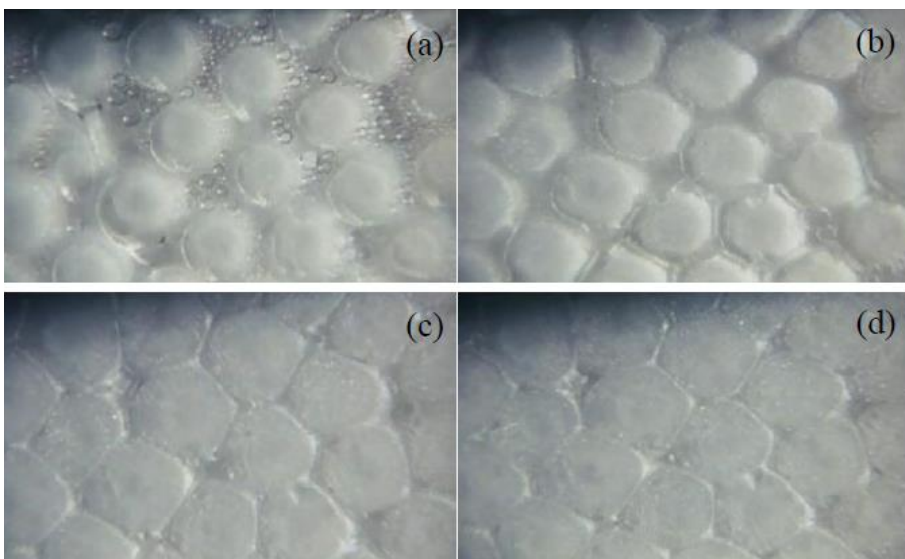


Figure 3. EPS final expansion into the mould whit steam (a) and molding stages from (b) to (d) adapted from [7].

Application as a Construction Material

EPS is used in many aspects of building work including large structures such as roads, bridges, railway lines, public buildings or even small family residences. Due its characteristics, EPS is suitable for use as lightweight filler (in roads, for example to facilitate land drainage), thermal insulation and as an element for decorating or imaginative touches [6]. The growing need for new roads may, in many cases, require construction over soft or loose soils that are incapable of supporting additional loads [8]. Engineers must identify innovative materials and construction techniques to address the problem of building on soft soils or where sensitive existing utilities or wetlands are present while, at the same time, accelerating project schedules [8]. EPS geofoam can be used to replace compressible soils or in place of heavy fill materials to prevent unacceptable loading on underlying soils and adjacent structures [8]. The high compressive resistance of EPS geofoam makes it able to adequately support traffic loadings associated with secondary and interstate highways. Construction with EPS geofoam also saves time because EPS geofoam is easy to handle without the need for special equipment. Figure 4 shows the application of EPS geofoam used during the construction of a roadway.

The following properties are important for EPS applications as a construction material:

Low thermal conductivity: due to its closed air-filled cell structure, it acts as a barrier that inhibits the passage of heat or cold resulting in a high capacity for thermal insulation [6]. The thermal conductivity at 25°C for density values between 10 and 28kg/m³ generally ranges between 0.0430-0.0352 W/mK [9].

Low weight: densities usually of between 10 and 35kg/m³ allow light and safe construction works. However, EPS geofoam blocks can reach density values up to about 45 kg/m³ [8].

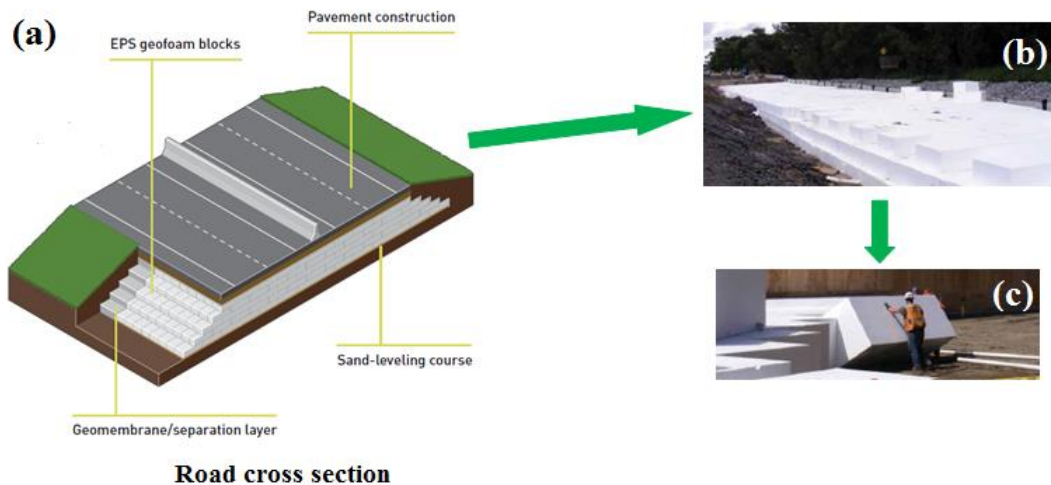


Figure 4. Road construction cross section scheme (a) using EPS for make the base of the pavement system (b) and a detail of the EPS blocks (c) [8].

Mechanical resistance: EPS has excellent mechanical properties making it good choice for load-bearing roof insulation, sub-pavement flooring, road-building among other applications [6]. The compressive resistance at 1% usually ranges between 15-100 kPa for density values in the range of 10-35kg/m³ [8].

Low water absorption: EPS does not absorb moisture and its thermal and mechanical properties are unaffected by damp, humidity or moisture [6]. For densities values between 10 and 28kg/m³ the rate of water vapor transmission (max) measured parallel to rise at 23°C ranges between 710-400 µg/m²s [9].

Chemical resistance: EPS is completely compatible with other materials used in construction including cements, plasters, salt, fresh water and so on [6]. Also, EPS can be cut into the shape or size required by the construction project. In addition the EPS present ageing resistance because all of its properties are retained over the whole of the material's life [6]. So, the properties of the material will not be altered by external agents such as fungi or parasites since they find no nutritional value in the material as long as the building lasts.

Other Applications

The versatility of EPS allows it to be used for a huge variety of different purposes. The possibilities include furniture products as chairs, book covers, snow sports helmet, infant car seats, air conditioning units, houses, paralympic sailors, load-bearing structurally insulated panels (SIP's) [6] (as can be seen in Figure 5 below), among others.

CONSUMPTION, CAPACITIES AND RECYCLING RATES

The consumption of EPS has continuously grown around the world in the last years. Whereas worldwide consumption in 2001 reach 3.251 million ton; it has increased by nearly to 80% to 5.833 million ton in 2011 [11]. Table 1 reflects the enormous growth that has taken place in EPS market in the last years.

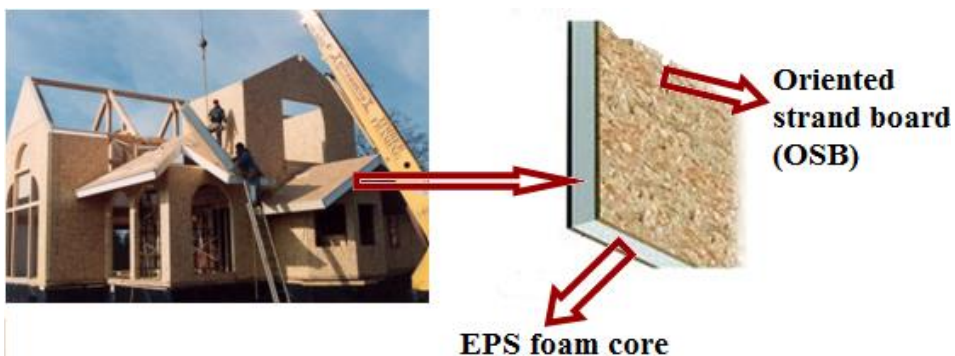


Figure 5. Structural insulated panels made with EPS and oriented wood strand board, adapted from [10].

Table 1. Global EPS consumption between 2001 and 2011 [11]

Consumption (million ton)						
Region	2001	2003	2005	2007	2009	2011
Asia	1.447	1.903	1.943	2.330	2.493	3.079
Europe (incl. Russia)	1.118	1.266	1.266	1.624	1.614	1.801
North America	0.518	0.640	0.640	0.610	0.488	0.513
Rest of world	0.168	0.250	0.250	0.347	0.382	0.440
Global consumption	3.251	3.765	4.099	4.911	4.977	5.833

According to Table 1, between 2001 and 2011, the growth of the Asian EPS market was around 110%. China alone shared about 40% of the demand for EPS in 2012 [12]. The increase in Europe (including Russia) was around 60 %, while EPS consumption in North America, contrary to the general trend, stagnated [11]. So, Asia is the largest customer with currently 53% of the global consumption, followed by Europe with 31 % and North America with 8.8%, as can be seen in Figure 6. The global consumption in 2011 was 5.833 million ton and the global production capacities totaled 9.676 million ton [11]. By far the greatest EPS capacities can be found in Asia: 6.694 million ton, or 69 % of the total [11] (as presented in Figure 6).

According to Global Business Intelligence Research [13], demand for polystyrene and expandable polystyrene (EPS) is rising in developing countries such as China, India, Iran, Saudi Arabia and Brazil. Asian consumption of all types of polystyrene is forecast to increase at an average annual rate of slightly over 3% during 2010-2015. North American demand is expected to decrease 0.5% and Western Europe will show only moderate growth of 1.6% over the next five years [13]. In the forecast period of 2010-2020, the global demand for polystyrene and EPS is expected to grow at a compound annual growth rate (CAGR) of 4.7%, increasing the overall demand for polystyrene and EPS to 23.5 million metric tons by 2020 [13]. With the fastest-growing economy of China, the Asia-Pacific dominance in the polystyrene and expandable polystyrene market is expected to increase further, to achieve 62.8% of the global demand share by 2020 [13]. As can be seen in Figure 7, the global EPS consumption in 2013 is dominated by Asia-Pacific region followed by Europe and North America. The Middle East is expected to retain its demand share of 1.7% by 2020 due the developing countries as Iran and Saudi Arabia [13]. Due to the comparatively slow demand growth from all other regions, their demand shares are expected to decline in this period. The global polystyrene market reported a marginal decline in net profit in demand over the past decade, whereas the global EPS demand increases at a CAGR of 5.5% during the same period (2000-2010) [13]. Major portion of this demand growth came from China, which consumed more than half of the global EPS demand in 2010. China's demand for EPS is expected to increase continually at a high rate over the forecast period, while other developing countries are expected to support the overall growth. Therefore, during the forecast period 2010-2020, the EPS demand is expected to increase at a CAGR of 7.3% in comparison with the polystyrene's expected of 2.8% during the same period [13]. Globally, packaging was the dominant end-use sector for both polystyrene and expandable polystyrene. The packaging industry consumes 41.5% of global polystyrene demand and 47.9% of global expandable polystyrene demand in 2010 [13]. After packaging, the construction industry was the second major polystyrene consuming industry, accounting for 47.8% of EPS and 7.7% of polystyrene

consumption at a global level, along with furniture and building industries. These two industries are expected to lead the global demand for polystyrene and expandable polystyrene in the forecast period as well [13]. The global EPS market (2012) is worth \$11.9 billion and is estimated to reach \$19.1 billion in 2018, growing at a CAGR of 8.2% from 2013 to 2018 [12]. The high demand across industries such as building and construction, packaging, and others will increase the overall EPS consumption [12]. Enormous research and development investments, followed by new product launches by key industry players better describes the expanded polystyrene market in 2012. More than 100 companies around the world are manufacturing EPS and this number is expected to increase to more than 200 in the next five years until 2018. Thus, there are more than 1,000 companies and institutions that are actively engaged in EPS' research and development [12].

There are also large differences regarding the main applications of EPS. In Europe, nearly 80% of EPS consumption is related to building construction, whereas this portion lies around 50% for the rest of the world. The consumption for applications in building construction in North America is approximately 41% which is especially low when compared with Europe. Also, the 20% consumption for packaging in Europe is the smallest portion worldwide. By contrast, it is nearly half in Asia. In all regions, it is expected that applications of EPS in building construction will increase faster than for the packaging sector [11].

On the other hand, the EPS recycling rate percentage continues to grow steadily around the world. In the United States the post-consumer EPS recycling increased from 1.7% in 1990 to 30% in 2012. This is supported by advances in EPS recycling technology, collaborative collection programs and new end-use markets that have continued to broaden EPS recycling opportunities. In addition, the EPS industry fosters ongoing development of new and innovative recycling technologies that will promote further EPS recycling growth [15]. In Japan, the recycling rate increases from 12.6% in 1991 to 87.5% in 2009. Among plastic materials in Japan, EPS is what maintains the highest recycling rate. The main recycling methods used in Japan include mechanical and thermal ones. In 2009, 56.8% of all recycled EPS in Japan was processed by mechanical methods whereas thermal recycled was responsible for 30.7% [16]. In South Korea the recycling rate is also high. It increased from 33.1% in 1996 to 75.1 in 2011 [17].

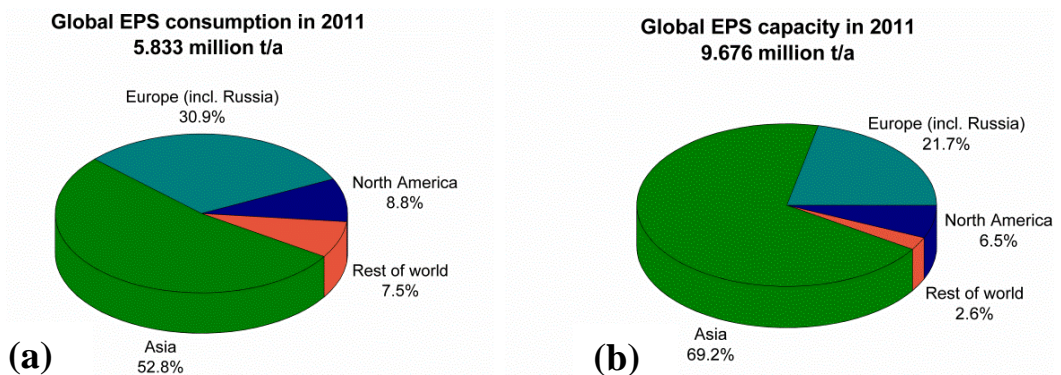


Figure 6. Global EPS consumption (a) and capacities (b) according to regions in 2011 [11].

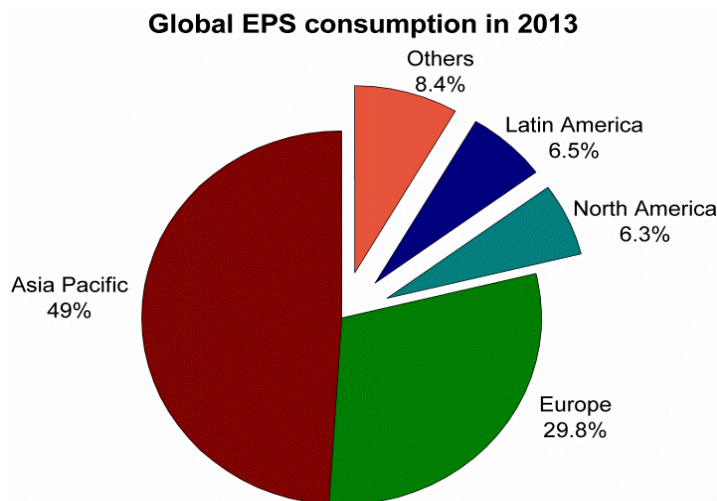


Figure 7. Global EPS consumption by regions in 2013, adapted from [14].

In Australia, it is estimated that more than 40,335 ton of expanded polystyrene from packaging were thrown away by year. According to the Plastics and Chemical Industry Association (PACIA) only 2,775 ton of EPS was collected and recycled in Australia during 2011-2012, which represents a recycling rate of 6.9% [18]. In Brazil the recycling rate grew from 6.7% in 2007 to 9.3% in 2009 [19] mainly due to mechanical recycling process.

Common Methods for Recycling EPS

Since the first industrial scale production of synthetic polymers (plastics) took place in the 1940s, the production, consumption and waste generation rate of plastic solid waste has increased considerably [20]. Plastics are used in our daily life in a number of applications. From greenhouses, coating and wiring, to packaging, films, bags, containers, in construction activities and other several applications. It is reasonable to find a considerable amount of plastic solid waste in the municipal landfill. So, environmental and economic concerns have caused much interest in developing new techniques to solve the problem of plastic waste. Since plastic waste materials are not usually biodegradable, their disposal can become a serious problem. Landfill and incineration are reasonable cheap methods, but give rise to major environmental issues problems. Therefore, alternative methods for recycling will be required. For this reason, various techniques for recycling of plastic waste materials effectively by chemical, thermal and mechanical have been actively developed [21].

Four different approaches have been proposed for the waste polymer recycling which include [22]: Primary recycling, referring to “in plant” recycling of scrap materials; Mechanical recycling, where there are a separation and removal of the contaminants associated with plastic and after, the material is reprocessed by melt extrusion or other techniques; Chemical or feedstock recycling leads to total depolymerization of the monomers, or partial degradation to other secondary valuable materials. Finally, Energy recovery, an effective way to reduce the volume of organic materials by incineration. However, the two main alternatives are energy and mechanical recycling [23]. In the former, environmental

argumentations such as toxic emissions have received much attention and resistance from concerned parties against incineration process (British Plastic Federation). In the latter, mechanical recycling is a popular recovery path for manufacturers and is carried out on single-polymer waste streams. Anyway, the market for recycled materials only worth if the quality of the final product is close to that of the original. Despite these drawbacks, mechanical plastic recycling is thought to be the most used, when ones takes into account the waste's energy, natural resources and environmental pollution [22, 24-25].

Expanded polystyrene (EPS) is commonly used for insulation and packing materials. However, the EPS used for packing materials is often discarded after their first use, which results in a large amount of polymer waste. Continuous disposal of EPS in landfills leads to serious environmental problems. Due to the increase in landfill costs and the decrease of the landfill space, alternatives for the disposal of polystyrene materials must be developed [25-26]. Recycling of this waste has recently received significant attention all over the world due to the changes in both regulatory and environmental issues [26].

Generally the EPS recycling has three types of methods. The first one is the material recycling, where there is a reduction in the volume of EPS by heating, solvent or friction. Then, PS can be recovered and re-used as raw material in daily products, construction materials and so on. The second one is chemical recycling, which is aimed at recovering the styrene monomer to re-use it as chemical resource. The third one is thermal recycling, an effective method for the contaminated EPS waste, which it can be used for energy production through combustion. Because the bulk volume of the waste EPS (due contains so much air), it becomes unfeasible to transport to recycling facilities [27]. So, many researchers have been developing potential solvents for this problem. Noguchi et al. [28-30] developed a new recycling system for waste EPS using a natural solvent. In their study, the authors proposed a new system for EPS recycling, which uses orange oil (*d*-limonene) as the EPS shrinking agent. This recycling process can reproduce polystyrene (PS) with the same mechanical properties of the original. Additionally, the limonene can be re-used at least 10 times. In a study performed by Amianti and Botaro [31], a new recycling method of waste EPS was demonstrated. Concrete was impregnated with polystyrene (CIP) by dissolving EPS in a mixture of acetone and cyclohexane. As a consequence, it resulted in an economic, efficient and easily applied material, which reduces the permeability of pre-cast concrete surfaces. Thereby, reducing the rate of degradation and increasing overall durability. Shin et al. [21] proposed a method for recycling EPS using N,N-dimethylacetamide, tetrahydrofuran and dimethylformamide as solvents. The authors developed submicron and nanofibers of recycled EPS from electrospinning process by mixing these fibers with the conventional glass filter media. The results showed that the addition of the nanofibers improved the efficiency of the filter media from 68 to 88%. However, the dissolution of waste EPS in solvents has some drawbacks. Unfortunately, these chemical techniques usually involve the use of hazardous solvents that can cause health diseases. On the other hand, after use, these solvents can be recovery, recycled or properly disposed without causing environmental damage.

On the other hand, chemical recycling is used to obtain styrene monomers and others chemical products. In contrast to condensation polymers as poly(ethylene terephthalate) [33], PS cannot be easily recycled to its monomer by simple chemical methods. So, thermochemical recycling techniques such as pyrolysis are generally applied. PS can be thermally depolymerized at relatively low temperatures in order to obtain the monomer styrene with high selectivity [22]. Kaminsky [34-35] reached a 65 wt% yield of styrene using

a fluidized bed reactor at 580°C. Ward et al. [36] in a later publication using the same experimental reactor at 520°C reported the generation of an oil composed of 82.8% w/w of styrene. This was achieved by further distillation of the liquid fraction after pyrolysis. Furthermore, Liu et al. [37] studied the pyrolysis of PS in a laboratory fluidized bed reactor in the temperature range of 450–700°C. The yield of styrene reached a maximum of 78.7 wt% at 600°C. The same yield of styrene monomer from the pyrolysis of polystyrene has been reported by Bouster et al. [38]. The uncatalyzed pyrolysis of polystyrene has been reported to produce 83 wt% conversion of low viscosity oil consisting mainly of styrene, with a gas and char yield each with less than 5 wt% [39]. Fast heating rates such as those produced in a fluidized bed reactor and higher temperatures result in the thermal cracking of the pyrolysis vapors and a higher yield of gas and lower yield of oil [40]. Miskolczi et al. [41] studied thermal degradation of waste EPS into fuel like diesel oil. The temperature range of 410–450°C was used in the process. They found out that an increase in the degradation temperature improved yield of both gas and liquid. Nearly complete cracking could be attained at 450°C. The addition of organic compounds such as naphthalene in the pyrolysis of polystyrene waste has been shown to enhance styrene yield [42]. In contrast, the addition of other polymers as polyethylene, led to higher gas release rates and lower liquid release rates [43]. The use of different solid-acid catalysts such as zeolites, alumina and silica-alumina at a temperature of around 350°C has been reported to significantly modify the selectivity of the styrene, since the main products are benzene, ethylbenzene and cumene [44]. Zhang et al. [45] used several basic catalysts and noted an increase of the yield of the monomer when compared to thermal or acid-catalyzed degradation. Barium oxide was proposed as the most effective catalyst for the pyrolysis of waste polystyrene. The monomer yield was of 76 wt% at 350.8°C in a batch reactor with a continuous nitrogen flow. Finally, it has been shown that the pyrolysis products can be a strong function of the raw material, reactor configuration, polymer-catalyst contacting pattern and the average molecular weight of the polymer [22, 38, 44, 46]. The pyrolysis of EPS and others plastic materials to fuel is gaining momentum and being adopted due to its efficiency over the others recycling processes [47].

According to the literature review, waste EPS can be recycled in many ways when it comes to the end of its life. The recycling method takes into account the technical, economic and environmental considerations [48]. Alternative systems using recycled materials contribute to environmental waste reduction and the development of sustainable products. EPS thermo-mechanical recycling process is a cheap alternative to recycle EPS without using hazardous solvent or generate toxic emissions. In addition, it can promote the integration of pickers and industries for the development of recycling-based materials. Generally, the addition of wood flour waste to recycled EPS results in a composite feasible from both mechanical and environmental point of view [49-50].

THERMAL-MECHANICAL RECYCLING OF EPS AND ITS COMPOSITES WITH WOOD FLOUR

Experimental Methods

Materials

The EPS waste was obtained from Associação de Recicladores Serrano, a sorting unit from Caxias do Sul, Brazil, with melt flow index (MFI) of 20g/10min (200°C/5 kg). Wood flour (WF) of *Pinus elliottii* was obtained from Madarco Co., Caxias do Sul, Brazil, with a particle size ranging between 53-105 μm . The wood flour used in this study is a waste from the lumber industry without any kind of preliminary chemical treatment. The poly(styrene-co-maleic anhydride) oligomer supplied by Sartomer Co., Exton/USA (SMA2000) used as the coupling agent, contains 30 wt% of maleic anhydride groups and a weight average molecular weight of 7500 g/mol. The amount of coupling agent incorporated was 2 wt%.

EPS thermo-mechanical recycling and composite preparation

The waste EPS samples were acquired from the packaging of electronic goods and home appliances. The adhesives and papers were removed before EPS recycling. EPS was molded by compression in a hot press at 130°C during 5 min in order to reduce the apparent density. Then, the resulting EPS plates were grinded in a rotary knife mill to obtain EPS flakes. The methodology used for recycling EPS waste is shown in Figure 8. The wood flour was dried in an oven with air circulation at 105°C for 24 h. Samples with 10, 20, 30 and 40 wt% of wood flour with and without 2 wt% of SMA2000 and EPS flakes were processed in a co-rotating twin-screw extruder at 200 rpm. The nine barrel temperature zones were controlled at between 160°C and 190°C. Specimens for mechanical tests were injection molded at a barrel temperature of 180°C and mold temperature of $40 \pm 2^\circ\text{C}$.

Mechanical testing

The tensile tests were conducted according to ASTM D638 at a crosshead speed of 5 mm.min⁻¹, with a 50-mm extensometer, using an EMIC DL 3000 analyzer. The flexural tests were performed on the same equipment according to ASTM D790 at a crosshead speed of 1.5 mm.min⁻¹. Izod impact strength was measured with a CEAST Resil 25 pendulum using unnotched specimens according to ASTM D256. Each test value was calculated as the average of at least five independent measurements.

Density and morphological study

The density values for five waste EPS samples, before and after the compression molding, were determined according to NBR 11949-07 and calculated as the mass volume ratio. The EPS samples had a volume superior of 30 cm³. For the EPS-r (recycled EPS), obtained after extrusion and injection molding, and the composite material, the density was determined according to ASTM D792-00. Void content was determined according to ASTM D2734.

Studies on the morphology of the composites were carried out using a SHIMADZU Superscan SS-550, scanning electron microscope (SEM). The cryo-fracture surface specimens were sputter-coated with gold.

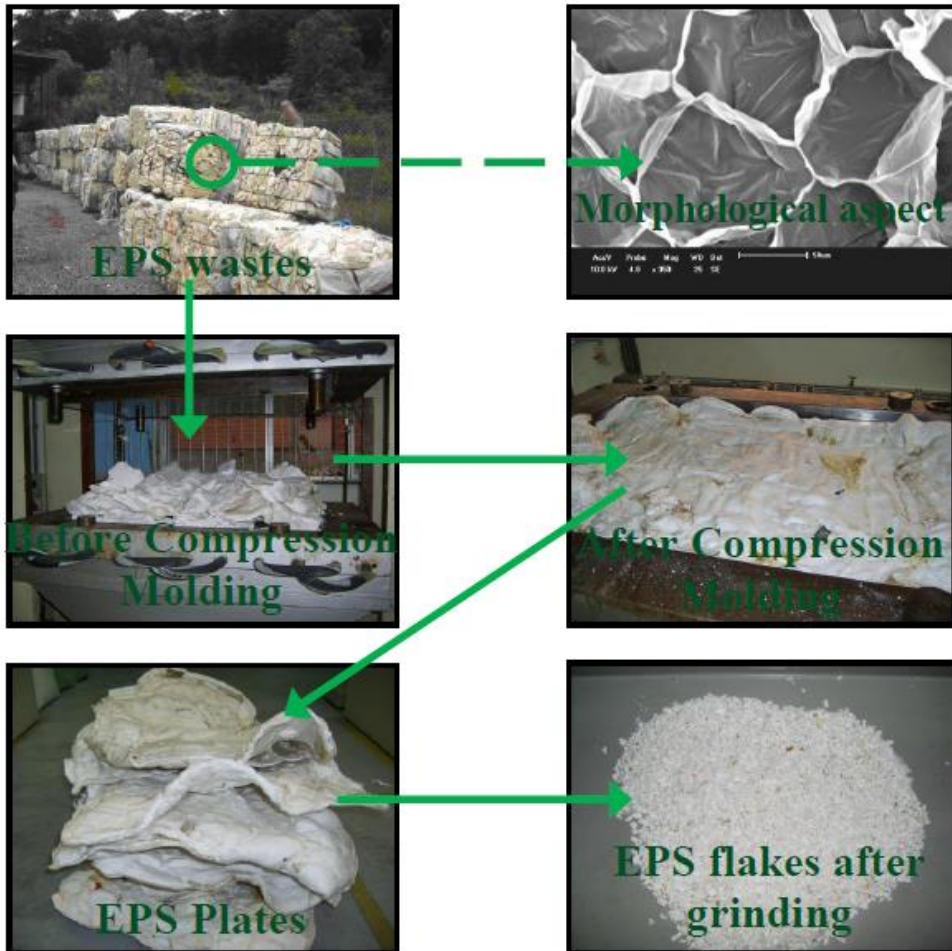


Figure 8. Thermo-mechanical process used for EPS recycling.

Results and Discussion

EPS recycling

The EPS waste density from the sorting unit was found to be equal to $0.022 \pm 0.001 \text{ g/cm}^3$. However, the density after compression molding increased to $0.552 \pm 0.047 \text{ g/cm}^3$. The process of compression molding led to a decreased volume, as well as a 25-fold increase in the density of the EPS wastes. Thus, after compression molding and grinding, the waste EPS can be extruded directly along with the wood flour, eliminating one extrusion process step and reducing the recycling costs. The lower void content of the composite samples (as presented in section density and void content below (Table 5)) confirms that the EPS can be used directly in composite formulations after compression molding and grinding. After the extrusion and injection processes, the apparent density of EPS obtained was equal to $1.072 \pm 0.001 \text{ g/cm}^3$, representing an increased by around 48-fold when compared to the as-received waste. Furthermore, the values being slightly higher than those reported in the literature, between $1.04\text{-}1.05 \text{ g/cm}^3$ [2].

Mechanical properties

The tensile strength, tensile strain and Young's modulus of the composites as a function of wood flour and coupling agent are presented in Table 2. As can be seen, the tensile strength of the composites without SMA decreased with increasing of wood flour content. This is due to the weak interfacial adhesion and low compatibility between wood flour and polymer matrix [49, 51]. In general, the introduction of wood flour reduced the tensile strength when compared to the unfilled EPS-r without the presence of the coupling agent. The expected incompatibility between the two components gave a poor transferring stress from the EPS-r matrix to the wood flour. Consequently, the composite failure at lower tensile strength. The introduction of 2 wt% of SMA2000 improved the tensile strength of the composites, as can be seen in Table 2. The tensile strength of the composites containing coupling agent increased when compared with the composites without SMA 2000. The introduction of the coupling agent improved the stress transfer efficiency by promoting chemical bonds between the hydrophilic filler and the hydrophobic matrix [51-52]. Also, the tensile strength of compatibilised composites increases.

On the other hand, the tensile modulus increased almost linearly by wood flour incorporation. This behavior is due to the reinforcing capacity of the wood flour [53]. The tensile modulus obtained was approximately 2 times higher in the composites with 40 wt% wood flour than in the EPS-r polymer matrix. However, composites with coupling agent presented higher tensile modulus values than composites without SMA, due to the improved interfacial adhesion. The tensile strain was almost the same for composites with and without coupling agent.

The flexural strength values of the composites with and without coupling agent are shown in Table 3. The flexural strength exhibits a similar behaviour to that of the tensile strength. The addition of 2 wt% of SMA to the polymer matrix significantly improved the flexural strength in relation to the composites without coupling agent. The flexural strength reached a maximum value with 40 wt% of wood flour and 2 wt% of SMA. The composite presented a flexural strength 22% higher than the polymer matrix. Due to the similar mechanism, as explained earlier, the flexural strength of the composites with SMA as a coupling agent increased when compared to that of non-treated composites.

Table 2. Tensile properties of the EPS-r composites with and without coupling agent

Sample	Tensile strength (MPa)	Tensile strain (%)	Young Modulus (MPa)
EPS-r	37.23 ± 0.57	1.17 ± 0.02	3494 ± 64
EPS-r/10wt% WF	31.47 ± 1.54	0.74 ± 0.08	3870 ± 66
EPS-r/20wt% WF	35.21 ± 0.90	0.86 ± 0.04	4208 ± 34
EPS-r/30wt% WF	35.32 ± 1.14	0.81 ± 0.01	4525 ± 103
EPS-r/40wt% WF	35.39 ± 1.53	0.64 ± 0.06	5615 ± 116
EPS-r/10wt% WF/2wt% SMA	35.55 ± 1.38	0.82 ± 0.02	3877 ± 59
EPS-r/20wt% WF/2wt% SMA	36.43 ± 0.60	0.86 ± 0.04	4426 ± 126
EPS-r/30wt% WF/2wt% SMA	34.98 ± 0.97	0.76 ± 0.03	4985 ± 104
EPS-r/40wt% WF/2wt% SMA	37.23 ± 1.18	0.71 ± 0.05	5810 ± 72

Table 3. Flexural properties of the EPS-r composites with and without coupling agent

Sample	Flexural strength (MPa)	Flexural strain (%)	Flexural Modulus (MPa)
EPS-r	46.10 ± 1.53	1.56 ± 0.06	3315 ± 189
EPS-r/10wt% WF	52.35 ± 0.77	1.51 ± 0.02	3621 ± 62
EPS-r/20wt% WF	49.09 ± 1.68	1.22 ± 0.04	4072 ± 22
EPS-r/30wt% WF	44.70 ± 1.17	0.97 ± 0.02	4844 ± 99
EPS-r/40wt% WF	46.51 ± 1.75	0.89 ± 0.04	5726 ± 86
EPS-r/10wt% WF/2wt% SMA	53.07 ± 1.09	1.54 ± 0.03	3655 ± 19
EPS-r/20wt% WF/2wt% SMA	52.33 ± 2.34	1.30 ± 0.02	4167 ± 40
EPS-r/30wt% WF/2wt% SMA	53.26 ± 1.58	1.16 ± 0.06	4886 ± 45
EPS-r/40wt% WF/2wt% SMA	56.04 ± 1.98	1.08 ± 0.04	5745 ± 94

There were no significant differences between the flexural modulus values for the composites with and without coupling agent, as presented in Table 3. However, the treated composites seem to have a slightly higher flexural modulus than the composites without SMA. In general, the flexural strain for composites with and without coupling agent presented a similar behaviour.

Impact strength

The Izod impact strength of the composites decreased by wood flour incorporation, as can be seen in Table 4. The poor interfacial bonding between the filler and the polymer matrix causes micro-cracks that are easy-to-propagate in the composite without coupling agent [52]. These micro-cracks decrease the impact strength of the composites. The addition of wood flour leads to the creation of a weak interface between the filler and the EPS-r matrix, which creates a stress concentration and crack initiation point causing a significant reduction of the impact strength. The filler also seems to reduce the polymer chain mobility, thereby reducing the ability of the composite to absorb energy during fracture propagation [54].

Composites with coupling agent exhibited better impact strength than the composites without treatment. With the addition of the coupling agent, the interfacial bonding between the wood flour and EPS-r matrix was considerably improved. The coupling agent promotes the interfacial adhesion between filler and matrix and also improved the dispersion of the wood flour, leading to a more uniform distribution of the applied stress. Therefore, more energy for debonding and fiber pull-out is required [54-55] increasing the impact strength of these composites.

Density and void content

Mechanical properties of polymer composites are well known to be strongly affected by internal defects such as voids [56]. Consequently, the density and void content usually serve as good indicators for composite performance [56-57]. A linear relationship can be observed between the density and the composite wood flour content, as presented in Table 5. The composites without coupling agent showed slightly lower density values than composites containing SMA. In addition, the treated composites had a density only 11% higher than the polymer matrix. However, the mechanical properties increased in comparison to EPS-r, which

makes these composites attractive for automotive applications that requires the combination of strong materials with low density. The incorporation of 40 wt% wood flour did not increase significantly the density of composites, which makes the development of the material particularly attractive to industry. Especially for application in automobiles since this requires composites with good mechanical properties, but with low density and void content values.

Table 4. Impact strength of the EPS-r composites with and without coupling agent

Sample	Impact strength (J/m)
EPS-r	123.77 ± 6.96
EPS-r/10wt% WF	96.87 ± 4.82
EPS-r/20wt% WF	92.17 ± 3.89
EPS-r/30wt% WF	78.62 ± 4.00
EPS-r/40wt% WF	71.47 ± 5.85
EPS-r/10wt% WF/2wt% SMA	107.53 ± 4.71
EPS-r/20wt% WF/2wt% SMA	100.35 ± 3.24
EPS-r/30wt% WF/2wt% SMA	96.58 ± 1.82
EPS-r/40wt% WF/2wt% SMA	81.33 ± 1.47

Table 5. Density and void content of the EPS-r composites with and without coupling agent

Sample	Density (g/cm ³)	Void content (%)
EPS-r	1.072 ± 0.001	---
EPS-r/10wt% WF	1.091 ± 0.001	1.653 ± 0.030
EPS-r/20wt% WF	1.114 ± 0.002	2.239 ± 0.184
EPS-r/30wt% WF	1.139 ± 0.001	2.973 ± 0.039
EPS-r/40wt% WF	1.180 ± 0.002	2.224 ± 0.159
EPS-r/10wt% WF/2wt% SMA	1.092 ± 0.001	1.228 ± 0.064
EPS-r/20wt% WF/2wt% SMA	1.122 ± 0.001	1.730 ± 0.103
EPS-r/30wt% WF/2wt% SMA	1.150 ± 0.002	2.214 ± 0.181
EPS-r/40wt% WF/2wt% SMA	1.188 ± 0.001	1.819 ± 0.054

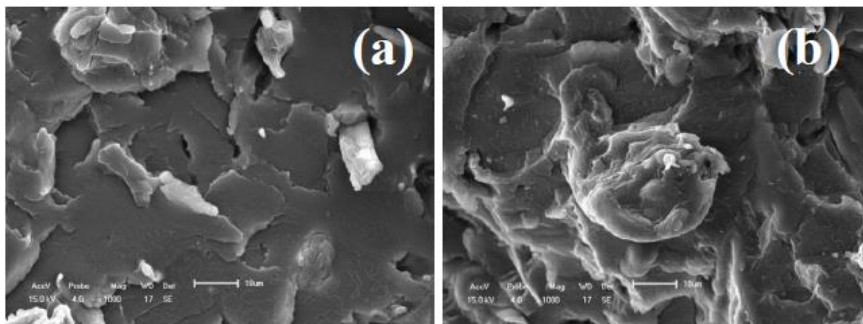


Figure 9. SEM images for composite fracture surfaces without (a) and with (b) coupling agent.

The void content values for the two types of composites were compared and were found to be lower for the treated composites than for the non-treated composites. According to Padma Priya et al. [58], for composites with good mechanical properties the void content values should be less than 3%. Composites with coupling agent had void content values less than 2%, while the non-treated composite values were close to 3%. Thus, the treated composites showed lower void content values and better mechanical properties than the non-treated ones. The decreased in void content for treated composites may indicate the existence of a good bonding between the wood flour and EPS-r matrix in the composite.

Morphology characteristics

The SEM micrographs of the non-treated composites and those treated with 20 wt% of wood flour are shown in Figure 9(a) and (b), respectively. In Figure 9(a), examination of the cryo-fracture surface of the composite without coupling agent indicated the presence of voids which are the main responsible for fiber pull-out and larger gaps between the wood flour and the EPS-r matrix. This causes a weak interfacial adhesion at the interface [51, 55]. The SEM micrograph of the treated composite in Figure 9(b) shows strong bonding and a reduced evidence of fiber pull-out. This result demonstrates that SMA addition to the composites provides strong interfacial adhesion and good wetting. This is confirmed by the almost complete absence of voids in the polymer matrix and gaps between the fiber and the matrix [51, 54].

FUTURE TRENDS

The trend toward EPS materials with better insulation and mechanical strength continues to be studied and developed. Novel EPS materials that aim to reduce the thermal conductivities for potential uses in special applications are under development. The global demand for EPS and its production is steadily increasing and according to the last surveys, it will grow at a CAGR of 8.2% from 2013 to 2018. The increase in EPS production necessitates the intensification of recycling efforts around the world. The technology to recycle polystyrene already exists and others will be invented. However, the high cost associated with transporting the waste EPS to recycling facilities generally is a huge obstacle [59]. The cost can be lowered considerably by reducing the volume of the waste, preferably at the point of origin [60]. Recycling polystyrene certainly shows great promise and more ways of utilizing recycled polystyrene will be discovered in the future [60]. Hopefully, the promise of sustainable EPS chain without cause environmental pollution will encourage companies, organizations and governments to work together to step up polystyrene recycling efforts [60].

CONCLUSION

EPS is a versatile material. The applications in packaging, construction and many others demonstrate the potential of this material. The increasing in demand, production and development of EPS also demonstrated that this material is far away to be replaced by others foam materials. On the other hand, recycling efforts need to be promoted by all members

involved in the EPS chain. Many processes can be used for recycling EPS and others will be created. However, the choice of an EPS recycling method needs to be based on technical, environmental and economic considerations. The thermal-recycling method presented in this work is an alternative to recycle EPS wastes and also contributes to the development of the EPS recycling. In addition, development composite materials with higher mechanical properties and low density can be used by industries as an interesting option to enclose environmental and economic benefits.

REFERENCES

- [1] Pohleman, HG; Echte, A. Fifty years of polystyrene. *Polym. Sci. Overview, ACS Symposium Series*, 175 (1981), 3685-3689.
- [2] Rubin, I. *Handbook of plastics materials and technology*, John Wiley & Sons, New York, 1990.
- [3] Dow Styrofoam invention. Available: <http://building.dow.com/about/invention.htm>.
- [4] Snijders, EA. *Water Expandable Polystyrene (WEPS) Computational and Experimental Analysis of Bubble Growth*, Technische Universiteit Eindhoven, Eindhoven, 2003.
- [5] EUMEPS, *EPS foam insulation – Environmental product declaration*, 2011.
- [6] EPS Packaging Group, *Expanded polystyrene (EPS) and the environment*. Available: http://www.eps.co.uk/pdfs/eps_and_the_environment.pdf.
- [7] ACEPE, *EPS components and transformation – Processes used*. Available: <http://www.acepe.pt/index.php/eps/composicao-transformacao>.
- [8] EPS Industry Alliance, *Expanded Polystyrene (EPS) Geofoam Applications & Technical Data*, EPS Industry Alliance, Crofton.
- [9] Australian Urethane & Styrene, *EPS technical data*, New South Wales, 2011.
- [10] Insulspan, *Structure Insulation Panel System*. Available: <http://www.insulspan.com/>.
- [11] Winterling, H; Sonntag, N. *Kunststoffe*, 10 (2011), 18-21.
- [12] Markets and Markets, *Expanded polystyrene (EPS) market, by applications (Building & Construction, Packaging & Others), & geography (North America, West Europe, Asia-Pacific & Rest of the World) – Global Trends & Forecast to 2018*, Dallas, 2013.
- [13] Plastemart, *Rise in global demand for polystyrene and expandable polystyrene is led by demand from Asia Pacific*, 2013. Available: <http://www.plastemart.com/Plastic-Technical-Article.asp?LiteratureID=2032&Paper=rise-global-demand-polystyrene-expandable%20polystyrene-EPS-led-by-asia-pacific>.
- [14] Merchant Research & Consulting, Ltd, *Expandable Polystyrene (EPS): 2014 World Market Outlook and Forecast up to 2018*, 2014. Available: <http://mcgroup.co.uk/researches/expandable-polystyrene-eps>.
- [15] EPS Industry Alliance, *2012 EPS recycling rate report*, EPS Industry Alliance, Crofton, 2012.
- [16] Japan Expanded Polystyrene Association (JPESA), *EPS recycling is steadily increasing*, JEPSA, Japan, 2010.
- [17] Korean Foam-Styrene Recycling Association (KFRA), *Waste EPS recycling status*, KFRA, Seoul, 2012.

-
- [18] Metropolitan Waste Management Group (MWMG), *Polystyrene Recycling*, MWMG, Melbourne, 2014.
- [19] Plastivida, *Repensar project*, Plastivida, São Paulo, 2010.
- [20] Al-Salem, SM; Lettieri, P; Baeyens, J. *Waste Manage.*, 29 (2009), 2625-2643.
- [21] Shin, C. *J. Colloid Interface Sci.*, 302 (2006), 267-271.
- [22] Achilias, DS; Kanellopoulou, I; Megalokonomos, P; Antonakou, E; Lappas, AA. *Macromol. Mater. Eng.*, 292 (2007), 923-934.
- [23] Garforth, A; Ali, S; Hernandez-Martinez, J; Akah, A. *Curr. Opin. Solid State Mater. Sci.*, 8 (2004), 419-425.
- [24] Borsoi, C; Scienza, LC; Zattera, AJ. *J. Appl. Polym. Sci.*, 128 (2013), 635-659.
- [25] Poletto, M; Dettenborn, J; Zeni, M; Zattera, AJ. *Waste Manage.*, 31 (2011), 779-784.
- [26] García, MT; Gracia, I; Duque, G; de Lucas, A; Rodríguez, JF. *Waste Manage.*, 29 (2009), 1814-1818.
- [27] Shin, C; Chase, GG; Reneker, DH. *Colloids Surf.*, A 262 (2005), 211-215.
- [28] Noguchi, T; Miyashita, M; Inagaki, Y; Watanabe, H. *Packag. Technol. Sci.*, 11 (1998), 19-27.
- [29] Noguchi, T; Inagaki, Y; Miyashita, M; Watanabe, H. *Packag. Technol. Sci.*, 11 (1998), 29-37.
- [30] Noguchi, T; Tomita, H; Satake, K; Watanabe, H. *Packag. Technol. Sci.*, 11 (1998), 39-44.
- [31] Amianti, M; Botaro, VR. *Cem. Concr. Compos.*, 30 (2008), 23-28.
- [32] Shin, C. *Packag. Technol. Sci.*, 18 (2005), 331-335.
- [33] Kosmidis, V; Achilias, DS; Karayannidis, GP. *Macromol. Mater. Eng.*, 286 (2001), 640-647.
- [34] Kaminsky, W. *Makromol. Chem., Macromol. Symp.*, 48/49 (1991), 381-393.
- [35] Kaminsky, W; Predel, M; Sadiki, A. *Polym. Degrad. Stab.*, 85 (2004), 1045-1050.
- [36] Ward, PG; Goff, M; Donner, M; Kaminsky, W; O'Connor, KE. *Environ. Sci. Technol.*, 40 (2006), 2433-2437.
- [37] Liu, Y; Qian, J; Wang, J. *Fuel Proc. Technol.*, 63 (2000), 45-55.
- [38] Bouster, C; Vermande, P; Veron, J. *J. Anal. Appl. Pyrolysis*, 15 (1989), 249-259.
- [39] Williams, PT; Williams, EA. *Energy and Fuels*, 13 (1999), 188-196.
- [40] Williams, PT; Williams, EA. *J. Inst. Energy*, 71 (1998), 81-93.
- [41] Miskolczi, N; Bartha, L; Deák, Gy. *Polym. Degrad. Stab.*, 91 (2006), 517-526.
- [42] Karaduman, A. *Energy Sources*, 24 (2002), 667-674.
- [43] Kiran, N; Ekinçi, E; Snape, CE. *Resour. Conserv. Recycling*, 29 (2000), 273-283.
- [44] Audisio, G; Bertini, F; Beltrame, PL; Carniti, P. *Polym. Degrad. Stab.*, 29 (1990), 191-200.
- [45] Zhang, Z; Hirose, T; Nishio, S; Morioka, Y; Azuma, N; Ueno, A; Okhita, H; Okada, M. *Ind. Eng. Chem. Res.*, 34 (1995), 4514-4519.
- [46] Ukei, H; Hirose, T; Horikawa, S; Takai, Y; Taka, M; Azuma, N; Ueno, A. *Catal. Today*, 62 (2000), 67-75.
- [47] Panda, AK; Singh, RK; Mishra, DK. *Renew. Sust. Energ. Rev.*, 14 (2010), 233-248.
- [48] Kan, A; Demirboğa, R. *J. Mater. Process. Tech.*, 209 (2009), 2994-3000.
- [49] Adhikary, KB; Pang, S; Staiger, MP. *Composites Part B*, 39 (2008), 807-815.
- [50] Ashori, A; Nourbakhsh, A. *Waste Manage.*, 29 (2009), 1291-1295.

- [51] Kim, H-S; Lee, B-H; Choi, S-W; Kim, S; Kim, H-J. *Composites Part A*, 38 (2007), 1473-1482.
- [52] Yang, H-S; Kim, H-J; Park, H-J; Lee, B-J; Hwang, T-S. *Composite Structures*, 77 (2007), 45-55.
- [53] Bengtsson, M; Le Baillif, M; Oksman, K. *Composites Part A*, 38 (2007), 1922-1931.
- [54] Nygård, P; Tanem, BS; Karlsen, T; Brachet, P; Leinsvang, B. *Compos. Sci. Technol.*, 68 (2008), 3418-3424.
- [55] Ashori, A; Nourbakhsh, A. *Waste Manage.*, 30 (2010), 680-684.
- [56] Takagi, H; Asano, A. *Composites Part A*, 39 (2008), 685-689.
- [57] Borja, Y; Rieb, G; Lederer, K. *J. Appl. Polym. Sci.*, 101 (2006), 364-369.
- [58] Padma Priya, S; Ramakrishna, HV; Rai, SK. *J. Reinf. Plast. Compos.*, 25 (2006), 339-345.
- [59] Salhofer, S; Schneider, F; Obersteiner, G. *Waste Manage.*, 27 (2007), S47-S57.
- [60] Rubio, MR. Trends in Recycling of EPS Foam, Environment, Recycling, Waste Management, 2013. Available: <http://www.ecomena.org/recycling-eps-foam/>.

Chapter 4

GIGAPOROUS POLYSTYRENE MICROSPHERES AND THEIR APPLICATIONS IN HIGH-SPEED PROTEIN CHROMATOGRAPHY

Jian-Bo Qu^{1,}, Fang Huang¹, Wei-Qing Zhou²,
Fei Gao² and Guang-Hui Ma^{2,#}*

¹Center for Bioengineering and Biotechnology,
China University of Petroleum (East China), Qingdao, P.R. China

²National Key Laboratory of Biochemical Engineering,
Institute of Process Engineering, Chinese Academy of Sciences,
Beijing, P.R. China

ABSTRACT

Modern chromatography media have developed over the years, providing improved binding capacity, faster mass transfer, better chemical resistance, and greater selectivity. Compared with silica and conventional separation media (e.g. dextran and agarose), there is an increasing interest in the use of poly(styrene-divinylbenzene) (PS) microspheres as chromatographic packing materials for proteins and antibodies owing to their excellent mechanical properties and good chemical stability over a wide pH range. However, for conventional porous microspheres with normal pore size of 10-100 nm, slow mass transfer rate is the factor that restricts their application in biomacromolecule separation. It is imperative to develop efficient separation media with high resolution, high speed and high capacity for a broad range of business areas including pharmaceuticals, nutrition and health products, bioenergy, environmental protection and so on.

Gigaporous PS microspheres with pore diameter around 300-500 nm are very promising in high-speed protein chromatography, which can effectively reduce the resistance from stagnant mobile phase mass transfer by inducing convective flow of mobile phase in the gigapores of medium. Unfortunately, the native PS beads are not suitable for protein chromatography medium due to their high hydrophobicity causing

* Corresponding author. Email: jbqu@upc.edu.cn.

Corresponding author. Email: ghma@home.ipe.ac.cn.

non-specific adsorption and denaturation of proteins. This chapter describes the current development of gigaporous PS microspheres and their application in high-speed protein chromatography, with emphasis on our recent contributions to this field.

1. INTRODUCTION AND BACKGROUND

Liquid chromatography (LC) has dominated biomacromolecules purification for more than five decades because of its high resolution and mild separation conditions. The properties of stationary phase are crucial to the performance of liquid chromatography. Bioseparation of high value products is mainly based on packed beds, and the progress of the stationary packings expands its application in bioseparations [1, 2]. The key aspect of LC is choice of a suitable stationary packing. Modern chromatography media have developed over the years, providing improved binding capacity, faster mass transfer, better chemical resistance, and greater selectivity.

During the past several decades, the progress of stationary phase has experienced several stages. In 1950s, the polysaccharide soft gels, such as cellulose, dextran and agarose, were the most popular matrix for protein chromatography because of their easy derivatization, high biocompatibility, high porosity and high surface area [3]. However, these soft gels have poor mechanical strength and can only be operated under low pressure [4]. In the early 1970s, the emergence of inorganic supports, such as silica, increased both the resolution and the operation speed of protein chromatographic columns, but these supports have poor chemical stability at low (pH <2) or high pH (pH >7.5) [5]. Due to the polysaccharides and inorganic material's shortcomings, organic resins have been widely studied as alternatives since the late 1970s. Organic resins usually possess higher mechanical strength than soft gel and can tolerate extreme environmental conditions such as pH1-12. Nevertheless, conventional polymer-based porous media with pore size in 10-30 nm have stagnant mobile phase mass transfer problem, which restricts the application of these microspheres in separation of biological macromolecules [6]. In order to solve the problem, the small non-porous microspheres were introduced in 1980s. Unger et al. reported that small (1-3 μm) nonporous particles can separate five proteins in 10 s owing to slow diffusion within the nonporous particles is eliminated and column may be operated at least an order of magnitude [7, 8]. However, their low loading capacity and high column backpressure made these columns less attractive for preparative-scale proteins separation [9].

Poly(styrene-divinylbenzene) (PS) microspheres are of increasing interest to chromatographers over silica and conventional separation media (e.g. dextran and agarose) as chromatographic packing materials for proteins and antibodies owing to their excellent mechanical properties and a good chemical stability over a wide pH range [10, 11]. In the beginning of 1990s, there emerged an alternative approach to solve the stagnant mobile phase mass transfer problem. A novel medium, referred as POROS perfusion adsorbent [12], with some pores approaching a micron in diameter was introduced by PerSeptive Biosystems, USA. The POROS support allow mobile phase to flow through chromatographic sorbents and transport solutes into the interior of packing materials by convection [5, 13]. From then on a few superporous poly (glycidyl methacrylate) (PGMA) microspheres have also been developed for high-speed protein chromatography [14-16]. There are however, limitations with PGMA microspheres. Weak chemical stability of ester group in PGMA cannot promise

the long-term use of substrates. The mechanical strength of PGMA microspheres is not as well as polystyrene particles. Inspired by HIPE (high internal phase emulsion) method [17, 18], Ma et al. developed a novel surfactant reverse micelles swelling method to prepare gigaporous PS microspheres with pore size of about 300-500 nm [19]. The gigaporous PS microspheres showed excellent performance in separation and purification of biomolecules with super-large molecular weight and can be used as perfusion chromatographic supports.

As described above, gigaporous PS microspheres, with their excellent mechanical properties, good chemical stability and convective transport mode, are very promising in high-speed protein chromatography. This review describes the current status of the research on gigaporous PS microspheres and their application in high-speed protein chromatography, with emphasis on our recent contribution to this field.

2. PREPARATION OF GIGAPOROUS POLYSTYRENE MICROSPHERES

Gigaporous PS microspheres with interconnected through pores provide an alternative approach besides diffusion to transport the biomacromolecules into interior of particles by convection. Also, the interconnected through pores can greatly shorten the diffusive distance from outer particle to inner particle. These merits make gigaporous PS microspheres outstanding as packing materials in high-speed protein chromatography. The preparation methods of gigaporous PS microspheres are described as follows.

2.1. POROS Microspheres

Gigaporous PS microspheres were first introduced by Lloyd et al. (Polymer Laboratories, Shropshire, UK) [20]. The particle diameter is 8-10 μm , and the average pore size is 400 nm. The high speed separation performance of the gigaporous PS microspheres was evaluated in reversed-phase HPLC and anion-exchange HPLC modes.

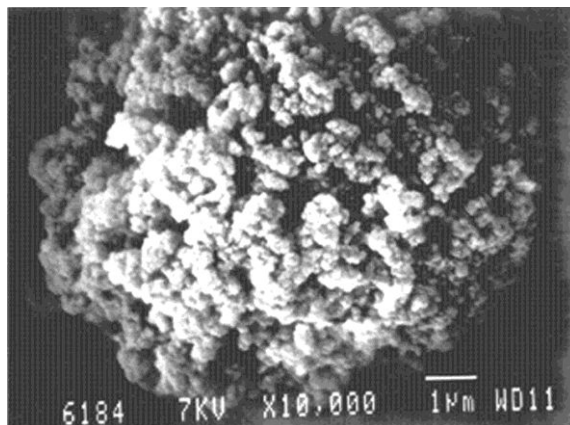


Figure 1. Scanning electron micrograph of POROS R/H. (From Ref. [5] with permission).

According to the separation mechanism of medium, Afan et al. named the media with perfusion chromatographic media, which means the separation mode of combining diffusion and convection just like the perfusion system in human body [5]. The trade name of this kind of media is POROS. There are mainly three kinds of POROS media, i.e. POROSTM Q (strong anion-exchange), S (strong cation-exchange) and R (reversed-phase) produced by PerSeptive Biosystems (Cambridge, MA, USA). They have been prepared by nanomicrospheres' agglomeration method and classified to the desired particle size range (nominal diameters are 10 μm for H series and 20 μm for M series). Figure 1 shows the scanning electron image of commercial POROS R/H, which has two sets of pores: through pores (600-800 nm) and diffusive pores (80-150 nm). The interconnected through pores bring intraparticle convective transport into the bead and diffusive pores provide a substantial surface area. So, this kind of stationary phase can be operated at high speed while maintaining high column efficiency and dynamic binding capacity [21-23]. Even though, the preparation method of POROS is complicated and the diameter of the two sets of pores is difficult to control. The particles were built from porons to produce small poron clusters, and then to aggregate the clusters, and then to agglomerate the aggregates to form particles of macroscopic size. The through pores and the diffusive pores were formed by the interstices between the small particles and their clusters. Therefore, the pores were difficult to control, and the reproducibility needs to be improved. There are few reports about application of POROS in protein separation in recent years after its flourish in 1990s.

2.2. Magnapore Microspheres

Barby et al. developed a high internal phase emulsion (HIPE) method to produce polyHIPE materials in 1985 [24]. HIPE is the emulsion with the volume concentration of internal phase over 70%. As normal emulsion, HIPE includes W/O and O/W styles. Styrene/divinylbenzene polyHIPE was prepared through W/O HIPE. After polymerization, the monolith polymer has a macroporous structure containing interconnected cavities, which are formed by the internal water phase in HIPE. The diameter of the cavities is very large, from one to tens of micrometer. Walsh et al. evaluated the effect of water/monomer ratio and mixing time on the structure of obtained polyHIPE materials [25]. Besides enough mixing time, the water content in the emulsion droplets must be higher than 95% to assure the open-pore structure. Good structure of polyHIPE can be obtained when the ratio of water/monomer and the mixing time is 20/1 and 1h, respectively. In 1996, Li and Benson developed an alternative strategy to prepare polyHIPE beads with porosity up to 90 %, i.e., Magnapore [26-29]. They dispersed the HIPE into the third medium (forming W/O/W or O/W/O three phase systems or double emulsion) where they are subsequently solidified by polymerization (Figure 2). However, the main drawbacks of Magnapore are their fragile mechanical strength and poor emulsion stability. After Li and Benson patented the preparation procedure in 1998, not much research has been done on polyHIPE beads.

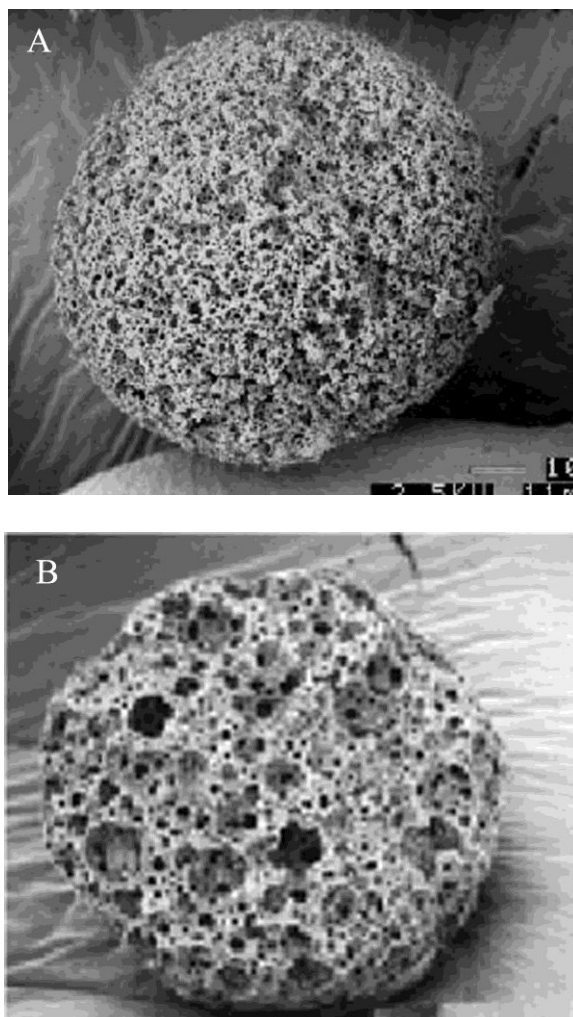


Figure 2. Scanning electron micrographs of Magnapore particles. A: External morphology; B: Internal morphology. (From Ref. [26] with permission).

2.3. Microspheres Prepared by Surfactant Reverse Micelles Swelling Method

Inspired by HIPE method, Ma et al. developed a novel surfactant reverse micelles swelling method to prepare gigaporous PS microspheres with pore size of about 500 nm, which overcomes the preparation problems of POROS medium and Magnapore particles described above and can be used as perfusion chromatographic supports [19]. By adjusting the amount of surfactant in the oil phase, the gigaporous microspheres can be more easily prepared by one-step suspension polymerization than HIPE method. The difference from conventional suspension polymerization was that surfactant with a higher concentration was applied in the oil phase. The effects of the amount and type of surfactants on the morphology of microspheres were investigated in detail.

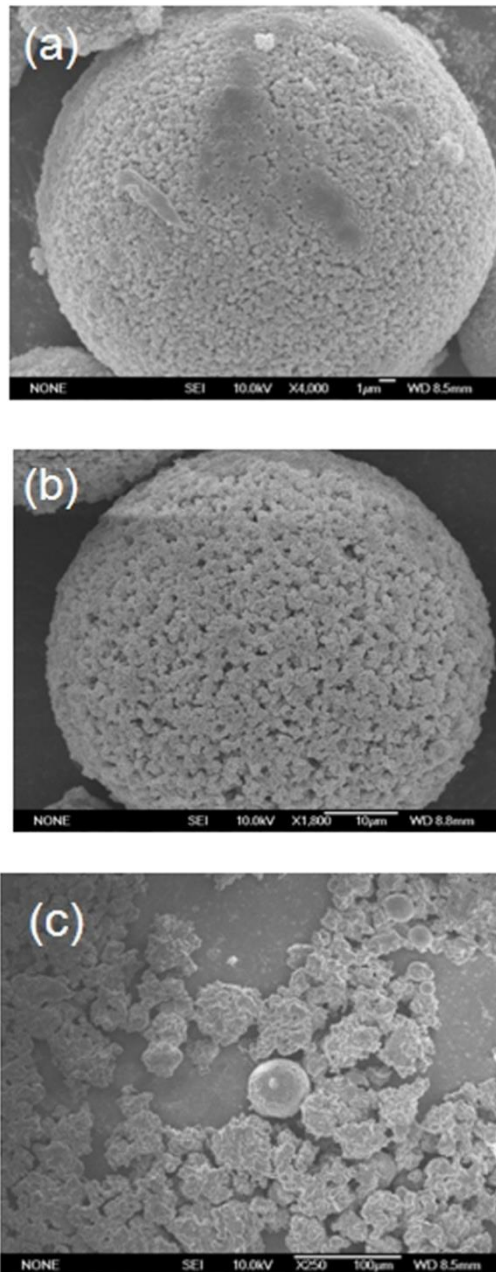


Figure 3. Effect of amount of Span 80 on the morphology of microspheres (crosslinking degree was 13.8%). (a) 30%; (b) 40%; (c) 50%. (From Ref. [30] with permission).

Taking Span 80 as an example, it was observed that the amount of Span 80 in oil phase had an important effect on the morphology of microspheres, as shown in Figure 3. When the amount of Span 80 was below 30% (based on the total amount of styrene and divinylbenzene), the pore size was not so large. When it was increased to 40%, the pore size became very large, around 500 nm. However, when the concentration of Span 80 exceeded 50%, the polymer beads were broken.

As for surfactant type, three surfactants (Span80, Span 85 and PO-500) were chosen to study their effects on the morphology of the particles. The effect of Span 85 was similar with that of Span 80, i.e., the pore size increased with surfactant concentration. However, more Span 85 was needed in order to get similar pore size. For example, in order to get the microspheres with large pore size showed in Figure 4, the necessary concentration of Span 85 was 60%, higher than the case of Span 80 (40%). This phenomenon was related to the hydrophobic hydrophilic property of the surfactants. The HLB (hydrophilic-lipophilic balance) of Span 85 is 1.8, and it is lower than that of Span 80 (HLB 4.3). This implied that Span 85 was more hydrophobic, and its ability of absorbing water was weaker than that of Span 80 under the same concentration, therefore, relatively smaller pores were formed when using Span 85. When it comes to PO500, the pore size also increased with surfactant concentration, and was about 1 μm when the PO-500 concentration increased to 40%, but the microspheres were not spherical as shown in Figure 5. This was probably because PO-500 (HLB 4.9) was more hydrophilic than Span 80 and the reverse micelles tended to move near the surface of the droplet. Thus, a lot of water was absorbed near the surface, so the surface was destroyed easily during polymerization.

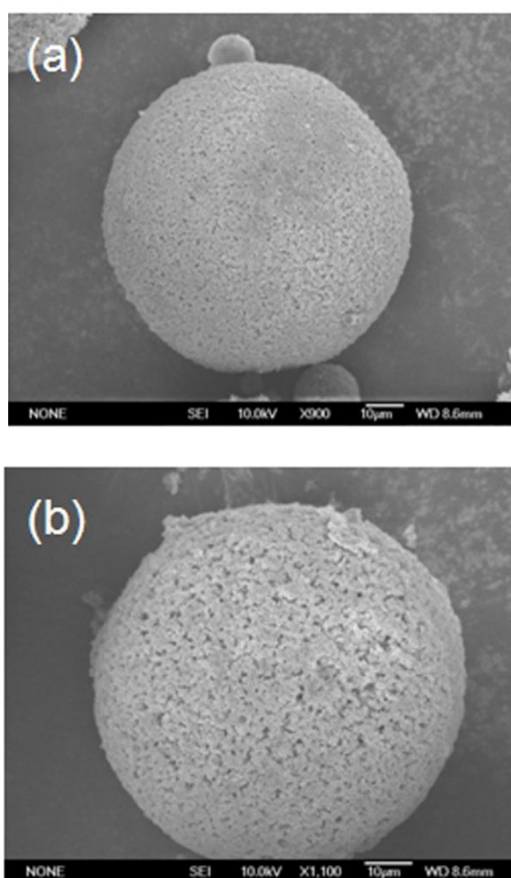


Figure 4. Microspheres prepared with different amount of Span 85. (a) 50%; (b) 60%. (From Ref. [30] with permission).

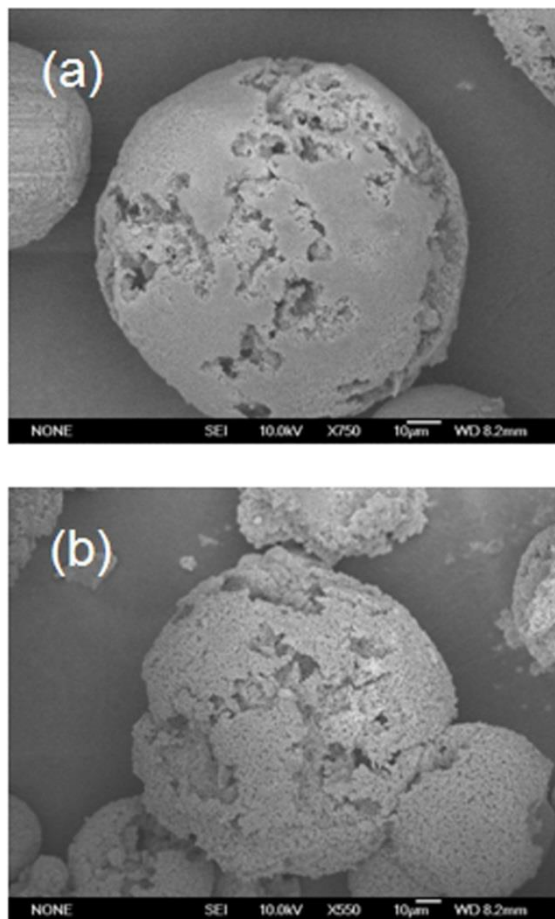


Figure 5. Microspheres prepared with different amount of PO 500. (a) 30%; (b) 40%. (From Ref. [30] with permission).

The formation mechanism of the big pores in the polymeric microspheres was also investigated by Ma et al. through laser confocal scanning microscope (LCSM) and conductivity measurements [30]. There are two crucial factors in the preparation of gigaporous PS microspheres: the high concentration of reverse micelles existed in the oil phase and the water absorbed by the reverse micelles from the external aqueous phase. It was found that the surfactant reverse micelles in oil droplets absorbed water and formed a bicontinuous emulsion. The absorbed water then aggregated into aqueous channels and became large pores after polymerization. Figure 6 shows the formation mechanism of gigapores in gigaporous PS microspheres. Candau et al. also found in the study of microemulsion polymerization that oil-water bicontinuous structure would form if the ratio of water/oil/surfactant was suitable [31]. The oil-water bicontinuous structure contributed to the through pores like POROS medium in the gigaporous PS microspheres, which would be a promising material in enzyme immobilization and separation of biomolecules with high molecular weight.

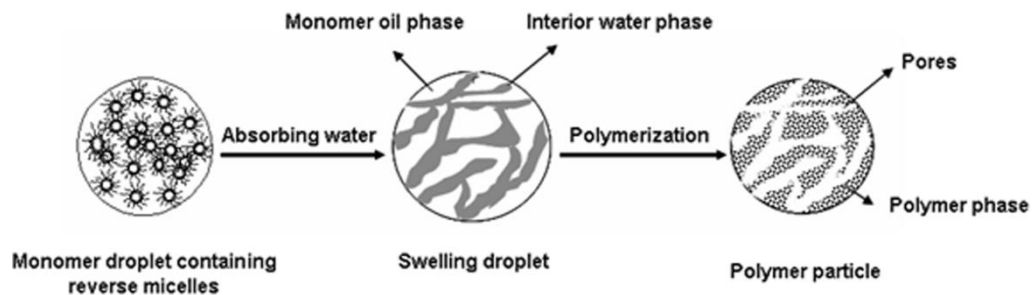


Figure 6. Schematic image showing the formation of macropores in monomer droplet. (From Ref. [30] with permission).

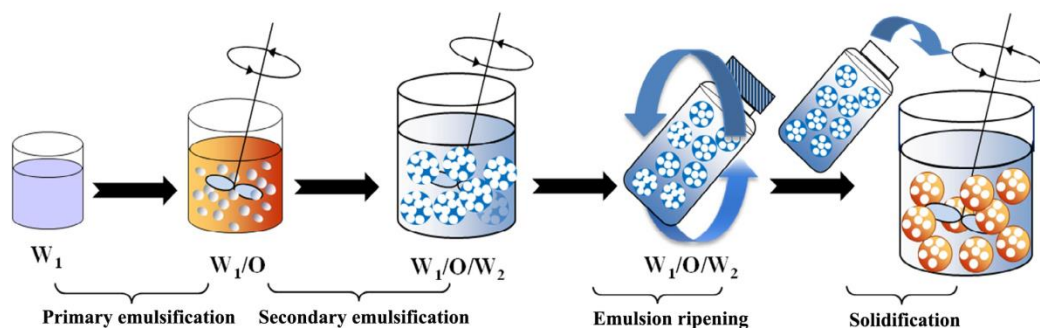


Figure 7. Fabrication procedure for double emulsion-templated gigaporous microspheres.

2.4. Double Emulsion-templated Microspheres

Ma et al. developed a novel method using double emulsion as template to prepare porous PS microspheres that possessed flow-through pores without adding any porogen [32]. Poly (vinylbenzyl chloride) (PVBC) was employed as the major component of the particle material and amphiphilic polymer methoxy poly (ethylene glycol)-*b*-poly (D,L-lactide) (PELA) was employed as an essential additive. Gigaporous microspheres that possess flow-through pores ranging from submicron to micron scale were prepared by two-step emulsification, emulsion ripening, and solvent extraction (Figure 7). It is expected that high porosity microspheres were templated from a well-stabilized $W_1/O/W_2$ system, where each oil globule possessed quite a number of W_1 droplets.

PELA is an ideal amphiphilic stabilizer to stabilize the W/O and $W/O/W$ emulsion systems because it has both hydrophilic and hydrophobic groups. The author observed that the amount of PELA in oil phase had an important effect on the morphology of microspheres and also on the surface porosity. When the $W_1/O/W_2$ system was not well stabilized with enough PELA, many entrapped W_1 droplets would coalesce quickly before solvent removing, fewer or even no pores were obtained. On the other hand, when too much PELA was dosed in the mixture, the spherical morphology could be destroyed.

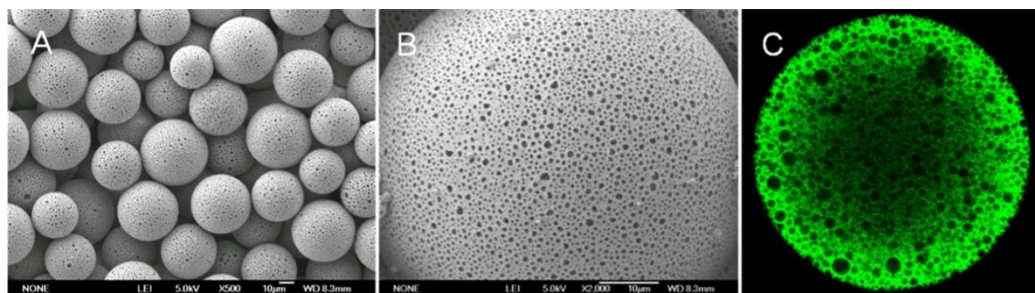


Figure 8. SEM images of pore morphology of PVBC microspheres with different magnifications (a, 500 \times ; b, 2000 \times) and LCSM image of PVBC porous microsphere (c).



Figure 9. The scheme of side-on (left) and end-on (right) polymer configurations.

The gigaporous structure of PVBC microspheres was shown in Figure 8a and 8b, which present homogeneous honeycomb-like pores on the particles. LCSM image in Figure 8c reflects the internal structure of PVBC microsphere that was dyed by fluorescein isothiocyanate (FITC) in advance. It can be seen from Figure 8c that hollow compartments existed deeply in the particles. Such microspheres are also promising candidates of chromatographic media for super large biomacromolecules separation.

3. HYDROPHILIZATION OF GIGAPOROUS POLYSTYRENE MICROSPHERES

Gigaporous PS microspheres not only have good chemical stability and mechanical strength, but also have interconnected gigapores within the particles which can effectively solve the stagnant mobile phase mass transfer problem in chromatography. It is very promising in high-speed preparative protein chromatography. Unfortunately, the native PS beads are limited in the chromatography for protein separation due to their highly hydrophobic property, which will lead to nonspecific adsorption and denaturation of proteins. As a good bioseparation substrate, it is necessary and indispensable to hydrophilize the gigaporous PS microspheres. Also, the hydrophilic coating should have active groups which can facilitate the substrate to be further derivatized.

There are a lot of literatures about hydrophilization of PS materials (PS latex particles, macroporous PS microspheres and nonporous PS nanoparticles). The hydrophilic coating methods mainly include physical adsorption and chemical grafting: (1) Physical adsorption coating is normally achieved by adsorbing a layer of hydrophilic polymer in advance, and the layer was further crosslinked to improve the stability of the coating. The specific surface energy of PS particles would decrease significantly after coating and therefore the non-

specific adsorption of proteins on PS particles can be effectively inhibited. (2) Chemical grafting method needs to first functionalize the benzene ring with active groups, such as hydroxyl, amino and carboxyl groups. Hydrophilic polymers can be grafted onto PS particles through classical chemical reactions. Until now, physical adsorption and chemical grafting have both turned out to be efficient.

Physical adsorption mainly has two modes at present (i.e., electrostatic adsorption and hydrophobic adsorption). For electrostatic adsorption, the surface of PS materials was negatively functionalized in advance by chlorosulfonic acid/chromic acid, then a thin organic polyamine layer, such as polyethyleneimine (PEI), can be adsorbed onto PS materials surface through ion-pairing between sulfonic acid /carboxyl groups and amine [33]. Rounds et al. prepared a PS based strong anion-exchange packing material by adsorption of PEI onto sulfonated macroporous PS microspheres [34, 35]. Performance of the resultant medium in the anion-exchange mode testifies to the effectiveness of the crosslinked PEI film in the shielding protein from the hydrophobic matrix underneath. Compared with electrostatic adsorption, the adsorption of amphiphilic polymers onto PS materials surface seems to be more eye-catching. The amphiphilic polymers can be adsorbed onto hydrophobic surface of PS materials through hydrophobic force. In most situations the adsorption style belongs to Langmuir model. The hydrophobic parts of amphiphilic polymers will tend to anchor the PS surfaces and the hydrophilic parts tend to stretch the outside. Therefore the hydrophilic modification can be realized. At present, the amphiphilic polymers reported in literatures mainly were poly (vinyl alcohol) [36-38], amphiphilic polysaccharides [39-45] and polyoxyethylene-polyoxypropylene-polyoxyethylene block copolymer [46-49]. Among them the amphiphilic polysaccharides seem to be more profitable for the further derivatization of the support due to their hydroxyl- rich sugar-rings.

Compared with physical adsorption, fewer studies about PS materials with chemical grafting polymer layers were reported [50-55], possibly due to the complicated steps and heterogeneous coatings. For chemical grafting, there are two kinds of polymer configuration on the PS materials surfaces, i.e. side-on and end-on (Figure 9). The former configuration was obtained by coupling hydrophilic polymers through side-chain group reaction, while the latter was often seen in coupling polymers through the terminal group reaction. Harris et al. compared the fibrinogen-rejecting ability and the effect on electrophoretic mobility of three polymer coatings bound to polystyrene [53]. The three polymers were side-bound dextran, end-bound dextran, and end-bound PEG. The results show that end-on PEG and side-on dextran are much more effective at reducing protein adsorption than is end-on dextran. In addition, packing density is more important than layer thickness in reducing protein adsorption. The great efficiency of small amounts of surface-bound PEG in reducing protein adsorption is consistent with the large molecular exclusion volume and heavy hydration of PEG.

Up to now most of previous works were concerned on coating of PS plate materials or nanoparticles, while few studies about adsorption of hydrophilic polymers onto PS based chromatographic porous particles are reported in literatures [38, 41]. The main challenge was the pore channels of conventional particles were easily blocked and hydrophilic macromolecules could not conveniently enter inner pores. On the contrary, the large pores of gigaporous PS microspheres could facilitate the coating with hydrophilic macromolecules. POROS microspheres have been successfully hydrophilized by coating a thin, crosslinked polymer film at the surface of the support [13, 56]. However, there is no detailed information

about how to modify the POROS microspheres probably due to trade secret. Herein we will describe our own investigation in the field of hydrophilization of gigaporous PS microspheres.

3.1. Physical Adsorption of Phenoxy Agarose on Gigaporous PS Microspheres

Agarose, a hydroxyl-rich and very biocompatible natural polymer, can not only effectively shield PS surface from hydrophobic interaction but also provide an easily derivative layer because: (1) the average molecular weight of agarose is too large (usually more than 10 kDa) to maintain the porous structure of conventional microspheres, and (2) the adsorption forces between hydrophobic materials and agarose chains are very weak, it is difficult to cover the interior surface completely with agarose. Qu et al. reported an effective way to hydrophilize gigaporous polystyrene microspheres with modified agarose (Agap) [57]. After modification, the molecular weight of agarose decreased significantly, which provided an advantage that the coating of Agap onto PS microspheres was facilitated. Also, the introduction of phenoxy groups on agarose leads to a derivative which can be adsorbed on polystyrene porous surface by means of hydrophobic sites.

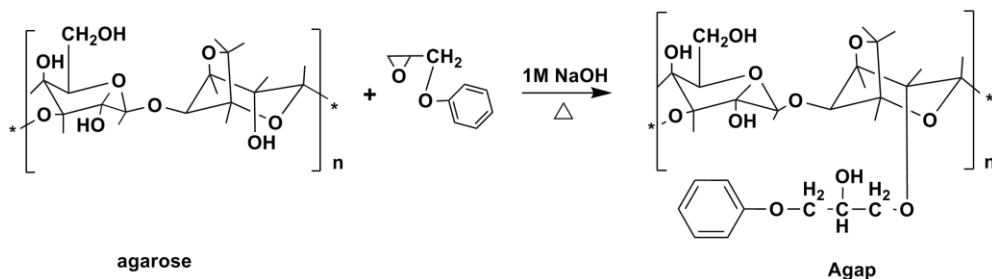


Figure 10. The fixation of phenoxy groups on agarose. (From Ref. [57] with permission).

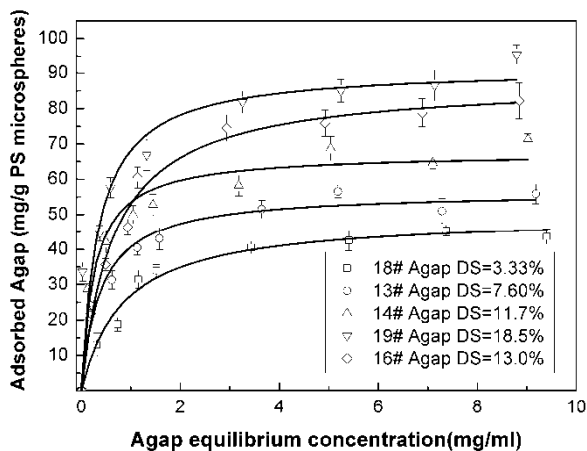


Figure 11. Adsorption isotherm of Agap on gigaporous PS microspheres. (From Ref. [57] with permission).

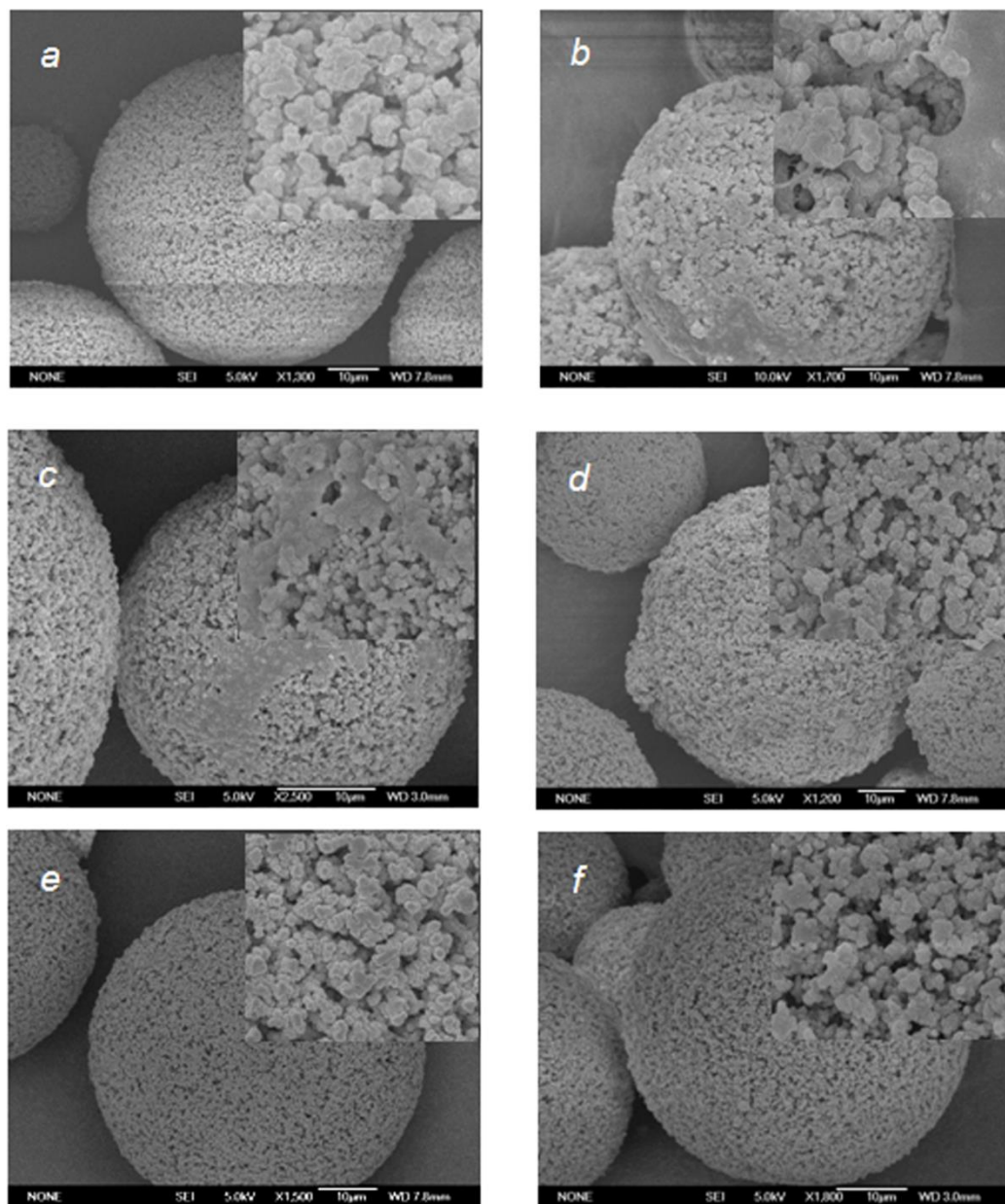


Figure 12. SEM images of gigaporous PS microspheres before and after adsorption. (From Ref. [57] with permission).

The introduction of aromatic group on agarose chains was performed according to Figure 10, and nine Agap samples with various degree of substitution (DS) were prepared. Figure 11 shows the coating amount of Agap with different DS on gigaporous PS microspheres. There was an increase in the amount of Agap adsorbed as DS increased, mainly because the adsorption forces between Agap and PS surface are hydrophobic forces, and phenoxy groups worked as hydrophobic anchors in the adsorption process.

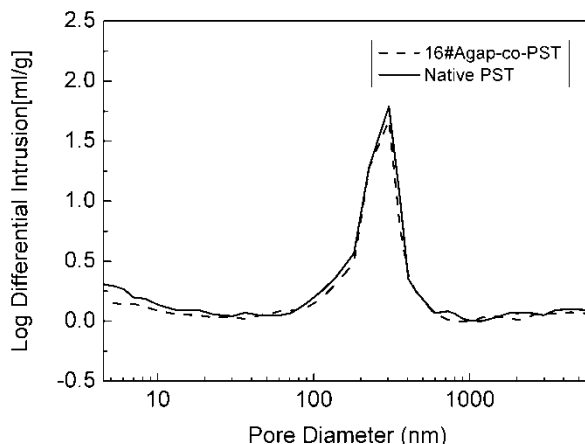


Figure 13. Pore size distribution curves of gigaporous PS microspheres before and after coating. (From Ref. [57] with permission).

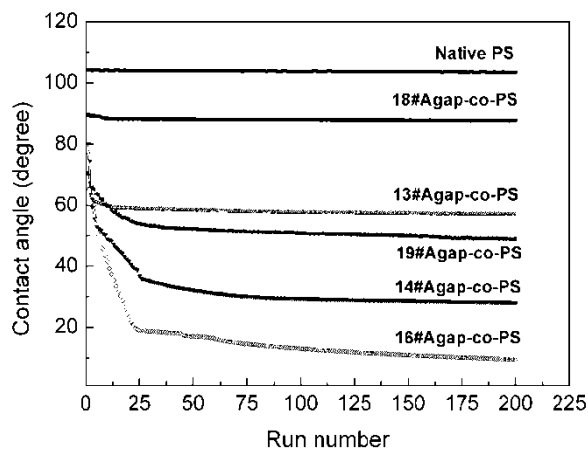


Figure 14. Dynamic contact angle of PS microspheres surface before and after coating. The DS values for 18#, 13#, 14#, 16# and 19# Agap were 3.33%, 7.60%, 11.7%, 13.0% and 18.5%, respectively. (From Ref. [57] with permission).

The SEM images of gigaporous PS microspheres coated with agarose and Agap were shown in Figure 12. When agarose was directly adsorbed onto PS microspheres, the coating was heterogeneous and agarose chains might plug the pore channels of PS microspheres. As adsorption of Agap was concerned, the same phenomena still existed when DS was lower (Figure 12 c, d). With the increase of DS (Figure 12 e, f), the aggregation of Agap on PS microspheres surface disappeared, and the coating became homogeneous. These results indicate that higher phenoxo content contributed to maintain the gigaporous structure of particles and homogeneity of the coating, which is desired as a chromatographic support.

Mercury porosimetry measurement was carried out to characterize the pore size distribution curves of gigaporous PS microspheres before and after coating. Figure 13 shows that the gigaporous structure of PS microspheres was well maintained after modification.

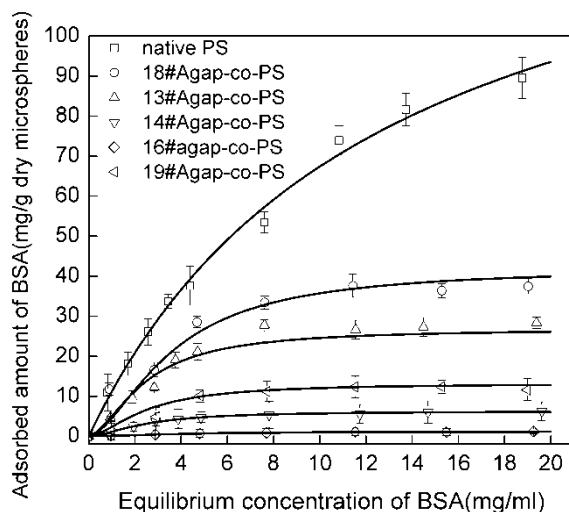


Figure 15. Adsorption isotherms of BSA on gigaporous PS microspheres before and after coating. (From Ref. [57] with permission).

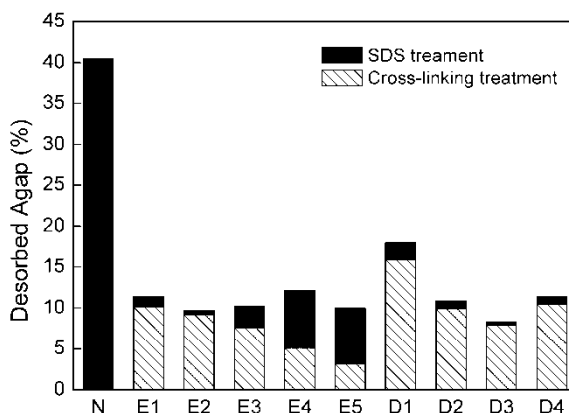


Figure 16. Relative Agap desorption from 19#-5 Agap-co-PS sample (77.48mg Agap/g PS microspheres) after cross-linking and SDS treatment. N was uncrosslinked sample. E1, E2, E3, E4 and E5 were crosslinked with EPCl (the concentration was 0.13M, 0.26M, 0.64M, 1.02M and 1.53M respectively). D1, D2, D3 and D4 were crosslinked with EDGE (the concentration was 0.13M, 0.32M, 0.64M and 0.93M, respectively). (From Ref. [57] with permission).

The hydrophilicity of gigaporous PS microspheres was evaluated by dynamic contact angle measurement and protein adsorption experiment [58, 59]. After coating, the contact angle of all samples decreased significantly (Figure 14). This indicates that the hydrophilicity of microspheres surface increased greatly. The contact angle of particles after coating decreased firstly and then rose again with the increase of DS, indicating there are optimum numbers of phenoxy groups on Agap chains. When DS was lower (lower than 13.0), the Agap chains cannot cover the PS surface sufficiently and the coating layer were loosely packed. For higher DS (higher than 18.5), the coating was packed tightly but excess phenoxy groups

would expose on the coating layer. Correspondingly, the hydrophilicity of PS surface would decrease again.

In protein adsorption experiment, bovine serum albumin (BSA) was chosen to evaluate the surface hydrophilization efficiency of microspheres after modification (Figure 15). The amount of BSA absorbed on microspheres decreased sharply after coating, which was ascribed to the surfaces of PS microspheres masked well by hydrophilic agarose chains. The adsorbed amount of BSA on 16# Agap-co-PS sample at the plateau (1.18mg/g dry microspheres) was 75.8 times lower than that of PS microspheres (89.55mg/g dry microspheres). Compared with the dynamic contact angle of particles, it was found that there was a consistency with the protein adsorption and microspheres surface hydrophobicity, i.e., the adsorbed amount of proteins on Agap-co-PS microspheres surface decreased firstly and then increased again with the increase of phenoxy content.

In order to avoid desorbing of Agap coatings in the later application, the coatings were chemical crosslinked with epichlorohydrin (EPCl) and ethylene glycol diglycidyl ether (EDGE), respectively. The stability of the coatings was evaluated by immersing the particles into 2% sodium dodecyl sulfate solution (SDS) at 50 °C for 24h. It was suggested that the performance of EDGE is better than that of EPCl, and the optimum concentration of EDGE was 0.64M at 25 °C in 0.4M NaOH (Figure 16, D3 group, the total amount of relative desorbed Agap was 8.33%).

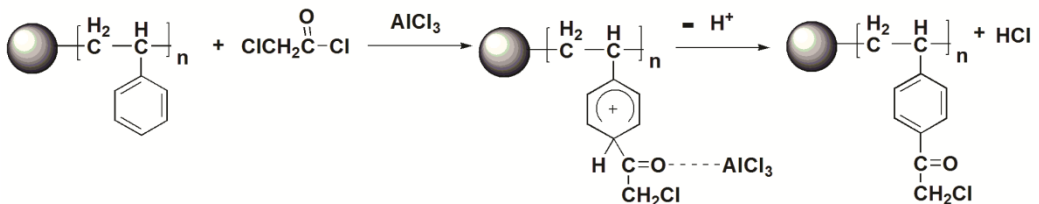


Figure 17. Chloroacetylation of gigaporous PS microspheres. (From Ref. [60] with permission).

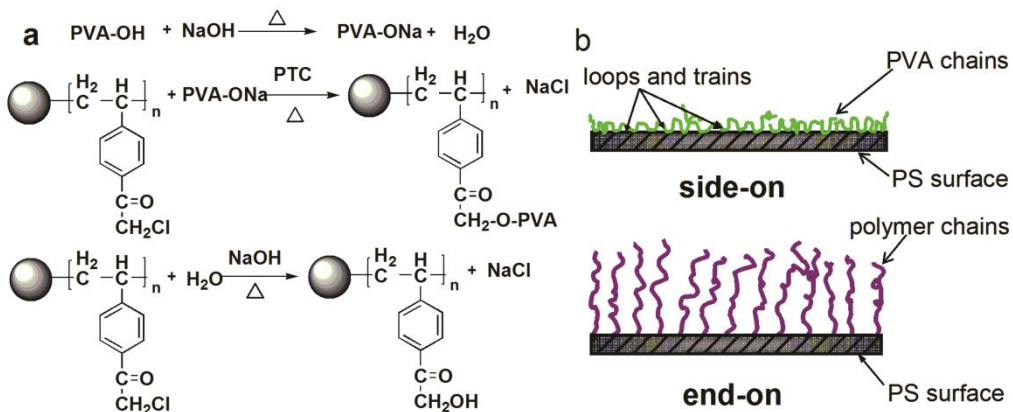


Figure 18. (a) Reacting route of PS-Cl coupled with PVA and (b) the side-on and end-on configuration of polymer chains on PS microspheres surfaces. (From Ref. [60] with permission).

In summary, the hydrophilicity and biocompatibility of gigaporous PS microspheres were greatly enhanced after modification, while the gigaporous structure can be well maintained. The non-specific adsorption of proteins was nearly reduced to zero through the optimization of both the phenoxy content and the cross-linking conditions of adsorbed layer. This study provided a hydrophilic chromatographic support for different types of chromatography such as ion-exchange or affinity chromatography since the agarose coatings may be easily derivatized by classical methods.

3.2. Chemical Grafting Poly (Vinyl Alcohol) (PVA) on Gigaporous PS Microspheres

With physical adsorption there is a problem of coating desorption over time. In order to obtain a permanent hydrophilic coating, Ma et al. have attempted to hydrophilize the gigaporous PS microspheres using PVA and chemical grafting [60]. PVA is also a hydroxyl-rich and very biocompatible polymer, not only can effectively shield the PS surface from hydrophobic interactions, but also provide a layer that can be easily derivatized. The gigaporous PS microspheres were chloroacetylated through Friedel-Crafts acetylation with chloroacetyl chloride (Figure 17), and modified with hydrophilic PVA through Williamson reaction afterwards (Figure 18). Because all the hydroxyl groups along the PVA chains are reacting sites, which is unlike coupling PEG through terminal group reaction, the configuration of PVA chains on PS microspheres surface is side-on but not end-on. The side-on configuration of PVA chains is favorable to maintain the gigapore structures of PS microspheres (Figure 19).

Table 1 presents the amount of coupled PVA under various conditions (temperature, time, base amount, PVA concentration and phase transfer catalyst). Because the reaction was in a heterogeneous system, phase transfer catalyst played an important role in this reaction. Among other factors, the control of temperature seemed to be very critical. Whether the temperature was higher or lower than 70 °C, the amount of coupled PVA both reduced. The amount of NaOH is also crucial for the reaction. Insufficiency of NaOH led to incomplete reaction of chloroacetyl groups, while over loading of NaOH resulted in dehydration of PVA chains. For reacting time, the coupling amount of PVA basically reached to stabilization when the reaction proceeded to 24 h later. Finally, we found exorbitant concentration of PVA (25 mg/ml) was neither necessary nor economical, and coupling amount of PVA also came to 110.6 mg/g (31#-39) when the concentration of PVA reached 10 mg/ml.

The composition of gigaporous PS microspheres before and after modification was characterized by Fourier transform infrared (FT-IR) spectra (Figure 20) and X-ray photoelectron spectroscopy (XPS) (Figure 21) respectively. In the spectrum of PS-PVA, the intensity of peak at 3433 cm^{-1} was greatly increased, the absorption peaks present at the 1114 cm^{-1} indicated the C-O-C asymmetric stretching vibration, and the absorption peak at 647 cm^{-1} (C-Cl stretching vibration) disappeared. For XPS C1s spectrum of PS-PVA, peak area ratio of Peak2 (C-O-C/C-OH, 286.1eV)/Peak1 (C-C/C-H, 284.7eV) increased to 0.55, but peak area ratio of Peak3 (O-C=O, 288.3eV)/Peak1 declined to 0.099. The results both confirmed that PVA had been successfully coupled onto PS microspheres.

Table 1. The amount of PVA coupled onto PS microspheres under various reactive conditions [60]

Run ^a	Catalyst ^b	Temperature (°C)	Reacting time (h)	Amount of NaOH ^c	PVA concentration (mg/ml)	Amount of coupling PVA(mg/g dry resin)	Specific surface area(m ² /g)
30#-1	/	70	24	5	25	39.7	24.34
30#-2	TBAB	70	24	5	25	65.2	24.19
31#-6	TBAB	70	24	8	25	108	22.49
31#-17	TBAB	70	24	2	25	22.8	24.51
31#-13	TBAB	70	24	8	25	115.5	22.08
31#-16	TBAB	70	24	15	25	95.2	23.15
31#-20	TBAB	40	24	8	25	68.5	24.07
31#-22	TBAB	85	24	8	25	71.8	23.44
31#-25	TBAB	70	6	8	25	70.3	23.89
31#-30	TBAB	70	18	8	25	103.9	22.57
31#-32	TBAB	70	30	8	25	115.0	22.50
31#-34	TBAB	70	24	8	5	74.2	23.54
31#-39	TBAB	70	24	8	10	110.6	22.37
31#-44	TBAB	70	24	8	10	91	23.64
31#-45	TBAB	70	24	8	10	97.4	23.38
31#-46	TBAB	70	24	8	10	95.3	23.30
31#-47	TBAB	70	24	8	10	96.5	23.21
32#-1	TBAB	70	24	8	25	42.4	126.86

^a The type of PVA coupled onto samples in Table 2 is PVA13000~23000 except 31#-44 (PVA2000), 31#-45 (PVA22000) and 31#-46 (PVA9000~10000).

^b Amount of catalyst is 0.5 times of chloride molar content in PS-Cl.

^c Feed quantity of NaOH is on the basis of chloride content of PS-Cl (molar ratio). The chloride content of 30#, 31# and 32#PS-Cl is 14.52%, 14.57% and 14.02% respectively.

^d For 30#-1, 2, 31#-17, 25, 30 samples, there were residual ester group (confirmed by FT-IR) and residual chloride on PS-PVA. In order to avoid experimental errors, they are further hydrolyzed at 80°C in 8wt% NaOH solution for 4h.

^e 32# macroporous PS microspheres was chose as control experiment, the average pore diameter was about 30nm (10~50nm range), and the specific surface area was 269.5m²/g.

The hydrophilicity of the gigaporous PS microspheres before and after modification was also evaluated by BSA adsorption experiment. Figure 22 shows the BSA amount adsorbed on microspheres decreased sharply after modification, which was contributed to the hydrophilic surfaces of modified PS microspheres masked well by PVA chains. The adsorbed amount of BSA on 31#-45 sample at the plateau (7.72 mg/g dry microspheres) was 12.5 times lower than that of PS microspheres (89.55 mg/g dry microspheres). In addition, the adsorbed amount of proteins decreased gradually along with the increase of PVA molecular weight, which was also corresponded to the coupled amount of PVA on PS microspheres. Compared with the adsorbed amount of BSA on Agap-co-PS (1.18 mg/g) microspheres, however, the adsorbed amount of BSA on PS-PVA (7.72 mg/g) is not satisfied. This indicates that the natural polysaccharides turn out to be excellent for the hydrophilization of hydrophobic gigaporous PS particles.

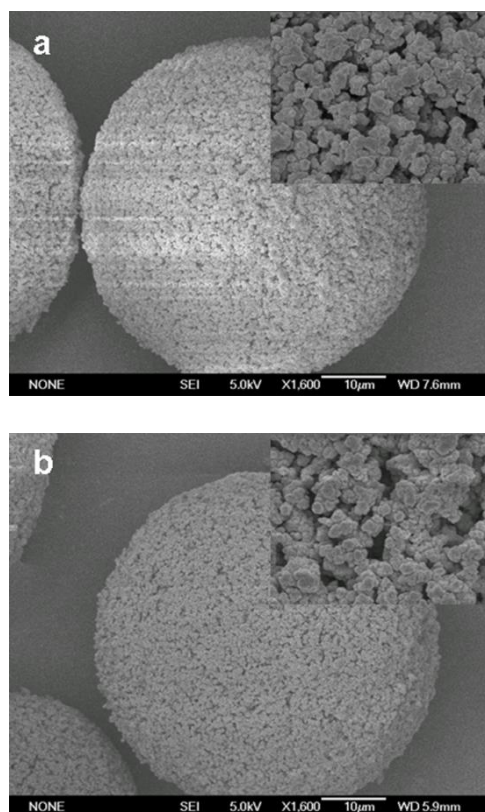


Figure 19. SEM images of microscopic morphology of (a) PS microspheres and (b) 31#-6 PS-PVA. (From Ref. [60] with permission).

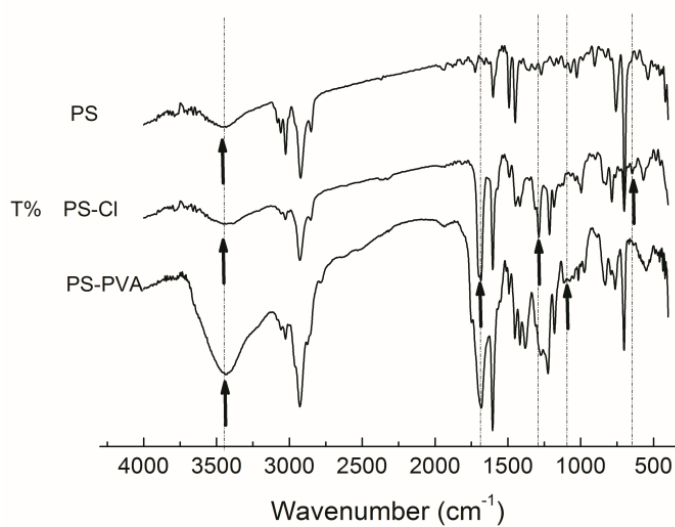


Figure 20. FT-IR spectra of PS microspheres, 31# PS-Cl and 31#-13 PS-PVA. (From Ref. [60] with permission).

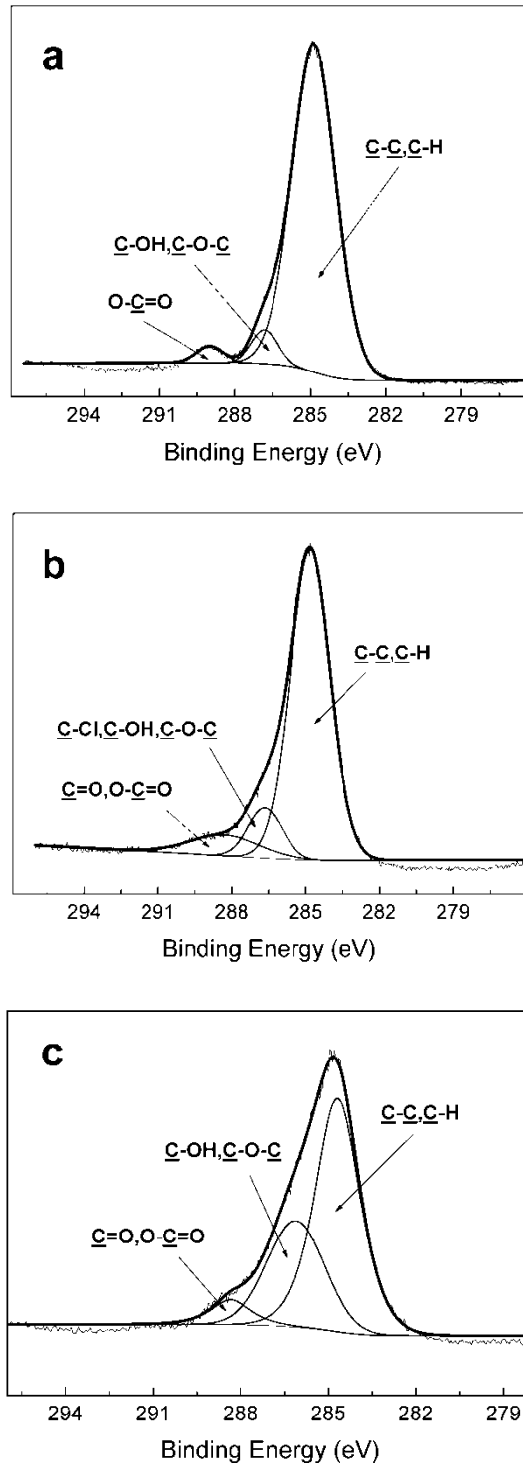


Figure 21. Characteristic C1s XPS curves for (a) PS, (b) 31# PS-Cl (chloride content is 14.57 wt. %), and (c) 31#-13 PS-PVA surfaces. (From Ref. [60] with permission).

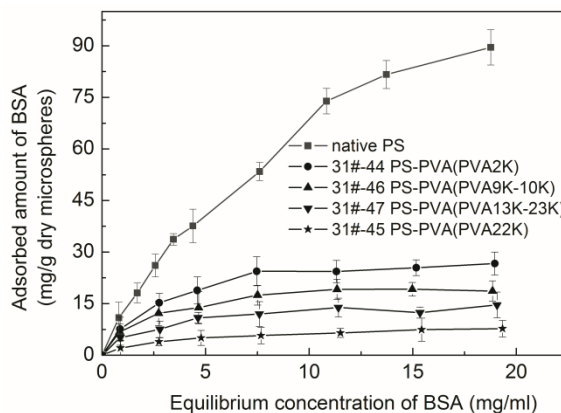


Figure 22. Adsorption isotherm of BSA on PS microspheres before and after coupling PVA at pH7.4, temperature 25 °C. (From Ref. [60] with permission).

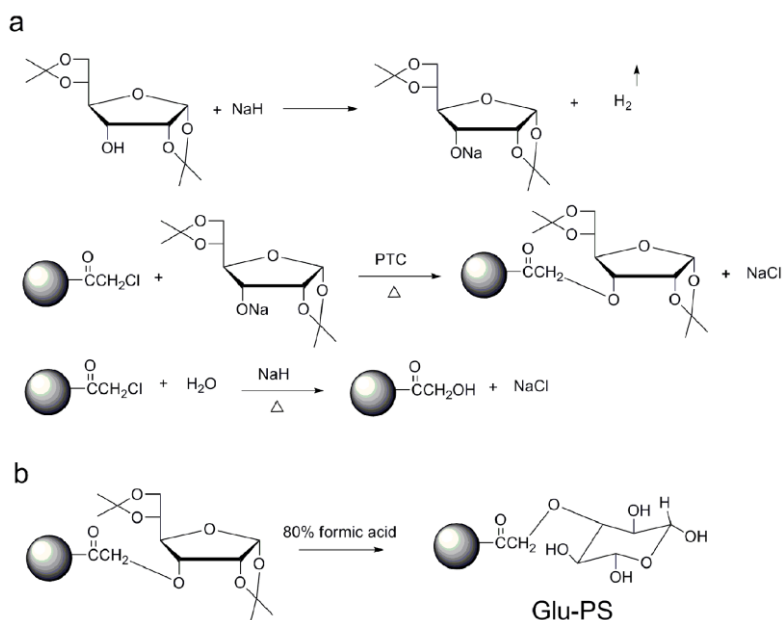


Figure 23. (a) Reaction mechanism of PS-Cl coupled with DAGlu and (b) the transformation of DAGlu-PS into Glu-PS. (From Ref. [61] with permission).

3.3. Chemical Coupling Saccharide on Gigaporous PS Microspheres

Natural polysaccharides have turned out to be more biocompatible than man-made synthetic polymers in our previous study [57, 60]. In order to obtain a permanent hydrophilic coating, chemical coupling saccharide seems to be a smart way. Recently Qu et al. reported the hydrophilization of gigaporous PS microspheres with natural saccharide as high-speed protein chromatography base support [61]. The microspheres were chloroacetylated according to the method we reported previously [60], and then coupled with diacetone-D-glucose

(DAGlu) through the Williamson reaction, and the protecting groups were removed on DAGlu (Figure 23).

Table 2. The amount of DAGlu coupled onto PS-Cl under various reactive conditions [61]

Run	Catalyst ^a	Temperature (°C)	Reacting time (h)	DAGlu Concentration (mol/l)	Amount of NaH ^b	Amount of coupling DAGlu (mmol/g resin)
7#	/	70	24	0.08	4	0.185
28#	TBAB	70	24	0.08	4	0.637
29#	TBAB	70	24	0.11	4	0.701
30#	TBAB	70	24	0.13	4	0.779
31#	TBAB	70	24	0.16	4	0.660
37#	TBAB	40	24	0.13	4	0.292
38#	TBAB	50	24	0.13	4	0.439
40#	TBAB	60	24	0.13	4	0.593
39#	TBAB	80	24	0.13	4	0.488
33#	TBAB	70	24	0.13	2	0.493
35#	TBAB	70	24	0.13	3	0.630
36#	TBAB	70	24	0.13	5	0.573
42#	TBAB	70	6	0.13	4	0.476
43#	TBAB	70	12	0.13	4	0.680
48#	TBAB	70	18	0.13	4	0.718
47#	TBAB	70	30	0.13	4	0.775

^a Amount of catalyst is 0.5 times of chloride molar content in PS-Cl. The chloride content of PS-Cl is 14.05%.

^b Feed quantity of NaH is on the basis of DAGlu (molar ratio).

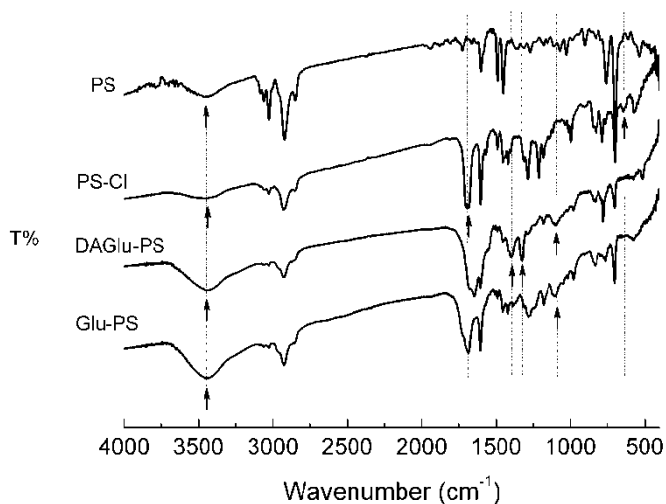


Figure 24. FT-IR spectra of PS microspheres, PS-Cl, DAGlu-PS and Glu-PS. (From Ref. [61] with permission).

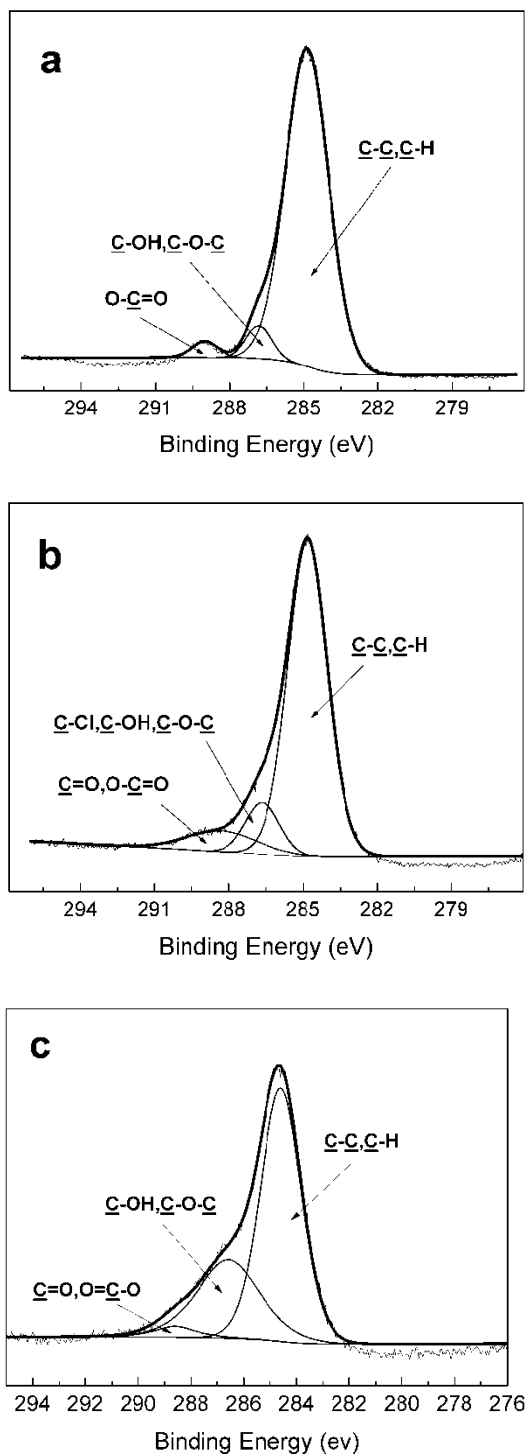


Figure 25. Characteristic C1s XPS curves for (a) PS microspheres, (b) PS-Cl and (c) 30# Glu-PS surface. (From Ref. [61] with permission).

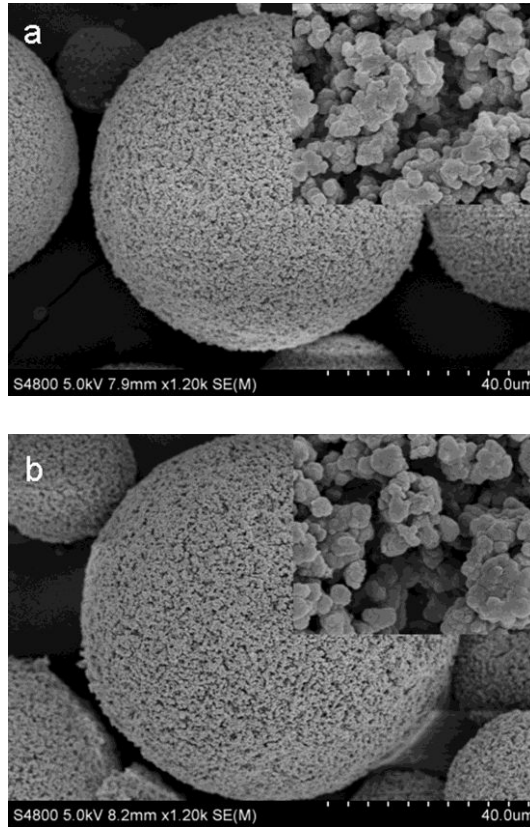


Figure 26. SEM images of microscopic morphology of (a) PS microspheres and (b) 30# Glu-PS. (From Ref. [61] with permission).

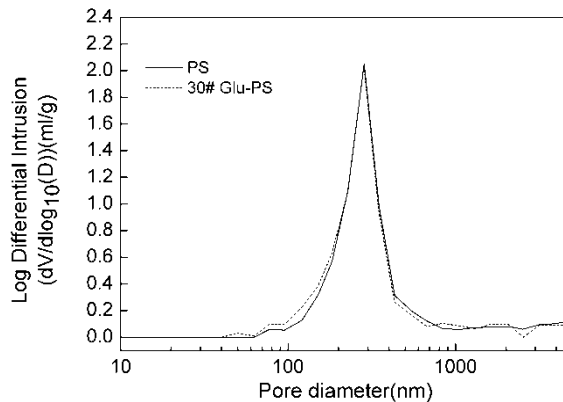


Figure 27. Pore size distribution curves of gigaporous PS microspheres before and after coating. (From Ref. [61] with permission).

Like coupling PVA, the effect of reactive conditions on the amount of DAGlu coupled onto gigaporous PS microspheres was also investigated (Table 2). Phase transfer catalyst still played an important role in the reaction. The optimal temperature was 70 °C due to lower temperature would lead to reduced activity of hydroxyl group on DAGlu with NaH, while

higher temperature would facilitate the occurrence of side reaction, i.e., hydrolysis of chloroacetyl groups. For NaH, there also exists an optimal quantity (30#). Lower addition (33#, 35#) led to incomplete reaction of chloroacetyl groups, while higher addition (36#) resulted in the hydrolysis of chloroacetyl groups. The coupling amount of DAGlu reached a plateau after 24 hrs in the proper concentration of DAGlu (0.13M).

FT-IR spectra (Figure 24) and XPS (Figure 25) were utilized to testify the composition changes of gigaporous PS microspheres before and after modification. Like coupling PVA, the results confirmed that glucose had been successfully coupled onto PS microspheres. SEM images and mercury porosimetry measurement suggested that there were no obvious changes on the pore morphology between these two kinds of particles, and the gigaporous of Glu-PS was well maintained (Figure 26, 27). This indicated that the glucose coatings did not block the pore channels of PS microspheres, which is a desirable feature for chromatographic supports.

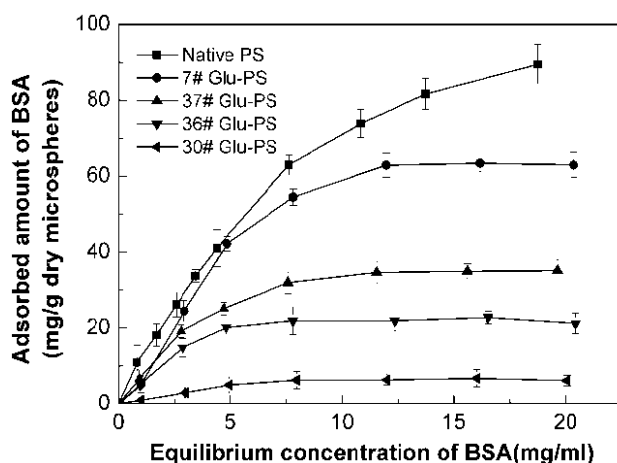


Figure 28. Adsorption isotherm of BSA on PS microspheres before and after modification at pH7.4, temperature 25°C. (From Ref. [61] with permission).

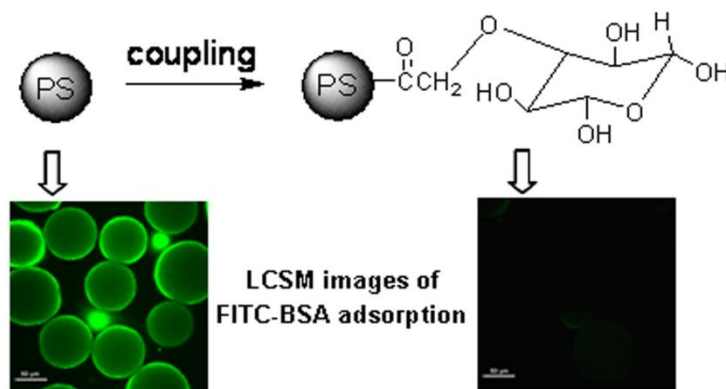


Figure 29. LCSM images of (a) PS and (b) 30# Glu-PS microspheres after incubated with FITC-BSA. (From Ref. [61] with permission).

Compared with physical adsorption of Agap and chemical grafting PVA, the effect of shielding protein from the hydrophobic PS underneath with chemical coupling glucose is medium. Figure 28 shows the adsorption isotherm of BSA on microspheres before and after modification. The adsorbed amount of BSA on 30# Glu-PS sample at the plateau was 6.86 mg/g dry microspheres, which is higher than Agap-co-PS (1.18 mg/g) and lower than PS-PVA (7.72 mg/g) microspheres. The results indicate that polysaccharide has some advantages over the smaller glucose molecule in masking the hydrophobic surface. Chemical grafting of polysaccharide on PS microspheres is now in progress in our laboratory.

The hydrophilicity of PS microspheres and Glu-PS was also evaluated by adsorption of FITC-BSA at 25 °C. As shown in Figure 29, strong fluorescence from the BSA was observed on the native PS microspheres, while little fluorescence was detected in Glu-PS. This comparative study also confirms that the adsorption of BSA on PS microspheres decreases strongly after modification, i.e., the hydrophobic surface of PS microspheres is effectively masked after coupling with glucose.

4. APPLICATIONS TO PROTEIN SEPARATION

With the quick development of biotechnology, more and more bioproducts with large molecule size such as proteins and plasmid DNA need to be separated. Gigaporous PS microspheres, with their inherent characteristics, are very promising in high-speed separation and purification of proteins, peptides and nucleotides to preparative scale. POROS media have been functionalized and run in different perfusion chromatography modes used for proteins and peptides: reversed-phase, ion-exchange, hydrophobic interaction, and affinity [5, 13, 21-23, 62-64]. Compared with conventional chromatographic supports, the bimodal pore distribution of POROS media enables intraparticle convection of biomacromolecules, which can separate the biomacromolecules in shorter analysis times without compromising resolution and loading capacity. The theory developed for perfusion chromatography derived that efficiency of a separation and loading capacity was independent of the flow velocity. Furthermore, perfusion supports present much higher efficiencies at high mobile phase velocities than conventional supports. The reduced plate height is only weakly dependent on the flow-rate in perfusive supports. Garcia et al. have reviewed the perfusion chromatography from characteristics, theory and media composition of perfusion chromatography to experimental conditions used in perfusion chromatography [62]. In addition, there are few reports recently about application of POROS in protein separation. Therefore, the applications of POROS media in various perfusion chromatography modes will not be discussed anymore. Our recent findings of gigaporous PS microspheres used in ion-exchange and immobilized-metal affinity chromatography are discussed below.

4.1. Ion-Exchange Chromatography

Using agarose coated gigaporous polystyrene microspheres as a base support, Ma et al. developed a novel anion exchanger (DEAE-AP) in high-speed protein separation. DEAE groups were introduced onto Agap-co-PS microspheres according to the method reported by

Wang and Su [65, 66]. The gigaporous structure, static adsorption behavior, and chromatographic properties of DEAE-AP medium were characterized and compared with those of commercial available resin DEAE Sepharose Fast Flow (DEAE-FF).

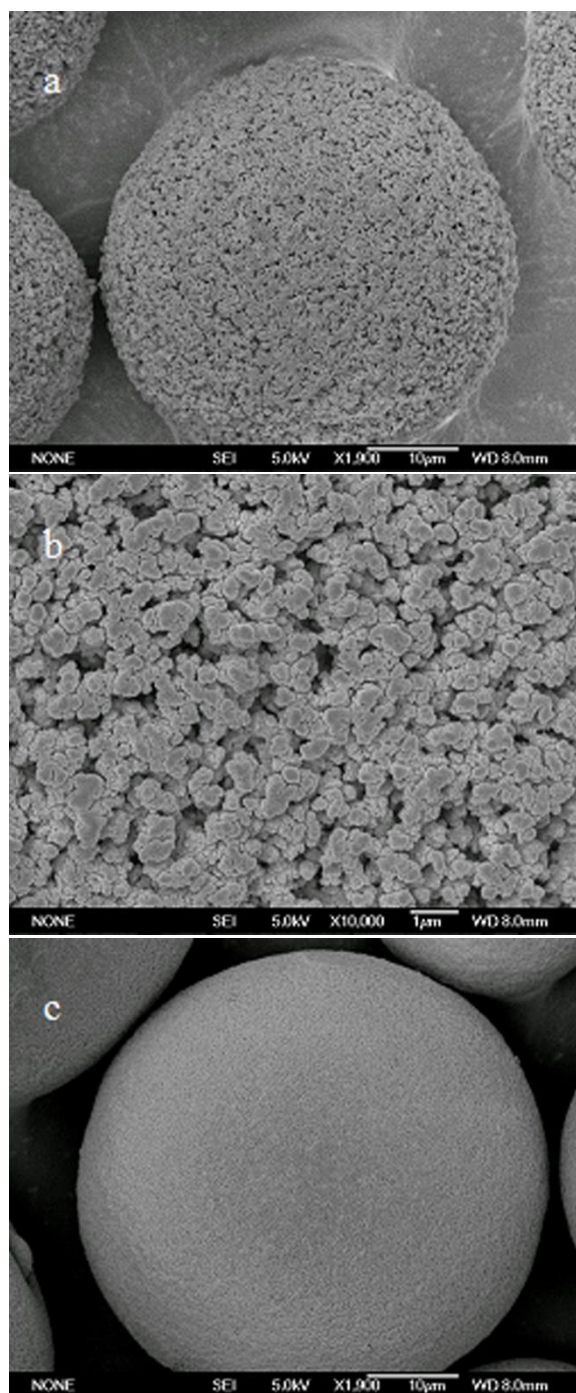


Figure 30. (Continued).

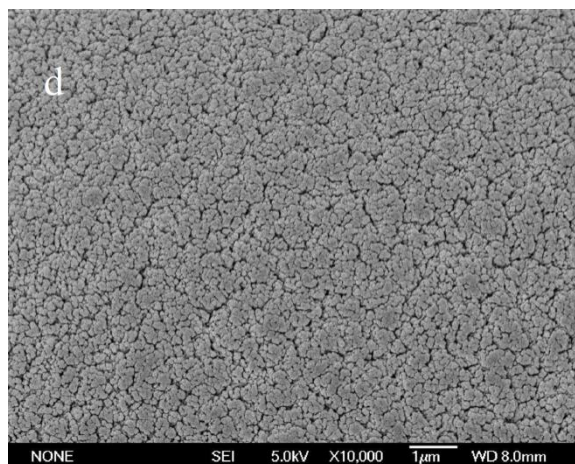


Figure 30. SEM images of DEAE-AP (a, 1900×; b, 10,000×) and DEAE-FF (c, 1900×; d, 10,000×) microspheres. (From Ref. [65] with permission).

Table 3. Physical properties of DEAE-FF and DEAE-AP media [65]

Media	\bar{n}_w (mg/ml)	Water content (%)	Anion exchange capacity (mmol/ml)	$\bar{\alpha}_p^a$ (-)	K (m ²) × 10 ¹⁰
DEAE-FF	1.02	90.18	0.1365	0.491	0.83
DEAE-AP	1.03	62.76	0.1336	0.599	2.77

^a Effective porosity for BSA.

SEM images of DEAE-AP and DEAE-FF microspheres at different magnifications are shown in Figure 30. It was suggested that there was significant difference on pore structure between DEAE-AP and DEAE-FF particles. At larger magnification, some highly reticular gigapores larger than 500 nm can be observed on DEAE-AP microspheres (Figure 30b) as compared with the small pores on DEAE-FF microspheres (Figure 30d). Consequently, the effective porosity of DEAE-AP microspheres for BSA was about 22% higher than that of DEAE-FF microspheres (Table 3). These gigapores in DEAE-AP microspheres are expected to provide an interconnected path for convective flow in chromatography.

The mechanical stability and permeability of DEAE-AP and DEAE-FF microspheres were evaluated through flow hydrodynamics, and the bed permeability (K) can be calculated by the Darcy's law in a laminar flow region [67].

$$K = \frac{\mu u L}{\Delta P} \quad (1)$$

where μ is the viscosity of the mobile phase (Pa·s), u the superficial velocity (cm/s), L the length of column (cm), and ΔP the column pressure-drop (Pa). Figure 31 shows the effect of flow velocity on the back pressures of DEAE-FF and DEAE-AP columns. The linear relationship was obtained on DEAE-AP column for flow velocity up to 3612 cm/h, while on DEAE-FF column the flow velocity was only up to 1668 cm/h owing to DEAE-FF resins' low mechanical stability. Moreover, it can be seen that the back pressure of DEAE-AP

column was much lower than that of DEAE-FF column under the same flow velocity. Correspondingly, the value of K for DEAE-AP column was 3.34 times higher than that for DEAE-FF column (Table 3). The lower back pressure of DEAE-AP column is an evidence for the presence of flow-through pores which reduced the flow resistance. It has been confirmed that mobile phase in the column flowed not only through the spaces between matrix but also through the gigapores of particles in previous study [57], i.e. the existence of through pores in gigaporous microspheres. For DEAE-AP column, we calculated 63.38% of flow was through the inter-spaces between the particles, and about 36.62% of the flow was possibly through the intra-pores of the particles, which can not only induce convective flow within particles but also greatly shorten the diffusive distance from outer particle to inner particle.

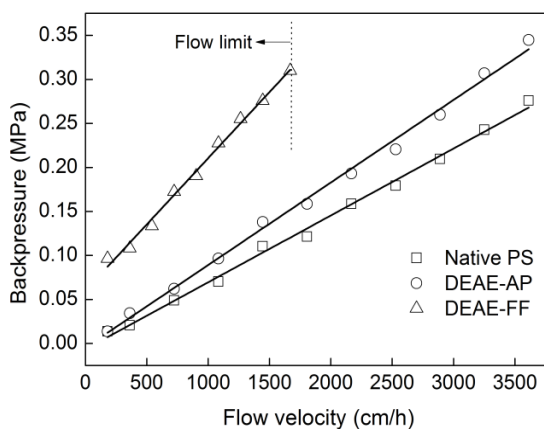


Figure 31. Relationship between the column back pressure and flow velocity. Column, 100×4.6 mm i.d.; mobile phase, high-purity water. (From Ref. [65] with permission).

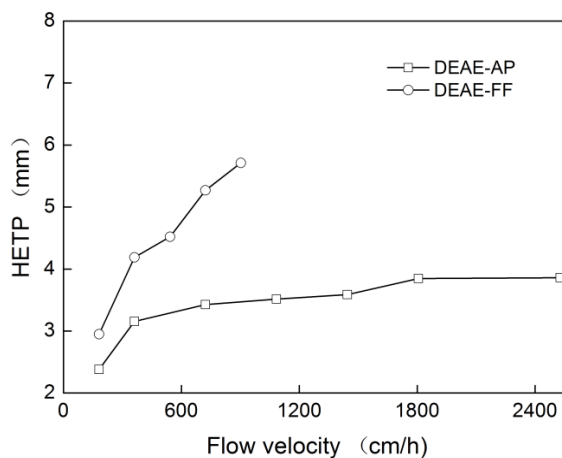
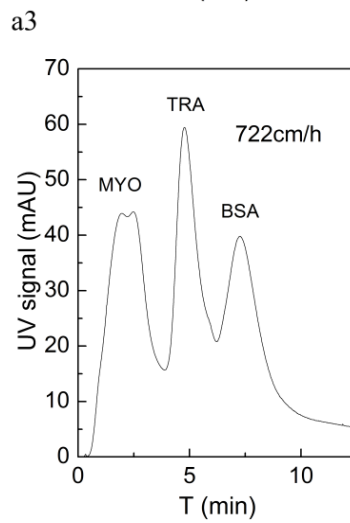
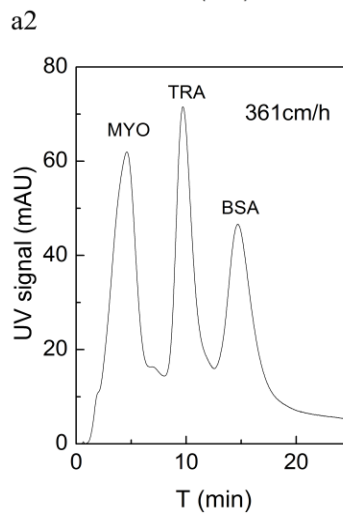
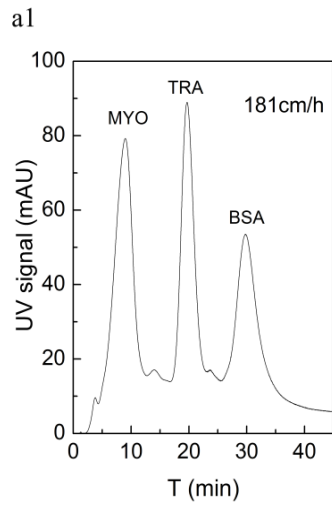


Figure 32. Column efficiency versus flow velocity. Column, 100×4.6 mm i.d.; sample, 2 mg/ml BSA; mobile phase, 1mol/l NaCl in 20 mM Tris-HCl buffer, pH8.0. (From Ref. [65] with permission).



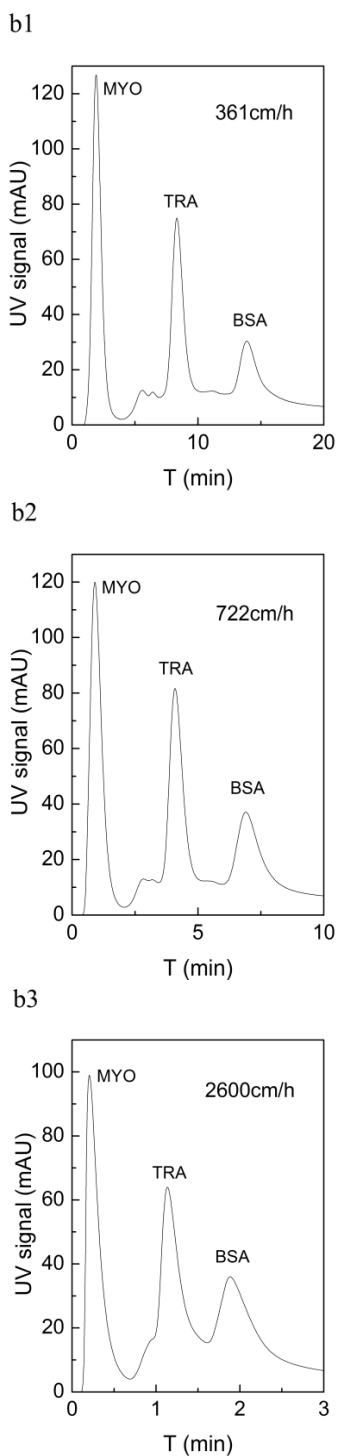


Figure 33. Separation of modern proteins on (a) DEAE-FF column and (b) DEAE-AP column. Column, 100mm×4.6mm I.D.; 20mMTris–HCl buffer, pH 8.0; injection size, 100 μ l; linear gradient, 100% buffer A to 50% buffer B in 30ml eluate; protein concentrations: myoglobin 5 mg/ml, transferrin 5mg/ml, BSA 10mg/ml. (From Ref. [65] with permission).

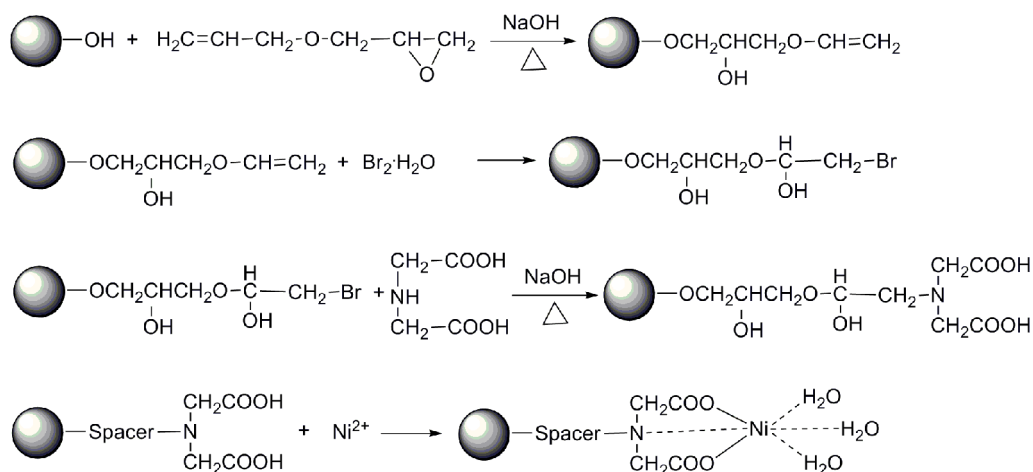


Figure 34. Synthetic route of immobilized-nickel affinity chromatography medium. (From Ref. [69] with permission).

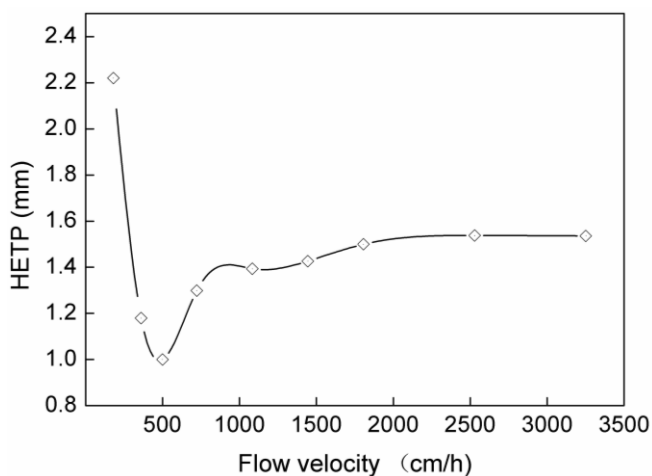


Figure 35. Column efficiency versus flow velocity. Column, 100×4.6 mm I.D.; sample, 2 mg/ml BSA; mobile phase, 20 mM sodium phosphate, 500 mM NaCl, 500 mM imidazole, pH 7.4. (From Ref. [69] with permission).

HETP (the height equivalent to a theoretical plate) is a typical criterion to describe the overall column efficiency. The advantage of intraparticle convective mass transfer to diffusive mass transfer can be seen in Figure 32. For DEAE-FF columns, HETP rapidly increased with the increase of flow velocity, which is in accordance with the Van Deemter equation [68]. It indicates that the mass transfer resistance in the DEAE-FF resins was dominated by the intraparticle term. However, the HETP of DEAE-AP column was nearly independent of flow velocity in a wide range of flow velocities (up to 2528 cm/h). The presence of flow-through pores in DEAE-AP microsphere contributed to intraparticle convective mass transfer for BSA and significantly lessened the stagnant mobile phase mass transfer of particle by reducing the diffusive distance.

The superiority of DEAE-AP column in retention mapping was shown in Figure 33. It can be seen in Figure 33 that individual separation of the mixture in question can be achieved

at the mobile phase velocity up to 2600 cm/h within 3 min. For DEAE-FF column, however, the resolution decreased significantly with the increase of the flow velocity. At the flow velocity of 722 cm/h, the separation chromatogram changed markedly, which indicates that the column probably slightly collapsed and formed flow channeling owing to the poor mechanical strength of agarose beads.

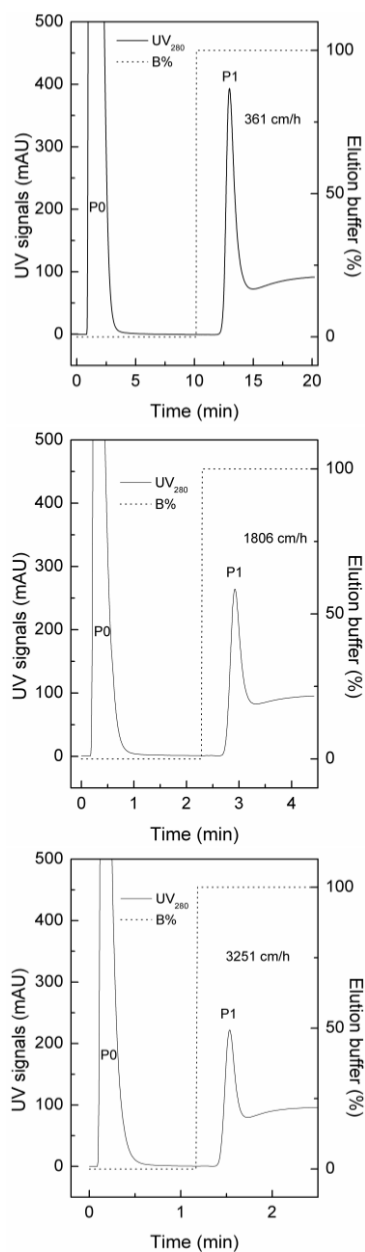


Figure 36. Chromatograms of SOD on APS-Ni column under different flow velocities. Column, 100×4.6 mm i.d.; 20 mM sodium phosphate, 500 mM NaCl, 100 mM imidazole, pH 7.4; injection size, 100 μ l; step gradient, 100% buffer A to 100% buffer B after washing step; P0, breakthrough peak; P1, elution peak. (From Ref. [69] with permission).

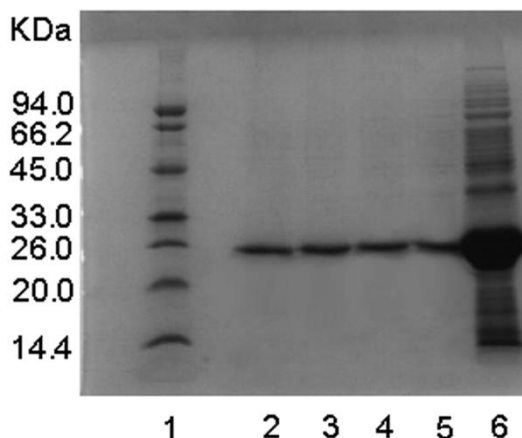


Figure 37. SDS-PAGE analysis of SOD samples purified from crude enzyme solution under different flow velocities. Lanes: 1, molecular weight marker; 2, 3, 4 and 5 is SOD sample purified under flow velocities of 361, 1084, 1806 and 2528 cm/h, respectively; 6, feedstock. (From Ref. [69] with permission).

4.2. Immobilized-metal Affinity Chromatography (IMAC)

IMAC medium (APS-Ni) was derivatized from agarose coated gigaporous polystyrene microspheres by classical surface chemistry in four steps (Figure 34). The amount of chelated ions on particles was $40.5 \mu\text{mol/ml}$ medium. After packing the bed permeability (K) of APS-Ni column is $2.71 \times 10^{-10} \text{ m}^2$, which is 3.26 times higher than DEAE-FF column [65, 69].

BSA was used as a probe and the HETP of APS-Ni column was measured under the non-retained condition (Figure 35). When the flow velocity was lower than 500 cm/h, HETP exhibited a typical curve defined by the Van Deemter equation, which indicated that the longitudinal diffusion occupies dominant effect in this regime. However, when the flow velocity was higher than 500 cm/h, the HETP of APS-Ni was nearly independent of flow velocity up to 3250 cm/h. This is accordance with POROS and DEAE-AP media, which was ascribed to convective mass transfer of through pores in the particles.

Figure 36 shows the chromatograms of superoxide dismutase (SOD) from *E. coli* feedstock on APS-Ni column under different flow velocities. It is seen in Figure 36 that the APS-Ni column can purify SOD within 2 min at velocity up to 3251 cm/h. In electrophoretogram all the purified SOD samples exhibit one major band near 24 kDa, which is consistent with the primary band in the feedstock (Figure 37). The average purification fold, SOD recovery and purity were 16.4, 95.6 % and 84 %, respectively. At a flow velocity of 3251 cm/h, the SOD recovery and purity can still reach 89.6 % and 79 %, respectively.

CONCLUSION

Gigaporous PS microspheres, with excellent mechanical strength, good chemical stability and high mass transfer rate, are of increasing interest to chromatographers in recent years. After proper hydrophilization and derivatization, these particles can be used as high-speed

protein chromatography packing materials in both preparative and analytical modes. The gigapores of microspheres enable intraparticle convection and accelerated mass transfer rate, making possible the separation of biomacromolecules with high molecular weights in shorter analysis times than with conventional chromatographic supports without compromising resolution and loading capacity. Accelerated mass transfer induced by convective flow of mobile phase through the gigapores in the media has been demonstrated by their high column efficiency and high protein resolution at high flow velocity. In conclusion, the gigaporous PS microspheres are very promising in high-speed protein chromatography, which has significant implications for analysis, on-line monitoring and scale-up, etc.

Of course, as with other relatively new fields, much more is expected to be accomplished in the near future. The methods of hydrophilization of gigaporous PS microspheres, no matter physical adsorption or chemical grafting, are relative complicated and high-cost. Particularly promising would be the preparation of hydrophilic gigaporous PS microspheres in one-pot polymerization. Preparation of dual-pore hydrophilic PS microspheres is now in progress in our laboratory.

ACKNOWLEDGMENTS

We would like to thank the financial support of National Natural Science Foundation of China (No. 21176257), the Natural Science Foundation of Shandong Province (No. ZR2010BM001), the key Science and Technology Program of Qingdao Economic & Technical Development Zone, and the Fundamental Research Funds for the Central Universities.

REFERENCES

- [1] A. Jungbauer. Chromatographic media for bioseparation. *J. Chromatogr. A*, 2005, 1065, 3-12.
- [2] G. Y. Sun, Q. H. Shi, Y. Sun. Novel biporous polymeric stationary phase for high-speed protein chromatography. *J. Chromatogr. A*, 2004, 1061, 159-165.
- [3] J. Porath, P. Flodin. Gel filtration: A method for desalting and group separation. *Nature*, 1959, 183, 1657-1659.
- [4] L. E. Weaver Jr, G. Carta. Protein adsorption on cation exchangers: Comparison of macroporous and gel-composite media. *Biotechnol. Progr.*, 1996, 12, 342-355.
- [5] N. B. Afeyan, N. F. Gordon, L. Mazasaroff, L. Varady, S. P. Fulton, Y. B. Yang, F. E. Regnier. Flow-through particles for the high-performance liquid chromatographic separation of biomolecules, perfusion chromatography. *J. Chromatogr.*, 1990, 519, 1-29.
- [6] M. C. Garcia, M. L. Marina, M. Torre. Perfusion chromatography: an emergent technique for the analysis of food proteins. *J. Chromatogr. A*, 2000, 880, 169-187.
- [7] K. K. Unger, G. Jilge, R. Janzen, H. Giesche, J. N. Kinkel. Non-porous microparticulate supports in high-performance liquid chromatography (HPLC) of biopolymers — concepts, realization and prospects. *Chromatographia*, 1986, 22, 379-380.

-
- [8] K. Kalghati, C. Horvath. Rapid peptide mapping by high-performance liquid chromatography. *J. Chromatogr.*, 1988, 443, 343-354.
- [9] J. Horváth, E. Boschetti, L. Guerrier, N. Cooke. High-performance protein separations with novel strong ion exchangers. *J. Chromatogr. A*, 1994, 679, 11-22.
- [10] D. P. Lee, Reversed-Phase HPLC from pH 1 to 13. *J. Chromatogr. Sci.*, 1982, 20, 203-208.
- [11] X. Huang, S. Zhang, G.A. Schultz, J. Henion, Surface-alkylated polystyrene monolithic columns for peptide analysis in capillary liquid chromatography –electrospray ionization mass spectrometry. *Anal. Chem.*, 2002, 74, 2336-2344.
- [12] N. B. Afeyan, F. E. Regnier, R. C. Dean. Perfusion chromatography. U.S. Patent No. 5,019,270, 1991.
- [13] N. B. Afeyan, S. P. Fulton, F. E. Regnier. Perfusion chromatography packing materials for proteins and peptides. *J. Chromatogr. A*, 1991, 544, 267-279.
- [14] G. Y. Sun, Q. H. Shi, Y. Sun. Novel biporous polymeric stationary phase for high-speed protein chromatography. *J. Chromatogr. A*, 2004, 1061, 159-165.
- [15] Y. Shi, Y. Sun. Fabrication and characterization of a novel biporous spherical adsorbent for protein chromatography. *Chromatographia*, 2003, 57, 29-35.
- [16] L. Wu, S. Bai, Y. Sun. Development of rigid bidisperse porous microspheres for high-speed protein chromatography. *Biotechnol. Prog.*, 2003, 19, 1300-1306.
- [17] Li N. H, Benson J. R. Polymeric Microbeads and Methods of Preparation. U.S. Pat. 5 653 922, 1996.
- [18] Li N. H, Benson J. R, Kitagawa N. Polymeric Microbeads. U.S. Pat. 5 863 957, 1999.
- [19] W. Q. Zhou, T. Y. Gu, Z. G. Su, G. H. Ma, Synthesis of Macroporous Poly (styrene-divinyl benzene) Microspheres by Surfactant Reverse Micelles Swelling Method. *Polymer*, 2007, 48, 1981-1988.
- [20] Lloyd L. L, Warner F. P. Preparative High-performance Liquid Chromatography on a Unique High-speed Macroporous Resin. *J. Chromatogr.*, 1990, 512, 365-376.
- [21] M McCoy, K. Kalghatgi, F. E. Regnier, N. B. Afeyan. Perfusion chromatography-characterization of column packings for chromatography of proteins. *J. Chromatogr. A*, 1996, 743, 221-229.
- [22] D. Whitney, M. McCoy, N. Gordon, N. B. Afeyan, Characterization of large-pore polymeric supports for use in perfusion biochromatography. *J. Chromatogr. A*, 1998, 807, 165-184.
- [23] J. M. Heras, M. L. Marina, M. C. García. Development of a perfusion ion-exchange chromatography method for the separation of soybean proteins and its application to cultivar characterization. *J. Chromatogr. A*, 2007, 1153, 97-103.
- [24] D. Barby, Z. Haq. Low density porous cross-linked polymeric materials and their preparation and use as carriers for included liquids. US Patent 4 522 953, 1985.
- [25] D. C. Walsh, J. I. T. Stenhouse, L. P. Kingsbury. PolyHIPE Foams: Production, Characterisation, and Performance as Aerosol Filtration Materials. *J. Aerosol. Sci.*, 1996, 27, 629-630.
- [26] N. H. Li, J. R. Benson. Polymeric microbeads and method of preparation. US Patent 5 583 162, 1996.
- [27] N. H. Li, J. R. Benson, N. Kitagawa. Polymeric microbeads and method of preparation. US Patent 5 653 922, 1997.

-
- [28] N. H. Li, J. R. Benson, N. Kitagawa. Polymeric microbeads. US Patent 5 863 957, 1999.
- [29] N. H. Li, J. R. Benson, N. Kitagawa. Polymeric microbeads and methods of preparation. US Patent 6 100 306, 2000.
- [30] W. Q. Zhou, J. Li, W. Wei, Z. G. Su, G. H. Ma. Effect of solubilization of surfactant aggregates on pore structure in gigaporous polymeric particles. *Colloid. Surface A: Physicochem. Eng. Aspects*, 2011, 384, 549-554.
- [31] F. Candau, F. Heatley, C. Price, R. B. Stubbersfield. An investigation of the structure of micelles formed by a polystyrene-b-poly(ethylene/propylene) block copolymer in paraffinic solvents using ¹H and ¹³C-nuclear magnetic resonance. *Eur. Polym. J.*, 1984, 20, 685-690.
- [32] S. F. Chen, F. Gao, Q. B. Wang, Z. G. Su, G. H. Ma. Double emulsion-templated microspheres with flow-through pores at micrometer scale. *Colloid Polym Sci*, 2013, 291, 117-126.
- [33] W. Kopaciewicz. Ph.D. dissertation, Purdue University, West Lafayette, in 1984.
- [34] M. A. Rounds, W. D. Rounds, F. E. Regnier. Poly (styrene-divinylbenzene)-based Strong Anion-exchange Packing Material for High-performance Liquid Chromatography of Proteins. *J. Chromatogr.*, 1987, 397, 25-38.
- [35] M. Chanda, G. L. Rempel. A New Method of Gel-coating Polyethyleneimine (PEI) on Organic Resin Beads. High capacity and Fast Kinetics of PEI Gel-coated on Polystyrene. *Ind. Eng. Chem. Res.*, 2001, 40, 1624-1632.
- [36] A. Tuncel, A. Denizli, D. Purvis, C. R. Lowe, E. Piskin. Cibacron Blue F3G-A-attached Monosize Poly(vinyl alcohol)-coated Polystyrene Microspheres for Specific Albumin Adsorption. *J. Chromatogr.*, 1993, 634, 161-168.
- [37] M. Leonard, C. Fournier, E. Dellacherie. Polyvinyl Alcohol-coated Macroporous Polystyrene Particles as Stationary Phases for the Chromatography of Proteins. *J. Chromatogr. B* 1995, 664, 39-46.
- [38] D. C. Nash, G. E. McCreath, H. A. Chase. Modification of polystyrene matrices for the purification of proteins— effect of the adsorption of poly(vinyl alcohol) on the characteristics of poly(styrene-divinylbenzene) beads for use in affinity chromatography. *J. Chromatogr. A* 1997, 758, 53-64.
- [39] S. Simon, L. Picton, D. Le Cerf, G. Muller. Adsorption of amphiphilic polysaccharides onto polystyrene latex particles. *Polymer* 2005, 46, 3700-3707.
- [40] M. Malmsten, F. Tiberg. Hydrophilization of polystyrene surfaces with ethyl (hydroxyethyl) cellulose. *Langmuir* 1991, 9, 2412-2414.
- [41] Fournier, M. Leonard, I. Le Coq-leonard, E. Dellacherie. Coating polystyrene particles by adsorption of hydrophobically modified dextran. *Langmuir* 1995, 11, 2344-2347.
- [42] A. D. Sousa Delgado, M. Leonard, E. Dellacherie. Surface Modification of Polystyrene Nanoparticles Using Dextrans and Dextran-POE Copolymers: Polymer Adsorption and Colloidal Characterization. *J. Biomater. Sci. Polym. Edit.*, 2000, 12, 1395-1410.
- [43] D. Sousa Delgado, M. Leonard, E. Dellacherie. Surface Properties of Polystyrene Nanoparticles Coated with Dextrans and Dextran-PEO Copolymers: Effect of Polymer Architecture on Protein Adsorption. *Langmuir*, 2001, 17, 4386-4391.
- [44] Duval-Terrie, J. Huguey, G. Muller. Self-assembly and Hydrophobic Clusters of Amphiphilic Polysaccharides. *Colloids Surf. A: Physicochem. Eng. Aspects*, 2003, 220, 105-115.

- [45] E. Osterberg, K. Bergstorm, K. Holmberg, T. P. Schuman, J. A. Riggs, N. L. Burns, J. M. Van Alstine, J. M. Harris. Protein-rejecting ability of surface-bound dextran in end-on and side-on configurations: comparison to PEG. *J. Biomed. Mater. Res.* 1995, 29, 741-747.
- [46] Shar J. A, Obey T. M, Cosgrove T. Adsorption Studies of Polyethers: Part 1. Adsorption onto Hydrophobic Surfaces. *Colloids Surf. A: Physicochem. Eng. Aspects*, 1998, 136, 21-23.
- [47] G. P. H. Schroen, M. A. Cohen Stuart, K. V. Maarschalk, A. Van der Padt, K. Vantriet. Influence of Preadsorbed Block Copolymers on Protein Adsorption: Surface Properties, Layer Thickness, and Surface Coverage. *Langmuir*, 1995, 11, 3068-3074.
- [48] O. E. Cassidy, G. Rowley, I. W. Fletcher, S. F. Davies, D. Briggs. Surface Modification and Electrostatic Charge of Polystyrene Particles. *Inter. J. Pharma.*, 1999, 182, 199-211.
- [49] J. H. Lee, P. Kopeckova, J. Kopecek, J. D. Andrade. Surface Properties of Copolymers of Alkyl methacrylates with Methoxy(polyethylene oxide) Methacrylates and their Application as Protein-resistant Coatings. *Biomater.*, 1990, 11, 455-464.
- [50] Y. S. Lee, B. D. Park, H. I. Lee. U.S. Pat. 5 466 758, 1995
- [51] D. Park, H. I. Lee, S. J. Ryoo, Y. S. Lee. Convenient Method for Preparing Polystyrene Having β -hydroxy Group: Its Application to the Synthesis of Polyethylene Glycol-grafted Polystyrene Resin. *Tetrahedron Letters*, 1997, 38, 591-594
- [52] S. J. Ryoo, J. Kim, J. S. Kim, Y. S. Lee. Efficient Methods of converting hydroxyl Groups into amino groups in poly(ethylene glycol)-grafted polystyrene resin. *J. Combin. Chem.*, 2002, 187-190.
- [53] Osterberg, K. Bergstorm, K. Holmberg, T. P. Schuman, J. A. Riggs, N. L. Burns, J. M. Van Alstine, J. M. Harris. Protein-rejecting ability of surface-bound dextran in end-on and side-on configurations: comparison to PEG. *J. Biomed. Mater. Res.*, 1995, 29, 741-747.
- [54] S. Roller, H. Turk, J. F. Stumbe, W. Rapp, R. Haag. Polystyrene-graft -polyglycerol resins: A new type of high-loading hybrid support for organic synthesis. *J. Combin. Chem.* 2006, 8, 350-354.
- [55] M. Malmsten, K. Emoto, J. M. Van Alstine. Effect of chain density on inhibition of protein adsorption by poly(ethylene glycol) based coatings. *J. Colloid Interface Sci.* 1998, 202, 507-517.
- [56] Y. B. Yang, F. E. Regnier. Coated hydrophilic polystyrene-based packing materials. *J. Chromatogr. A*, 1991, 544, 233-247.
- [57] J. B. Qu, W. Q. Zhou, W. Wei, Z. G. Su, G. H. Ma. An Effective way to Hydrophilize Gigaporous Polystyrene Microspheres as Rapid Chromatographic Separation Media for Proteins. *Langmuir*, 2008, 24, 13646-13652.
- [58] M. Leonard, C. Fournier, E. Dellacherie. Polyvinyl alcohol-coated macroporous polystyrene particles as stationary phases for the chromatography of proteins. *J. Chromatogr. B*, 1995, 664, 39-46.
- [59] J. Y. Yoon, J. H. Kim, W. S. Kim. The relationship of interaction forces in the protein adsorption onto polymeric microspheres. *Colloids Surf. A*, 1999, 153, 413-419.
- [60] J. B. Qu, W. Q. Zhou, W. Wei, Z. G. Su, G. H. Ma. Chemical modification and characterization of gigaporous polystyrene microspheres as rapid separation of proteins base supports. *J. Polym. Sci. Part A: Polym. Chem.*, 2008, 46: 5794-5804.

-
- [61] J. B. Qu, H. H. Shao, J. Li, G. L. Jing, J. G. Liu, W. Q. Zhou. Hydrophilization of gigaporous polystyrene microspheres with saccharide as high-speed protein chromatography base support. *Reactive & Functional Polymers*, 2012, 72, 606-612.
- [62] M. C. Garcia, M. L. Marina, M. Torre. Perfusion chromatography: an emergent technique for the analysis of food proteins. *J. Chromatogr. A*, 2000, 880, 169-187.
- [63] M. Pratap, J. L. Strominger. Perfusion chromatography for very rapid purification of class I and II MHC proteins. *J. Immun. Metho.*, 2000, 234, 83-88.
- [64] McCarthy, G. Vella, R. Mhatre, Y. P. Lim. Rapid purification and monitoring of immunoglobulin M from ascites by perfusion ion-exchange chromatography. *J. Chromatogr. A*, 1996, 743, 163-170.
- [65] J. B. Qu, X. Z. Wan, Y. Q. Zhai, W. Q. Zhou, Z. G. Su, G. H. Ma. A novel stationary phase derivatized from hydrophilic gigaporous polystyrene-based microspheres for high-speed protein chromatography. *J. Chromatogr. A*, 2009, 1216, 6511-6516.
- [66] G. H. Wang, F. G. Nie, Z. G. Su, Coupling reaction of diethylaminoethyl (DEAE) onto agarose gel. *Chin. Chem. React. Eng. Technol.*, 2002, 18, 80-85.
- [67] R. M. De La Vega, C. Chenou, J. M. Loureiro, A. E. Rodrigue. Mass transfer mechanisms in Hyper D media for chromatographic protein separation. *Biochem. Eng. J.*, 1998, 1, 11-23.
- [68] J. J. van Deemter, F. J. Zuiderweg, A. Klinkenberg. Longitudinal diffusion and resistance to mass transfer as causes of non ideality in chromatography. *Chem. Eng. Sci.*, 1956, 5, 271-289.
- [69] J. B. Qu, Y. D. Huang, G. L. Jing, J. G. Liu, W. Q. Zhou, H. Zhu, J. R. Lu. A novel matrix derivatized from hydrophilic gigaporous polystyrene-based microspheres for high-speed immobilized-metal affinity chromatography. *J. Chromatogr. B*, 2011, 879, 1043-1048.

Chapter 5

FUNCTIONAL STRUCTURES FABRICATED FROM SUBMICRON-SCALE POLYSTYRENE SPHERICAL PARTICLES

Akira Emoto^{1,2} and Takashi Fukuda²*

¹Doshisha University, Kyotanabe, Kyoto, Japan

²National Institute of Advanced Industrial Science and Technology (AIST),
Higashi, Tsukuba, Ibaraki, Japan

ABSTRACT

Spherical polystyrene (PS) particles dispersed in colloidal suspensions have been used to fabricate photonic crystal structures, nano- and micro-scale templates, and functional surface structures. In this chapter, we describe methods for forming many of these functional structures from submicron PS spheres. We propose a thin sandwich-type cell to fabricate adjacent structures of different photonic crystals. In addition, the order of the crystals can be controlled by the evaporation rate of the colloidal suspension, creating unique, structure-dependent, optical characteristics. Monolayers of metal-coated PS spheres are also used for plasmonic sensor chips. A replication process using silicone rubber molds can form them repetitively and accurately. The resultant structures and optical characteristics can be modified *via* mold deformation during the replication process. In particular, significant anisotropic, dichroic reflections can be observed under certain elongation conditions. Finally, unique porous films can be formed with PS spheres. We discuss a simple method for the fabrication of pores having outer shells, and where submicron-scale pores are formed by spin-coating colloidal mixtures.

* Corresponding author: aemoto@mail.doshisha.ac.jp.

1. INTRODUCTION

Polystyrene (PS) spherical particles are often used as particle size standards for the calibration of other particles. Thus, many commercial products with accurate and traceable sizes are available as colloidal suspensions of aqueous solution. Generally, a small amount of surfactant such as sodium dodecyl sulfate is added to stabilize the particle dispersion [1]. The colloidal particle sizes have a range from several tens of nanometers to micrometers, and mono-dispersed PS colloidal particles are used for precise nano- and micro-scale structures or hierarchical structures [2, 3]. Because the PS particles are dispersed in a colloidal suspension, structure formation is most likely a wet process. However, there are benefits to this as well. For example, self-assembly of particles *via* solution evaporation forms highly regulated arrangements of two- and three-dimensional structures, as described in section 2.

Two-dimensional PS particle arrays (*i.e.*, monolayers) are often used for nano-scale patterning or templating of other materials. These procedures are often called “sphere lithography” or “colloidal lithography” [2, 4, 5], and are depicted in Figure 1. When certain materials such as metals or molecules are deposited on the particle monolayer, the deposits can reach the bottom substrate through the narrow spaces (interspaces) between the particles (Figure 1(a)). After removal of the particles, a pattern of small islands of the deposited material remains [6]; the pattern is determined down to the nano-scale by the particle diameter [4]. When a monolayer of isolated particles is used, the remaining material pattern is an array of isolated rings after ion beam etching (Figure 1(b)) [7]. A receding meniscus in the interspaces among closed-packed monolayers of spheres can also be used to form ring structures on the substrate *via* vapor deposition of solution reactive materials [8] or simple additive solutions using the wettability of substrate surfaces (Figure 1(c)) [9]. Such monolayers can be used as an etching mask, resulting in the formation of ordered pillars (Figure 1(d)) [10, 11]. These strategies for structure formation *via* particle arrays are broadly applicable to various combinations of materials, substrates, chemical reactions, and physical processes.

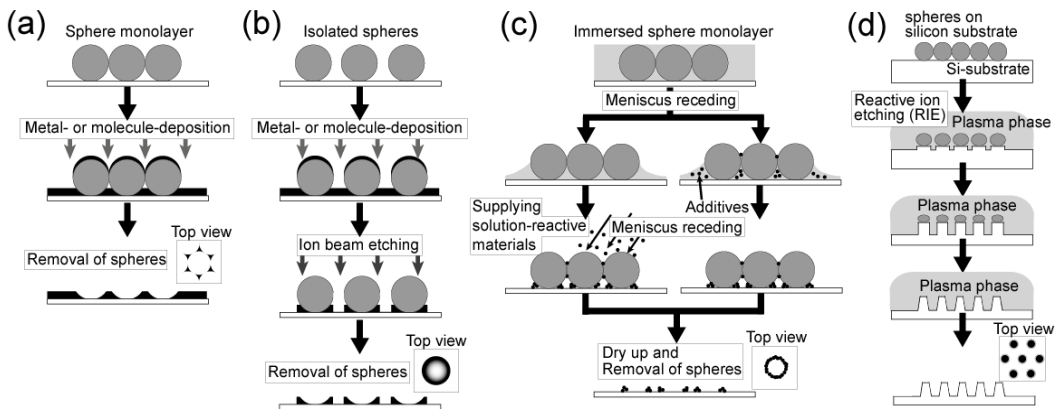


Figure 1. “Sphere lithography” or “colloidal lithography” for nano- or micro-structuring or templating. (a) Triangles created by material (metallic, molecular) deposition. (b) Rings created by material deposition on isolated spheres. (c) Rings created by solution meniscus receding toward the interspaces of spheres. (d) Pillars from reactive ion etching.

Self-assembled spherical particles with ideal three-dimensional crystal structures have received considerable attention when they are used as photonic crystals [12]. These close-packed arrays exhibit significant photonic band gaps and are often colored. In contrast, random structures of particles can exhibit random lasing because of the localization of light, as described in section 2. The photonic properties of colloidal crystals can be combined with the plasmonic behavior of adjacent metallic regions to create various optical functions [13].

In summary, structures of small particles such as PS spheres play an important role in applied physics. Studies involving particle sizes, arrangement style, chemical properties, and physical phenomena are becoming increasingly important for future applications. In this chapter, we describe several topics in our investigations of PS spherical particles, and cite related studies.

2. COLLOIDAL CRYSTALS

A close-packed self-assembly of spherical colloidal particles can be used to form colloidal crystals [14]. The formation mechanism is based on particle behavior in the solvent meniscus region, as illustrated in Figure 2 [15, 16, 17]. Monolayer formation requires a shallow region of the aqueous solution at the edge of the meniscus. Lateral capillary forces arise between particles immersed in this shallow region. Because the forces are attractive and are exerted on each particle, the particles are stacked each other as a close-packed monolayer. Solvent evaporation from the stacking area is accelerated by the shallow meniscus on the particle surfaces and interspaces. The accelerated evaporation enhances a convective flow of particles inside the meniscus, which enables continuous self-assembly of the colloidal crystal.

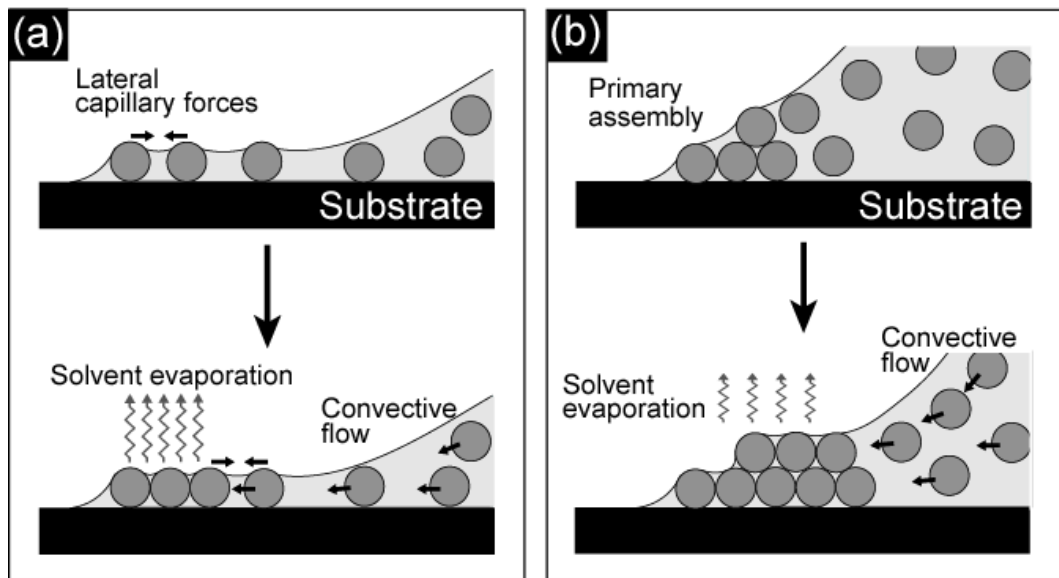


Figure 2. (a) Monolayer and (b) multilayer formation of colloidal spherical particles.

Multilayer formation requires a relatively thick solvent region at the meniscus edge [18, 19]. The trigger for the initial assembly of multilayers involves particle aggregation in the meniscus edge, particle stacking driven by a slight convective flow, and the lateral capillary forces. Accelerated evaporation and the subsequent convective flow enhancement enable multilayer formation as they did for monolayer formation. Continuous particle self-assembling results in a face-centered cubic crystal structure. Various methods have been developed to form highly ordered colloidal crystals, including vertical deposition by dip-coating [18, 20, 21], spreading [22, 23], glass cells (see below), or wedge cells [24, 25, 26], and meniscus formation in a ring [27].

Three-dimensional colloidal crystals produced by multilayer formation often exhibit coloration as a function of the lattice constant (*i.e.*, the particle diameter). This corresponds to the generation of forbidden bands in photonic crystals [28, 29]. The wavelength of the reflection spectrum maximum (λ_{\max}) can be determined by Bragg's law, as given by: [30, 31]

$$\lambda_{\max} = 2d\sqrt{n_{\text{eff}}^2 - \sin^2 \theta}, \quad (1)$$

where d is the lattice constant for the [111] in-plane, θ is the angle between the incident beam and the normal to the [111] plane, and n_{eff} is the effective refractive index. When the spherical particle diameter is denoted as D , the value of d equals to $D\sqrt{2/3}$. For PS spherical particles, n_{eff} is defined by general effective medium theory as $n_{\text{eff}} = \sqrt{n_{\text{PS}}^2 f + n_{\text{air}}^2 (1 - f)}$, where n_{PS} and n_{air} are the refractive indices of PS and the air in the void, respectively, and f is the filling factor of the PS particles. Thus, λ_{\max} can be obtained by the rewriting Eq. 1 as $\lambda_{\max} = 1.633Dn_{\text{eff}}$, assuming $\theta = 0$, $n_{\text{PS}} = 1.59$, $n_{\text{air}} = 1.0$, and $f = 0.74$.

A thin glass cell can be used to fabricate highly ordered colloidal crystals. Here, the PS particles are arrayed along the planar glass substrates that make up the cell because of solvent evaporation from the colloidal suspension (Figure 3(a)). Different colloidal crystals from different PS particle diameters can be formed adjacent to the last colloidal crystal in the cell, repetitively and alternately [24, 32, 33]. Examples of adjacent colloidal crystals are shown in Figure 3(b). Brilliant structural colors depending on the sphere diameters are captured in reflection images, and the ordered PS sphere arrays are confirmed by scanning electron microscopy (SEM). As shown in Figure 3(c), specular reflection spectra can be acquired with a reflection microscope. Each stripe of colloidal crystal is formed along the edge of the glass cell. When the shape of the edge was modified *e.g.*, by employing a patterned plastic plate for the cell, this changed the pattern of the colloidal crystals [33]. Patterning of colloidal crystals in the epitaxial direction is possible by means of layer transfer [34]. More recently, direct patterning by inkjet printing was used to create patterns of structural colors based on the photonic band gap [35].

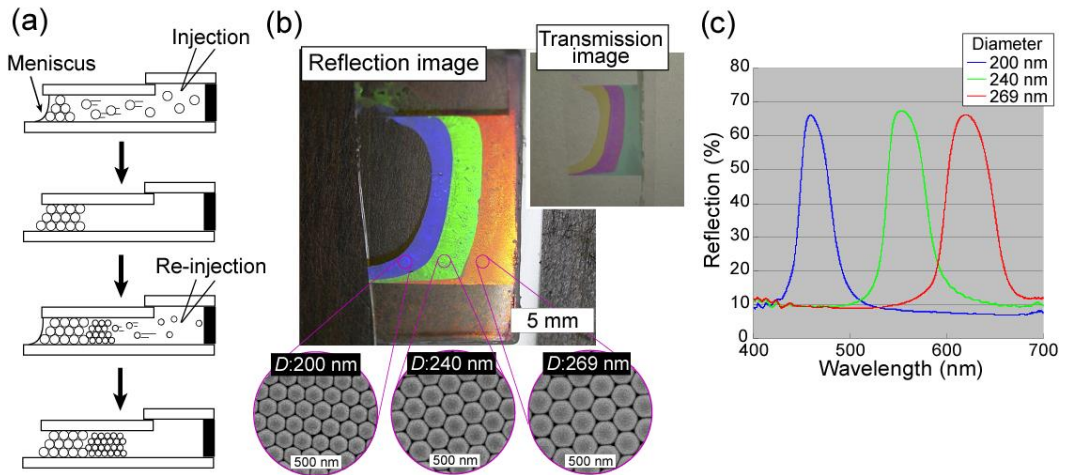


Figure 3. Colloidal crystal formation in a glass cell. (a) Fabrication process. (b) Optical and SEM images of colloidal crystals formed from PS particles having diameters of 200 nm, 240 nm, and 269 nm, respectively. (c) Reflection spectra.

In the thin glass cells, the order in the PS particle array is also controlled by the evaporation rate of the colloidal solvent (Figure 4(a)). In turn, the evaporation rate can be controlled *via* the relative humidity. Thus, crystalline and amorphous phases of PS particle arrays can be formed adjacent to each other, in repetitive fashion [36]. The crystal phase is a photonic crystal, whereas the amorphous phase is a photonic glass [12] that exhibits unique characteristics in optical propagation (Figure 4(b)). In such random structures, the optical path is randomly localized, *i.e.*, Anderson localization for light, and is used to investigate random lasing [37].

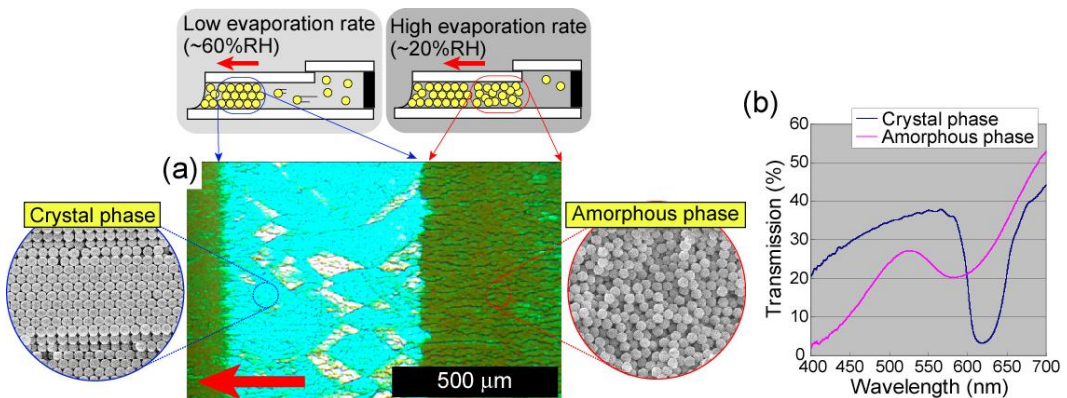


Figure 4. Tailored assembly of PS spherical particles with a diameter of 269 nm. (a) Optical microscope image of adjacent crystal and amorphous structures, with inset SEM images of crystalline and amorphous phases formed in the glass cell under conditions of relatively high and low humidity, respectively. Red arrows indicate the directions of convective flow in the glass cell. (b) Transmission spectra.

Binary colloidal crystals of mixed PS particles can be fabricated by single- or multi-step self-assembly. Single-step formation is performed using a mixed colloidal suspension of PS particles having two different diameters [38, 39, 40]. Self-assembly of both particles occurs simultaneously, generating a complex crystal structure where smaller particles are arrayed in the interstitial sites of the larger particle arrays. Binary colloidal crystals can also be formed by the multi-step process shown in Figure 5 [41, 42]. The optical properties include reflection spectra with features from each colloidal crystal component. This has the potential to perform as a platform for arrays of two types of functional particles.

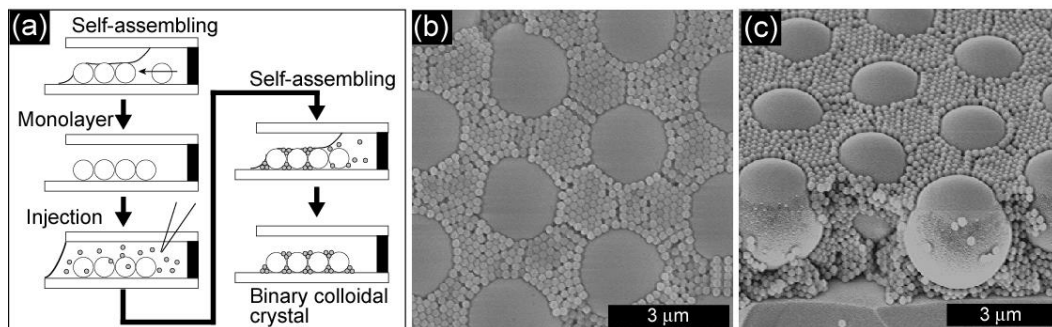


Figure 5. Fabrication of a binary colloidal crystal monolayer in a glass cell using PS particles having diameters of 3 μm and 200 nm. (a) Fabrication process. SEM images of (b) top and (c) perspective views.

Colloidal crystals such as those discussed above have been recently applied in the development of laser cavity mirrors [43, 44], a functional reflector [45], colloidal laser cavities [46], full-color displays [47], and colorimetric sensors [48]. In addition, they are being applied in bio-science areas such as cell scaffold fabrication [49], biomolecular confinement [50] and separation [51], and molecular sensing [52]. Thus structural, optical, and photonic properties of colloidal crystals will continue to have wide-ranging applications.

3. METAL-COATED PS-PARTICLE ARRAYS AND REPLICA FABRICATION

Spherical particle monolayers are effective templates for chemical and biological sensors. For example, a non-close-packed PS sphere monolayer coated with a thin film of Au exhibited spectral shifts induced by biotin-avidin bound molecules [53]. In this technique, optical reflection from the Au film is monitored as a function of wavelength, and the peak wavelength of the extinction spectrum shifts with the ambient environment because of refractive index changes induced by the molecular adsorption. In a different optical technique using surface enhanced Raman scattering, glucose was detected quantitatively on Ag-coated spherical particle monolayers made from carboxyl-substituted PS [54].

The optical characteristics of metal-coated spherical particle monolayers are determined by relationships between the structural properties and the incident optical wavelengths. In general, the resonant wavelengths are determined primarily by the structural periodicity given by the sphere diameter [55, 56]. Therefore, the “diffraction limit” is also strongly related to

the spectral characteristics [57]. Whereas, the width (or sharpness) of a spectral resonance is determined mainly by the nature of the metals and its thickness [55, 58]. Furthermore, the shift in resonant wavelength depends on the ambient refractive index, allowing us to use the metal-coated spherical particle arrays as sensing devices.

Figure 6 shows a PS sphere monolayer on a glass substrate where the 400-nm-diameter spheres are coated with a 100-nm-thick Ag layer (Figure 6(a) and 6(b)) [59]. Extinction spectra were acquired with an optical reflection arrangement (Figure 6(c)). The resonant extinction peak was observed around 600 nm, which corresponds to the observation of a bright blue appearance in reflection (Figure 6(a)). Spectral shifts, plotted in Figure 6(c) are dependent on the ambient refractive index (1.333, 1.375, 1.411, and 1.456), as shown for water, isopropyl alcohol (IPA), decane, and triethylene glycol (TEG), respectively. The extent of the spectral shift is assessed by a figure of merit determined from the wavelength shift per refractive index unit change (RIU^{-1}), as plotted in Figure 6(d), and where the constant 550 nm/RIU is obtained by the linear fit [53].

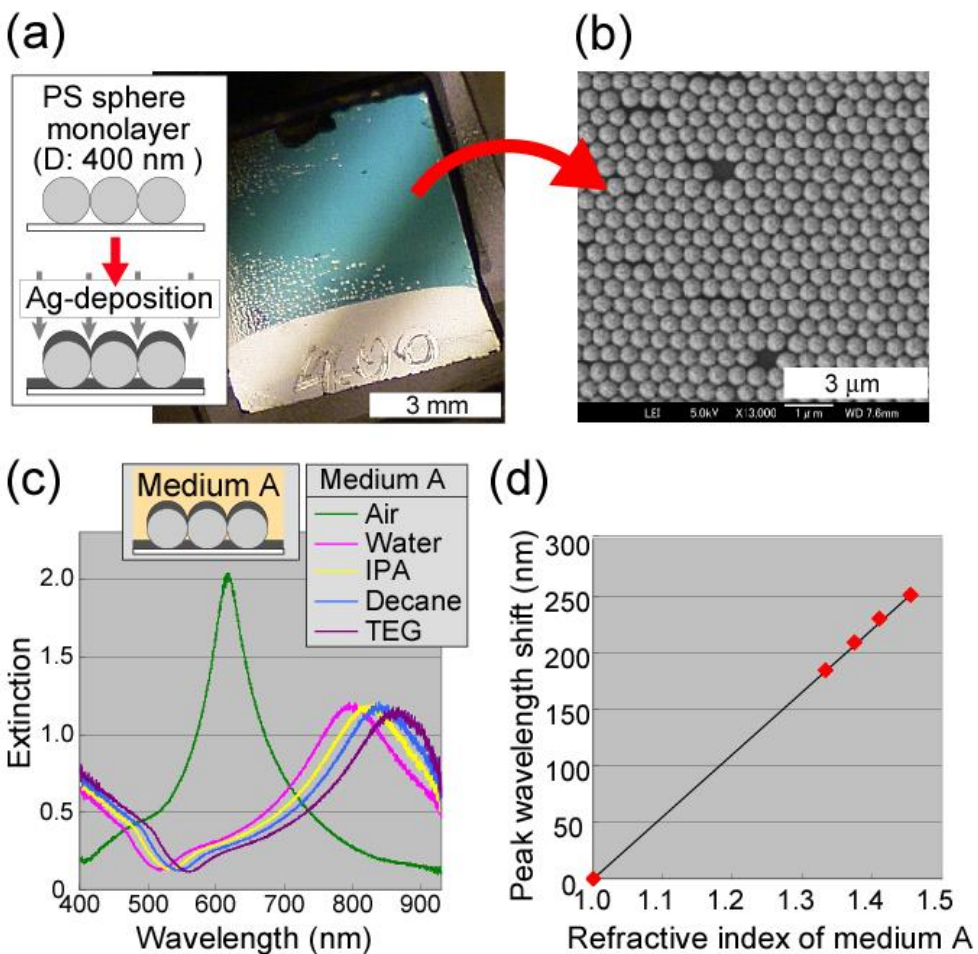


Figure 6. (a) Ag-coated PS sphere array. (b) SEM image of the surface. (c) Extinction spectra in a reflection optical arrangement where the peak shifts depend on the ambient medium A. (d) Peak wavelengths as a function of the refractive index of medium A.

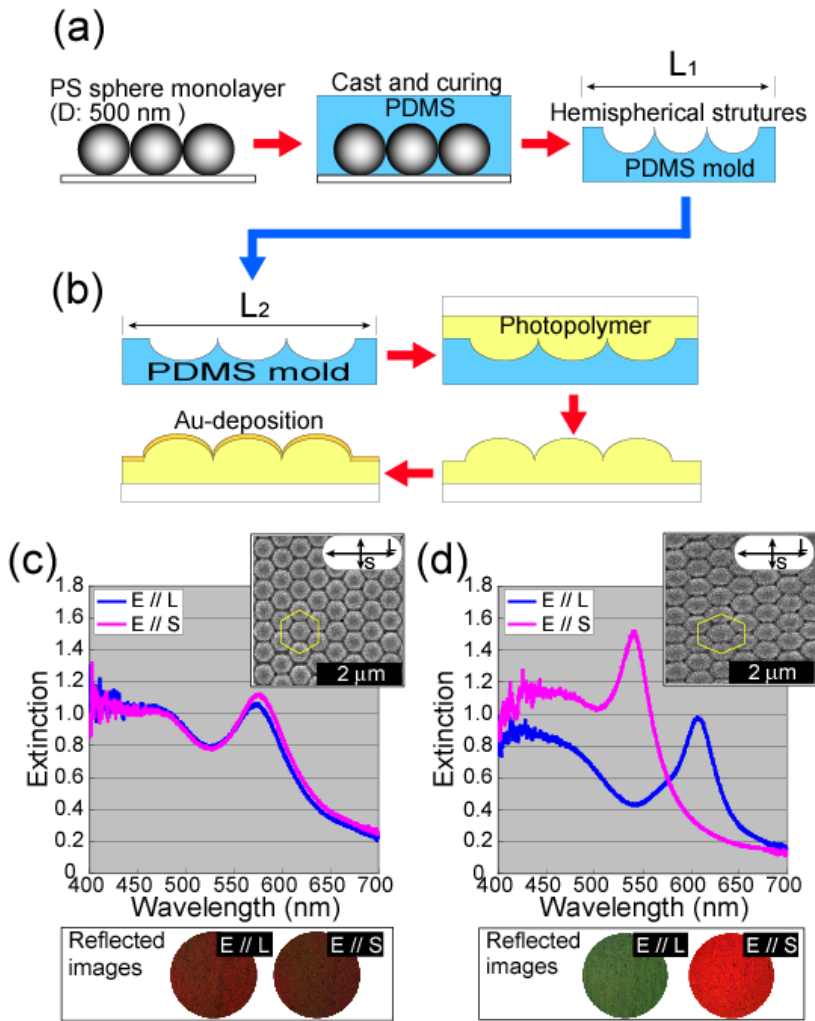


Figure 7. (a) Hemispherical PDMS mold based on a PS particle monolayer. (b) Replication with stretched PDMS mold. (c), (d) Extinction spectra for replicas with elongation ratios (L_2/L_1) of 1.0 and 1.3, respectively. A letter of “E” denotes the polarization direction of incident light. The insets show SEM images of the surface structures.

Self-assembly is an easy way to produce these spherical particle monolayers. However, structural consistency in self-assembled structures cannot be guaranteed, even at the macro scale. This irreproducibility is a problem for fundamental studies. One solution is using a replication process where the original spherical particle array is copied with a silicone rubber mold [60, 61]. The soft silicone structure can be modified by stretching [62, 63]. The fundamental procedure is illustrated in Figure 7(a) [64], where the silicone rubber material, poly(dimethylsiloxane) (PDMS) pre-polymer, was cast on a PS sphere monolayer. The pre-polymer covered the monolayer, including interspaces among the spheres. After thermal polymerization, the PDMS forms a hemispherical mold of the structure array when it is removed from the monolayer. This technique is dependent on the adhesive forces between the PDMS and bottom (glass) substrate [65]. The spherical structure of the original PS array is completed by a sequence of photopolymer injection into the mold, ultraviolet curing, removal

from the mold, and thin metal layer deposition (Figure 7(b)). Because of the softness of the silicone mold, anisotropic modification by mold stretching [*e.g.*, from L_1 to L_2 in Figure 7(c,d)] can be introduced in the fabrication sequence. Because the optical properties originate from the configuration of the metal film (*i.e.*, the upper half of metal-coated spheres) [55], optical resonances in the reflective spectra can be obtained as before from the hemisphere array. This can be seen in Figure 7(c), and also in Figure 7(d) where anisotropic changes were observed in the extinction spectra depending on both the elongation ratio and the incident polarization direction [64]. Along with the spectral changes in Figures 7(c) and (d), the corresponding reflected images also changed anisotropically. For an elongation ratio of 1.3, an “anisotropic dichroic reflection” was observed, where green and red reflections were observed for incident polarizations (E) parallel to L and S directions, respectively. The anisotropic resonance wavelengths also shift with the ambient refractive index, similar to that observed for Ag-coated spheres in Figure 6 [66].

These significant spectral shifts should be applicable to a wide region of sensing technologies. Because the surfaces are coated with conductive metals, the accuracy and/or the sensitivity of the spectral shifts can be increased by combining with electrochemical measurements [67, 68]. Such highly sensitive sensor chips can be introduced into fluidic cells to enable medical point-of-care devices [69]

4. FUNCTIONAL PORE FORMATION

Nano- and micro-scale channels such as pores or grooves have been widely studied for sensor applications, particularly in the rapid advancing field of biosensors [70, 71, 72]. In general, the sensing mechanism is based on changes in optical spectra, or in electrical conductivity, owing to molecular adsorption. Therefore, an effective approach will be to stably capture large amounts of targets in the sensor channels. Concave and convex structures have been reported, where the effect of fluid collection is based on the meniscus receding during solvent evaporation [73, 74]. However, the entrapment of the targets in such channels is not sufficient to withstand the shearing force exerted by repetitive wet processes such as rinsing. Thus, protective mechanisms are expected to be employed for the pore structures, as demonstrated recently [75, 76]. Such protective and effective pore structures can also be fabricated using PS spherical particles at a submicrometer scale, as shown in Figure 8 [77]. In this case, an aqueous mixture of a cationic poly(vinyl alcohol) (PVA) and a PS colloidal suspension was spin-coated on a substrate. The resultant film was then immersed in a toluene bath to dissolve the PS spheres, leaving pores with an outer shell (POS).

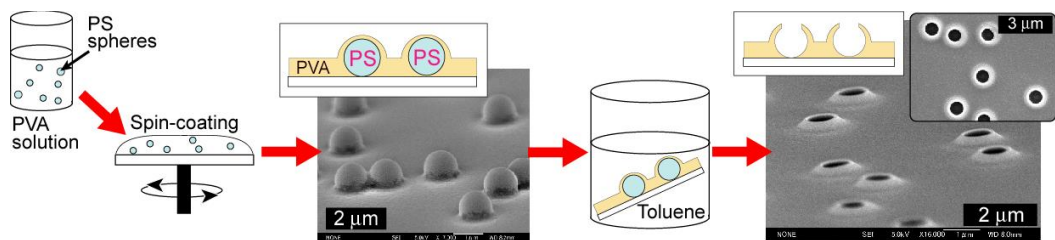


Figure 8. Schematic illustration of POS formation process. The PS particle diameter is 1 μm .

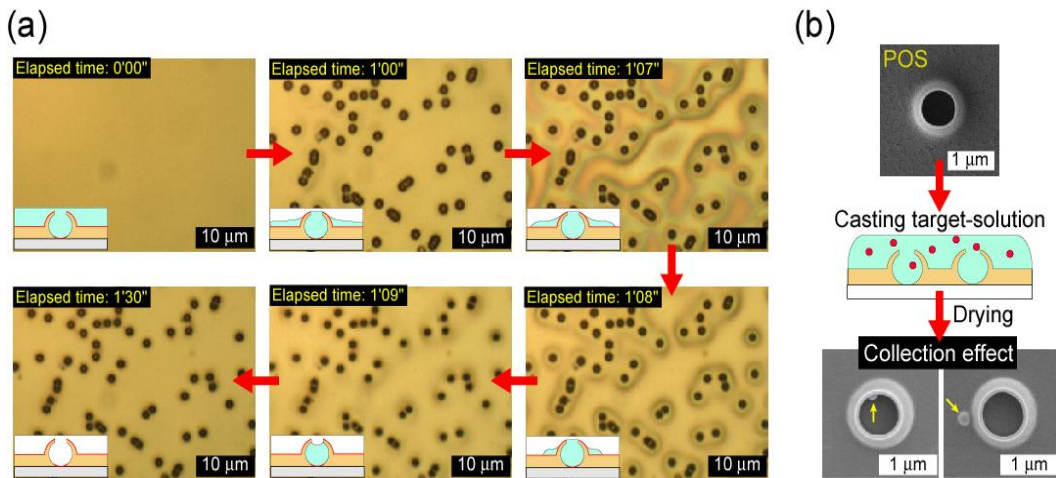


Figure 9. Experimental results of the collection effect on the POS. (a) Optical microscope images of the meniscus receding toward the POS. (b) The collection effect for smaller PS particles into each POS and vicinity.

When a solution of the target is cast on the POS, the shell structure generates molecular or particle migration toward the POS. Figure 9 shows the experimental images of this collection effect. The POS was coated with a 30-nm-thick Au layer to prevent collapse from PVA swelling (Figure 9(a)). The meniscus edge of ethanol solvent cast on the POS recedes towards the pores during evaporation, which eventually deposits the condensed target molecules or particles at the POS. The targets are thus collected inside each POS, and in the vicinity of the outer shell, as shown in Figure 9(b). The efficiency of the collection effect is closely related to the POS in-plane density and the properties of the shell structure. POS fabrications using submicrometer PS particles (500-nm diameter) and using a photo-cross-linkable PVA have also been demonstrated by the use of the same process, individually [77]. The POS with photo-cross-linkable PVA can be formed without photoreaction. Therefore, photo-cross-linking of PVA can be used for POS reinforcement or immobilization of collected targets in the POS.

For metallic spherical shells with openings (pores), electric fields induced by optical irradiation are localized along the edges of the pores [78, 79]. Therefore, the localization is expected for the openings in the POS when coated with ideal metallic layers.

CONCLUSION

In this chapter, several applications of PS spherical particle arrays are described along with related applied physics studies. The PS spherical particles are versatile in that they can form many types of two- and three-dimensional arrays as a function of spherical shape, size (diameter), and self-assembling process. Future applications will be expanded by variations in chemical composition and by advanced fabrication strategies that are simpler, more precise, and unique.

REFERENCES

- [1] Sefcik, J.; Verduyn, M.; Storti, G.; Morbidelli, M. *Langmuir* 2003, 19, 4778-4783.
- [2] Zhang, J.; Li, Y.; Zhang, X.; Yang, B. *Adv. Mater.* 2010, 22, 4249-4269.
- [3] Cong, H.; Yu, B.; Tang, J.; Li, Z.; Liu, X. *Chem. Soc. Rev.* 2013, 42, 7774-7800.
- [4] Hulteen, J. C.; Van Duyne, R. P. *J. Vac. Sci. Technol. A* 1995, 13, 1553-1558.
- [5] Li, Y.; Cai, W.; Duan, G. *Chem. Mater.* 2008, 20, 615-624.
- [6] Hase, A. J.; Van Duyne, R. P. *J. Am. Chem. Soc.* 2002, 124, 10596-10604.
- [7] Larsson, E. M.; Alegret, J.; Käll, M.; Sutherland, D. S. *Nano Lett.* 2007, 7, 1256-1263.
- [8] Li, J.-R.; Lusker, K. L.; Yu, J.-J.; Garno, J. C. *ACS Nano* 2009, 3, 2023-2035.
- [9] Chen, X.; Chen, Z.; Fu, N.; Lu, G.; Yang, B. *Adv. Mater.* 2003, 15, 1413-1417.
- [10] Whitney, A. V.; Myers, B. D.; Van Duyne, R. P. *Nano Lett.* 2004, 4, 1507-1511.
- [11] Zhang, X.; Zhang, J.; Ren, Z.; Li, X.; Zhang, X.; Zhu, D.; Wang, T.; Tian, T.; Yang, B. *Langmuir* 2009, 25, 7375-7382.
- [12] Galisteo-López, J. F.; Ibisate, M.; Sapienza, R.; Froufe-Pérez, L. S.; Blanco, Á.; López, C. *Adv. Mater.* 2011, 23, 30-69.
- [13] Romanov, S. G.; Korovin, A. V.; Regensburger, A.; Peschel, U. *Adv. Mater.* 2011, 23, 2515-2533.
- [14] Velev, O. D.; Jede, T. A.; Lobo, R. F.; Lenhoff, A. M. *Nature* 1997, 389, 447-448.
- [15] Denkov, N. D.; Velev, O. D.; Kralchevsky, P. A.; Ivanov, I. B.; Yoshimura, H.; Nagayama, K. *Langmuir* 1992, 8, 3183-3190.
- [16] Dimitrov, A. S.; Nagayama, K. *Langmuir* 1996, 12, 1303-1311.
- [17] Tan, K. W.; Koh, Y. K.; Chiang, Y.-M.; Wong, C.-C. *Langmuir* 2010, 26, 7093-7100.
- [18] Zhou, Z.; Zhao, X. S. *Langmuir* 2005, 21, 4717-4723.
- [19] Malaquin, L.; Kraus, T.; Schmid, H.; Delamarche, E.; Wolf, H. *Langmuir* 2007, 23, 11513-11521.
- [20] Iskandar, F.; Abdullah, M.; Yoden, H.; Okuyama, K. *J. Appl. Phys.* 2003, 93, 9237-9242.
- [21] Zhang, J.; Liu, H.; Wang, Z.; Ming, N. *J. Appl. Phys.* 2008, 103, 013517 1-4.
- [22] Matsushita, S.; Miwa, T.; Fujishima, A. *Langmuir* 1997, 13, 2582-2584.
- [23] Yang, H.; Jiang, P. *Langmuir* 2010, 26, 13173-13182.
- [24] Li, H.-L.; Marlow, F. *Chem. Mater.* 2005, 17, 3809-3811.
- [25] Ishii, M.; Nakamura, H.; Nakano, H.; Tsukigase, A.; Harada, M. *Langmuir* 2005, 21, 5367-5371.
- [26] Yamasaki, T.; Tsutsui, T. *Jpn. J. Appl. Phys.* 1999, 38, 5916-5921.
- [27] Sakai, T.; Takeoka, Y.; Seki, T.; Yoshida, R. *Langmuir* 2007, 23, 8651-8654.
- [28] Bogomolov, V. N.; Gaponenko, S. V.; Germanenko, I. N.; Kapitonov, A. M.; Petrov, E. P.; Gaponenko, N. V.; Prokofiev, A. V.; Ponyavina, A. N.; Silvanovich, N. I.; Samoilovich, S. M. *Phys. Rev. E* 1997, 55, 7619-7625.
- [29] Reynolds, A.; López-Tejeira, F.; Cassagne, D.; García-Vidal, F. J.; Jouanin, C.; Sánchez-Dehesa, J. *Phys. Rev. B* 1999, 60, 11422-11426.
- [30] Kopnov, F.; Lirtsman, V.; Davidov, D. *Synth. Met.* 2003, 137, 993-995.
- [31] Aguirre, C. I.; Reguera, E.; Stein, A. *Adv. Funct. Mater.* 2010, 20, 2565.
- [32] Gates, B.; Xia, Y. *Adv. Mater.* 2000, 12, 1329-1332.

-
- [33] Emoto, A.; Kamei, T.; Shioda, T.; Kawatsuki, N.; Ono, H. *J. Appl. Phys.* 2009, 105, 123506 1-5.
- [34] Yan, Q.; Teh, L. K.; Shao, Q.; Wong, C. C.; Chiang, Y.-M. *Langmuir* 2008, 24, 1796-1800.
- [35] Wang, J.; Wang, L.; Song, Y.; Jiang, L. *J. Mater. Chem. C* 2013, 1, 6048-6058.
- [36] Emoto, A.; Fukuda, T. *Appl. Phys. Lett.* 2012, 100, 131901 1-4.
- [37] Wiersma, D. S. *Nature Phys.* 2008, 4, 359-367.
- [38] Kitaev, V.; Ozin, G. A. *Adv. Mater.* 2003, 15, 75-78.
- [39] Wang, L.; Wan, Y.; Li, Y. Cai, Z.; Li, H.-L.; Zhao, X. S.; Li, Q. *Langmuir* 2009, 25, 6753-6759.
- [40] Kumnorkaew, P.; Gilchrist, J. F. *Langmuir* 2009, 25, 6070-6075.
- [41] Huang, X.; Zhou, J.; Fu, M.; Li, B.; Wang, Y.; Zhao, Q.; Yang, Z.; Xie, Q.; Li, L. *Langmuir* 2007, 23, 8695-8698.
- [42] Emoto, A.; Uchida, E.; Fukuda, T. *Colloids Surf. A* 2012, 396, 189-194.
- [43] Furumi, S.; Fudouzi, H.; Miyazaki, H. T.; Sakka, Y. *Adv. Mater.* 2007, 19, 2067-2072.
- [44] Furumi, S.; Fudouzi, H.; Sawada, T. *J. Mater. Chem.* 2012, 22, 21519-21528.
- [45] Huang, K.-M.; Chang, H.-J.; Ho, C.-L.; Wu, M.-C. *IEEE Photonics Technol. Lett.* 2012, 24, 1298-1300.
- [46] Feng, J.; Bian, S.; Long, Y.; Yuan, H.; Liao, Q.; Cai, H.; Huang, H.; Song, K.; Yang, G. *J. Mater. Chem. C* 2013, 1, 6157-6162.
- [47] Puzzo, D. P.; Arsenault, A. C.; Manners, I.; Ozin, G. A. *Angew. Chem. Int. Ed.* 2009, 48, 943-947.
- [48] Burgess, I. B.; Lončar, M.; Aizenberg, J. *J. Mater. Chem. C* 2013, 1, 6075-6086.
- [49] Liu, Y.; Wang, S.; Lee, J. W.; Kotov, N. A. *Chem. Mater.* 2005, 17, 4918-4924.
- [50] Zeng, Y.; Harrison, D. J. *Electrophoresis* 2006, 27, 3747-3752.
- [51] Nazemifard, N.; Bhattacharjee, S.; Masliyah, J. H.; Harrison D. J. *Angew. Chem. Int. Ed.* 2010, 49, 3326-3329.
- [52] Ye, X.; Li, Y.; Dong, J.; Xiao, J.; Ma, Y.; Qi, L. *J. Mater. Chem. C* 2013, 1, 6112-6119.
- [53] Himmelhaus, M.; Takei, H. *Sens. Actuators B* 2000, 63, 24-30.
- [54] Shafer-Peltier, K. E.; Haynes, C. L.; Glucksberg, M. R.; Van Duyne, R. P. *J. Am. Chem. Soc.* 2003, 125, 588-593.
- [55] Landström, L.; Brodoceanu, D.; Bäuerle, D.; Garcia-Vidal, F. J.; Rodrigo, S. G.; Martin-Moreno, L. *Opt. Express* 2009, 17, 761-772.
- [56] Farcău, C.; Aștilean, S. *Appl. Phys. Lett.* 2009, 95, 193110 1-3.
- [57] Farcau, C.; Giloan, M.; Vinteler, E.; Astilean, S. *Appl. Phys. B* 2012, 106, 849-856.
- [58] Landström, L.; Brodoceanu, D.; Piglmayer, K.; Bäuerle, D. *Appl. Phys. A* 2006, 84, 373-377.
- [59] Unpublished data.
- [60] Yabu, H.; Shimomura, M. *Langmuir* 2006, 22, 4992-4997.
- [61] Nam, H. J.; Jung, D.-Y.; Yi, G.-R.; Choi, H. *Langmuir* 2006, 22, 7358-7363.
- [62] Choi, H. K.; Im, S. H.; Park, O. O. *Langmuir* 2009, 25, 12011-12014.
- [63] Wang, T.; Li, X.; Zhang, J.; Ren, Z.; Zhang, X.; Zhang, X.; Zhu, D.; Wang, Z.; Han, F.; Wang, X.; Yang, B. *J. Mater. Chem.* 2010, 20, 152-158.
- [64] Emoto, A.; Noguchi, N.; Fukuda, T. *Colloids Surf. A* 2013, 429, 106-111.
- [65] Emoto, A.; Kobayashi, T.; Noguchi, N.; Fukuda, T. *J. Appl. Polym. Sci.* 2014, 131, 39927 1-7.

-
- [66] Unpublished data.
- [67] Dick, L. A.; McFarland, A. D.; Haynes, C. L.; Van Duyne, R. P. *J. Phys. Chem. B* 2002, 106, 853-860.
- [68] Abdelsalam, M.; Bartlett, P. N.; Russell, A. E.; Baumberg, J. J.; Calvo, E. J.; Tognalli, N. G.; Fainstein, A. *Langmuir* 2008, 24, 7018-7023.
- [69] Chin, C. D.; Linder, V.; Sia, S. K. *Lab Chip* 2012, 12, 2118-2134.
- [70] de la Escosura-Muñiz, A.; Merkoçi, A. *ACS Nano* 2012, 6, 7556-7583.
- [71] Kocer, A.; Tauk, L.; Déjardin, P. *Biosens. Bioelectron.* 2012, 38, 1-10.
- [72] Ingham, C. J.; ter Maat, J.; de Vos, W. M. *Biotechnol. Adv.* 2012, 30, 1089-1099.
- [73] Choi, S.; Stassi, S.; Pisano, A. P.; Zohdi, T. I. *Langmuir* 2010, 26, 11690-11698.
- [74] Dai, Q.; Chen, Y.; Liu, C.-C.; Rettner, C. T.; Holmdahl, B.; Gleixner, S.; Chung, R.; Pitera, J. W.; Cheng, J.; Nelson, A. *Langmuir* 2013, 29, 3567-3574.
- [75] Lee, S.-H.; Jeong, H.-E.; Park, M.-C.; Hur, J.-Y.; Cho, H.-S.; Park, S.-H.; Suh, K. Y. *Adv. Mater.* 2008, 20, 788-792.
- [76] Yue, W.; Li, C.-W.; Xu, T.; Yang, M. *Biosens. Bioelectron.* 2013, 41, 675-683.
- [77] Emoto, A.; Noguchi, N.; Kobayashi, T.; Fukuda, T. *Langmuir* 2013, 29, 12601-12607.
- [78] Ye, J.; Van Dorpe, P.; Van Roy, W.; Borghs, G.; Maes, G. *Langmuir* 2009, 25, 1822-1827.
- [79] Ye, J.; Lagae, L.; Maes, G.; Borghs, G.; Van Dorpe, P. *Opt. Express* 2009, 17, 23765-23771.

Chapter 6

SYNTHESIS AND APPLICATIONS OF IONIC POLYSTYRENES DERIVED FROM IMIDAZOLIUM- BASED POLYMERIZABLE IONIC LIQUIDS

*Jun-ichi Kadokawa**

Graduate School of Science and Engineering, Kagoshima University, Korimoto,
Kagoshima, Japan

ABSTRACT

Polystyrene is one of the representative high-performance and commercially successful synthetic polymers. The main-chain structure of polystyrene has been employed in a variety of polymeric materials for carrying functional groups. For example, polymerization of styrene monomers, which have some substituted functional groups on the aromatic rings has led to polystyrene-based functional materials. On the other hand, ionic liquids, which are salts with a low melting point have been noted as new solvents and functional materials for the use as catalysts, environmentally benign solvents, photomaterials, and so on. One of the representative cationic structures in the ionic liquids is an imidazolium group. The polymer forms of ionic liquids, which are produced by polymerization of ionic liquids having polymerizable groups, are expected to lead to new functional polymeric materials.

On the basis of the above background, in this chapter, the author review the synthesis and applications of ionic polystyrenes derived from imidazolium-based polymerizable ionic liquids. For the study, vinylbenzylimidazolium ionic liquids have been prepared, which can be converted into a polystyrene main-chain by radical polymerization.

In the first topic in this chapter, the author describes the use of the vinylbenzylimidazolium ionic liquids for the production of composite materials with polysaccharides such as cellulose. The investigations have been based on the viewpoint that imidazolium ionic liquids have good affinity with polysaccharides and thus have been used as good solvents for them. Consequently, the author found that polysaccharide-ionic polystyrene composite materials were facilely obtained by in-situ radical polymerization of the vinylbenzylimidazolium ionic liquids in the mixtures with polysaccharides. Clay-ionic polystyrene composite materials were also prepared by the

* Corresponding author: Tel: +81-99-285-7743, Fax: +81-99-285-3253, E-mail: kadokawa@eng.kagoshima-u.ac.jp.

similar in-situ polymerization approach. The second and third topics of this chapter deal with the applications of ionic polystyrenes derived from the vinylbenzylimidazolium ionic liquids as absorbents for CO₂ and sorbent coatings for microextraction, respectively.

1. INTRODUCTION

In the research field of the synthetic polymer chemistry, polystyrene and its derivatives are one of the most representative materials because of some unique properties that make them useful in a wide range of products [1]. The commercial success of polystyrene is due to transparency, ease of fabrication, thermal stability, relative high modulus, and low cost. Polystyrene derivatives having various functional substituents on the aromatic rings have also been synthesized by both the polymerization of the corresponding styrene derivative monomers and substitution reactions of the suitable polystyrene substrates with reactants. Over the past decade, the synthesis of ionic polystyrene derivatives having imidazolium groups, which are mostly connected to the aromatic rings through a methylene has also been reported on the basis of the viewpoints of poly(ionic liquid)s research field [2].

Poly(ionic liquid)s are defined as the polymers obtained by polymerization of ionic liquids having polymerizable groups [3]. Therefore, poly(ionic liquid)s are often called ‘polymerized ionic liquids’ or ‘polymeric ionic liquids.’ Ionic liquids, which are low-melting point salts that form liquids at temperatures below the boiling point of water, have been used as green solvents for environmental protection because of their properties of excellent thermal stability and negligible vapor pressure. Beyond such traditional properties, recently, ionic liquids have received much attention as designer substrates with controllable physical and chemical properties and specific functions, so-called ‘Task-Specific Ionic Liquids [4].’ Therefore, they have been used not only as alternative solvents in many reaction and extraction systems, but also as substrates in functional materials. Poly(ionic liquid)s are termed just the polymeric forms of ionic liquids, but they are not necessary to exhibit liquid form at room temperature or even at some ambient temperatures. The major advantages for providing the poly(ionic liquid)s are to be enhanced stability and improved processability and feasibility in application as practical materials. The imidazolium-based polymerizable ionic liquids as a source of the most common poly(ionic liquid)s are available by incorporating the polymerizable groups at anionic or cationic site [5] because an imidazolium group is one of the most common cationic structures in ionic liquids. In the latter case, polymerizable groups having a C=C bond are present as a *N*-substituent on the imidazolium group. A vinylbenzyl group is one of the most conventional polymerizable groups appeared in the imidazolium-based ionic liquids, which leads to a polystyrene main-chain by its radical polymerization (Figure 1). The reaction of vinylbenzyl chloride with 1-alkylimidazoles gives polymerizable ionic liquids (**1**) having the vinyl benzyl group connected to the imidazolium group through a methylene. The radical polymerization of **1** with radical initiator such as AIBN produces a linear ionic polystyrenes (**2**) (Figure 1(a)). Furthermore, when vinylbenzyl chloride is reacted with 1-vinylimidazole, a polymerizable ionic liquid (**3**) having two polymerizable groups are produced. Because the resulting ionic liquid can be converted into an insoluble and stable ionic polystyrene (**4**) with the cross-linked structure by radical polymerization (Figure 1(b)),

leading to enhanced stability and improved flexibility and durability, it has a highly potential as the source of functional components in practical materials.

On the basis of the above backgrounds, in this chapter, the studies on the preparation of ionic polystyrene-based functional materials by means of radical polymerization of the polymerizable ionic liquids having the vinylbenzyl group are reviewed. In-situ approach exploiting the radical polymerization has been studied, giving rise to composite materials of the ionic polystyrenes with polysaccharides and clays. Furthermore, applications of the ionic polystyrenes such as absorbents for CO₂ and sorbent coatings for microextraction have also been investigated.

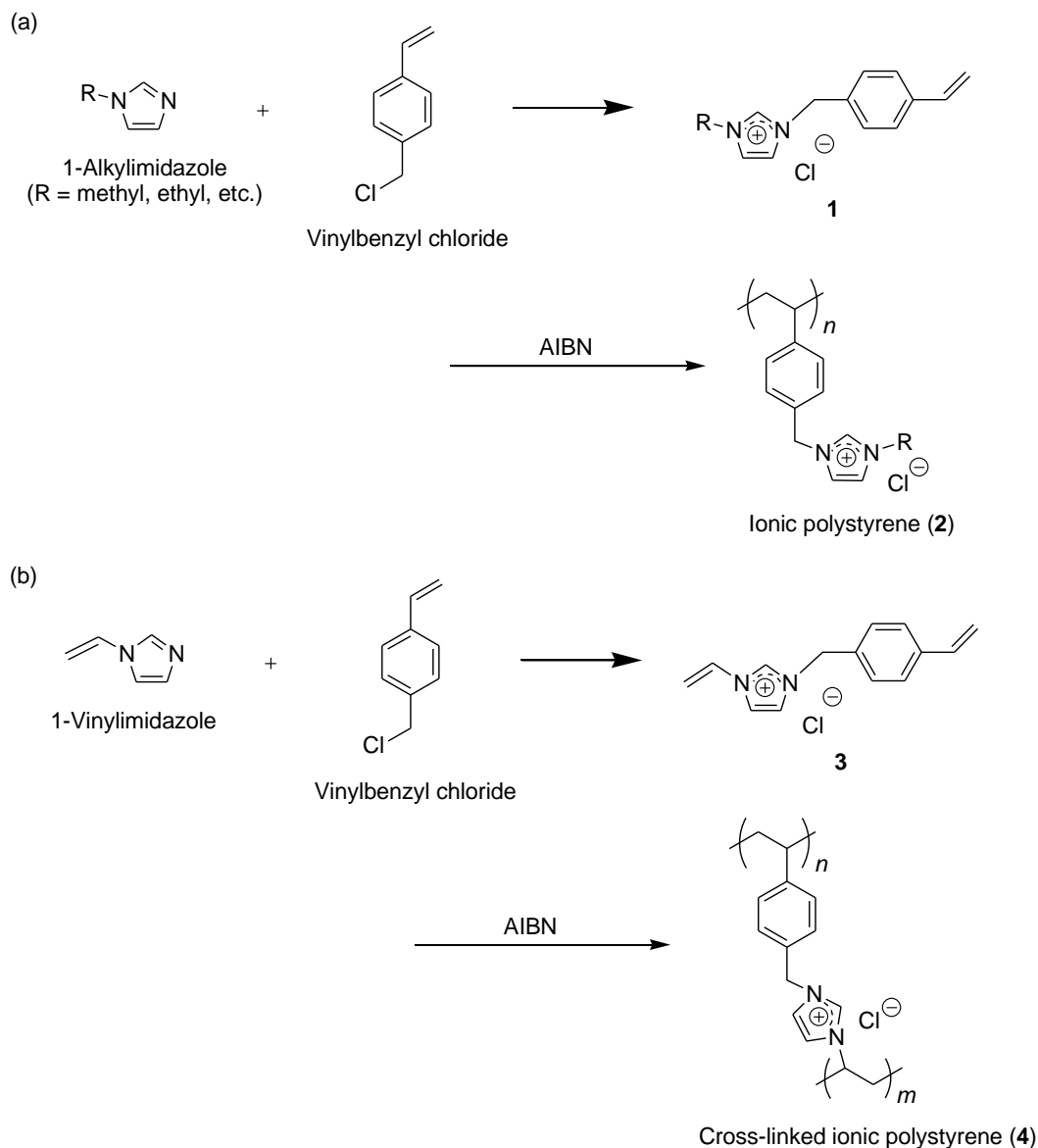


Figure 1. Synthesis of vinylbenzylimidazolium polymerizable ionic liquids (**1** and **3**) and their radical polymerization to produce ionic polystyrenes (**2** and **4**).

2.2. Preparation of Ionic Polystyrene Composites by in-Situ Polymerization

Composite materials of the ionic polystyrene with cellulose were prepared by in-situ radical polymerization of **3** (Figure 2) [6]. Cellulose is the most abundant biological macromolecule on the earth, which is a glucose polymer consisting of β -(1 \rightarrow 4)-linked glucose repeating units [7]. Cellulose has been studied on its fundamental chemical and physical properties. However, it has limited applications besides traditional purposes because of the strong inter- and intramolecular hydrogen bonds between the hydroxy groups of the glucose residues in the polymer chains. Even in recent years, therefore, considerable efforts have been still devoted to compatibilization of cellulose with synthetic polymers for improvement of the processability of cellulose. In-situ polymerization method, for example, has been useful for the fabrication of composites from cellulose [8].

For the preparation of the composite materials of cellulose with the ionic polystyrene by in-situ polymerization of **3**, the author found that **3** showed the ability for partially disrupting crystalline structure of cellulose by pre-treatment, indicating that **3** acted not only as a source of the ionic polystyrene, but also as a swelling agent of cellulose. Therefore, the target composite materials were prepared as follows. Cellulose (9.1–50.0 wt%) was first pre-treated with **3** by standing their mixtures at 7 °C for 24 h. The X-ray diffraction (XRD) profile of the pre-treated system (33.3 wt%) showed diminution of the crystalline peaks of cellulose (Figure 3(a) and (b)). The thermal gravimetric analysis (TGA) result of the pre-treated mixture (33.3 wt%) exhibited an onset weight loss at around 250 °C due to the thermal degradation of cellulose, which was ca. 50 °C lower than that of a standard cellulose. The XRD and TGA data indicated that cellulose chains were partially swollen in the pre-treated system using **3**.

After AIBN was added to the pre-treated mixtures, the systems were heated at 80 °C for 24 h for the progress of radical polymerization of **3**. Consequently, the composites were obtained without any isolation and purification procedures. The XRD (Figure 3(c)) and TGA results of all the composites indicated the partial disruption of the crystalline structure of cellulose. The compatibility between the ionic polystyrenes and cellulose in the composites was also evaluated by the scanning electron microscopic (SEM) measurement. The SEM image of the composite (Figure 4(b)) showed the completely different morphology from that of the original cellulose (Figure 4(a)), suggesting good compatibility between two components in the composite.

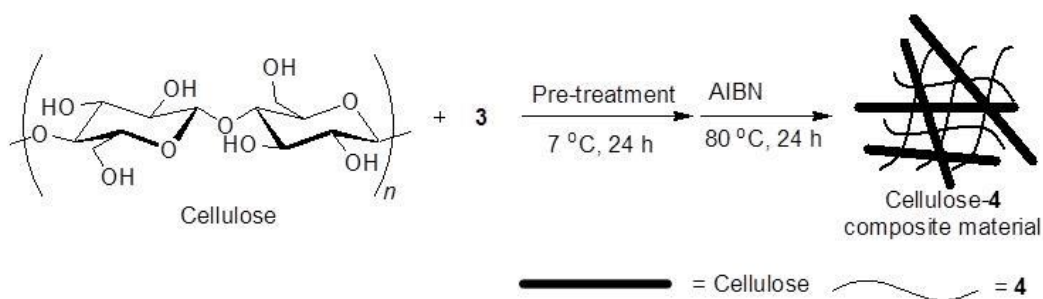


Figure 2. Preparation of cellulose-4 composite material by in-situ polymerization of **3**.

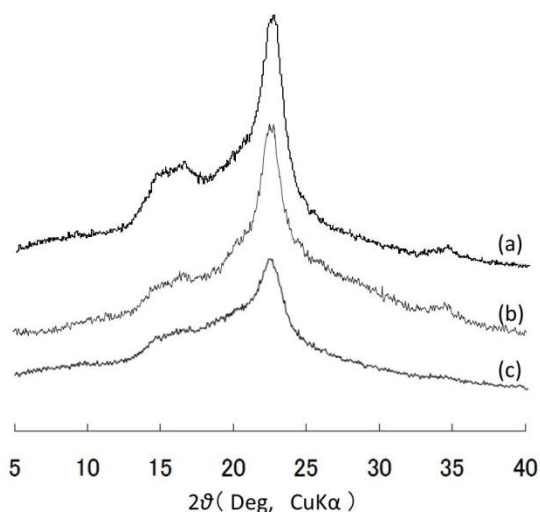


Figure 3. XRD profiles of cellulose (a), pre-treated mixtures of cellulose with **3** (b), and cellulose-**4** composite material (c).

The mechanical properties of the composites with 9.1, 33.3, and 50.0 wt% cellulose contents were evaluated by tensile testing. The composites sustained the stresses in the range 2.5–6.5 MPa and the strains at break were 1.3–2.0%. The higher content of cellulose in the composite (50 wt%) resulted in a brittle property. However, the appropriate content of cellulose affected to sustain higher stress. Consequently, the composite containing cellulose of 33.3 wt% exhibited good mechanical property.

The above approach for the preparation of composites by in-situ polymerization of the ionic liquids **1** and **3** having the vinylbenzyl group was extended to employ other polysaccharide such as fenugreek gum (FG) and ι -carrageenan [9]. These polysaccharides are used as hydrocolloids for a stabilizer, a viscous agent, and a structure provider in food industries [10]. The former is one of the representative galactomannans, well-known hydrocolloid polysaccharides, which is composed of galactose/mannose ratios of ca. 1:1.

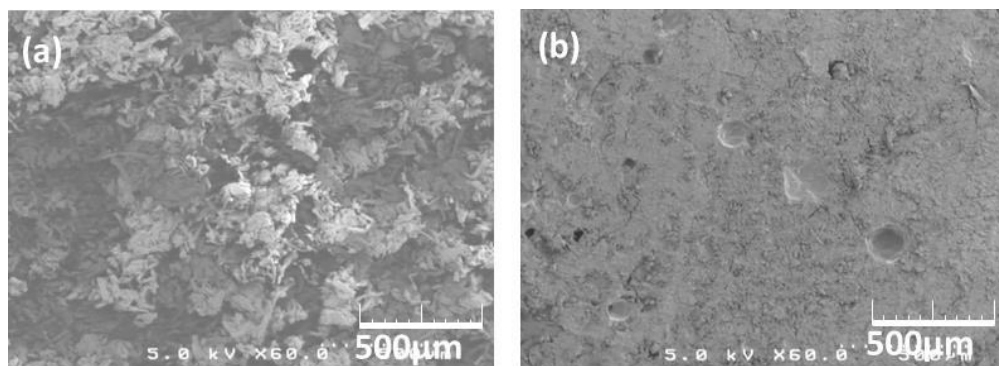


Figure 4. SEM images of cellulose (a) and cellulose-**4** composite material (b).

An attempt to prepare FG films compatibilized with the ionic polystyrene was made by means of in-situ radical polymerization of polymerizable ionic liquids in mixtures of FG with an ionic liquid solvent, 1-butyl-3-methylimidazolium chloride (BMIMCl) (Figure 5). In this approach, such BMIMCl was used as the solvent for film formation by regeneration from the solution because BMIMCl has been used as a good solvent for polysaccharides [11] and applied for the gel formations of polysaccharides [12]. Furthermore, two polymerizable ionic liquids, **1** and **5**, were used in this approach to produce the composite film with FG by in-situ polymerization; the latter has two polymerizable groups, acrylate and vinyl, and thus, acts as a cross-linking agent in the polymerization. It has already been found that the combination of **1** with **5** gave a cross-linked and stable ionic polystyrene (poly(**1-co-5**)) by radical copolymerization, which showed an ability for the formation of a transparent film [13]. For the fabrication of FG-ionic polystyrene composite film, a suspension of FG, **1**, and **5** with AIBN in BMIMCl was thinly casted on a Petri dish. Then, the suspension was heated at 100 °C for 9 h simultaneously for the dissolution of FG with BMIMCl and the progress of radical copolymerization. The resulting homogeneous material was left standing at room temperature for 3 h for the gelation. The gel-like product was subjected to Soxhlet extraction with ethanol to remove BMIMCl and unreacted **1** and **5**, followed by drying under reduced pressure to give the composite film. The strain values at break under tensile mode increased with increasing the unit ratios of **1** in the ionic polystyrenes, whereas the fracture stress values decreased. These data indicated the lower cross-linking density in the ionic polystyrenes affected to exhibit higher elasticity of the composite films. The similar approach by means of in-situ copolymerization of **1** with **5** was extended to the cellulose/chitin composite system [14] because chitin is one of the representative biological macromolecules comparable to cellulose [15].

ι -Carrageenan is a water-soluble phycocolloid extracted from red algae. Because of the presence of the anionic charges, it is expected to form well-miscible composites with cationic polystyrenes through cross-linking via ionic exchange, which possibly contribute to improving the mechanical properties of the materials. It has also been considered that the material may exhibit the electrical conductivity due to the ionic nature. Therefore, the preparation of the ι -carrageenan-ionic polystyrene **4** composite material by in-situ polymerization of **3** was performed according to the similar manner as that of the aforementioned cellulose composite material (Figure 6). The CP-MS ^{13}C NMR and IR spectra of the resulting composite fully supported the structure composed of ι -carrageenan and **4**. The mechanical property of the composite evaluated under compressive mode showed the fracture stress of 102.0 MPa with the strain of 10.7% at break. These values were larger than those of the aforementioned cellulose composite with **4**. The good mechanical property of the ι -carrageenan-**4** composite was reasonably explained by the formation of good miscibility, which was probably owing to the cross-linking through the ionic exchange between ι -carrageenan and **4**. The electrical conductivity of the composite was measured to be $1.6 \times 10^{-4} \text{ S cm}^{-1}$, which was comparable to the conductance of semiconductor and higher than that of the cellulose composite with **4** ($2.8 \times 10^{-5} \text{ S cm}^{-1}$). The higher electrical conductivity of the ι -carrageenan composite indicated the role of the effective ionic exchange during the formation of the composite due to the presence of charges in ι -carrageenan.

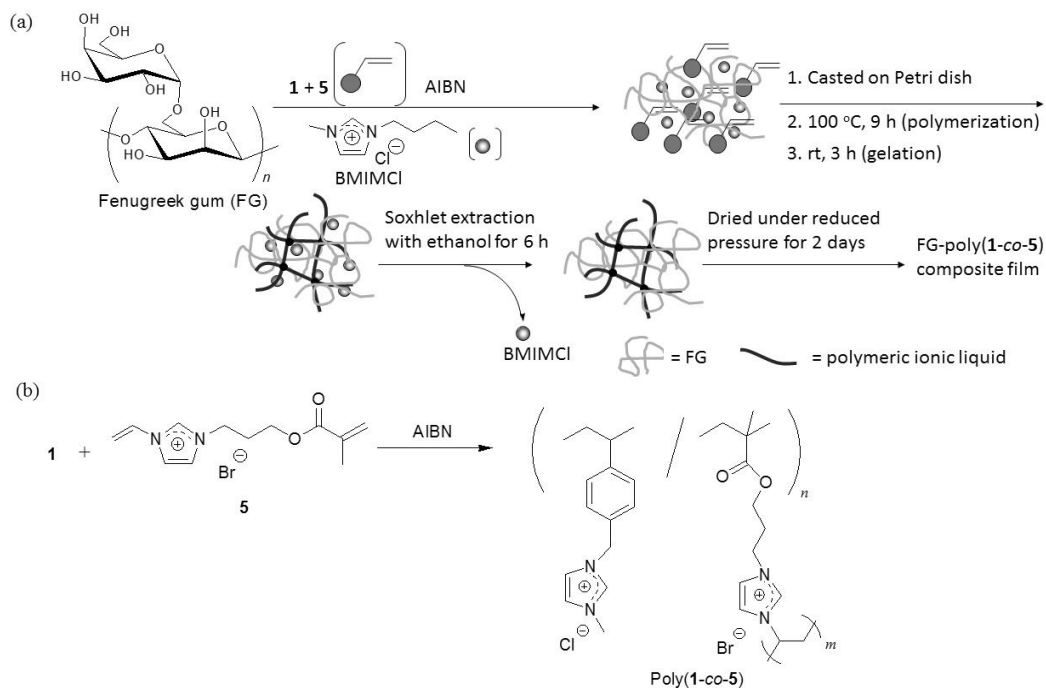


Figure 5. Preparation of FG-poly(1-co-5) composite film by in-situ copolymerization of polymerizable ionic liquids **1** and **5** (a) and radical copolymerization of **1** with **5** (b).

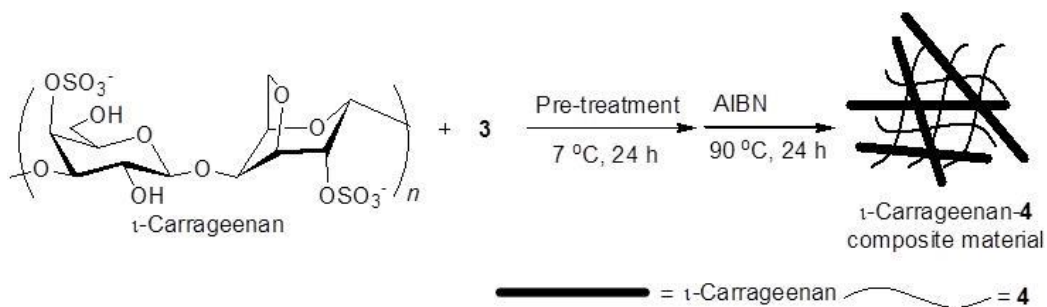


Figure 6. Preparation of ι -carrageenan-4 composite material by in-situ polymerization of **3**.

Clay-ionic polystyrene composites were also prepared by in-situ polymerization of polymerizable ionic liquids having the vinylbenzyl group. A simple chemical route for the exfoliation of kaolinite by in-situ polymerization of **1** and the resulting obtainment of an exfoliated nanocomposite was reported [16]. Kaolinite is a 1:1 dioctahedral layered mineral whose layers are formed of siliceous tetrahedral sheets linked to aluminium octahedral sheets [17]. The exfoliated nanocomposite of kaolinite with the ionic polystyrene **2** was produced by the intercalation and in-situ polymerization of **1** in a urea kaolinite pre-intercalate. The morphology of the resulting nanocomposite consisted of individual exfoliated layers of kaolinite dispersed in a continuous mixture of **2** and remaining urea. The same approach was

used with a DMSO kaolinite pre-intercalate. In this case, the resulting composite was a mixture of partially exfoliated individual layers of kaolinite and collapsed ones. These results indicated that the choice of the starting pre-intercalate of kaolinite was critical for the nature of the resulting composites.

Vinylbenzylimidazolium ionic liquids with methyl (**1**), hexyl (**6**), and dodecyl (**7**) as pendant alkyl substituents on the imidazolium group (Figure 7) were used as cation exchange monomers for clay montmorillonite (MMT)-Na⁺ [18]. Ionic polystyrene (**2**, **8**, and **9**)-MMT composites were subsequently prepared by in-situ intercalative radical polymerization of the vinylbenzylimidazolium polymerizable ionic liquids containing dispersed organophilic MMT. The ionic polystyrenes **2** and **8** prepared by in-situ polymerization of **1** and **6** with the shorter pendant groups appeared as conventional and microstructured composites with the silicate platelets dispersed within the continuous matrix as phase-separated micro-sized aggregates. In contrast, a high degree of organophilic clay dispersion in the ionic polystyrene **9** was obtained starting from the MMT functionalized using **7** likely to be due to exfoliation of the silicate layers occurring during in-situ radical polymerization of **7**.

3. IONIC POLYSTYRENES AS ABSORBENTS FOR CO₂

It has been found that CO₂ is remarkably soluble in imidazolium-based ionic liquids [19]. Therefore, the ionic liquids have been explored as reversible absorbents for CO₂ separation. The CO₂ solubility and selectivity can be tuned by choice of cation, anion, and substituents [20].

It has been found that poly(ionic liquid)s have higher CO₂ absorption capacity than room temperature ionic liquids [21]. The CO₂ sorption and desorption of the poly(ionic liquid)s are very fast and the sorption is completely reversible. For example, the ionic polystyrenes with the different counter anions (**14-16**) were synthesized by anion exchange of a vinylbenzylimidazolium chloride (**10**) with the corresponding sodium salts, and subsequent radical polymerization of the resulting polymerizable ionic liquids (**11-13**) (Figure 8). The ionic polystyrenes had enhanced CO₂ sorption capacities and fast sorption/desorption rates compared with room temperature ionic liquids. The ionic polystyrene (**15**) with PF₆⁻ counter anion had the highest CO₂-sorption capacity, while those (**14** and **16**) with BF₄⁻ or Tf₂N⁻ counter anions had the same capacities. The sorption was selective over H₂, N₂, and O₂. The Henry's constant of **14** was measured to be 26.0 bar, which was lower than that of a similar room temperature ionic liquid. The mechanism study indicated that the CO₂ sorption of the polymer particles was more absorption (the bulk), but less adsorption (the surface).

Copper-mediated atom transfer radical polymerization of the vinylbenzylimidazolium ionic liquid **11** with BF₄⁻ counter anion was carried out [22]. When the effect of various initiator/catalyst systems, monomer concentrations, solvent polarities, and reaction temperatures on the polymerization were examined, it was found that CuBr/1,1,4,7,10,10-hexamethyltriethylenetetramine or CuBr/2,2-bipyridine as the catalyst/initiator system gave the controlled fashion of the polymerization. Characterizations by the TGA, differential scanning calorimetric (DSC), and XRD analyses showed that the resulting ionic polystyrene was amorphous and had excellent thermal stability with a glass-transition temperature of 84 °C. The polymer absorbed 0.30% (w/w) CO₂ at room temperature and 0.78 atm.

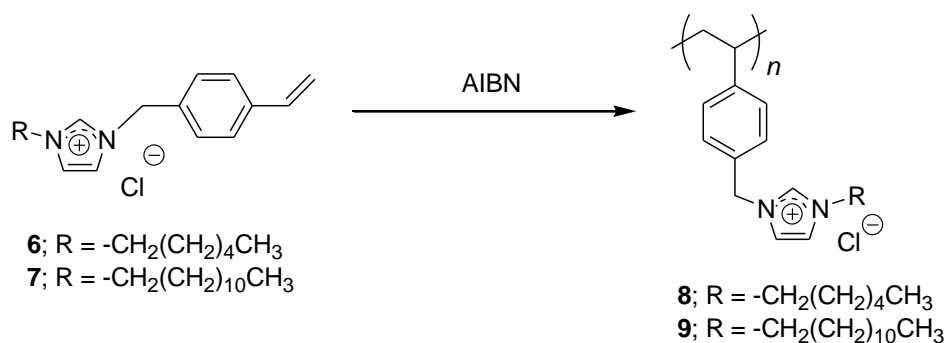


Figure 7. Radical polymerization of polymerizable ionic liquids (**6** and **7**) with different alkyl groups.

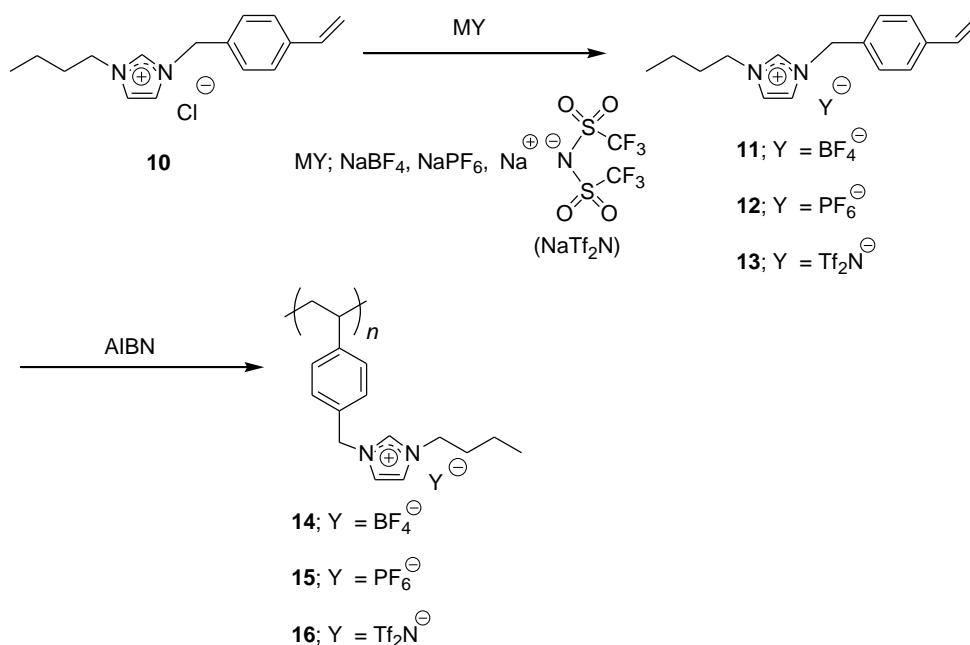


Figure 8. Synthesis of ionic polystyrenes (**14-16**) with different counter anions.

4. IONIC POLYSTYRENES AS SORBENT COATINGS FOR SOLID-PHASE MICROEXTRACTION

The ionic polystyrenes with long or bulky substituent on the imidazolium ring have been used as sorbent coatings for solid-phase microextraction. For example, a vinylbenzylimidazolium ionic liquid (**17**) having a hexadecyl group with Tf₂N[⊖] counter anion was polymerized by AIBN (Figure 9) and the resulting ionic polystyrene **19** showed impressive selectivity towards the extraction of polycyclic aromatic hydrocarbons from aqueous samples when it was used as a sorbent coating in direct-immersion solid-phase microextraction [23]. The ionic polystyrene **19** was imparted with aromatic character to enhance π - π interaction between the analytes and sorbent coating.

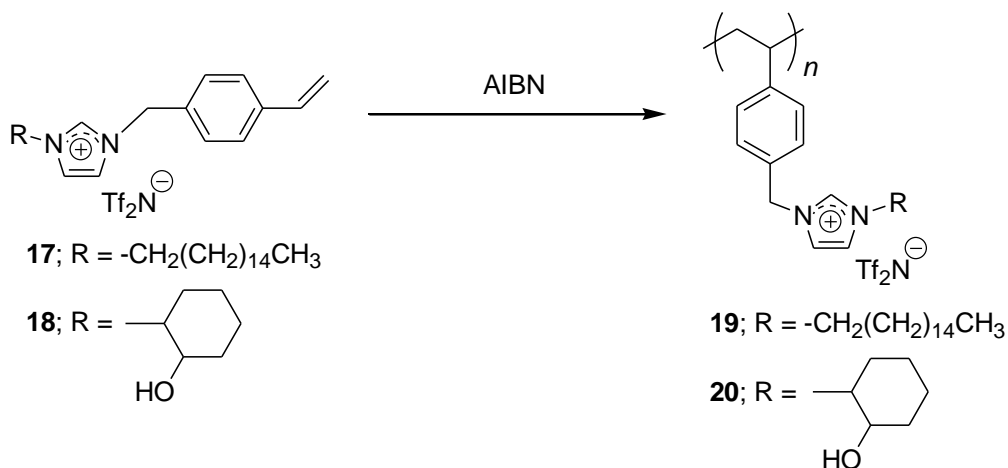


Figure 9. Synthesis of ionic polystyrenes (**19** and **20**).

An ionic polystyrene **20** having a hydroxycyclohexyl group in place of the hexadecyl group of the above was also used as a sorbent coating for solid-phase microextraction, which exhibited good film stability, high thermal stability, and long lifetime [24]. The mechanism of extraction for ionic polystyrene-based solid-phase microextraction sorbent coatings was also investigated [25]. The results were compared with conventional coatings, a polydimethylsiloxane/divinylbenzene coating and a polyacrylate coating, which were known to extract analytes primarily through adsorption and partitioning mechanisms, respectively. The study revealed that the ionic polystyrene-based coatings extracted analytes via a non-competitive partitioning mechanism.

CONCLUSION

This chapter reviewed the synthesis and applications of the ionic polystyrenes derived by radical polymerization of the vinylbenzylimidazolium polymerizable ionic liquids. The designed polymerizable ionic liquids were synthesized by the reaction of vinylbenzyl chloride with imidazoles having prospective substituents and the subsequent anion exchange. The polysaccharide-ionic polystyrene composite materials were prepared by in-situ polymerization of the vinylbenzylimidazolium polymerizable ionic liquids in the mixtures with polysaccharides such as cellulose (with chitin), FG, and ι -carrageenan. The similar in-situ polymerization approach produced the clay-ionic polystyrene composite materials. It was found that the ionic polystyrenes had enhanced CO_2 sorption capacities and fast sorption/desorption rates compared with room temperature ionic liquids. Furthermore, the ionic polystyrenes with long or bulky substituent on the imidazolium ring have been used as sorbent coatings for solid-phase microextraction. This review concludes with the further aspect that the ionic polystyrenes derived from the vinylbenzylimidazolium ionic liquids described herein have a high potential as functional materials and thus, will be used in practical application field in the future.

REFERENCES

- [1] Wünsch, J. R. (2000). *Polystyrene: Synthesis, production and applications*. Shropshire: iSmithers Rapra Publishing.
- [2] Green, O., Grubjesic, S., Lee, S. & Firestone, M. A. (2009). The design of polymeric ionic liquids for the preparation of functional materials. *J. Macromol. Sci., Part C: Polym. Rev.*, *49*, 339–360.
- [3] (a) Mecerreyes, D. (2011). Polymeric ionic liquids: broadening the properties and applications of polyelectrolytes. *Prog. Polym. Sci.*, *36*, 1629–1648. (b) Yuan, J., Mecerreyes, D. & Antonietti, M. (2013). Poly(ionic liquid)s: An update. *Prog. Polym. Sci.*, *38*, 1009–1036.
- [4] Giernoth, R. (2010). Task-specific ionic liquids. *Angew. Chem. Int. Ed.*, *49*, 2834–2839.
- [5] Kadokawa, J. (2011). Preparation of polysaccharide-based materials compatibilized with ionic liquids. In: Kokorin A. (Ed.), *Ionic liquids, Application and perspectives*, 95–114, Rijeka: InTech.
- [6] Kadokawa, J., Murakami, M. & Kaneko, Y. (2008). A facile method for preparation of composites composed of cellulose and a polystyrene-type polymeric ionic liquid using a polymerizable ionic liquid. *Compos. Sci. Technol.*, *68*, 493–498.
- [7] (a) Klemm, D., Heublein, B., Fink, H.-P. & Bohn, A. (2005). Cellulose: Fascinating biopolymers and sustainable raw material. *Angew. Chem. Int. Ed.*, *44*, 3358–3393. (b) Klemm, D., Kramer, F., Moritz, S., Lindström, T., Ankerfors, M., Gray, D. & Dorris, A. (2011) Nanocelluloses: A new family of nature-based materials. *Angew. Chem. Int. Ed.*, *50*, 5438–5466.
- [8] (a) Murakami, M.; Kaneko, Y. & Kadokawa, J. (2007). Preparation of cellulose-polymerized ionic liquid composite by in-situ polymerization of polymerizable ionic liquid in cellulose-dissolving solution. *Carbohydr. Polym.*, *69*, 378–381. (b) Takegawa, A.; Murakami, M.; Kaneko, Y. & Kadokawa, J. (2009). A facile preparation of composites composed of cellulose and polymeric ionic liquids by in situ polymerization of ionic liquids having acrylate groups. *Polym. Compos.*, *30*, 1837–1841. (c) Prasad, K.; Mine, S.; Kaneko, Y. & Kadokawa, J. (2010). Preparation of cellulose-based ionic porous material compatibilized with polymeric ionic liquid. *Polym. Bull.*, *64*, 341–349. (d) Kadokawa, J. (2013). Preparation of polysaccharide-polymeric ionic liquid composite materials. *J. Biobased Mater. Bioenergy*, *7*, 3–11.
- [9] (a) Prasad, K. & Kadokawa, J. (2010). Preparation of composite materials composed of ι -carrageenan and polymeric ionic liquids. *Polym. Compos.*, *31*, 799–806. (b) Kadokawa, J., Kato, T., Setoyama, M. & Yamamoto, K. (2013). Preparation of galactomannan-based materials compatibilized with ionic liquids. *J. Polym. Environ.*, *21*, 512–519.
- [10] Stephen, A. M., Philips, G. O. & Williams, P. A. (1995). *Food polysaccharides and their applications*. London: Taylor & Francis.
- (a) Swatloski, R. P., Spear, S. K., Holbrey, J. D. & Rogers, R. D. (2002). Dissolution of cellulose with ionic liquids. *J. Am. Chem. Soc.*, *124*, 4974–4975. (b) Seoud, O. A. E., Koschella, A., Fidale, L. C., Dorn, S. & Heinze, T. (2007). Applications of ionic liquids in carbohydrate chemistry: A windows of opportunities. *Biomacromolecules*, *8*, 2629–264. (c) Liebert, T. & Heinze, T. (2008). Interaction of ionic liquids with

- polysaccharides 5. Solvents and reaction media for the modification of cellulose. *BioResources*, 3, 576-601. (d) Feng, L. & Chen, Z. -I. (2008). Research progress on dissolution and functional modification of cellulose in ionic liquids. *J. Mol. Liq.*, 142, 1-5. (e) Pinkert, A., Marsh, K. N., Pang, S. & Staiger, M. P. (2009). Ionic liquids and their interaction with cellulose. *Chem. Rev.*, 109, 6712-6728. (f) Zakrzewska, M. E., Lukasik, E. B. & Lukasik, R. B. (2010). Solubility of Carbohydrates in Ionic Liquids. *Energy Fuels*, 24, 737-745.
- [11] (a) Kadokawa, J., Murakami, M., and Kaneko, Y. (2008). A facile preparation of gel materials from a solution of cellulose in ionic liquid. *Carbohydr. Res.*, 343, 769-772. (b) Kadokawa, J., Murakami, M., Takegawa, A., and Kaneko, Y. (2009). Preparation of cellulose starch composite gel and fibrous material from a mixture of the polysaccharides in ionic liquid. *Carbohydr. Polym.*, 75, 180-183. (c) Prasad, K., Murakami, M., Kaneko, Y., Takada, A., Nakamura, Y., and Kadokawa, J. (2009). Weak gel of chitin with ionic liquid, 1-allyl-3-methylimidazolium bromide. *Int. J. Biol. Macromol.*, 45, 221-225. (d) Prasad, K.; Kaneko, Y. and Kadokawa, J. (2009). Novel gelling systems of κ -, λ - and ι - carrageenans and their composite gels with cellulose using ionic liquid. *Macromol. Biosci.*, 9, 376-382. (e) Takegawa, A., Murakami, M., Kaneko, Y., and Kadokawa, J. (2010). Preparation of chitin/cellulose composite gels and films with ionic liquids. *Carbohydr. Polym.*, 79, 85-90. (f) Prasad, K.; Izawa, H.; Kaneko, Y. and Kadokawa, J. (2009). Preparation of temperature-induced shapeable film material from guar gum-based gel with an ionic liquid. *J. Mater. Chem.*, 19, 4088-4090. (g) Izawa, H., Kaneko, Y., and Kadokawa, J. (2009). Unique gel of xanthan gum with ionic liquid and its conversion into high performance hydrogel. *J. Mater. Chem.*, 19, 6969-6972. (h) Izawa, H. and Kadokawa, J. (2010). Preparation and characterizations of functional ionic liquid-gel and hydrogel of xanthan gum. *J. Mater. Chem.*, 20, 5235-5241. (i) Mine, S., Prasad, K., Izawa, H., Sonoda, K., and Kadokawa, J. (2010). Preparation of guar gum-based functional materials using ionic liquid. *J. Mater. Chem.*, 20, 9220-9225.
- [12] (a) Wakizono, S., Yamamoto, K. & Kadokawa, J. (2011). FRET function of polymeric ionic liquid film containing rhodamine moieties for exhibiting emissions by excitation at wide wavelength areas. *J. Photochem. Photobiol. A: Chem.*, 222, 283-287. (b) Wakizono, S., Yamamoto, K. & Kadokawa, J. (2012). Tunable multicolor emissions of polymeric ionic films carrying proper fluorescent dye moieties. *J. Mater. Chem.*, 22, 10619-10624.
- [13] Setoyama, M., Kato, T., Yamamoto, K. & Kadokawa, J. (2013). Preparation of chitin/cellulose films compatibilized with polymeric ionic liquids. *J. Polym. Environ.*, 21, 795-801.
- [14] (a) Kurita, K. (2006). Chitin and chitosan: functional biopolymers from marine crustaceans. *Mar. Biotechnol.*, 8, 203-226. (b) Rinaudo, M. (2006). Chitin and chitosan: properties and applications. *Prog. Polym. Sci.*, 31, 603-632. (c) Pillai, C. K. S., Paul, W., Sharma, C. P. (2009). Chitin and chitosan polymers: chemistry, solubility and fiber formation. *Prog. Polym. Sci.*, 34, 641-678.
- [15] Letaief, S., Leclercq, J., Liu, Yun. & Detellier, C. (2011). Single kaolinite nanometer Layers prepared by an in situ polymerization exfoliation process in the presence of ionic liquids. *Langmuir*, 27, 15248-25254.

- [16] (a) Bailey, S. W. (Ed.), *Hydrous phyllosilicates*, Washington DC: American Mineralogical Society, 1988. (b) Newman, A. C. D. & Brown, G. The chemical constitution of clays. Newman, A. C. D. (Ed.), In *Chemistry of clays and clay minerals*; Longman Scientific and Technical. Monograph, n6., Chapter 1, London: Mineralogical Society, 1987.
- [17] Pucci, A., Liuzzo, V., Melai, B., Pomelli, C. S. & Chiappe, C. (2012). Polymerizable ionic liquids for the preparation of polystyrene/clay composites. *Polym. Int.*, *61*, 426-433.
- [18] Blanchard, L. A., Hancu, D., Beckman, E. J. & Brennecke, J. F. (1999). Green processing using ionic liquids and CO₂. *Nature*, *399*, 28-29.
- [19] (a) Tang, J., Tang, H., Sun, W., Radosz, M. & Shen, Y. (2005). Low-pressure CO₂ sorption in ammonium-based poly(ionic liquid)s. *Polymer*, *46*, 12460-12467. (b) Blasig, A., Tang, J., Hu, X., Tan, S. P., Shen, Y. & Radosz, M. (2007). Carbon dioxide solubility in polymerized ionic liquids containing ammonium and imidazolium cations from magnetic suspension balance: P[VBTMA][BF₄] and P[VBMI][BF₄]. *Ind. Eng. Chem. Res.*, *46*, 5542-5547. (c) Bhavsar, R. S., Kumbharkar, S. C. & Kharul, U. K. (2012). Polymeric ionic liquids (PILs): Effect of anion variation on their CO₂ sorption. *J. Membr. Sci.*, *389*, 305-315.
- [20] (a) Tang, J., Sun, W., Tang, H., Radosz, M. & Shen, Y. (2005). Enhanced CO₂ absorption of poly(ionic liquid)s. *Macromolecules*, *38*, 2037-2039. (b) Tang, J., Tang, H., Sun, W., Plancher, H., Radosz, M. & Shen, Y. (2005). Poly(ionic liquid)s: a new material with enhanced and fast CO₂ absorption. *Chem. Commun.*, 3325-3327. (c) Tang, J., Tang, H., Sun, W., Radosz, M. & Shen, Y. (2005). Poly(ionic liquid)s as new materials for CO₂ absorption. *J. Polym. Sci., Part A: Polym. Chem.*, *43*, 5477-5489.
- [21] Tang, H., Tang, J., Ding, S., Radosz, M. & Shen, Y. (2005). Atom transfer radical polymerization of styrenic ionic liquid monomers and carbon dioxide absorption of the polymerized ionic liquids. *J. Polym. Sci., Part A: Polym. Chem.*, *43*, 1432-1443.
- [22] Meng, Y. & Anderson, J. L. (2010). Tuning the selectivity of polymeric ionic liquid sorbent coatings for the extraction of polycyclic aromatic hydrocarbons using solid-phase microextraction. *J. Chromatogr. A*, *1217*, 6143-6152.
- [23] González-Álvarez, J., Blanco-Gomisa, D., Arias-Abrodo, P., Pello-Palmaa, J., Ríos-Lombardía, N., Bustob, E., Gotor-Fernández, V. & Gutiérrez-Álvarez, M. D. (2013). Analysis of beer volatiles by polymeric imidazolium-solid phase microextraction coatings: Synthesis and characterization of polymeric imidazolium ionic liquids. *J. Chromatogr. A*, *1305*, 35-40.
- [24] Ho, T. D., Cole, W. T. S., Augusto, F. & Anderson, J. L. (2013). Insight into the extraction mechanism of polymeric ionic liquid sorbent coatings in solid-phase microextraction. *J. Chromatogr. A*, *1298*, 146-151.

Chapter 7

HYPERCROSSLINKED POLYSTYRENE: A NEW LIFE FOR THE OLD POLYMER

*M. P. Tsyurupa, A. V. Pastukhov, Z. K. Blinnikova,
L. A. Pavlova, M. M. Il'in, Yu. A. Davidovich
and V. A. Davankov**

Nesmeyanov-Institute of Organoelement Compounds,
Russian Academy of Sciences, Moscow, Russian Federation

ABSTRACT

Hypercrosslinked polystyrene (HP) has been obtained by an intensive crosslinking of strongly solvated pre-formed polystyrene chains with numerous rigid bridges. This approach results in obtaining uniformly crosslinked single-phase open-network polymers with developed intrinsic nanoporosity and a unique ability to swell in any liquid and gaseous media. Noteworthy, HP is characterized by a non-typical physical state, it belongs neither to glassy, nor rubber-like polymers. Owing to its special open network structure and high permeability, HP represents an excellent adsorbing material for large-scale water purification, separation of organic or inorganic compounds, solid-phase extraction of trace components in analytical chemistry, efficient detoxification of blood, etc. Polystyrene with ultimate crosslinking densities, up to a nominal 500%, displays a particularly high affinity even to small polar organic compounds and mineral electrolytes.

1. INTRODUCTION

Polystyrene represents one of the oldest and the most widespread polymers in the world. Its history started as far back as 1839 when a German apothecary Edmon Simon distilled an oily liquid named styrol from the resin of Turkish sweet gum trees. In several days the apothecary found out that sterol converted into a jelly product that he thought to be the result of the oxidation process. For that reason, the jelly product received the name styroloxide. Six years later it became clear that the formation of the jelly product also proceeds in the absence

of oxygen and the product was renamed as metastyrol/styroloxide. In 1866 famous French chemist Berthelot identified the formation of metastyrol from styrol as a polymerization process. (It is quite interesting to note here that the term “polymer” already existed. It was coined by the great scientist Berzelius as early as 1833 to describe organic compounds having an identical empirical formula but differing in overall molecular weight, so that the use of the new term “polymerization” was fully justified). Only in the beginning of the 20th century it was realized that heating of styrol (as well as its storage at room temperature) initiates a chain reaction leading to the formation of macromolecules. Eventually the product received its present name, polystyrene.

In 1931, scientists of IG. Farben (today’s BASF) developed a way to commercially manufacture polystyrene. However, the real breakthrough in commercial polystyrene production dates to the end of the 1930s when scientists at Dow Chemical Company developed an inhibitor of styrene polymerization. It proved to be a key component that enabled the production of high purity styrene and polystyrene at a low cost. The commercial product was named STYRON Polystyrene and in 1937 it was introduced to the U.S. market. From that moment on, the practical use of polystyrene became more and more intensive. At present, polystyrene is employed in the construction and armaments industry, medicine, electrical engineering, electronics, in private life and many other fields of human activity.

Apart from linear polystyrene, styrene copolymers, in particular, copolymers with butadiene and divinylbenzene (DVB) also represent large-tonnage products all over the world. The latter crosslinked copolymers are irreplaceable matrices for ion exchange resins. For the first time a styrene-DVB copolymer was obtained by Staudinger and Heuser in 1934 [1]. In 1942 D’Alelio developed a sulfonation process of the copolymer [2] and in 1944 he was granted a patent for the synthesis of strongly acidic ion exchange resins [3] and weakly basic exchangers, the latter being obtained by nitration styrene-DVB copolymers followed by the reduction of $-\text{NO}_3$ groups to $-\text{NH}_2$ groups [4]. Two years later, McBerney [5] invented the strongly basic ion exchangers by chloromethylation and amination of styrene-DVB copolymers. Besides, this procedure offered the way for preparing anion exchange resins with any basicity as well as numerous ion-selective sorbents. Since then, ion exchange resins based on styrene-DVB copolymers are widely used in hydrometallurgy, nuclear industry, wastewater treatment, polishing of potable water, food industry, etc.

In due time the diversity of fields of exchangers’ practical applications resulted in developing styrene-DVB copolymers of different physical structures. In general, three generations of polystyrene matrices and sorbents have to be distinguished.

The first generation comprises styrene-DVB copolymers having a single-phase, homogeneous (gel-type) structure. These historically first copolymers are obtained by free radical copolymerization of monomers in the absence of diluents. Transparent spherical beads of the copolymer have no pores; they are capable of swelling only in media with high thermodynamic affinity to polystyrene, such as toluene, ethylene dichloride, tetrahydrofuran etc. These gel-type styrene-DVB copolymers represent the most widespread matrix for making ion exchange resins of high sorption capacity by introduction of various functional groups, usually, sulfonic groups, amino groups or carboxylic groups. The polar functions make the polymeric network hydrophilic and provide it with the capability of swelling in water and alcohols. As was already mentioned above, the first accessible information on polystyrene-type exchangers appeared as early as 1944 [3, 4], but even nowadays, world-

wide, the water demineralization processes are deemed impossible without employing ion exchange resins of the first, gel-type generation.

Still, the decades-long experience of working with gel-type ion exchangers revealed their basic disadvantage, namely, resins with less than 5-6% DVB have unsatisfactory mechanical properties, but only they swell in water strongly enough to become permeable for relatively large ions and organic molecules. Mechanics can be enhanced by raising the degree of matrix crosslinking (i.e. its DVB content), however, at that point the permeability of gel-type resins drops. The problem of isolation and purification of large organic molecules became more and more important, while neither silica gels nor activated carbons met the requirements of practice. Therefore, extensive investigations were implemented in the 1950-1960s to develop styrene-divinylbenzene copolymers with improved kinetic characteristics [6].

The second generation of polystyrene-type matrices and sorbents comprise two-phase, heterogeneous materials. They have been obtained by free radical copolymerization of styrene with a large amount (more than 6-8%) of DVB in the presence of an inert diluent. As polymerization proceeds, nano-sized crosslinked particles form which precipitate from the initial homogeneous solution of comonomers. Subsequently they aggregate, agglomerate and eventually form an opaque macroporous material. Depending on the type of diluent used one may distinguish between two reasons for phase separation.

The first reason of microphase separation consists of thermodynamic incompatibility of growing polymeric chains or microgels with the inert diluent, if the latter mixes with monomers but precipitates polystyrene (at a certain moment when the major part of monomeric styrene was consumed). Aliphatic hydrocarbons and alcohols are typical examples of such diluents.

The second reason for microphase separation consists of limited swelling of growing crosslinked microgels in the inert diluent even if the latter represents a thermodynamically good medium for polystyrene, for example, toluene or xylene. At a certain enlarged DVB content the amount of the solvating diluent present in the system may prove to be larger than the growing three-dimensional network can incorporate. In this case the swollen microgel particles of styrene-DVB copolymer separate from the excess solvent, aggregate and agglomerate, while the non-absorbed solvent remains between the microgel particles and their connected supramolecular formations.

In the both cases, the resulting product represents two segregate phases, one of which is the crosslinked polymer and the other is the diluent. After the removal of the solvent, large pores remain between dense polymeric particles in the first case, whereas in the second case, in addition to large pores, micropores run through the polymeric micro particles.

Many scientific studies concerning the influence of various factors on the structure of macroporous copolymers resulted in developing a whole series of ion exchange resins and neutral sorbents of the second generation which exhibit excellent adsorption kinetics. Among them macroporous polystyrene sorbents of Amberlite XAD series produced by Rohm & Haas (USA) are the most reputed adsorbing materials.

The fields of practical application of macroporous copolymers are diversified. They encompass ion exchange of organic ions, catalysis of many organic reactions, gas and liquid chromatography, adsorption of organics from gaseous and aqueous media, etc.

At the same time, because of the high crosslinking degree of the polymeric microphase, the majority of organic substances adsorb on the pore surface, only, so that frequently the sorption capacity of macroporous copolymers proves to be insufficient for commercially

justified processes. This shortcoming was set in the very principle of preparing macroporous copolymers and cannot be eliminated without deterioration of either sorption capacity or kinetic properties of macroporous copolymers of the second generation.

Sorbents of the third generation have appeared and flourished on the base of hypercrosslinked polystyrene. In the beginning of the 1970s, Davankov and Tsyurupa [7] recognized that the synthesis of sorbents combining a good permeability with a good adsorption capacity is possible only if one approaches the problem of network formation from fundamentally different positions. The authors proposed a new concept that consists of the formation of a rigid homogeneous strongly expanded network. Such a network can be obtained by post-crosslinking polystyrene chains in solution, or in a swollen state, by a large amount of rigid bridges. When using reactive bifunctional crosslinking agents, it was possible to connect all phenyl rings of initial polystyrene chains and obtain a rigid homogeneous expanded openwork structure. Of course, these new and very useful materials required a new name. Therefore, the networks prepared in accordance with the aforementioned principle and, with the degree of crosslinking being higher than 40%, were named “hypercrosslinked polystyrene”.

Hypercrosslinked polystyrene owes its excellent adsorption properties to the unique network structure, which in turn, is determined by the conditions of network synthesis. Therefore it seems to be purposeful to first consider the basic principles of preparing hypercrosslinked polystyrene, its unusual properties and specific structural features, and then look at the most interesting aspects of its practical application.

One can find comprehensive information about hypercrosslinked polystyrene in the book written recently by V.A. Davankov and M.P. Tsyurupa "Hypercrosslinked Polymeric Networks and Adsorbing Materials" [8].

2. HYPERCROSSLINKED POLYSTYRENE

2.1. Basic Principle of Hypercrosslinked Polystyrene Preparation. Conditions of Synthesis

The basic principle of preparation of a hypercrosslinked polystyrene network consists of intensive crosslinking of sufficiently long polymeric chains in solution (or in a strongly swollen gel of a styrene-DVB copolymer) with rigid bridges [9]. These bridges-struts must maintain polymeric chains at a certain distance from each other in both swollen and dry networks.

Bis-chloromethylated aromatic hydrocarbons, monochlorodimethyl ether, methylal or other bifunctional compounds react with polystyrene in the presence of Friedel-Crafts catalysts and can be used as crosslinking agents. Figure 1 depicts the principal scheme of network synthesis by an example of the most frequently used reaction of monochlorodimethyl ether (MCDE) with polystyrene. The reaction proceeds in two stages. At first, chloromethyl groups are introduced in phenyl rings and then, the chloromethyl groups alkylate adjacent phenyls of neighbor chains, thus binding them by methylene $-CH_2-$ groups:

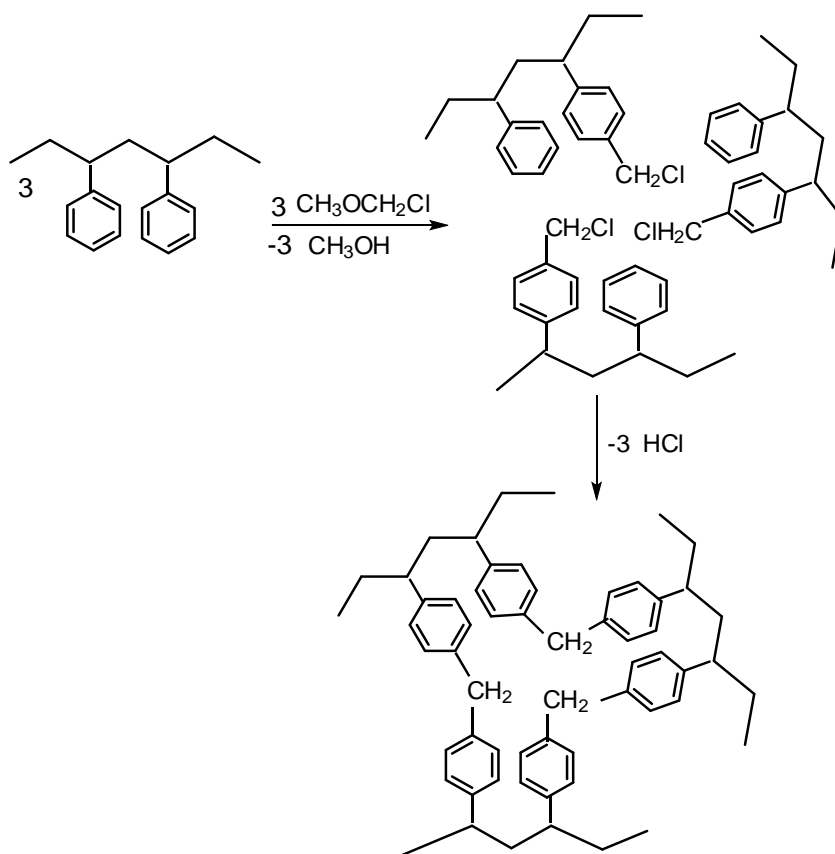


Figure 1. The scheme of hypercrosslinked polystyrene synthesis.

Under optimal conditions (80°C, 10-16 hrs, one mole SnCl_4 per one mole of MCDE, ethylene dichloride as reaction medium), the crosslinking agent reacts comprehensively with polystyrene and connects phenyl rings with methylene links. Therefore, the nominal crosslinking degree may be calculated from the ratio of the MCDE to styrene repeating units. In this Chapter we will define the degree of crosslinking based on the number of $-\text{CH}_2-$ groups binding each phenyl ring to neighboring phenyls. Thus, when 1 mole of polystyrene repeating units react with 0.5 mole of bifunctional MCDE, theoretically, one methylene group connects each two phenyl rings of polystyrene chains. In this case, each phenyl appears to be involved into bridging and the crosslinking degree of the resulting hypercrosslinked polystyrene (HP) network can be considered to amount to 100% (HP-100). Crosslinking of polystyrene with one mole of MCDE per phenyl ring leads to a network in which each phenyl ring participates twice in the formation of crosslinks. The degree of crosslinking of such polymer amounts to 200% (HP-200). In the case when polystyrene reacts with 1.5, 2.0 or 2.5 mole of the crosslinking agent, 3, 4 and 5 $-\text{CH}_2-$ groups bind each phenyl to its spatial neighbors and the formal degree of crosslinking, respectively, amounts to 300% (HP-300), 400% (HP-400) and 500% (HP-500).

Table 1. Conversion of monochlorodimethyl ether on crosslinking styrene-0.5% DVB copolymer

Polymer	MCDE mol/mol PS	Number of CH ₂ groups per phenyl	Conversion of MCDE, %	Unreacted chlorine, %
HP-43	0.3	0.6	100	None
HP-100	0.5	1	98	0.5
HP-200	1.0	2	-	0.8
HP-300	1.5	3	98.5	0.8
HP-400	2.0	4	-	2.3
HP-500	2.5	5	98.5	2-3

It is hard to believe the possibility of obtaining such ultimately crosslinked networks, however, gas chromatography shows that after accomplishing the crosslinking reaction, only traces of unreacted crosslinking agent remain in the reaction medium (Table 1). The ultimate extent of substitution on benzene rings is also confirmed by the absence of adsorption band at 3030 cm⁻¹ (vibration of aromatic C-H groups) in the FTIR spectrum of HP-500. At the same time the final network with the nominal crosslinking density of 500% contains a surprisingly small amount of unreacted chloromethyl groups, only 2-3% chlorine. (This chlorine content remains unchangeable after prolonged washing of the polymer with water, indicating substantial stability of the residual ClCH₂-groups at neutral pH and room temperature). Thus, we can assume the real crosslinking density of networks to be close to the calculated nominal one.

The chloromethylation reaction of polystyrene with the monochlorodimethyl ether was noted long ago to be accompanied by partial crosslinking polystyrene chains with methylene groups. In fact, we use this by-reaction as the main process for preparing hypercrosslinked polystyrene. In fact, when alkylating phenyl rings in a styrene-DVB copolymer, MCDE may also react with the occasionally remaining pendent double bonds of DVB units [10], however, in copolymers with 0.5-1% DVB, which we usually employ, the amount of pending double bonds is negligible. We also checked that SnCl₄ applied to catalyze the main Friedel-Crafts reaction does not catalyze alkylation of polystyrene with ethylene dichloride, reaction medium; it neither causes destruction or chlorination of polystyrene. Therefore, formation of -CH₂- links is definitely the main process in the crosslinking reaction. Naturally, industrial procedures for manufacturing hypercrosslinked polystyrene sorbents exploit other proprietary protocols for first introducing chloromethyl groups into the initial beaded copolymer and then involving them for the post-crosslinking, using less expensive catalysts. Copolymers of styrene with vinylbenzylchloride are also amenable to post-crosslinking. Other than MCDE, bifunctional crosslinking agents may also be used. Provided that basic conditions are met for the formation of a highly solvated rigid open network, properties of all products will point to their hypercrosslinked internal structure.

In the FTIR spectrum of the hypercrosslinked polystyrene sample HP-43 (Table 1) one can see the same characteristic bands that are present in the spectrum of polystyrene as such, namely, 3025 and 2922 cm⁻¹ referring to the vibration of aromatic CH and CH₂ groups, respectively, the bands in the range of 1600-1450 cm⁻¹ corresponding to the vibrations of aromatic rings, as well as bands at 760 and 700 cm⁻¹ that are ascribed to the vibration of

unsubsidized phenyl rings. By increasing the crosslinking density up to 300%, 400% and 500%, an additional intensive band appears at 1700 cm^{-1} [11]. Usually, this band has been ascribed to carbonyl groups. If judging by the high intensity of this band, the concentration of C=O groups should be sufficient for revealing them by means of characteristic organic reactions. However, treatment of the above polymers with hydroxylamine, sodium bisulfite, ethylorthoformate or LiAlH_4 causes neither disappearance of the band at 1700 cm^{-1} , nor emergence of corresponding new characteristic bands. The ^{13}C NMR method also confirms the absence of carbonyl groups in the chemical structure of ultimately crosslinked polymers. We believe therefore that the band at 1700 cm^{-1} in the FTIR spectra reflects the hindered vibrations of the C-C bonds and/or valence angles in a network with a high extent of mutual connection of its aromatic fragments. The correctness of our supposition was confirmed by the calculation of an IR-spectrum for a model fragment of HP-400 [12] where, indeed, a band shows up at 1697 cm^{-1} . On the reduction of aromatic rings by sodium in liquid ammonia, the band of interest disappeared and new bands at $1650\text{-}1680\text{ cm}^{-1}$ emerged.

2.2. Structure of Hypercrosslinked Polystyrene

Intensive crosslinking of strongly solvated polystyrene chains with numerous rigid bridges results in obtaining a single-phase rigid strongly expanded network.

Homogeneity of hypercrosslinked polystyrene structure. It is important to understand that crosslinking of polystyrene chains in solutions or in strongly swollen gel-type copolymers (both states may be achieved only in a thermodynamically good solvent) is not accompanied by phase separation and leads to a homogeneously crosslinked single-phase network. Indeed, before the reaction starts, all components are uniformly distributed throughout the entire volume of the initial solution. All polystyrene chains remain solvated by the good solvent both before and during the overall process of network formation. The crosslinking reaction starts simultaneously in many occasional points of contacts between polymeric chains. Only several seconds are required after the onset of the reaction to fix these chains in space by rigid bridges and deprive them of the possibility of approaching each other and forming a separate (from the solvent) polymeric phase. Indeed, X-ray scattering under small and large angles confirms the single-phase character of the hypercrosslinked polystyrene network. In fact, the scattering pattern resembles that of a polystyrene solution.

Statistical distribution of crosslinks in hypercrosslinked networks. In solvated atactic polystyrene, two neighboring phenyl rings in a zigzag chain are twisted about 120° [13]. If one bridge forms between the two chains, the next phenyls along the chains will locate far from one another and most likely will react with other chains. In other words, the formation of one bridge hampers the formation of the neighboring bridges between phenyl groups of the same pair of chains and precludes the emergence of domains with increased density of crosslinks. Thus, formation of a statistically uniform crosslinked network seems to be the most probable. All methods that were used to investigate the porosity of the hypercrosslinked polystyrenes testify to the rather uniform "pore" (free space between polystyrene chains) size distribution [14].

The basic structural element of hypercrosslinked polymer. All surprising properties of hypercrosslinked polystyrene manifest themselves at the degree of crosslinking of no less than 40%. In this case, each six of ten phenyl rings participate in the formation of three

bridges. If the crosslinking degree is 100%, virtually all phenyl rings are connected between each other, while at a crosslinking degree of 200% the majority of phenyls participate twice in bridge formation. Several traditional notions such as junction point, the distance between neighboring junction points, inter- and intramolecular crosslinks, etc., are inapplicable to hypercrosslinked networks. In order to understand specific properties of a hypercrosslinked network, it seems to be most correct to represent it as an openwork ensemble of mutually condensed and interpenetrating meshes. In the hypercrosslinked polystyrene network, the smallest and nearly unstressed mesh can be composed of three pairs of neighboring phenyl rings belonging to three different polystyrene chains and connected by three methylene groups (Figure 2). Importantly, this mesh contains a large amount of C-C bonds and, in principle, can change its spatially distorted conformation.

Each mesh in the network is condensed with many other meshes as illustrated by a scheme in Figure 2. More recently, publications appeared on modeling hypercrosslinked polystyrene by atomistic molecular dynamics [15, 16].

Since the hypercrosslinked network contains no long flexible chain fragments between the macrocycles, any change in the conformation of one mesh unavoidably involves corresponding changes in the conformation of its neighboring meshes. Importantly, appropriate cooperative conformational rearrangement of a large number of meshes should, in principle, enable relatively large alterations of the total network volume, which, indeed, takes place on drying and swelling of all hypercrosslinked polymers.

Still, the cooperative conformational rearrangement of network meshes is possible only under the condition that all meshes have a sufficient extent of freedom to change. In the first place, this mesh flexibility depends upon the existence of free space inside the mesh, i.e., on the number of alien chains (belonging to other meshes) that are embraced by the mesh. The extent of such interpenetration of meshes is unambiguously determined by the concentration of polystyrene chains in the initial solution subjected to the crosslinking.

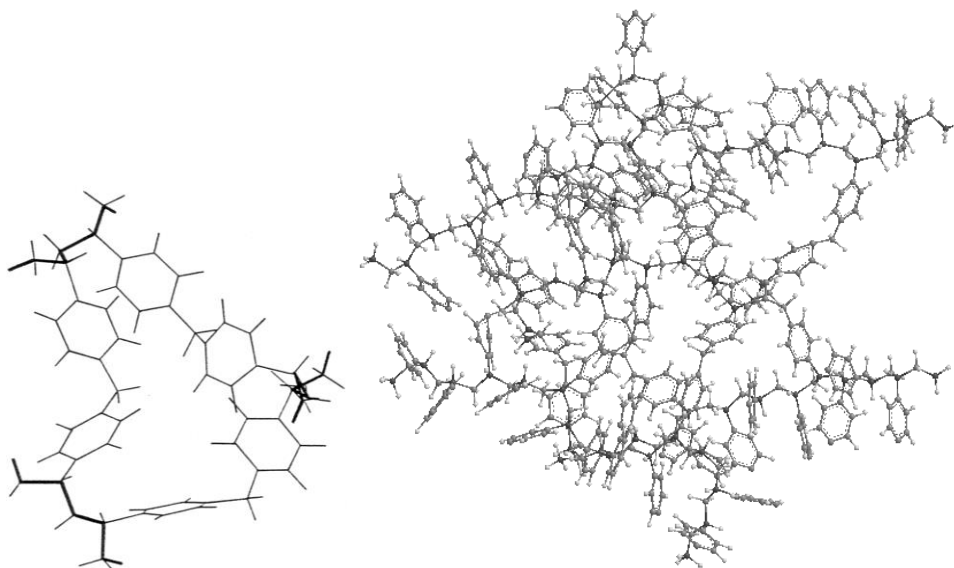


Figure 2. The smallest and nearly unstressed network mesh and a scheme of the open network structure. Reprinted from [8] with kind permission of Elsevier Publishing Company.

The higher the polymer concentration in the unit volume of the solution, the more alien mesh fragments will be entrapped in the closing mesh, thus strongly restricting the conformational mobility of the latter. Thus, the average size of meshes and the extent of their mutual entanglement are basic topological factors determining the mobility of the three-dimensional network as a whole. The unprecedented mobility of hypercrosslinked polystyrene networks is the logical consequence of the fact that they were obtained in the presence of a large amount of a good solvent and, hence, the extent of mesh interpenetration is sufficiently low.

2.3. Unusual Properties of Hypercrosslinked Polystyrene

Intensive crosslinking of polystyrene chains in solution results in obtaining single-phase rigid swollen hypercrosslinked gel. Removing the solvent from the gel leaves a transparent low-density polymer. Three basic properties distinguish this polymer from any other type of network polymers.

2.3.1. Compatibility of Hypercrosslinked Polystyrene with Different Media

The first unique property of the polymer is the presence of strong inner stresses of shrinkage in the dry hypercrosslinked material. The complete removal of solvent from the gel-type product of hyper-crosslinking leads to a significant decrease in gel volume, which implies a cooperative conformational rearrangement of the whole mesh system. However, the decrease in network volume is inevitable accompanied by appearance and rapid growth of strong inner stresses of shrinkage, which reflect two opposite tendencies. On the one hand, desolvated polystyrene chains tend to be densely packed; on the other hand, high rigidity of the openwork hypercrosslinked system makes the shrinkage more and more difficult. The inner stresses show up and accumulate in the form of distorted valence angles and bond length. Eventually, the inner stresses equilibrate the dispersion attraction between the desolvated network fragments and stop further shrinkage, despite the continuing solvent evaporation. The strongly stressed state distinguishes dry hypercrosslinked products from other three-dimensional polymers.

However, a stressed hypercrosslinked polystyrene network tends to relax through expansion and size increase right up to the volume in which it was formed and which is characterized by the smallest deviations from equilibrium conformations of all meshes. This tendency manifests itself in the unique ability of hypercrosslinked polystyrene to swell in any liquid and gaseous media irrespective of the thermodynamic affinity between the medium and polystyrene-precursor.

In general, the ability of hypercrosslinked polystyrene to swell decreases in the sequence:

Organic liquids of various classes	>	perfluorinated hydrocarbons	>	water	>	N ₂ , Ar at 77 K	>	N ₂ , CO ₂ at room temperature.
--	---	--------------------------------	---	-------	---	--------------------------------	---	---

Among other conditions of network synthesis, swelling of homogeneous single-phase hypercrosslinked polystyrenes in organic liquids depends, above all, on the concentration of polystyrene chains in the starting solutions subjected to crosslinking. When measured by weight, swelling varies between 1 and 5 mL/g. Swelling in water is noticeably smaller, but

may reach 2-2.5 mL/g. As regards the swelling in inert gases at low temperature, one may readily notice this effect when analyzing the adsorption isotherms. Indeed, for conventional microporous and mesoporous adsorbents with constant porosity, the adsorption of inert gases at 77 K and relative pressures close to unity is known to equal pore volume measured for the same sample by helium densitometry or any other appropriate method (with the exception of mercury intrusion, see [14]). In the case of hypercrosslinked polystyrenes, the pore volume calculated from gas adsorption isotherms proves to be substantially larger than the pore volume of dry material. This deviation, in combination with the shape of the hysteresis loop that extends throughout the entire range of relative pressures, gives evidence to network swelling even at the temperature of liquid nitrogen. Interestingly, the adsorption isotherms for N₂ and CO₂ at room temperature also exhibit a clear-cut hysteresis loop, although everybody understands that capillary condensation of these gases at room temperature is impossible. Only the rearrangement of network meshes under the influence of sorbate molecules, i.e. swelling of hypercrosslinked polymers with the gas, can explain the hysteresis phenomenon.

Two comments must also be said about the above sorbate sequence. First, hypercrosslinked polystyrene is hydrophobic and water cannot wet it directly. To overcome the wetting obstacle, the polymer should be first treated with acetone or ethanol (or any other solvent miscible with water) and then the latter should be removed by washing the polymer with excess water. Even the weak dispersion interactions of water with exposed aromatic structures prove to be sufficient to slide the network towards a partially relaxed, partially swollen state.

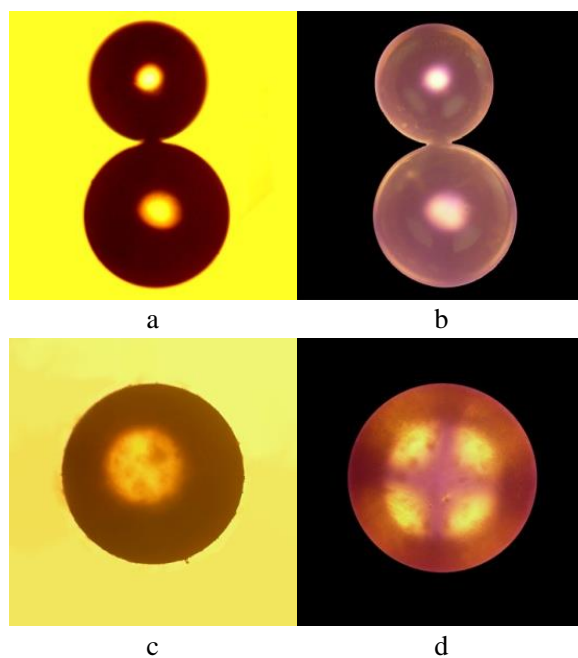


Figure 3. Optical micrographs of (a, b) dry beads of initial styrene-0.5% DVB copolymer and (c, d) dry beads of HP-100, taken in common light (a, c) and in polarized light (b, d). Reprinted from [17] with kind permission of Akademizdatsentr “Nauka”.

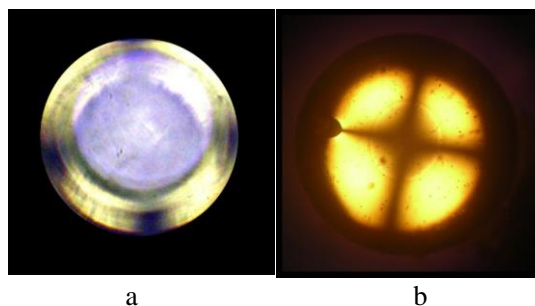


Figure 4. Optical micrographs of toluene-swollen beads of (a) HP-100 and (b) gel-type styrene-0.5% DVB copolymer taken in polarized light. Reprinted from [17] with kind permission of Akademizdattsentr “Nauka”.

Second, various organic liquids cause different swelling of hypercrosslinked networks, although the distinctions are pretty small. For instance, a hypercrosslinked material obtained by post-crosslinking a styrene-0.5% DVB copolymer with MCDE until a 100% degree of crosslinking increases its volume in toluene, *n*-hexane and methanol by factors of 1.91, 1.72 and 1.65, respectively. Though the values are similar, nevertheless, the thermodynamic affinity of these solvents to polystyrene and its hypercrosslinked network is different. One may easily make certain of the difference by using a polarization optical microscope [17].

Both the initial gel-type copolymer bead and hypercrosslinked product based on the copolymer appear in common light as isotropic transparent spheres (Figure 3a and 3b). If one crosses the polarizer and analyzer, the beads of starting copolymer remain unchanged while in the hypercrosslinked bead, the so-called Maltese cross shows up (Figure 3c and 3d). Since there are not any ordered supramolecular structures in the bead of hypercrosslinked polystyrene, its anisotropy is unambiguously caused by the presence of inner stresses in the dry material.

Strong solvation of hypercrosslinked polystyrene networks with a thermodynamically good solvent, toluene, leads to the appearance of expansion stresses, which are opposite in sign to those existing in dry beads. The strong swelling affects the network junction points that prevent the material from dissolution. (The same is true for conventional styrene-DVB copolymers). Under a polarization microscope, one can see a different type of Maltese cross (Figure 4a and 4b). Obviously, in the course of swelling with toluene, the initial stresses of shrinking within a dry hypercrosslinked polystyrene bead change into the stresses of expansion. Consequently, at some moment of the expansion process, the hypercrosslinked network must have passed an unstressed isotropic state. In fact, we observed this isotropic state when following the swelling process of a dry HP-100 bead in toluene under cross-polarized conditions.

Optical anisotropy of swollen hypercrosslinked polystyrene depends on the type of solvent used (Figure 5). Water is characterized by low affinity to the aromatic polymer. Beads weakly swollen with water partially preserve the stresses of the shrinkage, which are characteristic of dry beads. Methanol causes a significant increase in the volume of the hypercrosslinked network. Methanol transforms the dry stressed network into a completely isotropic swollen material. By analogy with unperturbed polymeric chains in diluted solutions in a Θ -solvent, one may assume that the hypercrosslinked polystyrene network swollen with methanol acquires a Θ -state.

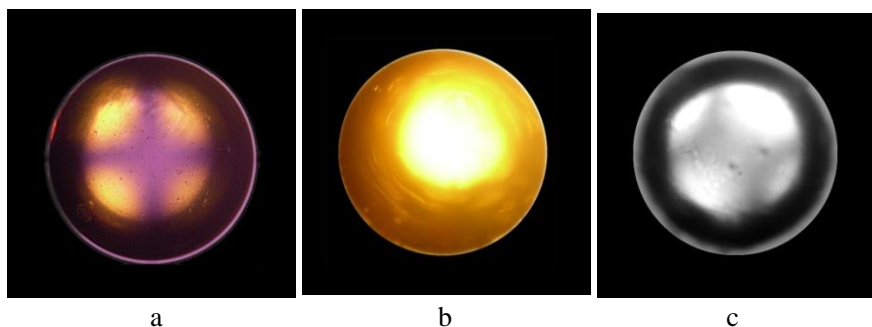


Figure 5. Optical micrographs made in polarized light of HP-100 swollen in (a) water, (b) methanol and (c) *n*-hexane. Reprinted from [17] with kind permission of Akademizdatsentr “Nauka”.

The affinity of *n*-hexane to polystyrene is higher than that of methanol; the network swells in hexane to a greater extent. Still, the aliphatic hydrocarbon fails to solvate and expand the aromatic network as effectively as toluene does. Therefore we see only the first signs of emerging inner stresses of expansion in the bead swollen with hexane (Figure 5).

2.3.2. Porosity of Hypercrosslinked Polystyrene

The second unusual property of hypercrosslinked polystyrene is its high porosity of a new type. Shrinkage of synthesized rigid hypercrosslinked gels during solvent removal stops long before the moment when the polymeric chains achieve a dense packing, which is normally characteristic of conventional polystyrene and its gel-type copolymers of the first generation. The free volume remaining in the dry low-density single-phase hypercrosslinked material is so large, up to $0.6 \text{ cm}^3/\text{g}$, that it might be thought to present true porosity. However, this type of porosity is fundamentally new. Up until now, porosity of conventional milky-white two-phase macroporous copolymers was known to result from the micro-phase separation during their synthesis. Alternatively, the single-phase hypercrosslinked materials are transparent. They do not scatter visible light. They scatter X-rays like a homogeneous polystyrene solution, rather than macroporous polystyrene copolymers.

The highly porous hypercrosslinked networks absorb very large amounts of inert gases at low temperature. It is important to understand, however, that the specific internal surface of $1500\text{-}2000 \text{ m}^2/\text{g}$ calculated from gas adsorption data is not a real surface of pore walls. In the single-phase hypercrosslinked open-type network the “pores” are nothing other than spaces between loosely packed chains, while the high specific surface area values simply reflect the high capability of the polymer to absorb gases. That is why we use the term “apparent inner surface area”.

The dimensions of the “pores” are pretty small, and their precise determination proved to be a real challenge. Nevertheless, relying on data obtained using a number of methods, we arrived at the conclusion that, on average, the diameter of the “pores” is about 2-3 nm. This size is adjacent to real micropores (below 2 nm, in accordance with the IUPAC recommendations), and, using the modern terminology, we consider the hypercrosslinked polystyrene as the first nanoporous polymeric material.

2.3.3. Non-trivial Physical State of Hypercrosslinked Polystyrene

The third striking property of hypercrosslinked polystyrene consists in that this polymer exists in a non-typical physical state. In addition to extremely large volume changes on swelling or drying, the high mobility of a rigid loosely packed hypercrosslinked network manifests itself in large deformations of the polymer when exposed to an external mechanical force. In order to understand the specific features of deformation of hypercrosslinked polystyrenes let us first consider the deformation of the conventional crosslinked styrene copolymers (Figure 6). (The behavior of networks was tested under uniaxial compression using a specially developed technique that operates with a single spherical bead [18, 19]). The copolymer incorporating 3% DVB exhibits two physical states, glassy and rubbery, with a narrow transition zone centered around 100°C (glass transition temperature, T_g), provided that the pressure applied to the sample is small, i.e., 10 grams per bead. An increase in the load to 400 grams per bead causes a 10°C shift in T_g toward lower temperatures, because of the development of forced high elasticity. It results in an increase from 17 to 40% in the deformation when the copolymer reaches rubber-like elasticity. The highly crosslinked conventional copolymer with 34% DVB and poly-DVB retain their glassy state up to the temperature of chemical degradation (over 300°C), while only exhibiting small thermal expansion up to about 200°C.

Contrary to gel-type styrene-3% DVB copolymer, the hypercrosslinked polystyrene HP-100 shows under the small load of 10 g a noticeable deformation only at 140°C. Under pressure of 400 g (which is still 20 times smaller than the breakdown limit at 25°C), the bead deformation starts at temperatures as low as -50°C. Such a broad temperature range of incipient deformation, from 140 to -50°C, is not typical of conventional gel-type glassy polymers. (Also, this effect has little in common with the deformation behavior of interpenetrating networks, semi-penetrating networks or polymeric blends composed of several constituent components).

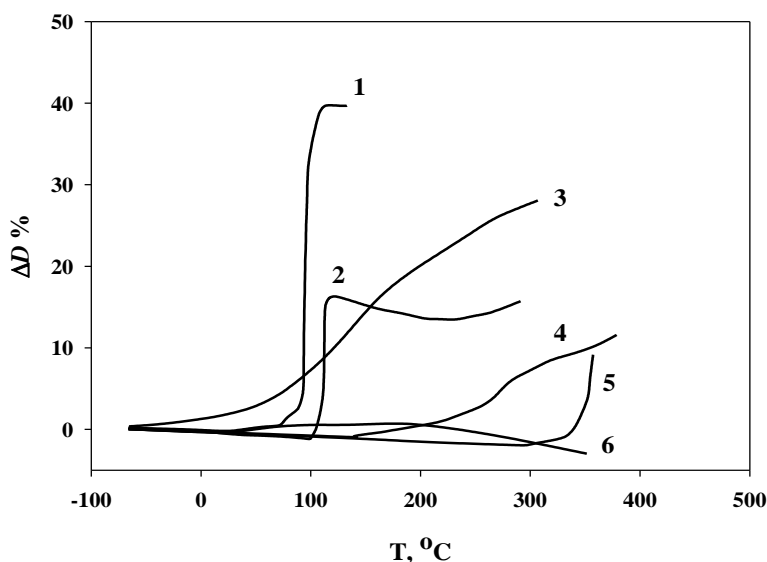


Figure 6. Thermomechanical plots for styrene copolymers containing (1, 2) 3% DVB and (5) 34% DVB, (6) polydivinylbenzene, as well as for (3, 4) HP-100 based on styrene-0.57% DVB copolymer. Loading: (2, 4, 5) 10 g and (1, 3, 6) 400 g per bead. ΔD_0 is the change in bead size along the axis of compression. Reprinted from [18] with kind permission of Wiley & Sons, Inc.

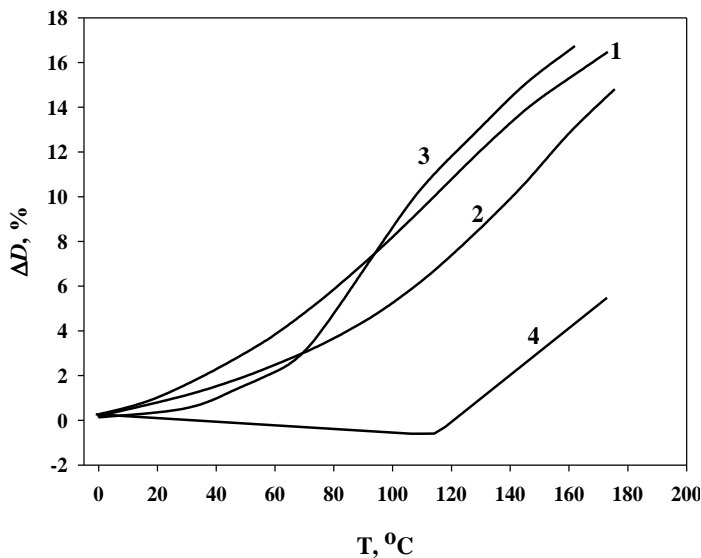


Figure 7. Effect of the pre-treatment of the network (obtained by crosslinking styrene-0.57% DVB copolymer with monochlorodimethyl ether to 100 %) on the position and form of thermomechanical deformation curves: (1) control sample; (2) the sample heated up to 136°C under a loading of 400 g and relaxed at 164°C for 2 hrs. without pressure; (3) the sample heated up to 136°C, then cooled under a loading of 400 g (12% residual deformations), and finally subjected to swelling and drying; (4) the sample heated up to 136°C and then cooled down under a loading of 400 g (10% residual deformations). D_0 is the change in bead size along the axis of compression. Reprinted from [18] with kind permission of Wiley & Sons, Inc.

Quite interesting is the fact that the deformation can achieve a high value of almost 30% when the temperature approaches 300°C. That high deformation is usually characteristic of elastomers, rather than glassy material. However, the hypercrosslinked polystyrene cannot be ascribed to rubbery-state materials, because no elasticity plateau shows up on the thermomechanical curves. On the other hand, all deformations are reversible. Indeed, Figure 7 gives sufficient evidence for the reversibility of the residual deformation, which implies maintenance of the whole network structure of the bead.

Several individual hypercrosslinked beads of HP-100 were heated to 136°C under a pressure of 400 g and then were allowed to cool down to ambient temperature under that pressure. During the second cycle of heating under the same pressure, the deformation of these pre-treated beads was observed to start only at elevated temperatures (Figure 7, plot 4). The sample obviously stored the information of the first cycle of deformation, possibly, by achieving higher mechanical strength along the axis of compression. Such information storage would be unthinkable in a plastically deformed sample. Plots 2 and 3 in Figure 7 demonstrate that both the non-elastic deformation and the “memory” effect in the pre-compressed network largely disappear if the deformations are allowed to relax. Plot 2 shows the behavior in the second cycle of deformation of beads relaxed at 146°C for 2 hours without any pressure applied. Plot 3 relates to another set of beads with “frozen” deformations that were allowed to swell with acetone, followed by washing with water and drying at 80°C. As can be seen, the deformation behavior of compressed and then relaxed beads does not differ substantially from the plots registered in the first cycle of deformation (Figure 7, plot 1).

Taking into account the normal scattering of the results registered for individual beads, one can state that residual “frozen” deformations in hypercrosslinked materials are completely reversible.

2.3.4. Astonishing Properties of Hypercrosslinked Polystyrene with Ultimate Crosslinking Densities

High mobility, high porosity of a new type, and compatibility with any liquid and gaseous media are inherent to all rigid single-phase loose hypercrosslinked polystyrene networks. However, a simple increase in polymer crosslinking density up to an ultimate 300%, 400% and 500%, imparts the polymer with new additional unexpected properties. In the first place, it should be said that HP-500 is colored black and is no longer a typical dielectric. Its specific electric resistance decreases by six orders of magnitude compared to that of initial styrene-0.5% DVB copolymer, 10^{10} ohm·m against 10^{16} ohm·m, respectively. For comparison, the resistance of a typical semi-conductor is 10^5 - 10^8 ohm·m [20].

The above three polymers with maximum possible crosslinking degrees give a sufficiently strong EPR signal (2×10^{16} - 1.2×10^{17} N/g) which is comparable with that of carbonaceous pyrolysis products prepared from hypercrosslinked polystyrene. Uncoupled electrons in the polymers probably emerge during the desolvation of synthesized gels, by rupture of some overstressed chemical bonds.

Figure 8 depicts absorption spectra of hypercrosslinked polystyrenes in the UV-VIS range of 240-850 nm. As the crosslinking degree of polymers increases from 43% to 500%, absorption bands become wider and wider while band maximums shift to a longer wavelength range. This change in the band form and its position appear to be caused by a change in the electronic structure of aromatic chromophores with the rising extent of their substitution. Interestingly, samples HP-300, HP-400 and HP-500 absorb in the visible spectrum range and are black in color.

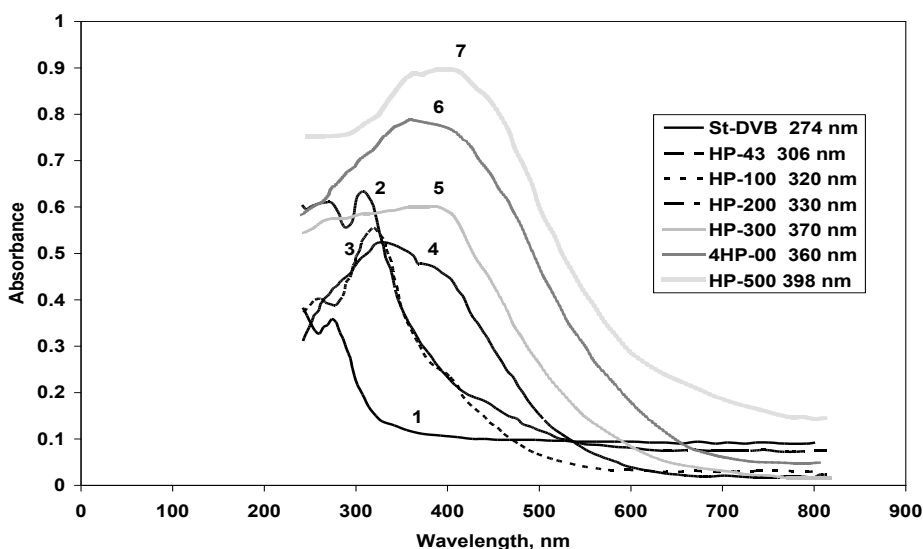


Figure 8. Absorption spectra of hypercrosslinked polystyrenes: (1) initial styrene-0.5% DVB copolymer, (2) HP-43, (3) HP-100, (4) HP-200, (5) HP-300, (6) HP-400, (7) HP-500; the insert indicates the positions of band maximum. After [20].

3. HYPERCROSSLINKED POLYSTYRENE ADSORBING MATERIALS

3.1. Commercial Types of Hypercrosslinked Polystyrene Sorbents and Fields of Their Practical Application

Owing to unique physico-chemical properties, hypercrosslinked polystyrene presents undoubted interest for the theoretical perception of relations between structural features and behavior of hypercrosslinked polymers. At the same time, the polystyrene-type material is of a great importance from a practical viewpoint. Indeed, one of the basic distinguishing features of the single-phase highly-porous hypercrosslinked matrix is that its polymeric chains are separated by statistically distributed, long and rigid bridge-struts and therefore, remain permanently exposed to gaseous or liquid environment. Being deprived of close contacts to one another, these chains generate a strong uncompensated force field. For this reason the permeable hypercrosslinked polymer attracts and retains a wide variety of organic compounds from the surrounding medium and concentrates them in the interior of the network. In contrast to common macroporous styrene-DVB adsorbents in which only the surface of pores is accessible to sorbate molecules, the hypercrosslinked polystyrene resin sorbs compounds by its entire network volume. That is why the third-generation hypercrosslinked resins exhibit exceptionally high sorption activity and high loading capacity towards both non-polar compounds due to general dispersion interactions and also highly polar organic substances, such as phenol or triazine pesticides, due to additional electronic effects. The latter are mainly represented by π - π type interactions emerging between polar functional and/or aromatic groups of the sorbate and exposed aromatic rings of the resin. This π -selectivity, in addition to the above-mentioned high permeability of the matrix, can be considered as the distinguishing feature of the new, third generation of polymeric adsorbents.

Our idea of post-crosslinking highly swollen styrene-DVB copolymers with a bifunctional reagent, published in a USSR patent as early as 1969 and soon in patents of 16 other leading countries [7], was later picked up by many researchers [21-24]. In 2005, Dow Chemical Company's web site advertised five hypercrosslinked polystyrene products of the Dow OptiporeTM series, V493, V503, SD-2, L493 and L323, all being designed to remove organics from water or air [25]. These sorbents have a (apparent) specific surface area above 1100 m²/g, V493 and L493 being biporous products with a pore volume of 1.16 cm³/g and an average pore size of 46 Å. Another company, Bayer AG in Germany, also advertised two hypercrosslinked sorbents, Lewatit VP OC 1163 [26] and Lewatit S 7768 [27], having both a macroporous and microporous structure with specific surface area values of over 1500 and 1300 m²/g, respectively. The pore volume of both versions is similar, 0.6-0.8 cm³/g, and the pore diameters are indicated as 0.5-10 nm. Importantly, the Lewatit resins have a narrow bead size distribution of 0.45-0.55 mm in diameter. In China, Jiangsu N&G Environmental Technology Co Ltd. quite recently began manufacturing the hypercrosslinked adsorbents NG-99 and NG-100. However, we are not aware of the real large-scale production at Dow and Bayer of the hypercrosslinked products.

Still, hypercrosslinked polystyrene sorbents appeared on the world market already in 1994 when Purolite International Ltd. (UK and the USA) began to produce, with our active participation, the Hypersol-MacronetTM (MN) series of resins on an industrial scale. At

present, a broad assortment of hypercrosslinked adsorbing materials is available (Table 2) that are intended for application in various large scale sorption technologies.

Table 2. Macronet-Hypersol™ adsorbing materials produced by Purolite International Ltd. [28]

Hypersol Macronet™	Type	Volume capacity eq/L	Pore diameter Å*	Surface area m ² /dry g**	Moisture retention %
MN100	WBA	0.1-0.3 (FB-form)	900	900	57-61 (Cl form)
MN102	WBA	-	750	700	49-60 Base-form
MN200	Inert	-	900	900	57-61
MN202	Inert	-	750	700	50-60
MN270***	Inert	-	25	1200	35-50
MN500	SAC	0.8-1.0 (Na form)	900	900	52-57 H ⁺ -form
MN502	SAC	0.8-1.0 (Na form)	750	700	52-57 H ⁺ -form

*Hg intrusion method; **one point BET; ***pore volume 0.2-0.4 mL/g.

Table 3. Commercial suppliers of hypercrosslinked sorbents for SPE applications. Reprinted from [8] with kind permission of Elsevier Publishing Company

Sorbent (Company)	Particle size, µm	Surface area, m ² /g	Pore volume, cm ³ /g	Pore diameter, nm	Ref.
Purosep 200 <i>Purolite International, UK</i>	40-140	1000	1.1	2-3 and 85-100	[29]
Isolute ENV <i>International Sorbent Technology, UK</i>	40-140	1100	1.1	2-3 and 85-100	[30]
LiChrolut EN <i>E.Merck, Germany</i>	40-120	1200	0.75	3	[31-33]
HYSphere-1 <i>Spark Holland</i>	5-20	>1100	-	-	[34]
HR-P <i>Macherey Nagel, Germany</i>	40-120	1300	-	2.5	[35]

Later, hypercrosslinked polystyrene sorbents also came into routine use in analytical chemistry. They were found to present excellent solid-phase extraction (SPE) materials for pre-concentration of trace amounts of organic contaminants in natural waters, food products, biological fluids, waste flows, gases, etc. Concentrated extracts from the SPE cartridges greatly enhance accuracy of determining target analytes, usually in combination with various chromatographic techniques. By now many companies offer fine beads or small particles of

efficient sorbents for SPE, sometimes without mentioning their hypercrosslinked polystyrene nature. Main characteristics of popular SPE sorbents are presented in Table 3.

Table 4. List of hypercrosslinked polystyrene practical applications

Hypercrosslinked polystyrene practical applications	Ref.
Decolorizing of sugar syrups	[36]
Removal of caffeine from extract of coffee green beans	[37]
Removal of colored bodies from fermentation liquid	[8]
Removal of bitterness from citrus juices	[38]
Removal of chloroform from industrial wastewater	[39]
Removal of benzene and chlorobenzene vapors from gaseous HCl	[40]
Solid-phase extraction	[8]
Hemosorption	[8]
Metal-selective impregnated resins for hydrometallurgy	[40]
Decontamination of soil	
Potable water treatment	
Removal of smell from industrial off-gases	

Commercially manufactured hypercrosslinked polystyrene resins showed themselves to good advantage over the world as excellent adsorbing materials for removing organic compounds from aqueous environment and air. Table 4 shows a selective list of industrial processes in which the use of hypercrosslinked polystyrenes proved to be beneficial, if not crucial. One can find detailed information on these processes in the cited publications.

Some interesting aspects of the already described applications as well as new suggestions of high potential importance will be discussed in the next Sections. Here we will mention just two emerging possibilities. One is the preparation of excellent microporous activated carbon-type materials by thermal carbonization of some variants of hypercrosslinked polystyrene sorbents. These microporous materials form with high carbon yield (of up to 50%) and present mechanically rigid perfect spheres with high adsorption capacity [41, 42]. One can consider the possibility of making such carbons by thermal utilization of contaminated and used-up hypercrosslinked polystyrene sorbents.

Another instructive example of utilization of low-quality batches of hypercrosslinked sorbents came from the practice of Purolite International Company (UK), the manufacturer of the resins. The company came up on the market in 1994 with a series of hypercrosslinked polystyrene sorbents Hypersol Macronet™ MN produced at the plant in Ponticlun, Wales. Several years ago Purolite transferred the production of resins under consideration to new enterprises in China and Romania. When closing the old plant in Wales the company faced the problem of remediation of the territory that was already contaminated many decades ago by previous plant owners. A simple and witty solution to the problem consisted of digging up the plant territory, providing it with drains and wetting it abundantly. Drainage water with all soil contaminants was sent through a container with hypercrosslinked sorbents. In a few days the territory was completely decontaminated and the polymer was then burned down.

3.2. Hypercrosslinked Polystyrene Sorbents for Solid-phase Extraction of Organic Contaminants

Dramatic growth of industry and agriculture in the later half of the 20th century has led to a significant contamination of the Earth's aquatic pool with a wide variety of toxic organic compounds. Among them pesticides are the most widespread pollutants due to the enormous scale of their application around the world. As an example, in the European Union countries the annual scale of pesticides application increased from $291,895 \times 10^3$ to $327,280 \times 10^3$ kg during the period from 1992 to 2001. Within the same period, the annual pesticide usage in the USA declined from $426,377 \times 10^3$ to $402,790 \times 10^3$ kg [43]. Following the intended benefit from an increase in crops, pesticides and their metabolites readily enter the surface and ground waters (the latter being a source of potable water in many countries) thus raising the risk of harmful effects on human health.

The family of hazardous pollutants also includes phenol and its nitro- and chloro-derivatives, which go directly into the aquatic environment through wastewaters from many industries. They also form in potable water due to the reaction of natural humic and fulvic acids with chlorinating disinfectors. The U.S. Environmental Protection Agency included 26 phenolic compounds and 32 pesticides and their metabolites in the list of priority contaminants. In accordance with regulatory requirements, the allowed tolerance limit of these pollutants must not exceed 0.1 $\mu\text{g/L}$ for individual species and 0.5 $\mu\text{g/L}$ for the sum of pesticides or phenols in water intended for human consumption [44].

A variety of other organic compounds contaminate soil, water and air. Carcinogenic polyaromatic hydrocarbons, surfactants, chlorinated hydrocarbons, freons, heterocyclic compounds, medical preparations and others resulting from human activity pose a real or potential threat for human, flora and fauna. All of these contaminants are present in the environment at a very low concentration so that their direct measurement is impossible even though modern high-tech equipment is used. Therefore, the pre-concentration of pollutants on porous solids, largely, polymeric sorbents, has become very popular because of its simplicity, flexibility, high efficiency and throughput, its possibility to be automated [45] and a relatively low laboratory cost. Since the number of publications concerning the use of hypercrosslinked sorbents for solid-phase extraction (SPE) of contaminants exceeds a hundred, in this Section we will describe only those examples that provide insight into the hypercrosslinked sorbents' high potential in analysis of aquatic environment.

3.2.1. Basic Principle of SPE Trace Enrichment

The basic principle of SPE trace enrichment consists of the transfer of target analytes from a large volume of diluted analytes solution to the surface of a polymeric sorbent in a small pre-column and subsequent elution of the adsorbed moieties with a small volume of an appropriate solvent. As a result of such operation, the concentration of the analytes in the eluate increases manifold, even by several orders of magnitude compared to their concentration in the initial solution. Afterwards, the analytes are separated, identified and measured quantitatively by gas chromatography (GC), high performance liquid chromatography (HPLC), capillary electrophoresis (CE) or other appropriate methods.

When SPE protocol involves a subsequent chromatographic analysis, two modes of the method's combination have been used, off-line and on-line. Off-line trace enrichment is

carried out separately from the further chromatographic procedure. After passing the sample solution through the small sorbent cartridge, followed by the clean-up step (flushing the sorbent with an appropriate solvent to remove interferences from the initial sample matrix), the polymer-retained analytes are desorbed with a portion of strong eluent. If necessary, the eluate may be evaporated additionally to raise the analyte concentration. Finally, an aliquot of the concentrate is injected into the analytical column. The off-line performance mode is appealing due to its flexibility, simplicity of equipment required and broad selection of acceptable solvents and mobile phases. On the other hand, numerous manipulations with the sample increase the risk of loss of volatile analytes and additional contamination [46].

On-line configuration permits conducting the SPE pre-concentration and subsequent chromatographic analysis within one set of analytical equipment. When the HPLC technique is used, a small sorbent-filled pre-column is connected as a sample loop to a multi-port injector valve of the chromatograph. In the position of loop disconnected from the flow of the mobile phase, a sample of solution to be analyzed, e.g. contaminated water, is percolated through the pre-column. Then, by switching the valve, the cartridge is directly coupled to the analytical column, and the flux of mobile phase (in back flush mode) transports the analytes from the pre-column to the analytical one [47]. On-line procedure is very convenient and permits conducting analysis within a short period of time. This configuration is free from the risk of sample loss or contamination. At the same time, analytes that are strongly retained in the pre-column require a strong solvent in order to be transported into the main column within a small volume. This strong solvent, however, deteriorates the final chromatogram that is usually obtained on a C-8 or C18 silica-based reversed phase analytical column, (silica gel with grafted octyl or octadecyl aliphatic chains). This drawback limits the number of useful combinations of sorbents in the pre-column and analytical column.

Three key parameters characterize SPE efficiency:

- (i) breakthrough volume of the analyte which depends on the retention power of the SPE adsorbing material and determines the volume of water sample percolated until the analyte appears at the cartridge outlet;
- (ii) recovery, R , of analyte that is determined as the portion of the analyte that was spiked to the sample matrix, subjected to a full solid-phase-extraction procedure, and finally detected after the chromatographic column. Recovery of 100% implies a complete retention of the target compound in the SPE cartridge from the sample solution and complete elution of the analyte from the SPE sorbent with an appropriate liquid phase;
- (iii) limit of detection (LOD) is the lowest concentration of a compound that can be detected in a given analytical procedure at the signal-to-noise ratio $s/n=3$, and limit of quantification (LOQ) that is estimated at $s/n=10$. They both depend on the extent of pre-concentration of the analyte and the quality of its purification from interfering components of the matrix, which the SPE procedure can offer.

Nowadays, hypercrosslinked polystyrene adsorbing SPE materials dominate in environmental monitoring, first of all in tracking rather polar pollutants like phenols, pesticides and their polar metabolites, pharmaceuticals, organic acids and other miscellaneous organic compounds presented both in industrial wastewaters and biological liquids. However,

in this Section we will briefly consider only the most complicated and vivid examples of employing hypercrosslinked polystyrenes for SPE trace enrichment.

3.2.2. Trace Enrichment of Phenolic Compounds

Many inorganic and polymeric sorbents have been tested for SPE pre-concentration of phenol and its derivatives before hypercrosslinked sorbents became commercially available. Early studies showed that silica-based C18 reverse phase SPE cartridges do not provide retention of phenol and its polar derivatives. The list of polymeric sorbents also carefully tested for SPE enrichment of phenols includes Styrogel resins, PRLP-S, Envi-Chrom P, Amberchrom 161m, PRP-1, Amberlite XAD-4 and other macroporous styrene-DVB sorbents. While proving suitable for enrichment of many less polar organic pollutants, not one of sorbents examined could provide a desirable level of pre-concentration for the unsubstituted phenol in natural waters. Therefore, benefits of hypercrosslinked polystyrene for solid-phase extraction of phenol and other polar organic pollutants were valued at once after the emergence of the sorbent on the world market. At present, several types of hypercrosslinked polystyrene-type SPE sorbents are commercially available. Their characteristics and manufacturers are listed in Table 3.

Obviously, our first report [48] on removing phenol from dilute aqueous solutions using an in-house made hypercrosslinked polystyrene sample Styrosorb 2 with a 100% crosslinking degree gave a powerful incentive to a burst of studies in the same direction. In these experiments 6 mg of Styrosorb 2 beads of 70 to 80 μm in diameter were placed in a 16 μL valve loop for the on-line SPE enrichment of the analytes followed by subsequent HPLC separation and quantification using a C18 analytical column and UV detection. Irrespective of the method used for the cartridge loading, namely, by pumping of up to 2.0 mL of 0.5 mg/L phenol solution or by introducing 1 mL solutions with the concentrations ranging from 0.05 to 1 mg/L, the plot of chromatographic peak heights versus the amount of phenol introduced into the pre-column was found to be linear. It implies that 6 mg of Styrosorb 2 absorb quantitatively at least 1 μg phenol injected in 2 mL of water and then release it completely with an aqueous acetonitrile mobile phase into the analytical column. Moreover, peak broadening caused by the Styrosorb-packed SPE 16 μL pre-column was found to be less significant than that caused by the empty pre-column. By using the same on-line SPE approach, 100% recoveries were also obtained on concentrating 2-chlorophenol, 2,4- and 2,6-dichlorophenols and 2,4,6-trichlorophenol.

Puig and Barceló [49] compared macroporous styrene-DVB resin PLRP-S, hypercrosslinked sorbents LiChrolut EN, Isolute ENV and porous graphitic carbon in on-line pre-concentration of phenols followed by LC analysis and arrived at the conclusion that LiChrolut EN and Isolute ENV are the most suitable sorbents for monitoring phenols except for 2-amino-4-chlorophenol. The latter is protonated in acidic solutions and is not retained on neutral polymers (Table 5). Both hypercrosslinked sorbents show very good breakthrough volumes and identically acceptable recoveries but the former demonstrates a slightly better limit of detection due to smaller bead size.

Hypercrosslinked biporous Isolute ENV+ was involved in the analysis of alkylphenolic pollutants [50]. Being the degradation products of non-ionic surfactants, these compounds were found to induce a hormonal imbalance in fish. The high extent of enrichment achieved in the off-line pre-concentration from 1 L samples and recoveries close to 100% permitted the

determination of 4-*n*-hexylphenol, 4-*tert*-octylphenol, 4-*n*-heptylphenol, nonylphenol and 4-*n*-octylphenol at the level of 0.1 µg/L.

Isolute ENV demonstrates exceptionally strong retention of chlorophenols [51]. No breakthrough of the analytes was registered after loading a 200 mg Isolute ENV cartridge with 2 L water samples containing 5 ng/L of chlorophenols, with a flow rate as high as 100 mL/min. Notably, complete elution of all the analytes from the loaded cartridge with 4 mL methanol was attained only in back-flush mode, thus implying the retention of the chlorophenols at the very top of the pre-column bed. The recoveries obtained were almost 100%, while the limit of quantification was very low ranging from 0.05 to 0.13 µg/L.

Finally, Figure 9 shows chromatogram of all sixteen EPA priority phenols off-line pre-concentrated on Purosep 270 with nearly 100% recoveries, thus demonstrating a high potential of hypercrosslinked polystyrenes for analysis of phenolic compounds.

Table 5. Mean percentage recoveries ± standard deviations of phenolic compounds from groundwater using different sorbents and working with on-line 10x2 mm I.D. stainless steel SPE pre-columns; spiking, 4 µg/L of each phenolic compound; sample volume, 100 mL, except for phenol, catechol and 2-amino-4-chlorophenol (50 mL), pH=2.5.

Analyte	Sorbent, particle size			
	PLRP-S 16-18 µm	LiChrolut EN 15-40µm	Isolute ENV 40-140µm	PGC
Catechol	<20	55±9	57±8	61±7
Phenol	34±5	67±7	62±7	54±6
4-Methylphenol	69±6	75±6	82±5	52±7
2,4-Dimethylphenol	81±4	98±4	92±4	nd
2-Nitrophenol	76±5	88±5	88±5	nd
4-Nitrophenol	78±5	84±6	100±4	nd
2,4-Dinitrophenol	100±4	102±5	98±4	nd
2-Amino-4-chlorophenol	<20	<20	<20	87±6
4-Chloro-3-methylphenol	85±5	92±6	88±5	nd
2-Chlorophenol	76±4	86±6	81±4	85±7
3-Chlorophenol	78±6	83±5	79±5	88±6
4-Chlorophenol	85±6	84±5	80±4	88±5
2,4-Dichlorophenol	81±3	94±5	92±3	nd
2,4,6-Trichlorophenol	96±4	103±5	99±5	nd
2,3,5-Trichlorophenol	94±5	96±4	101±6	nd
2,3,4-Trichlorophenol	95±5	101±4	105±6	nd
3,4,5-Trichlorophenol	93±5	99±4	98±4	nd
Pentachlorophenol	100±4	100±3	99±5	nd

PGC = porous graphitic carbon;

nd = not detected.

Reprinted from [49] with kind permission of Elsevier Publishing Company.

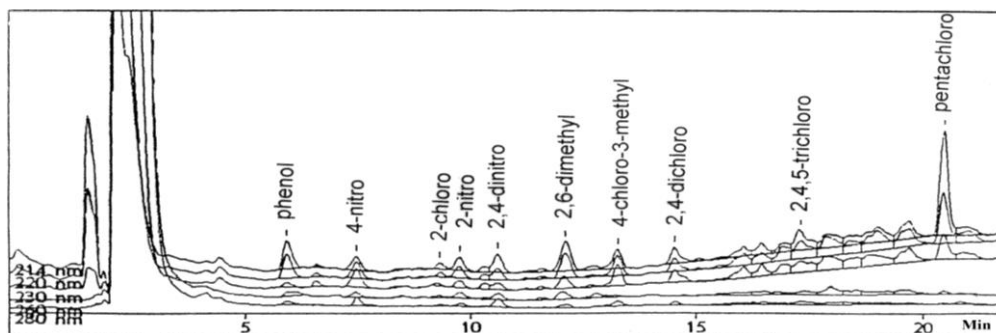


Figure 9. Gradient-mode HPLC separation of 18 priority phenolic contaminants off-line pre-concentrated on Purosep 200.

3.2.3. SPE Enrichment of Pesticides

Atrazine and related triazines represent the most widespread herbicides used throughout the world for the protection of crops from broadleaf weeds and for non-agricultural purposes, such as soil sterilization and road maintenance. Being hit upon the soil, the herbicides are subjected to oxidation, photolysis, thermal or microbial impacts. Triazines and their metabolites are very resistant compounds and may be found in soil, river and even seawater several years after application. Taking into account the enormous scale of pesticides' consumption, over three million metric tons per year, the control of contamination of water, soil and food with very toxic compounds is of great importance. The European Commission regulations set the maximum allowed concentration of an individual pesticide in drinking water to 0.1 $\mu\text{g/L}$. Obviously, the analysis of such diluted solutions is deemed to be impossible without SPE enrichment.

The comparative study of LiChrolut EN (40-120 μm particles), a restricted access material alkyl-diol-silica (25 μm), reversed-phase C18 (10 μm), mono-functional C18 (40-70 μm) and, finally, styrene-DVB Empore extraction disks in SPE enrichment of herbicides revealed a decisive superiority of the hypercrosslinked sorbent LiChrolut EN in retention of very polar didealkylatrazine, and desethyltriazine [52]. However, the strong retention power of LiChrolut EN causes significant band broadening when analysis is performed in on-line SPE-HPLC mode with conventional analytical equipment. To lessen this shortcoming, the elution of analytes from the loaded pre-column must be conducted in the back-flush mode.

A significant peak broadening was observed during the on-line extraction of pesticides with a hypercrosslinked polystyrene sorbent SDB-1 (J.T. Baker), followed by their HPLC separation and quantification on a C18 analytical column [53]. The problem was solved by replacing the silica-based separating medium in the analytical column with porous graphitic carbon. This on-line combination provided trace determination of most polar pesticides such as clopyralid, methomyl, deisopropylatrazine, picloram, etc. with detection limits at the low 0.1 $\mu\text{g/L}$ level for 100-mL drinking water samples.

Curini et al. [54] tested a series of SPE sorbents for the extraction of 52 herbicides belonging to twelve chemical classes from dilute aqueous solutions. Authors arrived at the conclusion that graphitized carbon black is the preferred one in monitoring environmental waters for trace pesticides; recoveries of all analytes were close to 100%. The necessity to acidify water samples to enhance the sorption of pesticides on LiChrolut EN or Envi-Chrom P results in a partial loss of imazethapyr and haloxyfop, which are unstable in acidic solutions.

Of 40 pesticides studied in [55], LiChrolut EN does not recover only very polar desethyldeisopropyl atrazine. Also, the polymer poorly retains tris(2-ethylhexyl)phosphate (recoveries were between 40 and 50%). Recoveries of other compounds from various aqueous matrices were pretty high and similar to those obtained with graphitized carbon black. Loos et al. [56] reported strong retention of very polar hydroxytriazine degradation products on LiChrolut EN at low pH values. LiChrolut EN was also found to demonstrate good recoveries for many organophosphorous pesticides present in various crop samples [57]. When comparing the retention power of the hypercrosslinked sorbents LiChrolut EN+ and Isolute ENV towards pesticides, one cannot notice any marked difference between them [58]. The retention power of LiChrolut EN, Isolute ENV+ and Hysphere-q with respect to some polar pesticides, such as oxamyl, atrazine, diuron, desethylatrazine, etc. was also reported in [59] to be comparable.

3.2.4. SPE Pre-concentration of Pharmaceuticals

Many residual pharmaceutical products and their metabolites enter ground waters because of their incomplete elimination from wastewaters of sewage treatment plants. Traces of many carcinogenic, mutagenic, and reproductive toxic pharmaceuticals attack receptors of non-target aquatic organisms that are sensitive to individual pharmaceuticals or to their combinations exhibiting synergetic effects. That is why pharmaceuticals belong to the family of compounds of growing concern. Nevertheless, only a few publications describe the use of hypercrosslinked sorbents for their determination in different waters.

Sachner et al. [60] described pre-concentration of 50 pharmaceuticals using off-line SPE on reversed phase C18 silica and hypercrosslinked sorbents, followed by gas chromatography-mass spectrometry or HPLC-electrospray-mass-spectrometry. The authors wrote that LiChrolut EN poorly retains very polar iodinated X-ray contrast media, such as Iopamidol or Iomeprol, while Isolute ENV+ poorly recovers sulfonamide antibiotics. On the contrary, good extent of enrichment was achieved for macrolide and penicillin antibiotics when using Isolute ENV+ extracting cartridges. The publication [61] documented 75-85% recovery of iodinated contrast medium, Iohexol, when LiChrolut EN was involved into analysis of canine serum and rat urine. The application of Purosep 200 was also found to be promising for the analysis of phenobarbital in aqueous matrix [62].

However, the first study on pharmaceutical determination in hUmAn blood dates back to the end of the 1980s [61, 63]. These studies dealt with the pharmaco-kinetics of drugs in the blood of cardiac patients. Since commercial production of hypercrosslinked sorbents did not yet exist, laboratory made Styrosorb 2 was the sorbent of choice for drug pre-concentration. This sorbent was found to belong to the so-called restricted access materials which pores are open for low molecular weight compounds but inaccessible even for relatively small protein molecules. Because of this property of microporous hypercrosslinked polymers, prior to analysis no deproteinization of blood plasma was required; 200 µl plasma sample was directly applied and pushed through a 3x1 mm I.D. glass column by centrifugation. Then, the column was washed with 200 µl acetonitrile, also applying centrifuge, and an aliquot of the extract was analyzed by HPLC. Table 6 demonstrates the obvious superiority of Styrosorb 2 over reversed phase C-8 silica.

Table 6. Recoveries (%) of some pharmaceuticals on Styrosorb 2 and reversed-phase C18 silica cartridges from human plasma. After [8]

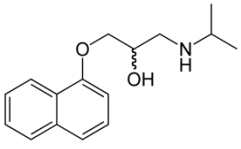
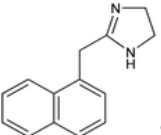
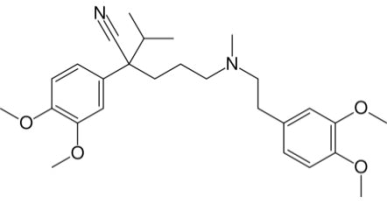
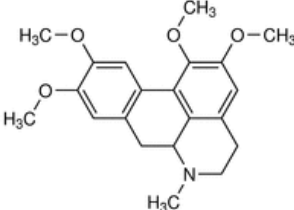
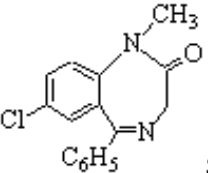
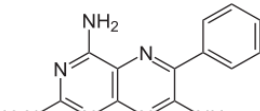
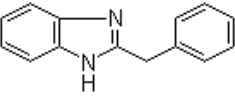
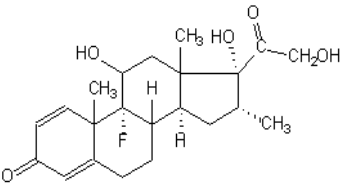
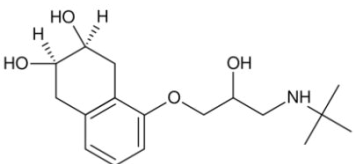
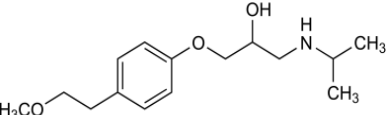
Formula and name	SPE	
	Styrosorb 2	RP-8
 <p>Propranolol (Alindol, Obsidan, Propral, Avlocardil)</p>	99±4	29±12
S-Propranolol glucuronid (metabolite of propranolol)	89±4	55±8
R-Propranolol glucuronid (metabolite of propranolol)	92±5	65±15
4-hydroxypropranolol sulphate (metabolite of propranolol)	98±6	72±9
 <p>Sanorine (Naphazoline Privin, Rhinazin)</p>	96±3	94±10
 <p>Verapamil (Isoptin, Veramil, Finoptin)</p>	95±4	-
 <p>Glaucine (Tussiglaucin)</p>	90±6	-
 <p>Seduxen (Apozepam, Diazepam, Relanium)</p>	85±3	-

Table 6. (Continued)

Formula and name	SPE	
	Styrosorb 2	RP-8
 Triamterene (Anteren, Diutac, Dyrenium, Noridyl)	80±3	-
 Bendazol (Bendazole, Tromasedan)	99±5	-
 Prednisalon (Arcodexan, Cortadex, Decardan)	72±8	-
 Nadolol (Anabet, Betadol, Corgard, Nadic)	48±6	-
 Metoprolol (Betalog, Blocksan, Neobloc, Opresol)	99±5	-

SPE conditions: off-line configuration, 3x1 mm ID cartridge packed with 80-125 µm beads of Styrosorb 2, 200µl of plasma, 200µl acetonitrile for desorption;
 HPLC conditions: 200x4 mm ID analytical column with Nucleosil 5 SA, acetonitrile as mobile phase, fluorimetric detection.

3.2.5. SPE Pre-concentration of Miscellaneous Compounds

Many other organic compounds can be determined in water samples and biological fluids using extraction with hypercrosslinked adsorbing materials. Polybrominated diphenyl ethers (flame retardant agents) were determined in human plasma of workers at an electronic dismantling facility via pre-concentration on Isolute ENV+ cartridge with recovery over 70%

and LOD ranging from 0.0076 to 0.13 ng/g for individual congeners [64]. Isolute ENV+ was successfully used in the determination of N-methyl-2-pyrrolidone and its metabolites in human plasma and urine [65].

Not only useful compounds, such as fats, proteins, carbohydrates, amino acids, vitamins, salts, etc., but also many hazardous organic substances enter the human body with food and drinks and, therefore, food quality control is of growing concern. For instance, heterocyclic aromatic amines, in particular, 2-amino-1-methyl-6-phenylimidazo[4,5-b]pyridine (PhIP), a potentially mutagenic and carcinogenic compound, form when meat or fish are fried or grilled at 150 to 250°C. Concentration of the heterocyclic amine in blood is too low to be analyzed even by applying SPE, while in urine it drops very soon after food intake. However, human hairs preserve the amines and may serve as useful indicators of long or medium-term exposure of individuals to the above toxicant. PhIP was isolated from a NaOH hydrolysate of male hairs by successive solid-phase extraction on Isolute ENV+ and on a silica-based mixed-mode column with C8 and -SO₃H functional groups. After GC separation and mass-spectrometric identification the above compound was determined on the level between 0.25 and 25 ng per gram of hair [66].

Commercial hypercrosslinked sorbents were successfully applied for analysis of harmful and useful components in wine; LiChrolut EN proved to be very efficient in SPE-pre-concentration of 90 pesticides from water-acetone extracts of fresh fruits and vegetables [67]. Only the most polar pesticides (methamidophos, acephate and omethoate) could not be determined by this technique in fruits and juices [68]. The method includes SPE pre-concentration of a polar mycotoxin patuline on Purosep 200 (with its quantification by normal-phase HPLC) and provides recoveries over 90%, with LOD five times lower than the allowed tolerance limit, 50 µg/kg.

3.2.6. SPE from Non-aqueous Media

In all the above discussed examples of using SPE materials for adsorption and pre-concentration of trace organic compounds from aqueous or aqueous-organic solutions, the hypercrosslinked polymers basically function as a hydrophobic adsorbing media. Still, hypercrosslinked polystyrene differs markedly from the well-known hydrophobic silica-C18 reversed-phase SPE material and macroporous styrene-DVB copolymers in that the former also retain much stronger weakly hydrophobic and even hydrophilic aromatic compounds such as phenol or catechol and polar cyclic and aliphatic compounds. The reason for the enhanced retention of such compounds, in particular those containing aromatic and heteroaromatic fragments, carbon-carbon double bonds as well as carbonyl functional groups, is that these analytes are capable of entering π - π type interactions with π -electronic systems of exposed phenyl rings of the open network hypercrosslinked polymer. These selective π - π interactions contribute substantially to trivial hydrophobic interactions when the above polar analytes are adsorbed from aqueous media. Even more important these electronic interactions become in the case of sorption from non-polar media, hexane or other aliphatic hydrocarbons where the hydrophobic-type interactions do not operate any more. This feature of hypercrosslinked polystyrene opens a unique possibility to selectively isolate the above π -electron-containing classes of organic compounds from non-polar media.

This possibility was demonstrated by selectively extracting four polar furan derivatives, 5-hydroxymethylfurfural, furfural, 2-acetylfuran and 5-methylfurfural, from transformer oil, which is mostly composed of higher aliphatic hydrocarbons. Being the degradation products of cellulose-type electric insulation in transformers, the furan-derived compounds serve as specific markers for the insulation diagnostics. To this end, 2 mL pure oil were diluted with

10 mL hexane, spiked with 100 µg/L of each analyte component and then 2 mL of the final solution was percolated through a 20x8 mm I.D. cartridge packed with 500 mg 70-140 µm particles of Purosep 200. The loaded cartridge was flushed with hexane and dried in the gentle flow of nitrogen. After eluting with an acetonitrile-water 1:1 mixture the above analytes were quantified by HPLC-UV [69]. Purosep 200 almost completely recovers the analytes with excellent reproducibility. At that, the LOD of each component does not exceed 30 µg/L, which permits determination of the target analytes at 1% level of their allowed tolerance limit. Similarly, by using the same approach, it proved to be possible to control the presence of priority polycyclic aromatic hydrocarbons or pesticides in vegetable oil [70]. The recoveries of polycyclic aromatic hydrocarbons vary between 80 and 99%. The above suggested pre-concentration of aromatic hydrocarbons from hexane extracts of fatty food products eliminates the most unpleasant stage of previously applied analytical techniques, which was the alkaline hydrolysis of oils and fats of the sample into sodium salts of fatty acids. Complete extraction of target analytes from the latter surfactants was also problematic.

3.2.7. Pre-concentration of Volatile Organic Compounds in Air

We could make examples over and over confirming the prosperous employing of hypercrosslinked polystyrene sorbents, both commercially available and in-house made, for SPE pre-concentration of a wide variety of organic compounds present in an aqueous (or non-aqueous) environment. However, we believe that the above-mentioned publications provide adequate insight into the high adsorption power of the sorbents in question. In conclusion, we would like to mention that the hypercrosslinked sorbents could be used for the pre-concentration of traces of volatile organic compounds present in air. For instance, the commercial MN-200 sorbent was used successfully to determine eight selected compounds by SPE enrichment. Table 7 reports their breakthrough volumes. The latter were found to exceed 1 L/g, which was considered to be required for efficiently collecting the trace amounts of vapors. After thermal desorption at 210°C all recoveries were close to 100% with the exception of isooctane where it dropped to 98.2±0.2%. By comparison, Texan GR gave recovery of 25% for pentane and 35% for dichloromethane under equal experimental conditions. This is rather logical, since the specific surface area of Tenax GR is less than 35 m²/g against 1000 m²/g characteristic of MN-200 [71].

Table 7. Breakthrough volumes on MN-200 for 8 volatile organic compounds measured at 5 elevated temperatures (50 through 210°C) and then extrapolated to 20°C at “infinite dilution” of the vapors [8]

Compound	BTV, L/g
Pentane	13
Octane	109
Undecane	329
Methanol	5.8
Dichloromethane	5.1
Toluene	26
Isooctane	3.7
Cyclohexane	188

BTV is breakthrough volume.

4. PREPARATIVE FRONTAL SIZE EXCLUSION CHROMATOGRAPHY OF MINERAL ELECTROLYTES ON NANOPOROUS HYPERCROSSLINKED POLYSTYRENE

Many industrial enterprises face the challenge of utilization or separation of concentrated aqueous mixed solutions of inorganic acids, bases and salts. This problem arises from pickling of metallic surfaces, acidic or basic leaching of ores, manufacturing of mineral fertilizers and soda. Mineralized wastes also originate from many processes of basic organic synthesis. In many cases wastes represent acidic or basic salt solutions of lead, copper, iron, cobalt, titanium and other metals. Extraction of valuable metals from rather concentrated solutions by means of ion exchange resins is not very promising for many reasons including unsatisfactory selectivity of ion exchange and shrinkage of resin beads in concentrated electrolyte solutions. Both reasons diminish the column operation efficiency and abridge the exchanger's lifetime. A rapid depletion of ion exchange capacity on percolating a concentrated electrolyte solution through the column and, hence, the necessity of frequent resin regeneration dramatically increase the cost of process. Over and above, each cycle of regeneration produces new saline wastes, which also require a corresponding processing. Recovering of excess acid from useless salt solutions also presents problems.

Various approaches have been proposed to overcome the above problems of separating concentrated mixed electrolyte solutions into individual components. Of these approaches, the so-called "acid retardation" process [72] became the most popular. It consists of passing a concentrated mixed solution of acid and its salt through the column packed with an anion exchange resin in the same salt form. Under these conditions that exclude ion exchange, the separated salt leaves the column first, while the acid retards and arrives at the column outlet later. In accordance with the generally accepted perception, retardation of the acid is caused largely by its interaction with the styrene-DVB matrix of the anion exchanger or with its functional groups. Utterly surprising, however, is the fact that within the 50 years that passed since the pioneering publications of Hatch and Dillon [72, 73], nobody even tried to confirm the above supposition by direct and independent experiments. We carried out such a simple experiment. Figure 10 depicts the sorption isotherm for hydrochloric acid onto a strong basic anion exchange resin PCA-433 (Purolite Int., UK) taken in chloride form. As can be seen, the sorption of hydrochloric acid starts only when its equilibrium concentration exceeds 5 eq/L. At such high concentrations, HCl is probably capable of forming stable ionic pairs or even covalent-bound molecules, the latter being retained by dispersion interactions with the resin matrix. At lower concentrations that correspond to typical contents of acid and salt in industrial wastes (2-3 eq/L), PCA-433 *does not retain hydrochloric acid*, at all. Consequently, the retardation of hydrochloric acid by anion exchangers taken in Cl-form cannot be explained by the excessive adsorption onto the polystyrene matrix.

When speculating about the reasons for electrolytes' discrimination on anion exchange resins, we arrived at the conclusion that the effect of acid separation from its salt is conditioned upon steric inaccessibility of some free space (pores) in the bead of the gel-type exchanger to large hydrated metal cations, rather than any connecting interactions of acid with styrene-DVB matrix or functional groups of the anion exchanger. In other words, we believe that the separation of electrolyte mixtures proceeds via mechanism of exclusion chromatography.

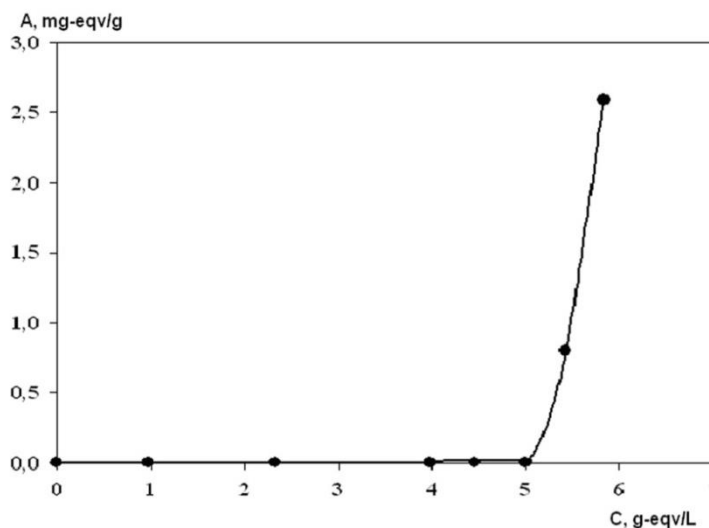


Figure 10. Sorption isotherm for hydrochloric acid onto strong basic anion exchange resin PCA-433 in chloride form.

4.1. Brief Description of Frontal Chromatography Experiment

A chromatographic column was filled with water (mobile phase) and water-swollen sorbent beads of 0.3-0.5 mm in diameter. To avoid the broadening of chromatographic zones due to convective fluxes, a heavier (compared to water) solution of electrolytes was sent upwards through the column until the column equilibrates with the initial solution. We called this part of the trial the “direct experiment”. Afterwards, the electrolytes were eluted from the column by pure water in the opposite direction. This is the “reversed experiment”. In all figures the breakthrough curves obtained in direct and reversed experiments were separated by a gap. In both experiments the eluate was collected by fraction of 1.2-1.5 mL in volume in which the concentration of electrolytes was determined by titration of constituent ions. A flow rate was 0.8-1.0 mL/min. The breakthrough volume of ions ($BV_{0.5}$) was determined at the middle of corresponding chromatographic zone fronts. The selectivity of separation in the direct experiment was calculated as the difference between $BV_{0.5}$ of separated components divided by bed volume. The self-concentrating effect of a separated electrolyte was determined as the ratio of its maximum concentration found in fractions to that in the initial mixture.

4.2. Basic Features of Frontal Size Exclusion Chromatography of Electrolytes

Exclusion chromatography separates compounds, macromolecules and particles in accordance with their size and ability to diffuse into pores of a stationary phase. Large species reside mostly in large pores and interstitial volume where they are quickly transported along the column by mobile phase. Smaller species also migrate into stagnant zones of both large

and small pores, that is why they achieve the column outlet later. However, to employ this method for separating the simplest hydrated mineral ions the diameter of which amounts to 6–10 Å, one needs to use a sorbent with very small pores. In this respect the nanoporous neutral (non-functionalized) hypercrosslinked polystyrene represents the adsorbing material of choice.

However, prior to discussion of electrolytes' separation within the scope of exclusion chromatography idea, and assuming that electrolytes are completely dissociated into constituent ions, we need to have the information about the dimensions of ions. Such information is ample but, unfortunately, different physical methods produce different results. Moreover, in each study the set of ions is limited. For that reason we made use of the data reported in publication [74] where, originating from the electroconductivity of diluted electrolyte solutions, the hydrated radii of a large number of cations and anions were estimated. It permits the comparison of ion dimensions between one another.

Let us now consider the results of two simple chromatographic experiments. Water-swollen hypercrosslinked sorbent NN-381 (Purolite Int., UK) was slurry packed in a glass column of 44 mL in volume. The interstitial volume on the packed column is 17.6 mL (40% of bed volume) [75]. Since one gram of dry sorbent beads incorporates 1.23 mL water on swelling, the total volume of the mobile phase in the column equals 36 mL. First of all, 3.45 N solution of CaCl_2 was sent through the column and then the salt was eluted with pure water. The same experiment was conducted with 3.48 N hydrochloric acid solution. Figure 11 shows the breakthrough and elution curves for the salt and the acid. Both in direct and in reversed experiments, the salt leaves the column before the acid. Indeed, in direct experiments CaCl_2 leaves the column at 32.5 mL while $\text{BV}_{0.5}$ of the acid amounts to 35.4 mL. In other words, the acid comes out of the column virtually with the volume of the mobile phase in the column. Consequently, *neutral nanoporous hypercrosslinked sorbent NN-381 retains neither calcium chloride, nor hydrochloric acid* (with the concentration of 3.48 N). It is also important that *practically all pores in the sorbent are accessible to hydrochloric acid whereas the salt is partially excluded from some small pores*. This difference is conditioned upon the fact that the radius of the hydrated double-charged cation of calcium is significantly larger than that of the chloride anion, 4.12 Å against 3.32 Å. It should also be noted that because of the partial CaCl_2 exclusion the two breakthrough curves diverge by 7% of the column bed.

The situation changes radically when the two electrolytes are simultaneously present in a mixed solution (Figure 12). Now CaCl_2 comes out of the column earlier, with the volume of 22.7 mL, rather than 32.5 mL as was observed in the previous experiment. On the contrary, the sorbent now seems to retain hydrochloric acid, since the latter leaves the column at 43 mL instead of 35.4 mL. In the direct experiment, the fronts of CaCl_2 and HCl diverged by one third of column volume. Another unprecedented chromatography phenomenon engages our attention, namely, the concentration of both separated components leaving the column rises compared to their concentration in the initial solution. At the maximum of concentration waves the concentration of calcium chloride and hydrochloric acid increases by a factor of 1.2 and 1.5, respectively. Thus, the behavior of the salt and acid mixture in the chromatographic column differs fundamentally from that of individual components.

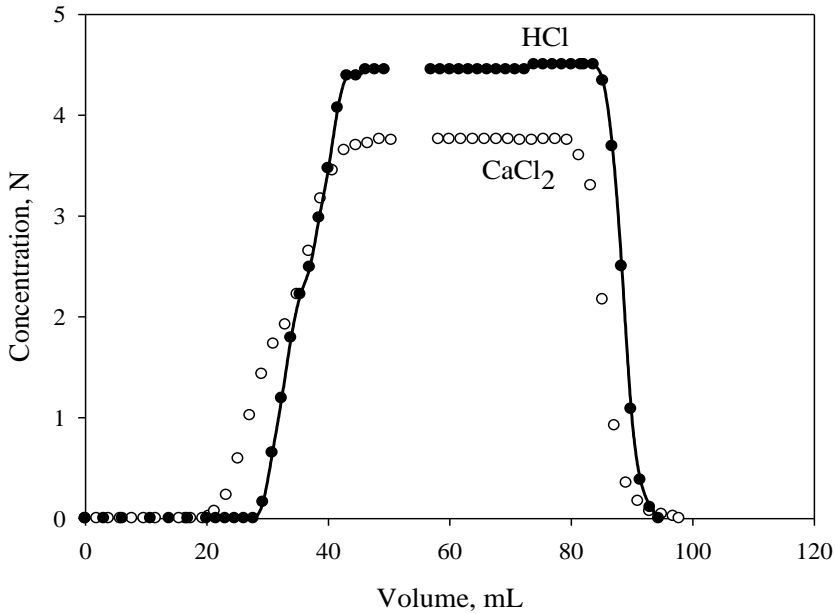


Figure 11. Breakthrough and elution curves for CaCl_2 and HCl obtained in separate experiments on 44 mL column with NN-381 [76].

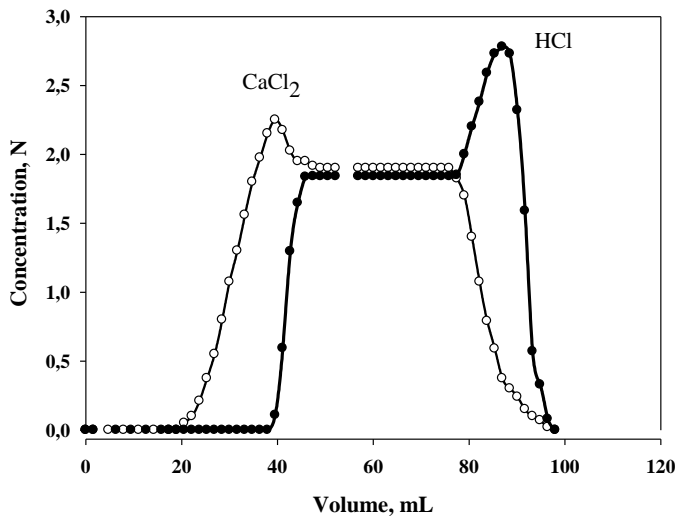


Figure 12. Breakthrough and elution curves of calcium chloride and hydrochloric acid, taken as a mixed solution, from 44 mL column with NN-381 [76].

In accordance with the principle of local electroneutrality, anions should move along the column in the vicinity of their cations. Our system is composed of two cations, calcium cation ($r_{\text{H}}=4.12 \text{ \AA}$) and proton ($r_{\text{H}}=2.82 \text{ \AA}$) and common chloride anion ($r_{\text{H}}=3.32 \text{ \AA}$). It should be noted, however, that protons and hydroxyl ions in electrophoretic and chromatographic processes can quickly appear in any point of the aqueous phase where there are water molecules bound to the rest of aqueous phase by hydrogen bonds, and where the maintenance

of electroneutrality is required. The emergence of a negative or positive charge on any water molecule in the required point proceeds via a simple shift of electrons along the chain of hydrogen bonds, so that the cations of hydroxonium and hydroxyl anions do not require their own place in sorbent pores in exclusion ion processes in aqueous media [77]. Therefore, when considering the separation of CaCl_2 and HCl , we may confine ourselves only to the analysis of behavior of Ca^{2+} and Cl^- .

In small pores of the nanoporous sorbent only those chloride anions reside that are formed on the dissociation of hydrochloric acid, since these pores can easily accommodate the equivalent amount of protons, but not Ca^{2+} -ions. At the same time, in large pores and interstitial liquid the chloride anions are disposed, which belong to both hydrochloric acid and calcium chloride. At that, the total concentration of two electrolytes in large pores appears to be higher than that of HCl in small pores. The great concentration gradient emerging between large and small pores, on the one hand, forces the acid to migrate additionally into small pores and accumulate there, and, on the other hand, pushes out the salt into the largest pores and the interstitial aqueous phase. This process continues until the concentration of chlorine ions (and hence the osmotic pressure) becomes equal throughout the entire aqueous system [78].

Under the conditions of exclusion chromatography, the above phenomenon results in an additional discrimination of two electrolytes and their spontaneous self-concentration in corresponding compartments of the liquid phase and, hence, corresponding eluate fractions. One can easily understand this effect within the scope of concept of the "ideal separation process" [77, 78]. The "ideal separation process" is the process which does not supplement any additional components (additional mobile phase in the system considered) into separated fractions. Distillation, crystallization and sieving belong to the family of such ideal separation processes. An automatic consequence of separating one component from the initial mixture is the unavoidable increase in the concentration of the residual component. Usually, chromatography has been dealing with *retention* of analytes on the stationary phase. Elution of retained species requires an additional volume of mobile phase, which leads to an inevitable increase in volume of the chromatographic zone of the substance and decrease in its concentration. In contrast to all other types of chromatography, *in exclusion chromatography substances are not retained on stationary phase and move along the column within the volume of injected probe* (and even faster than its mother solvent). Therefore, the effect of *redistribution of components within this volume portion* with increasing concentration of each of separated moieties becomes self-evident. Indeed, when calcium chloride, moving faster along the column than hydrochloric acid, leaves the chromatographic zone, the zone of the acid shrinks and the concentration of remaining hydrochloric acid increases automatically. From its part, the zone of calcium chloride also shrinks because of liberation from hydrochloric acid.

The following experiment documents the redistribution of electrolytes within the volume of introduced probe. A glass column was packed with beads of dry activated carbon prepared by pyrolysis of hypercrosslinked polystyrene (in contrast to hydrophobic hypercrosslinked polystyrene the carbonaceous product is water wettable material). An aqueous 0.6 N solution of ammonium sulfate was sent through the column until the equilibration of the column was reached. Then the latter was pushed out of the column by a water-immiscible organic solvent. Being confined between two sharp fronts, air/water and water/solvent, the aqueous solution moves along the column without any change in the volume of the aqueous phase.

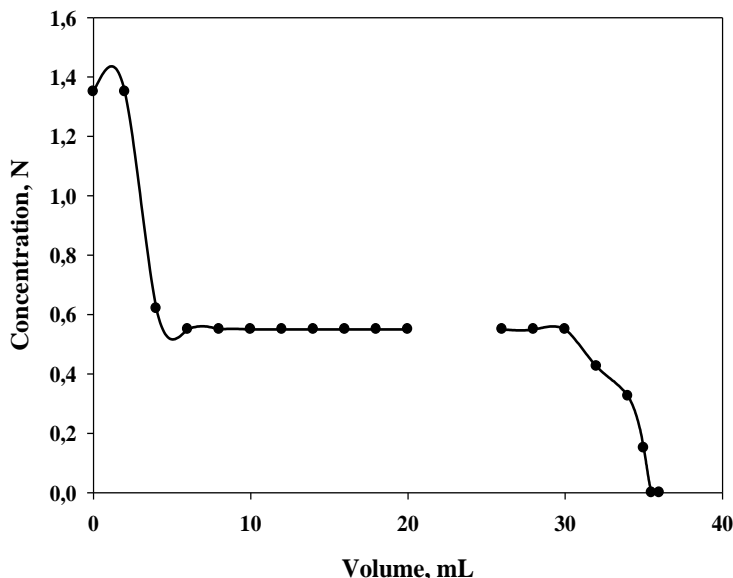


Figure 13. Redistribution of ammonium sulfate within the aqueous solution that passed through 28 mL column packed with dry activated Carbon D-4609 and then eluted by water-immiscible mixture of *n*-butanol/chloroform (1:1 v/v) [76].

Sulfate-anions are pretty large, $r_H=3.79 \text{ \AA}$, and tend to be excluded from fine sorbent pores. When moving along the column faster than water moves and at the same time having no possibility to escape the aqueous phase, SO_4^{2-} (together with NH_4^+) accumulates on the air/water boundary and, consequently the concentration of the salt in the first eluate fraction rises by a factor of 2.3. For the same reason, the concentration of salt in the last fractions of aqueous solution, displaced by the organic solvent, decreases and in the very last fraction the salt is absent, at all (Figure 13). Only the exclusion mechanism can explain the above phenomenon.

The above elaborated effects of separation of mineral electrolytes are based upon two fundamental suggestions, the exclusion of larger ions from small pores and the tendency of the system to level out any concentration gradients (or osmotic pressure gradients, or differences in the activity of water, which all are interdependent) between large and small pores. The reality of the both suggestions was strongly corroborated by a simple experiment [79]. Beads of water-swollen nanoporous hypercrosslinked polystyrene NN-381 were immersed into concentrated solutions of NH_4Cl , LiCl or H_3PO_4 . Small ions of Cl^- and NH_4^+ can occupy aqueous space both in large and small pores, so that the neutral polystyrene material experiences no changes, at all. In the other two electrolytes, on the contrary, surprisingly strong contraction of the beads is observed. Their volume decreases by 10% relative to the volume of *dry* beads (which, in its turn, is smaller than the initial volume of water-swollen beads by about 15%). A logical explanation of this remarkable phenomenon can be easily found in the combination of the above two suggestions. Ions of Li^+ and HPO_4^{2-} are large, so that electrolytes containing these ions cannot enter small pores of the sorbent. This causes a strong disproportion in the activity of water (or osmotic pressure) in large and small pores. The only way for the system to avoid the disadvantageous situation is reducing the water activity in small pores. A certain portion of water must migrate from the small pores

into greater pores, thus creating strong reduction of hydraulic pressure in the former. The consequence of the process is contraction of the hypercrosslinked matrix of sorbent beads. The high free volume and flexibility of the hypercrosslinked network allow the network to contract until the growing contraction stresses compensate for the reduced hydraulic pressure in small pores.

Understanding the nature of the processes that take place on the interaction between the hypercrosslinked sorbent interiors with a solution of electrolytes makes it possible to predict the outcome of the process and design new types of separations.

4.3. Acid Retardation Process

The above tendency of a system to level off the total concentration of a given pair of electrolytes throughout the entire volume of aqueous phase not only results in self-concentration of separating components in different parts of moving chromatographic zones but also significantly increases the selectivity of separation. Figure 14 depicts the chromatogram of separating a mixture concentrated in LiCl (3.9 N) and diluted in HCl (0.07 N). A strong concentration gradient of common chloride anions “salts out” the hydrochloric acid into the smallest pores where it accumulates until its concentration becomes close to that of LiCl in large pores and in the interstitial volume. Therefore, the breakthrough of HCl takes place only after percolation of four bed volumes of the initial solution. We can state with confidence that this is an acid “retardation” process, though there are no specific retentive interactions between the acid and neutral polymer. The accumulated portion of HCl elutes then in the reversed experiment in the form of a sharp concentrated peak.

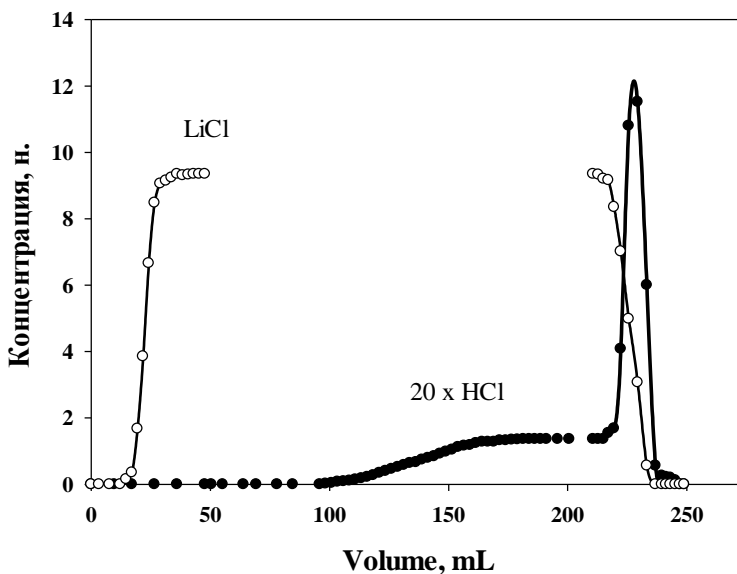


Figure 14. Chromatogram of separating 9.3 N LiCl/0.07 N HCl mixture on 28 mL column with NN-381. For visualization reasons the concentration of HCl on the plot was multiplied by a factor of 20 [76].

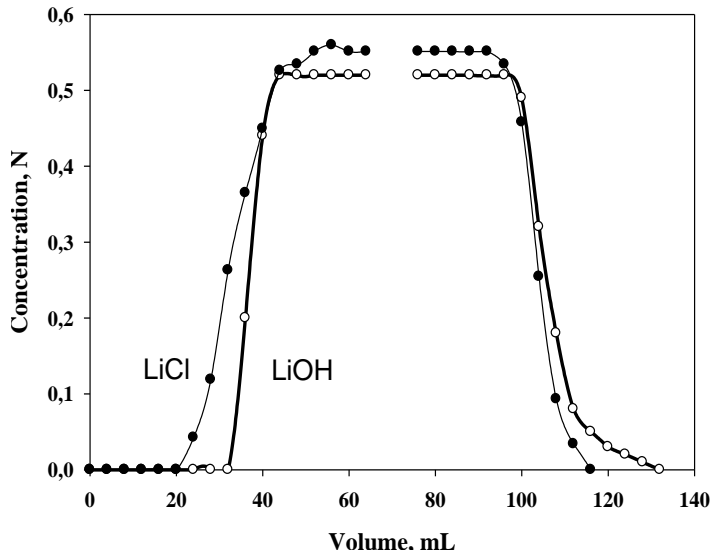


Figure 15. Chromatogram of 0.5 N LiCl/0.53 N LiOH mixture on 30 mL column with NN-381. After [81].

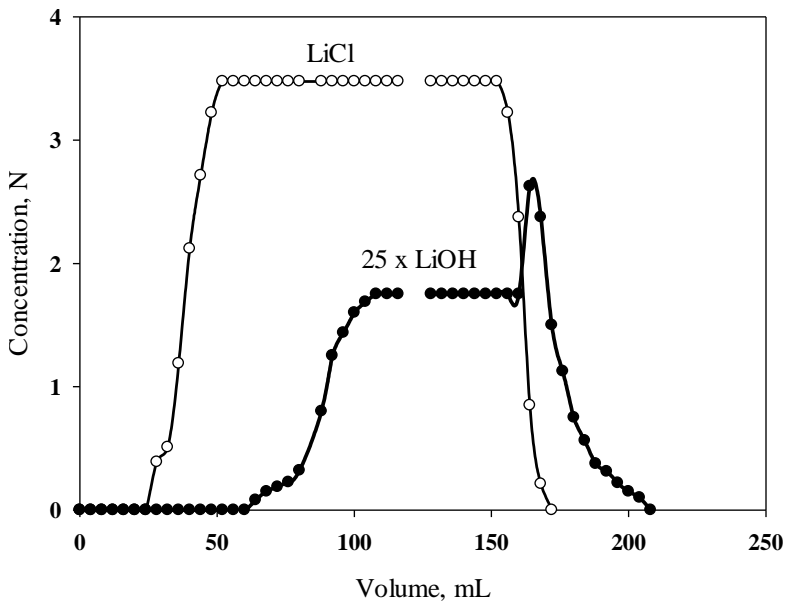


Figure 16. Chromatogram of separating 3.5 N LiCl/0.07 N LiOH mixture on 30 mL column with NN-381. For visualization reasons the concentration of LiOH on the plot was multiplied by a factor of 25. After [81].

4.4. Base Retardation Process

One may design a similar process for separating a base from its salt. Thus, one may expect that in a diluted 0.5 N mixture of LiCl and LiOH all constituent ions are highly

hydrated. The common for the both electrolytes lithium ion is large and must determine the rate of movement of fronts for both LiCl and LiOH. Indeed, both fronts appear at the column outlet before the dead volume. At that the fronts of base and salt diverge by 0.1 column bed volume (Figure 15). However, the selectivity of separation rises by a factor of 20 if the salt concentration increases till 3.5 N (Figure 16). In all probability, at high summary concentrations of electrolytes, LiOH the volume of which is smaller than that of LiCl, is forced to concentrate in small pores that are less accessible to hydrated ions of LiCl. (As was mentioned above, a hydroxyl-ion represents the deprotonated water molecule and does not need its own place in space, unlike chloride anions).

4.5. Salt Retardation Process

The above-discussed explanation of the mechanism of “acid retardation” and “base retardation” situations suggests that we may also achieve a similar “salt retardation” effect. Figure 17 shows the first example of such effect. It is related to the problem of separating small amounts of ammonium chloride from a concentrated solution of ammonium sulfate. In the course of manufacturing caprolactam, large quantities of sulfuric acid are neutralized to ammonium sulfate, which is then condensed to a crystalline fertilizer. Traces of chloride ions cause corrosion of evaporation equipment and impart the fertilizer hygroscopicity. As expected, a chromatographic column with nanoporous NN-381 demonstrates an express tendency for the small ions NH_4^+ and Cl^- to accumulate and retard in thin pores, which are inaccessible to large SO_4^{2-} ions. A large volume of pure ammonium sulfate can thus be obtained while a concentrated portion of ammonium chloride elutes in the reversed experiment. No ion exchange system would solve this particular problem of eliminating chloride ions from the sulfate brain.

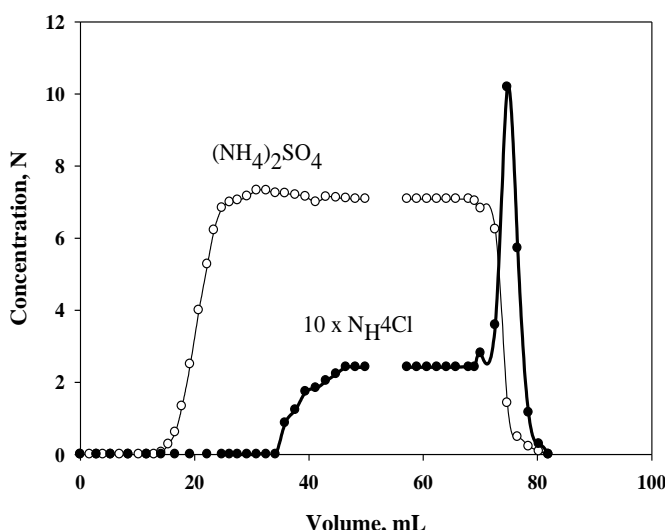


Figure 17. Chromatogram of separating 1% NH_4Cl from 40% $(\text{NH}_4)_2\text{SO}_4$ on 28 mL column with NN-381. In the plot the concentration of ammonium chloride was increased by a factor of ten. After [81].

4.6. Process of Acid Retardation on Other Types of Sorbents

It needs to be added here that separation of the model mixture of CaCl_2 and HCl , both on the neutral hypercrosslinked polystyrene adsorbing material NN-381 and other sorbents, such as neutral activated Carbon D-4609, strong basic anion exchange resins PCA-433, AV-17x8, Dowex 1x10 (in their Cl^- -forms) or hypercrosslinked weak basic anion exchanger MN-170 produces chromatograms identical to that shown in Figure 12 [80]. This unambiguously indicates that the type of functional groups and their very presence or absence in the material of the stationary phase by no means influences the nature of ion differentiation of the above mixture. A good separation of calcium chloride and hydrochloric acid on conventional anion exchangers containing 8-10% divinylbenzene points to the small size of 'pores' in their matrix and becomes evident in the light of the circumstance that chloromethylation of styrene-divinylbenzene matrix (the intermediate stage in synthesis of anion exchangers) is accompanied with a by-reaction of intensive crosslinking polystyrene chains. This significantly increases the real crosslinking density of the matrix leaving 'pores' and channels, which compare in their size with dimensions of hydrated ions, while the quaternary ammonium functional groups only provide swelling of the polystyrene-type matrix in aqueous media.

4.7. Conclusion

The new method of separating aqueous concentrated mixed electrolyte solutions into individual components by means of frontal size exclusion chromatography on neutral hypercrosslinked polystyrene sorbents is undoubtedly of great scientific and practical interest. From the preparative point of view the developed method is interesting in that it provides predictable and versatile possibilities, not restricted to salt-acid separations, the only amenable to the known method of acid retardation on anion exchangers. The main requirement for a successful separation consists of the difference in size of hydrated ions to be separated. The method is simple, does not require any chemicals, and does not produce mineralized wastes. The sorbent is stable in aggressive media and does not change its volume on transition from concentrated electrolyte solutions to water and vice versa. Also, to emphasize, is the possibility of exploiting the unique self-concentration effect and the circumstance that selectivity and productivity of the process increases with the concentration of the initial mixture rising. The whole process can be fully automated. No doubt, the method has a future in large-scale technologies.

5. DETOXIFICATION OF BLOOD BY HYPERCROSSLINKED HEMOSORBENTS

5.1. Basic Information on Extracorporeal Blood Purification

Extracorporeal blood purification is a modern medical procedure for removing toxic compounds from blood circulation, which is implemented outside the patient body. The

procedure may be divided into two main categories, hemoperfusion (hemisorption) and hemodialysis.

Hemoperfusion implies passing the blood through a cartridge packed with particles of an adsorbing material. In the general case, all blood circulating in body should pass twice through the sorption cartridge. Depending on disease, doctor determines the type of sorbent, its quantity and the number of recurring procedures.

Hemoperfusion is intended to be used in the following cases:

- exogenous intoxications by alcohol, narcotic drugs, medical products, etc.;
- endogenous intoxication caused by the accumulation of decomposition products and metabolites in the body of patients with sepsis, kidney or liver failure, hepatitis, pancreatitis;
- acute poisoning with medicines, salts of heavy metals, pesticides or other organic compounds;
- auto-immune diseases;
- diphtheria, acute viral hepatitis;
- psoriasis, eczema, dermatitis, food and drug allergy;
- endotoxiosis;
- some mental disorders.

Currently, two basic types of sorbents for hemoperfusion are in use. The first type incorporates non-specific sorbents, largely activated carbons. They simultaneously extract many organic compounds from the blood. Some polymeric sorbents may also be assigned to this type of materials. The second type is composed of selective sorbents, such as ion exchange resins, which are aimed at the removal of ammonium salts or excess potassium ions from blood. Synthetic bioaffine and immunoaffine sorbents, the structure of which incorporates specially designed ligands to remove some specific toxic compounds, also relate to the second type of hemosorbents.

Sorbents for extracorporeal blood purification must meet two fundamental requirements. First, they must extract effectively target compounds from whole blood or plasma and, second, they must be hemocompatible. The term “hemocompatibility” means that the sorbent in contact with blood does not cause any damage to blood cells, activate complement and cause clot formation, or extract inadmissibly large amount of albumin or other essential proteins. Frequently in scientific literature one may meet another term “biocompatibility”. It means compatibility of the material with patient tissue without causing any collateral body response, while still performing a necessary mechanical function or inducing the cellular or tissue response, which is necessary to achieve an optimal therapeutic effect.

The development of materials characterized by true hemocompatibility, in particular thrombo-resistance, represents a very complex problem. On the boundary of the internal vessel surface/blood in a healthy body, there exists a sensitive natural balance between complex systems of activation and inhibition of blood coagulation. The contact of circulating blood with a foreign surface, for example, with that of activated carbon, distorts the above equilibrium and results in adhesion of platelets on the sorbent and a lively clotting due to the activation of the internal fibrillation system. To preclude the highly undesirable consequences of clotting one introduces heparin into the blood stream. However, its application may be

accompanied with serious side-effects, such as internal bleeding, particularly, if a patient suffers from the stomach or intestine ulcers. One more negative feature of activated carbon is that it is mechanically fragile and easily produces particulates, which can cause an embolism of blood vessels.

To overcome the bad hemocompatibility and generation of fines, one covers particles of porous carbon with a thin film of a hemocompatible polymer. At that, however, the kinetic properties of adsorbing material greatly deteriorate. Polymeric adsorbing materials are usually more resistant to attrition, but also require careful chemical modification of the beads' outer surface to impart them hemocompatibility. This modification can be conducted by grafting on the outer surface of hydrophilic oligomeric or polymeric species, such as heparin, choline, chitosan, N-vinyl-pyrrolidone, etc. [82-85]. Again, the coating shell reduces the performance of polymeric adsorbing materials, which may anyway yield to those of activated carbons.

It has been noticed rather early that proteins barely adsorb on the surface of hypercrosslinked polystyrene beads. This observation led to a suggestion to design hemosorbents on the base of hypercrosslinked polymers. Indeed, first experiments showed that already small amounts of polar low-molecular-weight substituents on the surface of beads make them perfectly hemocompatible. Probably, the open network structure of the hypercrosslinked material does not present extended solid surfaces for platelets to adsorb. Another crucial requirement for modern hemosorbents is that they effectively adsorb toxins, including low-molecular-weight toxic proteins, but do not remove too much albumin and larger molecules from the blood. This requirement was met by making polydivinylbenzene materials that combined mesoporous general morphology with hypercrosslinked features of polymeric phase. Hemosorbents of this type finally received full approval in the clinics of the European Union, particularly for combating sepsis.

5.2. Hypercrosslinked Polydivinylbenzene-type CytoSorb™ for Treatment of Sepsis

Sepsis is the leading cause of mortality in intensive care units. Blood poisoning is usually accompanied by an uncontrolled rise of multiple toxic proteins, cytokines, the known representatives of which are numerous interleukins (IL). The reduction of cytokines' level in blood by hemoperfusion through a hypercrosslinked polydivinylbenzene-type adsorbent was found to be a powerful tool to improve the survival of patients in sepsis.

CytoSorb™ [86] is one of the families of hypercrosslinked mesoporous polydivinylbenzenes specially designed (with full involvement of authors of the present Chapter) to adsorb cytokines with molecular weights of 10 to 50 kDa. It is a highly porous beaded material having pores ranging from 2 to 70 nm in diameter and specific surface area of 500-700 m²/g. The inert polymeric material containing no biologics, cells, ligands or drug components is easily sterilized by gamma irradiation or steam treatment. The beads do not produce perishable or leachable materials. Their excellent hemocompatibility was confirmed by numerous *in vitro* and *in vivo* experiments.

Table 8 documents the superb adsorption ability of CytoSorb™ towards cytokines. In these experiments 8 mL of a horse serum spiked with 1000-5000 pg/mL of individual cytokines were percolated through 1 mL SytoSorb™ cartridge for 4 hours with a flow rate of about 1 mL/min [86].

Table 8. The removal of a broad spectrum of cytokines by hemoperfusion through SytoSorb™ [86]

Cytokines	Molecular weight kDa	Percent removal
IL-8	8	100
IL-1a	17	100
IL-1 α	17	100
IL-10	18	85
IL-6	26	87
HMGB1	30	80
TNF- α trimer	51	55

Table 9. Percent reduction of cytokine levels by SytoSorb™ plus standard of care therapy versus standard of care therapy alone [86]

Cytokines	CytoSorb™ + SOC		SOC alone	
	4 th day	7 th day	4 th day	9 th day
IL-6	- 45	-40	+ 50	+ 125
IL-8	- 30	-10	+ 50	+ 25
IL-1a	- 70	- 70	+ 50	0
NCP 1	- 40	- 40	+ 120	+ 20

“-“ means decrease in cytokine level, “+” means increase in cytokine levels.

CytoSorb™ was evaluated in a multi-center study in Germany in 43 patients with septic shock and respiratory failure. CytoSorb™ plus standard of care (SOC) therapy achieved a statistically significant 30-50% reduction of many key cytokines compared to standard of care therapy alone. Indeed, as an example, Table 9 shows the results of one experiment. Patients with septic shock and respiratory failure were treated with a 300 mL device for six hours a day for seven consecutive days (each day with a new device) at flow rates of 200-300 mL/min. In patients treated with the sorbent under study, the percentage reduction of plasma cytokine levels taken from a whole blood across the 4-day and 7-day periods amounts to 30-70% and 10-70%, respectively. Contrarily, in a control group of patients that received standard of care therapy alone, the concentration of cytokines rises on average by 40-60%.

The CytoSorb™ treatment of patients with highly elevated level of IL-6 ($\geq 1,000$ pg/mL) or IL-1a ($\geq 6,000$ pg/mL), which are known to be independent predictors of mortality in sepsis, resulted in statistically significant reduction in 28-day all-cause mortality: 0% versus 63% in the control group of patients treated conventionally and a trend to benefit in 60-day mortality, namely, 17% vs 63% control.

Thus, CytoSorb™ represents the first-class hypercrosslinked adsorbing material for extracorporeal cytokine removal with CE Mark regulatory approval. It can be used in patients with or without renal failure. CytoSorb™ therapy is safe and well tolerated. Also, the sorbent does not impact delicately balanced blood chemistries. It has been used in more than 650 human treatments without serious device-related adverse effects.

CytoSorbents Co. Corporation (USA), which optimized the hypercrosslinked polydivinylbenzene sorbent CytoSorb™ for detoxification of blood of patients with sepsis, further suggests a new and smart way of using the hemocompatible polymer for blood

purification. The corporation named this the HemoDefend technology platform [85]. The fact is that annually US hospitals require blood for over 15 million packed red blood cell (pRBC) transfusions. Transfusion of platelets, plasma, cryoprecipitate and other blood products double this number. Trauma, surgery, critical care illnesses, cancer, military usage, and inherited blood disorders are just some of the drivers of transfused blood products. However, transfusion is not a simple procedure. There is a low but still tangible (1-4%) risk of non-hemolytic febrile and allergic transfusion reactions, risks of allo-immunization, atypical infection, such as prions, or “mad-cow” disease, risk of transfusion related acute lung injury, anaphylaxis, angioedema, and hemolysis. Transfusion risk increases in patients receiving multiple pRBC units (e.g. trauma, surgery) and in “primed” susceptible patients (e.g. critical care and high risk surgery).

Donated blood can contain foreign antigens, antibodies, medications, infectious materials (e.g. prions, viruses) and other substances that can cause serious consequences. During blood storage, pRBC units also accumulate free hemoglobin due to hemolysis, and undergo in situ generation of bioactive lipids (e.g. lysophosphatidylcholine), cytokines, and other inflammatory mediators that can trigger severe transfusion reactions.

HemoDefend may be used in two configurations, as on-line filter and as “Beads in Blood”. When used as a dockable in-line filter between the blood bag and the patient at the point of transfusion, the filter can purify a unit of blood from antibodies, free hemoglobin, cytokines, other inflammatory mediators, toxins, drugs and other contaminants thus potentially extending the useful life of blood. In the unique “Beads in a Bag” treatment configuration, these beads are placed directly into a blood storage bag during bag manufacturing. They immediately begin to remove contaminants from the blood without the need to mix or agitate and continue their action thereafter. Unprecedented hemocompatibility of the hypercrosslinked polymer enables improvement of blood quality throughout the entire blood storage period.

5.3. Hypercrosslinked Polystyrene Sorbents Styrosorb Designed for Treatment of Sepsis

Hypercrosslinked polystyrene adsorbing materials of Styrosorb series (developed by authors of present Chapter in the early 1970^s) are known to be neutral highly porous polymers having a variable spectrum of pores between 0.2 nm 0.3 nm in diameter and high apparent specific surface area of around 1000 m²/g. Contrary to conventional macroporous copolymers, in the structure of which exists a real boundary between a densely packed polymeric phase of rigid pore walls and space filled with air or liquid; in the single-phase hypercrosslinked polystyrenes such a boundary does not exist. Here, virtually all polystyrene chains are separated from one another by numerous rigid struts and are therefore fully exposed to a surrounding medium. The openwork structure of hypercrosslinked polystyrenes provides an easy access of low molecular weight compounds to plural adsorption sites. In order to allow larger protein toxins with molecular weights of up to 40 kDa to enter the interior of the sorbent bead, the latter needs to be provided with another set of pores in the meso-range of up to 60 nm. This can be done by modifying the preparation protocol of the initial polymer. Besides, the surface of the beads must be modified [87] for tolerating prolonged contact with whole blood. According to these requirements, several batches of

hypercrosslinked polystyrene of the Styrosorb series have been prepared and carefully examined to estimate their suitability for extracorporeal blood purification.

Four specially designed samples of hypercrosslinked polystyrenes with an enhanced proportion of mesopores were in comparative study, Styrosorb 414, Styrosorb 514, Styrosorb 516 and Styrosorb 514M. The first three resins are beaded materials differing in surface chemistry, pore size and pore size distribution, the latter sorbent is a composite material containing nano-particles of ferric oxides (6.7 ± 3.8 nm, 8.7-8.9 % Fe) in the hypercrosslinked polystyrene matrix. For comparison reasons properties of commercial granulated activated carbon hemosorbent Adsorba 300C (Sweden) were also examined.

All sorbents under comparison have similar particle sizes (smaller than 1 mm) but different shapes. The polymeric materials present regular spheres with a rather narrow particle size distribution around 0.6-0.7 mm in diameter, while granules of activated carbon look like tiny cylinders of 2×0.8 mm (Figure 18).

More important is that all Styrosorb beads are rigid, mechanically and chemically stable, produce no leachables or particulates; the material is free of fines. On the contrary, activated carbons, though surface modified, are mechanically weak and generate fine particles on attrition. Carbon dust and fines on the surface of large particles are clearly seen in micrographs of Adsorba 300C. (It could be mentioned here that in this respect, activated carbons obtained by pyrolysis of beaded hypercrosslinked polystyrene sulfonated resin MN500HS or conventional macroporous sulfonated ion exchange resin CT275, have much better mechanical strength, 0.7-1.2 kg per bead [88]). Adsorba 300C was reported to have a specific surface area between 700 and 900 m^2/g , a well-developed mesoporosity and the ability to adsorb cytokine IL-1 β .

Already the very first sorption experiments under static equilibration conditions have demonstrated encouraging results for the Styrosorb series of materials. As Table 10 demonstrates, from a saline solution Styrosorb 414, Styrosorb 514 and Styrosorb 516 are good at taking up human recombinant cytokines, with the exception of interleukin IL-6, which has the highest molecular weight. Most probably, the low adsorption capacity in this case is caused by insufficient accessibility of the beads' interior for that large protein macromolecule.

Even better elimination effects for cytokines were observed in dynamic experiments where cytokine-spiked solutions in saline and plasma were sent through small cartridges packed with sorbents under comparison.



Styrosorb 514 and 516



Styrosorb 514M



Carbon Adsorba 300C

Figure 18. Optical micrographs of hemosorbents under comparison [89].

Table 10. The concentration of cytokines (pg/mL) in physiological solutions after their incubation with the sorbents Styrosorb [89]

Cytokines		Sorbents			Initial concentration
Type	Molecular weight, kDa	Styrosorb 516	Styrosorb 414	Styrosorb 514	
IL-8	8	232±15	718±15	196±4	724±22
IL-4	15	40±13	85±6,5	70±7	497±8
TNF α	17.4	265±29	513±13	86±6	778±25
IL-1 β	17	88±22	120±22	112±8	799±27
IL-10	18.6	203±14	273±18	340±14	701±21
TNF β	18.6	189±20	516±14	120±1	860±24
IL-6	20.8	610±18	694±21	610±18	701±20

Experimental conditions: 35 mg sorbent, 5 mL saline, spiked with individual cytokines, incubation in shaker for 1 hour at ambient temperature. Here and thereafter the statistic significance $p < 0.05$.

Beside cytokines, all hypercrosslinked sorbents actively absorb endotoxin lipopolysaccharide (LPS) *E. coli*. Under the same conditions from the solution in saline with the initial LPS concentration of $6,25 \pm 1,42$ U/mL Styrosorbs 514, 414 and 516 extract 77%, 78% and 54% endotoxin, respectively. As a whole, Styrosorb 514 has shown the best results; activated carbon Adsorba 300C and, in particular, Styrosorb 414 were less efficient for several types of cytokines. For these reasons in the following experiments we showed preference to Styrosorb 514.

The ability of the hypercrosslinked polystyrene sorbents, Styrosorb, proved surprising and extremely important in suppressing the growth of gram-positive bacteria. In an in vitro experiment, 450 mL blood of healthy donors were spiked with gram-positive (*S. aureus*) or gram-negative (*K. pneum. pneumoniae*) microorganisms and allowed to circulate five times through 10 mL columns packed with Styrosorbs. Then, the blood aliquot was sowed on a nutrient medium and in 24 hours the number of colonies was calculated. After hemoperfusion through Styrosorb 414 the number of colonies *S. aureus* decreased by 88%. The contact of blood with Styrosorb 514 and Styrosorb 516 also led to a sharp decrease in the number of grown colonies, by 63% and 51%, respectively. At the same time the growth of gram-negative *K. pneum. pneumoniae* was suppressed to a much smaller extent. The largest effect, 21%, was achieved for Styrosorb 414 while Styrosorbs 514 and 516 reduced the bacteria growth only by 2% and 10%, respectively [89]. Currently, the real reason for this pretty unusual effect is not yet clear. Nevertheless, this property of hypercrosslinked sorbents seems to be very useful from a practical point of view.

In addition, all sorbents examined were found to exert a pronounced influence on *S. cerevisiae* yeast suspended in canine blood by reducing their amount and decreasing the proportion of live fungi in the remaining fraction (by 82% and 26% for Styrosorb 514, 74% and 27% for carbon, and 76% and 12% for Styrosorb 514M, respectively) [90].

As was already repeatedly stressed, the most important characteristic of potential hemosorbents is their compatibility with blood. To evaluate the hemocompatibility of hypercrosslinked polystyrene Styrosorbs, Anisimova et al. examined the hemolysis of erythrocytes, which is a consequence of cell membrane damage, as well as the destruction of mononuclear leukocytes (ML) in blood of healthy donors after blood's contact with the

sorbents [90]. Four hours of contact with the donor blood polymers caused only a minimal damage of erythrocytes, proving a perfect hemocompatibility of Styrosorbs. The same is true for the one hour-long incubation of ML suspension with the sorbents; the survival of leukocytes remained on a level of 90-99%.

The obvious superiority in hemocompatibility of the polymers Styrosorb over granulated carbon hemosorbent becomes evident from the results of *in vitro* experiments with human blood. 10 mL of healthy donor blood stabilized with sodium citrate were recirculated 20 times through a miniature column with about 0.9 g sorbent at a flow rate of 1.3 mL/min. The averaged data are given in Figure 19. After a 20-fold percolation of the human blood samples through Styrosorb 514, the hemolysis of erythrocytes and the aggregation of platelets did not exceed 5%, thus demonstrating an excellent hemocompatibility of the polymer. Another hypercrosslinked sorbent, composite material Styrosorb 514M, under the same conditions also exhibits good hemocompatibility though it is slightly inferior to Styrosorb 514. Activated carbon-type hemosorbent, on the contrary, demonstrates an unsatisfactory performance.

Hypercrosslinked sorbents can also be used for the extracorporeal detoxification of lymphatic fluid [89]. This conclusion was drawn after percolating 700 mL lymph of an oncology patient in sepsis through an 80 mL column packed with Styrosorb 514. The comparison of biochemical and immunological lymph parameters before and after sorption procedure documented an insignificant lowering of total protein concentration and practically invariable albumin concentration. It is quite interesting that Styrosorb 514 extracts 20% urea and 39% creatinine and reduces the concentration of LPS endotoxin by a factor of 7.4. At the same time the level of the lipopolysaccharide-binding protein (LBP) rises by a factor of 1.34. The latter fact appears to be caused by the destruction of LPS-LBP complex, followed by the sorption of LPS. In addition, the hypercrosslinked polystyrene sorbent decreased the concentration of pro-inflammatory cytokines IL-6, IL-18 and IL-8 by a factor of 1.6, 1.6 and 2.4, respectively.

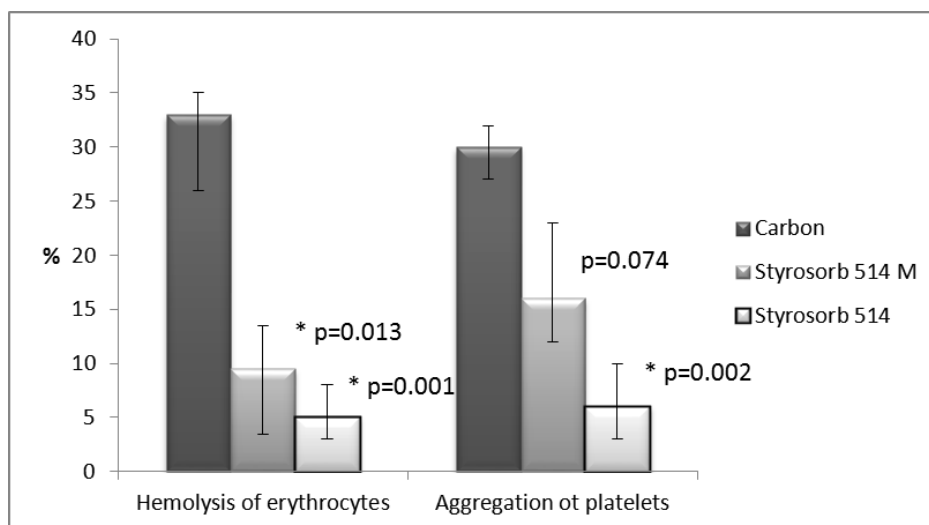


Figure 19. Hemolysis of erythrocytes and aggregation of platelets, % of initial, after 20-fold recirculation of human blood through hypercrosslinked polystyrene sorbents and activated carbon hemosorbent Adsorba 300C [89].

In view of all the above findings, it was pretty safe to start conducting *in vivo* experiments on rabbits, aimed at the detoxification of blood at an early stage of an artificial septic shock [91, 92]. A group of 6 rabbits received under narcosis a portion of heparin (50 U/kg) and an intravenous infusion of 5 ng/kg lipopolysaccharide LPS *Klebsiella pneumoniae* (Sigma, USA) and 1000 U/kg recombinant human TNF β (Biosource, USA). Blood circulation at a rate of 4 mL/min through 10 ml column with Styrosorb 514 was organized using a peristaltic pump. Three rabbits received hemoperfusion treatment during the first hour period while three other animals were left as the reference group. Both the LPS and hTNF β cytokine appeared in the venous blood of rabbits already three minutes after injection. But, LPS was almost completely eliminated from blood of experimental animals within a 1-hour hemoperfusion treatment, while in the reference group it dropped to half of the initial level, only. Similarly, concentration of hTNF β was reduced (to over 60%) in the blood of animals under hemoperfusion 2.3 times stronger than in the reference group. In the reference group of animals acute poisoning clearly manifested itself by a substantial drop in the neutrophils count and a rise in the leucocytes count, while no change in leucocytes and no hemolysis was registered in the group of animals that received hemoperfusion.

The above presented results of intensive *in vitro* and *in vitro* examination of three different samples of hypercrosslinked polystyrene-type sorbents, Styrosorbs 514, 516 and 414, as well as composite material Styrosorb 514M on the base of an analogous polymer, unambiguously prove their suitability for a practical application in the capacity of hemosorbents. They all outperform the commercially available surface-modified activated carbon-type hemosorbent Adsorba 300C. Styrosorb 514 was rated the best. While being fully hemocompatible, it must exert a complex action on sepsis patients, simultaneously removing from blood circulation bacterial lipopolysaccharide-type endotoxins, numerous cytokines, pro- and anti-inflammatory factors, and also block proliferation of gram-positive bacteria and even fungi.

Dogs with cancer and symptoms of multiple organ failure that accompany sepsis were chosen for further study. The animals were divided into two groups, five dogs in each. Hemosorption was carried out on “Hemos-HS” (Biotech-M, Russia) apparatus, basically consisting of a special peristaltic pump coupled with one of two types of columns (100 mL). “Hemos-KS” (Biotech-M, Russia) based on carbon sorbent were used for hemoperfusion in the control group of animals, while columns packed with Styrosorb 514 were used for the experimental animal group. Heparin load was 100-200 U/kg and the time of hemoperfusion treatment was two hours. All conditions of the study were similar for both groups of dogs.

As was observed, after hemoperfusion through the hypercrosslinked polystyrene column, the motor activity of the animals was normalized and their initially low systolic arterial pressure increased by $21 \pm 2.1\%$. As opposed to the control animals, the treatment in the experimental group didn't cause any changes in pH and ionic composition of blood serum, didn't lead to decreasing concentration of erythrocytes and platelets, nor did it change the blood coagulation tendency.

In comparison with the carbon sorbent, Styrosorb 514 was found to provide substantially more effective elimination of several toxic metabolites from animal blood (Table 11). Indeed, the polystyrene-based sorbent extracts 59% urea, 30% creatinine, and 77% bilirubin against 33%, 13% and 0%, respectively, for the carbon hemosorbent. The hypercrosslinked polystyrene does not deplete the concentration of albumin in the canine blood.

Table 11. Changes in blood levels of metabolites, bacterial endotoxin (LPS) and albumin after hemoperfusion in dogs with sepsis; median values for n=5 [89]

Analytes	Hemosorbent	Before hemisorption	After hemisorption	Norma for healthy dogs
Urea, mmol/L	Styrosorb 514	19	7.8	3.5-10.0
	Carbon	15	10	
Creatinine, μ mol/L	Styrosorb 514	148	104	45-140
	Carbon	152	132	
Bilirubin, μ mol/L	Styrosorb 514	53	12*	0-12
	Carbon	23	29	
LPS,U/mL	Styrosorb 514	0.114	0*	0-0.0001
	Carbon	0.100	0.005	
Albumin, g/L	Styrosorb 514	28	30	25-391
	Carbon	31	22*	

* $p < 0.05$.

Contrary to this, the carbon takes an inadmissible amount of the protein, 30%. Both sorbents completely eliminate the bacterial endotoxin LPS, however, the application of the polymeric column demonstrated a more prolonged detoxification effect.

The whole complex of results obtained thus far was regarded as a solid base for performing official clinical tests of the hemoperfusion device based on hypercrosslinked polystyrene hemosorbent Styrosorb. Twenty patients with 17 different diagnosis problems were given hemoperfusion treatments. The procedure was well tolerated by all patients who definitely felt better afterwards. No signs of hemolysis or thrombosis were noticed. Positive influence on several homeostasis systems was registered, including those of lipids, cytokine and blood cell composition. At the end, the simple and reliable device for extracorporeal detoxification via hemoperfusion with Styrosorb-type hemosorbent successfully passed all official clinical trials and was granted the approval of Ministry of Health of Russia for its use in clinical practice. Its application possibilities are versatile and manifold.

Introduction of hypercrosslinked polymeric hemosorbents have already saved many patients' lives. Popularity of hemoperfusion treatment will grow rapidly.

6. HYPERCROSSLINKED POLYSTYRENE WITH ULTIMATE CROSSLINKING EXTENT

All the above-discussed hypercrosslinked adsorbing materials, both industrial products and the majority of in-house made samples, have a crosslinking degree of up to 200%, which implies that in the last network each phenyl ring of polystyrene chains is connected too their neighbors with two methylene groups. As was mentioned in Section 3, these sorbents strongly retain organic compounds due to intensive universal dispersion interactions that can be fortified by π -interactions with aromatic or heteroaromatic rings, C=C double bonds or carbonyl functional groups of the adsorbate molecule. The π -type of interaction is especially effective in the hypercrosslinked open network matrix because the latter exposes many

electronic systems of its substituted aromatic rings to the guest molecule. The electron donating or accepting properties of these systems are strongly influenced by their geometry and degree of substitution. The latter can be further enhanced by involving into substitution more than one molecule of any bifunctional crosslinking agent per each phenyl ring of the initial polystyrene chains. This additional substitution of phenyls is in fact possible since the introduced alkyl groups do not reduce the activity of the benzene ring in Friedel-Crafts alkylation reactions. In section 2.1. of this chapter, it was explained that applying 1, 1.5, 2, and 2.5 moles of bifunctional agent, monochlorodimethyl ether, per each polystyrene phenyl ring, one arrives at hypercrosslinked networks with nominal degrees of crosslinking as high as 200% (HP-200), 300% (HP-300), 400% (HP-400) and 500% (HP-500) respectively. In these ultimately crosslinked networks, each phenyl ring appears bound to neighbor rings on the average by two, three, four and five methylene bridges, respectively. Such intensive condensation must cause distortion of initial planar rings, which must be telling on their electron-donating properties.

It turns out that the ultimately crosslinked polymers possess an unexpectedly high adsorption ability. They extract from the aqueous media polar low molecular weight organic compounds and, what is even more interesting, inorganic acids, bases and salts. Furthermore, these polymers are capable of adsorbing many organic substances from non-aqueous solvents. There is no other explanation than the enhanced activity of aromatic electronic systems of the network. Obviously, the reason lies with special properties of the aromatic network with a high extent of mutual connectivity and spatial distortion of its fragments as well as a partial overlap of electronic clouds of closely located rings.

6.1. Sorption of Organic Compounds on Ultimately Crosslinked Polystyrene from Aqueous Solutions

Despite the maximum possible crosslinking density, the non-functionalized polymers are capable of adsorbing relatively large molecules of synthetic organic dyes. From 0.3 g/L solutions of dyes they extract 120-140 mg/g (0.35-0.38 mmol/g) Malachite Green (MG) or about 50 mg/g (0.16 mmol/g) of Methylene Blue [93]. These dyes have similar molecular dimensions but Methylene Blue is disposed to form micelles. Obviously, in the structure of polymeric networks there exist relatively large meshes and canals between them, providing the migration of MG molecules (of 0.6x0.8 nm in size) or 0.9x1.3 nm MB molecules into the polymer interior. At the same time, even the largest pores are inaccessible to 3.0 nm globules of Cytochrome C (protein of 12 kDa molecular weight) which sorption is negligible.

The largely hydrophobic hypercrosslinked polymer HP-300 swells in water and takes up a surprisingly large amount of water, 1.3-1.6 mL/g. The high affinity of HP-300 even for a very polar compound, hydroxylamine, provides its adsorption loading of no less than 230 mg/g (7 mmol/g). From a 0.74 g/L aqueous solution HP-500 and HP-300 take up 40 and 60 mg/g (0.7-1.0 mmol/g) urea, respectively, whereas the capacity of industrial hypercrosslinked sorbents MN-200 and MN-202 is 20-26 mg/g, only. With increasing concentration of initial solutions till 2 M, the loading capacity of the ultimately crosslinked networks towards urea rises and reaches unprecedented 0.85-0.95 g/g that exceeds the capacity of industrial MN sorbents by a factor of about three [20].

The sorption of organic compounds is fully reversible although the stronger retained ones require longer washing with acetone and water for desorption from the polymer.

Table 12. Sorption of mineral acids onto ultimately crosslinked polystyrenes from 2.62 eq/L aqueous solutions [20]

Acid	HP-300		HP-500	
	C_{in} , mol/L	a, mmol/g	C_{in} , mol/L	a, mmol/g
HNO ₃	2.62	1.16	2.62	1.47
HF	2.62	0.93	2.62	1.06
HCl	2.62	0.79	2.62	0.70
H ₂ SO ₄	1,31	0.10	1,31	0.12
H ₃ PO ₄	0,87	0.077	0,87	0.09

Experimental conditions: 2.50 g polymer, 10 mL solution, 2 hours, 23°C.

6.2. Sorption of Inorganic Compounds on Ultimately Crosslinked Polystyrene from Aqueous Solutions

Sorption of mineral acids. Quite surprising is the ability of HP-300, HP-400 and HP-500 to absorb the simplest mineral acids, the maximum loading capacity being characteristic of HP-500 (Table 12). Sorption of mineral acids increases with rising concentration of initial solutions and pre-wetting the polymer. Irrespective of the polymer crosslinking degree and the concentration of initial solutions the sorption of acids decreases in the sequence HNO₃ > HF > HCl > H₂SO₄ > H₃PO₄. The retention of acids is probably balanced by the interaction of protons with electron-donating aromatic network fragments, on the one hand, and the exclusion of larger anions from the network's smallest pores, on the other hand. Therefore, the strong retention of HNO₃ is explained by the interaction of its protons with the aromatic network as well as dispersion interactions of small nitrate-anions, while the large phosphate anions are excluded from fine pores and so sorption of H₃PO₄ is negligible. Contrary to the ultimately crosslinked polymers, the HP-100 sample fails to absorb nitric acid, and the loading capacity does not exceed 0.06 mmol/g.

Interestingly, HP-300 polymer exhibits a high selectivity of extracting nitric acid. Indeed, from 1.63 M HNO₃/1.70 M HCl mixture the polymer takes up mostly nitric acid and even from the concentrated mixture, 3.75 M HNO₃/3.43 M HCl, the sorption of nitric acid is 1.5 times larger than that of HCl [20].

Sorption of hydrochloric acid was found to depend on the concentration of its solution. From diluted solutions HP-300 extracts no more than 1 mmol/g acid largely due to interactions of its protons with fully exposed to the aqueous phase electron-donating network fragments. When the concentration of solution exceeds 4 mol/L, the amount of water in it drastically drops. Now hydrogen chloride may exist in the form of stable ionic pairs or even covalent HCl molecules can appear in the solution. Such hydrogen chloride enters intensive dispersion interactions, thus increasing the adsorption load until one HCl molecule per one benzene ring of network, thus causing an increase in network volume by a factor of 1.6. To the same extent HP-300 swells in toluene.

Sorption of inorganic salts. The hypercrosslinked polymers HP-100, HP-300 and HP-500 take up 0.15-0.17 mmol/g ammonium nitrate from its 2.43 mol/L aqueous solution, which is conditioned by electrostatic interactions of ammonium cations and dispersion interactions of nitrate anions with aromatic networks. The three samples also adsorb 0.25, 1.40 and 0.46 mmol/g of potassium thiocyanate, respectively, due to the high polarizability of its large SCN⁻ anions [20].

As was found earlier, unmodified hypercrosslinked polymers retain salts of some transition metals, Hg(NO₃)₂ and Pb(NO₃)₂ as well as AgNO₃ from their acidified aqueous solutions. Thus, polymer HP-100 absorbs 2 mmol/g mercury(II) ions, 0.4 mmol/g lead(II) ions or 1.6 mmol/g silver ions [94]. The large loading capacity of HP-100 was suggested to result from the formation of charge-transfer or π -complexes of transition metal cations and network aromatic rings exposed to the surrounding solution. At that, one mercury(II) ion coordinates two phenyl rings. The formation of this complex requires time for rearrangement of rigid network fragments; hence the complexation is noticeably accelerated at elevated temperature. For that reason the sorption of the above salts onto ultimately crosslinked polystyrenes was conducted at 50°C. The loading capacity of HP-300 and HP-500 proved to be smaller even at higher equilibrium concentrations compared to adsorption ability of HP-100 (Table 13). The ions of mercury and lead are pretty large and exclusion effects may well reduce the sorption extent. Besides, HP-300 and HP-500 are more rigid networks than HP-100 and the rearrangement of their structure to form the above 1:2 complexes with metal ions is fairly hampered.

Sorption of the above salts is reversible. The salts may be removed by washing polymers with hydrochloric acid or ethylenediamine tetraacetic acid solutions.

Sorption of inorganic bases. Hypercrosslinked polymers HP-300 and HP-500 take up bases, such as KOH and NH₄OH. Figure 20 depicts the sorption isotherms for ammonium hydroxide onto two samples of hypercrosslinked polystyrenes, HP-100 and HP-300, as well as a sample of activated carbon D-4309 that was obtained by pyrolysis of hypercrosslinked polystyrene sulfonate. As can be seen, HP-100 does not take up ammonia while the loading capacity of HP-300, 6 mmol/g, proves to be even higher than that of conventional anion exchange resins. The sorption of ammonium cations appears to be due to their interaction with electronic systems of the aromatic matrix. In that case activated carbon would have to offer even stronger sorption sites, but in experiment it retains less ammonium hydroxide. Of course, HP-300 would expose more sorption sites. At the end, its interaction with NH₄OH is so intensive that in a 6 eq/L ammonium hydroxide solution the polymer increases its volume by a factor of 1.6, i.e. swells to the same extent as in concentrated hydrochloric acid and toluene.

Table 13. Sorption of salts of transition metals on hypercrosslinked polymers

Salt	HP-100		HP-300		HP-500	
	C _{eq} , mol/L	a, mmol/L	C _{eq} , mol/L	a, mmol/L	C _{eq} , mol/L	a, mmol/L
Hg(NO ₃) ₂	0.15	2	0,41	0,82	0,44	0,65
Pb(NO ₃) ₂	0.14	0.4	0,66	0,65	0,67	0,62
AgNO ₃	0.28	1.6	1,44	0,18	1,50	0,11

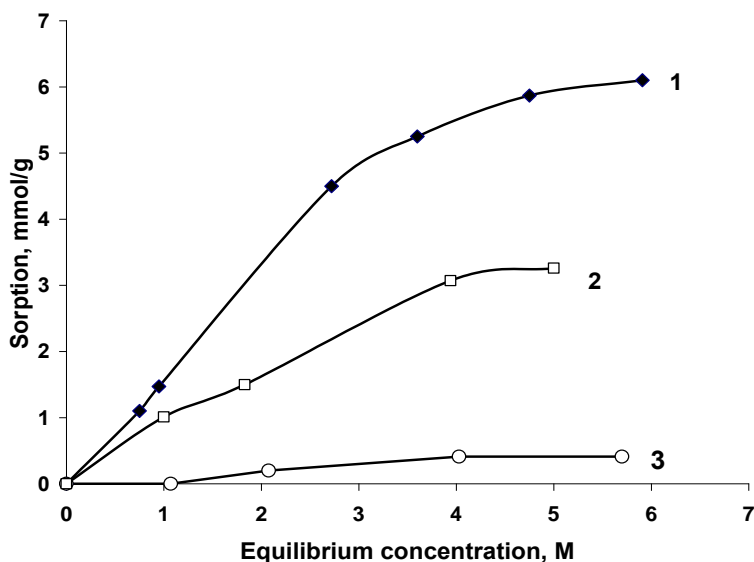


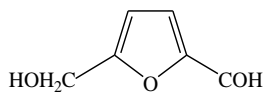
Figure 20. Sorption isotherms for ammonium hydroxide on (1) HP-300, (2) D4609 and (3) HP-100. Conditions: the pre-wetted sample contains 0.500 g dry polymer, 2-hour incubation in shaker at 23°C. After [20].

6.3. Sorption of Organic Compounds onto Ultimately Crosslinked Polystyrene from Non-aqueous Solutions

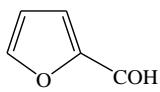
Marked electron-donating properties of ultimately crosslinked polystyrenes clearly manifest themselves on adsorption from non-aqueous media where general dispersive (“hydrophobic”) interactions degenerate almost completely. Two sets of organic compounds, furan derivatives and benzene derivatives, were in study.

In the nonpolar solvent, *n*-hexane, only specific interactions as dipole- and π -interactions, as well as hydrogen bonding must govern the retention of organic species. Obviously, they all condition the high adsorption of polar molecules of aniline on the HP-500 sample (Table 14). For the nonpolar toluene, only aromatic π -interactions can operate so its binding is noticeably weaker, the sorption loading for toluene does not exceed 0.09 mmol/g against 0.13 mmol/g for aniline. The introduction of chlorine into the CH_3 -group of toluene raises the polarity of the molecule and enhances its adsorption from *n*-hexane [95]. When used as the solvent, methanol strongly competes and practically eliminates all polar-type sorbent-solute interactions and also diminishes dispersive ones. Sorption from methanol is mainly due to remaining π -interactions, it is generally smaller than from hexane.

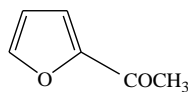
As for the furane derivatives, data are available only for sorption in methanol and acetonitrile, since the compounds examined do not dissolve in *n*-hexane. These series of solutes consists of a polar aromatic furane heterocycle that is prone to enter π -type interactions, and may also incorporate polar aldehyde, acetyl or hydroxymethyl groups.



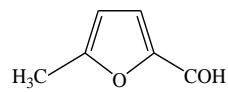
5-hydroxymethyl furfural



furfural



2-acetylfuran



5-methyl furfural

Though the highly polar solvents, methanol and, in particular, acetonitrile, severely compete for sorption sites with the analytes, adsorption on HP-500 is still astonishingly high (Table 14). As expected, the aldehyde group contributes to the adsorption more than acetyl, while the methyl group, on the contrary, increases the solute interaction with the solvent and reduces adsorption. A combined action of two polar groups provides for the extremely high adsorption of 5-hydroxymethyl furfural, 107 mg/g on HP-500 from methanol. Generally, acetonitrile solvates polystyrene more than methanol or hexane, which is also known for linear polystyrene that dissolves in acetonitrile, but not in the two other solvents. For this reason, adsorption from acetonitrile is smaller than from methanol and hexane.

Table 14. Sorption of organic substances from organic media on hypercrosslinked polystyrenes

Sorbate	Methanol		Acetonitrile		<i>n</i> -Hexane	
	a mg/g	a mmol/g	a mg/g	a mmol/g	a mg/g	a mmol/g
HP-500						
5-Hydroxymethyl furfural	107.0	0.85	42.9	0.34	-	-
2-Acetylfuran	4.0	0.04	1.6	0.01	-	-
Furfural	82.2	0.56	38.0	0.39	-	-
5-Methyl furfural	1.4	0.012	0	0	-	-
Aniline	28.7	0.31	-	-	33.1	0.36
Benzyl chloride	14.0	0.11	-	-	25.3	0.20
Toluene	4.2	0.04	-	-	12.7	0.14
Nitrobenzene	7.8	0.06	-	-	18.8	0.15
MN-200						
5-Hydroxymethyl furfural	6.2	0.05	2.6	0.02	-	-
2-Acetylfuran	2.8	0.02	0.2	0.001	-	-
Furfural	2.7	0.03	2.4	0.02	-	-
5-Methyl furfural	0.5	0.004	0	0	-	-
Aniline	0.2	0.002	-	-	17.1	0.18
Benzyl chloride	0.7	0.006	-	-	15.8	0.13
Toluene	1.1	0.012	-	-	7.9	0.09
Nitrobenzene	1.0	0.008	-	-	14.8	0.12

Experimental conditions: 0.125 g polymer, 10 mL of 0.1 mol/L initial concentration of solute solution, 5 hours, 23°C.

The data presented above lead to the conclusion that hypercrosslinked polystyrene with ultimate crosslinking densities present materials with unique, unprecedented adsorption properties. They may occupy a separate niche not only in solid phase extraction from non-

aqueous media, but also in special large-scale adsorption technologies, e.g. separation of exotic mixtures of HCl and HNO₃.

CONCLUSION

Some 45 years ago Davankov and Tsyurupa came up with a novel idea of making rigid open frameworks of polystyrene by an intensive crosslinking of its solvated chains. The hypercrosslinked polystyrene network proved to be of great interest both for practical use as a unique adsorbing material of a new generation, and also for the theory of polymeric networks.

It is hoped that the present Chapter gives sufficient information to corroborate these expectations. Indeed, in the decades of intensive study researchers enjoyed discovering many new unexpected properties of hypercrosslinked networks and new processes that emerged due to the use of the new material. It was not possible to outline all of them in this relatively short review chapter. More information can be found in the monograph on “Hypercrosslinked Polymeric Networks and Adsorbing Materials” [8]. But, a few of interesting topics, which remain outside the scope of this Chapter, can still be mentioned for the convenience of readers:

- Preparation of porous hypercrosslinked polystyrene-type monosized nanoparticles of circa 20 nm in diameter (“nanosponges”), which tend to self-assemble into regular clusters [96].
- Use of hypercrosslinked polystyrene microbeads of circa 5 μ as a rather universal and selective packing material for HPLC columns [97].
- Preparation and use of hypercrosslinked polystyrene monoliths for capillary liquid chromatography [98].
- Continuous separation of electrolyte mixtures with a spontaneous increase in the concentration of separated components [99].
- Partial resolution of a mineral salt into its parent acid and base by size-exclusion chromatography on hypercrosslinked polystyrene [100].
- Hypercrosslinked network-type non-polystyrenic polymers [101].
- Thermodynamic paradoxes in swelling of crosslinked polymers in vapors and liquids [102].

Indeed, in the frames of hypercrosslinked conception the old material called polystyrene has found an exciting new extension of life.

REFERENCES

- [1] Staudinger, H.; Heuer, W. *Berichte dtsch. Chem. Ges.* 1934, B, 1164-1172.
- [2] Ivanov, V.A.; Gorshkov, V.I. *Sorption and Chromatographic Processes.* 2006, 6, 5-31.
- [3] D’Alelio, G.I. Ion exchangers, Patent USA 2 366 007, 1944. *Chem. Abstr.* 39: 4418^{3,4}.
- [4] D’Alelio, G.I. Ion exchangers, Patent USA 2 366 008, 1944. *Chem. Abstr.* 39: 4418^{3,4}.
- [5] McBurney, C.M. Patent USA 2,591,573. 1952. *Chem. Abstr.* 46. 7364e.

-
- [6] Abrams, I.M.; Millar, J.R. *Reactive Funct. Polym.* 1997, 35, 7-22.
- [7] Davankov, V.A.; Rogozhin, S.V.; Tsyurupa, M.P. Patent USSR 299165 1969; *Chem. Abstr.* 1971, 75, 6841b; US Pat. 3,729,457.
- [8] Davankov, V.A.; Tsyurupa, M.P., "Hypercrosslinked Polymeric Networks and Adsorbing Materials. Synthesis, Structure, Properties, and Application", *Comprehensive Analytical Chemistry*, vol. 56, Elsevier, 2011, 670 pp.
- [9] Tsyurupa, M.P.; Davankov, V.A. *React. Funct. Polym.* 2002, 53, 193-203.
- [10] Bootsma, J.P.C.; Eling, B.; Challa, G. *Reactive Polym.* 1984, 3, 17-22.
- [11] Tsyurupa, M.P.; Blinnikova, Z.K.; Davidovich, Yu.A.; Lyubimov, S.E.; Naumkin, A.V.; Davankov, V.A. *React. Funct. Polym.* 2012, 72, 973-982.
- [12] Tsyurupa, M.P.; Borisov, Yu.A.; Blinnikova, Z.K.; Platonova, N.P.; Ul'yanov, S.V.; Buryak, S.K.; Davankov, V.A. *Protection of Metals & Phys. Chem. of Surf.* 2014, 50, 50-63.
- [13] Nikolaev, A.V.; Yakhin, V.S.; Yur'ev, G.S.; Bogatyrev, V.L. Theory and Practice of Sorption Processes (Russian), published by Voronezh State University. 1978, 12, 9-22.
- [14] Tsyurupa, M.P.; Davankov, V.A. *React. Funct. Polym.* 2006, 66, 768-779.
- [15] Lazutin, A.A.; Glagolev, M.K.; Vasilevskaya, V.V.; Khokhlov, A.R. *J. Chem. Physics* 2014, 140, 134903; doi: 10.1063/1.4869695.
- [16] Ferrante, F.; Celso, F. Lo; Duca, D. *Colloid Polym. Sci.* 2012, 290, 1443-1450.
- [17] Tsyurupa, M.P.; Papkov, M.A.; Davankov, V.A. *Vysokomol. Soedin. (Russia) Seria C.* 2009, 51, 1339-1345.
- [18] Pastukhov, V.A.; Tsyurupa, M.P.; Davankov, V.A. *J. Polym. Sci., Part B: Polym. Phys.* 1999, 37, 2324-2333.
- [19] Pastukhov, A.V.; Davankov, V.A. *Doklady Akad. Nauk Russ.* 2006, 410, 767-770.
- [20] Tsyurupa, M.P.; Blinnikova, Z.K.; Davankov V.A., *J. Sep. Sci.* 2014, in press.
- [21] Krauss, D.; Popov, G.; Schwachula, G.; Feistel, L.; Hauptmann, R.; Patent DDR 125,824, 1977.
- [22] Reed, S.F., US Appl. 927, 221, 24, 1978; *Chem. Abstr.* 1980, 93, 48118S.
- [23] Reed S.F.; Pinschmidt R.K.; Patent USA 4,191,813, 1980.
- [24] Stringfield, R.T.; Goltz, H.R.; Norman, S.I.; Bharwada, U.J.; LaBrie, R.L. Patent USA 4,950,332, 1990.
- [25] DOWEX Ion Exchange Resins and Adsorbents, Optipore L493 and V493, Product Information, 1998.
- [26] Bayer Chemicals, Levatit VP OC 1163, Product Information, 2003.
- [27] Bayer Chemicals, Levatit S 7768, Product Information, 2004.
- [28] Purolite Product Guide. Characteristics and applications, 2012.
- [29] Purosep SPEs – Solid Phase Extractants, Purolite, 1997.
- [30] Isolute ENV+, International Sorbent Technology, Catalog.
- [31] LiChrolut®, Merck, 1996.
- [32] Puig, D.; Barceló, D. *J. Chromatogr. A.* 1996, 733, 371-381.
- [33] Gun'ko, V.M.; Turov, V.V.; Zarko, V.I.; Nychiporuk, Y.M., et al. *J. Colloid Interface Sci.* 2008, 323, 6-17.
- [34] Less, M.; Schmidt, T.C.; von Löw, E.; Stork, G. *J. Chromatogr. A.* 1998, 810, 173-182.
- [35] Masqué, N.; Galià, M.; Marcé, R.M.; Borrull, F. *J. Chromatogr. A.* 1997, 771, 55-61.
- [36] Stringfield, R.T.; Goltz, H.R.; Norman, S.I.; Bharwada, U.J.; LaBrie, R.L. Patent USA 4,950,332, 1990.

- [37] Dawson-Ekeland, K.R.; Stringfield, R.T. Patent USA 5,021,253, 1991.
- [38] Norman, S.I.; Stringfield, R.T.; Gopsill C.C. Patent USA 4,965,083, 1990.
- [39] Dale, J.A.; Nikitin, N.V.; Moore, R.; Opperman, D.; Crooks, G.; Naden, D.; Belstein, E.; Jenkins, P. in: "Ion Exchange at the Millenium", ed. J.A. Greig, Imperial College Press, 2000, 261-268.
- [40] Troshkina, I.D.; Serbin, A.M.; Khaing, Z.N.; Ushanova, O.N.; Demin Yu.V.; Chekmarev, A.M. Sorption and Chromatographic Processes (Russia), 2006, 6, 1022-1027.
- [41] Alexienko, N.N.; Pastukhov, A.V.; Davankov, V.A.; Belyakova, L.D.; Voloshchuk, A.M. *Russ. J. Phys. Chem.* 2004,78, 1992-1998.
- [42] Pastukhov, A.V.; Aleksienko, N.N.; Tsyurupa, M.P.; Davankov, V.A.; Voloshchuk, A.M. *Russ. J. Phys. Chem.* 2005, 79, 1371-1379.
- [43] Planas, C.; Puig, A.; Rivera, J.; Caixach, J. *J. Chromatogr. A.* 2006, 1131, 242-252.
- [44] Fed. Reg., EPA Method 604, Phenols, Part VIII, 40 CFR Part 136, Environmental Protection Agency, 26 October 1984, 58-66.
- [45] Chilla, C.; Guillén, D.A.; Barroso, C.G.; Pérez-Bustamante, J.A. *J. Chromatogr. A.* 1996, 750, 209-214.
- [46] Liska, I. *J. Chromatogr. A.* 1993, 665, 163-176.
- [47] Berrueta, L.A.; Gallo, B.; Vicente, F. *Chromatographia.* 1995, 40, 474-483.
- [48] Tsyurupa, M.P.; Ilyin, M.M.; Andreeva, A.I.; Davankov, V.A. *Fresenius J. Anal. Chem.* 1995, 352, 672-675.
- [49] Puig, D.; Barceló, D. *J. Chromatogr. A.* 1996, 733, 371-381.
- [50] Kvistad, A.M.; Lundanes, E.; Greibrokk, T. *Chromatographia.* 1998, 48, 707-713.
- [51] Rodrigues, I.; Mejuto, M.C.; Bollaín, M.H.; Cela, R. *J. Chromatogr. A.* 1997, 786, 285-292.
- [52] Önerfjord, P.; Barceló, D.; Emnéus, J.; Gorton, L.; Marko-Varga, G. *J. Chromatogr. A.* 1996, 737, 35-45.
- [53] Guenu, S.; Hennion, M.-C. *J. Chromatogr. A.* 1996, 737, 15-24.
- [54] Curini, R.; Gentili, A.; Marchese, S.; Marino, A.; Perret, D. *J. Chromatogr. A.* 2000, 874, 187-198.
- [55] Tolosa, I.; Douy, B.; Carvalho, F.P. *J. Chromatogr. A.* 1999, 864, 121-136.
- [56] Loos, R.; Niessner, R. *J. Chromatogr. A.* 1999, 835, 217-229.
- [57] Laganà, A.; D'Ascenzo, G.; Fago, G.; Marino, A. *Chromatographia.* 1997, 46, 256-264.
- [58] Bagheri, H.; Saraji, M.; Barceló, D. *Chromatographia.* 2004, 59, 283-289.
- [59] Hogenboom, A.C.; Hofman, M.P.; Jolly, D.A.; Niessen, W.M.A.; Brinkman, U.A.Th. *J. Chromatogr. A.* 2000, 885, 377-388.
- [60] Sacher, F.; Lange, F.T.; Brauch, H.-J.; Blankenhorn, I. *J. Chromatogr. A.* 2001, 938, 199-210.
- [61] Pavlinov, S.A.; Piotrovskii, V.K. *Khim.-Farm. Zhurnal.* 1990, 24, 174-176.
- [62] Shkutina, I.V.; Stoyanova, O.F.; Selemenov, V.F. *Sorption and Chromatograph. Proc.* 2008, 8, 272-276.
- [63] Pavlinov, S.A.; Piotrovskii, V.K.; Metelitsa, V.I.; Filatova, N.P.; Bochkareva, E.V. *Khim.-Farm. Zhurnal.* 1990, 24, 17-19.
- [64] Karlsson, M.; Julander, A.; van Bavel, B.; Lindström, G. *Chromatographia.* 2005, 61, 67-73.
- [65] Cohen, A.S.; Jönsson, B.A.G. *Chromatographia.* 2007, 65, 407-412.

- [66] Hegstad, S.; Lundanes, E.; Reistad, R.; Haug, L.S.; Becher, G. A. *J. Chromatographia*. 2000, 52, 499-504.
- [67] Štajnbacher, D.; Zupančič-Kralj, L. *J. Chromatogr. A*. 2003, 1015, 185-198.
- [68] Sychev, C.S.; Eller, K.I.; Davankov, V.A. *Zavodskaya Laboratoriya*. 2004, 70, 17-19.
- [69] Proskurina, N.A.; Il'in, M.M.; Davankov, V.A.; Sychev, K.S.; Kostikov, S.Yu. *Russian J. Physical Chem.* 2007, 81, 424-427.
- [70] Sychov, C.S.; Davankov, V.A.; Proskurina, N.A.; Mikheeva, A.Yu. *LC-GC Europe*. 2009, 22, 20-27.
- [71] Baya, M.P.; Siskos, P.A.; Davankov, V.A. *Journal of AOAC International*. 2000, 83, 579-583.
- [72] Hatch, J.A.; Dillon, H.B. *Ind.&Eng. Chem., Process Design and Development* 1963, 2, 253-263.
- [73] Hatch, J.A.; Dillon, H.B.; Smith, H.B. *Ind.&Eng. Chem.* 1957, 49, 1812-1819.
- [74] Nightingale, E.R. *J. Phys. Chem.* 1959, 63, 1381-1387.
- [75] Manalo, G.D.; Turse, R.; Rieman III, W.M. *Anal. Chim. Acta.* 1959, 21, 383-391.
- [76] Blinnikova, Z.K. Frontal Preparative Exclusion Chromatography of Inorganic Electrolytes on Nanoporous Hypercrosslinked Polystyrene. Ph.D. Thesis, Moscow, 2009.
- [77] Davankov, V.A.; Tsyurupa, M.P. *J. Chromatogr.* 2005, 1087, 3-12.
- [78] Davankov, V.A.; Tsyurupa, M.P.; Blinnikova, Z.K.; Pavlova, L.A. *J. Sep. Sci.* 2009, 32, 64-73.
- [79] Pastukhov, A.V.; Davankov, V.A.; Tsyurupa, M.P.; Blinnikova, Z.K.; Kavalerskaya, N.E. *Russian J. Physical Chemistry A*. 2009, 83, 457-464.
- [80] Tsyurupa, M.P.; Blinnikova, Z.K.; Davankov, V.A. Ion Size Exclusion Chromatography on Hypercrosslinked Polystyrene as a Green Technology in Separating Mineral Electrolytes, in "Green Chromatographic Techniques", eds. Imannudin, Ali Mohammad, Springer, 2014, 19-54.
- [81] Tsyurupa, M.P.; Blinnikova, Z.K.; Pavlova, L.A.; Davankov, V.A. *IEX2008, Recent Advances in Ion Exchange Theory & Practice*, Ed. M. Cox, SCI, Cambridge, 2008, 77-83.
- [82] Brady, J.A.; Winchester, J.F.; Davankov, V.A.; Tsyurupa, M.P.; Pavlova, L.A.; Noris, F.M. Patent USA 7,846,650. 2010.
- [83] Brady, J.A.; Winchester, J.F.; Davankov, V.A.; Tsyurupa, M.P.; Pavlova, L.A.; Noris, F.M.; Quartararo, Jr. P.J.; Salsberg, J.A. Patent USA 7,556,768. 2009.
- [84] Brady, J.A.; Winchester, J.F.; Davankov, V.; Tsyurupa M.; Pavlova L.; Quartararo Jr. P.J.; Salsberg, J.A. Patent USA 7,312,023. 2007.
- [85] Brady, J.A.; Winchester, J.F.; Davankov, V.A.; Tsyurupa, M.P.; Pavlova, L.A.; Quartararo, Jr. P.J.; Salsberg, J.A. Patent USA 6,878,127. 2005.
- [86] www.Sytosorbents.com.
- [87] Davankov, V.A., Tsyurupa M.P., Pavlova L.A., Tur D.R., Patent RF 2,089,283. 1997.
- [88] Malika, D.J.; Warwick, G.L.; Venturi, M.; Streat, M.; Hellgardt, K.; Hoenich, N.; Dale, J.A. *Biomaterials*, 2004, 25, 2933-2940.
- [89] Anisimova, N.Yu. Pathogenetic Reasons for Use of Extracorporeal Detoxification of Cancer Patients with Sepsis. *Dr. Sci. Thesis*, Moscow; 2012.
- [90] Anisimova, N.Yu.; Dolzhikova, Yu.I.; Davankov, V.A.; Pastukhov, A.V.; Miljaeva, S.I.; Senatov, F.S.; Kiselevsky, M.V. *Russian Journal of Biotherapy*, 2012, 11, 23-29.

-
- [91] Anisimova, N.Yu.; Davankov, V.A.; Budnik, M.I.; Donenko, F.V.; Tuguz, A.R.; Kiselevsky, M.V. *Vestnik of Adyghe State University (Russian)*, 2011, 76, 91–98.
- [92] Anisimova, N.Yu.; Davankov, V.A.; Korniyushenkov, E.A.; Mitin, V.V.; Solov'eva, O.V.; Budnik, M.I.; Donenko, F.V.; Kiselevsky, M.V. *Russian Veterinary Journal*, 2011, 2, 23–25.
- [93] Tsyurupa, M.P.; Blinnikova, Z.K.; Davankov, V.A. *Russian J. Phys. Chem.*, 2010, 84, 1767-1771.
- [94] Tsyurupa, M.P.; Tarabaeva, O.G.; Pastukhov, A.V.; Davankov, V.A. *Intern. J. Polym. Materials*. 2003,52, 403-414.
- [95] Tsuzuki, S. in “Intermolecular Forces and Clusters”, 1 ed. Mingos, D.M.P.; vol. ed. Wales, D.J., Springer, Berlin, 2005, 149-194.
- [96] Davankov, V.A.; Ilyin, M.M.; Timofeeva, G.I.; Tsyurupa, M.P.; Yaminsky, I.V. *J. Polymer. Sci., Part A: Polymer Chem.*, 37, 1999, 1451-1455.
- [97] Sychov, C.S.; Ilyin, M.M.; Davankov, V.A.; Sochilina, K.O. *J. Chromatogr. A*, 1030, 17-24, 2004.
- [98] Urban J.; Svec F.; Fréchet J.M.J. *J. Chromatogr. A*. 2010, 1217, 8212-8221.
- [99] Laatikainen, M.; Sainio, T.; Davankov, V.; Tsyurupa, M.; Blinnikova, Z.; Paatero, E. *J. Chromatogr. A*. 2007, 1149, 245-253.
- [100] Davankov, V.; Tsyurupa, M. *J. Chromatogr. A*. 2006, 1136, 118-122.
- [101] Tsyurupa, M.P.; Davankov, V.A. *Reactive Funct. Polym.*, 2002, 53, 193-203.
- [102] Davankov V.A. *Z. Physik. Chem.* 2014, in press.

Chapter 8

SYNTHESIS AND CHARACTERIZATION OF POLYSTYRENE BASED NANOCOMPOSITES

Vesna V. Vodnik^{1,}, Enis S. Džunuzović²
and Jasna V. Džunuzović³*

¹Vinča Institute of Nuclear Sciences, University of Belgrade, Belgrade, Serbia

²Faculty of Technology and Metallurgy, University of Belgrade, Belgrade, Serbia

³Institute of Chemistry, Technology and Metallurgy (ICTM)-Center of Chemistry,
University of Belgrade, Belgrade, Serbia

ABSTRACT

Polystyrene, one of the most important material in the modern plastic industry and one of the major synthetic polymer in use today, offers an extremely broad range of applications, due to its good physical properties and low-cost. Significant change of mechanical, rheological, thermal, optical, fire retardancy and barrier properties of polystyrene has been obtained by its combination with different nanoparticles. Due to the extremely high interface area between nanoparticles and polystyrene, some new properties could also be generated, which are often necessary to provide in order to meet current and future demands for various significant applications in different fields. In this review, recent advances on nanocomposites based on polystyrene and different kinds of nanoparticles will be presented through the results obtained by authors of this chapter and results given in other literature reports. This chapter reviews the current understanding of polystyrene based nanocomposites with three particular topics: (i) the preparation conditions of nanoparticles for their efficient, homogeneous incorporation in polystyrene matrix, (ii) different approaches for the synthesis of nanocomposites based on polystyrene and (iii) the influence of the type, size and shape of incorporated nanoparticles on the properties of the polystyrene based nanocomposites. The potential applications of these nanocomposites are also highlighted.

* Corresponding author. E-mail address: vodves@vinca.rs (Vesna V. Vodnik).

INTRODUCTION

Polystyrene (PS) is discovered in 1839 by Eduard Simon, and represents one of the oldest commercial polymers (prepared by BASF in 1931 and by Dow in 1938), while some of its properties were firstly analyzed by Staudinger [1]. After polyolefins and polyvinyl chloride, polystyrene is one of the most often used thermoplastic material today. Polystyrene homopolymer (or general purpose polystyrene) is relatively cheap, amorphous, aromatic, crystal clear, glassy polymer with good gloss, stiffness, hardness and processability. It softens at around 75 °C and is liquid at around 100 °C, and thus it is easy to form. However, general purpose PS, sometimes called crystal polystyrene, is at the same time quite brittle material, it has relatively low melting point, poor chemical resistance, rather poor barrier properties to oxygen and water vapor, weak impact resistance, poor scratch resistance, low flexibility, electrostatic build-up, etc., which considerably limits its use in high-performance and engineering products. In order to overcome the mentioned disadvantages, polystyrene was modified and today its copolymers and blends represent one of the most versatile polymer materials. For example, the rubber toughening of PS led to the development of high-impact polystyrene (HIPS), which shows improved impact resistance and barrier properties, but reduced transparency. The presence of rubber provides flexibility and lowers the softening point, allowing easy thermoforming of HIPS. Furthermore, copolymerization of styrene with maleic anhydride, improved thermal performances, while by copolymerization of styrene with acrylonitrile, styrene-acrylonitrile (SAN) copolymers or acrylonitrile-butadiene-styrene (ABS) and acrylonitrile-styrene-acrylate (ASA) copolymers were obtained, which have excellent chemical and scratch resistance and improved gas barrier properties. Styrene-acrylonitrile copolymers are the most important representative of this class of PS products. Furthermore, the use of metallocene polymerization catalyst technology allowed development of semi-crystalline syndiotactic polystyrene (SPS), which has completely different properties than conventional PS. Syndiotactic PS has relatively high melting point of 270 °C and consequently high heat resistance and also high crystallization rate, to enable processing by extrusion and injection molding. Besides mentioned, the wide family of styrenic polymers is also consisted of a number of modified variants of polystyrene, such as foamed PS with a cellular microstructure, branched PS, hydrogenated PS, super PS (styrene-diphenylethylene copolymers), ethylene-styrene copolymers, oriented polystyrene sheet, extruded polystyrene, etc.

Because of its quite interesting performance profile, PS can be ranked between specialty and commodity polymers. One of the key factors for huge commercial success and high market share of PS and PS products are the low cost of PS per unit of weight, excellent cost/performance ratio and its possibility to substitute more costly polymers. It is expected that PS market will reach 34 million tons by 2016 [2]. Polystyrene is mainly used in building and construction (around 70%), packaging (around 25%) and other applications (around 5%), such as in consumer electronics, devices, in medical applications, for the production of toys, for garden equipment, kitchen and bath accessories, etc. [3].

At the moment, nanotechnology is present in almost every aspect of science and technology, and polymer nanocomposites (PNCs) represent one of its most important components and driving forces. The main purpose of nanotechnology is the development of new and considerably better materials within the nano-size range, which was not possible to

achieve using traditional micro-size fillers at normal loading levels. Polymer nanocomposite retains the inherent properties of nanoparticles (NPs), while the polymer matrix provides higher stability and processability and some interesting improvements caused by the nanoparticle–polymer interaction, and this represents the main reason for such extraordinary interest in this innovative materials which show unique and tunable characteristics that cannot be achieved by traditional materials. In addition, the resulting hybrid materials can also show some original properties, which are not fully observable from the properties of each component, derived from the local arrangements or organization of the nano-sized objects in the polymer matrix. Significant multidisciplinary research efforts of PS based nanocomposites (NCs), dedicated to the design, preparation and properties investigation, has broaden the application of PS and introduced its NCs as industrially and commercially important materials. Therefore, these materials have received tremendous attention from different scientists over the past few decades.

POLYSTYRENE: SYNTHESIS, PROPERTIES AND APPLICATION

Synthesis of Polystyrene

Polystyrene is produced by polymerization of monomer – styrene, as it is shown in Figure 1. General purpose PS can be considered as a linear polyethylene chain, which has laterally attached phenyl groups. Isotactic PS, where all phenyl groups are on the same side, is isomer of PS which is not commercially produced. Namely, although isotactic PS is a semi-crystalline polymer with a melting point of around 240 °C, its crystallization rate is too slow to be used in injection molding. SPS, where phenyl groups are placed on alternating sides of the polymer chain, has much faster crystallization rate than that of isotactic PS. Atactic PS which has randomly distributed phenyl groups on the both sides of the hydrocarbon backbone and consequently no crystallinity, is the most commercially significant isomer of PS.

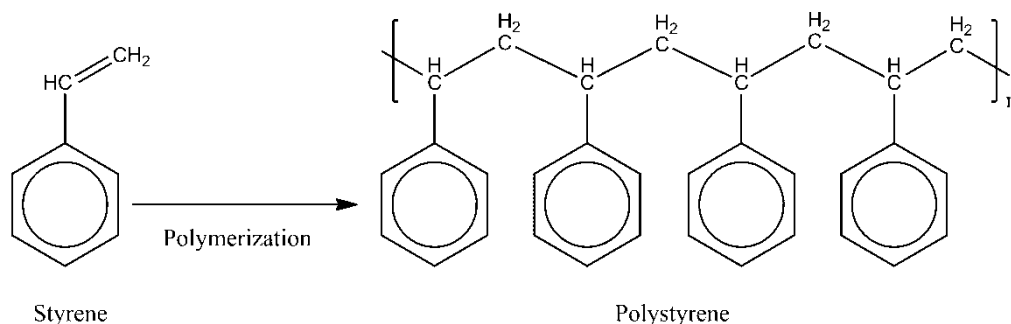


Figure 1. The reaction scheme for the synthesis of PS from monomer – styrene.

Because C-C double bond of styrene can act either as electron donating or as electron withdrawing center, the low polarity of the styrene and resonance stabilization of the growing polystyryl species in the transition state, synthesis of PS can be performed by free radical, anionic and cationic polymerization of styrene and using metal catalyzed conditions. Depending on the applied method for the synthesis, molecular structure of PS can be linear,

branched, star- and comb-like or dendritic. As an example, the mechanism of the free radical polymerization of styrene, using benzoyl peroxide as initiator, is presented in Figure 2 and Figure 3. Beside peroxides, other initiators, such as redox systems, azo components, etc. can be used to start the polymerization of styrene. Also, the reaction can be started thermally, without application of chemical initiator.

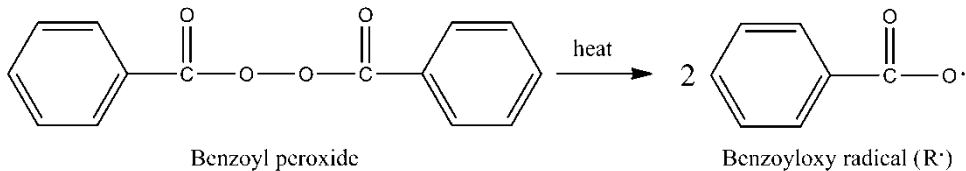
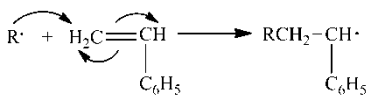
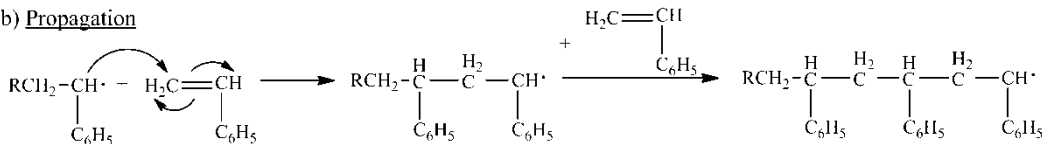


Figure 2. The reaction scheme for the formation of the radical initiator from benzoyl peroxide.

a) Initiation



b) Propagation



c) Termination

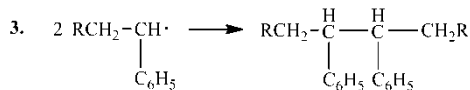
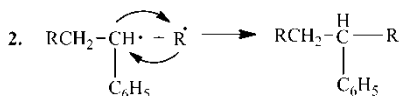


Figure 3. The reaction scheme for the free radical polymerization of styrene.

After formation of benzoyloxy radical (R•) from benzoyl peroxide, as shown in Figure 2, R• reacts with styrene and forms an active center (Figure 3a). In the propagation step, presented in Figure 3b, chain continues to grow until termination (Figure 3c). Besides termination, transfer reaction to other components of the polymerization reaction also occurs. Chain transfer agents can be the initiator, monomer, solvent, polymer or an added chemical agent. The transfer reactions have no effect on the polymerization rate, but can decrease the average molecular weight. By adequate use of transfer agent, such as mercaptanes, molecular weight of PS can be controlled [4]. Generally, it is very hard to control molecular weight, molecular weight distribution and molecular structure of the PS synthesized using free radical polymerization process. These disadvantages of radical polymerization reactions can be overcome by applying the substances called iniferters (*initiator-transfer agent-termination*), which act as initiators, transfer agents and termination agents. Iniferters react with growing

macromolecular radicals and form temporarily hidden species, minimizing in this manner termination by recombination and disproportionation [5,6]. Also, the presence of iniferters increases the concentration of reactive polymer chains in comparison to the concentration of free radicals, which lowers polymerization rate.

Free-radical PS can be prepared either by bulk, solution, suspension or emulsion technique. For the synthesis of PS by bulk process, pure styrene must be applied and as a result polymer with high clarity is obtained. Due to its poor control, this process is not used commercially. For the solution polymerization, styrene is dissolved in adequate solvent, which makes temperature control easier. However, the presence of solvents reduces molecular weight and polymerization rate. Both processes can be carried out in batch or continuously. The advantages of these kinds of PS synthesis are production of more uniform product and low volatile levels. In suspension polymerization, the polymerization system is composed of monomer suspended in water, stabilizing agents and initiators to speed polymerization. The advantages of suspension polymerization are easy heat control and removal of the final product. In emulsion polymerization water is used as carrier with emulsifying agents. This type of polymerization technique produces extremely small particles and it is usually used for the production of ABS copolymers [4].

Today the majority of general purpose PS is prepared using solution polymerization of styrene in a continuous process with heat removal by evaporation of styrene and solvent. Due to the consistent temperature, high product quality can be obtained with a narrow molecular weight distribution ($M_w/M_n = 2.2 - 2.4$) and high transparency. Depending of the synthetic procedure, three grades of general purpose PS are commercially produced: easy flow, medium flow and high heat. Easy and medium flow PS are used for injection molding, while high heat for the extrusion applications [7].

Properties of Polystyrene

Besides already mentioned properties, PS is appreciated for fair dimensional stability, fair density, versatility of processing methods, possibilities of food contact for specific grades, etc. General purpose PS is atactic and cannot crystallize. The presence of phenyl groups is responsible for the relatively high glass transition temperature (T_g) and high refractive index value (about 1.57 to 1.6). Besides, phenyl groups present in the polymer structure resist rotation of the chain and their effect makes the polymer stiff and brittle. Polystyrene has density of 1.05 g/cm^3 , which is higher than density of polyethylene and polypropylene. Because PS is amorphous, it does not have a sharp melting point. This is observed in gradual softening of the material over a wide range of temperatures. The T_g of the PS is between $74 \text{ }^\circ\text{C}$ and $105 \text{ }^\circ\text{C}$, and below its T_g PS is hard and brittle. Polystyrene softens at relatively low temperatures and it flows like a liquid at $100 \text{ }^\circ\text{C}$ or under stress, making it easy to thermoform or extrude. Service temperatures can be lower under stress because of modulus decay, creep, strain, relaxation, etc. Properties such as elongation at break and impact strength are especially heat sensitive. The mechanical properties of PS are generally fair and are characterized by low elongations at break and a brittle behavior at room temperature. General purpose PS is naturally highly transparent and due to that, certain grades are especially designed for adequate optical applications. Light transmission range from 80% up to 98% and haze can be as low as 0.65 [8]. Polystyrene has poor moisture barrier characteristics and is a

poor gas barrier. It is resistant to strong acids (except strong oxidizing acids) and alkalis, bases, vegetable oils, alcohols, aliphatic amines, beverages, condiments and various foodstuffs, polyglycols and numerous pharmaceuticals and is insoluble in aliphatic hydrocarbons and the lower alcohols, but it is soluble in esters, aromatic and aliphatic hydrocarbons, higher alcohols, aldehydes, aromatic amines, ethers, polyglycol ethers, ketones, chlorinated hydrocarbons insecticides, essential oils. Polystyrene resists hydrolysis well. Polystyrenes show good behavior under high-energy radiation, while fire resistance of PS is naturally weak and PS burns easily generating flames, even after the ignition source is removed. Even in a wet environment PS is good insulator and have high dielectric resistivity, fair rigidity and low loss factor.

Application of Polystyrene

As already mentioned, PS is used in packaging, appliances, in furniture industry, in refrigerators, for the production of toys, etc. ABS and SAN copolymers are mostly used in different sectors, such as: automotive and transportation, appliance, medicine, for the production of furniture, to build recreational vehicles, boats and others, etc. The consumption of expandable PS is 15–30% of the PS total. Polystyrene foam is usually used as an insulating material for heat-sensitive products, in packaging, and as a cushioning agent. Polystyrene is also quite often used as polymer matrix for the preparation of polymer based NCs.

POLYSTYRENE BASED NANOCOMPOSITES

General Consideration

Polymer based NCs represent a class of specific, multicomponent materials which are composed of a polymer matrix (thermoplastics, thermosets or elastomers) filled with small quantities of inorganic/organic nanoscale particles (nanoparticles), that show significant and unique influence on the macroscopic properties of the polymer matrix and are capable of interacting with polymer matrix at the molecular level [9,10]. Organic matrix, i.e. polymer forms a basis of the PNC, while NPs, such as clay, carbon-based NPs, metal NPs (gold (Au), silver (Ag), copper (Cu), aluminum (Al), nickel (Ni), cobalt (Co), iron (Fe)), metal oxides (titanium dioxide (TiO₂), zinc oxide (ZnO), magnetite (Fe₃O₄), hematite (Fe₂O₃), aluminum oxide (Al₂O₃), etc.), silicon dioxide or silica (SiO₂), and semiconductor NPs (cadmium sulfide (CdS), zinc sulfide (ZnS), lead sulfide (PbS), copper(I) sulfide (Cu₂S), cadmium selenide (CdSe), etc.) are dispersed in the polymer matrix. In the original definition of nanotechnology, NPs were considered to have the size range between 1 and 100 nm. However, it has been shown that particles larger than 50 nm show no significant improvement of the material properties as expected. The NPs can be zero-dimensional (such as fullerenes), one-dimensional (such as fibers and nanotubes), two-dimensional (such as graphene and layered minerals like clay), or three-dimensional (such as graphite and spherical particles). In all these cases, NPs are preferable to micron-sized ones due to their unique attributes [11]. Because of their high surface area-to-volume ratios, i.e. high aspect ratios, NPs show physical

and chemical properties distinctly different from their bulk materials and micro- and macro-additives [12]. In addition, the surface interactions of NPs with their environments become more and more important with decreasing particle size [13]. The disadvantages of micron-sized particles are: greater difficulty in their dispersing and appearance of sedimentation issues because of their larger densities and sizes, light scattering problem which is strongly size-dependent and can be completely avoided if NPs are used, etc. [14].

The main task during the preparation of PNCs is the prevention of aggregation of the NPs and formation of large-size agglomerates or undesirable assemblies, which can occur due to the high interfacial reactivity of NPs and their high surface tension energy. Agglomeration (aggregation) of NPs can occur in the initial reaction medium, such as solvent, or during the polymerization process. Besides, most polymers are hydrophobic, while surface of NPs is usually hydrophilic, leading to the incompatibility of the NPs with the polymer, absence of the uniform distribution through the polymer matrix, aggregation and extended phase separation between the NPs and polymer matrix. Because of that, PNCs will not show expected improvement of properties. Therefore, the manipulation with NPs in such way to prevent aggregation of NPs before, during and after dispersion or to achieve deagglomeration, efficient stabilization and uniform distribution of NPs in polymer matrix is essential in polymer nanotechnology. Methods which are usually used to improve dispersion of NPs and their compatibility with polymer matrix are: high-energy mechanical milling, application of ultrasonic treatment, treatment of NPs with surfactants (physical method), surface modification of NPs using adequate modifiers (chemical method), encapsulation of NPs by polymers, etc. [15]. The application of high-energy mechanical milling and ultrasound in most cases is not enough to achieve better dispersion of NPs in polymer matrix, since after elimination of ultrasonic treatment NPs are prone to agglomeration and sedimentation, depending on the viscosity of the medium. Besides, these methods do not completely break apart formed agglomerates. According to the literature, uniform distribution of NPs in polymer can occur after adequate treatment of the particle surface, i.e. its modification [16-20]. The application of surfactant molecules for the surface modification of NPs has proven to be quite efficient in preventing agglomeration [19,21]. Surfactant molecules contain one or more polar groups, such as OH, NH₂, NR₃⁺, COOH, COO⁻, SO₃H, SO₃⁻ and PO₄²⁻, and the aliphatic chain. During the surface modification of NPs, polar groups are adsorbed on the surface of NPs, where they form labile physical links with NPs, introducing in this manner hydrophobicity to the NPs and significant reduction of interface surface tension [15]. In contrast to the physical method, the chemical method of NPs surface modification is considered to be more efficient, due to the presence of chemical reactions [22]. The surface modification of NPs can be performed using monomer units, initiators, amphiphilic copolymers containing reactive functional groups, etc. The improvement of the NPs dispersion can also be obtained by their encapsulation in the protective shells of film-forming polymer, which acts as stabilizing agent [23].

Preparation of PNCs can be performed using various techniques which can be divided into two main categories: *ex situ* methods or direct compounding [24-30] and *in situ* methods [16-19,31-39]. In the *ex situ* methods NPs and polymer are prepared separately at first and then mixed in a solution or in melt or by application of mechanical forces. These methods are simple and give opportunity to the commercially available fillers to be used for the preparation of PNCs. However, issues considering aggregation, phase separation and limited dispersion of the NPs in the polymer matrix need to be overcome. The dispersion of NPs in

the polymer matrix depends on the processing conditions (temperature, time, shear force and configuration of the reactor), but this can be improved by application of complementary methods, such as functionalization of particles or the polymer matrix or both or by addition of appropriate dispersants or compatibilizers. On the other hand, *in situ* methods enable easier control of the dispersion of NPs and result in a more well-defined structure of PNCs. According to the different starting materials and fabrication processes, *in situ* methods can be divided into three approaches:

1. Nanoparticle precursors are preloaded into polymer matrix, where they are supposed to distribute uniformly. Then, the precursors are exposed to the adequate conditions necessary for the *in situ* synthesis of the target NPs [31].
2. In the second approach, monomers or prepolymers and the target NPs are used as the starting materials [34]. Nanoparticles are firstly dispersed into the monomers or prepolymers, and then the mixture is polymerized under desirable conditions. Using this method, NCs with tailored physical properties can be prepared.
3. The third approach is based on the simultaneous preparation of NPs and polymers by blending the precursors of NPs and the monomers with an initiator in proper solvent, and by subsequent polymerization of monomers [37].

Some other techniques can also be applied for the preparation of PNCs, such as phase separation, template synthesis, electro-spinning, self-assembly, etc.

The combination of NPs with polymers is known to have strong synergistic effects [40,41]. Properties of PNCs depend on the type of polymer matrix, type of NPs, their shape, size and concentration, and intensity of interfacial interactions between the polymer matrix and NPs. The choice of the polymer matrix usually depends on polymer mechanical and thermal behavior, hydrophobic/hydrophilic balance, chemical stability, bio-compatibility, optical and/or electronic properties and chemical functionalities (i.e. solvation, templating effect, wettability, etc.). It has been shown that even at extremely low loadings of the NPs into monomers and polymer matrices, significant change of the polymer matrix properties, such as mechanical, chemical, barrier, thermal, electro-physical, magnetic, optical, catalytic, and other can be observed [28-30,42-44]. Also, introduction of certain type of NPs, such as Ag, Au, and TiO₂ can induce or improve antimicrobial efficiency of polymer matrix [45-51]. One of the most interesting properties of polymers which can be influenced by the presence of NPs is the glass transition temperature, T_g , since changes in T_g are correlated with changes in polymer chains dynamics and chain relaxation behavior. Value of T_g depends on the nature and the molecular weight of the polymer, content of the NPs, thermal history of the NC, interparticle distances and mostly on the polymer–nanoparticle interface properties, i.e. on the interfacial interaction between the polymer matrix and NPs. This interaction can be attractive (leading to the reduction of dynamics of polymer chains and increase of T_g value) [16,25,26] or repulsive (leading to the acceleration of polymer chains dynamics and decrease of T_g value) [19,20,24,33]. If interfacial interactions between the polymer matrix and NPs are quite weak, then T_g value will not change, indicating that NPs have almost no impact on dynamics of polymer chains [17,18,32,38]. The presence of NPs can also improve [16,17,19,24,33,38] or reduce [26] thermal stability of polymer matrix, show certain [35,36,38,39] or no influence [16,17,33] on the molecular weight and polydispersity index of polymer matrix, change degree of crystallinity of polymer, [25] etc.

Polystyrene/Clay Nanocomposites

According to the very rich bibliography on polymer/clay NCs, nanoclays represent one of the most often used NPs for the preparation of polymer based NCs. This is due to the fact that clays are environmentally friendly, easily available and not expensive materials. Besides, nanoclays are composed of hundreds of layered nanometer scale platelets, which have high surface area (more than 750 m²/g) and high aspect ratio (100 to 500). Between the layers exists a regular van der Waals gap, called the interlayer or gallery. The layer surface of clays is composed of 0.25 - 0.9 negative charges per unit cell, while various types of exchangeable cations are present within the interlayer galleries. Between the layers and the intergallery cations strong electrostatic attractions exist. However, in order to take full advantage of high surface to volume ratio of clays, clay particles must be exfoliated as individual platelets and uniformly dispersed in polymer matrix.

Clay minerals can be divided into three major groups [52]:

- a) Kaolinite group (kaolinite, dickite, nacrite) with the general chemical formula: $\text{Al}_2\text{Si}_2\text{O}_5(\text{OH})_4$.
- b) Smectite group (montmorillonite, saponite, hectorite, vermiculate, talc, sauconite, and nontronite) with the general chemical formula: $(\text{Ca}, \text{Na}, \text{H})(\text{Al}, \text{Mg}, \text{Fe}, \text{Zn})_2(\text{Si}, \text{Al})_4\text{O}_{10}(\text{OH})_{2-x}\text{H}_2\text{O}$, where x represents the variable amount of water that members of this group contain.
- c) Mica-clay group (hydrated microscopic muscovites) with the general chemical formula: $(\text{K}, \text{H})\text{Al}_2(\text{Si}, \text{Al})_4\text{O}_{10}(\text{OH})_{2-x}\text{H}_2\text{O}$, and the structure similar to the smectite group.

Besides, clays can also be classified into two types: expanding (such as phyllosilicates and montmorillonite) and non-expanding (such as talc, mica, and kaolin) clays [53]. Among these, montmorillonite (MMT) is the most used layered silicate for the preparation of polymer/clay NCs. MMT has a sandwich structure with the top and bottom layers composed of tetrahedral structures of silica dioxide, while the center layer is composed of a metal oxide octahedral layer. Hydrated magnesium aluminum silicate platelets of MMT nanoclays are 1.45 nm thick and the lateral dimensions of layers can be 30-500 nm. The specific surface area of MMT is between 750 and 800 m²/g, while the modulus of each MMT sheet is around 178-220 GPa [54].

Depending on the affinity between clay and polymer, three different types of polymer/clay composites can be formed, as presented in Figure 4. If there is a poor affinity to the polymer, clay interlayer will not expand and only phase separated microcomposite (tactoid structure) will be formed. When moderate affinity between clay and polymer exists, then interlayer space of the clay gallery slightly expands, allowing polymer chains to penetrate into formed spacing of clay with a few nanometers of repeat distance, without changing shape of the layered platelets. In this manner intercalated structures are formed. Exfoliated structures are formed when layered platelets of clay are well separated into individual platelets and uniformly dispersed within the continuous polymer phase, due to the high affinity to the polymer. According to the literature, clay layer intercalation or exfoliation maximizes interfacial contact between the inorganic and organic phases and enhances bulk properties, such as mechanical, thermal, barrier, optical and fire retardancy of polymer

matrix. It has been shown that exfoliated systems generally show better properties than intercalated ones.

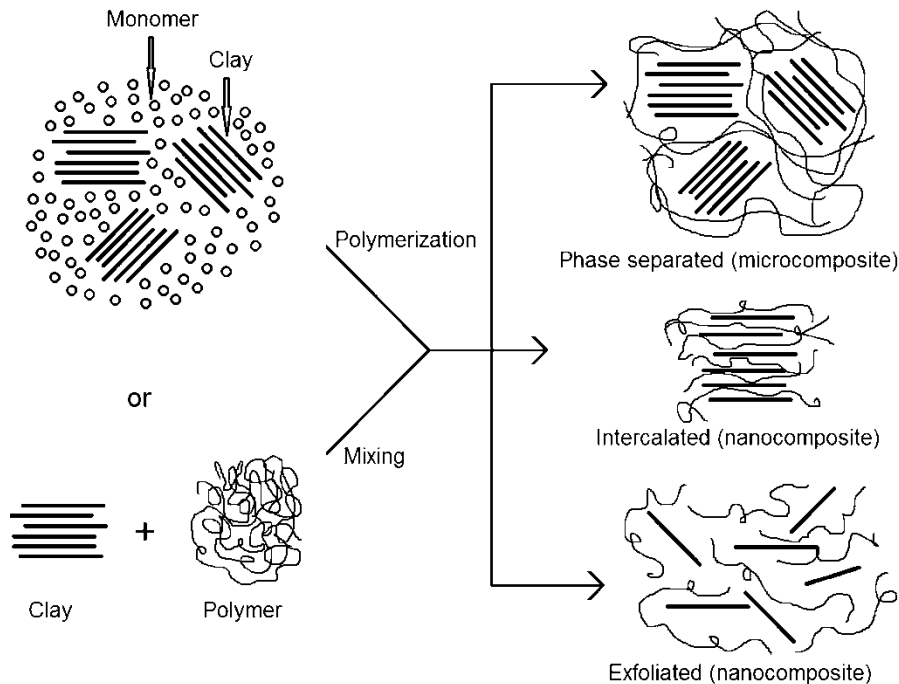


Figure 4. Different types of polymer/clay composites.

Modification of Clay

Exfoliation of clay particles can be achieved by application of high shear or by ultrasonic treatment in order to deaggregate platelet clusters. In addition, the compatibility of clay and polymer, their interactions and dispersion of clay platelets into polymer matrix can be improved by chemical modification of clay surface with adequate organo-modifier in order to make it more hydrophobic, since clays are hydrophilic. Without chemical modification of clay surface, pristine layered silicates are miscible only with hydrophilic polymers, such as poly(ethylene oxide) or poly(vinyl alcohol). In order to make clays miscible with other polymer matrices, such as PS, it is necessary to convert hydrophilic silicate surface to an organophilic one. The conversion of clays into organophilic can be performed by exchanging the cation present inside the clay galleries with the adequate cationic surfactants such as quaternary alkyl ammonium and alkyl phosphonium ions (ion-exchange reactions), which lower the surface energy of inorganic clay and consequently improve its wetting characteristics with polymer matrices [53]. Using these ion-exchange reactions, organophilic clay will be prepared, where alkyl ammonium or alkyl phosphonium cations are intercalated between the layers, while the interlayer height increases. The hydrophilicity-hydrophobicity and other clay properties can be adjusted by changing the type or length of alkyl chain or by adding some polar groups. The presence of alkyl chains increases the interlayer distance of the clay, allowing styrene to more easily approach into the clay layers. The attachment of other groups to the alkyl ammonium ions, such as aromatic, increases the interaction with the styrene monomer due to the similar nature of the organic groups. The conversion of clays into

organophilic can also be performed using silane grafting to the edge hydroxyl groups on the clay or between the clay layers on the clay surface. Such monofunctional silane modified montmorillonites were used to prepare PS based NCs, which showed intercalated morphology [55]. Different commercially available types of organophilic MMTs are today used for the preparation of polymer/clay NCs (different Cloisite® clays produced by Southern Clay Products, Inc. USA; clays produced by CO-OP Chemical Co., Ltd. Japan; clays produced by Nanocor Inc. USA, etc).

In some cases, the modification by conventional ammonium ions is not enough to achieve intercalation or exfoliation of clay interlayers by polymer. On the other hand, addition of reactive or polymerizable functionality has been often used to improve the clay dispersion in *in situ* prepared PS/clay NCs. The growing PS chain can polymerize from or through the reactive group present on the surfactant. Usually the reactive group has been based on styrene, although acrylic-based surfactants have also been used.

In order to achieve good dispersion of clay NPs in PS matrix and to obtain exfoliated morphology, it is necessary to take care about several important factors when choosing the adequate surfactant for clay [56]:

- the affinity of styrene monomer to swell the modified clays, which indicates the compatibility of monomer and clay,
- the presence of polymerizable group in a head position (adjacent to the ammonium ion and not at the end of the alkyl chain),
- the length of alkyl chain, since only chains longer than 12 C lead to the adequate swelling of the clay by styrene and formation of exfoliated structures [57],
- adequate solubility of surfactants in styrene in order to achieve complete swelling of the clay in the initial stages of the polymerization and
- sufficient concentration of surfactant used to exchange the clay.

Preparation Techniques for Polystyrene/clay Nanocomposites

In situ polymerization techniques are proved to be the best choice to produce well-dispersed PS/clay NCs. During the NCs formation, monomer penetrates into the intergallery space and then the polymerization reaction occurs between the clay layers, which are prerequisites for the formation of exfoliated structures. Besides possibility to choose an appropriate surfactant, *in situ* polymerization used to prepare PS/clay NCs can be performed using various techniques, i.e. cationic, anionic and free radical polymerization. Free radical polymerization is the most commonly used technique and it can be performed as bulk, solution, emulsion and dispersion free radical polymerization and as a controlled free radical polymerization techniques, such as atom transfer radical polymerization (ATRP), reverse addition-fragmentation transfer (RAFT) and nitroxide-mediated polymerization (NMP) of styrene.

Beside *in situ* polymerization, other two techniques can be applied for the synthesis of PS/clay NCs: solution casting and melt intercalation. The solution casting technique is based on a solvent system in which the polymer or prepolymer is soluble and the clay particles are swellable. During the solution casting, clay is first immersed into adequate solvent (water, chloroform or toluene) which penetrates into the clay galleries and expand them. Then, the polymer and clay solutions are mixed. Due to the lower viscosity, macromolecules easily

reach the surface of the platelets, and replace adsorbed solvent. After solvent removal, the intercalated structure remains, resulting in a polymer/clay NCs. During the melt intercalation, clay is mixed with polymer in the molten state using manual mixing, internal mixers or single- or double-screw extrusion. The dispersion of the clay into the polymer is achieved by application of shear and extrusion, while exfoliation of the clay is helped by high processing temperature (above the softening point of the polymer). Therefore, the selection of surfactant must be based on its thermal stability. Melt intercalation technique has certain advantages over solution casting, i.e. this technique is environmentally benign, due to the absence of organic solvents and it is compatible with current industrial processes, such as extrusion and injection molding.

Properties of Polystyrene/clay Nanocomposites

Mechanical Properties of PS/Clay NCs

Mechanical properties of PS/clay NCs considerably depend on the morphology of the synthesized NCs, as well as on the applied polymerization technique. It has been shown that desired and better improvements of mechanical properties can be obtained when PS/clay NCs have exfoliated structure. On the other hand, PS/clay NCs which have intercalated structures display a decrease in the tensile strength, which could be due to the formation of voids in the structure. The presence of voids weakens the interaction between clay and polymer, leading to the decrease of tensile strength and elongation. Uthirakumar et al., obtained 50% improvement of Young's modulus by addition of 5 wt.% of clay into PS by solution blending [58]. When PS/MMT NCs were prepared via bulk polymerization using a radical initiator that was exchanged onto the surface of MMT, than addition of 3 wt.% of modified clay led to the 45% improvement in tensile strength, improvements in Young's modulus by 25% and only a small decrease in the elongation at break [59]. Also, Zhu et al., have synthesized PS/MMT NCs by bulk polymerization using reactively modified clay [60]. They have observed improvements in tensile strength at break by 300% for exfoliated structures. Tseng et al., observed that addition of organically modified clay into PS by bulk polymerization improved flexural modulus and impact strength better than in the case where unmodified clay was used [61]. They have also showed that the flexural strength and modulus were significantly improved in comparison to the pure PS for exfoliated morphologies and less significantly for intercalated ones. Liu et al., obtained that addition of 5 wt.% of organoclay platelets into PS, using a melt intercalation approach, led to the 36% increase of flexural modulus, improvements in hardness by 32% and wear loss by 120%, while absorption of the impact energy was decreased by 21% [62]. The influence of different ammonium salt used for the modification of MMT on the mechanical properties of PS/MMT NCs was investigated by Arora et al. [63]. This group has used tetraethylammonium bromide (TEAB), tetrabutylammonium bromide (TBAB), and cetyltrimethylammonium bromide (CTAB) to prepare organoclay by cation exchange process. A significant improvement of the mechanical properties, such as tensile, flexural and Izod impact strength, of PS/clay NCs were observed, which followed the order as: PS/TBAB > PS/CTAB > PS/TEAB.

Rheological Properties of PS/Clay NCs

Since rheological properties of polymers considerably affect their processability, it is very important to investigate rheological behavior of the polymer after the addition of NPs. Dazhu et al., investigated PS/clay NCs prepared with organically modified clay and observed a decrease in flow behavior index along with increasing amount of organoclay [64]. Fu et al., obtained that storage modulus increase upon addition of MMT for PS/MMT obtained by bulk polymerization, while T_g decreased with increasing clay portion [65]. They have explained this behavior as an effect of the decreasing molecular weight as loading of MMT increased. Uthirakumar et al., observed that storage modulus increases with increasing concentration of MMT at all temperatures, while at temperatures close to the T_g storage modulus had the highest value [59]. This behavior was explained by the existence of the exfoliated structure of NCs. The increase of T_g with the increase of MMT concentration occurs because of the restriction of the polymer movements in the vicinity of the clay platelets and the exfoliated morphology indicates good dispersion of the clay platelets which could therefore affect a larger proportion of the polymer chains. The difference in the results of Fu et al., and Uthirakumar et al., is probably due to the different surface modification employed [65,59].

Thermal Properties of PS/Clay NCs

Inorganic clays are very stable at higher temperatures. For most clays the weight loss observed at 800 °C is only 5-7%, due to the presence of various forms of water molecules inside the clay layers. The organic treatment of clay surface reduces its thermal stability. However, it has been observed that generally, addition of organically modified clay NPs in small amounts into PS matrix enhances thermal stability of PS. Jang and Wilkie investigated the thermal degradation products of PS/MMT NCs and found that the degradation reactions of NCs were different in comparison to the pure PS [66]. Thermal degradation of pure PS occurs as chain scission followed by depolymerization (β - scission) through an intrachain reaction. On the other hand, thermal degradation of the prepared NCs was influenced by radical recombination reactions that took place in the intergallery spaces of the clay. The clay layers act as a barrier to heat and mass transfer, thus broadening the time of degradation and decreasing the peak degradation value. Samakande et al., observed that temperature at 10% of weight loss (T_{10}), obtained during thermogravimetric analysis (TGA) of PS/clay NCs, increased in comparison to the value obtained for the neat PS [67]. Also, according to the work done by Chiu and Su, the addition of organically modified MMT into the SPS enhances the thermal stability of polymer matrix, but at the same time inhibits the crystallization of SPS [68]. Wilkie et al., observed improvements in the onset temperature of the degradation up to 50 °C for the PS/MMT NCs in comparison to that of virgin PS [60]. The onset temperature was significantly increased even with as little as 0.1 wt.% of clay present in the NCs. They have also found that although alkyl phosphonium-modified clays had a higher thermal stability than reactively modified clay, the thermal stability of the resultant PS based NCs was higher for NCs based on reactively modified alkyl ammonium clay. They concluded that for thermal stability the final morphology of the prepared NCs was more important than the clay modification. Tang et al., investigated the thermal stability of PS/modified clay NCs, prepared by bulk co-polymerization, and observed that the thermal stability of the NCs prepared using coupling agent placed between the nanofillers and the PS matrix was better than for the pure polymer and those without coupling agents [69]. Uthirakumar et al., examined PS/MMT NCs prepared by bulk polymerization using a radical initiator attached to

the clay and observed that the thermal stability increased by increasing clay loading from 1 to 3 wt.% (exfoliated morphologies), but at 5 wt.% (intercalated morphology) there was no real increase in thermal stability [70]. This behavior was explained by existence of different morphologies of the obtained NCs and by the decrease of the molecular weight of the NCs containing higher levels of clay, which was attributed to the silicate platelets hindering the growth of polymer chains. On the other hand, Greesh et al., observed that PS/clay NCs, prepared via dispersion polymerization in polar medium using silane-functionalized montmorillonite NPs, show better thermal stability with intercalated structure (high clay loading) than with exfoliated structure (low clay loading) [71]. Alshabanat et al., have showed that different sonication time applied during the preparation of PS/organically modified MMT NCs has no significant influence on the thermal stability of the prepared NCs [72]. Greesh et al., investigated the influence of nanoclay shape on the thermal stability of PS/clay NCs, prepared by free radical emulsion polymerization, and obtained that when MMT (platelet-like structure) has been used at similar clay loading, thermal stability of NCs was better than for NCs prepared using attapulgite clay, which has a needle-like morphology [73]. The influence of different preparation techniques on the thermal stability of PS/clay NCs was investigated by Chigwada et al. [74]. They have observed that thermal stability of PS/modified clay NCs obtained by bulk polymerization was better than thermal stability of NCs obtained by melt blending technique. Giannakas et al., observed that better improvement in T_{10} and T_{50} values was obtained when NCs were prepared using CCl_4 solvent rather than CHCl_3 [75].

Using differential scanning calorimetry (DSC) Abate et al., detect T_g of PS/modified clay NCs, synthesized by bulk polymerization, and observed a small increase in the T_g and that the T_g increased as the alkyl chain length of the surfactant increased [76]. A larger increase in T_g value (5-13 °C) as the concentration of the clay increased was detected by Yeh et al., for PS/clay NCs, prepared by bulk polymerization [77]. However, these authors observed no relationship between the T_g and the morphology. The increase in T_g is usually ascribed to the restricted motion of PS chains located within or near the clay layers. Yang et al., observed that PS/clay NCs prepared via *in situ* emulsion polymerization using Na-MMT, and MMT modified with vinylbenzyl dimethyloctadecyl ammonium chloride (VC₁₈-MMT) and trimethyloctadecyl ammonium chloride (C₁₈-MMT) show different influence on the T_g , due to the different interaction between the polymer and clay layers [78]. They have found that T_g of PS/Na-MMT NCs with intercalated structure increased, while for the NCs with exfoliated structure the interactions between the polymer and the MMT layers become the key factor. Namely, the PS/VC₁₈-MMT NCs displayed higher T_g than the pure PS, while the T_g of PS/C₁₈-MMT NCs are slightly lower than that of PS.

Fire Retardant Properties of PS/Clay NCs

Generally, the addition of clay NPs into the polymer matrices has been known to improve flame retardancy in comparison to the pure polymers, which was explained by the formation of a carbonaceous - silicate char that control the flammability. During the degradation of polymer, the layered silicates can also act as an insulator and mass and energy transport barrier that slows the escape of generated volatile products. Zhu and Wilkie observed that the flame retardancy of the PS/MMT NCs was enhanced even when as little as 0.1% clay was added [79]. With increasing the fraction of clay, the amount of the char that can be formed increases, while the rate at which heat is released decreases [60]. It has been shown that various intercalated PS/clay NCs show reduced peak heat release rate (PHRR), less than

exfoliated NCs [80]. Chigwada et al., examined intercalated PS/MMT NCs prepared through bulk polymerization using MMT modified with quinolium and pyridinium surfactants, and obtained that clays reduced the PHRR by up to 50% at 7% clay loading, while the total heat release was not significantly decreased [81]. A decrease in the heat release rate is connected to the decrease in mass loss rate and decrease in the amount of energy released by the time that PS has ceased burning, as well as a certain increase in the time at which the peak heat release is achieved. The formation of a char barrier retains certain amount of PS, leading to the decrease of the released energy and the mass loss rate. It has been observed that the formation of NCs reduces production of smoke, but also increase of the clay content does not result in additional smoke reduction. Schutz et al., have discovered that both the aspect ratio of dispersed silicate layers and the preparation technique have significant influence on the fire retardant properties of PS/clay NCs [82]. Cai et al., observed that PS/clay NCs, prepared by melt blending using 3 and 5% of clay modified with one-chain benzimidazolium surfactant, exhibited substantial reduction of heat release rates [83].

Barrier Properties of PS/Clay NCs

It was shown that the presence of clay NPs in the PS matrix significantly improves polymer barrier properties, which is especially important in the applications such as packaging, where it is necessary to have adequate protection of food and drugs from the ingress of water vapor or oxygen. The permeability decrease is caused by the tortuous path toward the diffusing gas molecules. Nazarenko et al., have found that the permeability of oxygen decreases with increasing clay concentration and that exfoliated PS/MMT NCs exhibited lower permeability than microcomposites [84]. Arora et al., have found that PS/clay NC, prepared by melt blending using 2% tetrabutylammonium bromide modified MMT, show better oxygen barrier performance as compared to PS [63].

Polystyrene/Carbon Nanofillers Composites

The main advantages of carbon nanofillers are their excellent electrical and thermal conductivity properties. Carbon nanofillers can be divided according to their dimensionality into zero-dimensional fullerenes (buckyballs), one-dimensional carbon nanotubes and carbon nanofibers, two-dimensional graphene and three-dimensional graphite.

Polystyrene/Fullerene Nanocomposites

Fullerenes have spherical structure with C atoms arranged in the form of “closed-cage” hexagons or pentagons. They always have even number of C atoms and therefore have formula C_{2n} , where n is higher than 10. The most known fullerene is the spherical isomer of C_{60} , known as buckyball. The C_{60} molecule is composed of 20 hexagons and 12 pentagons with no two adjacent pentagons. The outer diameter of C_{60} molecule is 1.01 nm, while an average bond length is 0.144 nm. There are 1812 possible isomers of C_{60} , but only one is stable. The molecular weight of C_{60} is 720.66 g/mol, it appears as a stable black crystalline powder, melts above 280 °C and has a density of around 1.7 g/cm³. The C_{60} has a thermal conductivity of 0.4 W/mK and a resistivity of 1014 Ω/m. Fullerenes can be obtained by laser ablation of graphite.

Properties of Polystyrene/Fullerene Nanocomposites

Rheological Properties of PS/fullerene NCs

Tuteja et al., investigated the melt viscosity behavior of linear PS/C₆₀ NCs and obtained that at low shear frequencies the complex viscosity (η^*) of linear PS/C₆₀ NCs was higher than for pure PS when the weight average molecular weight (M_w) of linear PS was smaller than the critical molecular weight for the entanglement (M_c) of PS, and the η^* at low shear frequencies of linear PS/C₆₀ was lower than that of pure PS when the M_w of linear PS was larger than the M_c of PS [85]. However, Tan et al., obtained the opposite results for the six-arm star PS/C₆₀ NCs, i.e. when the molecular weight of the arm chain (M_a) of star PS was smaller than the M_c of PS, the η^* obtained at 0.05 rad/s of star PS/C₆₀ composites with a low content of C₆₀ was lower than that of pure star PS [86]. On the other hand, when M_a was larger than the M_c of PS, the η^* of the star PS/C₆₀ composites was higher than that of pure star PS. According to the Einstein–Batchelor law for the viscosity of a particle suspension, melt viscosity of polymer/nanoparticle composites is generally higher than that of the pure polymer, and with increasing volume fraction of NPs the monotonic increase of melt viscosity of the NCs occurs [87]. However, a reduction of the melt viscosity of the composites in comparison to the value obtained for pure polymer is found when adding small spherical NPs, such as fullerenes, to the entangled polymer matrix ($M_w > M_c$), such as PS, which have radius of gyration of polymer higher than radius of the NPs. Different explanations have been proposed for this behavior, such as dilution of the entanglement density of polymer chains, increase of excluded free volume induced around the NPs, constraint release of entangled polymer chains, etc. [85].

Thermal Properties of PS/Fullerene NCs

Fullerenes are considered as stabilizing agents for polymers, since they are radical scavengers. According to Wong et al., C₆₀ can be used to tune the properties of glass forming polymers [88]. Namely, they have used combination of calorimetry, incoherent neutron scattering and dielectric spectroscopy, and found that at concentration lower than 4%, C₆₀ hinder segmental motion of PS, leading to the increase of the T_g value, which corresponds to the increase of the fragility of glass formation.

Barrier Properties of PS/Fullerene NCs

Barnes et al., have prepared NCs from spun-cast PS films and C₆₀ NPs, and observed that up to the 1% of mass fraction of fullerene the immobilized C₆₀ particles form an enrichment layer at the solid boundary, leading to the suppression of dewetting [89].

Polystyrene/Carbon Nanotube Composites

Carbon nanotubes (CNTs) represent a thin hollow cylinders containing carbon and can be described as tubular derivatives of fullerenes or rolled-up graphene layers. Often, hemispherical caps of the buckyball structure seal both ends of the tube. CNTs can have several possible configurations, depending on how graphene layer is rolled up and properties of CNTs are strongly influenced by their configuration. For example, depending on the configuration of the CNTs, they can behave as either a metallic conductor or a semiconductor.

There are two types of CNT: single-wall nanotubes (SWCNTs) and multi-wall nanotubes (MWCNTs). SWCNTs are composed of single graphene layer and have diameter of 0.5-5 nm and lengths of the order of micrometer or centimeter. The main configurations of SWCNTs are armchair, zigzag and chiral, depending on the shape formed by adjacent C atoms in the cylinder. On the other hand, MWCNTs consist of a number of graphene layers coaxially rolled together, forming in this manner a cylindrical tube, with spacing between layers of around 0.34 nm and outer diameter of 3-10 nm. CNTs are considered as one-dimensional nanomaterials because of their very small diameter that confines electrons to move along their length. CNTs can be prepared by various techniques, such as growth in the arc discharge from a carbon electrode, by laser ablation of graphite and by chemical vapor deposition in which CNTs grow from the vapor on a metallic substrate of fine catalyst particles (iron, cobalt, nickel).

In the past twenty years CNTs have been extensively studied by researchers in various fields such as chemistry, physics, materials science, and electrical engineering, due to their high flexibility, low mass density, large aspect ratios (300-1000), large surface area (experimental: 150-1587 m²/g, theoretical: 3000 m²/g for SWCNTs), high Young's modulus of over 1 TPa, high tensile strength of over 200 GPa, the highest strength-to-weight ratio, thermal conductivity higher than 3000 W/mK, high corrosion resistance, high electrical conductivity ranging close to metallic conduction, etc. Armchair SWCNTs exhibit metallic conduction, while other CNTs behave as semiconductors. Because of these properties, CNTs are attractive nanofillers for the production of PS based NCs. PS/SWCNT NCs can be used mainly for electronic application, such as for device fabrication, for electromagnetic interference shielding, electrostatic protection, electrical contacts, etc. PS/MWCNT NCs has potential for radiation shielding due to its relatively high content of hydrogen. In order to achieve better interaction with polymers and to promote dispersion (especially in the case of MWCNTs) and to enhance interfacial adhesion with matrix it is required to apply physical and chemical surface modification of CNTs. Physical modification is performed using polymers such as PS and adequate surfactants to cover the outer surface of CNTs. Chemical modification can be performed by the use of surfactants, functionalization of end caps and by functionalization of sidewalls. For the production of polymer/CNT NCs, three different techniques are used: *in situ* polymerization, solution blending and melt compounding.

Properties of Polystyrene/Carbon Nanotube Composites

Mechanical and Rheological Properties of PS/CNT NCs

Nayak et al., have shown that PS/SWCNT NCs prepared by solution casting from tetrahydrofuran, using SWCNT with side walls functionalized with 4-vinylaniline, have higher values of the flexural modulus and tensile strength than PS/pure SWCNT NCs [90]. Using a surfactant assisted technique, Ayewah et al., have prepared PS/SWCNT NCs and investigated them with three-point bend test [91]. They have obtained that NC with 0.1 wt.% of SWCNT showed a decline in flexural strength and break strain, while the increase of the SWCNT content led to the improvement of flexural modulus, strength and break strain. In addition, prepared PS/SWCNT NCs had lower fracture toughness in comparison to the neat PS. The addition of 1 wt.% of MWCNTs to PS has been demonstrated to increase the elastic modulus by 42% and the stress at break by 25%, in comparison to the pure PS [92]. Choi and Ryu prepared SAN/MWCNT NCs by melt blending, by *in situ* ATRP and

SAN/functionalized MWCNT NC by *in situ* ATRP, and they have observed that SAN/functionalized MWCNT NC had improved mechanical properties due to the more uniform dispersion of functionalized MWCNT in SAN copolymer [93].

The rheological properties of PS/MWCNT NCs were investigated using a rotational rheometer with a parallel plate at a fixed temperature by Choi et al. [94]. Nanocomposites prepared without initiator (AIBN) showed increase of the η^* with increasing MWCNT portion in the low frequency region. The storage and loss modulus of PS/MWCNT NCs (with and without AIBN) increased with frequency and MWCNT loading. Srivastava et al., observed that PS/MWCNT NC with 6 wt.% MWCNT showed increase of storage modulus up to 122% at 80 °C, compared to PS [95]. Nanocomposite prepared from PS and 3 wt.% of ozone-treated MWCNTs has up to two orders of magnitude higher storage and loss modulus than PS [96]. Jia et al., investigated viscoelastic behavior of PS/MWCNT NCs during short-term creep and recovery under tensile cyclic loading and obtained that the creep strain of PS decreases with increasing MWCNTs content, with decreasing temperature and stress and with increasing cycle number [97]. This was explained by the network formation of molecule chains and MWCNT, which besides reduction of the creep strain induced the increase of the recovery ratio and the restriction of molecule chains mobility.

Thermal Properties of PS/CNT NCs

The presence of CNTs in PNCs leads to the enhancement of the thermal stability, which can be explained by the physical adsorption of the polymer molecules on the CNT surfaces or by the absorption of free radicals generated during polymer decomposition by the activated carbon surface [98]. Also, CNTs can restrict the mobility of polymer molecules and similar to other layered nanofillers, they can hinder the diffusion of the degradation products from the bulk of the polymer into the gas phase, which is especially pronounced in an inert atmosphere [99]. The incorporation of up to 2 wt.% MWCNT into PS using twin-screw extruder increased maximum temperature of PS degradation from 365 to 407 °C, as shown by Sathyanarayana et al. [100]. Bellayer et al., observed that the application of imidazolium-modified MWCNTs for the preparation of PS/MWCNT NCs increased thermal stability of PS for 20 °C, according to the TGA measurements [101].

The influence of SWCNTs on the T_g values of PS/SWCNT NCs in the bulk and in the thin films was investigated by Pham et al., using DSC and spectroscopic ellipsometry [102]. They observed that T_g value of NCs in the bulk increased by around 3 °C, while for the NC films thinner than 45 nm, T_g decreased with decreasing film thickness. Polystyrene grafting from the surface of carbon nanotubes has been proved to be effective way to produce PS/SWCNT NCs, having T_g higher than that of the pure PS [103]. Awad et al., have shown that addition of SWCNT or PS-grafted SWCNT into PS matrix leads to the increase of T_g value [104]. Furthermore, the increase of the MWCNT concentration led to significant increase of T_g value of PS/MWCNT NCs, as obtained by Srivastava et al. [95]. On the other hand, Sorrentino et al., performed the dynamic mechanical and DSC analysis of SPS/MWCNT NCs, prepared in twin-screw extruder, and obtained that T_g of these NCs is lower than for the neat SPS [105].

Electrical Properties of PS/CNT NCs

In order to achieve a conductive path through the polymer it is necessary to have three-dimensional network of conductive filler NPs, which is known as percolation. The percolation

threshold can be defined as the filler loading at which the electrical resistance of the NC sharply drops. According to the literature, the percolation threshold strongly depends on the particle shape, and the lower percolation threshold is obtained for the NPs with the higher aspect ratio. Because of their wide range of application, PS based NCs with high electrical conductivity are of great interest. Neat PS is an insulated material which has conductivity of around 1×10^{-12} S/cm. On the other hand, the addition of CNT to the PS drastically increases electrical conductivity of the PS/CNT NCs in comparison to the neat PS. High electrical conductivity and low percolation threshold of PS/SWCNT (with cellular structure) NCs, obtained by coating PS pellets with SWCNTs and then by hot pressing to get cellular structure of SWCNT, was obtained by Mu et al. [106]. According to the Ayewah et al., PS/SWCNT NCs showed electrical percolation occurring at 0.2 wt.% of SWCNT content, while prepared NCs were fully conductive at 1.0 wt.% [91]. Chang et al., have showed that initial thermal annealing of SWNT significantly improves their dispersion in PS and obtained NCs showed higher electrical conductivity and lower percolation threshold (lower than 0.3 wt.%) than the raw PS/SWCNT NCs [107]. Also, Cipriano et al., have showed that electrical conductivity of PS/MWCNT NCs decreased due to the applied processing (by twin-screw extrusion and compression molding), but this property can be recovered by annealing the NCs at high temperatures [108]. Surfactant removed NCs, prepared using monodispersed PS microspheres and SWCNT networks by compression molding, had drastic increase in the electrical conductivity with 0.8 wt.% of SWCNT, indicating that the percolation threshold for the formation of conductive SWCNT network in PS matrix is achieved [109]. PS/MWCNT prepared by mixing aqueous suspension of exfoliated MWCNTs and a PS latex (both stabilized with an anionic surfactant), followed by freeze drying and compression molding, showed low percolation threshold and high electrical conductivity above this threshold [110]. A low percolation threshold, less than 1.0 wt.% MWCNTs loading, is observed for PS/MWCNT NCs, prepared by *in-situ* bulk polymerization under the application of ultrasonication without any added initiator [111]. During the synthesis of these NCs, acid-treated MWCNTs were dispersed in styrene using ultrasound, and radicals generated after decomposition of monomer were used to initiate the polymerization. Also these authors have observed rapid increase in electrical conductivity of PS/MWCNT NCs when MWCNT content exceeds 0.5%. Ayesh et al., have observed that PS/ozone-treated MWCNT NCs have percolation threshold around 0.8 wt.% MWCNT, electrical conductivity up to six orders of magnitude higher than for PS, and that with increasing MWCNT content the relative dielectric permittivity, dielectric loss and loss tangent also increased [96]. According to the McClory et al., the addition of MWCNTs into HIPS increased electrical conductivity of HIPS by 12 orders of magnitude, while the electrical percolation increased with increasing screw speed during melt mixing of HIPS and MWCNTs [112]. Singh et al., obtained that ABS/MWCNT NCs prepared by melt blending of ABS and *in situ* polymerized PS/MWCNT NCs have electrical conductivity of around 1.27×10^{-6} S/cm with 0.64 wt.% MWCNTs content, which is quite lower than value obtained for the ABS/MWCNT NCs prepared by solution blending [113].

Polystyrene/Carbon Nanofibers Composites

Carbon Nanofibers (CNFs) are composed of concentric cylindrical layers of carbon, similar to MWCNT but with a length dependent diameter (few sub-micrometers to over 5 μ m). CNFs have morphology similar to a stack of cones or to a paper scroll. CNFs have

good thermal and electrical conductivity, excellent mechanical properties, high aspect ratio (up to 1000) and low cost. Carbon nanofibers are usually synthesized by chemical vapor deposition method. PS/CNF NCs can be used as an effective and practical electromagnetic interference shielding material.

Properties of Polystyrene/Carbon Nanofibers Composites

Mechanical and Rheological Properties of PS/CNF NCs

Shen et al., prepared PS/CNF NC foams, using batch and continuous extrusion process and CO₂ as blowing agent, and observed that CNFs served both as nucleants and the reinforcing agent for the PS foams [114]. Presence of CNFs in PS increased cell densities and decreased cell sizes, significantly enhanced mechanical properties (tensile and compressive) of PS foam and led to the 50% weight reduction of foam, compared to the bulk PS (for 5 wt.% CNF loading). The reinforcement of PS foam by the addition of CNFs was explained by the alignment of CNFs along the cell walls and the existence of absorbed PS layers around the fiber surface. Valle et al., observed that plasma treated CNFs can increase tensile modulus of PS/CNF NCs more than untreated CNFs [115].

Melt share rheological properties of PS/CNF NCs, prepared by solvent casting and melt blending, were investigated by Wang et al. [116]. PS/CNF NCs prepared by melt blending had uniformly dispersed CNFs, but the length of CNFs was about one-fourth of the original CNFs. On the other hand, in PS/CNF NCs prepared by solvent casting technique the dispersion of CNFs was not as uniform as for the NCs prepared by melt blending, but the length of CNFs was maintained. Authors have observed that storage and loss modulus and steady-state viscosity of both PS/CNF NCs increased with CNFs loading.

Thermal Properties of PS/CNF NCs

Xu et al., have observed that the presence of CNFs in PS matrix increased the onset and end thermooxidative decomposition temperature by approximately 60 °C, but has no influence on the T_g value of the NCs prepared by heterocoagulation technique [117].

Electrical Properties of PS/CNF NCs

Xu et al., obtained that PS/CNF NCs had the percolation threshold below 2 wt.% after molding NCs at 185 °C under a pressure of 25 MPa for 20 min [117]. Tjong et al., compared electrical properties of low density polyethylene/CNF, high density polyethylene/CNF and PS/CNF NCs and obtained that PS/CNF NCs exhibited the lowest percolation threshold due to the more uniform dispersion of CNFs in PS matrix [118].

Polystyrene/Graphene Nanocomposites

Graphene is obtained from inexpensive, environmentally friendly and chemically inert graphite, which is composed of regularly stacked, one-atom thick two-dimensional graphene layers. Small amount of graphene sheets can be obtained by graphite abrasion, for example by drawing a line with a pencil. Graphene represents a planar allotrope of carbon, where all carbon atoms (sp^2 -hybridized) form covalent bonds in a single plane, i.e. they are arranged in a six-numbered-ring plane (honeycomb structure). It has nanoscale dimensions and high specific surface area of 2600 m²/g, and unique chemical, physical and electrical properties

[119]. Graphene has very high electrical conductivity up to 6000 S/cm, good thermal conductivity (5000 W/mK), high thermal stability, high ultimate (intrinsic) strength of 130 GPa, etc.

Novoselov et al., were the first who obtained graphene using micromechanical exfoliation or peel-off method, which was performed by peeling off graphite on a piece of Scotch (adhesive) tape and transferring it to a stable SiO₂ substrate [120]. Methods which are usually used for the graphene production can be divided into:

- bottom-up processes, which include chemical vapor deposition, arc-discharge, epitaxial growth of graphene films on silicon carbide, chemical conversion, reduction of CO, unzipping of CNT, and self-assembly of surfactants, and
- top-down processes, which are based on the separation/exfoliation of graphite or graphite derivatives (such as graphite oxide and graphite fluoride) and production of, for example graphene oxide, which can be converted into graphene by chemical reduction. Analogous to graphite which is composed of stacks of graphene sheets, graphite oxide contains graphene oxide sheets stacked with an interlayer distance between 0.6 and 1.0 nm, depending on the water content [121].

The top-down processes generally provide routes to obtain larger amount of graphene, necessary to have for the production of PNCs. Also, interactions between graphene and polymer can be improved by functionalization, i.e. surface modification of graphene sheets. In this manner, the dispersion of the nanosheets, interactions between graphene and polymer, as well as mechanical properties of the prepared NC will be improved.

Because of very high aspect ratio, only small amount of graphene is sufficient to achieve percolation and network formation in a polymer matrix and to improve property profile of polymer, including electrical conductivity, barrier and electrooptical properties, fire retardancy, abrasion resistance, stiffness, etc. Due to that, graphene is today considered as very attractive alternative to the quite expensive CNTs. Three conventional techniques are usually used to prepare polymer/graphene NCs: *in situ* polymerization, solution blending and melt compounding. During the *in situ* polymerization technique, the intercalation of monomers into graphene interplanar spacing occurs, followed by the polymerization process. In the solution blending graphene dispersion in the polymers is carried out in a solvent medium and after solvent elimination, melt compounding usually follows. The disadvantage of this technique is large amounts of solvent and the high temperatures required to dissolve the polymer during the process. Melt compounding is performed with a twin-screw extruder, injection molding, twin-roller, or internal mixer under high shear conditions.

Properties of Polystyrene/Graphene Nanocomposites

Mechanical and Rheological Properties of PS/Graphene NCs

According to the different authors, the addition of graphene into the PS significantly improves PS mechanical properties. Ren et al., prepared PS/graphene NCs by *in situ* reduction of phenyl isocyanate functionalized graphite oxide in *N,N*-dimethylformamide in the presence of PS, and obtained that NCs containing only 0.5 wt.% of graphite oxide showed 28.4% increase in the Young's modulus and a 27.8% enhancement in the tensile strength,

which was the consequence of the excellent modulus, large lateral thickness ratio and high orientation of the graphene sheets [122]. The addition of 0.9 wt.% of covalently polymer modified graphene nanosheets to PS, led to the increase of 57% and 70% in Young's modulus and tensile strength, respectively, and in a 15 °C increase of T_g [123]. The addition of 1.94 vol.% of chemically converted graphene to the PS, by solution blending followed by compression molding, increased the storage modulus of the prepared NC in the glassy region by 28% [124]. Li et al., reported a facile approach for the production of PS/graphene NCs without application of surfactants and ultrasonic power, which included mixing of aqueous dispersion of graphene oxide with PS latex, their co-coagulation with sodium chloride to form stabilized particle suspension and *in situ* reduction of graphene oxide with hydrazine hydrate [125]. These PS/graphene NCs had greatly improved dynamic mechanical properties than pure PS. Basu et al., reported that storage modulus and relaxation time of PS/graphene NCs is higher than for the pure PS, and that loss modulus and η^* increase with increasing weight percentage of graphene [126].

Thermal Properties of PS/graphene NCs

Polystyrene/graphene NCs show improved thermal stability in comparison to the pure PS. According to the Li et al., the peak temperature of differential thermogravimetric analysis (DTG) curves is increased by 10 °C for PS/graphene nanosheets NCs in comparison to the pure PS [127]. The addition of 0.19 vol.% of chemically converted graphene to the PS increased the onset of decomposition temperature of the prepared NC by approximately 60 °C [124]. Ren et al., reported that incorporation of highly oriented graphene into the PS increased T_g and onset degradation temperature of PS from 96.6 and 427 to 103.2 and 439 °C, respectively [122].

Electrical Properties of PS/Graphene NCs

The electrical conductivity of PS can be greatly increased by incorporation of graphene, since graphene layers can provide percolated pathways for the electron transfer, especially if they are aligned parallel. Furthermore, the formation of three-dimensional compactly interconnected graphene network induces large increase of the electrical conductivity of PS NCs. Pham et al., observed that NC of PS and chemically converted graphene exhibited a percolation threshold as low as 0.19 vol.%, while NCs showed electrical conductivity of 72.18 S/m at 2.45 vol.% loading [124]. Zhang et al., reported that NCs based on PS and graphene sheets, obtained by γ -ray induced reduction of a graphene oxide suspension in *N,N*-dimethylformamide at room temperature, have a low percolation threshold of 0.24 vol.% and a high electrical conductivity of 45 S/m with only 2.3 vol.% graphene loading due to its uniform dispersion in PS matrix [128]. Qi et al., prepared PS/graphene NCs by solution mixing followed by compression molding and observed that conductivity of PS increases to ~3.49 S/m by increasing graphene content from ~0.11 to ~1.1 vol.%, which is of 2-4 orders of magnitude higher than for the PS/MWCNT NCs [129]. These authors have also concluded that the decrease of the percolation threshold of PS upon addition of graphene occurs due to the selective localization of graphene into the PS-rich regions. Using a self-assembly process Wu et al., have prepared highly conductive (1083.3 S/m) PS NC with 4.8 vol.% of graphene, which formed three-dimensional compactly interconnected network [130]. The electrical conductivity of the prepared NCs was greater than that of the PS/graphene NCs synthesized by solvent mixing method. Using latex-based technology for the NC formation, Tkalya et al.,

have prepared PS/graphene NCs which showed high conductivity of about 15 S/m by addition of 1.6-2 wt.% of graphene in PS [131]. PS/graphene NCs, prepared by Li et al., by latex mixing, co-coagulation and reduction of graphene oxide with hydrazine hydrate, exhibited electrical conductivity of 11 orders of magnitude higher than that of the pure PS at 8.0 wt.% loading of graphene [125]. Syurik et al., investigated the temperature dependence of electrical conductivity of PS/graphene NCs having 0.32 wt.% of nanofiller and obtained that it can be divided into three regions with different dominating mechanisms of conductance [132]. According to them, in the “high” temperature range (369-331 K) conductivity of the NC increases with temperature, and this was approximated by the mechanism of variable range hopping. This behavior is similar to the conductivity behavior of semiconductors. Further, the influence of hopping terminates with a decrease of temperature in the “medium” temperature range (331-305 K) and in this region results fit the fluctuation-induced tunneling of electrons between the neighboring graphene platelets. In the “low” temperature range (305-295 K) the conductivity grows with a decrease of temperature, which is caused by activation of polarization - a typical process for macromolecular compounds.

Polystyrene/Graphite Nanocomposites

Graphite is composed of thousands of graphene sheets stacked on the top of each other and separated by 0.337 nm. Firstly, graphite was intercalated with acid to obtain graphite intercalated compounds (GIC) and then it was thermally expanded to get expanded graphite (EG), which has been used as filler and flame retardant for polymers. By ultrasound sonication of the EG, a few nanometer thick stacks of graphene planes spaced by nanogalleries are formed, i.e. graphite nanoplatelets (GNPs) are obtained. Into these galleries polymer chains can intercalate. Filippone et al., prepared PS/GNP NCs by a combination of solution and melt mixing techniques and investigated elasticity of the formed GNP network in the PS matrix, using viscoelastic analysis [133]. The obtained results gave them an insight into the stress-bearing mechanism, which is usually responsible for the improvement of mechanical properties in PNCs. The influence of the process variables on the formation of PS/nanographite NC foams was investigated by Yeh et al. [134]. The NCs were prepared using direct compounding, pulverized sonication compounding and *in situ* polymerization, while foam was prepared using CO₂ as blowing agent. According to their results, *in situ* polymerization provided the best dispersion of NPs and the obtained foam had the finest cell size and the highest cell density.

Polystyrene/Metal Nanoparticles Composites

Metal NPs are among the most studied nanofillers for the synthesis of NCs, due to their outstanding size dependent properties. They show absorption bands or broad regions of absorption in the UV-visible range due to the interband transitions or excitation of surface plasmon resonance (SPR), the frequency at which conduction electrons, mainly on the metal surface, oscillate in response to the alternating electric field of incident electromagnetic radiation. Nevertheless, only metals with free electrons such as Au, Ag, and Cu have SPR band in the visible region of the electromagnetic spectrum, which causes intense colors of their colloidal dispersions. For this reason, these NPs are the metals of interest for a number of applications where SPR is used for enhancing the amount of reflected light just above the

plasmon frequency, such as plasmonic solar cells and optical surface plasmon sensors. Besides, since the SPR frequency is highly sensitive to the dielectric environment of the NPs [135], the role of metal NPs in bio- and chemical-sensing applications is important [136]. Therefore, surface plasmons of metal NPs have opened an avenue towards the possibility to amplify, concentrate and manipulate light at nanoscale, whether NPs are used independently or as nanofiller for PS or other polymer matrices. Since, the SPR depends on the particle size and shape, interparticle distance, and dielectric constant of the host medium [137], the size, size distribution, and morphology control of metal NPs have been the key to understand their optical and surface properties. These include efforts to improve physical properties of PS/metal nanoparticle composites, because such NCs can be useful in the field of optics and electronics.

The choice of the metal NPs for the preparation of PS based NCs is usually guided mainly by their optical, electrical, magnetic, mechanical, and thermal behavior. Ag, Au and Cu NPs are the metals of interest for the application of NCs in the field of optics and electronics. The Al and Cu NPs are often selected due to their high conductivity, Fe, Ni and Co NPs are applied because of their magnetic properties which can be changed from ferromagnetic to superparamagnetic. In applications for which costs are important, Cu NPs offer unequalled advantages over Ag and Au NPs. In addition, bimetallic NPs composed of two different metals, are also used as nanofillers and usually exhibit improved optical, magnetic, and catalytic properties resulting from electronic and structural effects of the bimetal [138,139].

Given the fact that the properties of the metal NPs are size-dependent, and also have a direct impact on composite properties, it is significant to be able to synthesize NPs with narrow size distributions. The successful synthesis of NPs involves three steps: nucleation, growth, and termination by the capping agent or ligand. Since the synthesis of metal nanoparticles is very sensitive to many experimental conditions like temperature, concentration of the reactants, and the rate of addition of the reactants, it is often impossible to independently control these steps and so the obtained NPs usually exhibit a distribution in size. Typically, the distribution is log-normal with a standard deviation of 10%. The most commonly-used analytical approach to obtain metal colloids is chemical synthesis, conventionally performed either in aqueous solutions via sodium citrate and sodium borohydride reduction of metal salts [140-143] or by Brust's and Schiffrin's liquid-liquid two phase method in an organic phase by sodium borohydride reduction of metal salts in the presence of an alkanethiol [144-146]. Better control of the NP size and size distribution was achieved in a single organic solvent using mild or strong reducing agent [33,147-150]. Because the as-prepared nanoparticles are often soluble in either the aqueous phase or the organic phase but not in both, a great amount of work is also being done toward the phase transfer of nanoparticles from an aqueous phase into an organic phase [19,28,151]. The selection of method for the synthesis of metal NPs is very important in the case when the pre-made metal NPs are used to prepare PS NCs, using *ex situ* or *in situ* methods. The both method used to prepare PS/Ag NCs were recently reported from our laboratories [16,17,24,33], as well as by other authors [152-154]. The first approach involves the incorporation of pre-made NPs-chemically synthesized with organically passivated surface into a PS matrix, with the use of a common blending solvent. In the second method, styrene monomer is polymerized in solution around the pre-made NPs, or in the presence of metal ions which are then reduced chemically, thermally, or by UV irradiation [33,155-163].

Despite the progress in the synthesis of PS/metal NPs composites, the efficient use of metal NPs is not without some challenges – stability and reactivity have to be controlled. Therefore, the stabilization of metal NPs is specifically required to prevent their uncontrollable growth, aggregation, to control their final shape and size and to allow particle solubility in various solvents. High surface energy of NPs, favors the aggregation of smaller particles into larger ones, whereas large contribution of surface atoms increases their reactivity. Surface free energy of the NPs determines both, matrix-NPs interaction, which has a pronounced effect on the mechanical properties of polymer, and particle-particle interactions which show influence on the aggregation of NPs. In addition to the surface free energy of the NPs, their specific surface area plays a crucial role in interfacial interactions and in the formation of the interface, which consists of a layer of high density polymer around the particle. Furthermore, the interface layer depends on the interparticle distance. When the content of the NPs is constant, reduction in particle size increases number of the NPs, bringing the particles closer to one another. Thus, the interface layers from adjacent particles overlap, altering the NC properties significantly. Understanding the nature of the interfacial region is essential in determining how this region impacts the overall bulk properties of the NC material.

Properties of Polystyrene/Metal Nanoparticles Composites

Electrical Properties of PS/Metal NCs

Some interesting properties of NCs can be produced using an anisotropic metal NPs (nanorods, nanowires, nanotubes, etc.), arising from interactions between macromolecules and NPs which have at least one dimension in the nanometer regime [164]. However, these properties are controlled by the size, concentration and orientation of the NPs during their distribution in the host polymer, which also determine the size of the polymer/particle interface. The atoms on different types of faces of a single crystal metal have different electronic structures and different densities of adsorption sites, and thus are expected to exhibit different catalytic properties [165]. Also, the sharp tips and edges found in NPs are regions of high electric field that greatly enhances optical effects [166]. Anisotropic NPs could reinforce polymers more than spherical NPs, and this effect increases with the anisotropy (aspect ratio) of the NPs. Besides, the morphology and distribution of the NPs may dramatically affect electrical percolation in composites. This is due to the ability of conductive metal NPs with high aspect ratio to produce a percolated, conducting network at much lower volume fractions than spherical carbon black or metal NPs, producing conductive or electrostatically dissipative NCs without reduction of polymer processability or degradation of polymer properties. Also, the NCs containing metal NPs with high aspect ratio should be considered as alternatives to CNT composites for use in electrostatic dissipation, electromagnetic interference, and other electronic applications [167]. Among all metals nanowires, Cu nanowires are the best one due to its high electrical and thermal conductivity. The electrical percolation threshold of PS/Cu nanowires composite material, as shown in the study of Al-Saleh et al., was just 0.24 vol.% [168]. Gelves et al., showed that individual dispersion, as well as aggregation and segregation of high aspect ratio of Ag and Cu nanowires up to 200 and 400, respectively, have contributed to the formation of electrically conductive networks at low concentrations of metal in the PS matrix [169]. The electrical percolation of metal nanowires in PS NCs has been demonstrated to occur at percentages of

0.50-0.75 vol.% for Ag nanowires and 0.25-0.75 vol.% for Cu nanowires. They also showed that volume electrical resistivity of PS containing metal nanowires decreases after percolation by about ten and eight orders of magnitude for Ag and Cu, respectively.

As we mentioned above, the conductivity of the PS containing dispersed conductive metal NPs depends on the size and shape of the metal NPs, their spatial distribution within a PS matrix, the interactions between the metal surface and the PS, and the contact resistance between adjacent NPs. All these factors determine the conditions of charge transport from one particle to another, i.e., the conductivity of the metal phase. For example, Scaldaferrri et al., investigated conductivity of composite consisting of PS matrix filled with Au NPs capped with 1-dodecanethiol and 8-hydroxyquinoline in different weight percentages [170]. Owing to the presence of two conductivity states which differ by several orders of magnitude, Ouyang et al., demonstrated the possibility to use such NCs as the basic material for programmable non-volatile memory devices [171].

Optical Properties of PS/Metal NCs

Optical properties of NC thin films, composed of metal NPs dispersed in solid dielectric materials such as PS, have been of increasing interest for practical reasons, largely because such NCs can be applied in photonics and electronics devices. The improvement of the optical performances of PS can be achieved by incorporation of the appropriate size Ag and Au NPs with strong plasma resonance absorption [24,33,153]. Since PS represents a colorless amorphous non-absorbing medium throughout the visible spectrum (with a refractive index similar to glass), whereas these NPs absorb light in narrow wavelength range, the controlled combination of these two dissimilar materials can lead to the formation of the NCs that display a resonance absorption peak in the visible spectral range. So prepared PS/metal NPs composites can be colored, made magnetic or fluorescent without losing their transparency, easily handled, and used for fabrication of optical devices for applications in different technological fields (linear optics, optoelectronics, magneto-optics, etc.). The effect of a surrounding PS on the surface plasmon of the Au and Ag NPs has been studied by several authors [24,33,172,173]. A red-shift in the plasmon absorption band of NPs after their incorporation in PS matrix, observed by our group, was due to the change in the refractive index of the NPs environment and dipole-dipole interaction between neighboring NPs in the NC films that occurred due to the decrease of average distance between them [24,33]. Carotenuto et al., prepared lightfast color filters (intensively and brightly colored) based on Ag NPs embedded in amorphous PS [174]. The intensity of the yellow coloration due to the SPR of the Ag NPs can be widely tuned simply by varying the cluster numerical density in the polymer matrix that depends on the Ag precursor concentration. The optical response of such PS/Ag nanostructures is dominated by the excitation of surface plasmons, which provides potential for using these materials as active surfaces in surface-enhanced Raman scattering, fluorescence control and optical biosensing [175-177]. It is important to note that interfacial physical and/or chemical interaction between PS and metal NPs may induce changes in the electronic band structure and optical interband transitions of the particle surface, and deviations of dielectric properties of PS-NP matrix interlayers from those of the bulk PS. In addition, aggregated particles have optical absorption different from that of isolated particles, i.e. at short interparticle distances, the interactions among particle dipoles cause a multiple splitting of metal SPR and a broad optical absorption appears. Consequently, optical characteristics of the NCs change. However, when the NCs are heated above the PS

glass transition temperature, expansion of aggregates with significant increase in the interparticle distance and transition from “collective” surface plasmon absorptions to “individual” particle optical absorptions occurs [178]. Such chromatic variation of PS/metal NPs films could find important technological application in the area of thermal and chemical sensors [179,180].

Thermal Properties of PS/Metal NCs

The introduction of metal NPs into PS matrix has a great influence on the thermal properties of PS, since the thermal properties of metal NPs significantly differ from those of PS matrix. Large differences in the thermal properties of the components, on the other hand, lead to the development of thermal stresses, which also influence the performance of the NC under external load. In the PS NCs, the thermal properties of the polymer component are often enhanced compared with those of the bulk PS, i.e. PS/metal NPs composites have better resistance to thermal degradation than neat PS, and it increases with the increase of metal NPs content [24,33]. The enhancement of thermal stability is attributed to the decrease in the mobility of polymer chains, as a result of the close interactions between the surface of the metal NPs and the polymer. For example, Kamrupi et al., reported that the thermal stability of the PS/Ag NCs is enhanced significantly up to around 30 °C [181]. The Ag NPs restrict the movement of the polymer chains and with the increase of the amount of NPs, this restriction increases considerably due to the interaction of NPs with the polymer chains. On the other hand, increase of free volume and chain segments mobility near the surface of metal NPs leads to the decrease of T_g of PS matrix. Also, the interface between metal NPs and PS matrix increases with the increase of the content of inorganic phase, resulting in a larger decrease of T_g . In some cases, the organic modification of NPs can result in a decrease in T_g due to plasticization [33]. Kim et al., explained the decrease of T_g with increasing amount of the Au NPs in PS with plasticizing effect of the metal NPs, which act as a low molecular weight fraction in a high molecular weight polymer, contributing to the increase of the free volume of the total plasticized polymers and to the reduction of intermolecular forces between PS molecules [162]. In another study, Hu et al., showed that PS/Au NC material has higher T_g than the corresponding pristine PS [161]. The difference is reduced with an increase in Au content, i.e. a decrease in the PS:Au weight ratio, because of the formation of larger Au NPs which provide a smaller total surface area for PS to anchor or to cover.

Antimicrobial Properties of PS/Metal NCs

The antimicrobial characteristic of PS/metal NCs is another interesting property of these materials, especially of PS containing Ag NPs. These materials can be used, for example, in medicine to reduce infections, as well as to prevent bacteria colonization on plastic devices such as prostheses, catheters, vascular grafts, and so forth [182]. Palomba et al., obtained Ag-doped PS material with very strong antimicrobial characteristics, which are comparable with the antimicrobial activity of a pure micrometric Ag powder, for Ag concentrations in the polymer higher than 30% by weight [183]. Kamrupi et al., demonstrated the high antimicrobial activity of the PS/Ag NC against *Bacillus circulens* BP2 culture type [181]. Moreover, Zhang et al. [184] showed that PS/Cu NCs display excellent antibacterial properties, such as relatively low minimal inhibitory concentrations against *Escherichia coli* and *Staphylococcus aureus*.

Polystyrene/Metal Oxide Nanocomposites

Metal oxide NPs such as TiO_2 , ZnO , Cu_2O , CuO , and Fe_3O_4 have a wide range of current and proposed applications, and rank among the highest production volume NPs. They are also used as fillers for PS matrix, due to their interesting optical, electrical, chemical, and antimicrobial properties. For example, TiO_2 is inexpensive and nontoxic material with unique electro-chemical and photo-catalytic properties, widely used as UV-resistant material and in the field of chemical fiber production, plastics, printing ink, coatings, self-cleaning glasses, self-cleaning ceramics, antibacterial materials, foods packing material, chemical industry, cosmetics, gas and moisture sensor, etc. [185-191]. Cu_2O and CuO NPs have peculiar physical and chemical properties such as chemical activity and thermal resistance, catalysis, antimicrobial, magnetic and optical properties which make them good candidates for optoelectronic devices and solar cells, ceramic resistors, gas sensors, magnetic storage media, photoconductive and photothermal applications, high-tech superconductors, etc. [192-196]. ZnO NPs have high chemical stability, low dielectric constant, large electromechanical coupling coefficient, high luminous transmittance, high catalysis activity, excellent electrical and optical properties, intensive ultraviolet and infrared absorption, and they are widely used in various fields such as UV-shielding, photocatalysis, field emission display, gas sensing, and thermoelectricity, for the production of voltage dependent resistor, image recording, antimicrobial and self-cleaning hygiene ceramics, floor tile, paints, and plastics [197-201]. Magnetic Fe_3O_4 NPs are currently intensely discussed for medical applications in vitro diagnostics due to their biocompatibility and for spintronic devices due to their half-metallic properties [202-204]. Introduction of metal oxide NPs into PS matrix, some of the above mentioned properties of these NPs can be used to improve or enhance properties of PS.

Properties of Polystyrene/ TiO_2 Nanocomposites

When the TiO_2 nanospheres [16,17] or nanotubes [205] were incorporated in PS by *in situ* bulk radical polymerization, the obtained PS/ TiO_2 NCs showed higher T_g and better thermal and thermooxidative stability than the pure PS. Sang et al., obtained the optimal properties, tensile performance and thermal stability of the PS/ TiO_2 NCs at 1.0 wt.% of TiO_2 loading, and the tensile strength increase of up to 43.6% compared to the pure PS [206]. The onset temperature at which 10% mass is lost is increased by 10 °C. On the other hand, the presence of TiO_2 NPs in PS films greatly promotes the photocatalytic degradation of the NCs, much faster than the simple photolysis of a pure PS sample, through its oxidative reaction with the active oxygen radicals [207-209]. In addition, the adsorption and photocatalytic properties of the PS/ TiO_2 NCs are efficient for the degradation of methylene blue dye solutions under UV irradiation [210]. Furthermore, Wang et al., showed that HIPS/ TiO_2 NCs have a satisfactory antibacterial effect against *Escherichia coli* and *Staphylococcus aureus* and better rheological behavior than bulk PS [211]. In another investigation of HIPS/ TiO_2 NCs, the notched impact strength, tensile strength, and tensile elastic modulus increased to their maximum when nano- TiO_2 content was 2% [212]. The TiO_2 NPs have both toughening and reinforcing effects on HIPS at 2% loading. The heat deflection temperature, flame retardancy, mechanical properties, and comprehensive performance of HIPS/ TiO_2 NCs are better than that of HIPS alone, so the NCs are useful for a wide range of applications. In another study, effect of PS/ TiO_2 NC dielectrics on thin film transistor performance has been explored [213]. These results provide a better understanding of how the

dielectric/semiconductor interface and especially the permittivity of the dielectric impact the transport properties of organic thin film transistors.

Properties of Polystyrene/ZnO Nanocomposites

In the case of the PS filled with ZnO NPs, Ma et al., reported that surface resistivity of PS/ZnO NCs falls as the amount of ZnO increases [214]. Addition of 30 wt.% of ZnO spherical particle and ZnO whisker reduced the surface resistivity of materials from 1.0×10^{16} to $8.98 \times 10^{12} \Omega/\text{cm}^2$ and to $9.57 \times 10^{10} \Omega/\text{cm}^2$, respectively. The ZnO in PS resin formed a conductive network, and hence, it produced a lower surface resistivity and improved the antistatic characteristics of the materials. T_g of the PS/ZnO NCs increased with ZnO content because ZnO restricted the segmental motion of the PS molecules and reduced the free volume of polymer chain folding. On the other hand, in some cases mechanical properties of NCs were decreased, because of aggregation NPs in polymer matrices. Chae et al., showed that introduction of 5wt.% ZnO nanoparticles into PS decreased both the tensile strength and elongation at break [215]. This implies that the interfacial adhesion is not strong enough to stand up to large mechanical forces, because the homogeneous dispersion of NPs was difficult. The presence of ZnO NPs in the PS film, highly transparent in the visible range, offers prospects of application of these NCs as transparent UV radiation protectors in the wavelength range from 200 to 360 nm [216]. Thus ZnO NPs enhance the UV absorption capacity of the NC films and modify the overall optical behavior of PS. This aspect offers the applications of the PS/ZnO NC films as UV protectors for UV shielding in plastics, textiles, paints, cosmetics, etc.

Properties of Polystyrene/Fe₃O₄ Nanocomposites

Zhong et al., incorporated magnetic Fe₃O₄ NPs in the PS by the facile *in situ* bulk radical polymerization [217]. They showed that saturation magnetization value of the PS/Fe₃O₄ was higher than that of the Fe₃O₄ NPs, because of the excellent dispersion of the magnetic NPs. This NC is expected to be applied for the large-scale industrial manufacturing of the superparamagnetic polymer NCs. Ali et al., also obtained PS/Fe₃O₄ NC film with superparamagnetic behavior and better thermal stability compared to those of the bulk polymer, suggesting that this NC could find applications as supercapacitor and chemical sensor [218].

Polystyrene/SiO₂ Nanocomposites

Silica NPs are attractive material due to their stability (chemical and thermal), low toxicity, possibility of controlling their particle size, ability to be functionalized with a range of molecules and polymers, biocompatibility, degradability under physiological conditions, low cost, etc. Mesoporous silica NPs with a large surface area and pores, which allow entrapping great amounts of cargo molecules, are receiving growing attention by the scientific biomedical community for their use as cell imaging, diagnosis, and drug/gene/protein delivery systems [219]. In addition, nanosilica can be widely used in batteries, paints, adhesives, cosmetics, glass, steel, chemical fibers and plexiglas, and many other fields of environmental protection. Silica NPs dispersed in rubber and plastics can significantly improve strength, toughness, wear and aging resistance [220,221]. Camkerten et al., observed

higher hardness and thermal stability of PS after introduction of SiO₂ NPs of 10 nm into PS [222]. Wu et al., reported that PS/poly(ethylene terephthalate)-SiO₂ NC films with 2 wt.% load of PS/encapsulated SiO₂ NPs possess the fastest poly(ethylene terephthalate) crystallization rate [223]. Whittington et al., [224] and Zhang et al., [225] found that PS/SiO₂ NCs showed much higher T_g than bulk PS. This enhancement in T_g value is attributed to the decrease in the mobility of the polymer chains, a result of the close interactions between the surface of the SiO₂ NPs and the polymer. Tethering and chain confinement are the two dominant contributions that affect mobility [226]. Another interesting NCs-shape memory materials were fabricated using chemically cross-linked PS as a matrix and SiO₂ (average grain size 15 nm) and Al₂O₃ (average grain size 80 nm) nanofillers as the reinforcing agents [227]. These NPs provide significant reinforcement for the PS, and the NCs exhibit better thermal and mechanical properties, including shape memory properties, than unreinforced PS.

Polystyrene/Semiconductor Nanocomposites

Semiconductor NPs (CdS, ZnS, Cu₂S, PbS, CdSe) are another most promising materials, because of their wide range of applications in optoelectronic, piezoelectronic, electroluminescent and semiconducting devices, light-emitting diodes, biological labels, and immune diagnosis [228-231]. Thermal stability of PS/semiconductor NCs is the important property from the application point of view. PS generally have the low thermal stability, which restrains it from the applications in higher temperature region. Improvement of the thermal stability of the PS matrix for about 50 K was found in the presence of the CdS NPs [232,233]. CdSe NPs also improve thermal stability of PS [234]. Besides the thermal stability, thermal conductivity of PS NCs is also a very important parameter for the industry. PS has very low thermal conductivity at room temperature 0.14 W/mK. To obtain PS NCs with higher effective thermal conductivity, Agarwal et al., studied the effect of the concentration, as well as temperature dependence of thermal conductivity of PS filled with CdS and ZnS NPs [235]. The obtained increase of effective thermal conductivity of PS/CdS and PS/ZnS NCs up to the loading of 4 wt.% NPs with increasing temperature up to the T_g , was attributed to the straightening of the chains and removal of defects. Almost constant value of thermal conductivity beyond T_g is explained on the basis of structure and vacant site scattering of phonons. As the concentration of CdS and ZnS fillers increases to 4 wt.% with uniform dispersion through the PS, the free volume decreases and makes the NCs more compact than the composite with 2 wt.% of CdS and ZnS. They reached the optimum compact structure for which the thermal conductivity of NCs is maximal. The transparent PS/CdS NC films, obtained by Xue et al.,, exhibited more optimized optoelectronic properties than that of CdS nanocrystals alone [236]. The NC films exhibited distinct luminescence properties of more stable emission and a narrower full-width at half-maximum than that of CdS nanocrystals in solution, which opens the possibility to use these films for fabricating novel optical sensors and microelectronic devices.

Recently, semiconductor CdSe-ZnS core-shells NPs with high-quantum yields, size-dependent wide optical tunability, and high color purity have been considered as the best fluorophores in biomedical and clinical applications [231,237,238]. CdSe semiconductor quantum dots have a good photostability compared to conventional fluorophore dyes of rhodamine or fluorescein derivatives without serious photobleaching problems for the

biomedical applications [239]. CdSe-ZnS semiconductor core-shells significantly enhance quantum yield and reduce photoblinkin. With PS encapsulation, semiconductor core-shells eliminate photoblinking and toxicity. In the interesting study on chip-based biosensor system with solid-phase immunoassay consisted of capture antibody, carboxylated PS/CdSe-ZnS core-shells, and detection antibody on the APTES/GA/Protein A, Kim et al., demonstrated that this system could be utilized to detect cardiac troponin I (cTnI) for sensing cardiovascular disease with a fluorescence readout technique. The glass chip biosensor successfully recorded the linear increase of fluorescence intensity as the concentration of cTnI antigen was increased [237].

In another study, a new smart polymer NC layer, based on metallic-semiconductor Cu_2S NPs embedded into a PS matrix, was developed for the detection of low-velocity impact damage in composite structures [240]. This material exhibits a combination of optical and electro-magnetic properties, in way that it can be employed to visualize in quick and effective manner barely visible impact damage, i.e. it can be employed in different *in situ* structural health monitoring applications.

CONCLUSION

The extensive research of polymer nanocomposites in recent years has proven that these materials give a powerful platform for the manipulation of physico-chemical and other properties of both components: polymers and NPs. Because of its low cost, dielectric properties and transparency, PS has been the extensively investigated for the preparation of PNCs. Currently, a significant amount of work is being published on PS NCs. In an attempt to further understand the synthesis, processing, and properties of PS NCs, a selection of representative and recent literature was chosen to highlight some of the issues related to the fabrication and behavior of PS matrix filled with different nanoparticles. Through the long list of preparation techniques, and combinations of large number of NPs, a different PS NCs can be produced. The construction of these NCs led to the fabrication of materials with new functionalities. In order to achieve that, it is necessary to establish guidelines for process optimization, discover methods that yield a desired properties or fabrication of hierarchically ordered NCs, and to understand PS-NPs property relationships in order to be able to predict the performances of final materials. Varying the NPs type and characteristics will lead to development of sophisticated PS NCs with tunable properties, capable for numerous future applications. A vigorous development of this field can be expected in the future, leading to the design of new PS NCs with better properties.

ACKNOWLEDGMENTS

This work was financially supported by the Ministry of Education, Science and Technological Development of the Republic of Serbia (research project numbers: 45020, 172056 and 172062).

REFERENCES

- [1] Staudinger, H. *Die Hochmolekularen Organischen Verbindungen*, Kautschuk und Cellulose; Springer: Berlin, Germany, 1932.
- [2] Polystyrene (PS) – A Global Market Watch, (2012) 2011-2016 http://www.researchandmarkets.com/reports/2364722/polystyrene_ps_a_global_market_watch_2011.
- [3] Faes, E. The Plastics Portal <http://www.plasticseurope.org/what-is-plastic/types-of-plastics-11148/polystyrene.aspx>.
- [4] Nuyken, O. In *Handbook of Polymer Synthesis*; Kricheldorf, H. R.; Nuyken O.; Swift, G.; Eds.; Second edition; Marcel Dekker: NY, USA, 2005; pp. 73-150.
- [5] Gretza, M. K.; Madereu, D.; Matyjaszewski, K. *Macromolecules* 1994, 27, 638-644.
- [6] Webster, O. E. *Science* 1991, 251, 887-893.
- [7] Wagner, P. A.; Sugden, J. In *The Wiley Encyclopedia of packaging technology*; Yam, K. L.; Ed.; Third edition; A John Wiley and Sons, Inc., Publication: USA, 2009; pp. 1009-1012.
- [8] Biron, M. *Thermoplastics and thermoplastic composites*; Butterworth-Heinemann, Elsevier: Oxford, UK, 2007.
- [9] Mancini, L. H. *Nanocomposites: Preparation, Properties and Performance*; Nova Science Publication, Inc.: New York, 2008; p. 272.
- [10] Nicolais, L. In *Metal Polymer Nanocomposites*; Carotenuto, G.; Ed.; John Wiley and Sons: New Jersey, 2005; p. 319.
- [11] Lan, Q.; Francis, L. F.; Bates, F.S. *J Polym Sci Part B: Polym Phys* 2007, 45, 2284-2299.
- [12] Kamat, P. V. *J Phys Chem B* 2002, 106, 7729-7744.
- [13] Manias, E.; Touny, A.; Wu, L.; Strawhecker, K.; Lu, B.; Chung, T. C. *Chem Mater* 2001, 13, 3516-3523.
- [14] Schmidtke, K.; Lieser, G.; Klapper, M.; Müllen, K. *Colloid Polym Sci* 2010, 288, 333-339.
- [15] Novakov, I. A.; Dang, N. K.; Vaniev, M. A.; Sidorenko N. V. *Russ Chem Bull International Edition* 2013, 62, 276-284.
- [16] Džunuzović, E.; Vodnik, V.; Jeremić, K.; Nedeljković, J. M. *Mater Lett* 2009, 63, 908-910.
- [17] Džunuzović, E. S.; Džunuzović, J. V.; Radoman, T. S.; Marinović-Cincović, M. T.; Nikolić, Lj. B.; Jeremić, K. B.; Nedeljković, J. M. *Polym Compos* 2013, 34, 399-407.
- [18] Džunuzović, E.; Jeremić, K.; Nedeljkovic, J. M. *Eur Polym J* 2007, 43, 3719-3726.
- [19] Vodnik, V. V.; Božanić, D. K.; Džunuzović, E.; Vuković, J.; Nedeljković, J. M. *Eur Polym J* 2010, 46, 137-144.
- [20] Pandis, Ch.; Logakis, E.; Kyritsis, A.; Pissis, P.; Vodnik, V. V.; Džunuzović, E.; Nedeljković, J. M.; Djoković, V.; Rodriguez Hernandez, J. C.; Gomez Ribelles, J. L. *Eur Polym J* 2011, 47, 1514-1525.
- [21] Safaei-Naeini, Y.; Aminzare, M.; Golestani-Fard, F.; Khorasanizadeh, F.; Salahi, E. *Iran J Mater Sci Eng* 2012, 9, 62-68.
- [22] Laachachi, A.; Ferriol, M.; Cochez, M.; Ruch, D.; Lopez-Cuesta, J.-M. *Polym Degrad Stab* 2008, 93, 1131-1137.

- [23] Oliveira, A. M.; Silva, M. L.; Alves, G. M.; de Oliveira, P. C.; Santos, A. M. *Polym Bull* 2005, 55, 477-484.
- [24] Vodnik, V.; Božanić, D. K.; Džunuzović, J. V.; Vukoje, I.; Nedeljković, J. *Polym Compos* 2012, 33, 782-788.
- [25] Vodnik, V. V.; Šaponjić, Z.; Džunuzović, J. V.; Bogdanović, U.; Mitrić, M.; Nedeljković, J. *Mater Res Bull* 2013, 48, 52-57.
- [26] Vodnik, V. V.; Abazović, N. D.; Stojanović, Z. A.; Marinović-Cincović, M.; Mitrić, M.; Čomor, M. I. *J Comp Mater* 2012, 46, 987-995.
- [27] Liang, J. Z. *Polym Int* 2002, 51, 1473-1478.
- [28] Vodnik, V. V.; Vuković, J. V.; Nedeljković, J. M. *Colloid Polym Sci* 2009, 287, 847-851.
- [29] Radoman, T. S.; Džunuzović, J. V.; Jeremić, K. B.; Marinković, A. D.; Spasojević, P. M.; Popović, I. G.; Džunuzović, E. S. *Hem Ind* 2013, 67, 923-932.
- [30] Marinković, A. D.; Radoman, T.; Džunuzović, E. S.; Džunuzović, J. V.; Spasojević, P.; Isailović, B.; Bugarski B. *Hem Ind* 2013, 67, 913-922.
- [31] Sanz, R.; Luna, C.; Hernandez-Velez, M.; Vazquez, M.; Lopez, D.; Mijangos, C. *Nanotechnology* 2005, 16, S278-S281.
- [32] Džunuzović, E.; Marinović-Cincović, M.; Jeremić, K.; Nedeljković, J. *Polym Degrad Stab* 2009, 94, 701-704.
- [33] Vukoje, I. D.; Vodnik, V. V.; Džunuzović, J. V.; Džunuzović, E. S.; Marinović-Cincović, M. T.; Jeremić, K.; Nedeljković, J. M. *Mater Res Bull* 2014, 49, 434-439.
- [34] Hsu, S. C.; Whang, W. T.; Hung, C. H.; Chiang, P. C.; Hsiao Y. N. *Macromol Chem Phys* 2005, 206, 291-298.
- [35] Džunuzović, E. S.; Marinović-Cincović, M. T.; Džunuzović, J. V.; Jeremić, K. B.; Nedeljković, J. M. *Hem Ind* 2010, 64, 473-489.
- [36] Džunuzović, E.; Marinović-Cincović, M.; Vuković, J.; Jeremić, K.; Nedeljković, J. M. *Polym Compos* 2009, 30, 737-742.
- [37] Cai, L. F.; Huang, X. B.; Rong, M. Z.; Ruan, W. H.; Zhang, M. Q. *Macromol Chem Phys* 2006, 207, 2093-2102.
- [38] Džunuzović, E. S.; Džunuzović, J. V.; Marinković, A. D.; Marinović-Cincović, M. T.; Jeremić, K. B.; Nedeljković, J. M. *Eur Polym J* 2012, 48, 1385-1393.
- [39] Džunuzović, E.; Marinović-Cincović, M.; Jeremić, K.; Vuković, J.; Nedeljković, J. *Polym Degrad Stab* 2008, 93, 77-83.
- [40] KICKELBICK, G. *Hybrid Materials: Synthesis, Characterization, and Applications*; John Wiley & Sons: New York, 2007.
- [41] Du, K.; Knutson, C. R.; Glogowski, E.; McCarthy, K. D.; Shenhar, R.; Rotello, V. M.; Tuominen, M. T.; Emrick, T.; Russell, T. P.; Dinsmore, A. D. *Small* 2009, 5, 1974-1977.
- [42] Laachachi, A.; Leroy, E.; Cochez, M.; Ferriol, M.; Lopez Cuesta, J. M. *Polym Degrad Stab* 2005, 89, 344-352.
- [43] Inkyo, M.; Tokunaga, Y.; Tahara, T.; Iwaki, T.; Iskandar, F.; Hogan, Jr., C. J.; Okuyama, K. *Ind Eng Chem Res* 2008, 47, 2597-2604.
- [44] Chen, X.; Mao, S. *Chem Rev* 2007, 107, 2891-2959.
- [45] Ilić, V.; Šaponjić, Z.; Vodnik, V.; Lazović, S.; Dimitrijević, S.; Jovančić, P.; Nedeljković, J. M.; Radetić, M. *Ind Eng Chem Res* 2010, 49, 7287-7293.

- [46] Mihailović, D.; Šaponjić, Z.; Vodnik, V.; Potkonjak, B.; Jovančić, P.; Nedeljković, J. M.; Radetić, M. *Polym Adv Technol* 2011, 22, 2244-2249.
- [47] Ilić, V.; Šaponjić, Z.; Vodnik, V.; Potkonjak, B.; Jovančić, P.; Nedeljković, J.; Radetić, M. *Carbohydr Polym* 2009, 78, 564-569.
- [48] Ilić, V.; Šaponjić, Z.; Vodnik, V.; Mihailović, D.; Jovančić, P.; Nedeljković, J.; Radetić, M. *Fiber Polym* 2009, 10, 650-656.
- [49] Radetić, M.; Ilić, V.; Vodnik, V.; Dimitrijević, S.; Jovančić, P.; Šaponjić, Z.; Nedeljković, J. M. *Polym Adv Technol* 2008, 19, 1816-1821.
- [50] Ilić, V.; Šaponjić, Z.; Vodnik, V.; Mihailović, D.; Jovančić, P.; Nedeljković, J. M.; Radetić, M. *J Serb Chem Soc* 2009, 74, 349-357.
- [51] Ilić, V.; Šaponjić, Z.; Vodnik, V.; R.; Molina, Dimitrijević, S.; Jovančić, P.; Nedeljković, J. M.; Radetić, M. *J Mater Sci* 2009, 44, 3983-3990.
- [52] Ray, S. S. *Clay-containing polymer nanocomposites: From fundamentals to real applications*; Elsevier: Oxford, UK, 2013; p. 5.
- [53] Panwar, A.; Choudhary, V.; Sharma, D. K. *J Reinf Plast Compos* 2011, 30, 446-459.
- [54] Chen, B.; Evans, J. R. G. *Scripta Mater* 2006, 54, 1581-1585.
- [55] Ianchis, R.; Donescu, D.; Petcu, C.; Ghiurea, M.; Anghel, D. F.; Stanga, G.; Marcu, A. *Appl Clay Sci* 2009, 45, 164-170.
- [56] Simons, R.; Qiao, G. G.; Powell, C. E.; Bateman, S. A. *Langmuir* 2010, 26, 9023-9031.
- [57] Chigwada, G.; Jiang, D. D.; Wilkie, C. A. *Thermochim Acta* 2005, 436, 113-121.
- [58] Uthirakumar, P.; Hahn, Y. B.; Nahm, K. S.; Lee, Y. S. *Eur Polym J* 2007, 41, 1582-1588.
- [59] Uthirakumar, P.; Song, M.-K.; Nah, C.; Lee, Y.-S. *Eur Polym J* 2005, 41, 211-217.
- [60] Zhu, J.; Morgan, A. B.; Lamelas, F. J.; Wilkie, C. A. *Chem Mater* 2001, 13, 3774-3780.
- [61] Tseng, C. R.; Wu, J. Y.; Lee, H. Y.; Chang, F. C. *J Appl Polym Sci* 2002, 85, 1370-1377.
- [62] Liu, S.-P.; Huang, I.-J.; Chang, K.-C.; Yeh J.-M. *J Appl Polym Sci* 2010, 115, 288-296.
- [63] Arora, A.; Choudhary, V.; Sharma, D. K. *J Polym Res* 2011, 18, 843-857.
- [64] Dazhu, C.; Haiyang, Y.; Pingsheng, H.; Weian, Z. *Compos Sci Technol* 2005, 65, 1593-1600.
- [65] Fu, X.; Qutubuddin, S. *Mater Lett* 2000, 42, 12-15.
- [66] Jang, B. N.; Wilkie, C. A. *Polymer* 2005, 46, 2933-2942.
- [67] Samakande, A.; Sanderson, R. D.; Hartmann, P. C. *Eur Polym J* 2009, 45, 649-657.
- [68] Chiu, F.-C.; Su, W.-I. *Mat Chem Phys* 2012, 132, 145-153.
- [69] Tang, Z.; Lu, D.; Guo, J.; Su, Z. *Mater Lett* 2008, 62, 4223-4225.
- [70] Uthirakumar, P.; Nahm, K. S.; Hahn, Y. B.; Lee, Y. S. *Eur Polym J* 2004, 40, 2437-2444.
- [71] Greesh, N.; Hartmann, P. C.; Sanderson, R. D. *Macromol Mater Eng* 2009, 294, 787-794.
- [72] Alshabanat, M.; Al-Arrash, A.; Mekhamer, W. *J Nanomater* 2013, Article ID 650725, 12 pages.
- [73] Greesh, N.; Ray, S. S.; Bandyopadhyay, J. *Ind Eng Chem Res* 2013, 52, 16220-16231.
- [74] Chigwada, G.; Wang, D.; Jiang, D. D.; Wilkie, C. A. *Polym Degrad Stab* 2006, 91, 755-762.
- [75] Giannakas, A.; Spanos, C. G.; Kourkoumelis, N.; Vaimakis, T.; Ladavos, A. *Eur Polym J* 2008, 44, 3915-3921.

- [76] Abate, L.; Blanco, I.; Bottino, F. A.; Pasquale, G.; Fabbri, E.; Orestano, A.; Pollicino, A. *J Therm Anal Calorim* 2008, 91, 681-686.
- [77] Yeh, J.; Liou, S.; Lin, C.; Chang, Y.; Yu, Y.; Cheng, C. *J Appl Polym Sci* 2004, 92, 1970-1976.
- [78] Yang, J.; Fan, H.; Bu, Z.; Li, B.-G. *Polym Eng Sci* 2009, 49, 1937-1944.
- [79] Zhu, J.; Wilkie, C. A. *Polym Int* 2000, 49, 1158-1163.
- [80] Bartholmai, M.; Schartel, B. *Polym Adv Technol* 2004, 15, 355-364.
- [81] Chigwada, G.; Wang, D.; Wilkie, C. A. *Polym Degrad Stab* 2006, 91, 848-855.
- [82] Schutz, M. R.; Kalo, H.; Lunkenbein, T.; Breu, J.; Wilkie, C. A. *Polymer* 2011, 52, 3288-3294.
- [83] Cai, G.; Feng, J.; Zhu, J.; Wilkie, C. A. *Polym Degrad Stab* 2014, 99, 204-210.
- [84] Nazarenko, S.; Meneghetti, P.; Julmon, P.; Olson, B. G.; Qutubuddin, S. *Polym Sci Part B: Polym Phys* 2007, 45, 1733-1753.
- [85] Tuteja, A.; Duxbury, P. M.; Mackay, M. E. *Macromolecules* 2007, 40, 9427-9434.
- [86] Tan, H.; Xu, D.; Wan, D.; Wang, Y.; Wang, L.; Zheng, J.; Liu, F.; Maa, L.; Tang, T. *Soft Matter* 2013, 9, 6282-6290.
- [87] Einstein, A. *Ann Phys* 1906, 17, 371-381.
- [88] Wong, H. C.; Sanz, A.; Douglas, J. F.; Cabral, J. T. *J Mol Liq* 2010, 153, 79-87.
- [89] Barnes, K. A.; Karim, A.; Douglas, J. F.; Nakatani, A. I.; Gruell, H.; Amis, E. J. *Macromolecules* 2000, 33, 4177-4185.
- [90] Nayak, R. R.; Lee, K. Y.; Shanmugaraj, A. M.; Ryu, S. H. *Eur Polym J* 2007, 43, 4916-4923.
- [91] Ayewah, D. O. O.; Davis, D. C.; Krishnamoorti, R.; Lagoudas, D. C.; Sue, H.-J.; Willson, M. *Composites: Part A* 2010, 41, 842-849.
- [92] Chen, J.; Liu, H.; Weimar, W. A.; Halls, M. D.; Waldeck, D. H.; Walker, G. C. *J Am Chem Soc* 2002, 124, 9034-9035.
- [93] Choi, W. S.; Ryu, S. H. *J Appl Polym Sci* 2010, 116, 2930-2936.
- [94] Choi, H.J.; Zhang, K.; Lim, J.Y. *J Nanosci Nanotechnol* 2007, 7, 3400-3403.
- [95] Srivastava, R. K.; Vemuru, V. S. M.; Zeng, Y.; Vajtai, R.; Nagarajaiah, S.; Ajayan, P. M.; Srivastava, A. *Carbon* 2011, 49, 3928-3936.
- [96] Ayesh, A. S.; Ibrahim, S. S.; Aljaafari, A. A. *J Reinforced Plastics and Composites* 2013, 32, 359-370.
- [97] Jia, Y.; Jiang Z.; Peng, J.; Gong, X.; Zhang, Z. *Composites: Part A* 43, 2012, 1561-1568.
- [98] Shaffer, S. P.; Windle, A. H. *Adv Mater* 1999, 11, 937-941.
- [99] Chatterjee, A.; Deopura, B. L. *J Appl Polym Sci* 2006, 100, 3574-3578.
- [100] Sathyanarayana, S.; Olowojoba, G.; Weiss, P.; Caglar, B.; Pataki, B.; Mikonsaari, I.; Hübner, C.; Henning, F. *Macromol Mater Eng* 2013, 298, 89-105.
- [101] Bellayer, S.; Gilman, J. W.; Eidelman, N.; Bourbigot, S.; Flambard, X.; Fox, D. M.; De Long, H. C.; Trulove, P. C. *Adv Funct Mater* 2005, 15, 910-916.
- [102] Pham, J. Q.; Mitchell, C. A.; Bahr, J. L.; Tour, J. M.; Krishnamoorti, R.; Green, P. F. *J Polym Sci Part B: Polym Phys* 2003, 41, 3339-3345.
- [103] Nayak, R. R.; Shanmugaraj, A. M.; Ryu, S. H. *Macromol Chem Phys* 2008, 209, 1137-1144.
- [104] Awad, S.; Chen, H. M.; Grady, B. P.; Paul, A.; Ford, W. T.; Lee, L. J.; Jean, Y. C. *Macromolecules* 2012, 45, 933-940.

- [105] Sorrentino, A.; Vertuccio, L.; Vittoria, V. *eXPRESS Polym Lett* 2010, 4, 339-345.
- [106] Mu, M.; Walker, A. M.; Torkelson, J. M.; Winey, K. I. *Polymer* 2008, 49, 1332-1337.
- [107] Chang, T.-E.; Kisliuk, A.; Rhodes, S. M.; Brittain, W. J.; Sokolov, A. P. *Polymer* 2006, 47, 7740-7746.
- [108] Cipriano, B. H.; Kota, A. K.; Gershon, A. L.; Laskowski, C. J.; Kashiwagi, T.; Bruck, H. A.; Raghavan, S. R. *Polymer* 2008, 49, 4846-4851.
- [109] Zhang, C.; Wen, B.; Gao, L.; Chen, Y.; Yang, M. *J Appl Polym Sci* 2011, 119, 155-161.
- [110] Grossiord, N.; Kivitt, P. J. J.; Loos, J.; Meuldijk, J.; Kyrylyuk, A. V.; van der Schoot, P.; Koning, C. E. *Polymer* 2008, 49, 2866-2872.
- [111] Kim, S. T.; Choi, H. J.; Hong, S. M. *Colloid Polym Sci* 2007, 285, 593-598.
- [112] McClory, C.; Pötschke, P.; McNally, T. *Macromol Mater Eng* 2011, 296, 59-69.
- [113] Singh, B. K.; Kar, P.; Shrivastava, N. K.; Banerjee, S.; Khatua, B. B. *J Appl Polym Sci* 2012, 124, 3165-3174.
- [114] Shen, J.; Han, X.; Lee, L. J. *J Cell Plast* 2006, 42, 105-126.
- [115] Ramos-deValle, L. F.; Neira-Velázquez, M. G.; Hernández-Hernández, E. *J Appl Polym Sci* 2008, 107, 1893-1899.
- [116] Wang, Y.; Xu, J.; Bechtel, S. E.; Koelling, K. W. *Rheol Acta* 2006, 45, 919-941.
- [117] Xu, Y.; Higgins, B.; Brittain, W. J. *Polymer* 2005, 46, 799-810.
- [118] Tjong, S. C.; Liang, G. D.; Bao, S. P. *Polym Eng Sci* 2008, 48, 177-183.
- [119] Bunch, J. S.; Verbridge, S. S.; Alden, J. S.; van der Zande, A. M.; Parpia, J. M.; Craighead, H. G.; McEuen, P. L. *Nano Lett* 2008, 8, 2458-2462.
- [120] Novoselov, K. S.; Geim, A. K.; Morozov, S. V.; Jiang, D.; Zhang, Y.; Dubonos, S. V.; Grigorieva, I. V.; Firsov, A. A. *Science* 2004, 306, 666-669.
- [121] Park, S.; Ruoff, R. S. *Nat Nanotechnol* 2009, 4, 217-224.
- [122] Ren, P.-G.; Yan, D.-X.; Chen, T.; Zeng, B.-Q.; Li, Z.-M. *J Appl Polym Sci* 2011, 121, 3167-3174.
- [123] Fang, M.; Wang, K.; Lu, H.; Yang, Y.; Nutt, S. *J Mater Chem* 2009, 19, 7098-7105.
- [124] Pham, V. H.; Cuong, T. V.; Dang, T. T.; Hur, S. H.; Kong, B.-S.; Kim, E. J.; Shina, E. W.; Chung J. S. *J Mater Chem* 2011, 21, 11312-11316.
- [125] Li, H.; Wu, S.; Wu, J.; Huang, G. *Colloid Polym Sci* 2013, 291, 2279-2287.
- [126] Basu, S.; Singhi, M.; Satapathy, B. K.; Fahim, M. *Polym Compos* 2013, 34, 2082-2093.
- [127] Li, Y.; Wang, Z.; Yang, L.; Gua, H.; Xue, G. *Chem Commun* 2011, 47, 10722-10724.
- [128] Zhang, Y.; Ma, H.-L.; Zhang, Q.; Peng, J.; Li, J.; Zhai, M.; Yu, Z.-Z. *J Mater Chem* 2012, 22, 13064-13069.
- [129] Qi, X.-Y.; Yan, D.; Jiang, Z.; Cao, Y.-K.; Yu, Z.-Z.; Yavari, F.; Koratkar, N. *ACS Appl Mater Interfaces* 2011, 3, 3130-3133.
- [130] Wu, C.; Huang, X.; Wang, G.; Lv, L.; Chen, G.; Li, G.; Jiang, P. *Adv Funct Mater* 2013, 23, 506-513.
- [131] Tkalya, E.; Ghislandi, M.; Alekseev, A.; Koning, C.; Loos, J. *J Mater Chem* 2010, 20, 3035-3039.
- [132] Syurik, J.; Ageev, O. A.; Cherednichenkob, D. I.; Konoplev, B. G.; Alexeev, A. *Carbon* 2013, 63, 317-323.
- [133] Filippone, G.; de Luna, M. S.; Acierno, D.; Russo, P. *Polymer* 2012, 53, 2699-2704.
- [134] Yeh, S.-K.; Huang, C.-H.; Su, C.-C.; Cheng, K.-C.; Chuang, T.-H.; Guo, W.-J.; Wang, S.-F. *Polym Eng Sci* 2013, 53, 2061-2072.

- [135] Kreibig, U.; Vollmer, M. *Optical Properties of Metal Clusters*, Springer Series in Materials Science; Springer-Verlag: New York, 1995.
- [136] McFarland, A. D.; Van Duyne, R. P. *Nano Lett* 2003, 3, 1057-1062.
- [137] Mulvaney, P. *Langmuir* 1996, 12, 788-800.
- [138] Beyene H. T.; Chakravadhanula, V. S. K.; Hanisch, C.; Elbahri, M.; Strunskus, T.; Zaporotchenko, V.; Kienle, L.; Faupel, F. *J Mater Sci* 2010, 45, 5865-5871.
- [139] Hatchett, D. W.; Josowicz, M. *Chem Rev* 2008, 108, 746-769.
- [140] Xiong, Y. J.; Washio, I.; Chen, J. Y.; Sadilek, M.; Xia, Y. N. *Angew Chem Int Ed* 2007, 46, 4917-4921.
- [141] Chen, J. Y.; McLellan, J. M.; Siekkinen, A.; Xiong, Y. J.; Li, Z. Y.; Xia, Y. N. *J Am Chem Soc* 2006, 128, 14776-14777.
- [142] Vodnik, V. V.; Nedeljković, J. M. *J Serb Chem Soc* 2000, 65, 195-200.
- [143] Vuković, V. V.; Nedeljković, J. M. *Langmuir* 1993, 9, 980-983.
- [144] Brust, M.; Walker, M.; Bethell, D.; Schiffrin, D. J.; Whyman, R. *Chem Commun* 1994, 801-802.
- [145] Leff, D. V.; Brandt, L.; Heath, J. R. *Langmuir* 1996, 12, 4723-4730.
- [146] Brown, L. O.; Hutchison, J. E. *J Phys Chem B* 2001, 105, 8911-8916.
- [147] Hiramatsu, H.; Osterloh, F. E. *Chem Mater* 2004, 16, 2509-2511.
- [148] Shen, C.; Hui, C.; Yang, T.; Xiao, C.; Tian, J.; Bao, L.; Chen, S.; Ding, H.; Gao, H. *Chem Mater* 2008, 20, 6939-6944.
- [149] Vodnik, V.V.; Božanić, D. K.; Bibić, N.; Šaponjić, Z. V.; Nedeljković, J.M. *J. Nanosci Nanotechnol* 2008, 8, 3511-3515.
- [150] Schulz-Dobrick, M.; Sarathy, K. V.; Jansen, M. *J Am Chem Soc* 2005, 127, 12816-12817.
- [151] Jana, N. R.; Peng, X. G. *J Am Chem Soc* 2003, 125, 14280-14281.
- [152] Zhang, K.; Fu, Q.; Fan, J. H.; Zhou, D. H. *Mater Lett* 2005, 59, 3682-3686.
- [153] Wang, D.; An, J.; Luo, Q.; Li, X.; Li, M. *J Appl Polym Sci* 2008, 110, 3038-3046.
- [154] Corbierre, M. K.; Cameron, N. S.; Sutton, M.; Laaziri, K.; Lennox, R. B. *Langmuir* 2005, 21, 6063-6072.
- [155] Tsuruoka, T.; Kumazaki, S.; Osaka, I., Nawafune, H., Akamatsu, K. *J Phys: Conference Series* 2013, 417, 012020, 6 p.
- [156] Lee, J.-M.; Jun, Y.-Doo; Kim, D.-W.; Lee, Y.-H.; Oh, S.-G. *Mater Chem Phys* 2009, 114, 549-555.
- [157] Wibawa, P. J.; Saim, H.; Agam, M. A.; Nur, H. *Bull Chem React Eng & Catalysis* 2013, 7, 224-232.
- [158] Wu, D. Z.; Ge, X. W.; Huang, Y. H.; Zhang, Z. C.; Ye, Q. *Mater Lett* 2003, 57, 3549-3553.
- [159] Tadd, E.; Zeno, A.; Zubris, M.; Dan, N.; Tannenbaum, R. *Macromolecules* 2003, 36, 6497-6502.
- [160] Kamrupi, I. R.; Phukon, P.; Konwer, B. K.; Dolui, S.K. *J Supercritical Fluids* 2011, 55, 1089-1094.
- [161] Hu, C.-W.; Yuming, H.; Tsiang, R. C.-C. *J Nanosci Nanotech*, 2009, 9, 3084-3091.
- [162] Kim, J. K.; Ahn, H. *Macromolecular Res* 2008, 16, 163-168.
- [163] Pullini, D.; Carotenuto, G.; Palomba, M.; Mosca, A.; Horsewell, A.; Nicolais, L. *J Mater Sci* 2011, 46, 7905-7911.

- [164] White, S. I.; Mutiso, R. M.; Vora, P. M.; Jahnke, D.; Hsu, S.; Kikkawa, J. M.; Li, J.; Fischer, J. E.; Winey, K. I. *Adv Funct Mater* 2010, 20, 2709-2716.
- [165] Cuenya, B. R. *Thin Solid Films* 2010, 518, 3127-3150.
- [166] Huang, X. H.; Neretina, S.; El-Sayed, M. A. *Adv Mater* 2009, 21, 4880-4910.
- [167] Chung, D. D. L. *J Mater Sci* 2004, 39, 2645-2661.
- [168] Al-Saleh, M.H.; Gelves, G. A.; Sundararaj, U. *Compos Part A: Appl Sci Manuf* 2011, 42, 92-97.
- [169] Gelves, G. A.; Lin, B.; Sundararaj, U.; Haber, J. A. *Adv Funct Mater* 2006, 16, 2423-2430.
- [170] Scaldaferrì, R.; Salzillo, G.; Pepe, G. P.; Barra, M.; Cassinese, A.; Pagliarulo, V.; Borriello, A.; Fusco, L. *Europ Phys J B* 2009, 72, 113-118.
- [171] Ouyang, J.; Chu, C.-W.; Szmanda, C.; Ma, L.; Yang, Y. *Nat Mat* 2004, 3, 918-922.
- [172] Carotenuto, G.; Palomba, M.; Longo, A., de Nicola, S.; Nicolais, L. *Sci Eng Compos Mater* 2011, 18, 187-190.
- [173] Carotenuto, G.; Giannini, C.; Siliqi, D.; Nicolais, L. *Polymers* 2011, 3, 1352-1362.
- [174] Carotenuto, G.; Palomba, M., Nicolais, L. *Sci Eng Compos Mater* 2012, 19, 195-197.
- [175] Farcau, C. A.; Astilean, S. J. *Optoelectron Adv Mater* 2005, 7, 2721-2725.
- [176] Nath, S.; Ghosh, S. K.; Kundu, S. *Mater Lett* 2005, 59, 3986-3989.
- [177] Baia, M.; Baia, L.; Astilean, S. *Chem Phys Lett* 2005, 404, 3-8.
- [178] Kreibig, U.; Quinten, M.; Schoenauer, D. *Phys Scripta* 1986, T13, 84-92.
- [179] Carotenuto, G.; Nicolais, L. In *Encyclopedia Polymer Science and Technology*; Nicolais, L.; Carotenuto, G.; Eds.; John Wiley and Sons: New York, 2003; p. 484.
- [180] Caseri, W. *Macromol Rapid Commun* 2000, 21, 705-722.
- [181] Kamrupi, I. R.; Phukon, P.; Konwer, B. K.; Dolui, S. K. *J Supercritical Fluids* 2011, 55, 1089-1094.
- [182] Dallas, P.; Sharma, V. K.; Zboril, R. *Adv Colloid Interface Sci* 2011, 166, 119-135.
- [183] Palomba, M.; Carotenuto, G.; Cristino, L.; Di Grazia, M. A.; Nicolais, F.; De Nicola, S. *J Nanomater* 2012, 2012, Article ID 185029, 7 pages.
- [184] Zhang, N.; Yu, X.; Hu, J. *Mater Lett* In press.
- [185] Fu, G.; Vary, P. S.; Lin, C.-T. *J Phys Chem B* 2005, 109, 8889-8898.
- [186] Sunada, K.; Watanabe, T.; Hashimoto, K. *Environ Sci Technol* 2003, 37, 4785-4789.
- [187] Linkous, A. C.; Carter, G. J.; Locuson, D. B.; Ouellette, A. J.; Slattery, D. K.; Simitha, L. A. *Environ Sci Technol* 2000, 34, 4754-4758.
- [188] Hagfeldt, A.; Gratzel, M. *Chem Rev* 1995, 95, 49-68.
- [189] Chen, X.; Mao, S. S. *Chem Rev*, 2007, 107, 2891-2959.
- [190] O'Regan, B.; Schwartz, D. T.; Zakeeruddin, S. M.; Gratzel, M. *Adv Mater* 2000, 12, 1263-1267.
- [191] Lakshmi, B. B.; Dorhout, P. K.; Martin, C. R. *Chem Mater* 1997, 9, 857-862.
- [192] Gan, J. H.; Yu, G. Q.; Tay, B. K.; Tan, C. M.; Zhao Z. W.; Fu Y. Q. *J Phys D: Appl Phys* 2004, 37, 81-85.
- [193] Huang, L. S.; Yang, S. G.; Li, T.; Gu, B. X.; Du, Y. W.; Lu, Y. N.; Shi, S. Z. *J Cryst Growth* 2004, 260, 130-135.
- [194] Balamurugan, B.; Aruna, I.; Mehta, B. R.; Shivaprasad, S. M. *Phys Rev B* 2004, 69, p165419-5p.
- [195] Jung, J. H.; Song, T. W. M. S.; Kim, Y.-H.; Yoo, k. H. *J Appl Phys* 2007, 101, p093708-4p.

- [196] Baek, Y.-W.; An, Y.-J. *Sci Total Env* 2011, 409, 1603-1608.
- [197] Xu, J. Q.; Pan, Q. Y.; Shun, Y. A.; Tian, Z. Z. *Sensor Actuator B* 2000, 66, 277-279.
- [198] Van Dijken, A.; Miulenkamp, E. A.; Vanmaekelbergh, D.; Meijerink, A. *J Luminesc* 2000, 9, 123-128.
- [199] Li, J. F.; Yao, L. Z.; Ye, C. H.; Mo, C. M.; Cai, W. L.; Zhang, Y. L.; Zhang, D. *J. Cryst Gr* 2001, 223, 535-538.
- [200] Wang, Z.; Li, H. *J. Appl Phys A* 2002, 74, 201-203.
- [201] Tsuzuki, T.; McCormick, P. G. *Scripta Mater* 2001, 44, 1731-1734.
- [202] Gupta, A. K.; Gupta, M. *Biomaterials* 2005, 26, 3995-4021.
- [203] Pankhurst, Q. A.; Connolly, J.; Jones, S. K.; Dobson, J. *J.Phys D: Appl Phys* 2003, 36, R167- R181.
- [204] Laurent, S.; Forge, D.; Port, M.; Roch, A.; Robic, C.; Elst, L. V.; Muller, R. *Chem Rev* 2008, 108, 2064-2010.
- [205] Wu, Y.; Song, L.; Hu, Y. *Polym-Plast Technol Eng* 2012, 51, 647-653.
- [206] Sang, X. M.; Wu, P.; Chen, X. G.; Hou, G. X. *Adv Mater Res* 2010, 139, 90-93.
- [207] Zan, L., Tian, L.; Liu, Z.; Peng, Z. *J Appl Catal A* 2004, 264, 237-242.
- [208] Shang, J.; Chai, M.; Zhu, Y. *J Solid State Chem* 2003, 174, 104-110.
- [209] Zan, L., Wang, S.; Fa, W.; Hu, Y.; Tian, L.; Deng, K. *Polym* 2006, 47, 8155-8162.
- [210] Herrera-Sandoval, G. M.; Baez-Angarita, D. B.; Correa-Torres, S. N.; Primera-Pedrozo, O. M.; Hernández-Rivera, S. P. *Mater Sci Appl* 2013, 4, 179-185.
- [211] Wang, Z.; Li, G.; Peng, H.; Zhang, Z. *J Mat Sci* 2005, 40, 6433-6438.
- [212] Zhang, J.; Wang, X., Lu, L.; Li, D., Yang, X. *J Appl Polym Sci* 2003, 87, 381-385.
- [213] Della Pelle, A. M.; Maliakal, A.; Sidorenko, A.; Thayumanavan, S. *Thin Solid Films* 2012, 520, 6262-6267.
- [214] Ma, C. C. M.; Chen, Y. J.; Kuan, H. C. *J Appl Polym Sci* 2006, 100, 508-515.
- [215] Chae, D. W.; Kim, B. C. *Polym Adv Technol* 2005, 16, 846-850.
- [216] Yao, T.; Li, Z.; Yi Zheng, J.; Chao, G.; Zhi Zhen, Y.; Ye Feng, Y.; Qing Ling, W., *J Mater Chem* 2010, 20, 1594-1599.
- [217] Zhong, W.; Liu, P.; Shi, H. G., Xue, D. S. *Express Polym Lett* 2010, 4, 183-187.
- [218] Ali, T.; Venkataraman, A. *Int J Adv Eng Technol* 2014, 7, 122-126.
- [219] Tang, L.; Cheng, J. *Nano Today* 2013, 8, 290-312.
- [220] Hsieh, T. H.; Kinloch, A. J.; Masania, K.; Sohn Lee, J.; Taylor, A. C.; Sprenger, S. *J Mater Sci* 2010, 45,1193-1210.
- [221] Kongsinlark, A.; Prasassarakich, P.; Rempel, G. L. *Chem Eng J* 2012, 193, 215-226.
- [222] Camkerten, R.; Erdogan, S.; Altinten, A.; Alpbaz, M. *Indian J Chem Technol* 2012,19, 185-190.
- [223] Wu, T.; Ke, Y. *Thin Solid Films* 2007, 515, 5220-5226.
- [224] Whittington, A. P.; Nguyen, S. T.; Kim, J.-H. *Nanoscape* 2009, 6, 26-29.
- [225] Zhang, H.; Xiping, L.; Zhixing, S.; Peng, L. *J Polym Res* 2007, 14, 253-260.
- [226] Savin, D. A.; Pyun, J.; Patterson, G. D.; Kowalewski, T. *J Polym Sci Part B: Polym Phys* 2002, 40, 2667-2676.
- [227] Xu, B.; Fu, Y. Q.; Ahmad, M.; Luo, J. K.; Huang, W. M.; Kraft, A.; Reuben, R.; Pei, Y. T.; Chend, Z. G.; De Hosson, J. Th. M. *J Mater Chem* 2010, 20, 3442-3448.
- [228] Vaccaro, K.; Davis, A.; Dauplaise, H. M.; Spaziani, S. M.; Martin, E. A.; Lorenzo, J. P. *J Electron Mater* 1996, 25, 603-609.

- [229] Lin, Y. F.; Song, J.; Ding, Y.; Lu, S. Y.; Wang, Z. L. *Appl Phys Lett* 2008, 92, 022105-1-022105-3.
- [230] Salata, O. V.; Dobson, P. J.; Sabesan, S.; Hull, P. J.; Hutchison, J. L. *Thin Solid Films* 1996, 288, 235-238.
- [231] Wang, H. Q.; Wang, J. H.; Li, Y. Q.; Li, X. Q.; Liu, T.-C.; Huang, Z.-L.; Zhao, Y.-D. *J Colloid Interface Sci* 2007, 316, 622-627.
- [232] Kuljanin, J.; Vucković, M.; Čomor, M. I.; Bibić, N.; Đoković, V.; Nedeljković, J. M. *Eur Polym J* 2002, 38, 1659-1662.
- [233] Jakovljević, J. K.; Cincović, M. M.; Stojanović, Z.; Krklješ, A.; Abazović, N. D.; Čomor, M. I. *Polym Degrad Stab* 2009, 94, 891-897.
- [234] Haritz, H.; Iñaki, Z.; Agnieszka, T.; Arantxa, E.; Galder, K.; Iñaki, M. *J Nanosci Nanotechnol* 2013, 13, 643-648.
- [235] Agarwal, S.; Patidar, D; Saxena, N. S. *Heat Mass Transf* 2013, 49, 947-953.
- [236] Xue, H. T.; Zhao, P. Q. *Appl Phys A* 2013, 110, 259-262.
- [237] Kim, S.; Seo, J.; Ramdon, R.; Pyo, H.-B.; Song, K.; Kang, B.H. *J Nanomater* 2012, 2012, Article ID 693575, 9 pages.
- [238] Han, M.; Gao, X.; Su, J. Z.; Nie, S. *Nature Biotech* 2001, 19, 631-635.
- [239] Michalet, X.; Pinaud, F. F.; Bentolila, L. A.; Tsay, J. M.; S. Doose, S.; Li, J. J.; Sundaresan, G.; Wu, A. M.; Gambhir, S. S.; Weiss, S. *Science* 2005, 307, 538-544.
- [240] Capezzuto, F.; Ciampa, F.; Carotenuto, G.; Meo, M.; Milella, E.; Nicolais, F. *Compos Structures* 2010, 92, 1913-1919.

Chapter 9

POLYSTYRENE SPHERES FOR TEMPLATE IN THE PRODUCTION OF NANOSTRUCTURED MATERIALS

Asep Bayu Dani Nandiyanto^{1,}, Takashi Ogi² and Kikuo Okuyama²*

¹Departemen Kimia, Fakultas Pendidikan Matematika dan Ilmu Pengetahuan Alam,
Universitas Pendidikan Indonesia, Bandung, Indonesia

²Department of Chemical Engineering, Graduate School of Engineering,
Hiroshima University, Higashi Hiroshima, Japan

ABSTRACT

Research progress in developing synthesis of polystyrene spheres with controllable physicochemical properties (i.e. size and charge) and showing effectiveness of these properties as a template for assisting the creation of material with various morphologies and pore structures is the main topic in this chapter. The available process parameters (e.g. temperature, amount of styrene, and type and concentration of initiator) to achieve a smart strategy that is capable of regulating interaction, reaction, and growth of styrene are introduced. By controlling this smart strategy, control of the physicochemical properties is possible. Indeed, this control offers great advantages as the template for creating innovative materials that have advanced performances and are applicable for various practical applications, such as phosphors, photocatalysts, and adsorbents.

Keywords: Polystyrene particles; nucleation and particle growth process; template; hollow particles; self-organization; zeta potential

1. INTRODUCTION

Polystyrene is a low-cost thermoplastic polymer that is easily produced, spherical shape with relatively monodisperse, and excellent properties (e.g. chemically stable, corrosion resistance, typically non-biodegradable, and relatively low refractive index). [1, 2] These

* Corresponding author: Email: nandiyanto@upi.edu

advantages make polystyrene to be the most useful plastics for wide range applications, such as a template [3], a fluorescent label [4], a protein adsorber [5], and a main component in the common facility products [1], such as cups, food containers, toys, home furniture, building materials, etc.

In this chapter, research progress in developing synthesis of polystyrene spheres with controllable physicochemical properties (i.e. size and charge) and showing effectiveness of these properties for assisting the creation of material with excellent nanostructures, including porous and hollow materials with control over hole cavity, internal structure, and external shape, is discussed. Examples of the effect of additional polystyrene template on the improvement of material performance, including phosphors, photocatalysts, and adsorbents, are also reported.

2. GENERAL STRATEGIES TO SYNTHESIZE POLYSTYRENE WITH CONTROLLABLE SIZE AND CHARGE

Several developments for the synthesis of polystyrene have been reported with no limitation to a particular type of process [6]: dispersion polymerization, emulsion polymerization, and seeded emulsion polymerization. Although the suggested methods have different synthetic procedures, the principle for all these processes is almost the same. The synthesis method involves polymerization of styrene monomer under the existence of initiator. This offers a potential way to synthesize polystyrene with specific physicochemical properties by regulating a smart strategy that is capable of controlling interaction, reaction, and growth of styrene during styrene polymerization. For achieving this smart strategy, optimization of synthesis parameters (i.e. reaction temperature, amount of styrene, and type and concentration of initiator) are inevitable. [7] Therefore, the following sub-sections discuss in detail about the effect of several parameters on properties of polystyrene.

2.1. Physicochemical Analysis of Polystyrene Spheres

To be effective for practical applications such as template, polystyrene must be spherical, monodisperse in size [8], and disperse in a specific solvent [9, 10]. To achieve this requirement, regulating the synthesis parameters (i.e. reaction temperature, amount of styrene, and type and concentration of initiator) is important. [7] Here, as a model, polystyrene is synthesized by a simple polymerization of styrene monomer using various synthesis parameters in an aqueous solution under surfactant-free conditions (Figure 1). [7] Scanning electron microscope (SEM) images shown in Figures 1a-d verify that relatively monodispersed particles with a spherical shape can be produced for all variations. Size of polystyrene is controllable from tens to hundreds of nanometers, depending on parameters used during the synthesis process. A photograph image in Figure 1e shows the dispersity of the polystyrene colloidal suspension. Turbidity of the polystyrene colloidal suspension depends on the size of polystyrene itself, where the smaller polystyrene results in the more transparent suspension gained. This informs the successful formation of polystyrene can be investigated directly by a visible observation.

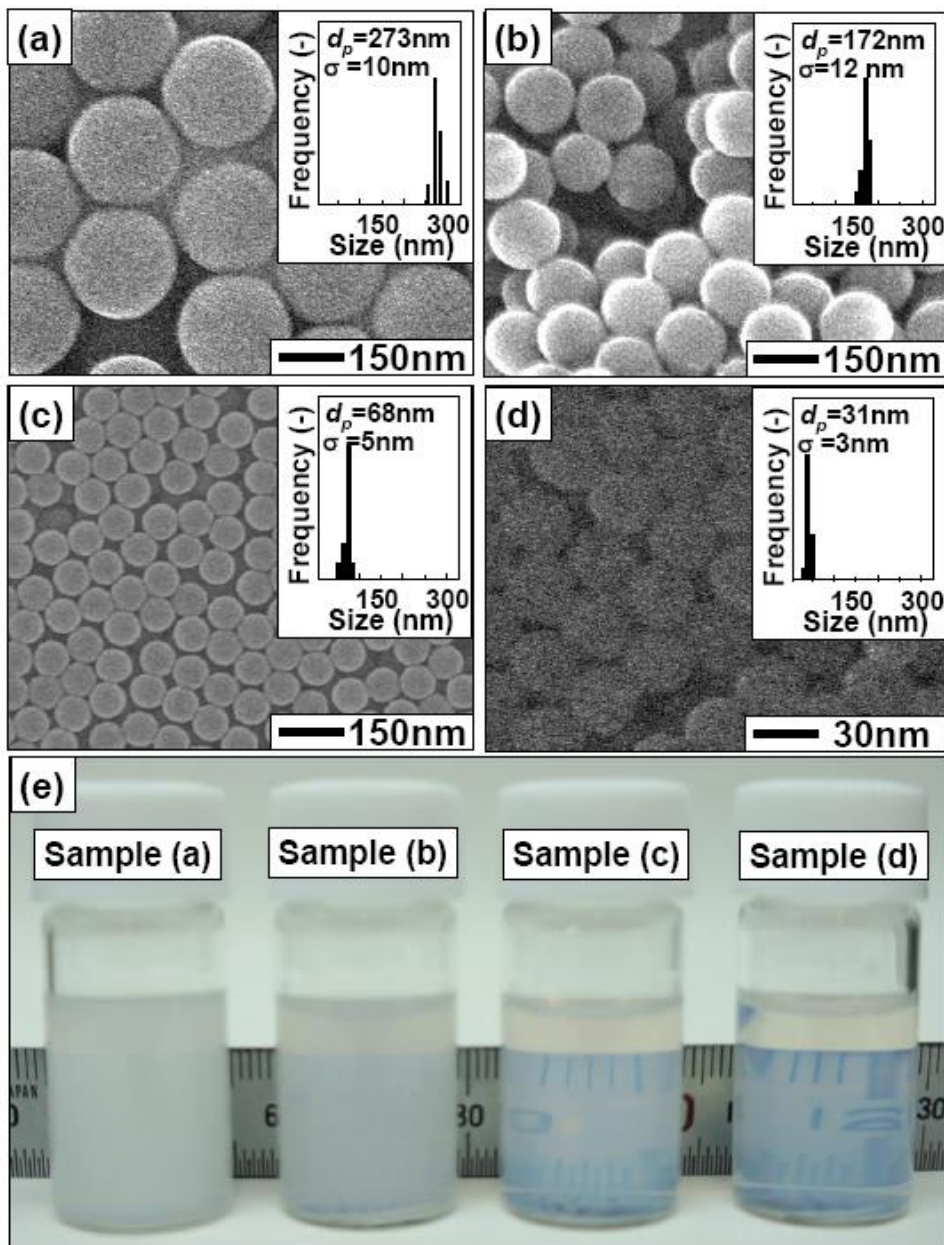


Figure 1. SEM images of polystyrene produced using various process parameters (temperature ($^{\circ}\text{C}$)/styrene amount (wt%)/AIBA initiator amount (wt%)): (a) 55/2.00/0.0400; (b) 55/0.80/0.0400; (c) 90/0.40/0.0400; and (d) 90/0.40/0.0040. Figure (e) is the photograph image of polystyrene samples. Figure was adopted from reference [7]. Note: d_p is the diameter of polystyrene. AIBA is 2,20-Azobis (2-methylpropionamide) dihydrochloride.

Due to absence of additive (e.g., chemicals, surfactants, polymers, salts, etc), all process parameters produce polystyrene material, confirmed by a fourier transmission infra red (FTIR) analysis in Figure 2. This verifies that the present process is reliable with respect to the quality of the polystyrene product. The change in the preparative conditions affects the

particle size only, driving the need for understanding the effect of the synthesis parameters for gaining polystyrene with specific physicochemical properties.

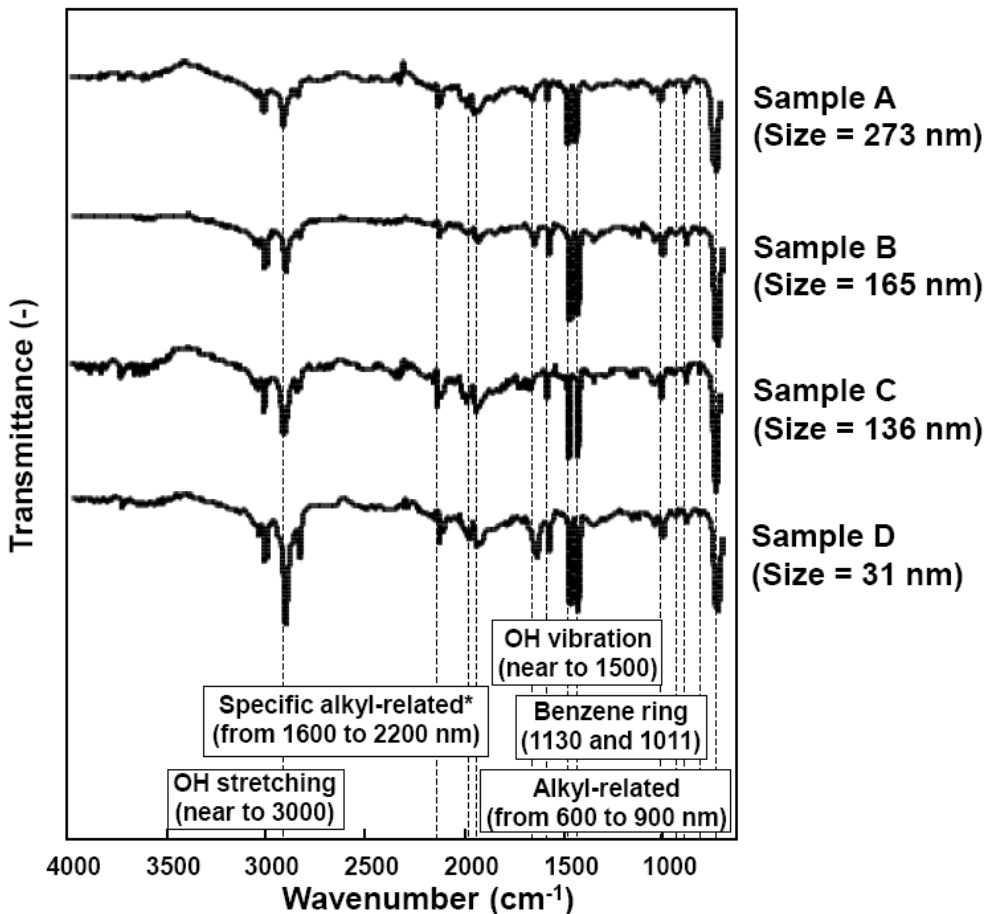


Figure 2. An FTIR analysis result of polystyrene with various sizes. Sample A, B, C, and D are the samples that were characterized in Figures 1(a), 1(b), 1(c), and 1(d), respectively. Figure was adopted from reference [7].

2.2. Effect of Temperature

One of the most contributed parameter involving the reaction is temperature. [11, 12] In the common polymerization process, this parameter might be responsible for the control of reaction via several roles: (i) improving reactant solubility in the solvent medium, (ii) enhancing initiation efficiency, (iii) making higher contact, interaction, and collision among the reactants, and (iv) increasing the propagation rate but at the same time reducing the possibility in the radical termination. [7, 13, 14] The roles suggest that high-temperature process makes high interaction of monomer and other reactants possible. [15] However, since this condition leads the consumption of monomers in the initial stage of the polymerization (i.e. the nucleus construction), the retardation of the particle growth step can be created. [7, 11, 16] As a consequence, the size decreases significantly with the increase in temperature

(shown in Figure 3). The impact of the temperature has been found for wide range of reactant compositions, as shown in Figures 3a-c that are processing the polymerization at a styrene concentration of 2.00, 0.80, and 0.40 wt%, respectively.

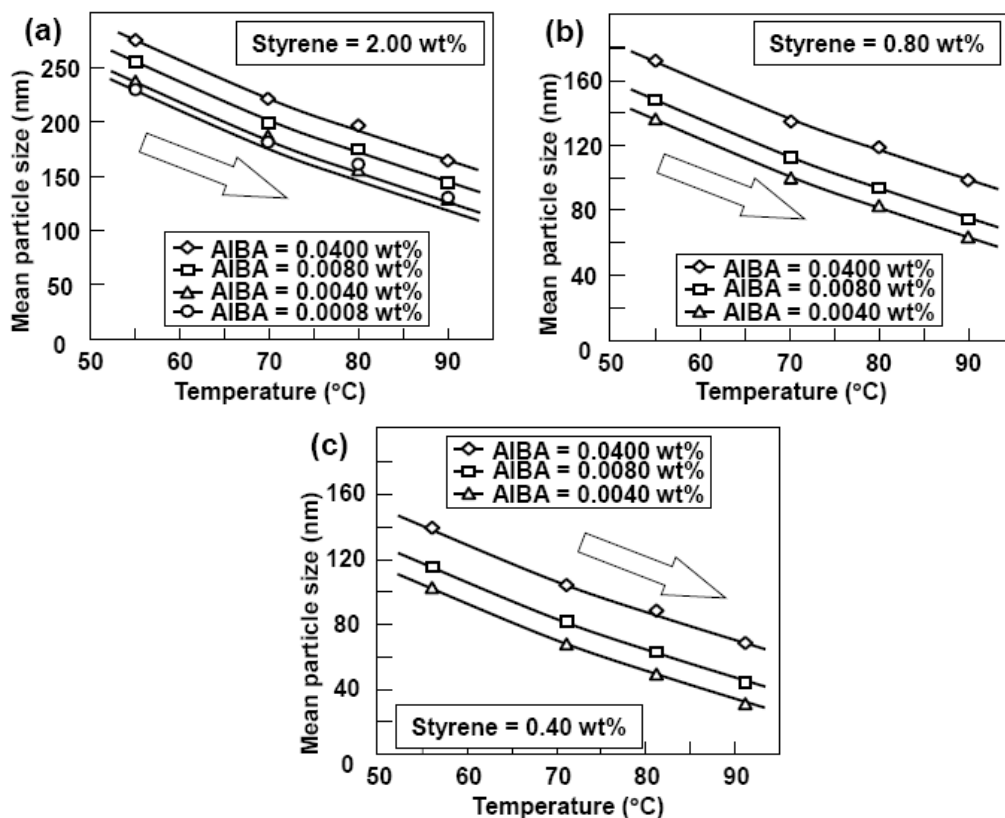


Figure 3. Effect of styrene concentration on the particle size under various temperatures: (a) 55, (b) 70, (c) 80, and (d) 90°C. Samples are also conducted with different initiator concentrations, ranging from 0.0008 to 0.400 wt%. As a model of initiator, AIBA was used. Figures were adopted from reference [7].

Although the change in temperature is excellent for controlling polystyrene size, the use of this parameter should be considered. [7] Too low temperature is not effective because it is related to the requirement of reaction time needed for converting styrene monomer into polystyrene. [17] On the contrary, too high temperature must be considered with the physicochemical properties of reactants and solvent.

2.3. Effect of Styrene Concentration

Other parameter that is also important for the polymerization process is styrene monomer. Styrene monomer is the main source for the formation of polystyrene; indeed, the increase in styrene concentration must have a positive impact to the progress in the polystyrene growth process. In the case of polystyrene synthesized using additive-free conditions, size of polystyrene increases from several tens to hundreds of nanometers as the

increase in styrene concentration (Figure 4). The trends of the effect of styrene amount on the polystyrene size are the same although the process is conducted with different temperatures (i.e. 55, 70, 80, and 90°C; corresponding to Figures 4a, b, c, and d, respectively).

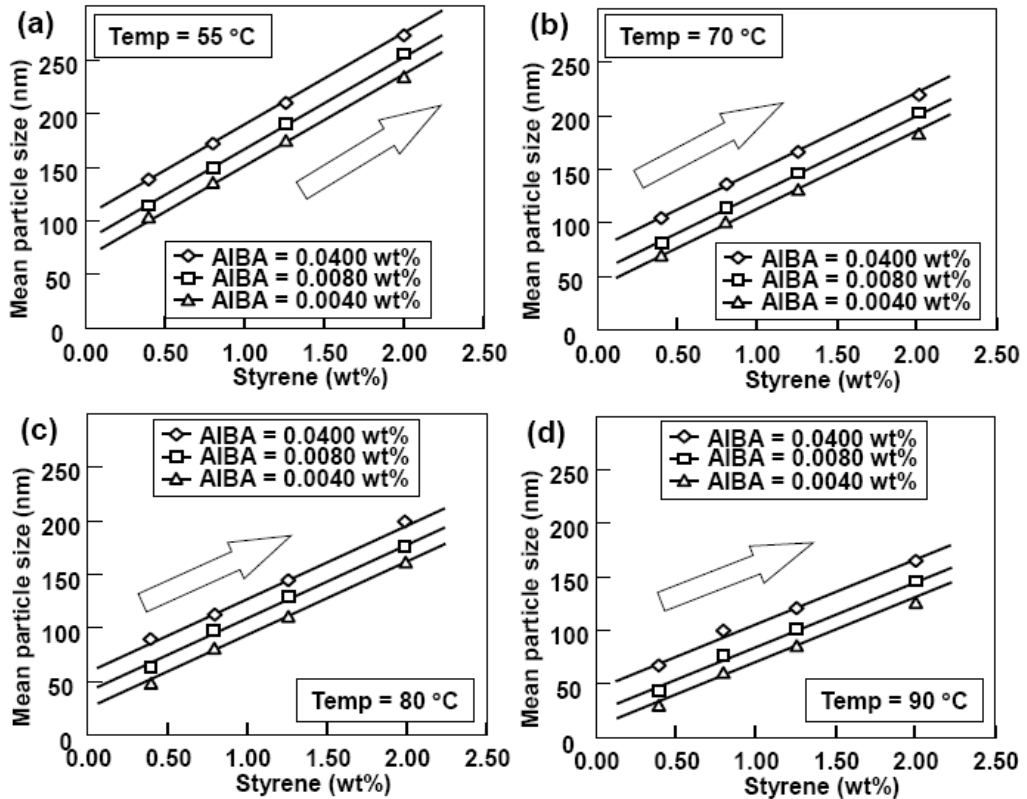


Figure 4. Effect of temperature on polystyrene size: (a) 55, (b) 70, (c) 80, and (d) 90°C. Samples are also synthesized using different initiator concentrations, ranging from 0.0040 to 0.0400 wt%. As a model of initiator, AIBA was used. Figures were adopted from reference [7].

Although increase in styrene concentration is effective to enlarge polystyrene size, the amount of styrene should be considered. [14] Excess styrene concentration would create problems in the polymerization process, such as solubility of styrene and radical polymerization.

These problems allow the production of polystyrene with a broad particle size distribution and the formation of a massive coagulum. [7] To minimize the radical polymerization process, additional techniques have been proposed, such as additional surfactant, water-alcohol system, and fed-batch reactor for the synthesis of polystyrene. [17] However, these techniques are not discussed in this chapter.

2.4. Effect of Initiator Type and Concentration

Beside temperature and styrene source, regulation of initiator is also important. Initiator decides number of ionic groups that have a positive impact to attack and activate styrene monomer. [7] With the existence of these active styrene component, a good progress in constructing longer oligomeric chain and forming larger particles can be achieved. [13, 17] As a consequence, polystyrene size depends on the amount of initiator used (Figure 5).

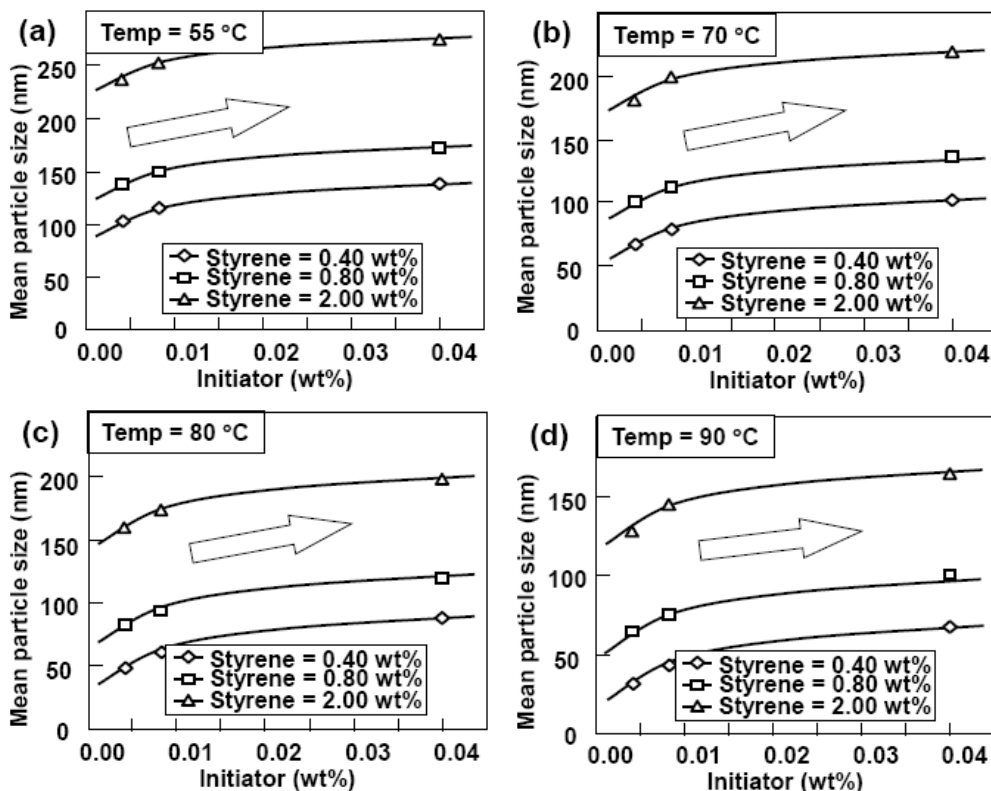


Figure 5. Mean particle size against detailed data on initiator and styrene concentrations under various temperatures: (a) 55, (b) 70, (c) 80, and (d) 90°C. Samples are also synthesized with different styrene concentrations ranging from 0.40 to 2.00 wt%. As a model of initiator, AIBA was used. Figures were adopted from reference [7].

Although changes in initiator amount have a direct correlation to number of ionic groups that have a positive outcome to the activation of styrene monomer, the concentration of initiator must be optimized. Too high or too low concentration of initiator has a correlation to the type of reaction.

In the case of too high concentration of initiator, this initiator does not make more efforts for enlarging polystyrene spheres. Excess initiator concentration causes production of unpredicted radical ionic groups that can allow reaction termination in the early stage. Indeed, this retards the growth process. [7]

Regarding to the case of too low concentration of initiator, anomaly results are possibly created. Number of ionic groups for activating styrene monomer are limited. As a consequence, some reactants are not converted well. Huge number of unreacted monomers in the solution remain. Finally, this condition would result the unpredictable polystyrene formation, such as broad size distribution.

In addition to the polystyrene size, type of initiator decides the type of polymerization (Figure 6). [7] Here, as a model of initiator, we show kalium persulphate (KPS) and 2,2,0-Azobis (2-methylpropionamide) dihydrochloride (AIBA). [9, 10] Different types of initiators have similar tendency on the polystyrene size (Figure 6a); However, when analyzing surface charge of the polystyrene produced, the change of initiator type can result different types of polystyrene (Figure 6b). The use of KPS allows the production of polystyrene with a negative zeta charge, whereas that of AIBA leads the formation of polystyrene with a positive zeta value. The change in the initiator concentration also influences to the magnitude of the polystyrene charge. The more initiator added results in the higher zeta charge value gained. These results confirm that to control polystyrene charge and magnitude, regulation of type and concentration of initiator is important.

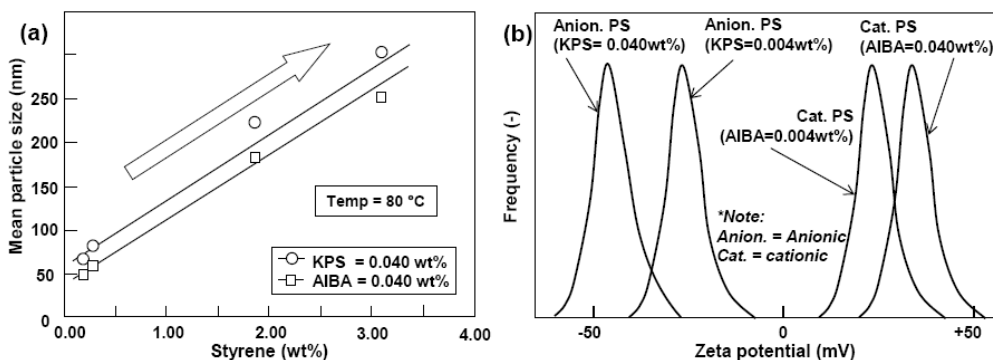


Figure 6. Effects of initiator type and concentration on physicochemical properties of prepared polystyrene. Figures were adopted from references [7, 9, 24, 25].

2.5. Empirical Formula for Predicting Polystyrene Size as an Effect of Several Parameters

Since the final polystyrene size can be interpreted as a wide range of preparative conditions (i.e. the temperature, the concentration of styrene, and the amount of initiator), prediction equation can be derived. [18] An example of overall predicting equation for the size of polystyrene reported by Nandiyanto et. al. [7] is shown in the following:

$$D_p = 71.80 \cdot S + 15.85 \cdot \ln(I) - 170.30 \cdot \ln(T) + 847.87 \quad (1)$$

where D_p , T , S , and I are the final particle size, the temperature, the concentration of styrene, and the amount of initiator, respectively.

Although the Nandiyanto's equation is purely empirical from the experimental data plot, this offers a useful guide to the selection and the adjustment of preparative conditions to provide a specific polystyrene size. For example, when intending the synthesis of polystyrene with a size of 100 nm in the fixed temperature of 70°C and the initiator concentration of 0.0200 wt%, the concentration of styrene that should be used is about 0.50 wt%.

3. PROGRESS IN THE ASSISTANCE OF POLYSTYRENE TEMPLATE FOR POROUS MATERIAL STRUCTURIZATION

Technology for the fabrication of porous material with a well-defined structure has been well-developed. [3] A number of techniques have been reported, and a template replication method using organic template is the best choice, known as the MCM-series, the SBA-series, and the HMM-series. [19] Although these methods show good utility for many applications, several limitations are noteworthy. For example, use of an organic surfactant has problems in the production of porous material with aspherical pores, bad pore arrangement and limited pore sizes. [20] Further, most of these processes have the limitation of producing film material only. [3] As an alternative, an organic particle, such as polystyrene, is the best choice because it produces spherical pores, permits maximal porosity, and allows the formation of homogeneous pore size and structure. [20]

To apply polystyrene as the template for assisting the creation of porous structures in the material, two steps of processes involve (Figure 7)[3]: (1) a self-assembly process of host component and polystyrene to form composite, and (2) a polystyrene removal process. By using this synthesis approach, innovative porous-structured material can be created.

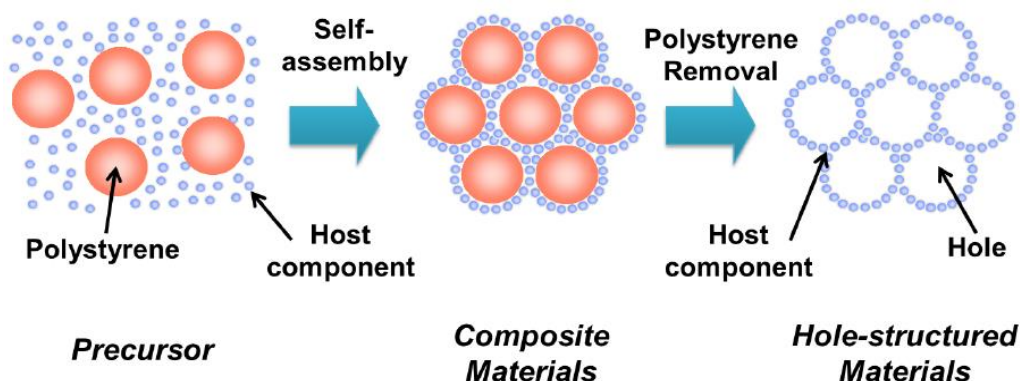


Figure 7. Schematic illustration of the use of polystyrene for assisting the creation of porous-structured material.

Since the pore is an inverse replica of the polystyrene, regulation of the self-assembly process is important. Based on the type of self-assembly process, there are two major parts of templating process: ex-situ and in-situ techniques. Both techniques are similar, except for the type of template used. The ex-situ technique uses colloidal polystyrene spheres directly. Although the pore size and shape can be predicted from the beginning of the templating

process, additional polystyrene synthesis procedure prior to the self-assembly process is required. Regarding the in-situ technique, the process involves polystyrene template formation at the same time with the self-assembly process in one-pot process. In simplification, the process is begun by adding initial host component and styrene monomer.

3.1. Ex-Situ Technique of Polystyrene Templating Method

As shortly described in the above definition about ex-situ technique, the process does not involve the formation of polystyrene during the self-assembly process. The size and shape of holes created are directly from the replication of those of polystyrene that are added in the precursor. [21] Here, several examples of the applications of ex-situ techniques for the production of porous and hollow material in film and particle forms are reported in the following:

3.1.1. Porous Film with Controllable Porous Structure

To produce material in film form, many methods have been well-documented [9, 10, 20, 21], such as dip-coating, spin-coating, bar-coating, dropped, spray method, etc. The main principle of the methods is the same, where the method is focused on how to self-assemble components on the surface of objective substrate. Prior to self-assembly process, the components typically is dissolved into specific solvent, namely precursor.

For adopting the ex-situ technique of polystyrene templating method in the coating method, polystyrene must be involved from the beginning of the coating process. Polystyrene must be added and combined with the host material in the initial precursor. This precursor then undergoes the self-assembly process.

Effect of additional polystyrene into the precursor on structurizing porous material in film form is shown in Figure 8. As a model of host material and polystyrene template, here we use 5-nm silica nanoparticles and 200-nm polystyrene spheres, respectively. When the precursor contains polystyrene only, self-assembly of precursor results in the formation of highly ordered polystyrene spheres on the surface of substrate (Figure 8a). When using precursor containing 5-nm silica and polystyrene, a composite film is produced (Figure 8b). Based on the conventional theory of multisize packing phenomena, hierarchical self-assembly process directly depends on the size of the component involved. The bigger component plays the role of structurizing agent for the smaller. As a result, a clear orientation of the hexagonal pattern, showing the act of polystyrene as a major building block while the silica nanoparticles in the void space between the polystyrene spheres, is found. After applying the polystyrene removal process to the composite film, polystyrene is removed from the composite, remaining porous structures in the final film product (Figure 8c). The formation of porous in all positions of the film are identical in structure, orientation, and dimension (shown in low-magnified SEM image in Figure 8d). FTIR analysis shows self-assembly of silica and polystyrene does not involve the chemical reaction [21], and the polystyrene removal process must be considered to remove polystyrene without changing the host material properties [22] (Figure 8e).

Based on the results in Figure 8, to be capable of regulating excellent interaction between polystyrene and host material, optimization of the amount and physicochemical properties (e.g. size and charge) of polystyrene is important factors (Figure 9). [9] Here, as a model,

silica (as a host material) and polystyrene are used and combined in the initial precursor. The parameters are described in the following.

To confirm the effect of amount polystyrene on porous structure, silica-to-polystyrene mass ratio is varied. Self-assembling precursor without polystyrene allows the formation of non-porous film (Figure 9a). However, when self-assembling precursor containing polystyrene, porous-structured film is obtained (Figures 9b, c). The additional polystyrene in the precursor initiates the creation of macroporous structure in the film, in which the number of pores increase with increasing polystyrene amount. Further excess in the polystyrene amount results in the formation of film with fragmented skeletal structures (Figure 9d). Interesting point gained from using this technique is the holes obtained in the film that are monodisperse in size and shape. "The size and shape" of holes follow "the size and the shape" of polystyrene identically.

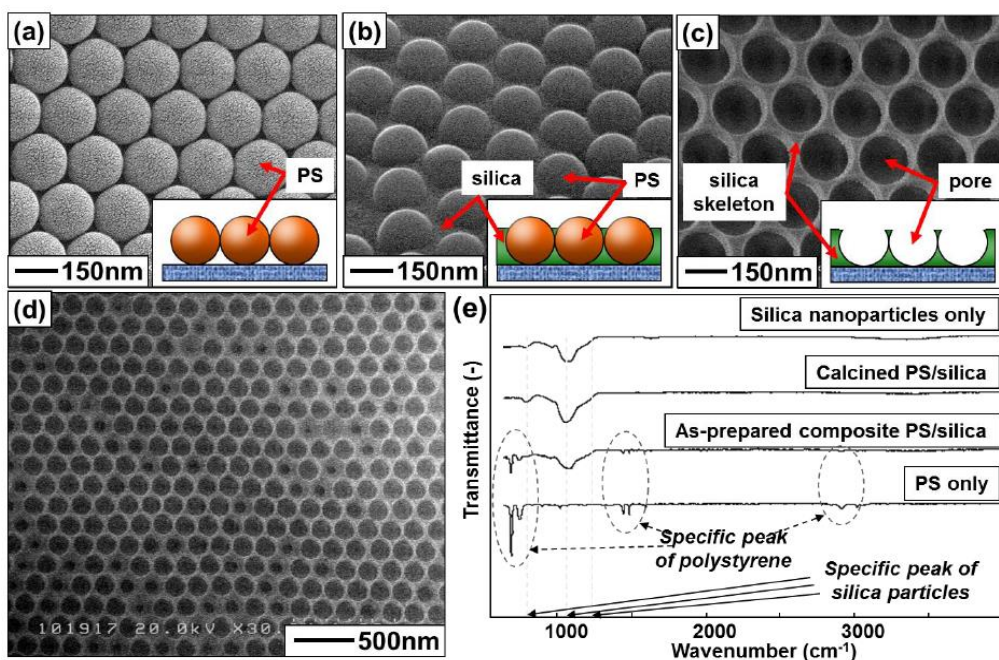


Figure 8. Effect of additional polystyrene on the preparation of porous-structured film. Figure (a) is the SEM image of coated film using precursor containing 200-nm polystyrene only, whereas Figures (b-d) are that using precursor containing 200-nm PS and 5-nm silica. Figures (b) and (c) are the SEM images of the coated film before and after the polystyrene removal, respectively. Panel (d) is a low-magnified SEM image of the film imaged for panel (c). Inset figure in (a-c) is the illustration of the silica and polystyrene configuration. Figures were adopted from reference [9].

According to the above hypothesis (shown in Figure 7), control of self-assembly process between host and polystyrene becomes the major factor. Therefore, understanding the influence of charge of host and polystyrene is inevitable. [23] In general, the charge decides what level of particle-particle interaction and repulsion forces during the self-assembly process. [9] These interactions drives the formation of porous film with different configurations (Figures 9c, e, and f). As shown in Figures 9c and e, the successful formation of porous film can be gained only by conducting the process with repulsive interactions

between the colloidal components. These repulsive interactions are achieved by using silica and polystyrene particles with negative zeta values. On the contrary, the use of polystyrene with a positive zeta charge results formation of hollow particles on the film (Figure 9f).

Aside from needing the same sign of surface charges for silica and polystyrene, the magnitude of component charge is also important. [24] Since silica is typically in the negative zeta charge and its charge magnitude cannot be changed using a simple technique, [9] control of porous structure mainly depends on the polystyrene charge. Only polystyrene with sufficient charge (surface charge ≤ -30 mV) leads to the creation of porous hexagonal arrangements (Figure 9c), whereas those with less charge enable only a non-optimal porous configuration to form (Figure 9e).

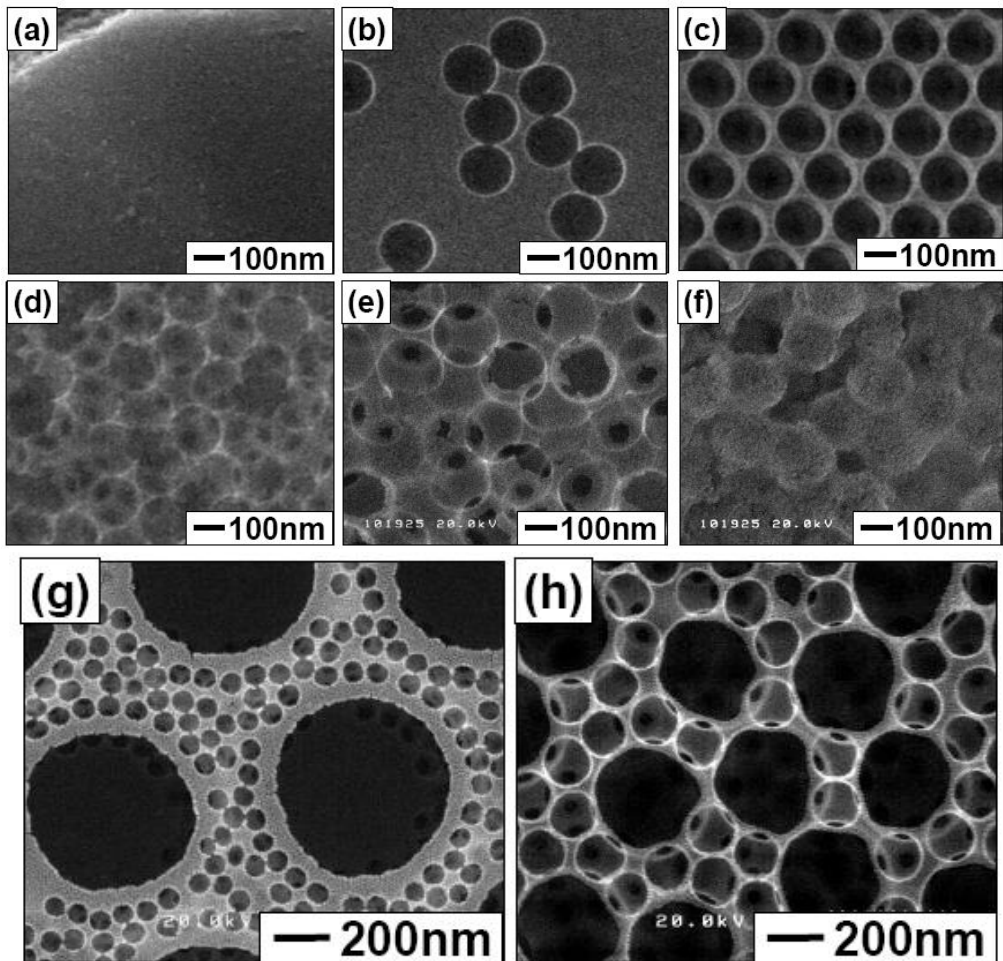


Figure 9. SEM images of the film prepared with various process parameters. Figures (a), (b), (c), and (d) are film prepared using silica-to-polystyrene mass ratios of "no polystyrene", 1.00, 0.50, and 0.10, respectively. Figures (b-d), (e), and (f) are film prepared using polystyrene with charge of -40, -25, and +40 mV, respectively. Figures (b-f), (g), and (h) are film prepared using polystyrene with a diameter of 200; 1000 and 100; (c) 500 and 200 nm, respectively. Figures were adopted from references [9, 20].

In addition, although higher magnitude value of polystyrene potentially assists the hexagonal porous structure, the production of this higher value has a relation to the amount of initiator used (discussed in the above Figure 6). In fact, higher amount of initiator would result the more number of ions (i.e. K^+ , SO_4^{2-} , and $S_2O_8^{2-}$) exist in the precursor that have negative impacts on the electrostatics and interactions between colloidal particles (e.g., coagulation, flocculation, etc.). Indeed, this creates problems in the porous structurization and skeleton strength. [24]

As discussed in the above, since pores are from reflection of polystyrene, this drives an idea that control of pore size is possible by changing the polystyrene size. Here, to clarify the impact of polystyrene size, Nandiyanto et al. reported the use of dual sizes of polystyrene as the template (Figures 9g, h). [20] As expected, evolution of pores is a function of the size of polystyrene template used. The use of polystyrene with size of "1000 and 100 nm" (Figure 9g) and "500 and 200 nm" (Figure 9h) is effective to produce film with pores of "1000 and 100 nm" and "500 and 200 nm", respectively.

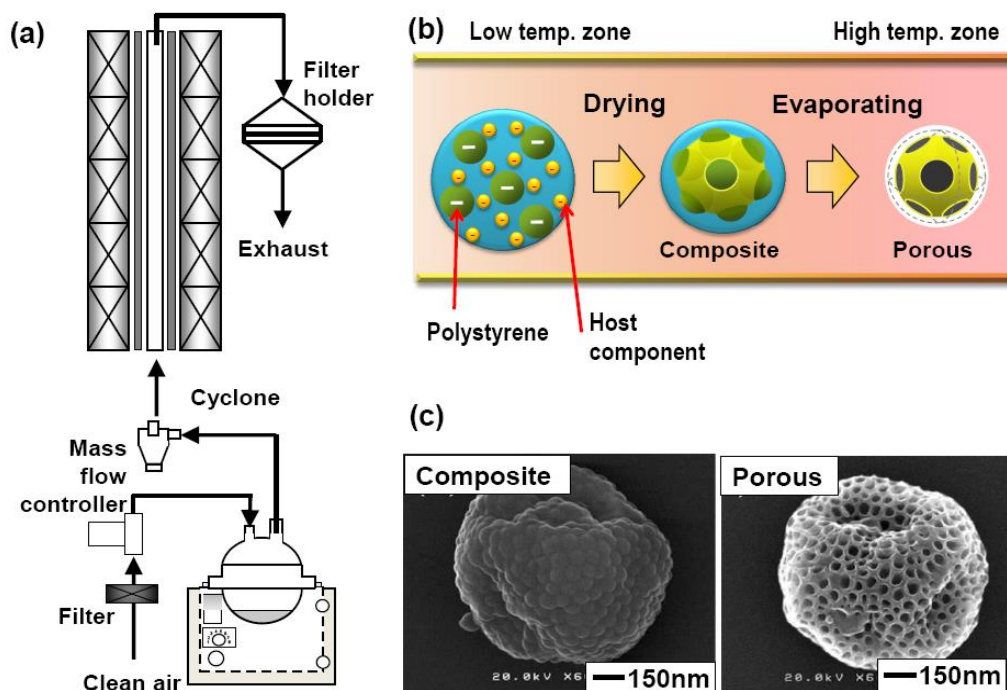


Figure 10. Schematic illustration of spray apparatus (a) with particle formation mechanism (b) and SEM result (c). Figures were adopted from references [10, 22].

3.1.2. Spray Method for Production of Particles with Controllable Hole Configuration

To produce particles, an aerosol-assisted self-assembly technique has been the most promising. [3] One of the method to get this technique is spray method. The main principle of this technique is to deliver and rapidly heat an initial solution/slurry via the direct injection of very small droplets.

Figure 10a is a schematic illustration of spray apparatus, and Figure 10b is mechanism of the assistance of polystyrene for creating porous-structured particles. In simplification, the

process is started by the atomization process to form droplet. The generated droplets are introduced to the droplet-to-particle conversion via solvent evaporation, forming composite host/polystyrene particles. The composites then undergo the polystyrene removal process to form porous-structured particles. Examples of the formation of composite and porous particles produced using a spray method are shown in the attached image in Figure 10c.

Based on the above mechanism, the key parameters to gain particles with unique morphology are (i) atomizer type (to control droplet size and charge), (ii) type, composition, and physicochemical properties of precursor, (iii) additional additive, and (iv) processing condition (temperature, pressure, etc). [3] Here, for investigating the effectiveness of polystyrene as the template in the ex-situ technique via a spray method, precursor containing silica (as a host material) and polystyrene is used as a model.

A potential advantage of polystyrene as the template in the spray method is shown in Figure 11. Similar to the above discussion in porous-patterned film formation in Figure 9, several parameters involve the porous particle formation. Here, parameters discussed are the mass ratio of silica-to-polystyrene, charge and size of polystyrene, and charge of droplet.

Spray-dried precursor with no additional polystyrene results in the production of spherical non-porous particles (Figure 11a). When using precursor containing polystyrene, it allows the formation of porous particles (Figures 11b-l). The roles of polystyrene as the template during the particle formation are found. Number of holes depend on the number of polystyrene added in the solution (Figure 11b), and excess polystyrene composition in the precursor leads to the formation of a broken particle (Figure 11c). Therefore, to develop maximal pore arrangements in the particle, the optimization of host-to-polystyrene composition is inevitable.

Figures 11b, d–f are the SEM images of particles prepared with various polystyrene surface charges. As discussed in the above section shown in Figures 9c, e, f, self-assembly process depends on the charge of the component and level of colloidal-colloidal interaction and repulsion forces. Since silica is a negative zeta charge, only the use of negatively charged polystyrene can assist the formation of porous particles (Figures 11b,d,e), whereas the process with positively charged polystyrene leads the creation of hollow particles (Figure 11f). The influence of charge magnitude allows the formation of porous particle with different hole configurations (shown in dashed red area). The use of polystyrene with high charge magnitude results in porous particles with kissing holes (Figure 11d), whereas those obtained with less magnitude exhibits fewer kissing holes (Figure 11e).

To confirm the effectiveness of polystyrene as the template, the use of various colloidal sizes (as the host material) and spray-drying process conditions is shown in Figures 11b,g–l. In spite of various particle morphologies, the appearance of holes that are identical to the polystyrene in size and shape verifies the effectiveness of polystyrene to replicate the hole formation. Changes in the host material transform only the skeleton structure (Figures 11g-i), while uses of polystyrene with different sizes can change the hole sizes (Figure 11j).

Effect of droplet charge is paneled in Figures 11k and l. As shown in these figures, the droplet charge affects the type of self-assembly process of component during the spray-drying process, which leads the change in the morphology and configuration of the hole inside the particle. The simplification of this discussion is in the following.

When utilizing uncharged droplet as common spray methods do, porous particles are produced (Figures 11b-j). Although various hole-structured particles (including porous and hollow particles) can be created, the shapes of particles produced are basically spherical. [3]

This is because the self-assembly phenomena involve the physicochemical properties of the colloidal nanoparticles only. However, when the spray-drying method is conducted under charged droplet conditions, consideration of additional factors in the self-assembly process phenomena must be added. The charge of droplet charging adds electrostatic interactions to the host and polystyrene during the self-assembly process. As a consequence, in addition to solvent evaporation and colloid-colloid interactions, several phenomena happen[10]: (i) attractive and repulsive interactions between the colloidal particle and the droplet surface, (ii) ion emission, and (iii) mass reduction (Rayleigh limit theory).

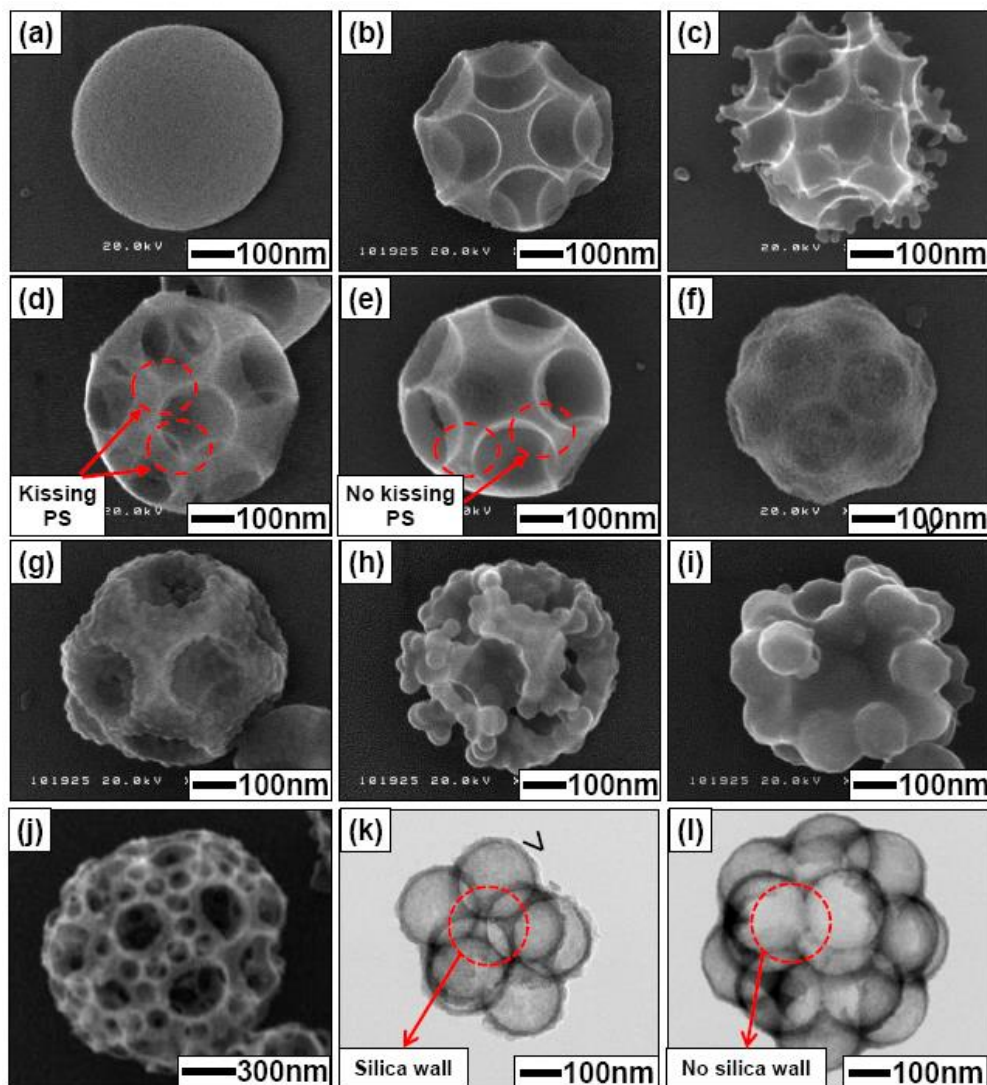


Figure 11. Electron microscope images of various porous silica particles prepared with various spray-drying process conditions. Figures were adopted from references [9, 10, 20].

Thus, combination of these factors in the self-assembly process results in the formation of particles with various morphologies, which are different from a common spray-drying method (shown by transmission electron microscope (TEM) images in Figures 11k and l). Then,

when this charge is combined with the charges of silica and polystyrene, different internal structures are found. Combination of silica and positively charged polystyrene results in the production of daisy-shaped particles with silica wall (Figure 11k), whereas those of silica and negatively charged polystyrene leads the formation of daisy-shaped particles without silica wall (Figure 11l).

3.1.3. Liquid-Phase Synthesis Method for Synthesis of Core-Shell and Hollow Particles with Controllable Shell Structural Properties

Beside film coating and spray methods, polystyrene is also effective for assisting porous structure in the common liquid-phase synthesis methods. [12, 24, 25] Similar to above methods in preparing porous-structured material in the ex-situ technique, several factors should be considered during the self-assembly process, specifically relating to the physicochemical properties of the polystyrene.

A schematic illustration of the self-assembly process in the liquid-phase synthesis method is shown in Figure 12. As a model, polystyrene is used as a core, whereas the reactants are the basic chemical for the formation of shell component. When polystyrene is contacted with reactants, interaction between polystyrene and shell component happens. This shell component involved in this process can be in several forms: monomers, clusters, nuclei, and particles. [11, 16] The resulting shell component products then interacts with the core component, namely the self-assembly process.

During the self-assembly process, three types of reactions are possible [12]: (i) individual formation (i.e. reactant interaction, reaction, nucleation, and growth processes; as indicated by the grey arrows), (ii) shell component deposition on the polystyrene core surface (as shown by the black and dashed arrows), and (iii) growth of shell component on the surface of polystyrene core (shown by the green arrows). Regarding deposition route shown by the black and dashed arrows, monomers/oligomers interacts with the core by several routes: diffusion-adsorption of monomers/oligomers on the polystyrene core surface (Routes R1 and R2), attraction and aggregation of clusters, nuclei, and nanoparticles to the polystyrene core surface (Routes R3–R5), and growth of the nuclei to form free nanoparticles.

Example of the above model for the interaction of polystyrene and magnesium fluoride (MgF_2) is shown in Figure 13. As a model of reactant, magnesium chloride (MgCl_2) and ammonium fluoride (NH_4F) are used as the magnesium and fluoride sources, respectively. In this approach, MgCl_2 and NH_4F quickly dissolve to form Mg^{2+} and F^- ions in solution, facilitating formation of MgF_2 monomers, clusters, nuclei, and particles. [11, 16]

Based on the model in Figure 13, control of self-assembly process is successfully achieved by carefully regulating how to control the interaction and reaction between the MgF_2 and polystyrene core. [12] The MgF_2 cluster can participate in three possible routes: (1) the cluster grows independently and is not influenced by the electrostatic attractive force exerted by the polystyrene core (Route a); (2) the cluster is attracted by the polystyrene core provided that the rate of MgF_2 formation is faster than that of MgF_2 deposition on the polystyrene surface (Route b); or (3) the cluster is attracted by the polystyrene core provided that the rate of MgF_2 formation is slower than that of MgF_2 deposition on the polystyrene surface (Route c).

To achieve the above hypothetical route, a smart strategy capable of controlling interaction, reaction, and growth of shell component on the surface of polystyrene can be achieved by managing several synthesis parameters. [24, 25] Route a proceeds when using

polystyrene with a positive zeta surface charge, whereas Routes b and c are achieved when employing polystyrene with a negative zeta surface charge. In the case of Routes b and c, both routes are tunable accordingly by controlling the reaction temperature and reactant composition. High-temperature process allows the formation of raspberry-like shell (Route b), whereas low-temperature process affords formation of shell with a smooth shell via (Route c). Additionally, modulation of the reactant composition enables the formation of shell with different shell thicknesses. Finally, additional template removal process to the synthesized composite $\text{MgF}_2/\text{polystyrene}$ particles is possible to afford the production of hollow MgF_2 particles with controllable shell structure.

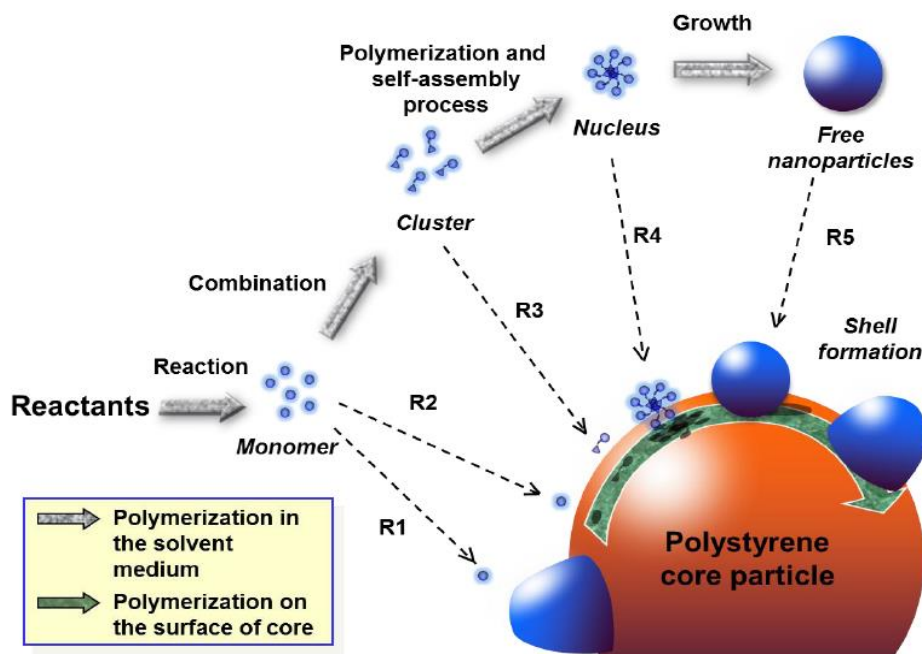


Figure 12. Schematic illustration of formation of host shell on the surface of polystyrene template. Figure was adopted from reference [12].

As shown in the Figure 13, the shape and size of the holes are identical to the that of polystyrene. This advantage makes it attractive to control the hole size by controlling polystyrene diameter. Examples of the use of polystyrene with different diameters for creating hollow particles are shown in Table 1.

Beside above model for the coating process, strategies for the successful shell component coating on the surface of core must be considered; Otherwise, the unsuccessful coating process can be obtained, as shown in Route a in Figure 13. Simplification illustration for the successful coating process is shown in Figure 14. Here, the way for the coating process can be classified into two options: (1) pure electrostatic and (2) additional additive. The fundamental process for both methods is the same, which relates only on how to attract/adsorb shell component on the surface of core.

The first strategy can be gained when the core and shell components are in the opposite charges (Figure 14a). On the contrary, the second strategy is when the core and shell components are in the same charge sign (Figure 14a). Regarding to the second strategy, since

the charges of core and shell can make repulsive phenomena, additional additive is required. This additive plays an important role to bridge and paste the shell component on the surface of core material.

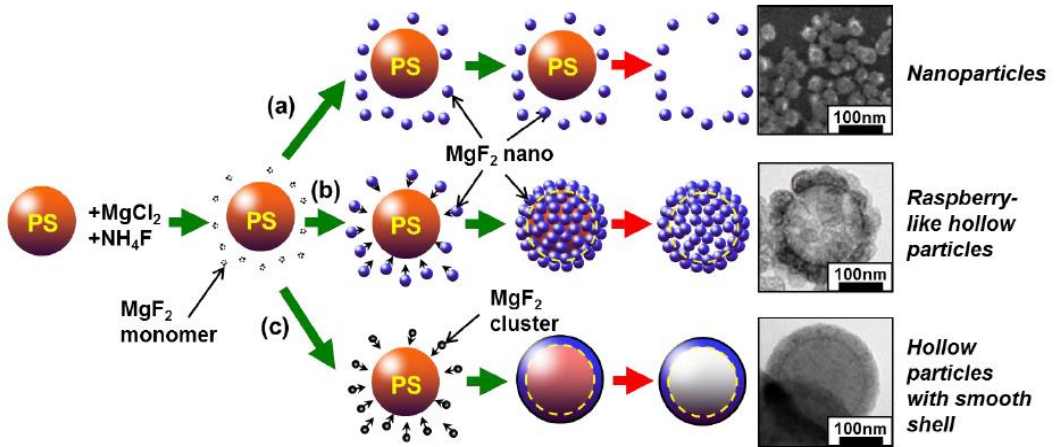
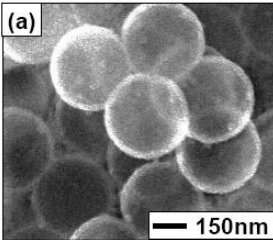
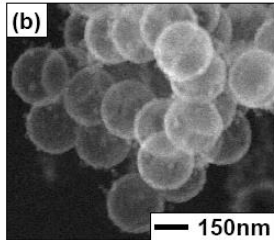
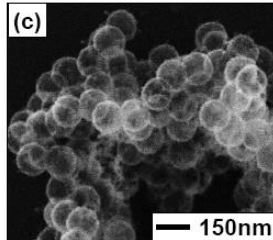
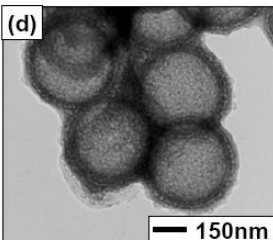
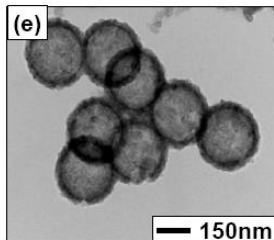
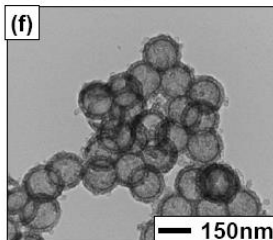


Figure 13. Schematic representation of formation of MgF_2 on the surface of polystyrene. Figure was adopted from reference [12]. Note: PS is the polystyrene.

Table 1. Electron microscope images of the hollow MgF_2 particles prepared with various polystyrene sizes: (a,d) 300, (b,e) 190, and (c,f) 100 nm. Figures were adopted from reference [12]

Analysis	Initial polystyrene size		
	300 nm	190 nm	100 nm
SEM			
TEM			

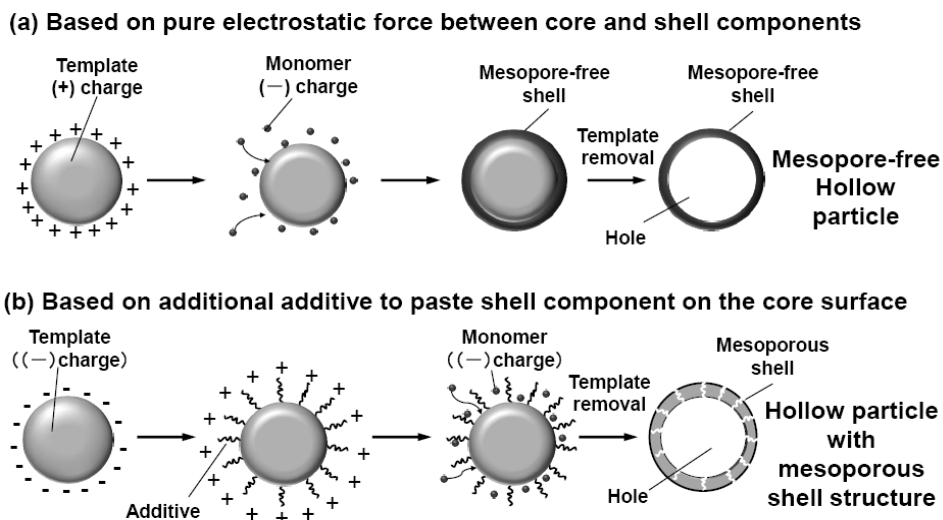


Figure 14. Schematic illustration of the synthesis of hollow particles.

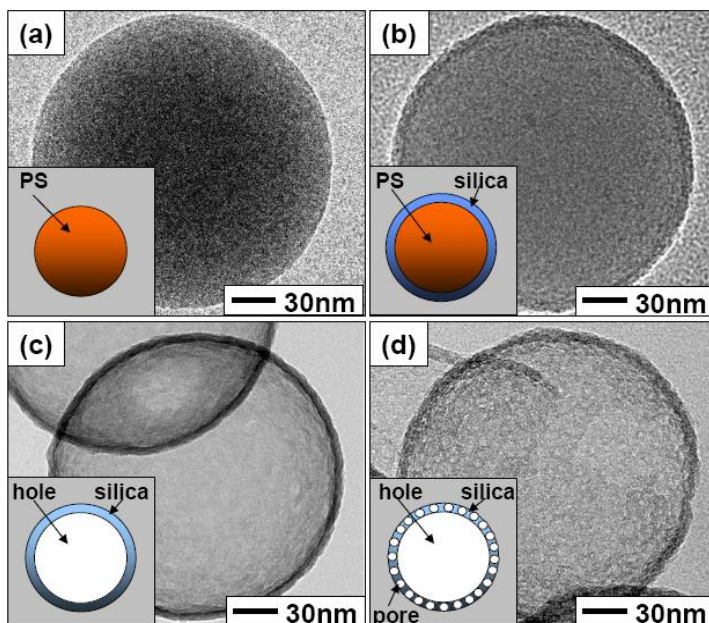


Figure 15. TEM images of the prepared particles: (a) polystyrene particles, (b) mesopore-free core-shell particles, (c) calcined mesopore-free core-shell particles, and (d) calcined conventional core-shell particles. Insert images in the TEM figures (a–d) are the illustration image of the prepared particle. Figures were adopted from references [24, 25]. Note: PS is the polystyrene.

The effectiveness of the hypothesis is not only for MgF_2 but also for other materials, such as silica (Figure 15). Figure 15a shows a high-magnified TEM image of polystyrene particle. After the silica coating process, the silica covers the polystyrene surface, forming core-shell particle (Figure 15b). By adding the calcination process (at 500°C) to the as-prepared core-shell particles, the hollow particle is produced (Figure 15c). Since the silica has a negative

zeta value, the above conditions are applicable only when using polystyrene with a positive zeta charge. Indeed, when using polystyrene with a negative zeta charge, additional additive is mandatory. Although the synthesis of core-shell or hollow particles are possible, the shell structural properties is different, depending on the initial reactants used. When conducting the reaction system under surfactant-free conditions (based on the purely electrostatic force), hollow particle with no mesoporous shell structure can be obtained (Figure 15c). When processing with additional additive, the shell with mesoporous structure is detected (Figure 15d). These results are in a good agreement with the above hypothesis in Figure 14.

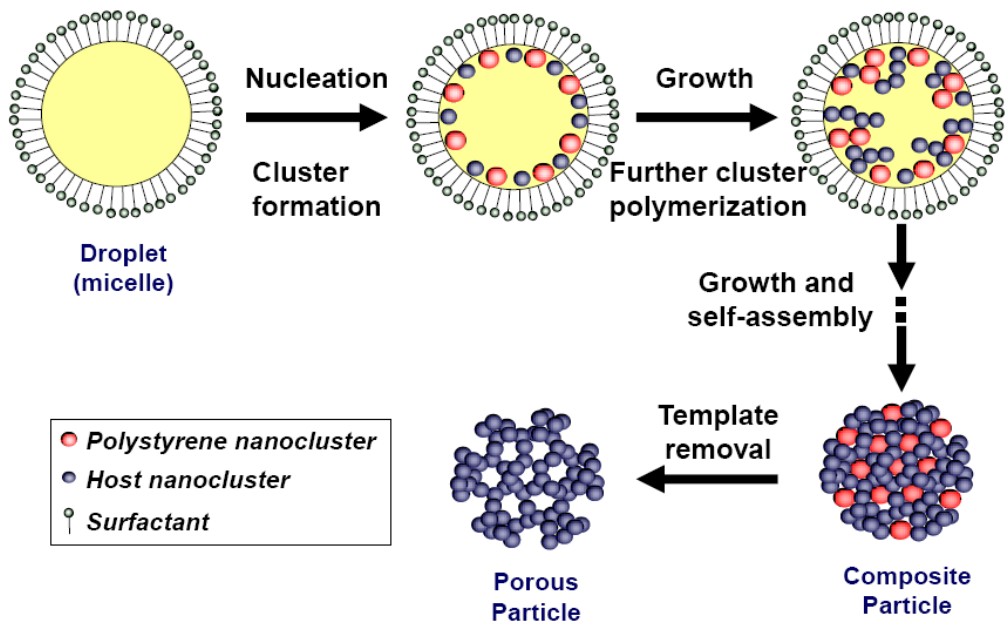


Figure 16. Schematic illustration of the synthesis of porous particles using in-situ technique of polystyrene templating method. Figure was adopted from reference [27].

3.2. In-Situ Technique of Polystyrene Templating Method

Although the ex-situ technique is effective for creating various porous-structured materials, this technique is somewhat impractical for some cases. Specifically, the problems appear when the particles with smaller outer diameter of particle and smaller pore size are required. [26] To solve the problems, the in-situ technique of polystyrene templating method is one of alternative methods.

As discussed in the above introduction about general strategies of porous-structured material synthesis, the synthesis procedure of in-situ technique of polystyrene templating method involves host and template components that are in monomer forms. Therefore, the self-assembly process is based on combination and reaction of these monomers in the in-situ synthesis system (Figure 16). As a model, when the reaction system contains host and styrene monomers, two types of reactions occur inside the micelle: host component formation and styrene polymerization. During the process, both host and polystyrene clusters combine and

interact with each other, forming composite nanoparticles. Then, after adding the polystyrene removal process, mesoporous nanoparticles are created.

Based on the above hypothesis in Figure 16, control of particle outer diameter and pore size can be obtained by regulating a smart strategy that is capable of controlling the formation and growth of host and polystyrene sources. Interestingly, application of this strategy, combining with the reaction under micrometer micelle reactor, tunable particle outer diameter and pore size are available in the nanometer range, in which this cannot be achieved by using ex-situ template technique. [27] Example of the applications of this in-situ technique is shown in Figure 17. Mesoporous silica nanoparticles with controllable pore size (from 3 to 20 nm; Figures 17a-c) and outer diameter (from 20 to 80 nm; Figures 17d-e) are producible. Application of this strategy in the formation of silica has been well known as Hiroshima Mesoporous Materials (HMM). [27]

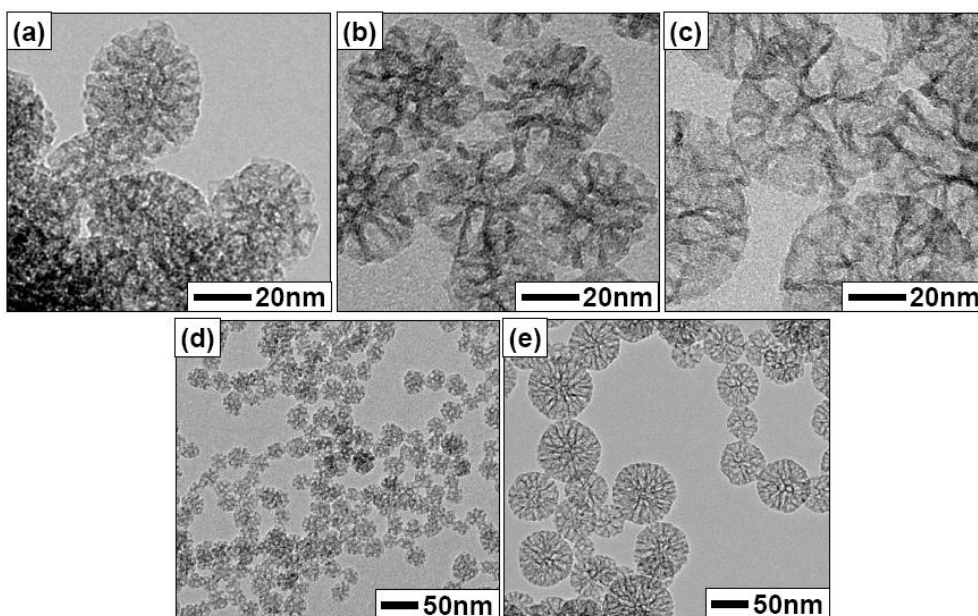


Figure 17. Electron microscope images of HMM with various outer diameters and pore sizes. Figures (a-c) are the HMM with controllable pore size, whereas Figures (d-e) are that with controllable outer diameter. Figures were adopted from reference [27].

4. APPLICATIONS OF POLYSTYRENE AS THE TEMPLATE FOR IMPROVING MATERIAL PERFORMANCE

4.1. Phosphor

Phosphors is inorganic materials that can be used for light-emitting diodes (LED) and biomarkers. This material emits light when exposed to various sources (e.g. photons, electrons, or X-rays). Since phosphors need rare-earth-metal ions (such as europium (Eu) or

cerium (Ce)) as doped component to improve luminescence properties, the application of phosphor must be optimized to be competitive for many practical uses. [26]

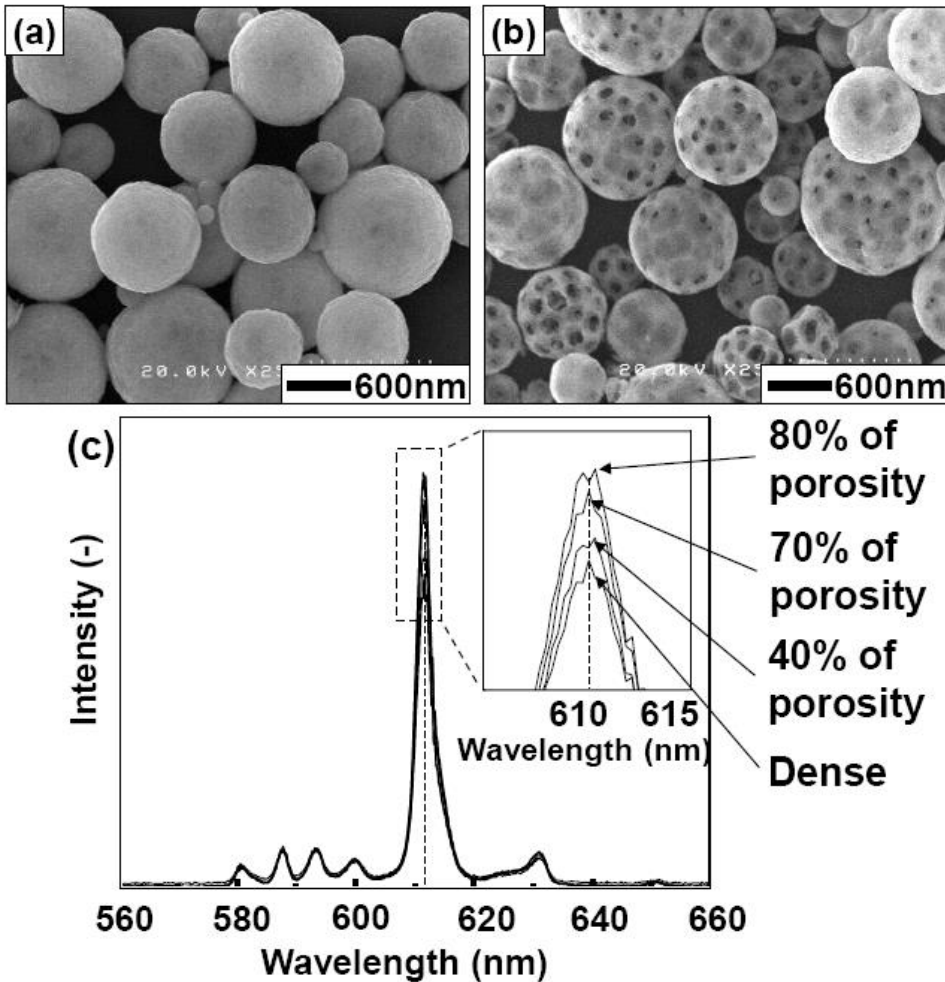


Figure 18. Effect of additional polystyrene on structurizing Y_2O_3 particles with photoluminescence performance. Figures were adopted from reference [26].

To optimize the use of raw material and improve material performance, porous-structured material can be used as one of the best alternative method. By adding porous structure, the amounts of expensive raw materials needed can be reduced. [28] Also, the existence of pores allows all the phosphor components in the particle to be activated and interact with light, thus increasing photoluminescence intensities. [26]

Application of polystyrene template in phosphor material (i.e. Eu-doped yttrium oxide ($Y_2O_3:Eu^{2+}$) particles) is shown in Figure 18. The particles were produced by spray-pyrolysis of a precursor containing a mixture of yttrium, europium nitrate, and colloidal polystyrene. As expected, photoluminescence characteristics of particles with porous structures is better than that of dense particles.

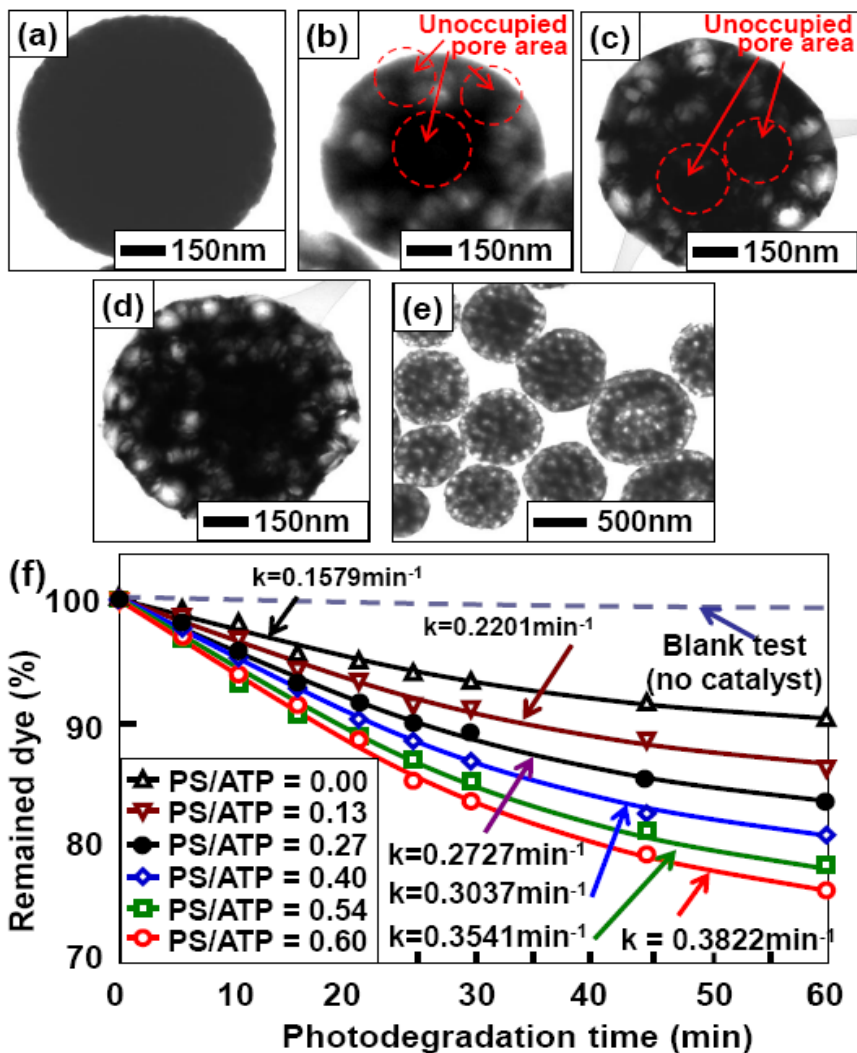


Figure 19. Effect of polystyrene amount on the porous structuration of WO_3 particles and photocatalytic ability. Figures (a), (b), (c), and (d) are the TEM images of particles produced using polystyrene of 0.00, 0.13, 0.40, and 0.60 respectively. Figure (e) is the photograph image of dye sample before and after photocatalytic process. Figure (f) is the photodegradation result of dye as a function of time. Figures were adopted from reference [28]. Note: k is the photodegradation rate.

4.2. Photocatalyst

Activity of catalyst depends on the surface active area available in the catalyst. This surface area can be improved by two ways: (i) decreasing particle size down to nanometer [8] and (ii) changing the porosity in the particle. [28] Since the decreasing particle size is somewhat impractical for industrial applications (due to high cost for downstream nanoparticle removal processes), a material with a porous structure that is larger than nano-size can be the best alternative to nano-catalysts. [29] The existence of pores would presumably produce catalytic activity similar to nanoparticles but without the high cost of

maintenance associated with nanoparticles, and the use of porous material with larger size can easily be re-collected or reused after catalytic treatment. [8]

Improvement of photocatalytic activity (i.e. tungsten trioxide (WO_3)) by additional porous structure is shown in Figure 19. When the photocatalyst is added into a dye under a light illumination, the concentration of dye decreases, shown by deterioration of color intensity as a function of time. Since the outer diameters and crystallite sizes of all the catalysts are the same, the fundamental reason for the different photocatalytic behaviors must be from the increase in the available surface area of the particles, and this can be achieved by the existence of pores. [28]

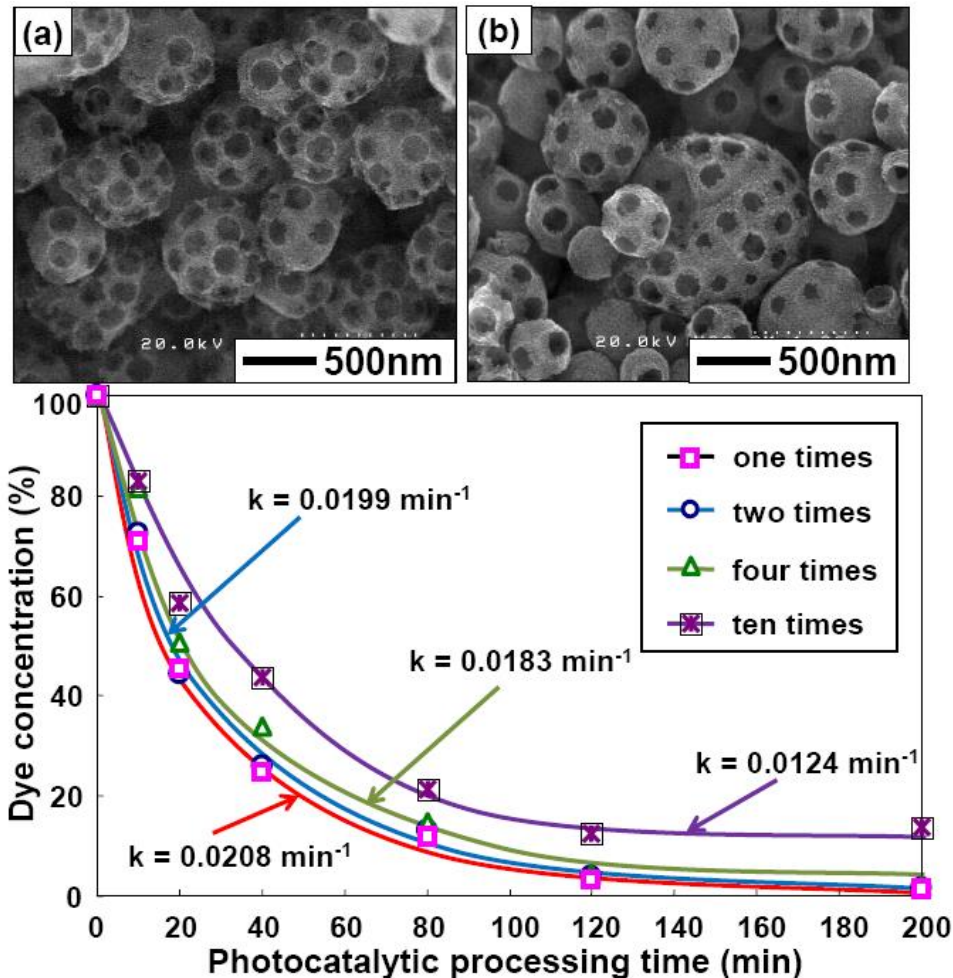


Figure 20. SEM images of titania porous particles before (a) and after photocatalytic process (b) and their recycle ability (c). Figures were adopted from reference [8].

The effectiveness of the porous particles is also trustable to be used for re-usable material. For example, in the case of titania nanoparticles, Okuyama group has shown the ability of porous-structured particles that can be used up to three times of the process, [8] while this cannot be achieved by nanoparticles (Figure 20).

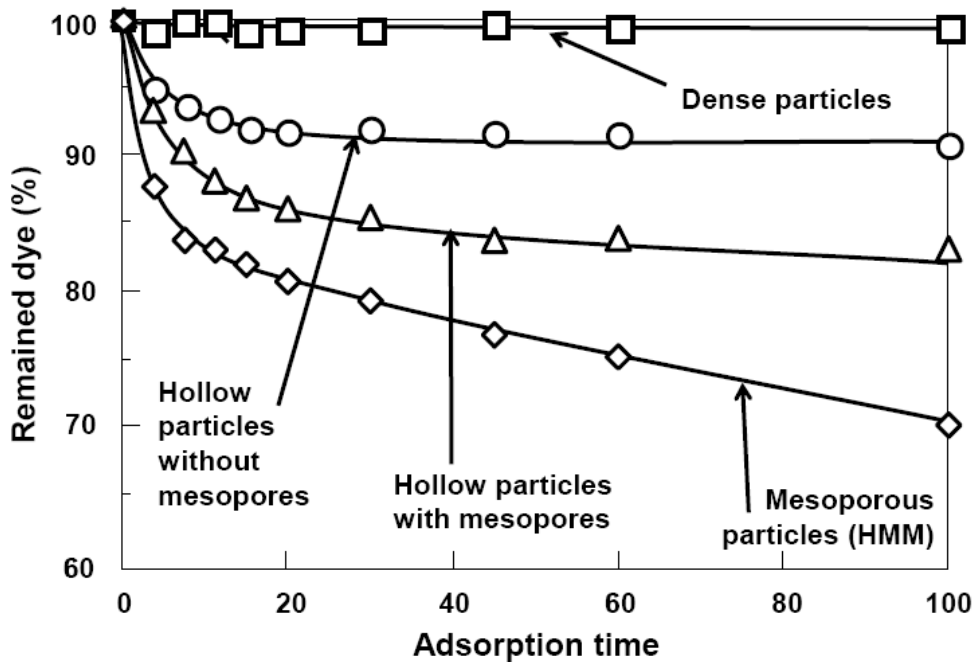


Figure 21. Adsorption performance of particles with various morphologies. Figure was adopted from reference [25].

4.3. Adsorbent

In the adsorption process, the adsorbed molecules are focused to interact directly with the outer surface of the adsorbent. To produce adsorbents that use less raw materials, there are three options: (i) creating porous-structured materials so that all of the adsorbent is accessible and can be active, [27] (ii) removing the inside of the particle (hollow particles), [24] and (iii) substituting the component inside the particle with a cheaper material (core-shell particles). [25]

Figure 21 shows effect of additional polystyrene on structurizing particle for improving adsorption performance. To compare these effects of particle nanostructurization, four types of adsorbents are compared: commercially non-porous particles, HMM nanoparticles, hollow particles with mesopore-free shells, and hollow particles with mesoporous shells. As the adsorbents are changed from dense to hollow to mesoporous structures, the adsorption ability of the particles increases, in which this is mostly because of their increased surface area that allow them to interact with more of the target molecules. However, for industrial applications, hollow particles have two advantages: (i) the use of raw component for hollow particles is less than that for nanoparticles, and (ii) the size of hollow particles (submicron range) offers this material available for recollecting/reuse process. In addition, although mesoporous and hollow-structured particles show a better performance of adsorbent than dense particles, the mechanical strength of the mesoporous and hollow-structured particles is questionable. For this reason, hybrid core-shell material can be used as an alternative technique to solve this problem. [26]

CONCLUSION AND PERSPECTIVE

Research progress in developing synthesis of polystyrene spheres with controllable physicochemical properties (i.e. size and charge) has been reviewed in this chapter. The synthesis of polystyrene particles with a controllable physicochemical properties (i.e. size and charge) has been made great advantages for assisting the creation of material with excellent nanostructures, including porous and hollow materials with control over hole cavity, internal structure, and external shape. We believe that insights gained from this type of research will contribute to more fabrication innovation and development materials for wide range of applications possible.

REFERENCES

- [1] Fihri, A.; Durand, R.; di Renzo, F.; Fajula, F.; Coq, B.; Roussel, T.; Vuillemin, B. *Appl. Catal. B*. 2010, 98, 224-228.
- [2] Ku, P.L. *Adv. Polym. Technol.* 1988, 8, 177 - 196.
- [3] Nandiyanto, A.B.D.; Okuyama, K. *Adv. Powder Technol.* 2011, 22, 1-19.
- [4] Liu, Q.-H.; Liu, J.; Guo, J.-C.; Yan, X.-L.; Wang, D.-H.; Chen, L.; Y, F.-Y.; Chen, L.-G. *J. Mater. Chem.* 2009, 19, 2018-2025.
- [5] Lee, J.; Martic, P.A.; Tan, J.S. *J. Colloid Interf. Sci.* 1988, 1, 252-266.
- [6] Liu, Q.; Li, Y.; Duan, Y.; Zhou, H. *Polym. Int.* 2012, 61, 1593-1602.
- [7] Nandiyanto, A.B.D.; Suhendi, A.; Ogi, T.; Iwaki, T.; Okuyama, K. *Colloid Surf. A* 2012, 396, 96-105.
- [8] Iskandar, F.; Nandiyanto, A.B.D.; Yun, K.M.; Hogan, C.J.; Okuyama, K.; Biswas, P. *Adv. Mater.* 2007, 19, 1408-1412.
- [9] Nandiyanto, A.B.D.; Suhendi, A.; Arutanti, O.; Ogi, T.; Okuyama, K. *Langmuir* 2013, 29, 6262-6270.
- [10] Suhendi, A.; Nandiyanto, A.B.D.; Munir, M.M.; Ogi, T.; Gradon, L.; Okuyama, K. *Langmuir* 2013, 29, 13152-13161.
- [11] Nandiyanto, A.B.D.; Ogi, T.; Ohmura, A.; Tanabe, E.; Okuyama, K. *KONA Powder Part. J.* 2011, 29, 141-157.
- [12] Nandiyanto, A.B.D.; Ogi, T.; Okuyama, K. *ACS Appl. Mater. Sci.* 2014, 6, 4418-4427.
- [13] Xu, J.; Li, P.; Wu, C. *J. Polym. Sci. A* 1999, 37, 2069 - 2074.
- [14] Lane, W. *Ind. Eng. Chem. Anal. Ed.* 1946, 18, 295-296.
- [15] Bas, S.Z.; Yildiz, S. *Colloid Surf. A* 2007, 298, 123-128.
- [16] Nandiyanto, A.B.D.; Iskandar, F.; Ogi, T.; Okuyama, K. *Langmuir* 2010, 26, 12260-12266.
- [17] Tseng, C.; Lu, Y.; El Aasser, M.; Vanderhoff, J. *J. Polym. Sci. A* 1986, 24, 2995-3007.
- [18] Goodwin, J.W.; Hearn, J.; Ho, C.C.; Ottewill, R.H. *Colloid Polym. Sci.* 1974, 252, 484-471.
- [19] Nandiyanto, A.B.D.; Iskandar, F.; Okuyama, K. *Chem. Lett.* 2008, 37, 1040-1041.
- [20] Nandiyanto, A.B.D.; Hagura, N.; Iskandar, F.; Okuyama, K. *Acta Mater.* 2010, 58, 282-289.

- [21] Nandiyanto, A.B.D.; Ogi, T.; Iskandar, F.; Okuyama, K. *Chem. Eng. J.* 2011, 167, 409-415.
- [22] Iskandar, F.; Nandiyanto, A.B.D.; Widiyastuti, W.; Young, L.S.; Okuyama, K.; Gradon, L. *Acta Biomater.* 2009, 5, 1027-1034.
- [23] Hagura, N.; Nandiyanto, A.B.D.; Iskandar, F.; Okuyama, K. *Chem. Lett.* 2009, 38, 1076-1077.
- [24] Nandiyanto, A.B.D.; Akane, Y.; Ogi, T.; Okuyama, K. *Langmuir* 2012, 28, 8616-8624.
- [25] Nandiyanto, A.B.D.; Iwaki, T.; Ogi, T.; Okuyama, K. *J. Colloid Interf. Sci.* 2013, 389, 134-146.
- [26] Ogi, T.; Nandiyanto, A.B.D.; Okuyama, K. *Adv. Powder Technol.* 2014, 25, 3-17.
- [27] Nandiyanto, A.B.D.; Kim, S.G.; Iskandar, F.; Okuyama, K. *Micropor. Mesopor. Mater.* 2009, 120, 447-453.
- [28] Nandiyanto, A.B.D.; Arutanti, O.; Ogi, T.; Iskandar, F.; Kim, T.O.; Okuyama, K. *Chem. Eng. Sci.* 2013, 101, 523-532.
- [29] Nandiyanto, A.B.D.; Iskandar, F.; Okuyama, K. *Chem. Eng. J.* 2009, 152, 293-296.

Chapter 10

APPLICATIONS OF POLYSTYRENE AND ITS ROLE AS A BASE IN INDUSTRIAL CHEMISTRY

Tanvir Arfin^{1,}, Faruq Mohammad^{2,*} and Nor Azah Yusof²*

¹Department of Chemistry, Uka Tarsadia University,
Maliba Campus, Gopal Vidyanagar, Bardoli, India

²Institute of Advanced Technology, Universiti Putra,
Serdang, Malaysia

ABSTRACT

In recent years, the activities related to polystyrene (PS), both in the fields of academic research as well as industrial usage are impressive and are increasing by the number of scientific papers and patent applications in general sense. The demanding interest of PS is due to its versatile applications and utility in various sectors is due to its hydrocarbon structure and ability to polymerize easily. PS is a thermoplastic polymer and is one of the most widely used plastic materials in the world, ranging from domestic, medical to automobiles. In addition, it is also an important ingredient in the manufacture of ionic membranes, disposable cutlery, plastic modelling, cases for compact disks, digital video disks, etc. The major application of PS is in packaging as an industrial base and specific additives are also included for achieving the product characteristics that are highly dependent on the usage at the end. It is transparent and can be fabricated easily to form products with enhanced mechanical and thermal properties. The chemical properties of PS are slightly brittle and soften at 100°C temperature and at higher temperatures, it gets degraded to a mixture of low molecular weight compound and styrene. The quality control and research protocols in the investigation of PS composition have resulted in different methodologies to be acting as a specific analyte. PS nanoparticles with some distinct particle morphology and surface composition can be achieved by using a simple and eco-friendly gentle free-radical micro-emulsion polymerization process. Based on these facts therefore, the current book chapter is aimed to demonstrate and discuss the applications and the role of PS in different aspect of analytical chemistry.

* Tel.: +91-7878366678; E-mail: tanvirarfin@ymail.com and farooqm1983@gmail.com.

Keywords: Polystyrene; Polystyrene aggregate concrete; PS-mediated inorganic composites; PS-mediated inorganic composites; PS –metallic membrane

INTRODUCTION

Polystyrene (PS) was first identified by Bonastre during 1831 by the distillation of Storax obtained from the “Tree of turkey,” and is commonly termed as liquidambar orientalis or oriental sweetgum or Turkish sweetgum. Following the investigation, Eduard Simon during 1839 has recorded the findings that the oxidation of styrene monomer can be activated by exposing it to the sun-light. Further, the industrial manufacture of PS from a specific monomer was discovered in 1869 by Berthelot and the patents were finally granted to F.E. Matthews for the use of styrene as an insulating material where the polymer was expensive and had various drawbacks related to crazing and colouring. After another thirty years, French chemists highlighted the agent that was able to retard the detrimental effects of polymerization [1]. In 1933, PS was recognized as a potentially viable moulding material because of its recommended characteristics such as mechanical strength, enhanced thermal, chemical stability and its applications in various fields. The commercial introduction of styrene as an insulating material has been hampered by the scientific community in which it was resided. This was happened mainly due to the lack of understanding and sophisticated information regarding the structurally relevant molecules, i.e. the relationship between benzene and its alkyl derivatives. For that, a separation of closely related benzene derivatives was inefficient and the derivatives were actually being co-distilled together because of their similar boiling points. In addition, it is also found that benzene, methylbenzene (toluene) and ethylbenzene can be readily separated on the basis of their boiling temperature where the other derivatives such as dimethylbenzenes have similar boiling points and lies in the range of 137-144°C.

PS structure and its production: PS is a specific *atactic* linear amorphous polymer and its monomeric form is shown in the Figure1.1. The configuration of monomer occurs through different processes as shown in Figure 1.2. According to method I, ethyl alcohol is the starting material which on combining with hydrogen chloride produces ethyl chloride and water. The formed ethyl chloride further reacts with benzene to form ethyl benzene which on subjection to superheated steam in a nickel tube forms styrene. Similarly, in method II, ethylene gas is allowed to react with benzene in the presence of aluminium chloride catalyst under heat and inert atmospheric pressure to form ethylbenzene. The formed ethylbenzene in the following step subjected to different conditions of heat, pressure and steam to produce styrene as shown in Figure1.2. If the formed ethylbenzene in the first step does not rupture to get styrene directly in method II, then the ethylbenzene is chlorinated to form chloroethyl benzene which further allowed passing through a nickel tube. This process is responsible for enhancing the production yielding rate and transmits less brittleness to the resulting polymer by thoroughly processing both the methods.

Polymerization and properties of PS: When ethylene and acetylene added to the reaction mixture in a nickel tube, the production of styrene also increases due to the enhanced reaction kinetics. The available specific methods are also dominated to be contaminated by the presence of two products such as cyclohexane and cyclohexadiene.

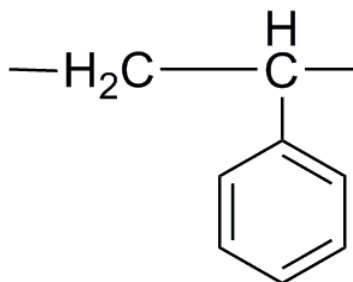
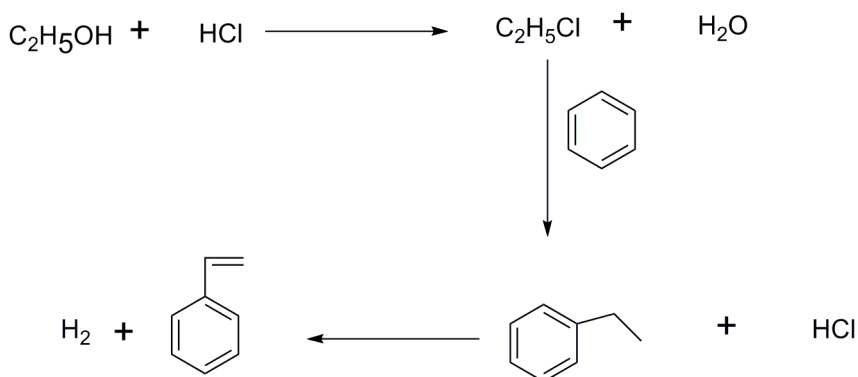


Figure 1.1. Monomer of PS and the polymer is the repeated unit of this monomer.

Method-1.



Method-2.

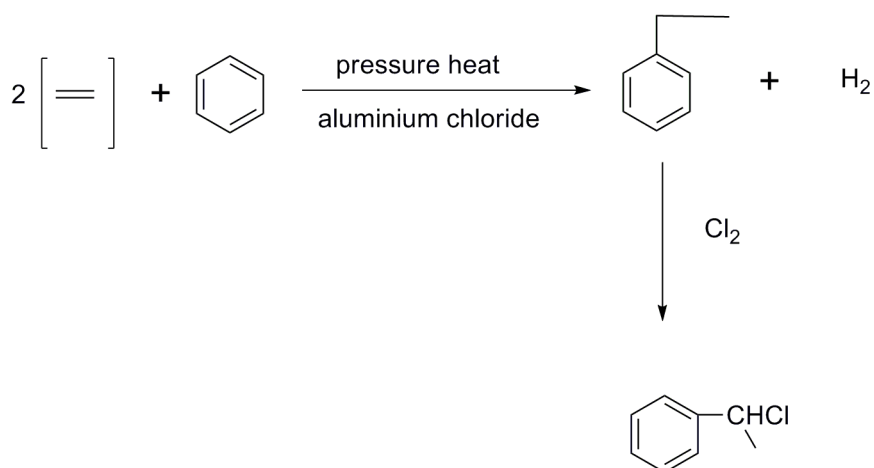


Figure 1.2. Reactions leading to the formation of styrene.

To start up with the polymerization, styrene and acetic acid are added together in the presence of sulphuric acid to form distyrene. The subjection of heat to the formed distyrene disputes the polymerization process and forms a glossy solid material known as matastyrene. When more amount of heat is supplied, it breaks the methyl group and polymerization occurs

which finally forms the PS as shown in Figure 1.3. The purity of the monomer traced by advance analytical methods such as chromatography leads to the commercial manufacture of PS [2]. The storage and polymerization of the styrene can be spoiled by the contamination which takes place in and around it. The specific and effective inhibitor such as *p-t*-butylcatechol (TBC) is generally added to keep it safe from the contamination leading to decomposition of the polymer. As per the specific application type, PS can be easily converted to hydrophilic, hydrophobic or ionic [3, 4]. There are several characteristics of PS which are highly important for industrial application point of view which includes: (a) its dimensional stability even at varying conditions of temperature, (b) low-loss dielectric constant, (c) infinitesimal water absorption, (d) inertness toward acids, bases and salts, (e) insolubility in aliphatic alcohols-petroleum hydrocarbons-glycol ethers, (f) high refractive index which helps to act as a substitute for glass and gems in jewellery, and (g) low specific gravity of 1.05.

The physical properties of PS are as follows: it is clear, transparent, can be easily fabricated, and possess high mechanical strength in addition to maintaining thermal properties. It is slightly brittle in nature and gets soften at 100°C which sustains it to be used in formulations that require sterilization. At elevated temperatures, a mixture having low molecular weight compound and styrene will be formed as decomposition products. PS is widely used for packing purposes and many other specific additives are integrated to get the product characteristics that are dependent on its usage [5-8].

The general additives of PS are antioxidants, UV-stabilizers, processing lubes, antistats and flame retardants. PS due to its difficult matrix of extraction and subsequent identification, the conventional solvent extraction and chromatographic separation methods are applied. In general, three major factors are mainly considered for developing an analytical method of polymer additives such as (a) the purity of additives (as they are not pure compounds by themselves), (b) the insoluble nature of PS in the additives, and (c) typical low concentration of additives. The polymer and additives must be basically distinguished from each other in order to use specific tools and techniques. The low molecular weight oligomers obtained during polymer extraction are removed due to their interference with the other analysis and this should be handled with utmost care so as to avoid any further decomposition.

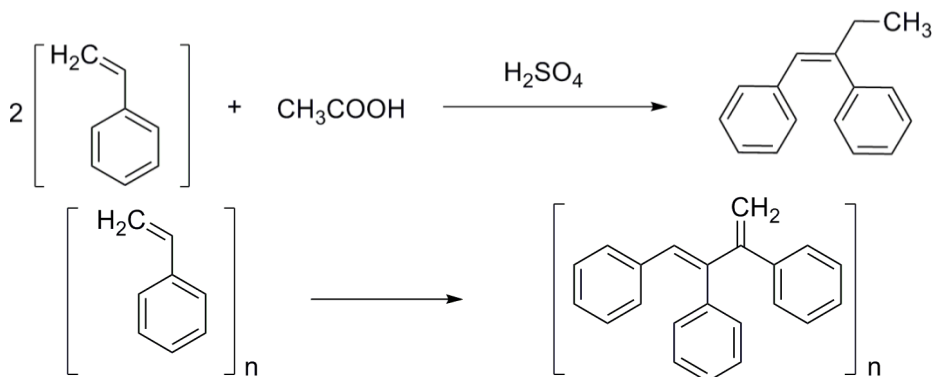


Figure 1.3. Reactions leading to the formation of PS from styrene.

For some duration, the antioxidants are unstable and the inconstant complex compounds acts as the decomposition products [9]. Many other important factors are needed to be considered while developing a technique or process for the variety of additives that are found in the polymer. Such factors include volatility, molecular weight, purity, stability of the analyte and other polymer matrix effects. Based on these characteristics, various analyte specific techniques are developed and are applied to improve the quality and compositional analysis of PS. The basic goal in this field is to identify the additives by both qualitative and quantitative aspects in order to minimize the problems appearing during the extraction process. In that process, the most promising challenge remains to be the development of a method that does not proved to interfere with the polymeric matrix [10].

The conventional methods of polymeric extraction employ large amounts of chlorinated solvents in the form of dissolution by means of Soxhlet extraction or precipitation extraction of polymer resin. These methods are time consuming and are generally restricted in terms of environmental concerns of the future prospects. It is also noticed that the traditional methods requires the actual liquid extraction and by doing this, a loss in the final amounts of the analytes were observed due to multistep extractions. In that view, the Supercritical fluid extraction (SFE) method is very appealing due to the possibility of less solvent consumption. In SFE, the extraction of substances are rapid with huge recoveries where we generally configure that it may be either off-line for method development or on-line where the analytes are objected in a direct way to a chromatograph or spectrometer for the analysis further [11].

Applications of PS: PS is a thermoplastic polymer, which is one of the most broadly used plastic materials and is also biodegradable on long standing and hence can be used as an important component in different sectors ranging from domestic, industrial to automobiles. The products formed from PS include the ionic membranes, disposable cutlery, plastic models including CD (compact disc) and DVD (digital video display) cases. Even though PS possesses some level of fragility and mechanical stability due to its plasticity nature and it was observed that the physical characteristics are greatly enhanced on integration with other materials.

(1) Polystyrene Aggregate Concrete (PAC)

Polystyrene aggregate concrete (PAC) is the material of lightweight with varying densities in the range of 1000 to 2000 kg/m³ and are produced by replacing partially coarse aggregate with reference of the normal weight concrete mixtures that is of equal volume chemically coated with PS beads. It can be used for both structural and non-structural applications due to its very attracting properties such as lightweight, thermal properties, insulating capacity, durable character and eco-friendly nature [12, 13]. All these characteristics are dependent on the amount of expanded PS used in an aggregate form. According to the structural application such as the structural self-weight, the foundation size can be reduced by decreasing the density. But yet many studies reported the data related to the PAC of lower strength only. In order to enlarge the utility of PAC and also to compete with both structural as well as functional demands, a series of PAC of 1410-2100 kg/m³ densities with corresponding strengths of at least 17 MPa has been designed [14].

The concrete undergoes a tiptoe in its amount that is dependent on the following factors: (a) magnitude of sustained loading, (b) age and strength of concrete while applying the stress,

and (c) time consume till the concrete is stressed. The specimen notifies the volumetric changes when the concrete is loaded which are irreversible for large extend. Such changes are because of the closure of voids in the concrete, gelatinous flow of the paste of cement-water having aggregate crystalline flow and flow of water out of the cement gel due to drying and loading [15]. It is very obvious that the properties of aggregate play a significant role in the creeping of concrete. It is believed that a concrete made with lightweight aggregate exhibits higher creep when compared with normal weight aggregate concrete. The high water absorption capability usually makes the creep potential of lightweight concrete to get influenced by the amount of moisture content and also the movement in lightweight aggregates [16, 17]. As such it is not the related matter in PAC as PS aggregates are impermeable having zero moisture content. On the other hand, PAC is supposed to be exhibiting higher creep and compressibility because it contains negligible deformation capacity that is offered by the low modulus PS aggregates. According to the study of Saaba and Ravindrarajah [18], it has been reported that the specified creep for PS concrete that are subjected to a density range of 1600-2000 kg/m³, inquires a stress/strength ratio of 0.30 for 150 days was between 47.2 and 206×10^{-6} /MPa for concrete with a cement content of 410 kg/m³. In their report, they stated that the higher creep potential for PAC is essentially because of the incapability of the low modulus PS aggregates for restraining the creep of the cement paste matrix. In addition, due to high compressibility, the PS aggregate particles are important area of interest for time-dependent volume changes. Ravindrarajah *et al.* [19] then studied the flexural creep of PS concrete composite that was recommended to a stress/strength ratio of 0.70 nearly for about 120 days. The present of PS concrete with higher creep is responsible for increasing the total deflection and cracking of the composite. For such notification, no clear evidence or proof has been formulated. Hanna [20] in his work reported that due to the lack of restraint to deformation that is offered by the property of the high compressibility of PS aggregates and the deformation of PAC resulting from creep would be comparatively greater than normal weight concrete. The slow development of creep for long period is enabling the difficulty in getting an exact prediction or possibility for the prescribed concrete from short term laboratory measurements.

The lightweight concrete is very much applicable as valuable ingredient in precast concrete products. The steam curing beds in precast concrete plants are usually framed for the highest temperature in the range of about 60-70°C for prohibiting the delay of ettingite formation that DEF in the concrete [21]. In general, the prolonged curing of steam is responsible for improving the strength of the binder and also the compressive strength of the concrete [22]. The concrete which is found to be of higher strength of time period which will basically have less creep formation that of the limited time period and equivalent loading. The time depended and mechanical properties of PAC are being affected by the initial curing and also the strong conditions.

(2) PS-Mediated Inorganic Composites

PS is generally studied as an organic substance for the synthesis of composites along with other inorganic materials. For example, Caruso using a layer-by-layer method prepared PS-silica composite particles with the core-shell structure and the formed structure found to exhibit morphological properties [23]. Similarly, Huang and Tang have prepared PS coated

Fe_3O_4 particles of spherical shape to be used as magnetic and structural properties [24]. Lenoble *et al.* Synthesized a PS matrix loaded with MnO_2 and studied on retention of As(V) and simultaneous of As(III) oxidation as well as the waste on this medium was analysed [25]. In a similar study, the formation of PS shell on the surface of ZnO (modified with oleic acid) by the microemulsion polymerization found to have water initiator as potassium persulfate (KPS) [26]. Pan and co-workers fabricated PS-supported ZrO_2 composites and studied their effect on the sorption enhancement of Pb(II) ions from water. It was observed from the studies that the fabrication of ZrO_2 with PS gave a specific result which had an influence on its use [27]. The photoactive TiO_2 particles are utilized in two ways, i.e. in the form of suspension or immobilization on a surface. The practical application of photoactive nanoparticles appear to be very difficult due to the lack of sophisticated and economical filtration procedures for the separation of suspended particles in the reaction medium after long treatment periods [28,29]. In search of suitable filtration a procedure, the immobilization of TiO_2 onto a surface is considered to overcome the disadvantages appeared in the treatment processing. However, the immobilization process seems to reduce the photocatalytic activity due to an increased amount of distance between the immobilized particle and the surface layer which is at the peak of degradation. As a result, it is very important to consider the interactions of TiO_2 immobilization on the material's surface whether it is physical or chemical and also tested to see as the produced material exhibiting unique characteristics of good separation performance or it just exhibiting some simple activity. To produce such hybrid materials, various immobilization techniques and other supporting systems are applied. In one approach, PS is more preferred because of its easiness of production, inert behaviour, buoyancy and less expensive character [30-38]. There have been a number of studies related to PS which deals with the preparation and photocatalytic properties of TiO_2 immobilized PS (TiO_2 -PS) [30-38]. In one of the study Fa *et al.* investigated that the embedding of the iron phytolocyanine immobilized TiO_2 nanoparticles into the commercial PS can lead to the solid-phase photocatalytic degradation of PS films [35]. Similarly, PS seems to be suitable as a template for the production of porous TiO_2 nanoparticles which had an exclusive effect [30, 31]. Other researchers have noticed that the immobilization of TiO_2 nanoparticles onto PS for degrading the waste PS itself [32-35] whereas TiO_2 -PS was used to debase methylene blue as a model pollutant [36-38].

Fabiyi and Skelton have organised a simple technique for the immobilization of TiO_2 nanoparticles on PS beads by utilizing the thermal attachment method [36]. On the basis of catalyst mass which range at 0.5-7g, it can be noticed that the degradation rates were 0.15–0.25 $\mu\text{mol min}^{-1}$. Magalhães and Lago [38] have reported that by grafting TiO_2 particles on the EPS surface, the preparation of TiO_2 immobilized is expanded on the PS (TiO_2 /EPS). The photocatalytic learning was assessed with 50 mgL^{-1} MB for 300 min irradiation at 254 nm Hg lamp that gave a clear conclusion of about 60% discoloration of the dye.

(3) PS in Different Metallic Membranes

Arfin and Mohammad have studied about DC electrical conductivity of nano-composite Polystyrene–Titanium–Arsenate (PS-Ti-As) membrane and found that the conductivity is dependent of the temperature. It was observed that the conductivity increased with an increase of temperature until 100°C, after that it decreased during 120-160°C. These changes expected

to be due to the loss of dopant HCl, as the dopant molecules are responsible for blocking the chemical reactions associated with it. It is also noticed that the perm-selectivity is attaining a value between zero and unity are dependent on the external electrolyte concentration for the PS-Ti-As membrane and the electrolyte pair [39-40]. The formed membrane is crystalline in nature and exhibited significant toxicological effects towards the H9c2 cardiomyoblasts due to the maintenance of cationic charge by the PS in the membrane. These cationic polymers due to their electron deficient character tries to absorb the electrons quickly from the intracellular components like DNA, protein etc and mediate many toxic responses through the initiation of free radical oxidative stress [41-42].

In a different study, Arfin and Yadav have reported in Polystyrene-Cobalt-Arsenate (PS-Co-As) membrane that at higher frequencies, the capacitances tend to be low and with an increase of frequency, the impedance gets decreased along with an increase in the corresponding phase angle [43]. At low frequencies, the impedance exhibited an absolute dependence of the phase angle, but is of cation independent. It is an evidential report that the PS-Co-As membrane displayed the particles in the nano range i.e. around 100 nm, in addition to showing the crystalline nature and uniform arrangement of particles without any marks of visible cracks [44-45].

Similarly, Arfin *et al.* experimentally showed that the Polystyrene-Titanium–Vanadium (1:2) phosphate (PS-Ti-V) membrane is cation selective and the selectivity of such membrane increased with the dilution rate and is due to the structural changes occurred in the electrical double layer at the specific solution membrane interface [46]. In a different study by Arfin and Rafiuddin, the Nickel-Arsenate (Ni-As) revealed that the membrane shows casual non-preferential orientation without any cracks which was basically composed of very dense small particles. Due to the rough surface of the Ni-As membrane and non-homogenous nature, the impedance spectra were diverged from the actual prediction that was at low frequency [47-48].

Arfin and Fatima has reported for the Polystyrene-Calcium phosphate (PS-CaP) membrane when tested under three different electrolyte solutions (LiCl, NaCl and KCl) that the resistivity was found to decrease for 1-1 electrolyte solutions in the order of $\text{Li}^+ > \text{Na}^+ > \text{K}^+$. The observed results are in accordance with the size of cations present in the electrolyte solutions, increase of cation size meaning that decreased resistivity [49].

(4) PS in Electronics

The electronic industry uses PS in the manufacturing of telivions and in computers as different types of emerging trends which follows the norms for its use such as combination of function, form and aesthetics and a high performance as well as cost ratio. With the advancement of disposable cutlery, the life of individual has become very easy and comfortable as the sheet or moulded form of PS is serving and the enormous utility in the production of plastic cutlery which is once used and thrown away.

It is also the preferred choice now a days as media enclosures, cassette tape and jewellery boxes for protecting CD's and DVD cases and many devices that are used in the information technology sector. PS is fit for manufacturing various household appliances like blenders, air conditioners, refrigerators, hot air and microwave ovens, hand-held vacuum cleaners. The increased uses of PS in the industrial sector is due to its easy production processing,

capability of imparting an easy and clear cut end of the appliances while meeting almost all the end product requirements. The consumer goods such as kitchen and bathroom accessories, lawn accessories are found to be produced by inculcating PS in the process of synthesis and manufacture. The availability of PS in economical prices compared with many other polymers and convenient to processing into desired shapes and sizes are especially making it to use in toys and other playing accessories, injection-molding, extrusion, thermoforming and smoke detecting alarms when the fire flares up [39-42].

(5) PS in Automotives

PS in automotives are quiet randomly used for various purposes by making of use of its characteristics such as thermal stability at a broader temperature range, high mechanical strength along with other elements, conductivity when used in ionic form, economical, recyclable, moisture free, etc. The commonly manufactured products in the automobile industry includes the bumper cores, boot in-fills, void fillers, roof liners, head rests, head impact, knee bolsters, side-impact protection, car seating, sun visors, car air conditioning liners, under bonnet battery liners, under bonnet sound deadening and material handling dunnage.

(6) PS in Food Packaging

PS is used as an insulator and food protector in the food packing process. The various food items like meat, fish, eggs, dairy products, salads, cold drink carry out meals can be prevented from decomposition/spoiling by packing it in PS material and is an easy and less expensive way of preserving food. Only because of PS role in packaging industry in terms of the goods packaging, refrigeration and transportation in developed countries ensured that only a 2% of food is that gets spoiled when compared with developing or underdeveloped countries where PS revolution has not started. The PS packaging materials are versatile and can serve as disposables for food having rigid packing and are recyclable. To transport other consumer goods and health care products (pharmaceuticals, nutraceuticals, etc) across the countries, they are packed in boxes along with PS as a supporting materials and also to provide insulation and protection from various external factors like moisture, air and temperature by maintaining its properties at all conditions.

(7) PS in Construction

PS resin, a long chain hydrocarbon has an excellent insulation capacity and so it can be used in building and construction industry as for insulating the ceilings, walls, floors, roofing, siding, panels, bath and shower units, in addition to lighting and plumbing fixtures to get rid of external temperature differences and humidity. The PS resin of chemical compound are mainly required for lighting and plumbing fixtures, panels and slidings used during the construction purposes. The polymers also find its utility in soundproofing walls of buildings

due to its properties of good processing ability and excellent performances at all climatic conditions.

(8) PS in Medical Sector

PS has a wide range of utility in medical field. The use of PS advances the technology to the patient and physician as its versatility had made it to be more suitable for use in the medical field. It is highly preferable for making medical equipments due to its excellent clarity which helps in good visibility and outstanding sterilization process. PS resins are used in the manufacturing of disposable medical appliances which includes the tissue culture plates, trays for conducting test, petri dishes, test tubes and kits for housing test which is involved in biomedical research. Many diagnostic test equipments and components made up of PS such as medical cups, medical keyboards, plastic boxes, vaginal dilator speculum are also under every day use.

(9) PS in Crafts

PS uses are also highly influencing the art and crafts sector. Extruded PS or Styrofoam is a special form of the polymer having closed cell which is used for art and craft projects. The material or the equipments are easily cut into various shapes and sizes for ornamenting it to amazing craft pieces which is of excellent beauty. Craft materials such as candle holders and ornaments for decorating christmas tree are generally made of Styrofoam. For making and manufacturing the model of architectural designs, PS is mainly used which can be replace in convenience for corrugated cardboards.

CONCLUSION

In conclusion we are reviewing the syntnesis, processing, importance, and applications of PS in the industrial sector. The chemistry associated with the structure of PS is playing the major for it to be used for the majority of applications by maintaining to be different from many other polymers at various conditions of temperature and other atmospheric conditions. The employment of PS polymer is not limited to a particular area as it is exclusively used due to its numerous advantages in many other areas. The attracting properties includes the portability, easiness of transportation due to its light weight, moisture resistant nature, easily affordable, recycled, visually appeals as good polymer.

REFERENCES

- [1] Nauth, R. The Chemistry and Technology of Plastics; Reinhold Publishing Corporation: New York, 1947.
- [2] Billmeyer, F. W. Textbook of Polymer Science, 3rd Ed., Wiley-Interscience: New York, 1984.

-
- [3] Rifi, E. H.; Rastegar, F.; Brunette. *Talanta*, 1995, 42, 811-816.
- [4] Wang, X.; Weiss, R. A. *Langmuir*, 2012, 28, 3298-3305.
- [5] Nghiem, L. D.; Mornane, P.; Potter, I. D.; Pereira, J. M.; Cattrall, R. W.; Kolev, S. D.; *J. Membr. Sci.*, 2006, 281, 7-41.
- [6] Peterson, J.; Nghiem, L. D. *Int. J. Environ. Tech. Manag.*, 12 (2010) 359-368.
- [7] Kebiche Senhadji, O.; Sahi, S.; Kahloul, N.; Tingry, S.; BenAmor, M.; Seta, P. *Sci. Technol. A.*, 2008, 27B, 43-50.
- [8] Upitis, A.; Peterson, J.; Lukey, C.; Nghiem, L. D. *Desalin. Water Treat.*, 2009, 6, 41-47.
- [9] Wheeler, D. A. *Talanta*, 1968, 15, 1315-1334.
- [10] Sulkowski, W. W.; Wolińska, A.; Pentak, D.; Maślanka, S.; Sulkowska, A. *Macromolecular symposia* 2006, 245-246, 315-321.
- [11] Cotton, N. J.; Bartle, K. D.; Clifford, A. A.; Dowle, C. J. *J. Appl. Polym. Sci.*, 1993, 48, 1607-1619.
- [12] Ferrandiz-Mas V.; Garcia-Alcocel E. *Constr. Build. Mater.*, 2013, 46, 175-182.
- [13] Chen B.; Liu, J.; Chen, I. Z. *J. Shanghai Jiaotong Univ.*, 2010, 15, 129-137.
- [14] ACI Committee 213 R-87. Guide for structural lightweight aggregate concrete ACI manual of concrete practice, Part 1. American Concrete Institute, Farmington Hills, 1987.
- [15] Naus, D. J. The effect of elevated temperature on concrete material and structures-a literature review. Technical Report, NUREG/CR-6900, U.S. Nuclear Regulatory Commission, Washington, DC, 2006.
- [16] Lopez, M.; Kahn, L. F.; Kurtis, K. E. *Cem. Concr. Res.*, 2009, 39, 610-619.
- [17] Zhuang, Y. Z.; Chen, C. Y.; Ji, T. *Constr. Build Mater.*, 2013, 46, 13-18.
- [18] Saaba, B.; Ravindrarajah, R. S. Engineering properties of lightweight concrete containing crushed expanded polystyrene waste. In: Proc. Materials research society 1997 fall meeting, Boston, 1997.
- [19] Ravindrarajah, R. S.; Camporeale, M. J.; Caraballo, C.C. Flexural creep of ferrocement-polystyrene concrete composite, ADCOM'96. In: second international conference on advances in composites, 18-20 December, Bangalore, India, 1996.
- [20] Hanna, A. N. *Res. Dev. Bull, Portland Cem. Assoc.*, 1978, Rd 055.01P.
- [21] Taylor, H. F. W.; Famy, C.; Scrivener, K. L. *Cem. Concr. Res.*, 2001, 31, 683-693.
- [22] Yazici, H. *Build. Environ.*, 2007, 5, 2083-209.
- [23] Caruso, F. *Adv. Mater.*, 2001, 13, 11-22.
- [24] Huang, Z.; Tang, F. *J. Colloid interface Sci.*, 2004, 274, 142-147.
- [25] Lenoble, V.; Laclautre, C.; Serpaud, B.; Deluchat, V.; Bollinger, J. C.; *Sci. Toatl. Environ.*, 2004, 326, 197-207.
- [26] Liu, P. *Colloid Surf. A: Physicochem. Eng. Asp.*, 2006, 291, 155-161.
- [27] Zhang, Q.; Du, Q.; Hua, M.; Jiao, T.; Gao, F.; Pan, B. *Environ. Sci. Technol.*, 2013, 47, 6536-6544.
- [28] Xiong, L.; Sun, W.; Yang, Y.; Chen, C.; Ni, J. *J. Colloid Interface Sci.*, 2011, 356, 211-216.
- [29] Okte, A. N.; Yilmaz, O. *Appl. Catal. A.*, 2009, 354, 132-142.
- [30] Dutschke, A.; Diegelmann, C.; Lobmann, P. *J. Mater. Chem.*, 2003, 13, 1058-1063.
- [31] Doongs, R.; Chang, S.; Hung, Y.; Kao, I. *Sep. Purif. Technol.*, 2007, 58, 192-199.
- [32] Zan, L.; Tian, L.; Liu, Z.; Peng, Z. *Appl. Catal. A: Gen.*, 2004, 264, 237-242.

- [33] Shang, J.; Chai, M.; Zhu, Y. *Environ. Sci. Technol.*, 2003, 37, 4494-4499.
- [34] Shang, J.; Chai, M.; Zhu, Y. *J. Solid State Chem.*, 2003, 174, 104-110.
- [35] Fa, W.; Zan, L.; Gong, C.; Zhong, J.; Deng, K. *Appl. Catal. B: Environ.*, 2008, 79, 216-223.
- [36] Fabiya, M. E.; Skelton, R. L. *J. Photochem. Photobiol. A. Chem.*, 2000, 132, 121-128.
- [37] Yang, J.-H.; Han, Y.-S.; Choy, J.-H. *Thin Solid Films*, 2006, 495, 266-271.
- [38] Magalhães, F.; Lago, R. M. *Solar Energy*, 2009, 83, 1521-1526.
- [39] Arfin, T.; Mohammad, F. *J. Ind. Eng. Chem.*, 2013, 19, 2046-2051.
- [40] Arfin, T.; Rafiuddin. *Electrochim. Acta*, 2009, 54, 6928-6934.
- [41] Arfin, T.; Rafiuddin. *Electrochim. Acta*, 2010, 55, 8628-8631.
- [42] Mohammad, F.; Arfin, T. *Bull. Environ. Contam. Toxicol.*, 2013, 91, 689-696.
- [43] Arfin, T.; Yadav, N. *J. Ind. Eng. Chem.*, 2013, 19, 256-262.
- [44] Arfin, T.; Rafiuddin. *Desalination*, 2012, 284, 100-105.
- [45] Arfin, T.; Rafiuddin, *Electrochim. Acta*, 2011, 56, 7476-7483.
- [46] Arfin, T.; Jabeen, F.; Kriek, R.J. *Desalination*, 2011, 274, 206-211.
- [47] Arfin, T.; Rafiuddin, *J. Electroanal. Chem.*, 2009, 636, 113-122.
- [48] Arfin, T.; Yadav, N. *Anal. Bioanal. Electrochem.*, 2012, 4, 135-152.
- [49] Arfin, T.; Fatima, S. *Asian J. Adv. Basic Sci.*, 2013, 2, 1-14.

Chapter 11

A NEW EQUATION FOR HOMOGENEOUS NUCLEATION FROM POLYSTYRENE SOLUTIONS

*John H. Jennings**

Jennings Research & Editing, Berkeley, CA, US

ABSTRACT

There have been various attempts since the two papers by (Han and Han) to predict the rise in superheat due to addition of polystyrene in solvents including toluene, benzene and cyclohexane. Calculation of the nucleation rate is a cumbersome way to attack the problem. The papers other than (Jennings) focus on getting a value for the nucleation rate J . In Jennings' formulation a simple vector calculus argument eliminates the need to calculate J . Each curve for (Jennings and Middleman) data is more or less a line and the object is to calculate the slope of the lines in the (w_2 , T) plane where w_2 is the weight fraction polystyrene in cyclohexane and T is temperature Kelvin. All lines meet at the point $(0, T_1)$ where J is equal for all 4 molecular weights and T_1 is the limit of superheat of pure cyclohexane at 1 atm. This Short Communication shows how Jennings' approach is simple and gives a beautiful effective equation. In expanded form I am proposing a new equation for the limit of superheat T , by extending the limiting equation published by (Jennings) because the data are lines. Because they are lines the limiting slope would be the true slope. The additional temperature rise in the superheat limit is inversely proportional to MW polymer and directly proportional to weight fraction polymer in the solution. It is a semi-empirical argument. One would believe that experiments with polystyrene in cyclopentane, n-hexane and n-heptane would give the same lines in the data as cyclohexane in the experimental setup used by (Jennings and Middleman).

NOMENCLATURE

a surface area of solvent molecule

B factor $\approx 2/3$

* jhjennings@juno.com

- d density of liquid
 d_i density of solvent (1) or polymer (2)
 d_G density of gas at equilibrium vapor pressure
 k Boltzmann constant
 M molecular weight of solvent molecule
 MW_i molecular weight of solvent or polymer
 N_o Avogadro's number
 P_e equilibrium vapor pressure of gas in bubble
 P_L ambient vapor pressure on solution droplet
 P_V vapor pressure of gas in bubble
 r ratio of molar volume of polymer to molar volume of solvent
 T_1 temperature of limit of superheat for pure solvent at 1 atm
 V_i molar volume of solvent (L) or vapor (e) in equilibrium
 w_2 weight fraction polymer
 δ Poynting correction factor
 σ_1 surface tension of solvent
 σ_2 surface tension of polymer
 ϕ_i volume fraction of solvent or polymer in interior of solution
 ϕ_{iS} volume fraction of solvent or polymer on surface of solution

INTRODUCTION

Bubble nucleation is a phenomenon known in pure liquids where a new gas phase appears upon superheating above the boiling point at 1 atm pressure. Classical nucleation theory, (Frenkel), is used to predict the temperature and many liquids, (Blander and Katz), exhibit it. Typically the superheating limit is 89% of the critical temperature. The earliest theory for the surface tension of polymer solutions was done by (Prigogine and Marechal) and was patterned after the famous Flory-Huggins lattice model for polymer solutions.

All of the efforts I know that attempted to arrive at an expression which predicts the superheat limit for polystyrene solutions made an effort to calculate J , the number of emerging bubbles/sec. The problem is that J is difficult and complicated to calculate. They all had limited success. (Han and Han (1990a) and (1990b)) came out with two papers, one with data and one with a theory for polystyrene in toluene. They used laser scattering and analyzed it with their theory, which gave an expression for J . (Kim et al) solved a molecular cluster model as their effort to get J for bubble nucleation in polymer solutions. Another effort, (Guo et al) involved CO_2 in polystyrene for this process and modeled it using an extension of diffuse interface theory but remark that classical nucleation theory is most successful for quantifying the nucleation process and that limited progress had been made for polymer solutions. (Yarin et al) studied devolatilization of differing polymer melts and their point was that bubble growth involves control by momentum transfer and diffusion.

These papers use many equations and complicated formalisms. The new equation I propose is beautiful and general for all polymer solutions, but in this case the data was measured for the polystyrene-cyclohexane system. The final equation in this Short Communication gives the linear slope, the correct trend in the slope and fairly accurately

gives the slopes for various molecular weights of polystyrene in cyclohexane of temperature as a function of weight fraction polymer.

MEASUREMENTS

(Jennings and Middleman) collected data on the superheat limit for the polystyrene-cyclohexane system for 2000 to 100,000 MW polymer. The values for the data points are tabulated in the Appendix of (Jennings) and in that appendix is presented all the other data necessary for this calculation.

The three figures are taken from (Jennings and Middleman). Figure 1 shows the typical linear rise in superheat with a binary solution, in this case pentane with addition of cyclohexane, by mass fraction. Figure 2 portrays the same linear rise with addition of styrene monomer and polystyrene of 2000 and 4000 MW and the curves are quite linear. Figure 3 gives the same linear rise, not as linear, but the trend is clear for 50,000 and 100,000 MW in that the rise is inversely proportional to the molecular weight and falls to zero as $MW \Rightarrow \infty$ and that is the result derived theoretically in (Jennings) paper. There is an additional rise that is felt to come from LCST or lower critical solution temperature, and this was noted in Jennings and Middleman. (Prud'homme and Gregory) used a similar apparatus to (Jennings and Middleman) for the benzene/polystyrene system but that data does not show the same straight lines and the high MW data drops off to a great degree, so what they got cannot be compared with the final equation here.

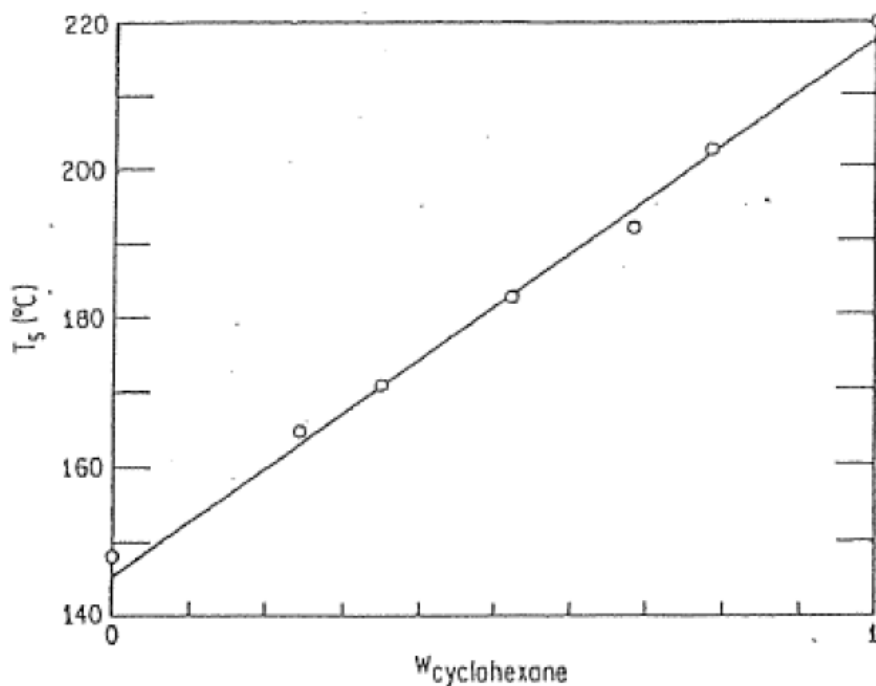


Figure 1. Data on limiting superheat for binary solutions of cyclohexane and pentane. Composition is mass fraction.

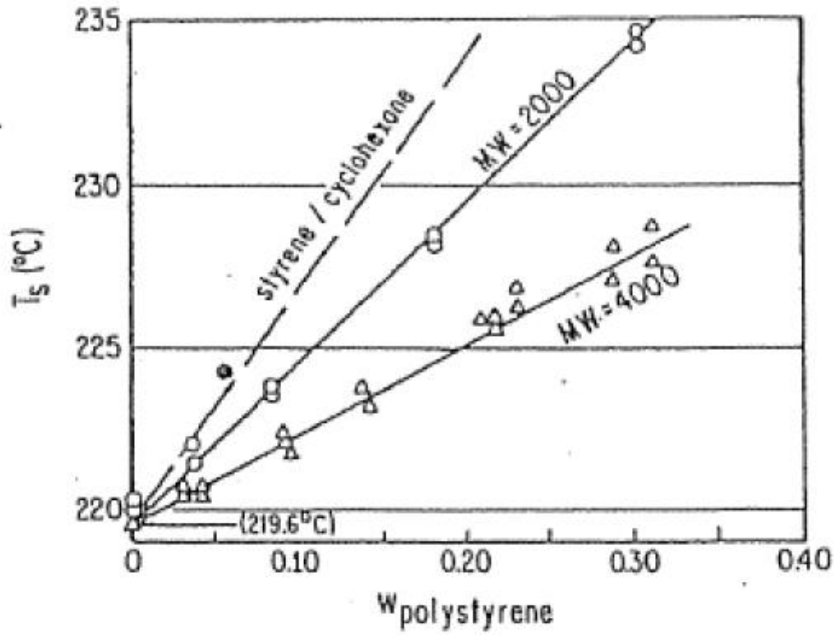


Figure 2. Data on limiting superheat for low molecular weight polystyrene in cyclohexane. T_s for pure cyclohexane is taken as 219.6 C.

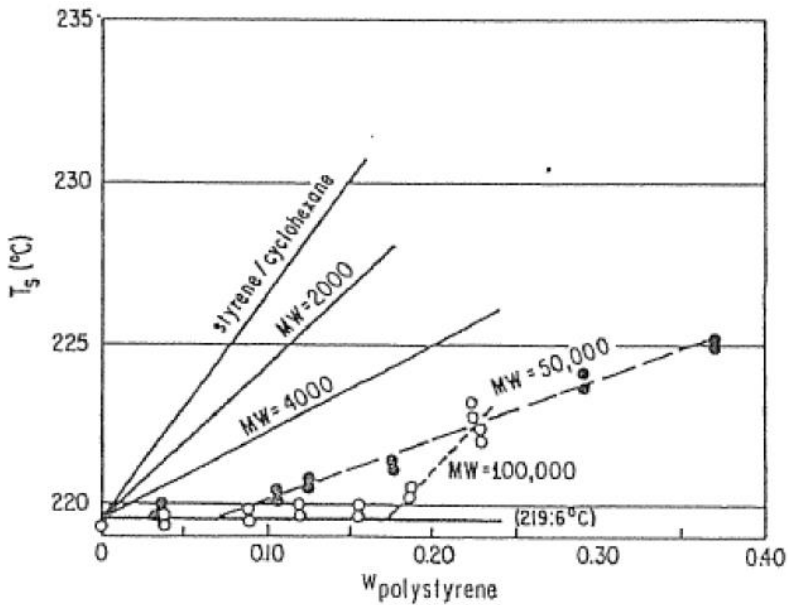


Figure 3. Data on limiting superheat for low molecular weight polystyrene in cyclohexane.

THEORY

According to (Blander and Katz) there is the following expression for the rate of nucleation J (number of bubbles formed per cm^3 per second).

$$J = 3.73 (10^{35}) (d^2 \sigma / M^3 B)^{1/2} \exp(-1.182(10^5) \sigma^3 / (T (P_V - P_L)^2)) \quad (1)$$

d is the liquid density, σ is the surface tension, M is the molecular weight of solvent, B is a correction factor (equation (6) below), T is the temperature in degrees Kelvin, P_V is the vapor pressure of the escaping gas molecules and P_L is the hydrostatic pressure on the droplet of solution.

The polymer is non-volatile and the "bubble surface gains or loses molecules" of molecular weight M (Blander and Katz). At a certain value of J nucleation takes place at the limit of superheat T_1 and we would expect J to be equal among the four molecular weights of polymer as the concentration of polymer approaches zero. This treatment proves that only what happens on the surface of the nucleating bubble matters. (Blander and Katz) say there is a Poynting correction factor δ that relates the vapor pressure of the superheated liquid, P_V , to the equilibrium vapor pressure, P_e , for small values of P_L , which is in this case atmospheric pressure. For this system, $P_e = 17.433$ atm and $P_L = 1$ atm, so this is satisfied, as $P_L / P_e = 0.057$. The Poynting correction factor is δ .

$$\delta = (P_V - P_L) / (P_e - P_L) \quad (2)$$

Assuming the gas is ideal in the equation, $d_G = P_e MW_1 / RT_1$, and

$$\delta \approx 1 - V_L / V_e + \frac{1}{2} (V_L / V_e)^2 = 1 - d_G / d + 0.5 (d_G / d)^2 \quad (3)$$

where the volumes and densities are for the liquid and gas in equilibrium. (Blander and Katz) give a proof for equation (3) and say it is generally accurate up to one atmosphere pressure, the condition in which the data was collected by (Jennings and Middleman).

When considering bubble nucleation for polymer solutions it seems that one should only look at the surface layer from which the solvent molecules are either escaping or adhering. Accordingly, the density would be the volume fraction weighted sum at the surface of the respective densities and the equilibrium vapor pressure would be directly proportional to the volume fraction of solvent at the surface. In polymer solutions, nucleation depends only on what is happening near the surface, so the density is essentially the density of the solvent and the equilibrium vapor pressure follows Raoult's Law.

$$d = d_1 \phi_{1S} + d_2 \phi_{2S} = d_1 + (d_2 - d_1) \phi_{2S} \quad (4)$$

$$P_e = P_e(0) \phi_{1S} = P_e(0) (1 - \phi_{2S}) \quad (5)$$

ϕ_{1S} and ϕ_1 and are the surface and interior volume fractions of solvent (the subscript 2 refers to the polymer). This is because the surface is the only thing the nucleating bubble "sees" and the rest of the interior could be regarded as having the same concentration as the surface. According to calculations made by (Siow and Patterson), for preferential solvent adsorption,

$\sigma_2 > \sigma_1$, the adsorption isotherm hardly changes with molecular weight above molecular weight 2500 so the surface volume fraction of polymer is essentially zero all the way up to $\phi_2 = 0.3$. When $\sigma_2 - \sigma_1 \approx 22$ dyne/cm there obtains preferential solvent adsorption, so in that case "there is little qualitative difference between the surface thermodynamics of a polymer solution and a mixture of spherical molecules". (The data that (Jennings and Middleman) gathered was only up to about weight fraction 0.3 and above that for high MW it was felt that the LCST phenomenon took over.) Below in Eq. (10) this is made quantitative.

In the equation for $J = A \exp(K)$ there is also a correction factor B which has little effect on the limit of superheat because for J large errors in the prefactor A "lead to very small errors in predictions of the superheats needed to cause homogeneous nucleation" (Blander and Katz).

$$B \approx 1 - 1/3 (1 - P_L/P_V) \quad (6)$$

The B factor accounts for the fact that the bubble is in mechanical equilibrium, is close to 2/3, and for the purposes of its calculation, $P_V = P_e$, as it has a negligible effect on the temperature of nucleation. The δ correction factor is needed because the nucleating droplet is under pressure $P_L = 1$ atm pressure (other than its equilibrium vapor pressure P_e) and must be included as it is in the exponent. It will be seen later that δ and the equilibrium vapor pressure drop out of the calculation for polymer solutions.

The following two equations apply for the athermal case ($dT = 0$) by a theory of (Siow and Patterson) for polymer solutions, where a = surface area of the solvent molecule and r = ratio of the molar volume of the polymer to that of the solvent. Eq. (7) gives the surface tension and Eq. (8) relates the surface and interior volume fractions.

$$(\sigma - \sigma_1) a / kT = \ln(\phi_{1S} / \phi_1) + ((r - 1) / r) (\phi_{2S} - \phi_2) \quad (7)$$

$$\ln((\phi_{2S} / \phi_2)^{1/r} / (\phi_{1S} / \phi_1)) = (\sigma_1 - \sigma_2) a / kT \quad (8)$$

Near $\phi_2 = 0$, Eq. (7) becomes

$$\partial\sigma/\partial\phi_2 = kT / ra \quad (9)$$

Near $\phi_2 = 0$, Eq. (8) becomes

$$\phi_{2S} = \phi_2 \exp(r(\sigma_1 - \sigma_2) a / kT) \quad (10)$$

Putting in the numbers, $\partial\phi_{2S}/\partial\phi_2 \approx 10^{-38}$ (for MW = 2000, $r = 13.4$) and even less for higher MW.

Thus, polymer is present in vanishingly small volume fraction in the surface for $w_2 \leq 0.3$ for which there is data. That is why the density and vapor pressure only apply to what is at the surface. The gas molecules escape or adhere to the surface of a bubble nucleating in the interior of the rising droplet of solution.

So, the following equations are true: $\partial\delta/\partial\phi_2 = 0$, $\partial d/\partial\phi_2 = 0$, $\partial P_e/\partial\phi_2 = 0$, and $\partial B/\partial\phi_2 = 0$ for w_2 near 0. The rate of nucleation is of the form $J = A \exp(K)$ and $(\partial \ln A / \partial w_2) / (\partial K / \partial w_2)$ and $(\partial \ln A / \partial T) / (\partial K / \partial T)$ are both small near the origin (0, T_1). It turns out that they both are

about - 0.2% and that establishes for any ray emanating from the origin, $\Delta J = J \Delta K$, so $\Delta J = 0 \rightarrow \Delta K = 0$. Therefore K can be taken as a constant where the 2000, 4000, 50,000 and 100,000 curves meet. An expression for $\partial T / \partial w_2$ can be derived from the fact that K dominates in nucleation and that is done in this theory.

For the weight fraction, this ratio is independent of the molecular weights and surface area of the solvent molecule. It is simply:

$$\lim w_2 \rightarrow 0 (\partial \ln A / \partial w_2) / (\partial K / \partial w_2) = 1 / (6K) = - 0.24\% \quad (11)$$

In the temperature direction, there are a number of terms, as each parameter depends on temperature. These expressions are for $T \rightarrow T_1$. See Appendix in Jennings' paper for values of parameters and partial derivatives.

$$\partial \ln A / \partial T = (\partial d_1 / \partial T) / d_1 + 0.5 (\partial \sigma / \partial T) / \sigma - 0.5 (\partial B / \partial T) / B = - 0.01251$$

$$\partial K / \partial T = - 1.182 \times 10^5 (3\sigma^2 (\partial \sigma / \partial T) / (T \delta^2 (P_e - P_L)^2) - \sigma^3 / (T^2 \delta^2 (P_e - P_L)^2) - 2\sigma^3 (\partial \delta / \partial T) / (T \delta^3 (P_e - P_L)^2) - (2\sigma^3 / (T \delta^2 (P_e - P_L)^3)) (\partial P_e / \partial T)) = 6.488$$

$$\lim T \rightarrow T_1 (\partial \ln A / \partial T) / (\partial K / \partial T) = - 0.19\% \quad (12)$$

The reason these two ratios do not agree exactly must be mainly in the estimation for the surface tension.

It is extrapolated far beyond the data up near the critical point. The pressure is close, except the Poynting correction may be off a bit. Otherwise, the approximation that $K = \text{const}$. is good, so it would hold for all the data.

Neglecting the change in the coefficient one can easily derive an expression for $\lim \varphi_2 \rightarrow 0$ for $\partial T / \partial \varphi_2$ where φ_2 is the volume fraction of polymer in the interior of the droplet. The exponent is then taken constant.

$$K = - 1.182 \times 10^5 \sigma^3 / T (P_V - P_L)^2 \quad (13)$$

So, solving for T, then differentiating (using partial derivatives throughout this paper).

$$\lim \varphi_2 \rightarrow 0 \partial T / \partial \varphi_2 = T_1 ((3 / \sigma_1) \partial \sigma / \partial \varphi_2 - (2 / (P_V - P_L)) \partial P_V / \partial \varphi_2) \quad (14)$$

In Siow and Patterson's theory for polymer solutions, the surface volume of solvent and interior volume of solvent are used here in the simple athermal ($dT = 0$) case. Their theory is for the surface tension of a polymer solution against a liquid and in the experimental conditions the droplet rose in a column of heated glycerol where the temperature rises as the droplet ascends in the column. This surface tension is taken to be the surface tension of the nucleating bubble within the droplet. Substituting (2) into (14) and using the fact that $\partial \delta / \partial \varphi_2 = 0$ for w_2 near 0:

$$\lim \varphi_2 \rightarrow 0 \partial T / \partial \varphi_2 = T_1 ((3 / \sigma_1) \partial \sigma / \partial \varphi_2 - (2 / (P_e - P_L)) \partial P_e / \partial \varphi_2) \quad (15)$$

The result (using (9) and (15)) along with the fact that $\partial P_e / \partial \varphi_2 = 0$ near $\varphi_2 = 0$ is:

$$\lim_{\phi_2 \rightarrow 0} \partial T / \partial \phi_2 = 3 k T_1^2 / \sigma_1 r a \quad (16)$$

where k = Boltzmann constant, T_1 = limit of superheat of cyclohexane, σ_1 = surface tension of cyclohexane at T_1 , r = ratio of molar volume of polymer to molar volume of solvent at T_1 and a = surface area of the solvent molecule at T_1 .

One adjustment made to (Siow and Patterson) was in the calculation of the surface area of the cyclohexane molecule, according to the formulas for a sphere

$$a = (4 \pi / (4 \pi / 3)^{2/3}) V^{2/3} = 4.836 V^{2/3} \quad (17)$$

where V is the molar volume of cyclohexane at T_1 divided by Avogadro's number.

RESULTS

Following is a table comparing theory with experiment. In this simplified equation, all quantities are at the limit of superheat for the solvent.

$$\lim_{w_2 \rightarrow 0} \partial T / \partial w_2 = (MW_1 / MW_2) (3kT_1^2 / \sigma_1 a) \quad (18)$$

Table 1. Theory vs. experiment for polystyrene in cyclohexane

Molecular weight	2000	4000	50,000	100,000
$\partial T / \partial w_2$ T in °C				
Theory	52.58	26.29	2.10	1.05
Experiment	48.48	28.78	3.62	2.66
ΔT in °C for $w_2 = 0.2$	+0.82	-0.50	-0.30	-0.32

Extrapolating Eq. (18) does reasonably well at predicting the limit of superheat for all the data.

The average deviation in the slope for the two lower MWs is about 8%, but since the temperature rise is only about 10-15 °C at 30 weight percent, if the athermal slope is used, the prediction gives an error of 0.5 or 0.8 °C at 20% weight fraction between theory and experiment.

Notice that as the MW of polymer grows large, the temperature rise from this phenomenon is much less; that is what is found for the data in (Jennings and Middleman) for low weight fraction and higher molecular weight. However, the slope is more accurate at low molecular weight.

Now, I am proposing the expanded form of the differential as a new equation general for all polymer solutions and presenting it here as Eq. (19). Since the data are quite linear for the two lower MW and the two higher MW follow the predicted trend, it seems appropriate to offer this formula as the correct one. This derivation did not require calculation of the nucleation rate because of the vector calculus argument. Eq. (19) could be easily tested for polystyrene by using cyclopentane, n-hexane and n-heptane using the rising drop method presented in (Jennings and Middleman).

$$T - T_1 = (MW_1/MW_2) (3kT_1^2 / \sigma_1 a) (w_2) \quad (19)$$

CONCLUSION

A new formula for the limit of superheat of polymer solutions is offered here. It resulted from the theory of surface thermodynamics of polymer solutions by (Siow and Patterson) and classical nucleation theory. Data of the superheat in polystyrene-cyclohexane solutions from 2000 to 100,000 molecular weight at 1 atm pressure collected by (Jennings and Middleman) agrees reasonably well with Eq. (19). However, the slope is more accurate at low molecular weight. The temperature rise above the limit of superheat of pure solvent by addition of polymer is directly proportional to weight fraction polymer and inversely proportional to molecular weight polymer.

ACKNOWLEDGMENTS

The Theory section is taken from John H. Jennings "Limit of Superheat of Polystyrene-Cyclohexane Solutions: Theory" *INTERNATIONAL JOURNAL OF THERMODYNAMICS* (2012) 15, 127-132. The figures are taken from Jennings, J.H. and Middleman, S. "Homogeneous Nucleation of Vapor from Polymer Solutions" *MACROMOLECULES*. (1985) 18, 2274-2276 © American Chemical Society. Finally, I acknowledge the staff and members of Creative Wellness Center of Berkeley, California for egging me on in the pursuit of science.

REFERENCES

- Blander, M. and Katz, J.L. Bubble Nucleation in Liquids. *AIChE J.* (1975) 21, 833-848.
- Frenkel, J. *Kinetic Theory of Liquids* (1955) Dover, New York, Chapter 7.
- Guo, Z., Burley, A.C., Koelling, K.W., Kusaka, I., Lee, L.J., and Tomasko, D.L. CO₂ Bubble Nucleation in Polystyrene: Experimental and Modeling Studies. *J. Appl. Polym. Sci.* (2012) 125, 2170-2186.
- Han, J.H. and Han, C.D. Bubble Nucleation in Polymeric Liquids. I. Bubble Nucleation in Concentrated Polymer Solutions. *J. Polym. Sci. Part B.* (1990a) 28, 711-741.
- Han, J.H. and Han, C.D. Bubble Nucleation in Polymeric Liquids. II. Theoretical Considerations. *J. Polym. Sci. Part B.* (1990b) 28, 743-761.
- Jennings, J.H. Limit of Superheat of Polystyrene-Cyclohexane Solutions: Theory *Int. J. Thermodynamics.* (2012) 15, 127-132.
- Jennings, J.H. and Middleman, S. Homogeneous Nucleation of Vapor from Polymer Solutions *Macromol.* (1985) 18, 2274-2276.
- Kim, K.I., Kang, S.L. and Kwak, H.Y. Bubble Nucleation and Growth in Polymer Solutions. *Poly. Eng. Sci.* (2004) 44, 1890-1899.
- Prigogine, I. and Marechal, J. The Influence of Differences in Molecular Size on the Surface Tension of Solutions IV. *J. Coll. Sci.* (1952) 7, 122-127.

- Prud'homme, R.K. and Gregory W.J. Homogeneous Nucleation Temperatures for Concentrated Polystyrene-Benzene Solutions. *J. Polym. Sci. Symp.* (1985) 72, 263-275.
- Siow, K.S. and Patterson, D. Surface Thermodynamics of Polymer Solutions. *J. Phys. Chem.* (1973) 77, 356-365.
- Yarin, A.L., Lastochkin, D., Talmon, Y., and Tadmor, Z. Bubble Nucleation During Devolatilization of polymer Melts. *AIChE J.* (1999) 45, 2590-2605.

INDEX

#

20th century, 144, 161

A

ABA, 40

absorbents, x, 130, 131, 136

absorption spectra, 157

access, 165, 166, 184

accessibility, 185

accounting, 61

acetic acid, 271

acetone, 64, 152, 156, 169, 191

acetonitrile, 163, 166, 168, 170, 193, 194

acetylation, 91

acid, 15, 17, 28, 33, 47, 65, 85, 171, 172, 173, 174,

175, 177, 179, 180, 191, 192, 195, 219, 223, 271

acidic, 28, 33, 42, 144, 163, 165, 171

acrylate, 34, 40, 134, 139, 202

acrylic acid, 32

acrylonitrile, 4, 26, 32, 202

activated carbon, 29, 145, 160, 175, 181, 182, 185,

186, 187, 188, 192, 218

activation energy, 9

active centers, 28

active oxygen, 228

active site, 41

acute lung injury, 184

additives, xi, 12, 19, 207, 269, 272, 273

adhesion, 71, 181

adhesives, 66, 229

adjustment, 249, 288

adsorption, 44, 84, 85, 86, 87, 88, 89, 90, 91, 92,

100, 101, 109, 111, 112, 120, 123, 136, 138, 145,

146, 148, 152, 154, 160, 169, 170, 171, 182, 184,

185, 190, 191, 192, 193, 194, 218, 225, 228, 256,

265, 285

adsorption isotherms, 152

advancement, 276

adverse effects, 183

aesthetics, 276

age, 273

aggregation, 43, 45, 46, 47, 88, 118, 187, 207, 225,
229, 256

agriculture, 32, 161

AIBN, 130, 132, 134, 137, 218

albumin, 181, 182, 187, 188, 189

alcohols, 55, 144, 145, 206, 272

aldehydes, 206

algae, 134

aliphatic amines, 206

aliphatic compounds, 169

alkaline hydrolysis, 170

alkane, 5, 12

alkenes, 12

alkylation, 148, 190

alkylation reactions, 190

allergy, 181

aluminium, vii, 2, 270

aluminum oxide, 19, 206

amine(s), 85, 169, 206

amino, 85, 112, 144, 163, 164, 169

amino acid(s), 169

amino groups, 112, 144

ammonia, 149, 192

ammonium, 141, 175, 176, 179, 181, 192, 193, 210,

211, 212, 213, 214, 256

ammonium salts, 181

amorphous phases, 119

anaphylaxis, 184

angioedema, 184

aniline, 193

anisotropy, 153, 225

annealing, 219

annual rate, 61

antibody, 231

antigen, 231
 antimony, 10, 13
 aqueous solutions, 163, 165, 191, 192, 224
 aqueous suspension, 219
 argon, 14
 aromatic compounds, vii, 1, 5, 7, 9, 10, 11, 12, 13, 15, 17, 19, 22, 169
 aromatic hydrocarbons, 13, 15, 17, 146, 170
 aromatic rings, ix, 5, 129, 130, 148, 158, 190, 192
 aromatics, vii, 1, 10, 14, 16, 19, 20, 21, 22, 27
 ascites, 113
 Asia, 61, 62, 72
 atmosphere, 24, 55, 218, 285
 atmospheric pressure, 13, 56, 270, 285
 atoms, 14, 215, 217, 225
 attachment, 210, 275
 automobiles, xi, 269, 273
 automotive application(s), 70

B

bacteria, 186, 188, 227
 band gap, 117, 118
 base, xi, 2, 28, 59, 91, 95, 100, 112, 113, 146, 178, 179, 182, 188, 189, 195, 269
 basicity, 144
 batteries, 229
 BD, 32
 beer, 141
 behaviors, 7, 264
 Beijing, 75
 beneficial effect, 14
 benefits, 17, 18, 72, 116, 163
 benign, ix, 129, 212
 benzene, vii, xi, 1, 6, 11, 12, 15, 47, 65, 85, 110, 148, 160, 190, 191, 193, 270, 281, 283
 benzoyl peroxide, 204
 beverages, 206
 bilirubin, 188
 biocompatibility, 76, 91, 181, 228, 229
 bioenergy, ix, 75
 biological fluids, 159, 168
 biomarkers, 261
 biomass, 29
 biomedical applications, 231
 biomolecules, 77, 82, 109
 biopolymers, 109, 139, 140
 biosensors, 123
 bioseparation, 109
 biotechnology, 32, 100
 biotic, 2
 biotin, 120
 bleeding, 182

blends, 32, 202
 blood, x, 143, 166, 169, 180, 181, 182, 183, 184, 186, 187, 188, 189
 blood circulation, 180, 188
 blood plasma, 166
 blood stream, 181
 blood vessels, 182
 blowing agent, 54, 55, 220, 223
 boils, 54
 Boltzmann constant, 282, 288
 bonding, 71, 193
 bonds, 2, 22, 148, 149, 150, 175
 bottom-up, 221
 brain, 179
 Brazil, 53, 61, 63, 66
 breakdown, 155
 brittleness, 270
 brominated flame retardants, 13, 16
 bromine, 16
 bulk materials, 207
 bulk polymerization, 212, 213, 214, 215, 219
 butadiene, 4, 26, 32, 144, 202
 butadiene-styrene, 4, 32, 202

C

Ca²⁺, 175
 cadmium, 206
 CAF, 22
 caffeine, 160
 calcium, 16, 173, 174, 175, 180
 calcium carbonate, 16
 calculus, xi, 281, 288
 calibration, 116
 calixarenes, 41
 calorimetry, 216
 canals, 190
 cancer, 184, 188
 candidates, 84, 228
 CaP, 276
 capillary, 110, 117, 118, 152, 161, 195
 caprolactam, 179
 carbohydrate(s), 139, 169
 carbon, vii, 2, 5, 7, 11, 14, 15, 16, 18, 20, 21, 26, 29, 141, 160, 163, 164, 165, 169, 182, 186, 187, 188, 189, 192, 206, 215, 216, 217, 218, 219, 220, 225
 carbon atoms, 14, 220
 carbon dioxide, 141
 carbon materials, 29
 carbon nanotubes, 215, 218
 carbonization, 160
 carbonyl groups, 149
 carboxyl, 85, 120

- carboxylic groups, 144
cardiovascular disease, 231
casting, 24, 211, 217, 220
catalysis, 145, 228
catalyst, 15, 16, 17, 22, 27, 28, 41, 65, 91, 92, 96, 98, 136, 202, 217, 263, 270, 275
catalytic activity, 16, 263
catalytic effect, 18
catalytic properties, 224, 225, 228
catalytic system, 4, 8, 12, 16, 22, 41
cation, 78, 109, 136, 173, 174, 210, 212, 276
cationic surfactants, 210
C-C, 5, 22, 91, 149, 150, 203
cell size, 220, 223
cellulose, ix, 14, 27, 76, 111, 129, 132, 133, 134, 138, 139, 140, 169
ceramic, 228
cerium, 262
CFR, 197
chain scission, 213
chain transfer, 9, 40, 42
challenges, 225
Char formation, vii, 1
charge density, 47
chemical bonds, 68, 157
chemical degradation, 155
chemical industry, 228
chemical interaction, 226
chemical properties, xi, 117, 130, 158, 207, 228, 269
chemical reactions, 18, 85, 116, 207, 276
chemical stability, ix, 75, 76, 77, 84, 108, 208, 228, 270
chemical vapor deposition, 217, 220, 221
chemicals, 2, 5, 22, 180, 243
children, 58
China, 61, 75, 109, 158, 160
chitin, 134, 138, 140
chitosan, 140, 182
chloride anion, 173, 174, 175, 177, 179
chlorinated hydrocarbons, 161, 206
chlorination, 148
chlorine, 13, 148, 175, 193
chlorobenzene, 160
chloroform, 160, 176, 211
choline, 182
chopping, 18
chromatograms, 108, 180
chromatographic supports, 77, 79, 99, 100, 109
chromatographic technique, 159
chromatography, viii, ix, 75, 76, 77, 84, 91, 95, 100, 102, 106, 109, 110, 111, 112, 113, 148, 161, 166, 171, 172, 173, 175, 180, 195, 272
circulation, 66, 188
clarity, 205, 278
classes, vii, 1, 2, 151, 165, 169
classical methods, vii, 1, 91
classification, 13, 15, 26
Clay, x, 129, 135, 209, 210, 211, 212, 213, 214, 215, 234
clay minerals, 141
cleaning, 228
cleavage, 2, 5, 6, 7, 12
clinical application, 230
clinical trials, 189
closure, 274
cluster model, 282
clusters, 78, 195, 210, 256, 260
CMC, 42, 43
CO₂, x, 2, 130, 131, 136, 138, 141, 151, 152, 220, 223, 282, 289
coal, 4, 11, 18, 19, 23, 26, 29
coal tar, 11, 26
Coast Guard, 54
coatings, x, 32, 44, 47, 85, 90, 91, 99, 112, 130, 131, 137, 138, 141, 228
cobalt, 15, 171, 206, 217
coffee, 160
coke, 15, 17
coke formation, 17
collateral, 181
colonization, 227
color, 120, 157, 226, 230, 264
combustion, 2, 9, 15, 64
commercial, 15, 54, 78, 101, 116, 130, 144, 166, 170, 185, 202, 270, 272, 275
commodity, vii, 31, 32, 202
community, 229, 270
compatibility, 44, 68, 132, 157, 181, 186, 207, 208, 210, 211
complexity, 5
composite materials, ix, 72, 129, 131, 132, 138, 139
composite wood, 69
composites, viii, 53, 66, 68, 69, 70, 71, 132, 133, 134, 135, 136, 139, 141, 209, 210, 216, 224, 225, 226, 227, 232, 254, 270, 274, 279
composition, vii, viii, xi, 1, 9, 12, 13, 15, 18, 19, 20, 22, 25, 31, 39, 43, 46, 91, 99, 100, 124, 188, 189, 254, 257, 269
compounds, x, 2, 10, 11, 12, 13, 14, 15, 16, 17, 18, 19, 20, 21, 22, 143, 146, 158, 161, 163, 165, 166, 169, 170, 172, 180, 181, 184, 193, 223, 272, 273
compressibility, 274
compression, viii, 53, 58, 66, 67, 155, 156, 219, 222
conception, 195
condensation, 64, 152, 190
conditioning, 18, 60, 277

conductance, 134, 223
 conduction, 217, 223
 conductivity, 59, 82, 134, 215, 217, 219, 221, 222, 224, 225, 226, 230, 275, 277
 conductor, 157, 216
 conference, 279
 configuration, 65, 85, 90, 91, 123, 162, 168, 184, 208, 216, 251, 252, 254, 270
 confinement, 120, 230
 conjugation, 5
 connectivity, 190
 conservation, vii, 1
 construction, 54, 57, 59, 60, 61, 62, 63, 64, 71, 144, 202, 231, 244, 277
 consumer goods, 57, 277
 consumers, 57
 consumption, 60, 61, 62, 63, 161, 165, 206, 244, 273
 contact time, 10
 containers, vii, 1, 7, 63, 242
 contaminated water, 162
 contamination, 161, 162, 165, 272
 control group, 183, 188
 COOH, 207
 cooling, 56, 57
 copolymer, 32, 33, 39, 41, 44, 45, 46, 47, 85, 111, 144, 145, 146, 148, 152, 153, 155, 156, 157, 218
 copolymerization, vii, 31, 32, 134, 135, 202
 copolymers, viii, 4, 31, 32, 33, 34, 36, 38, 39, 40, 41, 42, 43, 44, 45, 46, 47, 144, 145, 148, 149, 153, 154, 158, 169, 184, 202, 205, 206, 207
 copper, 18, 19, 29, 171, 206
 correlation, 247
 corrosion, 179, 217, 241
 cosmetics, 32, 228, 229
 cost, viii, x, 2, 26, 53, 54, 55, 57, 71, 109, 130, 144, 161, 171, 201, 202, 220, 229, 231, 241, 263, 276
 covalent bond, 2, 220
 cracks, 69, 276
 creatinine, 187, 188
 creep, 205, 218, 274, 279
 Croatia, 23
 crop(s), 161, 165, 166
 crude oil, 47
 crystal structure, ix, 115, 117, 118, 120
 crystalline, 4, 119, 132, 179, 202, 203, 215, 274, 276
 crystallinity, 203
 crystallization, 175, 202, 203, 213, 230
 crystals, ix, 115, 117, 118, 119, 120
 culture, 227, 278
 customers, 58
 cytokines, 182, 183, 184, 185, 186, 187, 188

D

decay, 205
 decomposition, 13, 16, 17, 25, 26, 28, 181, 218, 219, 220, 222, 272, 273, 277
 decomposition temperature, 13, 220, 222
 defects, 69, 230
 deformation, ix, 115, 155, 156, 274
 degenerate, 193
 degradation, 5, 6, 7, 11, 12, 22, 23, 24, 26, 63, 64, 65, 163, 166, 169, 213, 214, 218, 222, 225, 228, 275
 degradation mechanism, 22
 degradation rate, 12, 275
 degree of crystallinity, 208
 dehydration, 91
 denaturation, ix, 76, 84
 density values, 59, 60, 66, 69
 depolymerization, 17, 63, 213
 deposition, 116, 118, 123, 256
 deposits, 116, 124
 derivatives, 12, 40, 130, 161, 163, 169, 193, 216, 221, 230, 270, 287
 dermatitis, 181
 desorption, 89, 91, 136, 138, 168, 170, 191
 destruction, 148, 186, 187
 detection, 162, 163, 165, 168, 231
 detoxification, x, 143, 183, 187, 188, 189
 developed countries, 277
 developing countries, 61
 deviation, 152, 288
 dialysis, 42
 dielectric constant, 43, 44, 224, 228, 272
 dielectric permittivity, 219
 dielectrics, 228
 differential scanning, 136, 214
 differential scanning calorimetry, 214
 diffraction, 120
 diffusion, 18, 56, 76, 77, 78, 108, 113, 218, 256, 282
 diluent, 145
 dimensionality, 215
 dimethylformamide, 64, 221, 222
 dipoles, 226
 direct measure, 161
 discrimination, 171, 175
 diseases, 64, 181
 dispersion, 69, 116, 136, 151, 152, 158, 171, 189, 191, 192, 207, 210, 211, 212, 213, 214, 217, 218, 219, 220, 221, 222, 223, 225, 229, 230, 242
 dispersity, 42, 242
 dissociation, 175
 distillation, 65, 270

- distribution, vii, 1, 12, 14, 15, 16, 18, 24, 28, 54, 69, 88, 98, 100, 149, 158, 185, 207, 224, 225, 226, 246, 248
- diversity, 144
- DNA, 276
- dogs, 188, 189
- dominance, 61
- donors, 186
- double bonds, 5, 8, 148, 169, 189
- drainage, 59
- drawing, 220
- drinking water, 165
- drug carriers, 47
- drug delivery, 47
- drugs, 166, 181, 184, 215
- drying, vii, 1, 18, 134, 150, 155, 156, 219, 254, 255, 274
- DSC, 136, 214, 218
- durability, 64, 131
- dyes, 190, 230

E

- E.coli, 186
- eczema, 181
- elastic deformation, 156
- elastomers, 156, 206
- electric field, 124, 223, 225
- electrical conductivity, 123, 134, 217, 219, 220, 221, 222, 275
- electrical properties, 220
- electrical resistance, 7, 219
- electrolyte, 171, 172, 173, 180, 195, 276
- electromagnetic, 18, 217, 220, 223, 225
- electromagnetism, 43
- electron(s), 18, 66, 77, 78, 79, 132, 157, 169, 175, 190, 191, 193, 203, 217, 222, 223, 242, 255, 261, 276
- electronic structure, 157, 225
- electronic systems, 169, 190, 192
- electrophoresis, 161
- electrospinning, 64
- elongation, ix, 115, 122, 123, 205, 212, 229
- embolism, 182
- emission, 228, 230, 255
- employment, 278
- emulsifiers, viii, 31
- emulsifying agents, 205
- emulsion polymerization, viii, xi, 31, 47, 205, 214, 242, 269
- encapsulation, 207, 231
- endotoxins, 188
- energy, vii, 1, 2, 4, 10, 11, 18, 55, 58, 63, 64, 69, 84, 206, 207, 214, 225
- engineering, 144, 202, 217
- entrapment, 123
- environment(s), 2, 20, 72, 120, 158, 160, 161, 170, 206, 207, 224, 226
- environmental conditions, 76
- environmental crisis, 2
- environmental impact, 58
- environmental issues, 63, 64
- environmental protection, ix, 75, 130, 229
- Environmental Protection Agency, 161, 197
- enzyme, 82, 108
- enzyme immobilization, 82
- EPA, 164, 197
- epitaxial growth, 221
- EPR, 157
- EPS, viii, 4, 7, 53, 54, 55, 56, 57, 58, 59, 60, 61, 62, 63, 64, 65, 66, 67, 68, 69, 70, 71, 72, 74, 275
- equilibrium, 5, 40, 151, 171, 181, 192, 282, 285, 286
- equipment, 59, 66, 161, 162, 165, 179, 202
- erythrocytes, 186, 187, 188
- ester, 33, 76, 92
- etching, 116
- ethanol, 124, 134, 152
- ethers, 168, 206, 272
- ethyl alcohol, 270
- ethylbenzene, vii, 1, 6, 9, 11, 17, 19, 22, 65, 270
- ethylene, 4, 11, 26, 32, 39, 40, 47, 83, 90, 111, 112, 144, 147, 148, 202, 210, 230, 270
- ethylene glycol, 40, 83, 90, 112
- ethylene oxide, 32, 39, 47, 210
- Europe, 61, 62, 72, 198
- European Commission, 165
- European Union, 161, 182
- europium, 261, 262
- evaporation, ix, 115, 116, 117, 118, 119, 123, 124, 151, 179, 205, 254, 255
- everyday life, 2
- evidence, 71, 103, 152, 156, 274
- evolution, 24, 253
- excitation, 140, 223, 226
- exclusion, 85, 171, 173, 175, 176, 180, 191, 192, 195
- experimental condition, 20, 33, 100, 170, 224, 287
- exposure, 169
- extinction, 120, 121, 123
- extraction, x, 83, 130, 134, 137, 138, 141, 143, 159, 160, 161, 162, 163, 165, 168, 169, 170, 194, 272, 273
- extracts, 159, 169, 170, 187, 188, 191
- extrusion, viii, 53, 63, 66, 67, 202, 205, 212, 219, 220, 277

F

fabrication, ix, 83, 110, 119, 115, 120, 123, 124, 130, 132, 134, 208, 217, 226, 231, 249, 266, 275

families, 182

fatty acids, 170

feedstock(s), 2, 5, 12, 14, 18, 22, 26, 29, 63, 108

fermentation, 160

ferromagnetic, 224

fertilizers, 171

fiber(s), 64, 69, 71, 140, 206, 220, 228, 229

fibrillation, 181

fibrinogen, 85

fillers, 203, 207, 228, 230, 277

film formation, 134, 254

film thickness, 218

films, ix, 63, 115, 134, 140, 216, 218, 221, 226, 228, 229, 230, 275

filters, 226

filtration, 109, 275

financial, 2, 23, 109

financial support, 23, 109

fire resistance, 206

fire retardancy, x, 201, 209, 221

first generation, 144, 154

fish, 58, 163, 169, 277

fixation, 86

flame, 4, 13, 16, 17, 27, 55, 168, 214, 223, 228, 272

flame retardants, 13, 272

flammability, 214

flexibility, 131, 150, 161, 162, 177, 202, 217

flocculation, 47, 253

flooring, 60

flora, 161

flora and fauna, 161

flour, viii, 53, 65, 66, 67, 68, 69, 71

fluid, 10, 16, 123, 187, 273

fluid extract, 273

fluidized bed, 8, 10, 14, 22, 23, 26, 65

fluorescence, 42, 100, 226, 231

fluorophores, 230

foams, 54, 55, 220, 223

food, vii, 1, 17, 54, 57, 58, 109, 113, 133, 144, 159, 165, 169, 170, 181, 205, 215, 242, 277

food industry, 144

food intake, 169

food products, 159, 170

force, 85, 123, 155, 158, 208, 256, 260

Ford, 50, 235

6, 257, 258, 260, 261, 271, 272, 274, 275

formula, 39, 144, 209, 215, 288, 289

fracture stress, 134

fracture toughness, 217

fragility, 216, 273

fragments, 149, 150, 151, 169, 190, 191, 192

free energy, 5, 225

free radical copolymerization, 144, 145

free radicals, 40, 205, 218

free volume, 154, 177, 216, 227, 229, 230

freedom, 150

friction, 18, 64

fruits, 169

FTIR, 148, 243, 244, 250

fuel consumption, 58

fullerene, 215, 216

functionalization, 208, 217, 221

fungi, 60, 186, 188

furan, 169, 193

G

gas sensors, 228

gasification, 11, 15, 17, 26, 28

gel, 44, 45, 46, 76, 109, 113, 134, 140, 144, 145, 146, 149, 151, 153, 154, 155, 162, 171, 274

gel formation, 134

gelation, 44, 45, 46, 134

geography, 72

geometry, 47, 190

Germany, 54, 158, 159, 183, 232

glass transition, 42, 47, 155, 205, 208, 227

glass transition temperature, 47, 155, 205, 208, 227

glasses, 228

glassy polymers, 155

global demand, 61, 71, 72

glucose, 95, 99, 100, 120, 132

glycerol, 287

glycol, 121, 272

GNP, 223

good behavior, 206

governments, 71

grades, 54, 205

grain size, 230

granules, 185

graphene sheet, 220, 221, 222, 223

graphite, 206, 215, 217, 220, 221, 223

gravimetric analysis, 132

greenhouse(s), 2, 63

greenhouse gas, 2

groundwater, 164

growth, x, 39, 40, 41, 60, 61, 62, 151, 161, 186, 214, 217, 224, 225, 241, 242, 244, 245, 247, 256, 261, 282

growth rate, 61

guidelines, 231

H

hair, 169
 halogen, 41
 hardness, 202, 212, 230
 harmful effects, 161
 hazards, 57
 haze, 205
 HDPE, 4, 12, 29
 health, viii, ix, 53, 57, 64, 75, 231, 277
 health care, 277
 heat release, 214
 heat removal, 205
 heat transfer, 18
 heating rate, 12, 14, 16, 65
 heavy metals, 181
 heavy oil, 13, 14
 height, 100, 106, 210
 helium, 152
 hemisphere, 123
 hemocompatibility, 181, 182, 184, 186, 187
 hemodialysis, 181
 hemoglobin, 184
 hepatitis, 181
 heptane, xi, 281, 288
 hexabromocyclododecane (HBCD), 55
 hexane, xi, 11, 47, 153, 154, 169, 193, 194, 281, 288
 high density polyethylene, 220
 highways, 59
 history, 47, 143
 homeostasis, 189
 homogeneity, 88
 homolytic, 5
 host, 18, 224, 225, 249, 250, 251, 254, 255, 257, 260, 261
 hot pressing, 219
 housing, 4, 278
 HPLC-UV, 170
 human, 78, 144, 161, 167, 168, 169, 183, 185, 187, 188
 human activity, 144, 161
 human body, 78, 169
 human health, 161
 humidity, 58, 60, 119, 277
 hybrid, 112, 203, 265, 275
 hydrazine, 222, 223
 hydrocarbons, 2, 13, 14, 16, 17, 23, 25, 29, 54, 55, 145, 151, 161, 169, 206, 272
 hydrogen, 5, 7, 11, 12, 15, 17, 132, 174, 191, 193, 217, 270
 hydrogen abstraction, 5, 7
 hydrogen bonds, 132, 174
 hydrogen chloride, 191, 270

hydrogenation, 17
 hydrolysis, 23, 39, 40, 41, 99, 206
 hydrophilicity, 40, 47, 89, 91, 92, 100, 210
 hydrophobicity, ix, 75, 90, 207, 210
 hydroxide, 17, 28, 192, 193
 hydroxyl, 85, 86, 91, 98, 112, 174, 179, 211
 hydroxyl groups, 91, 211
 hygiene, 228
 hypothesis, 251, 259, 261
 hysteresis, 152
 hysteresis loop, 152

I

ID, 168, 234, 238, 240
 ideal, 54, 58, 83, 117, 124, 175, 285
 identification, 169, 272
 ignition source, 206
 IL-8, 183, 186, 187
 illumination, 264
 image(s), 44, 70, 78, 83, 84, 87, 88, 93, 98, 99, 102, 118, 119, 120, 121, 122, 123, 124, 132, 133, 228, 242, 243, 250, 251, 252, 254, 255, 258, 259, 261, 263, 264
 imidazolium group, ix, 129, 130, 136
 immersion, 137
 immobilization, 124, 275
 immunization, 184
 immunoglobulin, 113
 impact energy, 212
 impact strength, 54, 66, 69, 205, 212, 228
 improvements, 203, 212, 213
 in vitro, 182, 186, 187, 188, 228
 in vivo, 182, 188
 inadmissible, 189
 incompatibility, 45, 68, 207
 India, 61, 269, 279
 individuals, 169
 Indonesia, 241
 industrial wastes, 171
 industries, 18, 57, 62, 65, 72, 133, 161
 industry, viii, x, 16, 32, 57, 61, 62, 66, 70, 144, 161, 201, 206, 230, 276, 277
 infection, 184
 inflammatory mediators, 184
 information technology, 276
 inhibition, 112, 181
 inhibitor, 144, 272
 initiation, 69, 244, 276
 inorganic fillers, 2
 institutions, 62
 insulation, viii, 4, 53, 54, 58, 59, 60, 64, 71, 72, 169, 277

insulators, 22
 integration, 65, 273
 intensive care unit, 182
 interface, x, 43, 44, 69, 71, 201, 207, 208, 225, 227, 229, 276, 279, 282
 interface layers, 225
 interfacial adhesion, 68, 69, 71, 217, 229
 interfacial bonding, 69
 interfacial reactivity, 207
 interference, 217, 220, 225, 272
 intestine, 182
 intoxication, 181
 investments, 62
 iodinated contrast, 166
 ion exchangers, 110, 144, 145
 ion-exchange, 91, 100, 110, 113, 210
 ionic polystyrenes, ix, x, 129, 130, 131, 132, 134, 136, 137, 138
 ionization, 110
 ions, 44, 108, 145, 172, 173, 174, 175, 176, 178, 179, 180, 181, 192, 210, 211, 253, 256, 275
 IR spectra, 93, 96, 99, 134
 Iran, 61, 232
 iron, vii, 2, 11, 15, 16, 18, 171, 206, 217, 275
 irradiation, 18, 124, 182, 275
 islands, 116
 isolation, 132, 145
 isomers, 55, 215
 isotherms, 89, 152, 193
 issues, 18, 207, 231
 Italy, 1

J

Japan, 62, 72, 115, 129, 211, 241

K

K^+ , 253, 276
 KBr, 45
 ketones, 55, 206
 kidney, 181
 kinetic model, 7, 24
 kinetics, 24, 26, 145, 166, 270
 KOH, 192

L

laminar, 102
 landfills, viii, 2, 53, 64
 laser ablation, 215, 217
 leaching, 171

lead, ix, 5, 45, 62, 84, 98, 129, 171, 182, 188, 192, 194, 206, 211, 226, 227, 231, 275, 286
 learning, 275
 LED, 261
 leukocytes, 186
 liberation, 175
 life cycle, 2
 lifetime, 138, 171
 ligand, 224
 light, 2, 10, 13, 14, 16, 26, 58, 59, 117, 119, 122, 152, 153, 154, 180, 207, 223, 226, 230, 261, 262, 264, 270, 278
 light cycle, 10, 26
 light scattering, 207
 light-emitting diodes, 230, 261
 linear systems, 45
 lipids, 184, 189
 liquid chromatography, 76, 109, 110, 145, 161, 195
 liquid fraction, vii, 1, 12, 14, 15, 25, 65
 liquid monomer, 141
 liquid phase, 47, 162, 175
 liquid-phase synthesis, 256
 liquids, ix, 12, 15, 16, 20, 21, 22, 110, 129, 130, 131, 133, 134, 135, 136, 137, 138, 139, 140, 141, 151, 153, 162, 195, 282
 lithium, 179
 lithography, 116
 liver, 181
 liver failure, 181
 living radical polymerization, 40
 localization, 117, 119, 124, 222
 low density polyethylene, 220
 low temperatures, 25, 64, 205
 lubricating oil, 13, 27
 luminescence, 230, 262
 Luo, 48, 237, 239
 lymph, 187

M

machinery, 57
 macromolecular chains, 32
 macromolecules, 12, 43, 76, 85, 134, 144, 172, 211, 225
 macropores, 83
 magnesium, 17, 28, 209, 256
 magnetic properties, 224, 231
 magnetization, 229
 magnitude, 44, 45, 76, 157, 161, 218, 219, 222, 226, 248, 252, 253, 254, 273
 majority, 145, 150, 189, 205, 278
 Malaysia, 269
 man, 54, 95

- manganese, 17
manipulation, 207, 231
manufacturing, 55, 56, 62, 148, 158, 171, 179, 184, 229, 276, 278
mapping, 106, 110
market share, 202
masking, 100
mass, viii, ix, 15, 43, 54, 66, 75, 76, 84, 106, 108, 110, 113, 166, 169, 213, 214, 216, 217, 228, 251, 252, 254, 255, 275, 283
mass loss, 215
mass spectrometry, 110, 166
material handling, 277
materials science, 217
matrix, x, 32, 54, 68, 69, 71, 76, 85, 103, 113, 136, 144, 145, 158, 162, 166, 171, 177, 180, 185, 189, 192, 201, 203, 206, 207, 208, 210, 211, 213, 215, 217, 218, 219, 220, 222, 223, 224, 225, 226, 227, 228, 230, 231, 272, 273, 274, 275
matter, 109, 274
MB, 190
measurement, 88, 89, 99, 132
measurements, 66, 82, 123, 218, 274
meat, 58, 169, 277
mechanical properties, ix, 60, 64, 69, 71, 72, 75, 76, 77, 133, 134, 145, 205, 212, 218, 220, 221, 223, 225, 228, 229, 230, 274
media, viii, x, 43, 64, 75, 76, 78, 84, 100, 102, 108, 109, 113, 140, 143, 144, 145, 151, 157, 166, 169, 175, 180, 190, 193, 194, 195, 276
median, 189
medical, xi, 123, 161, 180, 181, 202, 228, 269, 278
medicine, 32, 144, 206, 227
melt, 57, 63, 66, 207, 211, 212, 214, 215, 216, 217, 219, 220, 221, 223
melt flow index, 66
melting, ix, 19, 129, 130, 202, 203, 205
melts, 54, 215
membranes, xi, 269, 273
memory, 156, 226, 230
mental disorder, 181
mercury, 88, 99, 152, 192
metabolites, 161, 162, 165, 166, 168, 181, 188, 189
metal ion(s), 192, 224, 261
metal nanoparticles, 224
metal oxides, 206
metal salts, 224
metals, 15, 18, 116, 121, 123, 171, 223, 224, 225
methacrylates, 112
methacrylic acid, 32
methanol, 10, 26, 153, 154, 164, 193, 194
methodology, viii, 14, 53, 66
methyl group, 194, 271
methylene blue, 228, 275
MFI, 66
Mg²⁺, 256
MHC, 113
microemulsion, 82, 275
microextraction, x, 130, 131, 137, 138, 141
microgels, 145
micrometer, 78, 111, 217, 261
microorganisms, 186
microporous materials, 160
microscope, 66, 82, 118, 119, 124, 153, 242, 255, 258, 261
microspheres, viii, ix, 75, 76, 77, 79, 80, 81, 82, 83, 84, 85, 86, 87, 88, 89, 90, 91, 92, 93, 95, 96, 97, 98, 99, 100, 102, 103, 108, 109, 110, 111, 112, 113, 219
microstructure, 202
microwave heating, 29
microwave radiation, 18
Middle East, 61
migration, 124, 190
military, 184
miniature, 187
Ministry of Education, 231
mixing, 10, 18, 47, 64, 78, 212, 219, 222, 223
modelling, xi, 30, 269
models, 273
modulus, 68, 69, 130, 205, 209, 212, 213, 217, 218, 220, 221, 228, 274
moisture, 39, 54, 60, 205, 228, 274, 277, 278
moisture content, 274
molar volume, 282, 286, 288
mold, ix, 57, 66, 115, 122
molds, ix, 115
mole, 147
molecular dynamics, 150
molecular structure, 203, 204
molecular weight, viii, xi, 2, 5, 9, 14, 17, 21, 22, 31, 32, 40, 42, 44, 45, 55, 65, 66, 77, 82, 86, 92, 108, 109, 144, 166, 182, 184, 185, 190, 204, 205, 208, 213, 214, 215, 216, 227, 269, 272, 273, 281, 282, 283, 284, 285, 287, 288, 289
molecular weight distribution, 40, 204, 205
molecules, 32, 43, 116, 120, 124, 145, 152, 158, 166, 171, 174, 182, 190, 191, 193, 207, 213, 215, 218, 227, 229, 265, 270, 276, 285, 286
molybdenum, 15
momentum, 65, 282
monolayer, 116, 117, 118, 120, 121, 122
monomers, vii, viii, ix, 2, 24, 31, 32, 33, 41, 42, 63, 64, 129, 130, 136, 144, 145, 208, 221, 244, 248, 256, 260
Moon, 25

morphology, 66, 79, 80, 81, 83, 84, 93, 98, 99, 132, 135, 182, 211, 212, 213, 214, 219, 224, 225, 254
 mortality, 182, 183
 Moscow, 143, 198
 motor activity, 188
 moulding, vii, 1, 270
 MR, 74
 municipal solid waste, 12
 myoglobin, 105

N

Na⁺, 136, 276
 NaCl, 45, 103, 106, 107, 276
 nanocomposites, x, 201, 203
 nanocrystals, 230
 nanofibers, 64, 215, 220
 nanomaterials, 217
 nanometer(s), 116, 140, 209, 223, 225, 242, 245, 261, 263
 nanometer scale, 209
 nanoparticles, x, xi, 84, 85, 195, 201, 203, 206, 224, 229, 231, 250, 255, 256, 261, 263, 264, 265, 269, 275
 nanoreactors, viii, 31
 nanorods, 225
 nanostructures, 226, 242, 266
 nanotechnology, 32, 202, 206, 207
 nanowires, 225
 naphthalene, 65
 narcotic, 181
 natural resources, 64
 NCP, 183
 Netherlands, 31
 network polymers, x, 143, 151
 neutral, 46, 145, 148, 163, 173, 176, 177, 180, 184
 neutrophils, 188
 New South Wales, 72
 NH₂, 41, 144, 207
 nickel, 106, 206, 217, 270
 nitrogen, 8, 9, 14, 16, 65, 152, 170
 nitroxide, 33, 40, 211
 NMR, 134, 149
 non-polar, 33, 42, 158, 169
 North America, 61, 62, 72
 nuclear magnetic resonance, 111
 Nuclear Regulatory Commission, 279
 nucleation, xi, 224, 241, 256, 281, 282, 284, 285, 286, 288, 289
 nuclei, 256
 nucleotides, 100
 nucleus, 244
 nutrient, 186

nutrition, ix, 75

O

OH, 17, 91, 207, 209
 oil, vii, 1, 10, 13, 14, 15, 19, 26, 27, 32, 44, 47, 48, 64, 65, 79, 80, 82, 83, 169
 olefins, 14, 27
 oleic acid, 275
 oligomerization, 15
 oligomers, 256, 272
 one dimension, 225
 opportunities, 62, 139
 optical properties, 120, 123, 228
 optimization, 24, 91, 231, 242, 250, 254
 optoelectronic properties, 230
 optoelectronics, 226
 ores, 171
 organ, 188, 212, 213
 organic compounds, x, 20, 65, 143, 144, 158, 160, 161, 162, 168, 169, 170, 181, 189, 190, 191, 193
 organic solvents, 212
 osmotic pressure, 44, 175, 176
 overlap, 190, 225
 ox, 19
 oxidation, vii, 2, 143, 165, 270, 275
 oxidative reaction, 228
 oxidative stress, 276
 oxygen, 15, 19, 39, 144, 202, 215
 ozone, 218, 219

P

PAA, 34, 39, 40, 41, 42, 44, 45, 46
 Pacific, 61, 72
 paints, 44, 228, 229
 pairing, 85
 pancreatitis, 181
 parallel, 60, 123, 218, 222
 parasites, 60
 particle morphology, xi, 269
 pasteurization, 18
 patents, 4, 54, 158, 270
 pathways, 5, 17, 24, 222
 PCA, 171, 172, 180
 penicillin, 166
 peptide(s), 100, 110
 percolation, 46, 177, 187, 218, 220, 221, 222, 225
 percolation theory, 46
 perfusion, 76, 78, 79, 100, 109, 110, 113
 periodicity, 120

- permeability, x, 64, 102, 108, 143, 145, 146, 158, 215
- permission, 77, 79, 80, 81, 82, 83, 86, 87, 88, 89, 90, 93, 94, 95, 96, 97, 98, 99, 102, 103, 105, 106, 107, 108, 150, 152, 153, 154, 155, 156, 159, 164
- permittivity, 229
- pesticide, 161, 165
- PET, 4, 12, 13, 14, 16, 27
- petroleum, 24, 75, 272
- pH, ix, 40, 44, 46, 47, 75, 76, 105, 106, 107, 110, 148, 164, 166, 188
- pharmaceutical(s), ix, 57, 58, 75, 162, 166, 167, 206, 277
- pharmacology, 32
- phenol, 158, 161, 163, 164, 169
- phenolic compounds, 161, 164
- phonons, 230
- phosphate, 106, 107, 166, 191, 276
- photobleaching, 230
- photocatalyst(s), x, 228, 241, 242
- photodegradation, 263
- photoluminescence, 262
- photolysis, 165, 228
- photonics, 226
- photons, 261
- physical characteristics, 273
- physical phenomena, 117
- physical properties, x, 15, 132, 201, 208, 224, 272
- physical structure, 144
- physicochemical properties, x, 241, 242, 244, 245, 248, 250, 254, 255, 256, 266
- physics, 117, 124, 217
- pitch, 11
- plants, 166, 274
- plasmid, 100
- plasmid DNA, 100
- plasticity, 273
- plasticization, 227
- plastics, 10, 12, 13, 15, 16, 17, 23, 24, 25, 26, 27, 28, 63, 72, 228, 229, 232, 242
- platelets, 136, 181, 182, 184, 187, 188, 209, 210, 212, 213, 214, 223
- platform, 120, 184, 231
- playing, 277, 278
- PMMA, 34, 38, 41
- point of origin, 71
- polar, x, 18, 40, 41, 143, 144, 158, 162, 163, 165, 166, 169, 182, 190, 193, 194, 207, 210, 214
- polar groups, 194, 207, 210
- polar media, 169
- polarity, 33, 193, 203
- polarizability, 192
- polarization, 122, 123, 153, 223
- pollutants, 161, 162, 163
- pollution, viii, 53, 64, 71
- poly(ethylene terephthalate), 4, 64
- poly(vinyl chloride), 4, 14
- polyamine, 85
- polybutadiene, 32
- polycyclic aromatic hydrocarbon, 9, 17, 137, 141, 170
- polydimethylsiloxane, 13, 138
- polydispersity, 5, 40, 208
- polymer chain(s), 40, 69, 90, 132, 203, 205, 208, 209, 213, 214, 216, 223, 227, 229, 230
- polymer composites, 69
- polymer materials, 202
- polymer matrix, 68, 69, 71, 203, 206, 207, 208, 209, 210, 213, 216, 221, 226, 273
- polymer melts, 282
- polymer molecule, 218
- polymer nanocomposites, 202, 231, 234
- polymer properties, 225
- polymer solutions, 46, 282, 285, 286, 287, 288, 289
- polymer structure, 43, 205
- polymer wastes, 23
- polymeric blends, 155
- polymeric chains, 145, 146, 149, 153, 154, 158
- polymeric materials, ix, 2, 8, 18, 22, 23, 110, 129, 185
- polymerizable groups, ix, 129, 130, 134
- polymerizable ionic liquids, ix, 129, 130, 131, 134, 135, 136, 137, 138
- polymerization process, 55, 144, 207, 221, 244, 245, 246, 271
- polymerization temperature, 55
- polyolefins, viii, 2, 24, 27, 53, 202
- polypropylene, 5, 23, 24, 26, 27, 205
- polysaccharide(s), ix, x, 76, 85, 92, 95, 100, 111, 129, 131, 133, 134, 138, 139, 140
- polystyrene latex, 111
- polyurethane, 54
- polyurethane foam, 54
- polyvinyl chloride, 202
- porosity, 76, 78, 83, 102, 149, 152, 154, 157, 249, 263
- porous media, 76
- portability, 278
- potassium, 181, 192, 275
- potassium persulfate, 275
- precedent, 17
- precipitation, 47, 273
- preparation, viii, x, 31, 40, 41, 66, 77, 78, 79, 82, 109, 110, 111, 131, 132, 133, 134, 139, 140, 141, 146, 160, 184, 201, 203, 206, 207, 208, 209, 211, 214, 215, 218, 224, 231, 251, 275

prevention, 207
 principles, 146
 prions, 184
 probability, 179
 probe, 42, 108, 175
 profit, 61
 pro-inflammatory, 187
 project, 59, 60, 73, 231
 proliferation, 188
 propagation, 40, 41, 69, 119, 204, 244
 propane, 55
 propranolol, 167
 propylene, 4, 41, 47, 55, 111
 prostheses, 227
 protection, 39, 57, 58, 165, 215, 217, 277
 protective mechanisms, 123
 proteins, viii, ix, 75, 76, 84, 85, 90, 91, 92, 100, 105, 109, 110, 111, 112, 113, 169, 181, 182
 protons, 174, 175, 191
 psoriasis, 181
 pure water, 43, 172, 173
 purification, 9, 76, 77, 100, 108, 111, 113, 132, 145, 162, 180, 181, 184, 185
 purity, 103, 108, 144, 230, 272, 273
 PVA, 90, 91, 92, 93, 94, 95, 98, 99, 100, 123, 124
 PVC, 4, 12, 13, 14, 16, 27
 pyrolysis, vii, 1, 2, 4, 5, 6, 7, 8, 9, 10, 11, 12, 13, 14, 15, 16, 17, 18, 19, 20, 22, 23, 24, 25, 26, 27, 28, 29, 30, 64, 157, 175, 185, 192, 262
 pyrolysis behaviour, vii, 1
 pyrolysis reaction, 11, 22, 24

Q

quality control, xi, 169, 269
 quantification, 162, 163, 164, 165, 169
 quantum dot(s), 230
 quantum yields, 230
 quartz, 14, 18
 quaternary ammonium, 180

R

radiation, 18, 22, 206, 217, 223
 radical copolymerization, 134, 135
 radical polymerization, viii, ix, x, 31, 33, 40, 42, 54, 55, 129, 130, 131, 132, 134, 136, 138, 141, 204, 211, 228, 229, 246
 radical reactions, 5
 radicals, 5, 7, 11, 19, 40, 205, 219, 228
 radio, 4
 radius, 45, 46, 173, 216

radius of gyration, 216
 raw materials, 262, 265
 reactant, 244, 256, 257
 reactants, 130, 224, 244, 245, 248, 256, 260
 reaction medium, 147, 148, 207, 275
 reaction rate, 40
 reaction temperature, 9, 10, 136, 242, 257
 reaction time, 10, 11, 15, 19, 22, 245
 reactions, 5, 7, 9, 10, 11, 12, 13, 15, 16, 17, 19, 22, 39, 40, 145, 149, 204, 210, 213, 256, 260
 reactivity, 39, 225
 reality, 176
 receptors, 166
 recombination, 5, 6, 205, 213
 recommendations, 154
 recovery, 22, 24, 25, 26, 27, 28, 32, 44, 47, 48, 63, 64, 108, 162, 166, 168, 170, 218
 recreational, 206
 recycling, vii, viii, 1, 2, 22, 23, 25, 26, 28, 53, 62, 63, 64, 65, 66, 67, 71, 72, 74
 red mud, 15, 16
 redistribution, 175
 refractive index, 118, 120, 121, 123, 205, 226, 241, 272
 refractive indices, 118
 regeneration, 134, 171
 regulations, viii, 53, 58, 165
 regulatory requirements, 161
 reinforcement, 124, 220, 230
 relaxation, 205, 208, 222
 remediation, 160
 renal failure, 183
 replication, ix, 115, 122, 249, 250
 repulsion, 44, 251, 254
 requirements, vii, 1, 10, 58, 145, 181, 184, 277
 researchers, vii, 1, 64, 158, 195, 217, 275
 residuals, 28
 residues, 132
 resins, 18, 76, 102, 106, 112, 144, 145, 158, 160, 163, 171, 180, 181, 185, 192, 278
 resistance, viii, ix, 13, 58, 59, 60, 64, 75, 76, 103, 106, 113, 157, 181, 202, 217, 221, 226, 227, 229, 241
 resolution, ix, 75, 76, 100, 107, 109, 195
 resources, 2
 respiratory failure, 183
 response, 21, 181, 223, 226
 retardation, 171, 177, 179, 180, 244
 retention power, 162, 165, 166
 rheology, viii, 31, 44, 46, 47
 rings, 19, 85, 116, 130, 146, 147, 148, 149, 169, 189, 190, 192
 risk(s), 57, 161, 162, 184

Romania, 160
 room temperature, 2, 9, 12, 13, 41, 130, 134, 136,
 138, 144, 148, 152, 205, 222, 230
 routes, 2, 17, 221, 256, 257
 rubber, ix, x, 18, 23, 24, 32, 54, 115, 122, 143, 155,
 202, 229
 Russia, 61, 188, 189, 196, 197

S

safety, 57, 58
 salinity, 44, 47
 salt concentration, 179
 salts, ix, 11, 44, 129, 130, 136, 169, 170, 171, 177,
 181, 190, 192, 224, 243, 272
 saturation, 229
 Saudi Arabia, 61
 savings, 58
 SBS rubber, 32
 scaling, 46
 scanning electron microscopy, 118
 scatter, 154
 scattering, 120, 149, 157, 216, 226, 230, 282
 scavengers, 216
 science, viii, 32, 120, 202, 289
 scientific papers, xi, 269
 scope, 32, 173, 175, 195
 SDS-PAGE, 108
 second generation, 145, 146
 sedimentation, 207
 segregation, 32, 225
 selectivity, viii, 11, 14, 16, 64, 75, 76, 136, 137, 141,
 158, 171, 172, 177, 179, 180, 191, 276
 self-assembly, viii, 31, 32, 116, 117, 120, 208, 221,
 222, 249, 250, 251, 253, 254, 255, 256, 260
 self-organization, 241
 SEM micrographs, 71
 semiconductor(s), 134, 206, 216, 217, 223, 229, 230,
 231
 sensing, 120, 121, 123, 224, 228, 231
 sensitivity, 123
 sensors, 120, 224, 227, 230
 sepsis, 181, 182, 183, 187, 188, 189
 septic shock, 183, 188
 Serbia, 201, 231
 serum, 90, 166, 182, 188
 serum albumin, 90
 sewage, 166
 shape, x, 18, 60, 118, 124, 152, 201, 208, 209, 214,
 217, 219, 224, 225, 226, 230, 241, 242, 249, 250,
 251, 254, 257, 266, 275
 shear, 45, 208, 210, 212, 216, 221
 shock, 54, 183, 188

showing, x, 45, 83, 241, 242, 250, 276
 signal-to-noise ratio, 162
 signs, 154, 189
 silane, 211, 214
 silica, viii, 17, 65, 75, 76, 145, 162, 163, 165, 166,
 167, 169, 206, 209, 229, 250, 251, 252, 254, 255,
 256, 259, 261, 274
 silica dioxide, 209
 silicon, 16, 28, 206, 221
 silver, 192, 206
 SiO₂, 206, 221, 229, 230
 SIP, 60
 skeleton, 253, 254
 SO₄²⁻, 176, 179, 253
 social problem, vii, 1
 society, 279
 sodium, 90, 106, 107, 116, 136, 149, 170, 187, 222,
 224
 solar cells, 224, 228
 sol-gel, 46
 solid phase, 141, 194
 solid surfaces, 182
 solid waste, 2, 63
 solubility, 33, 40, 136, 140, 141, 211, 225, 244, 246
 solvation, 153, 208
 solvent molecules, 285
 solvents, viii, ix, x, xi, 11, 18, 26, 33, 40, 53, 64,
 111, 129, 130, 153, 162, 190, 194, 205, 225, 273,
 281
 sorption, 136, 138, 141, 144, 145, 158, 159, 165,
 169, 171, 181, 185, 187, 190, 191, 192, 193, 194,
 275
 sorption experiments, 185
 sorption isotherms, 192
 South Korea, 62
 species, 5, 39, 40, 161, 172, 175, 182, 193, 203, 205
 specific adsorption, ix, 76, 85, 91
 specific gravity, 272
 specific surface, 84, 92, 154, 158, 170, 182, 184,
 185, 209, 220, 225
 spectroscopy, 216
 spin, ix, 115, 123, 250
 spintronic devices, 228
 SS, 40, 66
 stability, viii, 5, 42, 53, 57, 76, 78, 84, 90, 102, 130,
 138, 148, 203, 205, 213, 218, 225, 227, 229, 230,
 272, 273
 stabilization, 47, 91, 203, 207, 225
 stabilizers, viii, 31, 47, 272
 stable radicals, 39
 standard deviation, 164, 224
 star polymers, 45
 starch, 140

state(s), x, 143, 146, 149, 151, 152, 153, 155, 156, 157, 177, 203, 212, 220, 226

steel, 10, 11, 12, 229

sterol, vii, 143

stomach, 182

storage, 56, 57, 58, 144, 156, 184, 213, 218, 220, 222, 228, 272

storage media, 228

stress, 44, 68, 69, 133, 205, 217, 218, 223, 273

stretching, 91, 122

structural changes, 276

structure formation, 116

structuring, 116

style, 85, 117

styrene copolymers, 144, 155, 202

styrene polymerization, 9, 144, 242, 260

styroloxide, vii, 143

substitution, 22, 87, 130, 148, 157, 190

substitution reaction, 130

substrate(s), 77, 84, 116, 118, 121, 122, 123, 130, 217, 221, 250

sulfate, 17, 28, 90, 116, 175, 176, 179

sulfonamide, 166

sulfuric acid, 179

Sun, 48, 109, 110, 141, 279

superparamagnetic, 224, 229

suppliers, 57, 159

suppression, 216

surface area, 19, 76, 78, 154, 158, 206, 209, 217, 227, 229, 263, 264, 265, 281, 286, 287, 288

surface chemistry, 108, 185

surface energy, 210, 225

surface layer, 275, 285

surface modification, 207, 213, 217, 221

surface properties, 43, 224

surface structure, ix, 115, 122

surface tension, 42, 43, 207, 282, 285, 286, 287, 288

surfactant(s), 32, 40, 4, 77, 79, 81, 82, 111, 116, 161, 163, 170, 207, 211, 212, 214, 215, 217, 219, 221, 222, 242, 243, 246, 249, 260

survival, 182, 187

suspensions, ix, 115, 116

Sweden, 185

sweet gum trees, vii, 143

swelling, 77, 79, 124, 132, 144, 145, 150, 151, 153, 155, 156, 173, 180, 195, 211

swelling process, 153

symptoms, 188

synergistic effect, 208

synthesis, vii, viii, ix, x, 4, 11, 26, 27, 31, 32, 33, 41, 42, 47, 112, 129, 130, 138, 144, 146, 147, 151, 154, 171, 180, 201, 203, 205, 208, 211, 219, 223,

224, 225, 231, 241, 242, 244, 246, 249, 250, 256, 259, 260, 266, 274, 277

synthetic polymers, ix, 63, 95, 129, 132

T

talc, 209

tar, 11, 19, 26

target, 124, 132, 159, 161, 162, 166, 170, 181, 208, 265

techniques, viii, 53, 59, 63, 64, 170, 207, 208, 211, 214, 217, 221, 223, 231, 246, 249, 250, 272, 273, 275

technologies, 2, 4, 22, 62

technology, 2, 4, 10, 17, 22, 62, 71, 72, 184, 202, 222, 232, 278

TEG, 121

TEM, 255, 259, 263

temperature dependence, 223, 230

tensile strength, 68, 212, 217, 221, 228, 229

tension, 43, 207, 287

territory, 160

testing, 16, 66, 133

tetrabutylammonium bromide, 212, 215

tetrahydrofuran, 64, 217

tetrahydrofurane, 144

textiles, 229

TGA, 132, 136, 213, 218

therapy, 183

thermal decomposition, 23

thermal degradation, 24, 30, 65, 132, 213, 227

thermal expansion, 155

thermal history, 208

thermal insulator, vii, 1

thermal properties, xi, 58, 227, 269, 272, 273

thermal resistance, 228

thermal stability, 130, 136, 138, 208, 212, 213, 218, 221, 222, 227, 228, 229, 230, 277

thermodynamic incompatibility, 145

thermodynamics, 24, 285, 289

thermogravimetric analysis, 213, 222

thermolysis, 24

thermooxidative stability, 228

thermoplastics, 206

thermosets, 206

thin films, 218, 226

thinning, 45

thrombosis, 189

tissue, 181, 278

titania, 264

titanium, 171, 206

TNF, 183

TNF- α , 183

toluene, vii, xi, 1, 5, 6, 9, 11, 22, 39, 123, 144, 145, 153, 154, 191, 192, 193, 211, 270, 281, 282
top-down, 221
topology, 45
toxicity, 47, 229, 231
toys, 4, 57, 202, 206, 242, 277
trade, 78, 86
transferrin, 105
transformation, 54, 56, 72, 95
transfusion, 184
transfusion reactions, 184
transistor, 228
transition metal, 40, 192
transition temperature, 136, 227
transmission, 60, 205, 243, 255
transparency, 130, 202, 205, 226, 231
transport, 57, 58, 64, 76, 77, 78, 214, 226, 229, 277
transportation, 206, 277, 278
trauma, 184
treatment, 22, 66, 69, 89, 132, 144, 149, 156, 166, 182, 183, 184, 188, 189, 207, 210, 213, 264, 275, 285
trial, 172
tungsten, 264
tunneling, 223

U

UK, 23, 28, 77, 158, 159, 160, 171, 173, 232, 234
ultrasound, 207, 219, 223
uniform, 40, 55, 69, 149, 205, 207, 218, 220, 222, 230, 276
unique features, 18
United, 28, 54, 62
United States, 54, 62
urea, 135, 187, 188, 190
urine, 166, 168, 169
USA, 66, 76, 78, 145, 158, 161, 183, 188, 195, 196, 197, 198, 211, 232
USSR, 158, 196
UV, 157, 163, 223, 224, 228, 229, 272
UV irradiation, 224, 228
UV radiation, 229

V

vacuum, 9, 17, 25, 56, 276
valence, 149, 151
valve, 162, 163
vapor, 116, 130, 217, 282, 285, 286
variables, 223
variations, 11, 124, 242

vector, xi, 281, 288
vegetable oil, 170, 206
vegetables, 169
vehicles, 206
velocity, 17, 100, 102, 103, 106, 107, 108, 109, 231
versatility, viii, 53, 57, 60, 205, 278
vibration, 91, 148
vinylbenzylimidazolium, ix, 129
viruses, 184
viscosity, 20, 21, 44, 45, 46, 47, 65, 102, 207, 211, 216, 220
visualization, 177, 178
vitamins, 169
volatile organic compounds, 170
volatility, 273
volumetric changes, 274
vulcanization, 18

W

Wales, 160, 199
Washington, 141, 279
waste, vii, viii, 1, 2, 7, 11, 12, 13, 14, 15, 17, 22, 23, 24, 25, 26, 27, 28, 29, 53, 55, 57, 63, 64, 65, 66, 67, 71, 159, 275, 279
waste treatment, vii, 1
wastewater, 144, 160
water absorption, 60, 272, 274
water purification, x, 32, 143
water vapor, 58, 60, 202, 215
wavelengths, 120, 121, 123
wear, 212, 229
web, 158
weight loss, 11, 132, 213
weight ratio, 217, 227
weight reduction, 220
Western Europe, 61
wetlands, 59
wettability, 116, 208
wetting, 71, 152, 160, 191, 210
windows, 18, 139
wood, viii, 15, 53, 60, 65, 66, 67, 68, 69, 70, 71
workers, 57, 168, 275
World War I, 54
worldwide, 60, 62

X

xanthan gum, 140
XPS, 91, 94, 97, 99
X-ray diffraction (XRD), 132
X-ray photoelectron spectroscopy (XPS), 91

XRD, 132, 133, 136

Z**Y**

yeast, 186

yield, 5, 6, 9, 10, 11, 12, 13, 14, 15, 16, 17, 19, 20,
24, 25, 27, 44, 45, 64, 160, 182, 231

yttrium, 262

zeolites, 15, 16, 65

zinc, 206

zinc oxide, 206

ZnO, 16, 206, 228, 229, 275